P.O.Box 2345, Beijing 100023, China
Fax: +86-10-85381893
E-mail: wjg@wjgnet.com www.wjgnet.com

World J Gastroenterol 2003;9(4):635-640
World Journal of Gastroenterology
 ISSN 1007-9327

• REVIEW •

Preventive treatments for recurrence after curative resection of hepatocellular carcinoma - A literature review of randomized control trials

Hui-Chuan Sun, Zhao-You Tang

Hui-Chuan Sun, Zhao-You Tang, Liver Cancer Institute and Zhong Shan Hospital, Fudan University, Shanghai 200032, China
Correspondence to: Hui-Chuan Sun, MD, Associate Professor of Surgery, Liver Cancer Institute and Zhong Shan Hospital, Fudan University, 136 Yi Xue Yuan Road, Shanghai 200032, China. sunhc@zshospital.com
Telephone: +86-21-64041990 Ext 3056 **Fax**: +86-21-64037181
Received: 2002-09-13 **Accepted:** 2002-10-17

Abstract

To review the inhibitory effect of preventive approaches on recurrence after operation in patients with hepatocellular carcinoma (HCC), we summarized all available publications reporting randomized control trial indexed in PubMed. The treatment approaches presented above included pre-operative transcatheter arterial chemoembolization (TACE), post-operative TACE, systemic or locoregional chemotherapy, immunotherapy, Interferons and acyclic retinoic acid. Although no standard treatment has been established, several approaches presented promising results, which were both effective and tolerable in post-operative patients. Pre-operative TACE was not effective on prolonging survivals, while post-operative TACE was shown with both disease-free survival and overall survival benefits in some papers, however, it was also questioned by others. Systemic chemotherapy was generally not effective on prolonging survival but also poorly tolerated for its significant toxicities. Adoptive immunotherapy using LAK cells was proved to be beneficial to patients' survival in a recent paper. Interferon α and Interferon β can inhibit recurrence in HCC patients with HCV infection background, though the mechanism is not fully understood. Acyclic retinoic acid was shown to decrease multi-centric recurrence after operation, which was reported by only one group. In conclusion, several adjuvant approaches have been studied for their efficacy on recurrence in HCC patients in randomized control trials; however, multi-centric randomized control trial is still needed for further evaluation on their efficacy and systemic or local toxicities; in addition, new adjuvant treatment should be investigated to provide more effective and tolerable methods for the patients with HCC after operation.

Sun HC, Tang ZY. Preventive treatments for recurrence after curative resection of hepatocellular carcinoma - A literature review of randomized control trials. *World J Gastroenterol* 2003; 9(4): 635-640
http://www.wjgnet.com/1007-9327/9/635.htm

INTRODUCTION

Over the last two decades, the surgical techniques and peri-operative care have been improved, and the operative death (within 30 days after operation) decreased to 2.5 %[1], the 5-year overall survival after curative resection of hepatocellular carcinoma (HCC) increased to 25 %[1] or 46.7 %[2]. However, HCC is far from a curable disease because of high recurrence rate, the 5-year recurrence rate after curative resection was 38 %[1] and 61.5 %[2], the 5-year disease-free survival was 16 %[3] or 38.6 %[4] after curative resection of HCC, and the recurrence resulted in most deaths after resection[5].

People have tried a number of approaches to prevent recurrence, however, only a few of them were designed as randomized control trial (RCT), which provide evidence-based results for those treatment modalities. In this paper, the authors summarized those results from randomized control trials, attempting to find a more suitable treatment modality for prevention of recurrence.

IMPORTANT ISSUES RELATED TO EVALUATION OF EFFICACY OF PREVENTION

It is difficult to compare the results among different RCTs because of different study settings and patient collection; therefore, several important issues should be addressed in evaluation of efficacy of prevention of HCC recurrence.

The definition of "curative resection"

The most important issue is the definition of "curative resection" of HCC, because, the definition will greatly affect the recurrence rate. There is no consensus on this definition in the literature. Some authors described it as "complete removal of tumor tissues"[6]; others prefer to "complete removal of tumor tissues plus a clear resection margin ≥1 cm on pathological examination"[7]. And some authors used a strict criterion, in which negative findings by angiography followed by Lipiodol-CT and ultrasound one or two months after resection were also included[8]. The 1 year disease-free survival was 43.0 % by the first criteria[6], and 59.1 % by the second[7], and 69 % by the third[8]. The different definitions of curative resection and their results are listed in Table 1.

Bias in patient collection

The clinicopathological characteristics of patients enrolled in a study also influence the results. For example, tumor size, which was regarded as the age of tumor, affects the recurrence rates and survival after operation, thereafter, has great impact on the results (Table 1).

Origins of recurrence

The origin of recurrence can be divided into two sources, uni-centric and multi-centric origins[9], which could be discriminated by genetic markers, such as HBV integration sites[9,10] or p53 mutation types[11]. Uni-centric origin can also be named as intrahepatic metastatic recurrence or residual tumor, which means metastatic lesion spread from the primary main tumor, and left in the remnant liver. However, multi-centric recurrence is a newly developed lesion in the cirrhotic background. Generally two kinds of recurrences can be roughly divided according to the time of appearance. Twelve months[12] or 3-years[13] were set as a parameter to distinguish them by

different authors. A study may be needed to clarify the percentage of uni-centric and multi-centric recurrence by different set point.

Most preventive procedures are targeting the metastatic recurrence, which are used to control the residual tumor cells in the liver. Therefore, 1, 2, 3-year disease-free survival or recurrence rates are used to evaluate the efficacy of preventive procedures targeting metastatic recurrence; however, if a preventive procedure is targeting the multi-centric origin recurrence, 3 or 5-year disease-free survival or recurrence rate should be noticed.

Table 1 showed the overall survival and disease free survival are better when the tumor size decreases, and when a stricter criteria for curative resection was applied. Therefore, when evaluating a preventive treatment targeting residual tumors, it is suggested that a subgroup of patient with more invasive HCC should be enrolled. On the other hand, a subgroup of patient with less invasive HCC or selected by stricter criteria for curative resection should be recruited to investigate a preventive treatment targeting secondary HCC appearance.

LITERATURE REVIEWS OF RANDOMIZED CONTROL TRIALS (RCT) TO PREVENT RECURRENCE OF HCC

Pre-operative or post-operative TACE

TACE has been used to control the growth of HCC for a long time[17]. Pre-operative and post-operative TACE were investigated by RCT to clarify if it reduced the recurrence rate after curative resection of HCC (Table 2).

Wu *et al* have studied the effect of pre-operative TACE (preTACE) on resetability and curability in management of huge resectable HCC. Although preTACE induced tumor shrinkage as expected, the shrinkage of tumor didn' t result in an easy operation, on the contrary, the preTACE group had a longer operative time, more blood loss, more extra-hepatic metastasis, higher possibility of invading adjacent organs by tumors and removal of adjacent organs; furthermore, the disease-free survival (DFS) in preTACE group was not statistically different with that in the control group, the overall survival (OS) was even worse than that in control group. The author suggested that preTACE delayed the resection, which may leave tumor more time to develop intra-hepatic or distant metastasis; in addition, preTACE can' t eliminate tumor cells completely, therefore, preTACE for resectable huge HCC was not recommended[16].

In another study by Yamasaki *et al*, the efficacy of preTACE on small HCC was tested. The results confirmed that preTACE induced necrosis in tumor, but the results demonstrated again that it didn' t improve the DFS, because preTACE was not capable to inhibit the intrahepatic micrometastatic lesions and tumor thrombus in microvessel[17].

The first RCT study on post-operative TACE (postTACE) was reported by Izumi *et al* in1994. The authors enrolled 50 patients after curative resection of HCC with blood vessel involvement or intra-hepatic spreadings. The results showed that both DFS rate and DFS time were higher in postTACE group than those in control group. However, 1 and 3-year OS rates were similar in both groups (58.8 % *vs* 63.5 %; 30.5 % *vs*

Table 1 The important issues related to evaluation of efficacy of prevention of recurrence

Authors	Average tumor size	Definition of curative resection			1 year RR	1 year DFS	1 year OS
		Complete removal in operation	Negative in histology on surgical margin	Negative in post-operative exams			
Kubo[144]	2.6 cm	Yes	No	Yes	25%[a]	NA	92%
Lau[77]	3.8 cm	Yes	Yes	No	NA	59.1%	86.4%
Tang[155]	<5 cm, complete tumor capsule, without portal vein involvement	Yes	Yes	No	6.5%	NA	NA
Poon[12]	>5 cm[a]	Yes	No	No	46%	NA	55.5%
Izumi[6]	>5 cm[a]	Yes	No	No	51.7%	43.0%	81.0%
Lai[8]	10.4 cm	Yes	No	Yes	20-30%	69.0%	75%*

RR: recurrence rate; DFS: disease free survival; OS: overall survival; NA: data not available.
[a]estimated according to the authors' paper.

Table 2 Summary of RCTs to evaluate the efficacy of pre- and post-operative TACE on prevention of recurrence

Authors	Tumor factors	Treatment protocol	Sample size (Tx/Ctl)	Observation time	DFS (Tx *vs* Ctl)	OS (Tx *vs* Ctl)	Conclusions
Wu[18]	>10 cm; resectable	Pre-operative TACE	52 (24/28)	2-10 years	3-year 39% *vs* 46%[a]	3-year 31% *vs* 62%[a]	Harmful
Yamasaki[19]	2-5 cm; Single	Pre-operative TACE	97 (50/47)	4-6.6 years	39.1% *vs* 31.1%	NA	Not effective
Izumi[6]	With vessel involvement or intrahepatic spreading	Post-operative TACE, once L 3ml/m^2+A 20mg/m^2+M 10mg/m^2+G or: L 2ml/m^2+A+M	50 (23/27)	28.7 Months (median)	3-year 32% *vs* 11.7%	3-year 56.6% *vs* 53.4%	Postpone recurrence,but change over all survival
Lai[8]	Negative in lipiodol CT, angiography and ultrasound one month after operation	Post-operative TACE, 3 times L 10ml+C 10mg+EA(40mg/m^2 iv×8)	66 (30/36)	Median 28.3 months	3-year 18% *vs* 48%	3-year 65% *vs* 67%[a]	Harmful
Lau[7]	Surgical margin ≥1 cm	Post-operative TACE I^{131} Lipiodol	43 (21/22)	14.1-69.7 months	3-year 74.5% *vs* 36%	3-year 84.4% *vs* 46.3%	Beneficial

L: lipiodol; M: mitomycin; A: adriamycin, G: gelfoam; C: cis-platin; Tx: treatment; Ctl: control; DFS: disease free survival; OS: overall survival.
[a]estimated according to the figure in authors' paper.

33.9 %, *P*=0.7647), the median survival time in postTACE was shorter than that in the control group (644.5±129.4 days *vs* 759.9±137.5day, *P*<0.05). The authors concluded that postTACE may postpone but not eliminate the recurrence (60.9 % *vs* 81.5 %, *P*=0.106)[6].

In another RCT reported by Lau *et al*, the authors used ^{131}I-Lipiodol instead of conventional Lipiodol. The result showed that postTACE improved DFS and OS, decreased recurrence without major side-effects[7]. This is the only one RCT reporting a positive result for postTACE treatment. The authors suggested more effective agents should be used in postTACE.

However, in Lai *et al*' s study of postTACE, although the preventive treatment protocol was more aggressive than Izumi' s study, the result was even worse. The recurrence rate and extrahepatic metastasis rate were higher in postTACE group (recurrence rate: 23/30 *vs* 17/36, *P*=0.01) extrahepatic metastasis rate: 11/30 *vs* 5/36, *P*=0.03); 3-year DFS in postTACE group was lower than that in the control group (18 % *vs* 48 %, *P*=0.04). The OS in postTACE group was worse than that in the control group, especially in the first two years, but the difference was not statistically significant. Therefore, the authors concluded postTACE is harmful to patients after curative resection of HCC[8].

The reason of why conflicting results came from different RCTs is the selection of patients. Lai *et al*' s group of patients was selected by a highly rigorous standard; the rationale of preventive treatment was not solid enough to protect this group of patient with interventional treatment like postTACE. However, in Izumi and Lau' s studies, the authors selected a group of patients with more possibility of recurrence (invasive cancer or large cancer), so the results turned out to be effective.

In summary, preTACE is not helpful in terms of decreasing recurrence after resection of resectable HCC. PostTACE is only beneficial to the patients with invasive HCC, but not effective or even harmful to the patients after a "real" curative resection.

Systemic or locoregional chemotherapy

Systemic chemotherapy is generally not effective in most cases with HCC[18], only a few papers showed a favorable results of systemic chemotherapy[19]. Here is a summary of RCTs studying post-operative systemic and locoregional chemotherapy (Table 3).

Yamamoto *et al* studied systemic chemotherapy using HCFU 200 mg bid as a adjuvant treatment for the patients after curative resection of HCC. The result showed that systemic chemotherapy was effective in a subgroup of patients with mild cirrhosis and good liver function, but not effective in a subgroup of patients with severe cirrhosis and poor liver function. The authors discussed that systemic chemotherapy inhibited the growth of micro-metastatic lesions existing before operation or multi-centric carcinogenesis after operation, but jeopardized liver function as well, which resulted a negative effect on both OS and DFS, especially in patients with poor liver function reserve[20].

Kohno *et al* studied the result of an aggressive treatment combining systemic and one course of transcatheter arterial chemotherapy (TAC). There was no obvious side-effect of this treatment. However, the results showed this combination treatment did not improve the 3 and 5-yearOS and DFS compared with the control group with UFT treatment alone, and another control group without any specific treatment[21].

Ono *et al*' s treatment protocol was even more aggressive with combining systemic and multiple courses of TAC, however, the result was still negative. Furthermore, very aggressive protocol was intolerable to most enrolled patients, and too many cases withdrew from this study[22].

Ueno *et al*' s study showed multiple courses of TAC improved DFS after curative resection of HCC. The flaw of this study is too small sample size[23].

A recent meta-analysis also showed that systemic chemotherapy was not effective or even harmful as an adjuvant treatment in patients after resection of HCC[24]. Another meta-analysis showed that TAE (transcatheter arterial embolization) improved OS after resection of HCC compared with TAC, and no evidence showing TACE was more effective than TAE[25], which implied a very limited benefit of locoregional chemotherapy introduced by TACE overtopping TAE alone.

From the above data, it is suggested that systemic or locoregional chemotherapy didn' t inhibit the recurrence, and the tolerance was another important factor influencing the results.

Post-operative adoptive immunotherapy

Post-operative active or adoptive immunotherapy became a very attractive cancer treatment modality in early 1990s

Table 3 Summary of locoregional or systemic chemotherapy for prevention of recurrence

Authors	Entry criteria	Treatment protocol	Sample size (Tx / Crl)	Observation time	DFS (Tx *vs* Ctl)	OS (Tx *vs* Ctl)	Conclusions
Yamamoto[20]	Liver cacner study group of japan for UICC stage II HCC[a]	HCFU 200mg, bid	67(32 / 35)	6-10 years	Stage I[b] cirrhosis 62% *vs* 32% Stage II cirrhosis 0% *vs* 0%[c]	Stage I cirrhosis 79% *vs* 70% Stage II cirrhosis 59% *vs* 57%[c]	Beneficial only to patients with Stage I liver dys function
Kohno[21]	NA	UFT 300mg, qd *vs* UFT 300mg, qd+A (ia, 40mg / m^2, once)	88 (40 / 48)	NA	3-year 37% *vs* 32%	NA	Not effective
Ono[22]	NA	A 40mg / m^2 ia and 40mg / m^2 iv every 3 months for 2 years, and HCFU 300mg qd for 2 years	56 (29 / 27)	24 months	NA	NA	Not effective,with poor tolerance
Ueno[23]	NA	CDDP 50-80mg and MMC 10mg ia, 2-3 times	21 (11 / 10)	>1 year	70% *vs* 20%[c]	NA	Beneficial

NA: not available; A: adriamycin or Epirubicin; ia: intraarterially; iv: intravenously; DFS: disease free survival; OS: overall survival.
[a] complete excision of a solitary tumor, less than 5 cm in diameter, with a tumor capsule and no vascular invasion to the first or second branches of the portal vein, or for other stage II tumors, complete removal with a surgical margin from the tumor edge of more than 1 cm;
[b]see the original paper;
[c]estimated according to the figure in authors' paper.

because of a series of successful animal experiments[26]; however, it turned out to be not so effective as expected in a number of clinical trials[27-29]. At the same time, several clinical trials have been set up to test the effect of adoptive immunotherapy on recurrence in patients with HCC in early 1990s. The followings are a summary of these RCTs (Table 4).

Une *et al*' s study compared the effect of locoregional chemotherapy with locoregional chemotherapy plus systemic immunotherapy on recurrence after curative resection of HCC. The results showed that locoregional chemotherapy plus systemic immunotherapy decreased recurrence rate[30]. However, Kawata *et al*, reported from the same institution and used almost identical treatment settings, demonstrated immunochemotherapy didn' t present any survival benefit to the patients, although in a subgroup of patients with negative surgical margin (≥1 cm), the immunochemotherapy group had a better disease-free survival rate than the chemotherapy group[31]. The reason of the difference might come from the different observation time.

Lygidakis *et al* employed a protocol combining pre-operative and post-operative locoregional chemotherapy with systemic immunotherapy to prevent post-operative recurrence in HCC patients. The results showed this protocol decreased recurrence[32].

In Takayama' s study, which had a more than 5-year observation time, presented a clear survival benefit from adoptive immunotherapy in terms of DFS but not OS. To explain the reason of that, the authors discussed that adoptive immunotherapy may eliminate the micrometastatic lesion in the remnant liver, but can' t prevent multicentric recurrence; the second reason was, during a longer time of observation, the treatment choice for recurrence was not totally dependent on doctors' presetting, therefore different treatment modalities may affect the long term results[1].

In general, the immunotherapy may inhibit recurrence in patients after resection of HCC, especially in the first several years after operation, with a good tolerance. However, it needs more randomized control trial to confirm, and more powerful agents need to be discovered.

Post-operative Interfereon (IFN) treatment

The rationale of post-operative IFN treatment came from the several findings in HCV related HCC. First, a lower incidence of HCC was observed in many studies when IFN was used to clear HCV viremia[33]; second, recurrence after curative resection of HCC developed from multicentric origin, which was closely related to the HCC viremia status[14]. Third, IFN had anti-cancer effect on the early stage tumors, like micrometastatic lesions[34]. The following is the summary of post-operative IFN treatment (Table 5).

Ikeda *et al*[35]s results showed that, although the recurrence curve increased similarly in both groups in the first two years, but it remained the same in treatment group after that, which suggested that the effect of IFNβ on prevention of recurrence was not through direct inhibition of tumor cells per se, but depended on the clearance of HCV viremia, implying the mechanism of IFNα is through inhibition of multicentric recurrence. However, in Kubo *et al*' s study, the decrease of recurrence rate was associated with neither clearance of HCV nor normalization of serum ALT level, the actual reason was unknown, but the authors suggested that it might depend on direct antitumor effects or inhibition of carcinogenesis by HCV. Therefore, the mechanism of IFN' s effect on recurrence remains to be investigated further[14,36]. Recently, our data

Table 4 A summary of RCT results of adoptive immunotherapy to prevent recurrence

Authors	Entry criteria	Treatment protocol	Sample size (Tx/Ctl)	Observation time	DFS Tx *vs* Ctl	OS Tx *vs* Ctl	Conclusions
Une[30]	NA	A ia *vs* A+LAK and IL2 ia	24(12/12)	NA	50% *vs* 8.3%	NA	Beneficial
Kawata[31]	NA	A ia *vs* A +IL2+LAK ia	24(12/12)	NA	NS	NA	Not beneficial
Lygidakis[32]	NA	No Tx *vs* Chemoimmunotherapy	40(20/20)	NA	Recurrence: 0/18 *vs* 7/17	NA	Beneficial
Takayama[1]	Completely remove; histologically negative in surgical margin	LAK IV at the 2nd, 3rd, 4th, 12th, 24th week after operation	155 (76/79)	>5 years	3-year 48% *vs* 33% 5 year 37% *vs* 22%	5-year 68% *vs* 62%	Beneficial

ia: intra-arterially; iv: intravenously; NA: not available; NS: not significant; DFS: disease free survival; OS: overall survival; Tx: treatment; Ctl: control; LAK: lymphokine activated killer cells; NA: not available.

Table 5 Summary of RCTs of Interferon treatment

Authors	Entry criteria	Tx protocol	Sample size	Observation time	DFS Tx *vs* Ctl	OS Tx *vs* Ctl	Conclusions
Ikeda[35]	Complete remove by resection or PEI	IFNβ 6MU im biw×36 months	20(10/10)	2-34.6 months	1 year 0% *vs* 62.5%	NA	Beneficial
Kubo[14,36]	Complete remove, negative in CT scan 3-4 weeks after operation	IFNα 6MU biw×2 weeks then tiw×14 weeks then biw×88 weeks	30(15/15)	1817 days (Tx) and 1487 (Ctl)	Recurrence 9/15 *vs* 13/15 P=0.041	NA	Beneficial

Table 6 Summary of RCTs of acyclic retinoic acid

Authors	Entry criteria	Tx protocol	Sample size	Observation time	Recurrence Tx *vs* Ctl	OS Tx. *vs* Ctl	Conclusions
Muto[37,38]	Complete removal by resection or PEI, negative in postoperative Ultrasound or CT	ARA 300mg, bid	89(44/45)	62 months (Median)	27% *vs* 49% (P=0.04)	6 year 74% *vs* 46%	Beneficial

Tx: treatment; Ctl: control; OS: overall survival.

suggested anti-angiogenesis instead of the anti-proliferation property of IFNα involving in antitumor effect in animal models, and it may act through regulation of VEGF expression. A randomized control trial in HBV related HCC patients after curative resection was also conducted to test the effect of IFNα on recurrence in the authors' institution, the interim results showed that long-term IFNα treatment improved disease-free survival of patients through direct antitumor effect, which was not associated with serum conversion of HBeAg.

Acyclic retinoid acid

Retinoid acid is a inducer of differentiation. All-trans retinoic acid has been successfully used to treat a subtype of leukemia. Muto *et al* reported a serial results in patients with HCV-related HCC treated by post-operative acyclic retinoic acid (ARA), and showed long term ARA treatment improvement in OS and DFS[37,38]. A further study revealed the mechanism of ARA treatment was through inhibition of second primary liver cancer by deletion of a latent clonal hepatoma cells[39] (Table 6).

SUMMARY

A number of preventive treatment protocols to inhibiting recurrence after curative resection of HCC have been evaluated by RCT. Although no standard treatment has been proven to be effective to all patients, several approaches presented promising results, which were both effective and tolerable in post-operative patients. Generally systemic and locoregional chemotherapy or combined with embolization was not as effective as expected, meanwhile the side-effects, such as downstaging of liver function was noticed in this treatment; however, biological treatment approaches showed a better outcome, but need more evidence before being accepted widely.

REFERENCES

1 **Takayama T**, Sekine T, Makuuchi M, Yamasaki S, Kosuge T, Yamamoto J, Shimada K, Sakamoto M, Hirohashi S, Ohashi Y, Kakizoe T. Adoptive immunotherapy to lower postsurgical recurrence rates of hepatocellular carcinoma: a randomised trial. *Lancet* 2000; **356**: 802-807

2 **Tang ZY**, Yu YQ, Zhou XD, Ma ZC, Wu ZQ. Progress and prospects in hepatocellular carcinoma surgery. *Ann Chir* 1998; **52**: 558-563

3 **Poon RTP**, Fan ST, Lo CM, Ng IOL, Liu CL, Lam CM, Wong J. Improving survival results after resection of hepatocellular carcinoma: a prospective study of 377 patients over 10 years. *Ann Surg* 2001; **234**: 63-70

4 **Qin LX**, Tang ZY. The prognostic molecular markers in hepatocellular carcinoma. *World J Gastroenterol* 2002; **8**: 385-392

5 **Ikeda K**, Saitoh S, Tsubota A, Arase Y, Chayama K, Kumada H, Watanabe G, Tsurumaru M. Risk factors for tumor recurrence and prognosis after curative resection of hepatocellular carcinoma. *Cancer* 1993; **71**: 19-25

6 **Izumi R**, Shimizu K, Iyobe T, Ii T, Yagi M, Matsui O, Nonomura A, Miyazaki I. Postoperative adjuvant hepatic arterial infusion of Lipiodol containing anticancer drugs in patients with hepatocellular carcinoma. *Hepatology* 1994; **20**: 295-301

7 **Lau WY**, Leung TW, Ho SKW, Chan M, Machin D, Lau J, Chan ATC, Yeo W, Mok TSK, Yu SC, Leung NW, Johnson PJ. Adjuvant intra-arterial lipiodol iodine-131 for resectable hepatocellular carcinoma: a prospective randomised trial. *Lancet* 1999; **353**: 797-801

8 **Lai ECS**, Lo CM, Fan ST, Liu CL, Wong J. Postoperative adjuvant chemotherapy after curative resection of hepatocellular carcinoma: a randomized controlled trial. *Arch Surg* 1998; **133**: 183-188

9 **Sakon M**, Nagano H, Nakamori S, Dono K, Umeshita K, Murakami T, Nakamura H, Monden M. Intrahepatic recurrences of hepatocellular carcinoma after hepatectomy: analysis based on tumor hemodynamics. *Arch Surg* 2002; **137**: 94-99

10 **Yamamoto T**, Kajino K, Kudo M, Sasaki Y, Arakawa Y, Hino O. Determination of the clonal origin of multiple human hepatocellular carcinomas by cloning and polymerase chain reaction of the integrated hepatitis B virus DNA. *Hepatology* 1999; **29**: 1446-1452

11 **He B**, Tang ZY, Liu KD, Zhou G. Analysis of the cellular origin of hepatocellular carcinoma by p53 genotype. *J Cancer Res Clin Oncol* 1996; **122**: 763-766

12 **Poon RTP**, Fan ST, Ng IOL, Lo CM, Liu CL, Wong J. Different risk factors and prognosis for early and late intrahepatic recurrence after resection of hepatocellular carcinoma. *Cancer* 2000; **89**: 500-507

13 **Sugimoto R**, Okuda K, Tanaka M, Aoyagi S, Kojiro M. Metachronous multicentric occurrence of hepatocellular carcinoma after surgical treatment - clinicopathological comparison with recurrence due to metastasis. *Oncol Rep* 1999; **6**: 1303-1308

14 **Kubo S**, Nishiguchi S, Hirohashi K, Tanaka H, Shuto T, Yamazaki O, Shiomi S, Tamori A, Oka H, Igawa S, Kuroki T, Kinoshita H. Effects of long-term postoperative interferon-alpha therapy on intrahepatic recurrence after resection of hepatitis C virus-related hepatocellular carcinoma. A randomized, controlled trial. *Ann Intern Med* 2001; **134**: 963-967

15 **Tang ZY,** Yu YQ, Zhou XD. An important approach to prolonging survival further after radical resection of AFP positive hepatocellular carcinoma. *J Exp Clin Cancer Res* 1984; **4**: 359-366

16 **Wu CC**, Ho YZ, Ho WL, Wu TC, Liu TJ, P'Eng FK. Preoperative transcatheter arterial chemoembolization for resectable large hepatocellular carcinoma: a reappraisal. *Br J Surg* 1995; **82**: 122-126

17 **Yamasaki S**, Hasegawa H, Kinoshita H, Furukawa M, Imaoka S, Takasaki K, Kakumoto Y, Saitsu H, Yamada R, Oosaki Y, Arii S, Okamoto E, Monden M, Ryu M, Kusano S, Kanematsu T, Ikeda K, Yamamoto M, Saoshiro T, Tsuzuki T. A prospective randomized trial of the preventive effect of pre-operative transcatheter arterial embolization against recurrence of hepatocellular carcinoma. *Jpn J Cancer Res* 1996; **87**: 206-211

18 **Alsowmely AM**, Hodgson HJF. Non-surgical treatment of hepatocellular carcinoma. *Aliment Pharmacol Ther* 2002; **16**: 1-15

19 **Clavien PA**, Selzner N, Morse M, Selzner M, Paulson E. Downstaging of hepatocellular carcinoma and liver metastases from colorectal cancer by selective intra-arterial chemotherapy. *Surgery* 2002; **131**: 433-442

20 **Yamamoto M**, Arii S, Sugahara K, Tobe T. Adjuvant oral chemotherapy to prevent recurrence after curative resection for hepatocellular carcinoma. *Br J Surg* 1996; **83**: 336-340

21 **Kohno H**, Nagasue N, Hayashi T, Yamanoi A, Uchida M, Ono T, Yukaya H, Kimura N, Nakamura T. Postoperative adjuvant chemotherapy after radical hepatic resection for hepatocellular carcinoma (HCC). *Hepatogastroenterology* 1996; **43**: 1405-1409

22 **Ono T**, Nagasue N, Kohno H, Hayashi T, Uchida M, Yukaya H, Yamanoi A. Adjuvant chemotherapy with epirubicin and carmofur after radical resection of hepatocellular carcinoma: a prospective randomized study. *Semin Oncol* 1997; **24**(2Suppl 6): S618-S625

23 **Ueno S**, Tanabe G, Yoshida A, Yoshidome S, Takao S, Aikou T. Postoperative prediction of and strategy for metastatic recurrent hepatocellular carcinoma according to histologic activity of hepatitis. *Cancer* 1999; **86**: 248-254

24 **Ono T**, Yamanoi A, Nazmy El Assal O, Kohno H, Nagasue N. Adjuvant chemotherapy after resection of hepatocellular carcinoma causes deterioration of long-term prognosis in cirrhotic patients: metaanalysis of three randomized controlled trials. *Cancer* 2001; **91**: 2378-2385

25 **Camma C**, Schepis F, Orlando A, Albanese M, Shahied L, Trevisani F, Andreone P, Craxi A, Cottone M. Transarterial chemoembolization for unresectable hepatocellular carcinoma: meta-analysis of randomized controlled trials. *Radiology* 2002; **224**: 47-54

26 **Rosenberg SA**. Adoptive immunotherapy for cancer. *Sci Am* 1990; **262**: 62-69

27 **Hermans J**, Bonenkamp JJ, Boon MC, Bunt AM, Ohyama S, Sasako M, Van de Velde CJ. Adjuvant therapy after curative resection for gastric cancer: meta-analysis of randomized trials. *J Clin Oncol* 1993; **11**: 1441-1447

28 **Huncharek M**, Caubet JF, McGarry R. Single-agent DTIC versus

combination chemotherapy with or without immunotherapy in metastatic melanoma: a meta-analysis of 3273 patients from 20 randomized trials. *Melanoma Res* 2001; **11**: 75-81

29 **Hanna MG Jr**, Hoover HC Jr, Vermorken JB, Harris JE, Pinedo HM. Adjuvant active specific immunotherapy of stage II and stage III colon cancer with an autologous tumor cell vaccine: first randomized phase III trials show promise. *Vaccine* 2001; **19**: 2576-2582

30 **Une Y**, Kawata A, Uchino J. Adopted immunochemotherapy using IL-2 and spleen LAK cell-randomized study. *Nippon Geka Gakkai Zasshi* 1991; **92**: 1330-1333

31 **Kawata A**, Une Y, Hosokawa M, Wakizaka Y, Namieno T, Uchino J, Kobayashi H. Adjuvant chemoimmunotherapy for hepatocellular carcinoma patients. Adriamycin, interleukin-2, and lymphokine-activated killer cells versus adriamycin alone. *Am J Clin Oncol* 1995; **18**: 257-262

32 **Lygidakis NJ**, Pothoulakis J, Konstantinidou AE, Spanos H. Hepatocellular carcinoma: surgical resection versus surgical resection combined with pre- and post-operative locoregional immunotherapy-chemotherapy. A prospective randomized study. *Anticancer Res* 1995; **15**: 543-550

33 **Camma C**, Giunta M, Andreone P, Craxi A. Interferon and prevention of hepatocellular carcinoma in viral cirrhosis: an evidence-based approach. *J Hepatol* 2001; **34**: 593-602

34 **Jonasch E**, Haluska FG. Interferon in oncological practice: review of interferon biology, clinical applications, and toxicities. *Oncologist* 2001; **6:** 34-55

35 **Ikeda K**, Arase Y, Saitoh S, Kobayashi M, Suzuki Y, Suzuki F, Tsubota A, Chayama K, Murashima N, Kumada H. Interferon beta prevents recurrence of hepatocellular carcinoma after complete resection or ablation of the primary tumor-A prospective randomized study of hepatitis C virus-related liver cancer. *Hepatology* 2000; **32**: 228-232

36 **Kubo S**, Nishiguchi S, Hirohashi K, Tanaka H, Shuto T, Kinoshita H. Randomized clinical trial of long-term outcome after resection of hepatitis C virus-related hepatocellular carcinoma by postoperative interferon therapy. *Br J Surg* 2002; **89**: 418-422

37 **Muto Y**, Moriwaki H, Ninomiya M, Adachi S, Saito A, Takasaki KT, Tanaka T, Tsurumi K, Okuno M, Tomita E, Nakamura T, Kojima T. Prevention of second primary tumors by an acyclic retinoid, polyprenoic acid, in patients with hepatocellular carcinoma. Hepatoma Prevention Study Group. *N Engl J Med* 1996; **334**: 1561-1567

38 **Muto Y**, Saito A. Prevention of second primary tumors by an acyclic retinoid in patients with hepatocellular carcinoma. *N Engl J Med* 1999; **340**: 1046-1047

39 **Moriwaki H**, Yasuda I, Shiratori Y, Uematsu T, Okuno M, Muto Y. Deletion of serum lectin-reactive alpha-fetoprotein by acyclic retinoid: a potent biomarker in the chemoprevention of second primary hepatoma. *Clin Cancer Res* 1997; **3**: 727-731

Edited by Wu XN

P.O.Box 2345, Beijing 100023, China
Fax: +86-10-85381893
E-mail: wjg@wjgnet.com www.wjgnet.com

World J Gastroenterol 2003;9(4):641-644
World Journal of Gastroenterology
 ISSN 1007-9327

• REVIEW •

Current status and prospects of studies on human genetic alleles associated with hepatitis B virus infection

Fu-Sheng Wang

Fu-Sheng Wang, Division of Biological Engineering, Beijing Institute of Infectious Diseases, 100 Xi Si-Huan-Zhong Road, Beijing 100039, China
Supported by Key project grant from Natural Science Foundation of Beijing Municipal Government No: 7011005
Correspondence to: Dr. Fu-Sheng Wang, Professor of Medicine, Division of Bioengineering, Beijing Institute of Infectious Diseases, 100 Xi Si-Huan-Zhong Road, Beijing 100039, China. fswang@public.bta.net.cn
Telephone: +86-10-63831870 **Fax:** +86-10-63831870
Received: 2002-11-26 **Accepted:** 2002-12-18

Abstract

Chronic hepatitis B virus (HBV) infection can cause a broad spectrum diseases, including from asymptomatic HBV carriers or cryptic hepatitis, to acute hepatitis, chronic hepatitis, Liver cirrhosis and primary hepatocellular carcinoma. The variable pattern and clinical outcome of the infection were mainly determined by virological itself factors, host immunological factors and genetic factors as well as the experimental factors. Among the human genetic factors, major candidate or identified genes involved in the process of HBV infection fall into the following categories: (1) genes that mediate the processes of viral entry into hepatocytes, including genes involved in viral binding, fusion with cellular membrane and transportation in target cells; (2) genes that modulate or control the immune response to HBV infection; (3) genes that participate in the pathological alterations in liver tissue; (4) genes involved in the development of liver cirrhosis and hepatocellular carcinoma associated with chronic HBV infection, including genes related to mother-to-infant transmission of HBV infection; and (5) those that contribute to resistance to antiviral therapies. Most of the reports of human genes associated with HBV infection have currently focused on HLA associations. For example, some investigators reported the association of the HLA class II alleles such as DRB1*1302 or HLA-DR13 or DQA1*0501-DQB1*0301-DQB1*1102 haplotypes with acute and/or chronic hepatitis B virus infection, respectively. Several pro-inflammatory cytokines such as Th1 cytokines (including IL-2 and IFN-γ) and TNF-α have been identified to participate the process of viral clearance and host immune response to HBV. In contrast, the Th2 cytokine IL-10 serves as a potent inhibitor of Th1 effector cells in HBV diseases. The MBP polymorphisms in its encoding region were found to be involved in chronic infection. Thus, reports from various laboratories have shown some inconsistencies with regard to the effects of host genetic factors on HBV clearance and persistence. Since genetic interactions are complex, it is unlikely that a single allelic variant is responsible for HBV resistance or susceptibility. However, the collective influence of several single nucleotide polymorphisms (SNPs) or haplotype (s) may underlie the natural combinational or synergistic protection against HBV. The future study including the multi-cohort collaboration will be needed to clarify these preliminary associations and identify other potential candidate genes. The ongoing study of the distributions and functions of the implicated allele polymorphisms will not only provide insight into the pathogenesis of HBV infection, but may also provide a novel rationale for new methods of diagnosis and therapeutic strategies.

Wang FS. Current status and prospects of studies on human genetic alleles associated with hepatitis B virus infection. *World J Gastroenterol* 2003; 9(4): 641-644
http://www.wjgnet.com/1007-9327/9/641.htm

INTRODUCTION

Chronic hepatitis B virus (HBV) infection is one of the most common infectious diseases and leads to high morbidity and mortality due to the development of liver cirrhosis (LC) and hepatocellular carcinomas (HCC). It is estimated that HBV is present in a reservoir of more than 130 million chronic carriers, representing more than 10 % of Chinese population[1]. In particular, more than 23 million of Chinese HBV-infected subjects clinically manifest liver damage with abnormally elevated ALT levels and HBV active replication. Generally, exposure to HBV can cause a broad spectrum ranging from no infection to different clinical conditions[2]. What produces the individual or ethnic differences in infection, severity, and outcome? The reasons for this variation in the natural history of HBV infection are not fully understood, but are environmental factors and the following: (1) *Virological factors* such as viral load, genotype, and genetic divergence due to viral gene mutations. HBV mutates very rapidly and uses high genetic variability as an effective mechanism for escaping the host immune response[3]. (2) *Immunological factors* including the innate and adaptive immune responses against viral infection, which play important roles in modulating both the antiviral immune response and host susceptibility to HBV. The rapid mutations in HBV epitopes recognized by HBV-specific CTLs may cause both humoral and cell-mediated virus-specific immune responses to quickly lose their ability to efficiently control the virus[4,5]. (3) The *host genetic factors* are believed to be responsible for clinical outcomes of many infectious diseases[6-9].

In the last decade, the virological and immunological factors of HBV have been extensively studied, but the examination of the relationship between host genetics and HBV resistance is still in its infancy[10-12]. Therefore, this review focuses on the recent progress in study of human genetic alleles associated with chronic HBV infection, and discuss the unanswered questions and future directions in this field.

HOST GENETIC FACTORS INVOLVED IN HBV INFECTION

HBV-infected subjects generally fall into one of the following clinical types: (1) asymptomatic HBV carriers and cryptic hepatitis; (2) acute hepatitis; (3) chronic hepatitis; (4) liver cirrhosis with or without decompensated liver failure; and (5) primary hepatocellular carcinoma associated with HBV infection[2,13]. However, the pattern and clinical outcome of the infection are highly variable. Why is this? Previous epidemiological investigation in humans suggests that there is

a strong genetic component to affect the individual susceptibility to infectious pathogens[14-16], although to date, no single allele has not been clearly associated with HBV persistence or disease severity. However, the following reflects individual and ethnic differences in response to HBV infection.

(1) Infection with the same HBV virus has been found to cause various clinical outcomes in patients. In adults suffering from primary HBV infection, 90-95 % of the subjects can successfully clarify the virus through self-limiting hepatitis and only 5-10 % of adults become chronic HBV carriers[17]. Among the chronically infected subjects, 20-30 % lead to liver cirrhosis and -5 % develop hepatocellular carcinoma through a long-term disease progression. Of teen-ager subjects that acquire HBV infection from either perinatal or horizontal transmission, more than 90 % develop chronic infection. In China, mother-to-child transmission of HBV was once a common source of chronic infection.

(2) The long-term follow-up studies indicate that some individuals in high-risk groups (e.g. spouses in HBV-infected families) never develop the disease. This suggest the existence of an individual-specific resistance to HBV infection[1,3].

(3) There is a different incidence and infection rate among global ethnic groups. HBV infection is significantly endemic in Asia and Africa, and there is a significantly higher incidence of chronic HBV infection in Chinese compared to Caucasians[18].

(4) In clinic, HBV-infected individuals may display complete, partial or no response to interferon-a or Lamivudine antiviral therapy alone or in combination.

(5) Around 85 % of healthy subjects can produce the efficient protective anti-HBsAg antibody upon the HBV vaccination, while remaining fail.

The above-mentioned data suggests that the knowledge of understanding human genetic factors may provide critical clues not only to the ethnic diversity of HBV infection, but also to the issue of disparity in therapeutic response[19]. The human genome project has indicated that there are approximately thirty-five thousand genes in the human genome. Many of these alleles contain polymorphisms such as single nucleotide polymorphisms (SNPs) within the encoding or flanking regions. It is estimated that there are 3.5 million SNPs within human genome and there are likely to explain much of the genetic diversity of individuals and ethnic groups[13]. If a specific SNP version is associated with a favorable outcome and low risk of progression of HBV infection and liver disease, the allele may be considered an ' HBV resistant' allele. Conversely, a version of the SNP that confers an unwanted HBV phenotype (quick disease progression or high risk of severe infection) may be called a ' HBV susceptible' allele. Current research is focusing on the hunt and identification for these alleles.

SELECTION OF CANDIDATE ALLELES

Two strategies are currently used in the study involving genetic markers associated with disease phenotypes. The *candidate gene method* is the typing of markers located near genes that could be chemically related to the disease in question[20]. Conversely, a genome-wide search scans markers throughout the whole genome in search of chromosomal regions that could be associated with disease susceptibility or resistance. The choice of candidate genes for the first method is strongly determined by the function (or putative function) of the gene and its possible role in the host response to HBV infection and disease progression. Major genes involved in the process of HBV infection can be identified by characterizing host response to HBV exposure such as clinical response, biological response (intensity of infection), and immunological response (levels of antibodies, cytokines or cell-mediated response against HBV)[10]. These biological processes may then suggest genes of interest for screening. Many of the candidate genes fall into the following categories: (1) genes that mediate the processes of viral entry into hepatocytes, including genes involved in viral binding, fusion with cellular membrane and transportation in target cells; (2) genes that modulate or control the immune response to HBV infection; (3) genes that participate in the pathological alterations in liver tissue; (4) genes involved in the development of liver cirrhosis and hepatocellular carcinoma associated with chronic HBV infection, including genes related to mother-to-infant transmission of HBV infection; and (5) those that contribute to resistance to antiviral therapies[19,20]. This study is still in its early stages, and much more remains to be done on candidate genes, including the clarification of sequence, identification of mutant SNPs, functional evaluation of SNPs, and evaluation of their association with diseases.

ADVANCES ASSOCIATED WITH INDIVIDUAL GENETIC SUSCEPTIBILITY TO HBV INFECTION

Some candidate gene work has been completed at this time. Since both chemokine receptor and HLA genes play critical roles in host immune response to viral infection, they are among the first HBV candidate genes screened.

HLA class I and II alleles

The genes for HLA class I (HLA-A, -B, and -C) and class II (HLA-DRB1, -DQA1, -DQB1, -DPA1, and -DPB1) are located on the short arm of chromosome 6. As the primary modulator of host immune response, the HLA molecules present foreign antigens to both the CD4+ T lymphocytes and the CD8+ cytolytic T cells, leading to both humoral and cell-mediated immune response. The majority of the human genetic studies associated with HBV infection has focused on HLA associations[21]. Thursz et alinvestigated a large cohort of pediatric patients from Gambia and identified the association of the HLA class II allele DRB1*1302 with a self-limiting course of acute hepatitis B[23,24]. Hohler *et al*[17]. confirmed the effect of DBR1*1302 in Gambian adults that seemed to clear the HBV infection *in vivo*. Thio *et al*[25] examined the DQA1*0501, DQB1*0301 and DQA1-DQB1 haplotypes and found the haplotype cluster of DQA1*0501-DQB1*0301-DQB1*1102 had a significant association with viral persistence. However, Zavaglia *et al* reported that no correlation could be observed between the clearance of HBV or HCV virus and HLA phenotypes[22]. Recently, Diepolder *et al* reported that HLA-DR13 allele is less frequent in patients with chronic hepatitis B than in healthy controls or subjects with a self-limiting hepatitis B[26]. Additional study has confirmed a strong association between the HLA class II allele DR13 and a self-limiting course of acute HBV infection. Rapid progression to chronic hepatitis B is rare in these patients, suggesting that patients with HLA-DR13 can mount a more vigorous CD+ T cell response to HBV core antigen during acute HBV infection. The beneficial effect of HLA-DR13 allele on the outcome of HBV infection may either be the result of more proficient antigen presentation by the HLA-DR13 molecules themselves or of a linked polymorphism in a neighboring immunoregulatory gene. To date, no associations between HLA class I alleles and the viral persistence or disease progression in HBV-infected patients was found, though class I molecule mediates the cytotoxic T lymphocyte (CTL) response through the cytolytic and noncytolytic mechanisms[13]. Future studies have to investigate whether one of these polymorphisms or a yet unidentified immunoregulatory gene is possibly associated with a more successful immune response against HBV[27].

Cytokine and chemokines

Since individual variation in cytokine release is predominantly caused by polymorphisms near or within the genes[28,29], heterogeneity of the candidate gene in HBV-infected patients serves as a probable biomarker for influence the disease phenotypes. Several pro-inflammatory cytokines such as Th1 cytokines (including IL-2 and IFN-γ) and tumor necrosis factor-alpha (TNF-α) have been identified as participating in the viral clearance and the host immune response to HBV. In contrast, the Th2 cytokine IL-10 serves as a potent inhibitor of Th1 effector cells[30].

Tumor necrosis factor (TNF)-α is an important cytokine involved in noncytotoxic antiviral mechanisms[31]. This gene is located within the class III region of the MHC complex and has five polymorphisms in its promoter region, located at positions -1031(T/C), -863(C/A), -857(C/T), -308(G/A) and -238(G/A) respectively [negative numbers represent number of bases upstream from the transcription initiation site][32,33]. Miyazoe *et al* reported the TNF-α gene promoter polymorphisms were not linked to disease progression in HBV carriers in Japan[34], however both Hohler[35,36] found that the two polymorphisms such as -308(G/A) and -238(G/A) were significantly associated with HBV or HCV persistence in patients. It is thought that the polymorphism influences the expression of TNF-α, which may block HBV gene expression. Similar to TNF-α, IFN-γ clears HBV *in vivo* by a noncytolytic effect. Hoffmann *et al*[18]. showed that the Asian population contains more IFN-γ genotypes that result in low expression than do Caucasian populations, which suggests the possibility of an association between low IFN-γ expression in the highly HBV-susceptible Asian population.

The promoter region of IL-10 gene contains three SNPs at position -1082 (A/G), -819 (T/C), and -592 (A/C), which may assort into three different haplotypes[37]. Miyazoe *et al* analyzed the distributions of TNF-α and IL-10 promoter SNPs in Japanese HBV-infected petitents and found that the -819T and -592A wild-type alleles in the IL-10 gene promoter were significantly more common in asymptomatic carriers than in patients with chronic progressive liver diseases[32], suggesting that inheritance of the IL-10 gene promoter polymorphisms is relevant to progression in chronic HBV infection, perhapse due to decreased IL-10 production induced by -819T and -592A haplotype allele.

Mannose binding protein (MBP)

MBP is a calcium-dependent opsonin that plays an important role in innate immunity by activating the classical complement pathway and phagocytosis. There are three identified polymorphisms in the MBP gene encoding region (in codons 54, 57 and 52), leading to low serum concentrations and thus abolishing its ability to affect host immunity because of an opsonic defect. The middle surface protein of HBV viral envelope contains a mannose-rich oligosaccharide to which MBP could potentially bind. Thomas *et al* showed that 27 % of Caucasian patients chronically infected with HBV were homozygous or heterozygous for the codon 52 mutant allele whereas only 11 % of patients with acute infection and 4 % of controls carried the wild type allele, which suggests that the codon 52 mutant gene has been associated with persistence of HBV infection[38]. The higher frequency of the codon 52 mutation among the HBV patients than among controls is probably consistent with the fact that the mutation leads to the failure of opsonisation and phagocytosis of HBV. Yuen *et al*[39]. reported that the codon 54 mutation was associated with symptomatic persistent viral infection in Chinese patients. In German Caucasians and Gambians, these MBP polymorphisms were not associated with chronic infection[40].

Vitamin D receptor, cytochrome P450 and Complement four associated with HBV infection

The active form of vitamin D is an immunomodulatory hormone that inhibits the Th1 response and activates the Th2 immune reaction. Bellamy *et al*. studied two known Vitamin D receptor gene polymorphisms in Gambian HBV-infected patients and found that the tt genotype of one polymorphism was associated with viral clearance[41].

Thus far, reports from various laboratories have shown some inconsistencies with regard to the effects of host genetic factors on HBV clearance and persistence. This ambiguity may be attributable to one or more of the following reasons: (1) a complex interaction between the virus and host multiple alleles; (2) the ethnic differences in the studied groups; (3) an association with a gene in linkage disequilibrium with an HLA allele. Therefore, a global multicort studies may be needed to integrate the genetic data and the clinical data for fully clarification of underlying immunogenetic pathogenesis of HBV infection. In addition, further candidate genes must be identified and screened for associated polymorphisms.

PROSPECT FOR STUDY OF HBV RESISTANCE ALLELES

A growing body of evidence related to the genetic effects on infectious diseases has shown only a fraction of the total picture. The most successful example is the identification of CCR5 delta32 allele in HIV-1 infection[8,42]. Since genetic interactions are complex, it is unlikely that a single allelic variant is responsible for HBV resistance or susceptibility[43]. However, the collective influence of several SNPs or haplotype(s) may exert the natural combinational or synergistic protection against HBV. Recently developed genetic epidemiology strategies and dense genome-wide search, together with the growing availability of candidate alleles and suquence information supply a basic platform for identifying genes associated in HBV infection. These investigations will depend on the interactions of many different factors including the viral phenotypes, population traits, accurate measurement of environmental factors, and previous knowledge. Genetic resistance to HBV-induced persistent hepatitis is likely to involve a complex array of host genetic effects involving multiple variants and haplotypes. Because of this, future study including the multicohort collaboration will be needed to clarify these preliminary associations and identify other potential candidate genes[20]. In addition, it will be necessary to functionally characterize the identified associated genes, such as versions of HLA molecules and MBP, and see whether the mutations have functional significance in terms of individual susceptibility to HBV infection. The ongoing study of the distributions and functions of the implicated allele polymorphisms will not only provide insight into the pathogenesis of HBV infection, but may also provide a novel rationale for new methods of diagnosis and therapeutic strategies[44].

REFERENCES

1 **Gu CH**, Luo KX. Hepatitis B: Basic biology and clinical science. Second edition. Beijing, People's Medical Publishing House 2001: 1-6
2 **Iino S**. Natural history of hepatitis B and C virus infections. *Oncology* 2002; **62**(Suppl 1): 18-23
3 **Luo KX**. Hepatitis B: Basic biology and clinical science. Second edition. Beijing, People's Medical Publishing House 2001: 56-70
4 **Ferrari C**. Hepatitis B virus immunopathogenesis. *Annu Rev Immunol* 1995; **13**: 29-60
5 **Guidotti LG**, Chisari FV. Noncytolytic control of viral infections by the innate and adaptive immune response. *Annu Rev Immunol* 2001; **19**: 65-91
6 **Abel L**, Dessein AJ. The impact of host genetics on susceptibility

to human infectious diseases. *Curr Opin Immunol* 1997; **9**: 509-516
7 **McNicholl J**. Host genes and infectious diseases. *Emerg Infect Dis* 1998; **4**: 423-426
8 **McNicholl JM**, Cuenco KT. Host genes and infectious diseases. HIV, other pathogens, and a public health perspective. *Am J Prev Med* 1999; **16**: 141-154
9 **McGuire W**, Hill AV, Allsopp CE, Greenwood BM, Kwiatkowski D. Variation in the TNF-alpha promoter region associated with susceptibility to cerebral malaria. *Nature* 1994; **371**: 508-510
10 **Dean M**, Carrington M, O'Brien SJ. Balanced polymorphism selected by genetic versus infectious human disease. *Annu Rev Genomics Hum Genet* 2002; **3**: 263-292
11 **Hill AV**. Host genetics of infectious diseases: old and new approaches converge. *Emerg Infect Dis* 1998; **4**: 695-697
12 **Hill AV**. The immunogenetics of human infectious diseases. *Annu Rev Immunol* 1998; **16**: 593-617
13 **Thio CL**, Thomas D L, Carrington M. Chronic viral hepatitis and the human genome. *Hepatology* 2000; **31**: 819-827
14 **Kwiatkowski D**. Genetic dissection of the molecular pathogenesis of severe infection. *Intensive Carc Med* 2000; **26**(Suppl 1): S89-97
15 **Weatherall D**, Clegg J, Kwiatkowski D. The role of genomics in studying genetic susceptibility to infectious disease. *Genome Research* 1997; **7**: 967-973
16 **Powell EE**, Edwards-Smith CJ, Hay JL, Clouston AD, Crawford DH, Shorthouse C, Purdie DM, Jonsson JR. Host genetic factors influence disease progression in chronic hepatitis C. *Hepatology* 2000; **31**: 828-833
17 **Hohler T**, Gerken G, Notghi A, Lubjuhn R, Taheri H, Protzer U, Lohr HF, Schneider PM, Meyer zum Buschenfelde KH, Rittner C. HLA-DRB1*1301 and *1302 protect against chronic hepatitis B. *J Hepatol* 1997; **26**: 503-507
18 **Hoffmann SC**, Stanley EM, Cox ED, DiMercurio BS, Koziol DE, Harlan DM, Kirk AD, Blair PJ. Ethnicity greatly influences cytokine gene polymorphism distribution. *Am J Transplant* 2002; **2**: 560-567
19 **Knolle PA**, Kremp S, Hohler T, Krummenauer F, Schirmacher P, Gerken G. Viral and host factors in the prediction of response to interferon-alpha therapy in chronic hepatitis C after long-term follow-up. *J Viral Hepat* 1998; **5**: 399-406
20 **Abel L**, Dessein AJ. Genetic epidemiology of infectious diseases in humans: design of population-based studies. *Emerg Infect Dis* 1998; **4**: 593-603
21 **Almarri A**, Batchelor JR. HLA and hepatitis B infection. *Lancet* 1999; **344**: 1194-1195
22 **Zavaglia C**, Bortolon C, Ferrioli G, Rho A, Mondazzi L, Bottelli R, Ghessi A, Gelosa F, Iamoni G, Ideo G. HLA typing in chronic type B, D and C hepatitis. *J Hepatol* 1996; **24**: 658-665
23 **Thursz MR**, Kwiatkowski D, Allsopp CE, Greenwood BM, Thomas HC, Hill AV. Association between an MHC class II allele and clearance of hepatitis B virus in the Gambia. *N Engl J Med* 1995; **332**: 1065-1069
24 **Thursz MR**. Host genetic factors influencing the outcome of hepatitis. *J Viral Hepat* 1997; **4**: 215-220
25 **Thio CL**, Carrington M, Marti D, O'Brien SJ, Vlahov D, Nelson KE, Astemborski JA, Thomas DL. Class II of HLA alleles and hepatitis B Virus persistence African Americans. *J Infect Dis* 1999; **179**: 1004-1006
26 **Diepolder HM**, Jung MC, Keller E, Schraut W, Gerlach JT, Gruner N, Zachoval R, Hoffmann RM, Schirren CA, Scholz S, Pape GR. A vigorous virus-specific CD4+ T cell response may contribute to the association of HLA-DR13 with viral clearance in hepatitis B. *Clin Exp Immunol* 1998; **113**: 244-251
27 **Ahn SH**, Han KH, Park JY, Lee CK, Kang SW, Chon CY, Kim YS, Park K, Kim DK, Moon YM. Association between hepatitis B virus infection and HLA-DR type in Korea. *Hepatology* 2000; **31**: 1371-1373
28 **Westendorp RG**, Langermans JA, Huizinga TW, Verweij CL, Sturk A. Genetic influence on cytokine production in meningococcal disease. *Lancet* 1997; **349**: 1912-1913
29 **van Deventer SJ**. Cytokine and cytokine receptor polymorphisms in infectious disease. *Intensive Care Med* 2000; **26**(Suppl 1): S98-102
30 **Fiorentino DF**, Zlotnik A, Vieira P, Mosmann TR, Howard M, Moore KW, O'Garra A. IL-10 acts on the antigen-presenting cell to inhibit cytokine production by Th1 cells. *J Immunol* 1991; **146**: 3444-3451
31 **Knight JC**, Kwiatkowski D. Inherited variability of tumor necrosis factor production and susceptibility to infectious disease. *Proc Assoc Am Physicians* 1999; **111**: 290-298
32 **Hajeer AH**, Hutchinson IV. TNF-alpha gene polymorphism: clinical and biological implications. *Microsc Res Tech* 2000; **50**: 216-228
33 **Higuchi T**, Seki N, Kamizono S, Yamada A, Kimura A, Kato H, Itoh K. Polymorphism of the 5'-flanking region of the human tumor necrosis factor (TNF)-alpha gene in Japanese. *Tissue Antigens* 1998; **51**: 605-612
34 **Miyazoe S**, Hamasaki K, Nakata K, Kajiya Y, Kitajima K, Nakao K, Daikoku M, Yatsuhashi H, Koga M, Yano M, Eguchi K. Influence of interleukin-10 gene promoter polymorphisms on disease progression in patients chronically infected with hepatitis B virus. *Am J Gastroenterol* 2002; **97**: 2086-2092
35 **Hohler T**, Kruger A, Gerken G, Schneider PM, Meyer zum Buschenefelde KH, Rittner C. A tumor necrosis factor-alpha (TNF-alpha) promoter polymorphism is associated with chronic hepatitis B infection. *Clin Exp Immunol* 1998; **111**: 579-582
36 **Hohler T**, Kruger A, Gerken G, Schneider PM, Meyer zum Buschenfelde KH, Rittner C. Tumor necrosis factor alpha promoter polymorphism at position -238 is associated with chronic active hepatitis C infection. *J Med Virol* 1998; **54**: 173-177
37 **Edwards-Smith CJ**, Jonsson JR, Purdie DM, Bansal A, Shorthouse C, Powell EE. Interleukin-10 promoter polymorphism predicts initial response of chronic hepatitis C to interferon alfa. *Hepatology* 1999; **30**: 526-530
38 **Thomas HC**, Foster GR, Sumiya M, McIntosh D, Jack DL, Turner MW, Summerfield JA. Mutation of gene of mannose-binding protein associated with chronic hepatitis B viral infection. *Lancet* 1996; **348**: 1417-1419
39 Yuen MF, Lau CS, Lau YL, Wong WM, Cheng CC, Lai CL. Mannose binding lectin gene mutations are associated with progression of liver disease in chronic hepatitis B infection. *Hepatology* 1999; **29**: 1248-1251
40 **Hohler T**, Wunschel M, Gerken G, Schneider PM, Meyer zum Buschenfelde KH, Rittner C. No association between mannose-binding lectin alleles and susceptibility to chronic hepatitis B Virus infection in german patients. *Exp Clin Immunogenet* 1998; **15**: 130-133
41 **Bellamy R,** Hill AV. Genetic susceptibility to mycobacteria and other infectious pathogens in humans. *Curr Opin Lmmunol* 1998; **10**: 483-487
42 **Dean M**, Carrington M, Winkler C, Huttley GA, Smith MW, Allikmets R, Goedert JJ, Buchbinder SP, Vittinghoff E, Gomperts E, Donfield S, Vlahov D, Kaslow R, Saah A, Rinaldo C, Detels R, O'Brien SJ. Genetic restriction of HIV-1 infection and progression to AIDS by a deletion allele of the CKR5 structural gene. Hemophilia Growth and Development Study, Multicenter AIDS Cohort Study, Multicenter Hemophilia Cohort Study, San Francisco City Cohort, ALIVE Study. *Science* 1996; **273**: 1856-1862
43 **Griffiths PD**. Interactions between viral and human genes. *Rev Med Virol* 2002; **12**: 197-199
44 **Dean M**, Carrington M, O'Brien SJ. Balanced polymorphism selected by genetic versus infectious human disease. *Annu Rev Genomics Hum Genet* 2002; **3**: 263-292

Edited by Ren SY

P.O.Box 2345, Beijing 100023, China
Fax: +86-10-85381893
E-mail: wjg@wjgnet.com www.wjgnet.com

World J Gastroenterol 2003;9(4):645-649
World Journal of Gastroenterology
 ISSN 1007-9327

• ESOPHAGEAL CANCER •

Translocation of annexin I from cellular membrane to the nuclear membrane in human esophageal squamous cell carcinoma

Yu Liu, Hui-Xin Wang, Ning Lu, You-Sheng Mao, Fang Liu, Ying Wang, Hai-Rong Zhang, Kun Wang, Min Wu, Xiao-Hang Zhao

Yu Liu, Hui-Xin Wang, Fang Liu, Ying Wang, Min Wu, **Xiao-Hang Zhao**, National Laboratory of Molecular Oncology, Cancer Institute and Hospital, Chinese Academy of Medical Sciences & Peking Union Medical College, Beijing 100021, China
Ning Lu, Department of Pathology, Cancer Institute and Hospital, Chinese Academy of Medical Sciences & Peking Union Medical College, Beijing 100021, China
You-Sheng Mao, Department of Pectoral Surgery, Cancer Institute and Hospital, Chinese Academy of Medical Sciences & Peking Union Medical College, Beijing 100021, China
Hai-Rong Zhang, Kun Wang, Beijing Yanjing Hospital, Beijing 100037, China
Supported by the Major State Basic Research Development Program of China, No.G1998051205; the National Hi-Tech R & D Program of China, No.2001AA227091; the National Natural Science Foundation of China, No. 39990570 (Major Program) and No. 30171049 (General Program), and the National Science Fund for Distinguished Young Scholars (No.30225045)
Correspondence to: Dr. Xiao-Hang Zhao, National Lab. of Molecular Oncology, Cancer Institute and Hospital, Chinese Academy of Medical Sciences & Peking Union Medical College, Beijing P. O. Box 2258, Beijing 100021, China. zhaoxh@pubem.cicams.ac.cn
Telephone: +86-10-67709015 **Fax:** +86-10-67709015
Received: 2002-12-25 **Accepted:** 2003-01-05

Abstract

AIM: To investigate the alteration of the annexin I subcellular localization in esophageal squamous cell carcinoma (ESCC) and the correlation between the translocation and the tumorigenesis of ESCC.

METHODS: The protein localization of annexin I was detected in both human ESCC tissues and cell line via the indirect immunofluorescence strategy.

RESULTS: In the normal esophageal epithelia the annexin I was mainly located on the plasma membrane and formed a consecutive typical trammels net. Annexin I protein also expressed dispersively in cytoplasm and the nuclei without specific localization on the nuclear membrane. In esophageal cancer annexin I decreased very sharply with scattered disappearance on the cellular membrane, however it translocated and highly expressed on the nuclear membrane, which was never found in normal esophageal epithelia. In cultured esophageal cancer cell line annexin I protein was also focused on the nuclear membrane, which was consistent with the result from esophageal cancer tissues.

CONCLUSION: This observation suggests that the translocation of annexin I protein in ESCC may correlate with the tumorigenesis of the esophageal cancer.

Liu Y, Wang HX, Lu N, Mao YS, Liu F, Wang Y, Zhang HR, Wang K, Wu M, Zhao XH. Translocation of annexin I from cellular membrane to the nuclear membrane in human esophageal squamous cell carcinoma. *World J Gastroenterol* 2003; 9(4): 645-649
http://www.wjgnet.com/1007-9327/9/645.htm

INTRODUCTION

Annexin I is a member of annexins, an evolutionary conserved multigene family, which are calcium and phospholipid-binding proteins. Annexins consist of a conserved C-terminal domain that confers calcium-dependent phospholipid binding and a variable N-terminal domain that is responsible for the specific properties of each annexin I[1,2]. As a steroid-regulated protein annexin I has been found to participate in the cell differentiation and anti-inflammatory effects[3, 4]. It is also a major substrate of EGF receptor, which related to endocytic trafficking and sorting of EGFR in multivesicular endosomes[5]. The annexin I modulates the signal transduction through MAPK/ERK pathway and, specifically, inhibits the activities of phospholipase A2[6, 7]. Recent studies describe increased expression of annexin I in human hepatocellular carcinoma but it is absent in several types of carcinomas, such as human esophageal cancer and prostatic neoplasm[8, 9]. We have found that annexin I is clearly lost in ESCC, a kind of major diseases and the 4th killer of malignant tumors in China, and it seems that the annexin I protein plays an important role in the carcinogenesis.

It is well known that the protein subcellular localization is a very important way to better understand protein functions. The alteration of protein subcellular localizations and the membrane trafficking will facilitate the specific cellular functions as well as signal transduction. To detect the subcellular localizations of annexin I in both normal epithelia and ESCC mucosa will give us some clues to address the functions of annexin I in malignant tumors.

MATERIALS AND METHODS

Materials

Tissues specimens The esophageal specimens used for immunohistochemical (IHC) staining were obtained from patients who presented to the Cancer Hospital of Chinese Academy of Medical Sciences, Beijing, China and were diagnosed as esophageal squamous cell carcinoma without chemotherapy and radiotherapy by two senior pathologists. After surgical resections the specimens were fixed in 70 % ethanol or 40 mg· L^{-1}neutral formalin and embedded in paraffin.
Cell line Human ESCC cell line, EC0156 was generated in our laboratory from an ESCC tissue.
Antibodies Commercial available antibodies included annexin I monoclonal antibody (Santa Cruz Biotechnology Inc., Santa Cruz, CA, USA), goat anti-mouse TRITC and goat anti-mouse FITC antibodies (Jackson ImmunoResearch Laboratories, Inc., West Grove, PA, USA). All other reagents were of analytical grade.

Methods

Cell cultures The human esophageal cancer cell line EC0156 was cultured in Dulbecco' s modified Eagle' s medium (DMEM) with 10 % fetal bovine serum and antibiotics (penicillin and streptomycin) at 37 ℃ in a humidified atmosphere with 5 % CO_2.
Indirect immunofluorescence staining[10] For immunostaining, EC0156 cells were grown on glass-coverslips at 80 % confluence and fixed in 4 % paraformaldehyde in 100 mmol· L^{-1}

PBS (pH=7.4) for 15 min at room temperature. After three washes with the buffer (25 mmol· L^{-1} HEPES, 1 mmol· L^{-1} $CaCl_2$, 1 mmol· L^{-1} $MgCl_2$ and 10 g· L^{-1} BSA), the paraffin embedded tissue sections were deparaffinized and hydrated through xylenes and graded alcohol series, and then rinsed for 5 min in water. The fixed cells and deparaffinized tissue sections were incubated in blocking solution (0.1 % horse serum and 0.06 % Triton-X 100 in PBS) for 1 hour to decrease the non-specific binding of the antibodies and to improve the penetration of the antibodies through membranes. The blocking solution was also used for diluting the primary and secondary antibodies. After 1 hour, the blocking solution was changed for the primary antibody solution (anti-annexin I monoclonal antibody was diluted to 1:200 and PBS was used as negative control) and the cells were incubated at 4 ℃ overnight. After three washes, cells and tissues were incubated with the fluorescence-labeled secondary antibodies (1:300 diluted goat anti-mouse TRITC or the goat anti-mouse FITC) for 30 min at room temperature. This was followed by a last washing step (3×5 min, in PBS), then the cells were rinsed with distilled water, air dried and mounted on glass slides using Cytoseal 60 mounting medium (Stephens Scientific). Cells were then analyzed and images were obtained with a fluorescence microscope (Olympus BX51, OLYMPUS OPTICAL CO., LTD., Japan).

RESULTS

Localization of annexin I in normal esophageal epithelia

Annexin I protein was mostly located on the cell membrane in a granular pattern and some of them on the nucleus and cytoplasm as well through immunofluorescence staining in the normal esophagus epithelia (Figure 1. d, e, f and g). Consecutively and symmetrically expressed annexin protein on the cellular membrane makes typical trammel net. Annexin I also expressed in the cytoplasm and nuclei dispersively without specific localization on the nuclear membrane.

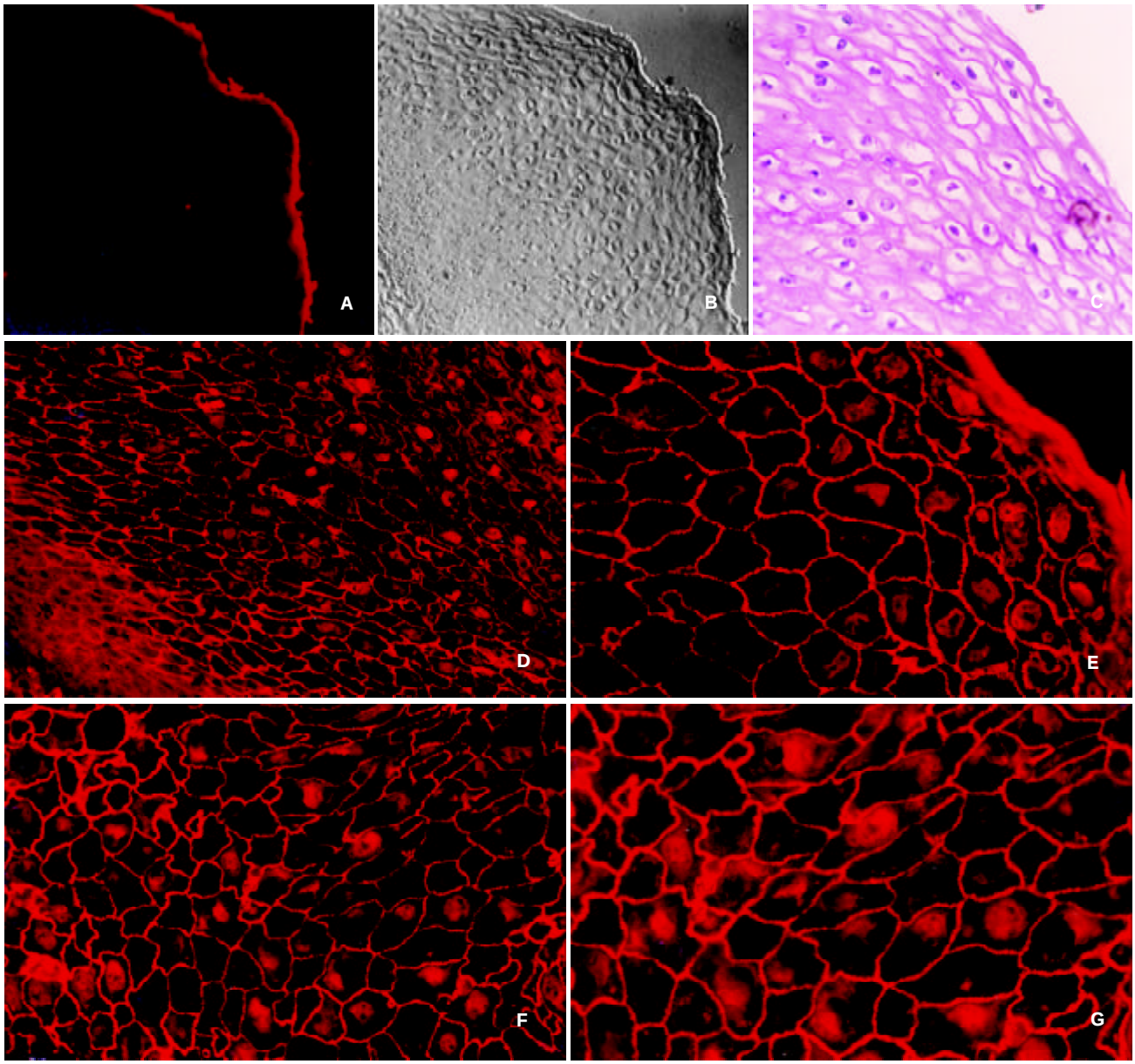

Figure 1 The localization of annexin I in normal esophageal epithelium. The normal esophageal epithelia on the paraffin-embedded tissues were detected with anti-annexin I monoclonal antibody and imaged with TRITC-conjugated goat anti-mouse antibody, and then observed under a fluorescence microscope (a, d, e, f and g). PBS was used as a negative control (a 50×), the tissue section was viewed under a Nomarski interference-contrast microscopy (b 50×) and the additional H & E staining was also performed (c 200×). The localization of annexin I protein in normal esophageal epithelium was shown from d to g (d 200×; e 400×; f 400× and g 400×). The orientation of the bottom left corner was the basal membrane of the esophageal mucosa.

Translocation of annexin I protein in ESCC

Figure 2 (c, d, e and f) showed clearly that the beautiful trammel net of annexin I protein on the esophageal epithelia had been broken and the holes of the net had been fused each other on the ESCC cellular membrane. The expression of annexin I on the cellular membrane decreased very sharply with unequal distribution or scattered disappearance. In the meantime, we also found the nuclear membrane localization of annexin I protein had appeared and increased very obviously (shown by the yellow arrows), which has never been found in normal esophageal epithelia. However, the expression of annexin I in nuclear plasma had been decreased distinctly.

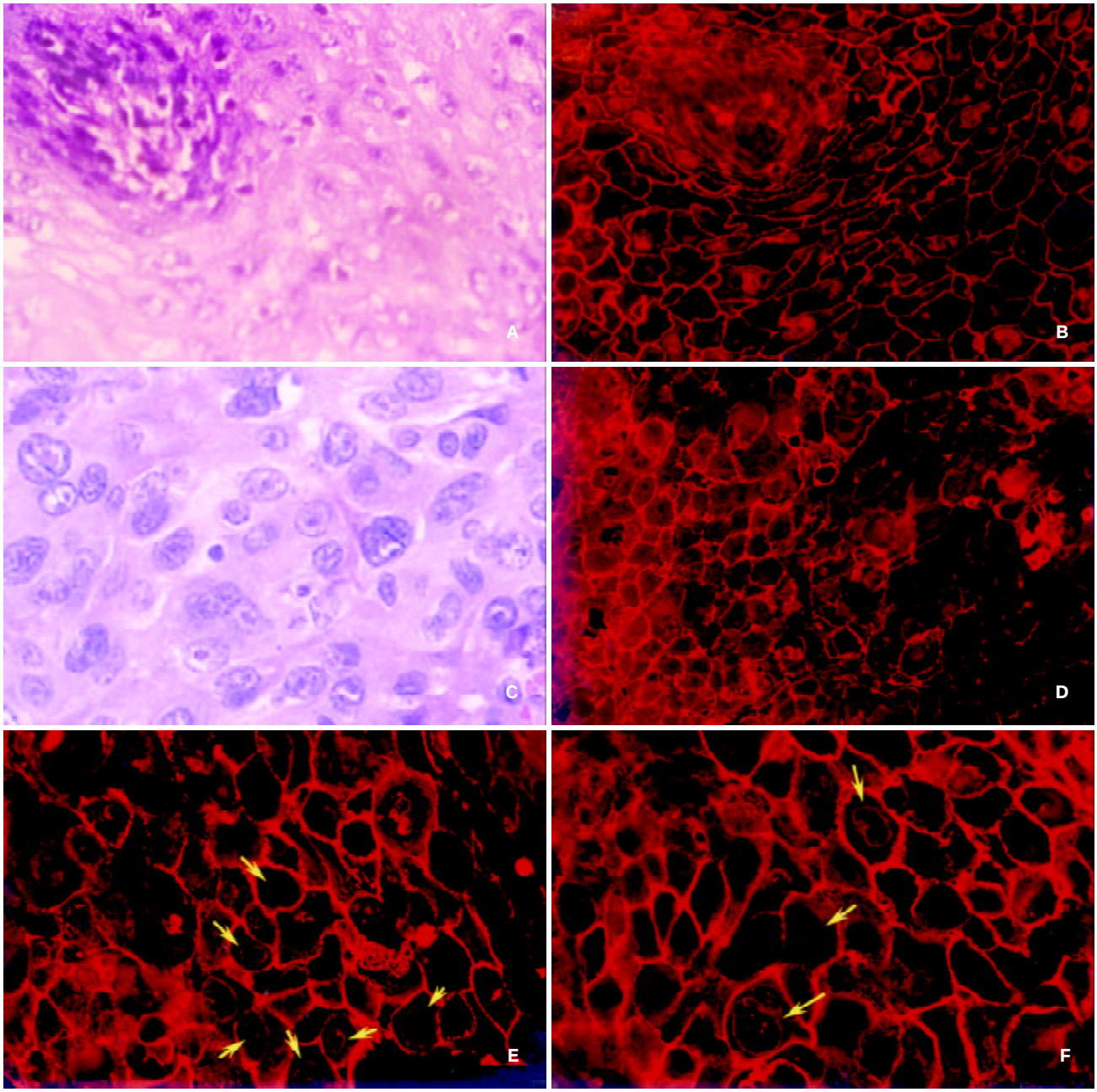

Figure 2 The translocation of annexin I protein in ESCC. Paraffin-embedded tissue sections of ESCC were detected with anti-annexin I antibody and annexin I protein was labeled by TRITC-conjugated secondary antibody. The fluorescence image was visualized under a fluorescence microscope (Olympus BX51, Japan). An H & E staining was performed (a 200×; c 400×). A hyperplasia of esophageal epithelia were shown in Figure 2 (a and b, b 200×) and there were basal papillae displaying boundary area of the epithelium, which consecutively expressed annexin I formed the typical trammel net on the cellular membrane. Annexin I protein was decreased sharply and translocated from cellular membrane to the nuclear membrane (d 200×; e 400×; f 400×). The yellow arrows showed the nuclear membrane localization of annexin I in ESCC and all of the materials were from a same ESCC case.

Nuclear membrane localization of annexin I on ESCC cell line

In order to further confirm the localization of annexin I protein in ESCC, a human esophageal cancer cell line, EC0156 was used to inspect the distributions of annexin I by indirect immunofluorescence staining. Annexin I protein was distinctly focused on the nuclear membrane (Figure 3, indicated by red arrows) of the EC0156 cells and it was consistent with what we saw in esophageal cancer tissues. On the cell line, annexin I proteins were also expressed on cytoplasm, cellular membrane and nuclear plasma as well.

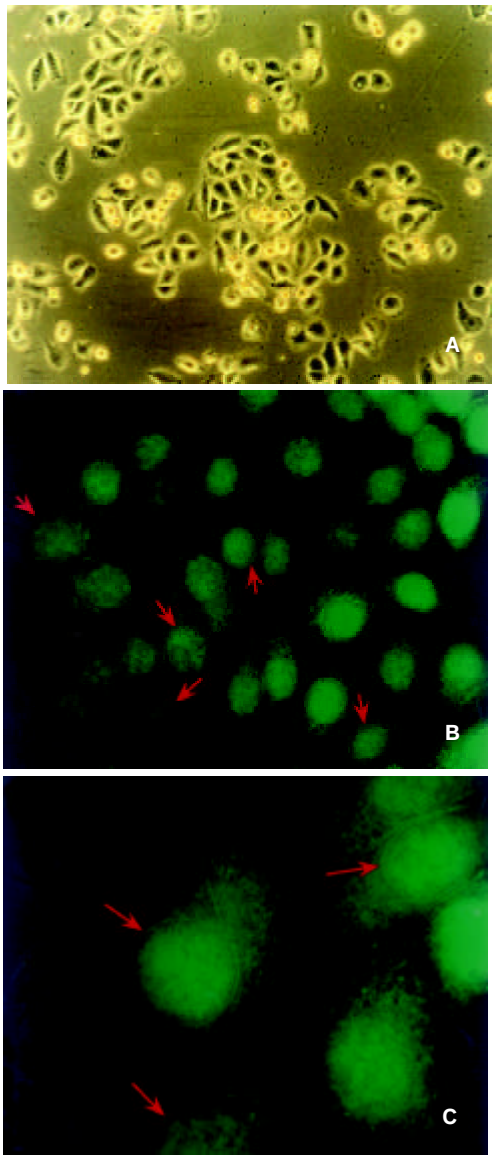

Figure 3 The localization of annexin I in ESCC cell line. EC0156 cells were grown on glass coverslips at 80 % confluence, detected with the anti-annexin I monoclonal antibody and visualized by FITC-conjugated secondary antibody under the fluorescence microscope. EC0156 cells were cultured in DMEM medium and photomicrographied under a phase-contrast microscopy (a 100×). Annexin I was observed by fluorescence microscope (b 400× and c 1 000×). The red arrows showed that annexin I protein was also located on nuclear membranes in EC0156 cells.

DISCUSSION

Annexin I protein belongs to a family of calcium-dependent phospholipid-binding proteins whose functions are presumed to participate in various membrane related events including membrane fusion in exocytosis and endocytosis as well as membrane organization. Previously studies have reported that in human epidermis annexin I was stained in a granular pattern in the monolayer but in an envelope pattern in the stratified keratinocytes[11]. The subcellular localization of annexins in rat was mainly found in the cytoplasm and nucleus of the mesangial cells[12], and in cytoplasm of mast cells[13]. By the localization of annexin I, II, VI and XIII in epithelial cells of intestinal, hepatic and pancreatic tissues of the rabbit, Massey-Harroche *et al*[14] showed that the basolateral domain of polarized cells appears to be the main site where annexins are located, and annexins may therefore be involved in the important cellular events occurring at this level. It suggests that the different localizations of annexin I contribute to its versatile functions.

Recently it has been found that annexin I is drastically down-regulated in esophageal cancer and assumed that the it may play a key role in the tumorigenesis of ESCC[8,15, 16]. To gain the insight into the localization of annexin I, its relationship with the processing of esophageal cancer and the possible functions of this protein, we investigated the subcellular localization of annexin I in ESCC cell line, normal and cancer esophageal epithelia by indirect immunofluorescence strategy. It was found that annexin I was mainly located on the membrane of the normal esophageal epithelia in granular pattern and formed a typical trammel net between the esophageal epithelia. Annexin I also expressed dispersively in the nuclei and cytoplasm without specific localization on the nuclear membrane. However, on the cellular membrane of ESCC the beautiful trammel net of annexin I had been broken and the holes on the net had been fused together. The expression of annexin I on the cellular membrane and nuclear plasma decreased very sharply, and the protein distributed unequally with scattered disappearance. Meanwhile, the nuclear membrane localization of annexin I had been appeared and increased obviously, which was never been found in normal esophageal epithelia. Additionally the distribution of annexin I on the human esophageal cancer cell line, EC0156 was also distinctly focused on the nuclear membrane. This finding suggests that the translocation of the subcellular localization of annexin I may be correlated with the tumorigenesis of ESCC. An IHC analysis of annexin I in ductal epithelial cells of various human breast tissues indicated that this annexin was not demonstrable in both the ductal luminal cells of normal breast and benign tumors, but was generally expressed in various types of breast cancer. Therefore it is most likely involved in an early stage of human breast cancer development. Annexin I expression might also correlate with breast cancer progress[17].

Annexin I appeared to be cleaved by neutrophil elastase at the N-terminal portion between Val-36 and Ser-37 to yield a 33 kDa protein. Cleavage of the N-terminal portion of annexin I was accompanied by a marked change in the annexin I isoelectric point (pI) value (from 6.0 to 8.5-9.0) and greatly diminished its functional activities. The findings demonstrate that annexin I degradation in epithelial lining fluid is closely related to lung inflammation[18].

The mechanisms of annexin I localization are a complexity. A study showed calcium induced translocation of annexin I into subcellular organelles and secretory vesicles in human neutrophils, which suggested annexin I might contribute to the secretory process in neutrophils[19]. Other studies also showed that dexamethasone and IL-6 could affect the localization of annexin I. In A549 human adenocarcinoma cell line dexamethasone could inhibit EGF-stimulated cytosolic PLA2 activation and arachidonic acid release. Annexin I participated in this regulated pathway. Dexamethasone induced annexin I phosphorylation and translocation mediated by glucocorticoids receptor, then brought about a competition between annexin I and Grb2 leading to a failure of recruitment of signaling factors to EGFR[6]. In U937 cells dexamethasone also caused translocation of annexin I from the intracellular compartment to the cell membrane[20]. Solito *et al* reported that induction of annexin I protein and its translocation to the cell membrane were stimulated by interleukin 6 and a unique 30 bp region of the annexin I promoter, which was critical for the responsiveness of the reporter gene to IL-6 and dexamethasone. IL-6 stimulation was mediated by a C/EBP beta-like transcriptional factor. Annexin I might participate in host defence system as a new acute class II phase protein[21].

Another study showed that stresses, treatment of A549 and

Hela cells with heat, hydrogen peroxide or arsenate, resulted in the translocation of annexin I from cytoplasm to nucleus and perinuclear region. There were different intracellular distributions of annexins in macrophage-like cells in phagocytosis, and reactions to hydrogen peroxide and sodium arsenate[22].

In summary, we have first detected the translocation of annexin I from cellular membrane to nuclear membrane in ESCC cells. It seems that the subcellular localizations of annexin I are closely related to its functions and the alterations are most likely involved in the tumorigenesis of ESCC, especially at the early stage. More investigations are doing to further clarify the mechanisms of annexin I subcellular-localization changes during tumorigenesis of human ESCC.

REFERENCES

1 **Kourie JI**, Wood HB. Biophysical and molecular properties of annexin-formed channels. *Prog Biophys Mol Biol* 2000; **73**: 91-134

2 **Rosengarth A**, Wintergalen A, Galla HJ, Hinz HJ, Gerke V. Ca2+-independent interaction of annexin I with phospholipid monolayers. *FEBS Lett* 1998; **438**: 279-284

3 **Solito E**, de Coupade C, Parente L, Flower RJ, Russo-Marie F. Human annexin 1 is highly expressed during the differentiation of the epithelial cell line A 549: involvement of nuclear factor interleukin 6 in phorbol ester induction of annexin 1. *Cell Growth Differ* 1998; **9**: 327-336

4 **Perretti M**. Lipocortin 1 and chemokine modulation of granulocyte and monocyte accumulation in experimental inflammation. *Gen Pharmacol* 1998; **31**: 545-552

5 **Futter CE**, Felder S, Schlessinger J, Ullrich A, Hopkins CR. Annexin I is phosphorylated in the multivesicular body during the processing of the epidermal growth factor receptor. *J Cell Biol* 1993; **120**: 77-83

6 **Alldridge LC**, Harris HJ, Plevin R, Hannon R, Bryant CE. The annexin protein lipocortin 1 regulates the MAPK/ERK pathway. *J Biol Chem* 1999; **274**: 37620-37628

7 **Croxtall JD**, Choudhury Q, Newman S, Flower RJ. Lipocortin 1 and the control of cPLA2 activity in A549 cells. Glucocorticoids block EGF stimulation of cPLA2 phosphorylation. *Biochem Pharmacol* 1996; **52**: 351-356

8 **Paweletz CP**, Ornstein DK, Roth MJ, Bichsel VE, Gillespie JW, Calvert VS, Vocke CD, Hewitt SM, Duray PH, Herring J, Wang QH, Hu N, Linehan WM, Taylor PR, Liotta LA, Emmert-Buck MR, Petricoin EF 3rd. Loss of annexin 1 correlates with early onset of tumorigenesis in esophageal and prostate carcinoma. *Cancer Res* 2000; **60**: 6293-6297

9 **Masaki T**, Tokuda M, Ohnishi M, Watanabe S, Fujimura T, Miyamoto K, Itano T, Matsui H, Arima K, Shirai M, Maeba T, Sogawa K, Konishi R, Taniguchi K, Hatanaka Y, Hatase O, Nishioka M. Enhanced expression of the protein kinase substrate annexin in human hepatocellular carcinoma. *Hepatology* 1996; **24**: 72-81

10 **Zhao X**, Varnai P, Tuymetova G, Balla A, Toth ZE, Oker-Blom C, Roder J, Jeromin A, Balla T. Interaction of neuronal calcium sensor-1 (NCS-1) with phosphatidylinositol 4-kinase beta stimulates lipid kinase activity and affects membrane trafficking in COS-7 cells. *J Biol Chem* 2001; **276**: 40183-40189

11 **Ma AS,** Ozers LJ. Annexins I and II show differences in subcellular localization and differentiation-related changes in human epidermal keratinocytes. *Arch Dermatol Res* 1996; **288**: 596-603

12 **Vervoordeldonk MJ**, Schalkwijk CG, Vishwanath BS, Aarsman AJ, van den Bosch H. Levels and localization of group II phospholipase A2 and annexin I in interleukin- and dexamethasone-treated rat mesangial cells: evidence against annexin mediation of the dexamethasone-induced inhibition of group II phospholipases A2. *Biochim Biophys Acta.* 1994; **1224**: 541-550

13 **Oliani SM**, Christian HC, Manston J, Flower RJ, Perretti M. An immunocytochemical and *in situ* hybridization analysis of annexin 1 expression in rat mast cells: modulation by inflammation and dexamethasone. *Lab Invest* 2000; **80**: 1429-1438

14 **Massey-Harroche D**, Mayran N, Maroux S. Polarized localizations of annexins I, II, VI and XIII in epithelial cells of intestinal, hepatic and pancreatic tissues. *J Cell Sci* 1998; **111**: 3007-3015

15 **Zhou G,** Li H, DeCamp D, Chen S, Shu H, Gong Y, Flaig M, Gillespie JW, Hu N, Taylor PR, Emmert-Buck MR, Liotta LA, Petricoin EF 3rd, Zhao Y. 2D Differential in-gel electrophoresis for the identification of esophageal scans cell cancer-specific protein markers. *Mol Cell Proteomics* 2002; **1**: 117-124

16 **Emmert-Buck MR**, Gillespie JW, Paweletz CP, Ornstein DK, Basrur V, Appella E, Wang QH, Huang J, Hu N, Taylor P, Petricoin EF 3rd. An approach to proteomic analysis of human tumors. *Mol Carcinog* 2000; **27**: 158-165

17 **Ahn SH**, Sawada H, Ro JY, Nicolson GL. Differential expression of annexin I in human mammary ductal epithelial cells in normal and benign and malignant breast tissues. *Clin Exp Metastasis* 1997; **15**: 151-156

18 **Tsao FH**, Meyer KC, Chen X, Rosenthal NS, Hu J. Degradation of annexin I in bronchoalveolar lavage fluid from patients with cystic fibrosis. *Am J Respir Cell Mol Biol* 1998; **18**: 120-128

19 **Sjolin C**, Stendahl O, Dahlgren C. Calcium-induced translocation of annexins to subcellular organelles of human neutrophils. *Biochem J* 1994; **300**: 325-330

20 **Solito E**, Nuti S, Parente L. Dexamethasone-induced translocation of lipocortin (annexin) 1 to the cell membrane of U-937 cells. *Br J Pharmacol* 1994; **112**: 347-348

21 **Solito E**, de Coupade C, Parente L, Flower RJ, Russo-Marie F. IL-6 stimulates annexin 1 expression and translocation and suggests a new biological role as class II acute phase protein. Cytokine 1998; **10**: 514-521

22 **Rhee HJ**, Kim GY, Huh JW, Kim SW, Na DS. Annexin I is a stress protein induced by heat, oxidative stress and a sulfhydryl-reactive agent. *Eur J Biochem* 2000; **267**: 3220-3225

Edited by Zhang JZ

P.O.Box 2345, Beijing 100023, China
Fax: +86-10-85381893
E-mail: wjg@wjgnet.com www.wjgnet.com

World J Gastroenterol 2003;9(4):650-654
World Journal of Gastroenterology
 ISSN 1007-9327

• ESOPHAGEAL CANCER •

Loss of clusterin both in serum and tissue correlates with the tumorigenesis of esophageal squamous cell carcinoma via proteomics approaches

Li-Yong Zhang, Wan-Tao Ying, You-Sheng Mao, Hong-Zhi He, Yu Liu, Hui-Xin Wang, Fang Liu, Kun Wang, De-Chao Zhang, Ying Wang, Min Wu, Xiao-Hong Qian, Xiao-Hang Zhao

Li-Yong Zhang, Hong-Zhi He, Yu Liu, Hui-Xin Wang, Fang Liu, Ying Wang, Min Wu, Xiao-Hang Zhao, National Laboratory of Molecular Oncology, Cancer Institute and Hospital, Chinese Academy of Medical Sciences & Peking Union Medical College, Beijing 100021, Beijing, China
You-Sheng Mao, De-Chao Zhang, Department of Pectoral Surgery, Cancer Institute and Hospital, Chinese Academy of Medical Sciences & Peking Union Medical College, Beijing 100021, Beijing, China
Wan-Tao Ying, Xiao-Hong Qian, Department of Genomics and Proteomics, Beijing Institute of Radiation Medicine, Beijing 100850, China
Kun Wang, Beijing Yanjing Hospital, Beijing 100037, China
Supported by the Major State Basic Research Development Program of China, No.G19980512 and No.2001CB510201; the National Hi-Tech R & D Program of China, No.2001AA227091 and No. 2001AA233061; National Natural Science Foundation of China, No. 39990570, No.30171049, 30225045 and No.39990600
Correspondence to: Dr. Xiao-Hang Zhao, National Laboratory of Molecular Oncology, Cancer Institute and Hospital, Chinese Academy of Medical Sciences & Peking Union Medical College, Beijing 100021, Beijing, China. zhaoxh@pubem.cicams.ac.cn
Telephone: +86-10-67709015 **Fax:** +86-10-67709015
Dr. Xiao-Hong Qian, Department of Genomics and Proteomics, Beijing Institute of Radiation Medicine, Beijing 100850, China. qianxh@nic.bmi.ac.cn
Telephone: +86-10-68279585 **Fax:** +86-10-68279585
Received: 2002-11-26 **Accepted:** 2002-12-18

Abstract

AIM: To identify the differentially secreted proteins or polypeptides associated with tumorigenesis of esophageal squamous cell carcinoma (ESCC) from serum and to find potential tumor secreted biomarkers.

METHODS: Proteins from human ESCC tissue and its matched adjacent normal tissue; pre-surgery and post-surgery serum; and pre-surgery and normal control serum were separated by two-dimensional electrophoresis (2-DE) to identify differentially expressed proteins. The silver-stained 2-DE were scanned with digital ImageScanner and analyzed with ImageMaster 2D Elite 3.10 software. A cluster of protein spots differentially expressed were selected and identified with matrix-assisted laser desorption/ionization time-of-flight mass spectrometry (MALDI-TOF-MS). One of the differentially expressed proteins, clusterin, was down-regulated in cancer tissue and pre-surgery serum, but it was reversed in post-surgery serum. The results were confirmed by semi-quantitative reverse-transcription (RT)-PCR and western blot.

RESULTS: Comparisons of the protein spots identified on the 2-DE maps from human matched sera showed that some proteins were differentially expressed, with most of them showing no differences in composition, shape or density. Being analyzed by MALDI-TOF-MS and database searching, clusterin was differentially expressed and down-regulated in both cancer tissue and pre-surgery serum compared with their counterparts. The results were also validated by RT-PCR and western blot.

CONCLUSION: The differentially expressed clusterin may play a key role during tumorigenesis of ESCC. The 2DE-MS based proteomic approach is one of the powerful tools for discovery of secreted markers from peripheral.

Zhang LY, Ying WT, Mao YS, He HZ, Liu Y, Wang HX, Liu F, Wang K, Zhang DC, Wang Y, Wu M, Qian XH, Zhao XH. Loss of clusterin both in serum and tissue correlates with the tumorigenesis of esophageal squamous cell carcinoma via proteomics approaches. *World J Gastroenterol* 2003; 9(4): 650-654
http://www.wjgnet.com/1007-9327/9/650.htm

INTRODUCTION

Esophageal squamous cell carcinoma (ESCC), the major histological form of esophageal cancer, is one of the most common malignant tumors in China especially in the north part of the country. Human ESCC carcinogenesis is a multistage process involving multifactorial etiology and genetic-environment interactions[1-3]. Patients with ESCC have a poor prognosis, with 5-year survival rates of less than 10 %, because of the rapid spread and of the cancer associated malnutrition due to dysphagia and cachexia[4]. The molecular mechanisms that underlie the tumor formation and progression are still not completely perspicuous, although several progresses based on alterations of gene expression[5] and disregulated proteins, such as annexin I[6] and tumor rejection antigen[7] in esophageal cancer via proteomic approaches have been reported recently. Discovery of new markers to discriminate tumorigenic from normal cells, as well as the different stage is critical important for early detection and diagnosis of ESCC. The success of the Human Genome Project and the initiation of human proteome are strongly facilitating these efforts as tremendous information of genes and proteins are currently available[8,9]. It would be possible to undertake comprehensive profiling of tumor at the proteomics level to identify protein alterations that are unpredictable at either the genomics or transcriptomics levels[10]. However there is no comprehensive study of esophageal cancer protein profiling or protein expression patterns have been generated, especially the tumor-associated serum protein biomarkers. To identify specific protein tumor markers both in serum and tissue by proteomics approaches is a currently critical issue[8,11,12].

Tumor associated proteins as well as post-translational modifications can be identified via proteomic methodologies. In the present study, we used the 2-DE/mass spectrometry (MS)-based proteomic analysis to profile the proteins in serum of ESCC patients. We analyzed 17 pairs of patient-matched pre- and post-surgery as well as normal and tumor sera from ESCC patients to discover the alterations of expression profiling. We first found the clusterin is loss in both serum and tissue of ESCC.

MATERIALS AND METHODS

Specimens and preparation

The esophageal specimens were from patients diagnosed with esophageal cancer by the pathologists in Cancer Hospital of Chinese Academy of Medical Sciences (CAMS) (Beijing, China). The study was approved by the Institutional Review Board of Cancer Institute of CAMS. The pre-surgery serum were obtained from the first physical examination after the patients presented to the hospital, ESCC tumor tissues were obtained immediately after surgical resection and the post-surgery serum were obtained from the matched patients during the day 8 to day 10 after surgery. Sera described in Table 1, were centrifuged at 3 000 g at 4 ℃ for 15 min. Both tissue and serum samples were snap-frozen in liquid nitrogen immediately and then stored at -80 ℃. The tissues were homogenized in five volumes of lysis buffer [8M urea, 4 % CHAPS, 2 % Pharmalyte, pH 3-10, 10 mM DTT] and centrifuged at 12 000 g at 4 ℃ for 40 minutes. The supernatant was removed and protein concentration was determined using the Bradford assay.

Table 1 The matched sera for 2-DE

No. of matched-sera	Gender	Age	Histopathological diagnosis
M51Q-M51H	M	59	MDSCC
M88Q-M88H	F	56	MDSCC
M88Q-M88H	M	62	MDSCC
M92Q-M92H	M	65	MDSCC
M93Q-M93H	M	65	MDSCC
M141Q-Nor86	F	62	MDSCC
M149Q-Nor67	M	67	PDSCC
M151Q-Nor24	M	64	MDSCC
M156Q-Nor87	F	70	PDSCC
M160Q-Nor15	M	68	MDSCC
M162Q-Nor34	M	72	MDSCC
M168Q- Nor16	M	70	MDSCC
M180Q- Nor66	F	65	HDSCC
M180Q- Nor10	F	65	HDSCC
M181Q- Nor97	M	57	MDSCC
M192Q- Nor36	M	68	MDSCC
M193Q- Nor19	F	66	HDSCC

The abbreviations used are: Q, pre-surgery; H, post-surgery; Nor, age and gender matched normal serum; MDSCC, moderate differentiated squamous Cell Carcinoma; PDSCC, poorly differentiated squamous Cell Carcinoma; HDSCC, Highly Differentiated squamous Cell Carcinoma.

Reagents

Electrophoresis reagents including acrylamide solution (40 %), N, N-methylenebisacrylamide, N, N, N', N'-tetramethylethylenediamine, tris base, glycine, SDS, DTT, CHAPS, Immobiline Drystrips, IPG buffer, IPG cover fluid, LMW protein marker were from Amersham Pharmacia Biotechnology Inc. (Uppsala, Sweden); Iodoacetamide was from Acros (New Jersey, USA); Sequence grade Trypsin was from Washington Biochemical Corporation; Trifluoroacetic acid (TFA) was from Fluka (Switzerland); Trizol™ Reagent and Transcriptase SuperScript II™ were from Gibco BRL; PVDF membrane was from Bio-Rad; Taq DNA polymerase and dNTPs were from TaKaRa; All other reagents were of analytical grade.

Analytical 2-DE

All sera or cell lysates were quantitated by Bradford assay. 2-DE was performed by standard procedures as described[8,12] using precast IPG strips (pH3-10 linear, 18 cm, Amersham Pharmacia Biotechnology Inc.) in the first dimension, isoelectric focusing (IEF). Briefly, 180 μg proteins were diluted to a total volume of 350 μl with the buffer [8 M urea, 2 % CHAPS, 0.5 % IPG buffer 3-10, 20 mM DTT and a trace of bromophenol blue]. After loaded on IPG strips, IEF was carried out according to the following protocol: 6 hours of rehydration at 0 V; 6 hours at 30 V; 1 hour at 500 V; 1 hour at 1 000 V and 5 hours at 8 000 V. The current was limited to 50 μA per gel. After IEF separation, the strips were immediately equilibrated 2×15 min with equilibration solution [50 mM Tris-HCl, pH6.8, 6 M urea, 30 % glycerol and 2 % SDS]. 20 mM DTT was included in the first equilibration solution, and 2 % (w/v) iodoacetamide was added in the second equilibration step to alkylate thiols. SDS-polyacrylamide gel electrophoresis (PAGE) was performed using 1 mm thick, 13 % SDS-PAGE gels. The strips were held in place with 0.5 % agarose dissolved in SDS/Tris running buffer and electrophoresis was carried out at constant power (2.5 W/gel for 40 min and 15 W/gel for 6 hours) and temperature (20 ℃) using Ettan Dalt II system (Amersham Pharmacia Biotechnology Inc.). Gels were stained with silver nitrate according to the instructions of the silver-staining kit (Amersham Pharmacia Biotechnology Inc.).

Gel scanning and image analysis

Silver stained 2-DE gels were scanned with ImageScanner and analyzed including spots detection, quantification and normalization with ImageMaster 2D Elite 3.10 (Amersham Pharmacia Biotechnology Inc.). Statistical analysis was performed using SPSS statistical software late.

In-gel protein digestion

Individual protein spot was excised from the gel by Ettan Spot Picker (Amersham Pharmacia Biotechnology Inc.), destained with the solution [15 mM potassium ferricyanide, 50 mM sodium thiosulfate] and washed till opaque and colorless with 25 mM ammonium bicarbonate/50 % acetonitrile. After dried with vacuum concentrator (SpeedVac Plus, USA) the gel was rehydrated with 3-10 μl trypsin solution (10 ng/μl) at 4 ℃ for 30 min and then incubated at 37 ℃ overnight. Tryptic peptides were eluted and dried on SpeedVac vacuum concentrator.

Protein identification by MALDI mass spectrometry

Digested peptides were dissolved with 0.5 % TFA, with saturated CHCA solution in 0.1 % TFA/50 % acetic acid as matrix and analyzed by M@LDI R (Micromass, Manchester, UK). Spectrum acquisition was externally calibrated with lock mass 2465.199 Da and internally calibrated with autodigested peaks of trypsin (MH^+: 2211.105 Da). The protein identification was performed by searching protein databases of Swiss-prot/trEMBL (http://www.expasy.ch/tools/peptident.html) and Mascot (http://www.matrixscience.com/). The error for peptide mass was set as 50 ppm and possible missed cleavage of trypsin was set as 1. The proteins with more than 4 matched peptides were thought significant.

RT-PCR

Total RNAs were isolated from esophageal cancer tissues using TRIzol reagent (Gibco BRL) according to the manufactures' instructions. First strand cDNA was reversely transcribed from 5 μg total RNAs using SuperScript II kit (Life Technologies) at 42 ℃ for 50 min. Clusterin was amplified by the primers (left: 5' ACCTCACGCAAGGCGAAGAC3', right: 5' TCTCACTCCTCCCGGTGCTT3') and a product with 232bp was generated.

Western blot

Total cells or tissues were lysated with the buffer [1 % SDS, 10 Mm Tris-Cl, pH 7.6, 20 μg/ml aprotenin, 20 μg/ml leupeptin

and 1 mM AEBSF]. The protein concentrations were determined using Bradford method. Five micrograms of protein were separated on 12 % of SDS-PAGE gels and transferred to PVDF membranes. After blocked with 10 % non-fat milk, the membranes were incubated with anti-clusterin monoclonal antibody (Santa Cruz Bitechnology Inc.) (1:1 000 dilution) at 4 ℃ overnight. After washing for three times the membranes were incubated with rabbit anti-mouse IgG at room temperature for 1 hour. The signals were developed with the ECL kit (Amersham Pharmacia Biotechnology Inc.) and using anti-α-tubulin antibody (Santa Cruz Biotechnology Inc.) as an internal control.

RESULTS

Clusterin was identified down-regulated in pre-surgery serum

A proteomic approach was used to determine the differentiated proteins profiling between the pre-surgery and post-surgery sera of ESCC. The proteins from five pairs of matched sera from pre- and post-surgery of ESCC patients were separated by 2DE. Figure 1 illustrates the proteomic profilings of the pre- and post-surgery sera from same individual and more than 600 proteins and polypeptides were detected on each gel. The matched rate of the five pairs gel was more than 87.2 % and the spots localized in pI 3-10 with the molecular mass range around 20-200 kDa. All the identified spots can be considered as abundant proteins since they are detectable with Coomassie Blue staining on the preparative 2-DE gel. After computer analysis for spots detection, background subtraction and volume normalization, we were able to identify 20 spots (corresponding to 5 different proteins) from the tryptic digestion via MALDI-TOF-MS analysis. The isoforms of clusterin were identified from 8 spots as multipeptides components, which were dramatically down-regulated in tumor sera (Figure 2 A and Figure 3).

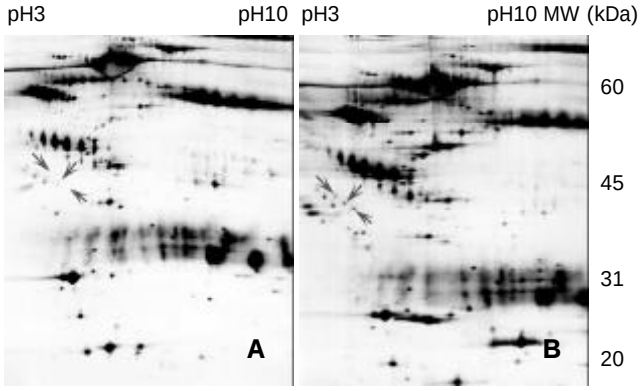

Figure 1 2-DE profiles of the pre- and post-surgery matched esophageal cancer sera from a same individual. One hundred and eighty microgram of protein was separated by 2-DE (IEF at pH 3-10, 13 % of SDS-PAGE) and stained by silver staining. LMW markers were from Amersham Pharmacia. (A) pre-surgery serum, (B) matched post-surgery serum.

Proteomic determination of esophageal cancer serum

We asked the question whether the loss of clusterin was induced by surgical attacks? In order to get rid of the interferences of the human immunoresponse after routine surgery, we additionally selected and matched 12 pairs of pre-surgery sera with the healthy sera from the same age and gender individuals who had no any surgical attacks and infections recently. We ran 2-DE profiling again between the two groups. Comparison with the healthy reference sera, clusterin proteins were also identified as more than four times lower in esophageal cancer serum after statistical analysis (Figure 2B).

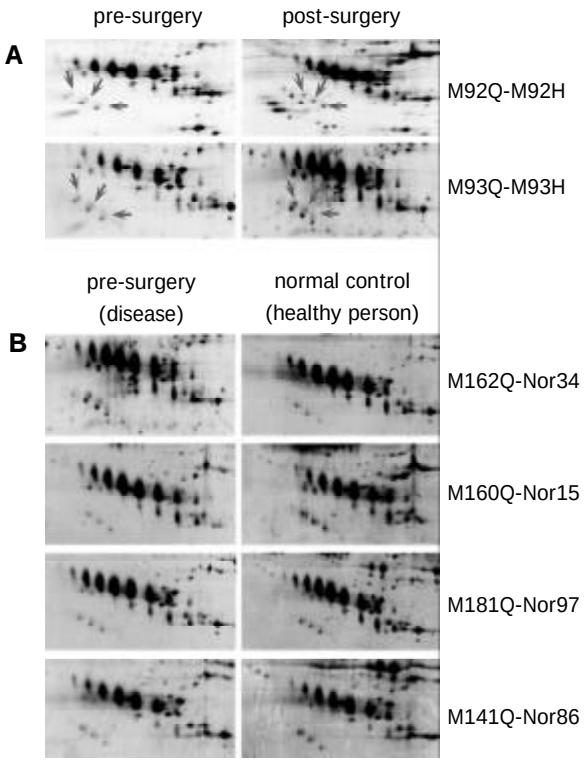

Figure 2 Representative regions of 2-DE patterns of more matched esophageal cancer sera. One hundred and eighty microgram of protein was separated by 2-DE (IEF at pH 3-10, SDS-PAGE 13 %) and stained by silver staining. LMW markers were from Amersham Pharmacia. (A) pre-surgery sera *vs* post-surgery sera, (B) pre-surgery sera *vs* normal control sera.

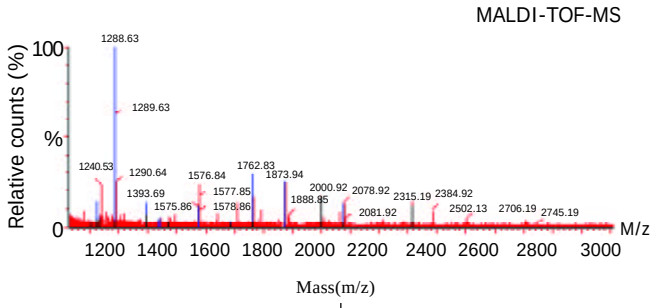

Mass(m/z)

Measured mass	Matched sequence	Residues
1575. 86	(K)YVNKEIQNAVNGVK(Q)	41-54
1232. 63	(K)TLIEKTNEER(K)	58-67
1393. 69	(R)ASSIIDELFQDR(F)	183-194
1434. 76	(R)ASSIIDELFQDR(F)	183-194
2000. 92	(R)EPQDTYHYLPFSLPHR(R)	199-214
1222. 52	(R)EGDDDRTVCR(E)	277-286
1203. 56	(R)HNSTGCLRMK(D)	290-299
2078. 92	(K)CREILSVDCSTNNPSQAK(L)	305-322
1762. 83	(R)EILSVDCSTNNPSQAK(L)	307-322
1444. 73	(R)RELDESLQVAER(L)	325-336
1288. 63	(R)ELDESLQVAER(L)	326-336
1471. 65	(K)YNELLKSYQWK(M)	341-351
1683. 75	(R)LANLTQGEDQYYLR(V)	372-385
2315. 19	(R)VTTVASHTSDSDVPSGVTEVVVK(L)	386-408
1873. 94	(K)LFDSDPITVTVPVEVSR(K)	409-425

MMKTLLLFVGLLLTWESGQVLGDQTVSDNELQEMSNQGSKYVNKEIQNAVNGVKQIKTLI
EKTNEERKTLLSNLEEAKKKKEDALNETRESETKLKELPGVCNETMMALWEECKPCLKQT 120
CMKFYARVCRSGSGLVGRQLEEFLNQSSPFYFWMNGDRIDSSLENDRQQTHMDDVMQDHF
SRASSIIDELFQDRFFTREPQDTYHYLPFSLPHRRPHFFFPKSRIVRSLMPFSPYEPLNF 240
HAMFQPFLEMIHEAQQAMDIHFHSPAFQHPPTEFIREGDDDRTVCREIRHNSTGCLRMKD
QCDKCREILSVDCSTNNPSQAKLRRELDESLQVAERITRKYNELLKSYQWKMLNTSSLLE 360
QLNEQFNWVSRLANLTQGEDQYYLRVTTVASHTSDSDVPSGVTEVVVKLFDSDPITVTVP
VEVSRKNPKFMETVAEKALQEVRKKHREE

Figure 3 The spectra of MALDI-TOF-MS obtained from one of the differentiated polypeptide spots matched with the tryptic peptide sequences of clusterin (characters in red).

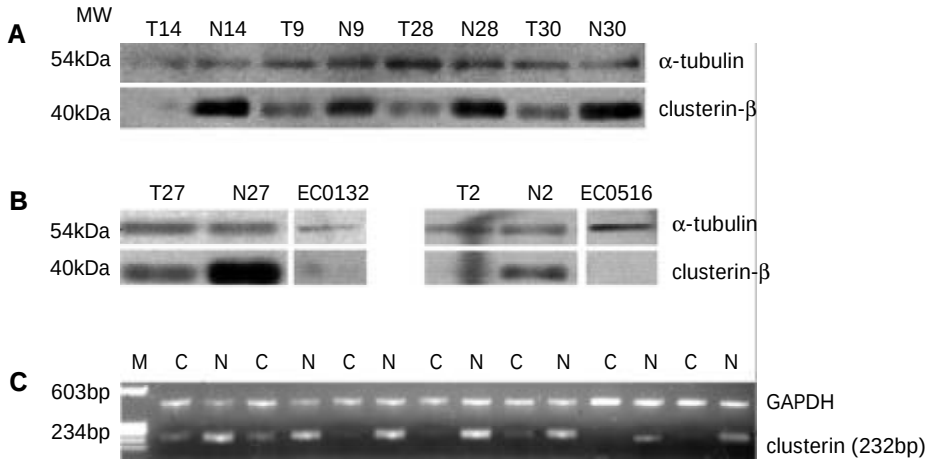

Figure 4 (A) Western blot analysis of clusterin proteins expressed in patient-matched normal and tumor epithelium; (B) Western blot analysis of clusterin proteins expressed in two kinds of esophageal squamous cell carcinoma, EC0156 and EC0132. Alpha-tubulin was used as a loading control. (C) Expression analysis of clusterin in patient-matched esophageal cancer tissues by semi-quantitative RT-PCR. GAPDH was used as an internal control.

Loss of clusterin in tumor epithelium

Immunoblot analysis of clusterin expressed in patient-matched normal and tumor epithelium from different ESCC individuals, whose sera had been found with low level of clusterin was performed. Using a commercially available antibody, clusterin has also been found down-regulated at different ESCC tissues (20/24), but absent in two kinds of cell lines of esophageal squamous cell carcinoma, EC1 and EC2 (Figure 4A, B). At the transcriptional level, clusterin was also found lower-expressed in 88 % of esophageal cancer tissues (22/25) by semi-quantitative RT-PCR (Figure 4C). The findings of tumor tissue and cell lines were consistent with the findings of ESCC serum.

DISCUSSION

To identify the differentially secreted proteins or polypeptides associated with tumorigenesis of esophageal squamous cell carcinoma, we carried out differentially proteomic analysis of human serum in two groups. First we compared the pre- and post-surgery sera of ESCC patient to identify the differentiated proteins from the same individuals. Second, the sera from the disease (pre-surgery) and age- and gender-matched healthy populations (normal control) had been analyzed through 2DE-MS strategy. There were 3 protein spots quantitatively changed between the two groups and were identified as clusterin, which was completely loss or dramatically down-regulated in pre-surgery serum of esophageal cancer compared with the post-surgery and the healthy controls. In addition, clusterin was also lost or decreased in tumor cell lines and tissues. Clusterin has never been known to be associated with esophageal cancer. This study reports identified clusterin as a candidate protein of a tumor-associated serum marker in esophageal squamous cell carcinoma via proteomic approaches for the first time.

Clusterin, so-called the testosterone-repressed prostate message-2[13], sulfated glycoprotein 2, complement-associated protein SP-40, complement cytolysis inhibitor, a 80 kDa heterodimeric highly conserved secreted glycoprotein expressed in a wide variety of tissues and was found in all human fluids. It responses to a number of diverse stimuli, including hormone ablation and has been attributed functions in several diverse physiological processes such as sperm maturation, lipid transportation, complement inhibition, tissue remodeling, membrane recycling, cell adhesion and cell-substratum interactions, stabilization of stressed proteins in a folding-competent state and promotion or inhibition of apoptosis[14-16].

Clusterin gene is differentially regulated by cytokines, growth factors and stress- inducing agents, while another defining prominent and intriguing clusterin feature is its upregulation in many severe physiological disturbances states and in several neurodegenerative conditions mostly related to advanced aging[17-22]. Active cell death (ACD) in hormone-dependent tissues such as the prostate and mammary gland is readily induced by hormone ablation and by treatment with anti-androgens or anti-estrogens, calcium channel agonists and TGF beta[23]. Clusterin has been found up-regulated in several cases of *in vivo* cancer progression and tumor formation such as human prostate carcinomas[18,24], renal cell carcinoma (RCC)[25,26], breast carcinoma[17], ovarian cancer[22], glioblastoma, testicular tumor cells, the normal and cancerous endometrium, hemangioma[21], anaplastic large-cell lymphomas[20], transitional cell carcinoma (TCC) of the bladder[27], as well as hepatoma cells. Clusterin, on the other hand, is a membrane-stabilizing protein that appears to be involved in limiting the autophagic lysis of epithelial cells during apoptosis. Recent studies have shown the clusterin expression mediates antiapoptotic activity against a wide variety of stimuli[28] and using antisense oligonucleotides of clusterin, also could enhance androgen sensitivity and chemosensitivity in prostate cancer therapy[29]. On the other hand, it has recently been shown that decreased synthesis and delayed processing of clusterin in testicular germ cell tumors, colorectal cancer[16,30] and human polycystic kidneys cells[31,32]. However, there is no definitive biochemical evidence to support a specific function for clusterin except for its role in the modulation of the immune system and the functional roles of clusterin are still enigmatic.

A robust antigen capture assay for the measurement of serum clusterin concentrations has been developed and validated for increased clusterin expression, and alterations in serum clusterin levels associated with a number of disease states[33]. Whether the decrease of clusterin in pre-surgery serum is a predictor of ESCC progression and prognosis, still need more efforts to address and the molecular mechanisms of clusterin implicated in tumorigenesis needs to be elucidated.

REFERENCES

1 **Zhang WH**, Bailey-Wilson JE, Li WD, Wang XQ, Zhang CL, Mao XZ, Liu ZH, Zhou CN, Wu M. Segregation analysis of esophageal cancer in a moderately high-incidence area of norther China. *Am J Hum Genet* 2000; **67**: 110-119

2 **Wang DX**, Li W. Advances on pathogenesis of esophageal cancer. *Shijie Huaren Xiaohua Zazhi* 2000; **8**: 1029-1030

3 **Hu SP**, Yang HS, Shen ZY. Study on etiology of esophageal carcinoma: retrospect and prospect. *Zhongguo Aizheng Zazhi* 2001; **11**: 171-174

4 **Oka M**, Yamamoto K, Takahashi M, Hakozaki M, Abe T, Iizuka N, Hazama S, Hirazawa K, Hayashi H, Tangoku A, Hirose K, Ishihara T, Suzuki T. Relationship between serum levels of interleukin 6, various disease parameters and malnutrition in patients with esophageal squamous cell carcinoma. *Cancer Res* 1996; **56**: 2776-2780

5 **Lu J**, Liu Z, Xiong M, Wang Q, Wang X, Yang G, Zhao L, Qiu Z, Zhou C, Wu M. Gene expression profile changes in initiation and progression of squamous cell carcinoma of esophagus. *Int J Cancer* 2001; **91**: 288-294

6 **Paweletz CP**, Ornstein DK, Roth MJ, Bichsel VE, Gillespie JW, Calvert VS, Vocke CD, Hewitt SM, Duray PH, Herring J, Wang QH, Hu N, Linehan WM, Taylor PR, Liotta LA, Emmert-Buck MR, Petricoin EF 3rd. Loss of annexin I correlates with early onset of tumorigenesis in esophageal and prostate carcinoma. *Cancer Res* 2000; **60**: 6293-6297

7 **Zhou G,** Li H, DeCamp D, Chen S, Shu H, Gong Y, Flaig M, Gillespie JW, Hu N, Taylor PR, Emmert-Buck MR, Liotta LA, Petricoin EF 3rd, Zhao Y. 2D differential in-gel electrophoresis for the identification of esophageal scans cell cancer-specific protein markers. *Mol Cell Proteomics* 2002; **1**: 117-124

8 **Xiong XD**, Xu LY, Shen ZY, Cai WJ, Luo JM, Han YL, Li EM. Identification of differentially expressed proteins between human esophageal immortalized and carcinomatous cell lines by two-dimensional electrophoresis and MALDI-TOF-mass spectrometry. *World J Gastroenterol* 2002; **8**: 777-781

9 **Li F**, Guan YJ, Chen ZC. Proteomics in cancer research. *Shengwu Huaxue Yu Shengwu Wuli Jinzhan* 2001; **28**: 164-167

10 **Wang H**, Hanash SM. Contributions of proteome profiling to the molecular analysis of cancer. *Technology in Cancer Research & Treatment* 2002; **1**: 1-8

11 **Vercoutter-Edouart AS**, Lemoine J, Louis H, Boilly B, Nurcombe V, Revillion F, Peyrat JP, Hondermarck H. Proteomic analysis reveals that 14-3-3 sigma is down-regulated in human breast cancer cells. *Cancer Res* 2001; **61**: 76-80

12 **Zhan XQ**, Chen ZC, Guan YJ, Li C, He CM, Liang SP, Xie JY, Chen P. Analysis of human lung squamous carcinoma cell line NCI-H520 proteome by two-dimensional electrophoresis and MALDI-TOF-mass spectrometry. *Ai Zheng* 2001; **20**: 575-582

13 **Parczyk K**, Pilarsky C, Rachel U, Koch-Brandt C. Gp80 (clusterin; TRPM-2) mRNA level is enhanced in human renal clear cell carcinomas. *J Cancer Res Clin Oncol* 1994; **120**: 186-188

14 **Trougakos IP**, Gonos ES. Clusterin / Apolipoprotein J in human aging and cancer. *Int J Biochem Cell Biol* 2002; **34**: 1430-1448

15 **Jones SE,** Jomary C. Clusterin. *Int J Biochem Cell Biol* 2002; **34**: 427-431

16 **Yang CR**, Leskov K, Hosley-Eberlein K, Criswell T, Pink JJ, Kinsella TJ, Boothman DA. Nuclear clusterin / XIP8, an x-ray-induced Ku70-binding protein that signals cell death. *Proc Natl Acad Sci USA* 2000; **97**: 5907-5912

17 **Redondo M**, Villar E, Torres-Munoz J, Tellez T, Morell M, Petito CK. Overexpression of clusterin in human breast carcinoma. *Am J Pathol* 2000; **157**: 393-399

18 **Behrens P,** Jeske W, Wernert N, Wellmann A. Downregulation of clusterin expression in testicular germ cell tumours. *Pathobiology* 2001; **69**: 19-23

19 **Tobe T**, Minoshima S, Yamase S, Choi NH, Tomita M, Shimizu N. Assignment of a human serum glycoprotein SP-40, 40 gene (CLI) to chromosome 8. *Cytogenet Cell Genet* 1991; **57**: 193-195

20 **Wellmann A**, Thieblement C, Pittaluga S, Sakai A, Jaffe ES, Siebert P, Raffeld M. Detection of differentially expressed genes in lymphomas using cDNA arrays: identification of as a new diagnostic marker for anaplastic large-cell lymphomas. *Blood* 2000; **91**: 398-404

21 **Hasan Q**, Ruger BM, Tan ST, Gush J, Davis PF. Clusterin / apo J expression during the development of hemangioma. *Hum Pathol* 2000; **31**: 691-697

22 **Hough CD**, Cho KR, Zonderman AB, Schwartz DR, Morin PJ. Coordinately up-regulated genes in ovarian cancer. *Cancer Res* 2001; **61**: 3869-3876

23 **Tenniswood MP**, Guenette RS, Lakins J, Mooibroek M, Wong P, Welsh JE. Active cell death in hormone-dependent tissues. *Cancer Metastasis Rev* 1992; **11**: 197-220

24 **Kadomatsu K**, Anzano MA, Slayter MV, Winokur TS, Smith JM, Sporn MB. Expression of sulfated glycoprotein 2 is associated with carcinogenesis induced by N-nitroso-N-methylurea in rat prostate and seminal vesicle. *Cancer Res* 1993; **53**: 1480-1483

25 **Miyake H**, Gleave ME, Arakawa S, Kamidono S, Hara I. Introducing the clusterin gene into human renal cell carcinoma cells enhances their metastatic potential. *J Urol* 2002; **167**: 2203-2208

26 **Hara I**, Miyake H, Gleave ME, Kamidono S. Introduction of clusterin gene into human renal cell carcinoma cells enhances their resistance to cytotoxic chemotherapy through inhibition of apoptosis both *in vitro* and *in vivo*. *Jpn J Cancer Res* 2001; **92**: 1220-1224

27 **Welsh J**. Induction of apoptosis in breast cancer cells in response to vitamin D and antiestrogens. *Biochem Cell Biol* 1994; **72**: 537-545

28 **Viard I**, Wehrli P, Jornot L, Bullani R, Vechietti JL, Schifferli JA, Tschopp J, French LE. Clusterin gene expression mediates resistance to apoptotic cell death induced by heat shock and oxidative stress. *J Invest Dermatol* 1999; **112**: 290-296

29 **Zellweger T**, Miyake H, Cooper S, Chi K, Conklin BS, Monia BP, Gleave ME. Antitumor activity of antisense clusterin oligonucleotides is improved in vitro and in vivo by incorporation of 2'-O-(2-methoxy)ethyl chemistry. *J Pharmacol Exp Ther* 2001; **298**: 934-940

30 **Yamori T**, Kimura H, Stewart K, Ota DM, Cleary KR, Irimura T. Differential production of high molecular weight sulfated glycoproteins in normal colonic mucosa, primary colon carcinoma and metastasis. *Cancer Res* 1987; **47**: 2741-2747

31 **Longo VD**, Viola KL, Klein WL, Finch CE. Reversible inactivation of superoxide-sensitive aconitase in Abeta1-42- treated neuronal cell lines. *J Neurochem* 2000; **75**: 1977-1985

32 **Zellweger T**, Chi K, Miyake H, Adomat H, Kiyama S, Skov K, Gleave ME. Enhanced radiation sensitivity in prostate cancer by inhibition of the cell survival protein clusterin. *Clin Cancer Res* 2002; **8**: 3276-3284

33 **Morrissey C**, Lakins J, Moquin A, Hussain M, Tenniswood M. An antigen capture assay for the measurement of serum clusterin concentrations. *J Biochem Biophy Methods* 2001; **48**: 13-21

Edited by Ren SY

P.O.Box 2345, Beijing 100023, China
Fax: +86-10-85381893
E-mail: wjg@wjgnet.com www.wjgnet.com

World J Gastroenterol 2003;9(4):655-659
World Journal of Gastroenterology
 ISSN 1007-9327

• GASTRIC CANCER •

Mutation and methylation of hMLH1 in gastric carcinomas with microsatellite instability

Dian-Chun Fang, Rong-Quan Wang, Shi-Ming Yang, Jian-Ming Yang, Hai-Feng Liu, Gui-Yong Peng, Tian-Li Xiao, Yuan-Hui Luo

Dian-Chun Fang, Rong-Quan Wang, Shi-Ming Yang, Jian-Ming Yang, Hai-Feng Liu, Gui-Yong Peng, Tian-Li Xiao, Yuan-Hui Luo, Department of Gastroenterology, Southwest Hospital, Third Military Medical University, Chongqing, 400038, China
Supported by the National Natural Science Foundation of China, No. 30070043, and "10.5" Scientific Research Foundation of Chinese PLA, No. 01Z075
Correspondence to: Dian-Chun Fang, M.D., Ph.D. Southwest Hospital, Third Military Medical University, Chongqing 400038, China. fangdianchun@hotmail.com
Telephone: +86-23-68754624 **Fax:** +86-23-68754124
Received: 2002-10-09 **Accepted:** 2002-11-14

Abstract

AIM: To appraise the correlation of mutation and methylation of hMSH1 with microsatellite instability (MSI) in gastric cancers.

METHODS: Mutation of hMLH1 was detected by Two-dimensional electrophoresis (Two-D) and DNA sequencing; Methylation of hMLH1 promoter was measured with methylation-specific PCR; MSI was analyzed by PCR-based methods.

RESULTS: Sixty-eight cases of sporadic gastric carcinoma were studied for mutation and methylation of hMLH1 promoter and MSI. Three mutations were found, two of them were caused by a single bp substitution and one was caused by a 2 bp substitution, which displayed similar Two-D band pattern. Methylation of hMLH1 promoter was detected in 11(16.2 %) gastric cancer. By using five MSI markers, MSI in at least one locus was detected in 17/68(25 %) of the tumors analyzed. Three hMLH1 mutations were all detected in MSI-H ($\geqslant$2 loci, n=8), but no mutation was found in MSI-L (only one locus, n=9) or MSS (tumor lacking MSI or stable, n=51). Methylation frequency of hMLH1 in MSI-H (87.5 %, 7/8) was significantly higher than that in MSI-L (11.1 %, 1/9) or MSS (5.9 %, 3/51) (P<0.01-0.001), but no difference was found between MSI-L and MSS (P>0.05).

CONCLUSION: Both mutation and methylation of hMLH1 are involved in the MSI pathway but not related to the LOH pathway in gastric carcinogenesis.

Fang DC, Wang RQ, Yang SM, Yang JM, Liu HF, Peng GY, Xiao TL, Luo YH. Mutation and methylation of hMLH1 in gastric carcinomas with microsatellite instability. *World J Gastroenterol* 2003; 9(4): 655-659
http://www.wjgnet.com/1007-9327/9/655.htm

INTRODUCTION

Our previous studies indicated that genetic instability may play an important role in gastric carcinogenesis[1]. There are at least two distinct genetic instabilities in gastric tumorigenesis: one is the chromosomal instability (or suppressor pathway) and the other is microsatellite instability (or MSI pathway). In the former, perhaps including tumors with low-frequency MSI (MSI-L) as well as microsatellite stable (MSS), accumulation of loss of tumor suppressor genes such as p53, Rb, APC, MCC and DCC play an important role in their carcinogenesis; whereas in the latter, consisting of a small subset of gastric cancer with high-frequency MSI (MSI-H), defective repair of mismatched bases results in an increased mutation rate at the nucleotide level, and the consequent widespread MSI[2-4].

Mismatch repair is required for the cell to accurately copy its genome during cellular proliferation. Deficiencies of this system result in mutation rates 100-fold greater than those observed in normal cells[5]. MSI is a hallmark of mismatch repair gene (MMR)-deficient cancers. MSI in tumors from patients with hereditary non-polyposis colorectal cancer (HNPCC) is caused by germline mutations in MMR genes, principally hMSH2 and hMLH1[6-10]. In contrast, somatic mutations in MMR genes are relatively rare in sporadic MSI+ colon cancers[9,11]. Rather, the majority of negative mutation, MSI+ cases involve hypermethylation of the hMLH1 promoter and subsequent lack of expression of hMLH1[12-16]. The details of the mechanisms of this epigenetic gene silencing remain to be elucidated in gastric cancer. The aim of this study was to define the mutation and methylation of hMLH1 in gastric carcinomas with MSI.

MATERIALS AND METHODS

Tissue samples

Sixty-eight cancer and corresponding normal tissues were obtained from surgically resected gastric carcinoma in our hospital. Each specimen was frozen immediately and stored at -80 ℃ until analyzed. A 5 μm section was cut from each tissue and stained with hematoxylin/eosin in order to ascertain whether the cancer cells in the tissues were predominant or not. Genomic DNA was isolated by standard proteinase-K digestion and phenol-chloroform extraction protocols. Of the 68 patients with gastric cancer, 45 were men and 23 were women with an age range of 30-76 years (a mean of 56.2 years at diagnosis). None of the patients included in the present series had a family history suggestive of HNPCC or had received chemotherapy or radiation therapy.

hMLH1 mutation analysis

PCR and heteroduplexing Primer pairs for long-chain and short-chain PCR and GC-clamped primers used were shown in Table 1[17]. PCR reactions were carried out in 50 μl reactions in thin-walled tubes in a Perkin-Elmer 2 400 thermocycler. A total of 200-400 ng of genomic DNA, varying concentrations of each primer, and the LA PCR kit (TaKaRa, Otsu, Shiga, Japan) were used for long PCR. Final concentrations of each LA PCR primer pair were as follows: hMLH1-4F and hMLH1-4R, 0.16 μM each; hMLH5-10F and hMLH5-10R, 0.125 μM each; hMLH11-13F and hMLH11-13R, 0.094 μM each; and hMLH14-19F and hMLH14-19R, 0.125 μM each. The reactions were carried out according to the manufacturer's instructions. In brief, the conditions were as follows: a hot start of 94 ℃ for 2 min, with the addition of Taq Pol in between,

followed by eight cycles of 98 ℃×20 sec, 69 ℃×1 min (with decrements of 0.5 ℃/cycle), and 68 ℃×12 min; six cycles of 96 ℃×20 sec, and 68 ℃×12 min; 16 cycles of 96 ℃×20 sec, and 68 ℃×12 min (with increments of 15 sec/cycle), and finally a chain extension of 72 ℃ for 10 min.

Table 1 Primer information for long and short PCR for HMLH1

A. Primer pairs for long-distance PCR

Exons 1-4
MLH1-4F GCG.GCT.AAG.CTA.CAG.CTG.AAG.GAA.GAA.CGT.GA[a]
MLH1-4R GGC.GAG.ACA.GGA.TTA.CTC.TGA.GAC.CTA.GGC.CC
Product size-10.8kb
Exons5-10
MLH5-10F GCG.CCC.CTT.GGG.ATT.AGT.ATC.TAT.CTC.TCT.ACT.GG
MLH5-10R GCG.CTC.ATC.TCT.TTC.AAA.GAG.GAG.AGC.CTG
Product size-10.5kb
Exons11-13
MLH11-13F CGG.CTT.TTT.CTC.CCC.CTC.CCA.CTA.TCT.AAG.G
MLH11-13R GGG.TTA.GTA.AAG.GAA.GAG.GAG.CTT.GCC.C
Product size-8.7kb
Exons14-19
MLH14-19F GGT.GCT.TTG.GTC.AAT.GAA.GTG.GGG.TTG.GTA.G
MLH14-19R GCG.CGC.GTA.TGT.TGG.TAC.ACT.TTG.TAT.ATC.ACA.C
Product size=10.5kb

B. Primer pairs for short PCR

Exon	Clamp[b]	Product size	T_m[c]	Primer sequence
1	5	258	64.13	GCA.CTT.CCG.TTG.AGC.ATC
	40			CCG.TTA.AGT.CGT.AGC.CCT
2	40	187	38.14	ATA.AAT.TAT.TTT.CTG.TTT
				CAT.CCT.GCT.ACT.TTG.AGG
3	40	237	32.22	GGA.AAA.TGA.GTA.ACA.TGA
	2			TGT.CAT.CAC.AGG.AGG.ATA
4	2	218	36.26	ACC.CAG.CAG.TGA.GTT.TT
	40			GCC.CAA.AAT.ACA.TTT.CAG
5	40	170	30.19	ATA.TTA.ATT.TGT.TAT.ATT
				CAA.TTT.ACT.CTC.CCA.TGT
6	40	228	35.58	TTT.CAA.GTA.CTT.CTA.TGA
				ACT.TTG.TAG.ACA.AAT.CTC
7		194	30.88	GAC.ATC.TAG.TGT.GTG.TTT
	40			CCC.CTT.TTT.TCT.TTT.CAT
8	5	213	42.21	GAC.AAT.AAA.TCC.TTG.TGT
	50			AAG.ATT.TTT.TTA.TAT.AGG
9	40	249	33.73	TTT.GAG.TTT.TGA.GTA.TTT
				TGG.GTG.TTT.CCT.GTG.AGT
10	50	240	41.47	CAC.CCC.TCA.GGA.CAG.TTT
				ACA.TCT.GTT.CCT.TGT.GAG
11.1	50	145	40.58	AGG.TAA.TTG.TTC.TCT.CTT
				GAA.GTG.AAC.TTC.ATG.CTT
11.2	40	224	60.81	TCC.CAA.GAA.TGT.GGA.TGT
	2			AAA.GGC.CCC.AGA.GAA.GTA
12.1	40	184	44.53	TTT.TTT.TTT.TTT.TAA.TAC.A
				AAT.CTG.TAC.GAA.CCA.TCT
12.2	8	366	53.23	TGG.AAG.TAG.TGA.TAA.GGT
	40			TGT.ACT.TTT.CCC.AAA.AGG
13	40	272	49.06	ATC.TGC.ACT.TCC.TTT.TCT
				AAA.ACC.TTG.GCA.GTT.GAG
14	45	235	48.94	TAC.TTA.CCT.GTT.TTT.TGG
	5			GTA.GTA.GCT.CTG.CTT.GTT
15	40	179	29.97	CAG.CTT.TTC.CTT.AAA.GTC
				CAG.TTG.AAA.TGT.CAG.AAG
16		261	47.56	CTT.GCT.CCT.TCA.TGT.TCT.TG
	40			AGA.AGT.ATA.AGA.ATG.GCT.GTC
17	40	199	47.01	ATT.ATT.TCT.TGT.TCC.CTT
				AAT.GCT.TAG.TAT.CTG.CCT
18	45	215	46.67	CCT.ATT.TTG.AGG.TAT.TGA.AT
				GCC.AGT.GTG.CAT.CAC.CA
19		282	43.43	TGT.TGG.GAT.GCA.AAC.AGG
	40			ATC.CCA.CAG.TGC.ATA.AAT

[a]Underlined nucleotides represented nucleotides added to modify the melting temperatures of the primers. [b]GClampsm are: 50clamp,CGC.CCG.CCG.CCG.CCC.GCC.GCG.CCC.CGC. GCC.CGT .CCC.GCC.GCC.CCC.GCC.CG; 45 GC clamp, CGC. CCG.CCG.CGC.CCC.CGC.CCC.GTC.CCG.CCG.CCC.CCG. CCC.GGC.CCG; 40 clamp, CGC.CCGCCG.CGC.CCC.GCG. CCC.GGC.CCG.CCG.CCC.CCG.CCC.G; 8 clamp, CGT.CCC. GC; 5 clamp, GCG. CG; 2 clamp,CG; [c]TM is given in %UF.

After checking and visualizing the long PCR products on a 0.8 % agarose gel, 1μl of the long PCR amplicons was used as template for subsequent extensive multiplex short PCR. The short PCR was performed in two multiplex groups of 11 and 10 amplicons, respectively. The final concentrations of each primer were shown in Table 2. The final concentrations of the PCR mix included 1×PCR buffer, 7 mM $MgCl_2$, and 0.25 mM each dNTP. Cycling conditions included a hot start of 3 min at 94 ℃ with the Taq Pol added after 2 min, followed by five cycles of 94 ℃×1 min, 52 ℃×45 sec (decrements of 1 ℃/cycle), and 72 ℃×1 min; 15 cycles of 94 ℃×1 min, 48 ℃×45 sec, and 72 ℃×1 min, 30 sec (with increments of 2 sec/cycle); 15 cycles of 94 ℃×1 min, 38 ℃×45 sec, and 72 ℃×1 min 30 sec. Each PCR reaction was teminated with a round of heteroduplexing: 72 ℃×10 min, 98 ℃×10 min, 45 ℃×30 min, and finally 37 ℃×30 min. Each tube reaction was directly mixed with 1/10 volume of 10×loading buffer, 6.5 μl of multiplex group I and 8.5 μl of multiplex group II were loaded onto a slab gel for size separation.

Table 2 Multiplex groups for short PCR

Multipex group I		Multipex group II	
Exon	Final concentration	Exon	Final concentration
11.1	0.375 μM	5	1.5 μM
15	0.5 μM	2	1.25 μM
12.1	0.375 μM	7	1.75 μM
17	0.5 μM	4	1.625 μM
8	0.375 μM	11.2	0.5 μM
18	1.25 μM	6	1.625 μM
14	1.25 μM	9	1.5 μM
3	0.625 μM	1	1.25 μM
10	0.625 μM	13	1.625 μM
16	1.0 μM	12.2	0.325 μM
19	1.75 μM		

Two-dimensional electrophoresis For two-dimensional electrophoresis, the DGGE instrument was from CBS Scientific Co. (Solana Beach, CA. Amplicons from each of the two multiplex reactions were mixed and subjected to electrophoresis in 0.5×TAE (Tris-Acetate EDTA). A 10 % polyacrylamide, 0.75 mm thick slab gel was used, the amplicons were fractionated at 140V for 7.5hr at 50 ℃. The separation pattern was detected by SYBR green staining and UV-transillumination of the slab gel. The 120-to 420-bp region in the middle of each lane was quickly cut out and applied to a 1mm thick DGGE gel.

The DGGE gel was prepared as a 1 mm thick slab gel with a 10-6.5 % reverse polyacrylamide gradient containing 25-70 % urea/formamide (UF) and 3-9 % glycerol gradients. Electrophoresis was carried out for 16 hr at 56 ℃ and 90-110V. After electrophoresis, the gels were stained with SYBR-green I and II for 30 min. The DGGE band patterns were detected and documented with a gel documentation system (Oncor, Gaithersburg, MD).

Sequence analysis Amplicons were prepared by PCR such that a standard M13 primer site was incorporated at one end. These products were sequenced on an ABI 377 sequencer (Foster

City, CA) with kits containing Taq FS DNA polymerase and dye primer technology, as recommended by the manufacturer.

hMLH1 methylation analysis

DNA methylation patterns in the CpG islands of hMLH1 gene were determined by Methylation-specific PCR(MSP) as described[18]. The primer sequences of hMLH1 for unmethylated reaction were 5' -TTTTGATGTAGATGTTTTATTAGGGTTGT-3' (sense) and 5' -ACCACCTCAT CATAACTACCCACA-3' (antisense), and for methylated reaction were 5' -ACGTAGACGTTTTATT AGGGTCGC-3' (sense) and 5' -CCTCATCGTAACTACC CGCG-3' (antisense).

MSI detection

MSI analyses included five microsatellite markers: BAT25, BAT26, BAT40, D2S123, and D5S346. PCR was performed as previous described[1]. MSI was defined as the presence of band shift in the tumor DNA that was not present in the corresponding normal DNA. Based on the number of mutated MSI markers in each tumor, carcinomas were characterized as MSI-H if they manifested instability in two or more markers, MSI-L if unstable in only one marker, and MSS if they showed no instability in any marker[19,20].

Statistical analysis

Chi-square test with Yates' correction were used. A P value <0.05 was considered significant.

RESULTS

MSI in gastric cancer

Alterations of electrophoretic patterns of PCR products of five microsatellite markers were compared between the tumor and the normal DNA in each patient (Figure 1). MSI affecting at least one locus was observed in 17 (25 %) of 68 tumors, among which eight (11.8 %) were MSI-H, nine (13.2 %) were MSI-L, and fifty-one (75 %) were MSS.

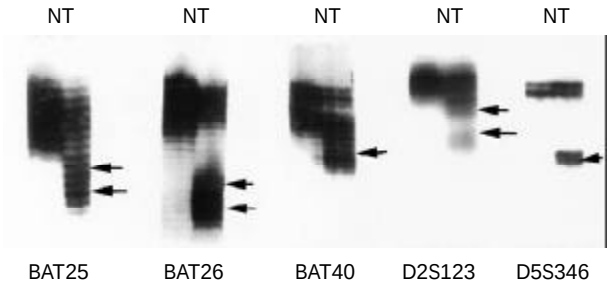

Figure 1 MSI in gastric cancer using 5 microsatellite loci (BAT-25, BAT-26, BAT-40, D2S123, and D5S346). Arrows indicate variant conformers. N: normal DNA pattern; T: tumor specimens containing variant conformers representing MSI.

hMLH1 mutation and MSI

Mutations and sequence alteration in various exons manifested as the four-spot pattern denoting a heterozygous variant (Figure 2). We found three mutations in 68 (4.4 %) gastric cancer by DNA sequencing. Two mutations were caused by a single bp substitution (exon 8 at codon 226, CGG→CTG, Arg→Leu; exon 9 at codon 252, TCA→TTA, Ser→Phe);. One identical change was caused by a 2 bp substitution (exon 12 at codon 409, CAG→CGT, Gln→Arg), which displayed similar DGGE band pattern. A comparison of MSI status with hMLH1 mutation was shown in Table 3. Three hMLH1 mutations were all detected in MSI-H, but no mutation was found in MSI-L or MSS.

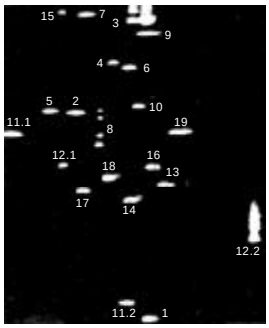

Figure 2 Detection of mismatching repair gene hMLH1 mutation in gastric cancer by two-dimentional DNA electrophoresis. Four-band pattern was observed at exon 8.

Table 3 The relevance of MSI and hMLH1 mutation

MSI Status	No.of cases	hMLH1 mutation
MSI-H	8	3
MSI-L	9	0
MSS	51	0

hMLH1 methylation status and MSI

To examine methylation of promoter region of hMLH1, we adapted MSP for the 5' CpG islands in this gene. The region chosen spaned the area of greatest CpG density immediately 5' to the transcription starting site, in an area previously studied for methylation changes[15]. In gastric mucosal samples without cancer, only unmethylated hMLH1 genes were present. Eleven of 68 (16.2 %) gastric cancers exhibited prominent methylation, which always had both methylated and nonmethylated hMLH1 genes (Figure 3). A comparison of MSI status with hMLH1 methylation status was shown in Table 4. Seven of 8 (87.5 %) cancers with MSI-H exhibited prominent methylation, whereas methylated hMLH1 gene was only found in 1/9 (11.1 %) gastric cancer with MSI-L and 3/51 (5.9 %) with MSS, suggesting that hMLH1 methylation was more correlated with gastric cancers with MSI -H than that with MSI -L or with MSS (P<0.01-0.001).

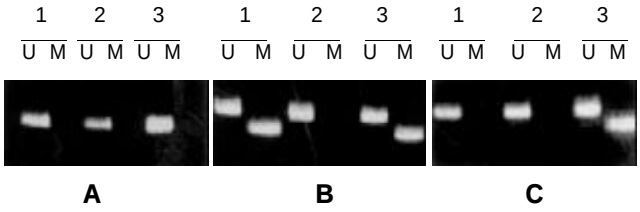

Figure 3 Methylation of hMLH1 in gastric cancer. A: No methylation was found in normal mucosa; B: Methylation of hMLH1 in MSI-H gastric cancer. Cases 1, 3 showed both hypermethylation and unmethylation; C: Methylation of hMLH1 in MSI-L gastric cancer. Case 3 showed both hypermethylation and unmethylation; U: Unmethylation; M: methylation.

Table 4 The relevance of methylation of hMLH1 and MSI

MSI status	Unmethylated	Hypermethylation(%)
MSI-H	1	7(87.5)
MSI-L	8	1(11.1)[b]
MSS	48	3(5.9)[d]

[b]P<0.01; [d]P<0.001 *vs* MSI-H group.

DISCUSSION

A significant portion of gastric cancers exhibit defective DNA mismatch repair, manifested as MSI. There is now evidence that MSI cancer comprises distinctive MSI-H and MSI-L categories[21-23]. MSI-H cancers are distingushed clinicopathologically and in their spectrum of genetic alterations from cancers showing MSI-L and MSS cancers[24-34]. Our previous studies indicated that MSI-H gastric cancers often showed lower frequency of LOH in APC, MCC and DCC genes than do MSI-L and MSS cancers[1]. In the present study, all three hMLH1 mutations were detected in MSI-H, but no mutation was found in those showing MSI-L or MSS. This result further indicates that hMLH1 is mutational target in MSI -H tumor cells and supported the notion that MIS-H tumors identified an alterative pathway of tumorigenesis that had been proposed by Vogelstein and co-workers[35].

Human cancers with MSI-H phenotype develop due to defects in DNA mismatch repair genes. Silencing of a DNA mismatch repair gene, hMLH1 gene, by promoter hypermethylation is a frequent cause of MSI-H phenotype[36-42]. In this study, 11 (16.2 %) of 68 gastric cancers exhibited prominent hMLH1 methylation, which is similar to previous studies[36]. It has been reported that MSI-H is related to methylation of the hMLH1 promoter but not hMSH1 mutations in sporadic gastric carcinomas[43]. It was also found that MSI-L gastric carcinomas share the hMLH1 methylation status of MSI-H carcinomas but not their clinicopathological profile[44]. In this study, 7/8 (87.5 %) cancers with MSI-H exhibited prominent methylation of the hMLH1 promoter, suggesting that methylation of the hMLH1 promoter is correlated with MSI-H gastric cancer. The frequency of methylation in MSI-H cancers is significantly higher than that in cancers with MSI-L and MSS, however no difference was found between cancers with MSI-L and MSS, indicating that MSI-H tumors identify a different methylation pathway from cancers with MSI-L and MSS, and MSI-L cancers involves the same methylation pathway as MSS tumors. This finding is in agreement with our recently published data on molecular pathway in the gastric carcinogenesis[2].

It has been found that colorectal cancer cell lines only had methylated hMLH1 genes, but had absent unmethylated hMLH1 genes[45]. In the present study, unlike the situation with the cell lines, however, the primary MSI+ gastric cancers always had both methylated and nonmethylated hMLH1 genes. It is likely that a significant fraction of the unmethylated genes is derived from the non-neoplastic cells (stromal, inflammatory, vascular, etc.), which are invariably present within the primary tumors but are not found in cultured cell lines. It has been reported that methylation of the hMLH1 promoter correlates with lack of expression of hMLH1 in sporadic colon tumors and mismatch repair-defective human tumor cell lines[13]. whereas demethylation of hMLH1 promoter results in reexpression of hMLH1 in tumor cells tested. Not only was the protein expressed, but MMR activity was restored. DNA methylation is a fundamental feature of the genomes and the control of their functions therefore it is a candidate for pharmacological manipulation that might have important therapeutic advantage.

REFERENCES

1 **Fang DC**, Jass JR, Wang DX, Zhou XD, Luo YH, Young J. Infrequent loss of heterozygosity of APC / MCC and DCC genes in gastric cancer showing DNA microsatellite instability. *J Clin Pathol* 1999; **52**: 504-508

2 **Fang DC**, Yang SM, Zhou XD, Wang DX, Luo YH. Telomere erosion is independent of microsatellite instability but related to loss of heterozygosity in gastric cancer. *World J Gastroenterol* 2001; **7**: 522-526

3 **Martins C**, Kedda MA, Kew MC. Characterization of six tumor suppressor genes and microsatellite instability in hepatocellular carcinoma in southern African blacks. *World J Gastroenterol* 1999; **5**: 470-476

4 **Wu BP**, Zhang YL, Zhou DY, Gao CF, Lai ZS. Microsatellite instability, MMR gene expression and proliferation kinetics in colorectal cancer with famillial predisposition. *World J Gastroenterol* 2000; **6**: 902-905

5 **Thomas DC**, Umar A, Kunkel TA. Microsatellite instability and mismatch repair defects in cancer. *Mutat Res* 1996; **350**: 201-205

6 **Peltomaki P**. Microsatellite instability and hereditary non-polyposis colon cancer. *J Pathol* 1995; **176**: 329-330

7 **Cai Q**, Sun MH, Lu HF, Zhang TM, Mo SJ, Xu Y, Cai SJ, Zhu XZ, Shi DR. Clinicopathological and molecular genetic analysis of 4 typical Chinese HNPCC families. *World J Gastroenterol* 2001; **7**: 805-810

8 **Modrich P**. Mismatch repair, genetic stability, and cancer. *Science* 1994; **266**: 1959-1960

9 **Papadopoulos N**, Lindblom A. Molecular basis of HNPCC: mutations of MMR genes. *Hum Mutat* 1997; **10**: 89-99

10 **Zhao B**, Wang ZJ, Xu YF, Wan YL, Li P, Huang YT. Report of 16 kindreds and one kindred with hMLH1 germline mutation. *World J Gastroenterol* 2002; **8**: 263-266

11 **Aaltonen LA,** Peltomaki P, Leach FS, Sistonen P, Pylkkanen L, Mecklin JP, Jarvinen H, Powell SM, Jen J, Hamilton SR. Clues to the pathogenesis of familial colorectal cancer. *Science* 1993; **260**: 812-816

12 **Miyakura Y,** Sugano K, Konishi F, Ichikawa A, Maekawa M, Shitoh K, Igarashi S, Kotake K, Koyama Y, Nagai H. Extensive methylation of hMLH1 promoter region predominates in proximal colon cancer with microsatellite instability. *Gastroenterology* 2001; **121**: 1300-1309

13 **Kane MF**, Loda M, Gaida GM, Lipman J, Mishra R, Goldman H, Jessup JM, Kolodner R. Methylation of the hMLH1 promoter correlates with lack of expression of hMLH1 in sporadic colon tumors and mismatch repair-defective human tumor cell lines. *Cancer Research* 1997; **57**: 808-811

14 **Garinis GA**, Patrinos GP, Spanakis NE, Menounos PG. DNA hypermethylation: when tumour suppressor genes go silent. *Hum Genet* 2002; **111**: 115-127

15 **Jones PA**. DNA methylation and cancer. *Oncogene* 2002; **21**: 5358-5360

16 **Ehrlich M**. DNA methylation in cancer: too much, but also too little. *Oncogene* 2002; **21**: 5400-5413

17 **Wu Y,** Nystrom-Lahti M, Osinga J, Looman MW, Peltomaki P, Aaltonen LA, de la Chapelle A, Hofstra RM, Buys CH. MSH2 and MLH1 mutations in sporadic replication error-positive colorectal carcinoma as assessed by two-dimensional DNA electrophoresis. *Genes Chromosomes Cancer* 1997; **18**: 269-278

18 **Herman JG**, Graff JR, Myohanen S, Nelkin BD, Baylin SB. Methylation-specific PCR: A novel PCR assay for methylation status of CpG islands. *Proc Natl Acad Sci USA* 1996; **93**: 9821-9826

19 **Boland CR**, Thibodeau SN, Hamilton SR, Sidransky D, Eshleman JR, Burt RW, Meltzer SJ, Rodriguez-Bigas MA, Fodde R, Ranzani GN, Srivastava S. A national cancer institute workshop on microsatellite instability for cancer detection and familial predisposition: Development of international criteria for the determination of microsatellite instability in colorectal cancer. *Cancer Res* 1998; **58**: 5248-5257

20 **Sood AK**, Holmes R, Hendrix MJ, Buller RE. Application of the national cancer institute international criteria for determination of microsatellite instability in ovarian cancer. *Cancer Res* 2001; **61**: 4371-4374

21 **Jass JR**, Biden KG, Cummings MC, Simms LA, Walsh M, Schoch E, Meltzer SJ, Wright C, Searle J, Young J, Leggett BA. Characterization of a subtype of colorectal cancer combining features of the suppressor and mild mutator pathways. *J Clin Pathol* 1999; **52**: 455-460

22 **Wahlberg SS**, Schmeits J, Thomas G, Loda M, Garber J, Syngal S, Kolodner RD, Fox E. Evaluation of microsatellite instability and immunohistochemistry for the prediction of germ-line MSH2 and MLH1 mutations in hereditary nonpolyposis colon cancer families. *Cancer Res* 2002; **62**: 3485-3492

23 **Kambara T**, Matsubara N, Nakagawa H, Notohara K, Nagasaka

T, Yoshino T, Isozaki H, Sharp GB, Shimizu K, Jass J, Tanaka N. High frequency of low-level microsatellite instability in early colorectal cancer. *Cancer Res* 2001; **61**: 7743-7746

24 **Miyoshi E**, Haruma K, Hiyama T, Tanaka S, Yoshihara M, Shimamoto F, Chayama K. Microsatellite instability is a genetic marker for the development of multiple gastric cancers. *Int J Cancer* 2001; **95**: 350-353

25 **Yamamoto H**, Min Y, Itoh F, Imsumran A, Horiuchi S, Yoshida M, Iku S, Fukushima H, Imai K. Differential involvement of the hypermethylator phenotype in hereditary and sporadic colorectal cancers with high-frequency microsatellite instability. *Genes Chromosomes Cancer* 2002; **33**: 322-325

26 **Halford S**, Sasieni P, Rowan A, Wasan H, Bodmer W, Talbot I, Hawkins N, Ward R, Tomlinson I. Low-level microsatellite instability occurs in most colorectal cancers and is a nonrandomly distributed quantitative trait. *Cancer Res* 2002; **62**: 53-57

27 **Young J**, Simms LA, Biden KG, Wynter C, Whitehall V, Karamatic R, George J, Goldblatt J, Walpole I, Robin SA, Borten MM, Stitz R, Searle J, McKeone D, Fraser L, Purdie DR, Podger K, Price R, Buttenshaw R, Walsh MD, Barker M, Leggett BA, Jass JR. Features of colorectal cancers with high-level microsatellite instability occurring in familial and sporadic settings: parallel pathways of tumorigenesis. *Am J Pathol* 2001; **159**: 2107-2116

28 **Lee JH,** Abraham SC, Kim HS, Nam JH, Choi C, Lee MC, Park CS, Juhng SW, Rashid A, Hamilton SR, Wu TT. Inverse relationship between APC gene mutation in gastric adenomas and development of adenocarcinoma. *Am J Pathol* 2002; **161**: 611-618

29 **Duval A**, Hamelin R. Genetic instability in human mismatch repair deficient cancers. *Ann Genet* 2002; **45**: 71-75

30 **Moran A**, Iniesta P, de Juan C, Gonzalez-Quevedo R, Sanchez-Prnaute A, Diaz-Rubio E, Ramon Y, Cajal S, Torres A, Balibrea JL, Benito M. Stromelysin-1 promoter mutations impair gelatinase B activation in high microsatellite instability sporadic colorectal tumors. *Cancer Res* 2002; **62**: 3855-3860

31 **Peiro G**, Diebold J, Lohse P, Ruebsamen H, Lohse P, Baretton GB, Lohrs U. Microsatellite instability, loss of heterozygosity, and loss of hMLH1 and hMSH2 protein expression in endometrial carcinoma. *Hum Pathol* 2002; **33**: 347-354

32 **Wu CW**, Chen GD, Jiang KC, Li AF, Chi CW, Lo SS, Chen JY. A genome-wide study of microsatellite instability in advanced gastric carcinoma. *Cancer* 2001; **92**: 92-101

33 **Ogata S**, Tamura G, Endoh Y, Sakata K, Ohmura K, Motoyama T. Microsatellite alterations and target gene mutations in the early stages of multiple gastric cancer. *J Pathol* 2001; **194**: 334-340

34 **Tamura G**, Sato K, Akiyama S, Tsuchiya T, Endoh Y, Usuba O, Kimura W, Nishizuka S, Motoyama T. Molecular characterization of undifferentiated-type gastric carcinoma. *Lab Invest* 2001; **81**: 593-598

35 **Vogelstein B,** Fearon ER, Hamilton SR, Kern SE, Preisinger AC, Leppert M, Nakamura Y, White R, Smits AM, Bos JL. Genetic alterations during colorectal tumor development. *N Engl J Med* 1988; **319**: 525-532

36 **Fleisher AS**, Esteller M, Tamura G, Rashid A, Stine OC, Yin J, Zou TT, Abraham JM, Kong D, Nishizuka S, James SP, Wilson KT, Herman JG, Meltzer SJ. Hypermethylation of the hMLH1 gene promoter is associated with microsatellite instability in early human gastric neoplasia. *Oncogene* 2001; **20**: 329-335

37 **Murata H**, Khattar NH, Kang Y, Gu L, Li GM. Genetic and epigenetic modification of mismatch repair genes hMSH2 and hMLH1 in sporadic breast cancer with microsatellite instability. *Oncogene* 2002; **21**: 5696-5703

38 **Norrie MW**, Hawkins NJ, Todd AV, Meagher AP, O'Connor TW, Ward RL. The role of hMLH1 methylation in the development of synchronous sporadic colorectal carcinomas. *Dis Colon Rectum* 2002; **45**: 674-680

39 **Sakata K**, Tamura G, Endoh Y, Ohmura K, Ogata S, Motoyama T. Hypermethylation of the hMLH1 gene promoter in solitary and multiple gastric cancers with microsatellite instability. *Br J Cancer* 2002; **86**: 564-567

40 **Baranovskaya S**, Soto JL, Perucho M, Malkhosyan SR. Functional significance of concomitant inactivation of hMLH1 and hMSH6 in tumor cells of the microsatellite mutator phenotype. *Proc Natl Acad Sci U S A* 2001; **98**: 15107-15112

41 **Deng G**, Peng E, Gum J, Terdiman J, Sleisenger M, Kim YS. Methylation of hMLH1 promoter correlates with the gene silencing with a region-specific manner in colorectal cancer. *Br J Cancer* 2002; **86**: 574-579

42 **Hawkins N,** Norrie M, Cheong K, Mokany E, Ku SL, Meagher A, O'Connor T, Ward R. CpG island methylation in sporadic colorectal cancers and its relationship to microsatellite instability. *Gastroenterology* 2002; **122**: 1376-1387

43 **Bevilacqua RA**, Simpson AJ. Methylation of the hMLH1 promoter but no hMLH1 mutations in sporadic gastric carcinomas with high-level microsatellite instability. *Int J Cancer* 2000; **87**: 200-203

44 **Pinto M**, Oliveira C, Machado JC, Cirnes L, Tavares J, Carneiro F, Hamelin R, Hofstra R, Seruca R, Sobrinho-Simoes M. MSI-L gastric carcinomas share the hMLH1 methylation status of MSI-H carcinomas but not their clinicopathological profile. *Lab Invest* 2000; **80**: 1915-1925

45 **Herman JG**, Umar A, Polyak K, Graff JR, Ahuja N, Issa JP, Markowitz S, Willson JK, Hamilton SR, Kinzler KW, Kane MF, Kolodner RD, Vogelstein B, Kunkel TA, Baylin SB. Incidence and functional consequences of hMLH1 promoter hypermethylation in colorectal carcinoma. *Proc Natl Acad Sci USA* 1998; **95**: 6870-6875

46 **Machover D**, Zittoun J, Saffroy R, Broet P, Giraudier S, Magnaldo T, Goldschmidt E, Debuire B, Orrico M, Tan Y, Mishal Z, Chevallier O, Tonetti C, Jouault H, Ulusakarya A, Tanguy ML, Metzger G, Hoffman RM. Treatment of cancer cells with methioninase produces DNA hypomethylation and increases DNA synthesis. *Cancer Res* 2002; **62**: 4685-4689

47 **Nichol K**, Pearson AC. CpG methylation modifies the genetic stability of cloned repeat sequences. *Genome Res* 2002; **12**: 1246-1256

48 **Karpf AR**, Jones DA. Reactivating the expression of methylation silenced genes in human cancer. *Oncogene* 2002; **21**: 5496-5503

49 **Christman JK**. 5-Azacytidine and 5-aza-2'-deoxycytidine as inhibitors of DNA methylation: mechanistic studies and their implications for cancer therapy. *Oncogene* 2002; **21**: 5483-5495

Edited by Wu XN

P.O.Box 2345, Beijing 100023, China
Fax: +86-10-85381893
E-mail: wjg@wjgnet.com www.wjgnet.com

World J Gastroenterol 2003;9(4):660-664
World Journal of Gastroenterology
 ISSN 1007-9327

• GASTRIC CANCER •

Tributyrin inhibits human gastric cancer SGC-7901 cell growth by inducing apoptosis and DNA synthesis arrest

Jun Yan, Yong-Hua Xu

Jun Yan, Yong-Hua Xu, Lab of Molecular and Cellular Oncology and Lab of Molecular Cell Biology, Institute of Biochemistry and Cell Biology, Shanghai Institutes for Biological Sciences, Chinese Academy of Sciences, Shanghai 200031, China
Supported by the Major State Basic Research (973) Program of China, (G1999053905) and National Natural Science Foundation of China, No. 30170207
Correspondence to: Dr. Yong-Hua Xu, Lab of Molecular and Cellular Oncology, Institute of Biochemistry and Cell Biology, Shanghai Institutes for Biological Sciences, Chinese Academy of Sciences, 320 Yue Yang Road, Shanghai 200031, China. yhxu@sunm.shcnc.ac.cn
Telephone: +86-21-54921361 **Fax**: +86-21-54921361
Received: 2002-10-09 **Accepted:** 2002-11-04

Abstract

AIM: To evaluate the effects of tributyrin, a pro-drug of natural butyrate and a neutral short-chain fatty acid triglyceride, on the growth inhibition of human gastric cancer SGC-7901 cell.

METHODS: Human gastric cancer SGC-7901 cells were exposed to tributyrin at 0.5, 1, 2, 5, 10 and 50 mmol·L^{-1} for 24-72 h. MTT assay was applied to detect the cell proliferation. [^{3}H]-TdR uptake was measured to determine DNA synthesis. Apoptotic morphology was observed by electron microscopy and Hoechst-33258 staining. Flow cytometry and terminal deoxynucleotidyl transferase-mediated dUTP nick end labeling (TUNEL) assay were performed to detect tributyrin-triggered apoptosis. The expressions of PARP, Bcl-2 and Bax were examined by Western blot assay.

RESULTS: Tributyrin could initiate growth inhibition of SGC-7901 cell in a dose- and time-dependent manner. [^{3}H]-TdR uptake by SGC-7901 cells was reduced to 33.6 % after 48 h treatment with 2 mmol·L^{-1} tributyrin, compared with the control (P<0.05). Apoptotic morphology was detected by TUNEL assay. Flow cytometry revealed that tributyrin could induce apoptosis of SGC-7901 cells in dose-dependent manner. After 48 hours incubation with tributyrin at 2 mmol·L^{-1}, the level of Bcl-2 protein was lowered, and the level of Bax protein was increased in SGC-7901, accompanied by PARP cleavage.

CONCLUSION: Tributyrin could inhibit the growth of gastric cancer cells effectively *in vitro* by inhibiting DNA synthesis and inducing apoptosis, which was associated with the down-regulated Bcl-2 expression and the up-regulated Bax expression. Therefore, tributyrin might be a promising chemopreventive and chemotherapeutic agent against human gastric carcinogenesis.

Yan J, Xu YH. Tributyrin inhibits human gastric cancer SGC-7901 cell growth by inducing apoptosis and DNA synthesis arrest. *World J Gastroenterol* 2003; 9(4): 660-664
http://www.wjgnet.com/1007-9327/9/660.htm

INTRODUCTION

Gastric cancer is one of the most common causes of malignancy-related death worldwide. In China, the annual average mortality rate of gastric carcinoma is as high as 16 per 100 thousand[1]. Environmental factors, diet that is high in salts and low in fresh fruit and vegetables are regarded as the risk of stomach cancer[2-6]. Although plenty of advances have been made in the gastrointestinal medicine, the inability to diagnose early and treat effectively of the gastric cancer remains an unsolved problem for clinicians[7-23].

Chemoprevention and chemotherapy including the use of natural products, synthetic compounds or dietary substances are promising ways to stop or reverse the process of carcinogenesis[24]. Large number of minor dietary components has been found to inhibit carcinogenesis at various stages[25]. Tributyrin is a neutral short-chain fatty acid triglyceride existed in some spice plants at low levels in nature[26], and has been approved as a food additive in the United States[27]. Tributyrin is also a pro-drug of natural butyrate synthesized by the bacterial fermentation of various complex carbohydrates unabsorbed in the digestive tract[28] and has been reported bearing anti-tumor effect on neoplastic cells[27, 29, 30] as well as inhibiting proliferation and stimulating differentiation in multiple cancer cell lines. Most importantly, tributyrin is more lipophilic compared with the butyrate and can be metabolized by the intracellular lipases, progressively releasing therapeutically effective butyrate directly in the cell[26, 31]. However, the underlying mechanisms of tributyrin against different types of tumor remain to be understood and so far, the effect of tributyrin on gastric cancer cells has not been reported yet.

In this study, we are trying to evaluate the ability of tributyrin to inhibit cell proliferation, arrest DNA synthesis and induce apoptosis in human gastric cancer SGC-7901 cells and go further into some apoptosis-related events in these processes.

MATERIALS AND METHODS

Cell lines and reagents

Human gastric cancer cell line SGC-7901 was provided by the Cell Bank of Shanghai Institute of Cell Biology, Chinese Academy of Sciences (Shanghai, China). Cells were cultured in Dulbecco's Modified Eagle Medium (DMEM; Life Technologies Inc., Grand Island, NY) supplemented with 10 % fetal calf serum (FCS; Life Technologies Inc., Rockville, MD), penicillin (100 kU·L^{-1}) and streptomycin (0.1 g·L^{-1}) at 37 ℃ in a 5 % CO_2-95 % air atmosphere. Antibodies against Bax, Bcl-2, PARP, and Actin were obtained from Santa Cruz. Other chemicals used in the study were purchased from Sigma Chemical Co (St. Louis, MO, USA). *In situ* cell death detection kit was purchased from Roche Diagnostics. [^{3}H]-TdR was obtained from Amersham Company.

Assessment of cell proliferation

MTT assay was conducted to determine the cell proliferation. SGC-7901 cells were seeded in a 96-well plate (1×10^4·$well^{-1}$) as described previously[32]. In brief, after 24 h incubation cells were treated with tributyrin for three days and untreated cells served as a control. Prior to the determination, 5 μL of the 2.5 g·L^{-1} stock solution of 3-[4,5-dimethylthiaolyl]-2,5-diphenyl-

tetrazolium bromide (MTT) was added to each well. After 4 h incubation, the culture media were discarded followed by addition of 100 μL of DMSO to each well and vibration for 10 min. The absorbance (A) was measured at 492nm with a microplate reader. The percentage of viable cells was calculated as follows:(A of experimental group/A of control group)×100 %.

[^{3}H]-TdR incorporation

The cells were treated with 2 mmol· L^{-1} Tributyrin for the indicated time as described previously[33]. 74kBq of [^{3}H]-TdR were added to cells 3 h before the end of the culture. Cells were then washed with ice-cold PBS and 5 % trichloroacetic acid and lyzed in 0.25 mol· L^{-1} NaOH. The lysates were neutralized with 3 mol· L^{-1} HCl and [^{3}H]-TdR uptake was measured with Beckman LS5000 TD liquid scintillation counter.

Transmission electron microscopy

The cultured cells treated with 2 mmol· L^{-1} tributyrin for 48 h were trypsinized and harvested, respectively. Subsequently the cells were immersed with Epon 821, embedded in capsules and converged at 60 ℃ for 72 h, then they were prepared into ultrathin section (60 nm) and stained with uranyl acetate and lead citrate. Cell ultrastructure was examined by transmission electron microscopy.

Morphological change of apoptosis

The morphological changes of cell apoptosis were determined under fluorescence microscope. Briefly, the experimental cells were pelleted and fixed in 200 ml· L^{-1} ethanol/phosphate-buffered saline (PBS), stained with 5 mg· L^{-1} Hoechst-33258 for 10min at room temperature, then visualized under fluorescence microscope.

TUNEL assay

Apoptosis of SGC-7901 cells was analyzed by using *in situ* cell death detection kit. The method is essentially based on the terminal deoxynucleotidyl transferase-mediated dUTP nick end labeling (TUNEL) technique. In brief, after cells were treated with or without tributyrin for the indicated time, they were fixed overnight in 100 g· L^{-1} formaldehyde, then treated with proteinase K and H_2O_2, labeled with fluorescein dUTP in a humid box at 37 ℃ for 1 h and visualized under fluorescence microscope. The cells without addition of TdT enzyme were used as negative control.

Flow cytometry

After harvested, the experimental cells were washed with PBS twice and fixed with 700 mL· L^{-1} ethanol at 4 ℃ overnight. The fixed cells were washed twice with PBS and stained with 800 μL propidium iodide and 200 μL deoxyribonulcease-free ribonuclease A in PBS. The fluorescence density of propidium iodide-stained nuclei was determined by flow cytometry.

Western blot analysis

The experimental cells were lysed in lysis buffer [25 mmol· L^{-1} HEPES, 1.5 % Triton X-100, 1 % sodium deoxycholate, 0.1 % SDS, 0.5 mol· L^{-1} NaCl, 5 mmol· L^{-1} EDTA, 50 mmol· L^{-1} NaF, 0.1 mmol· L^{-1} sodium vanadate, 1 mmol· L^{-1} phenylmethylsulfonyl fluoride (PMSF), and 0.1 g· L^{-1} leupeptin (pH7.8)] at 4 ℃ with sonication. The lysates were centrifuged at 15 000 g for 15 min at 4 ℃ and the proteins were separated on SDS-PAGE, transferred to nitrocellulose filter and incubated with antibodies against Bcl-2, Bax, PARP, and Actin, respectively. Then the membrane was incubated with peroxidase-conjugated secondary antibodies. Detection was performed with enhanced chemiluminescence reagent.

Statistical analysis

Student' s *t* test was used to assess statistical significance of differences. If $P<0.05$, the difference was considered statistically significant.

RESULTS

Inhibition of human gastric cancer SGC-7901 cell proliferation by tributyrin

The experimental SGC-7901 cells were treated with various concentrations of tributyrin for 1-3 days and the cell viability was determined as described above by MTT assay. As shown in Figure 1, tributyrin could inhibit the growth of gastric cancer cells in a dose- and time-dependent manner. Cell growth was suppressed by 24.9 %, 36.6 %, 50.3 %, 60.6 %, 84.1 % and 91.3 % after 72 h treatment with tributyrin at 0.5, 1, 2, 5, 10 and 50 mmol· L^{-1}, respectively. It was noted that tributyrin at 50 mmol· L^{-1} had an inhibitory effect of more than 90 % on the tumor cell growth after 48-72 h treatment. The IC_{50} value of tributyrin for SGC-7901 cell at 72 h was 2 mmol· L^{-1}.

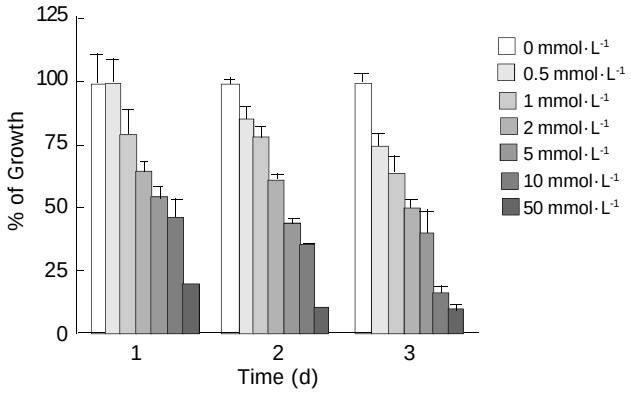

Figure 1 Effect of tributyrin on cell growth in SGC-7901 cells. The cells were treated with various concentrations of tributyrin for 24, 48 and 72 h. The antiproliferative effect was measured by MTT assay. Results were expressed as the means ±SD from three independent determinations.

DNA synthesis arrest by tributyrin

Since the IC_{50} value of tributyrin was 2 mmol· L^{-1}, the concentration was used for the following assay. Tributyrin inhibited the [^{3}H]-TdR uptake by SGC-7901 cells in a time-dependent manner. Compared with the control, the DNA synthesis of tumor cells was significantly reduced by 66.4 %, 92.2 % and 90.1 % after 48 h, 72 h and 96 h treatment with tributyrin, respectively, ($P<0.05$, Figure 2).

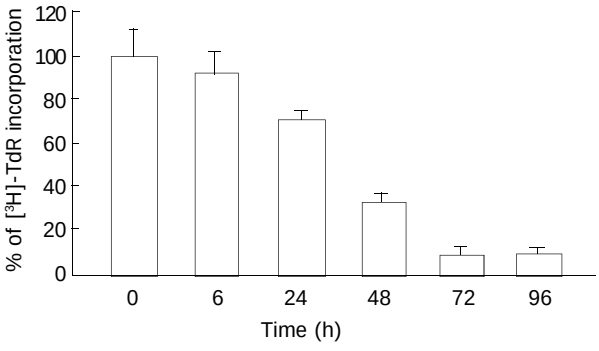

Figure 2 Inhibitory effect of tributyrin on DNA synthesis incorporated with ^{3}H-TdR. With the concentration of 2 mmol·L^{-1}, tributyrin inhibited the [^{3}H]-TdR uptake by SGC-7901 cells in a time-dependent manner. Results were expressed as means ±SD from three independent determinations.

Tributyrin induction of apoptosis

Morphological changes After 48 h of exposure to tributyrin, gastric cancer cells began to show morphologic features of apoptosis, which manifested as cell shrinkage, chromatin condensation and nuclear pyknosis, *etc* by transmission electron microscopy (Figure 3). The tributyrin-treated SGC-7901 cells labeled with Hoechst-33258 also showed apoptotic features including nuclear shrinkage or fragmentation by fluorescence microscopy (Figure 4).

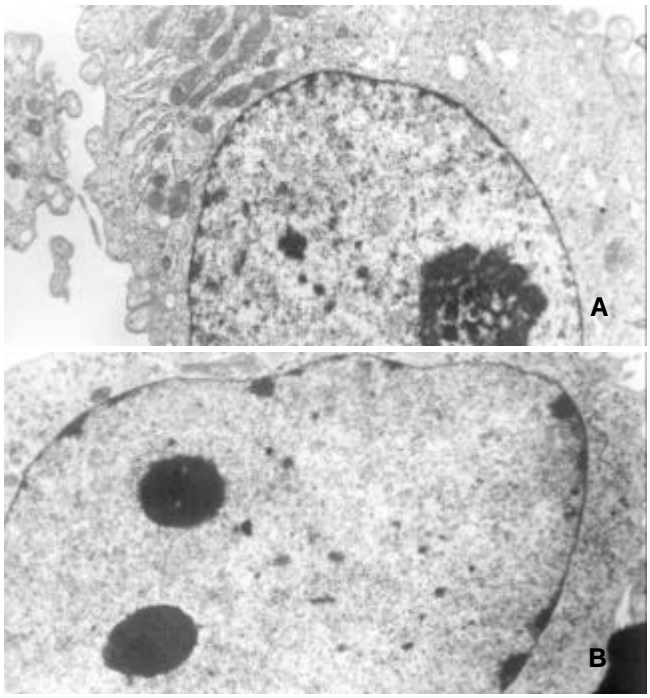

Figure 3 Ultrastructural changes of the gastric cancer cells treated with 2 mmol·L^{-1} tributyrin for 48 h. (A) The control SGC-7901 cell; (B) the experimental cell showing early changes of apoptosis in which nuclear chromatin condensation and cell shrinkage were observed (B).

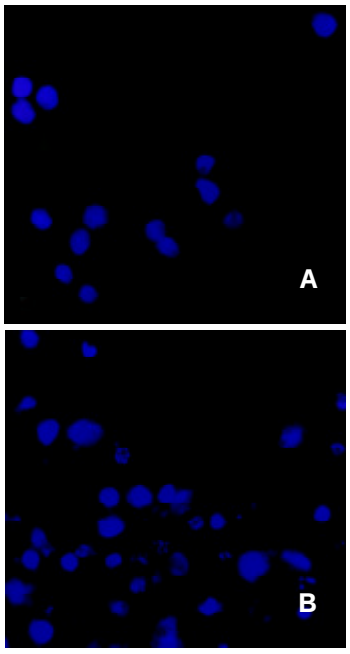

Figure 4 Tributyrin-induced apoptosis in SGC-7901 cells stained with Hoechst-33258. A: the control SGC-7901 cells; B: the experimental cells showing nuclear shrinkage or fragmentation.

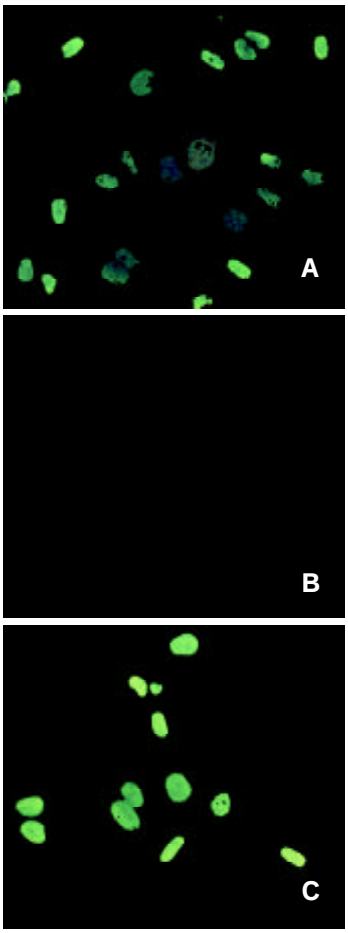

Figure 5 Tributyrin-induced apoptosis by TUNEL assay. A: the positive control cells; B: the negative control cells; C: the experimental cells treated with tributyrin at 2 mmol·L^{-1} for 2 days.

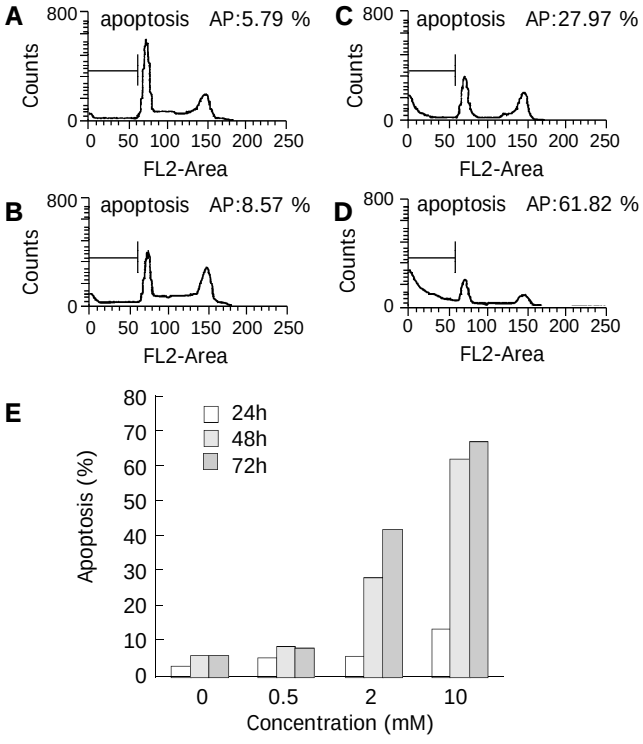

Figure 6 Tributyrin-induced apoptosis in SGC-7901 cells by flow cytometry. (A) The control cells, (B)-(D) The experimental cells treated with tributyrin at 0.5, 2 and 10 mmol·L^{-1} respectively for 48 h. (E) Apoptosis rates in SGC-7901 cells treated with 0.5, 2 and 10 mmol·L^{-1} or without tributyrin for the indicated times.

TUNEL assay

The TUNEL assay revealed that tributyrin could induce the apoptosis of SGC-7901 cells, while the negative control did not show any signs of fluorescence signals (Figure 5).

Flow cytometry

Cell cycle analysis in SGC-7901 cells treated with tributyrin revealed that a sub-G1 apoptotic peak appeared (Figure 6). The apoptosis rate in tributyrin-treated tumor cells was increased in a time- and dose-dependent manner. When treated with 2 mmol· L^{-1} tributyrin for 72 h, the experimental SGC-7901 cells showed a 41.5 % of apoptosis.

Differential expression of Bcl-2 and Bax protein and PARP cleavage in tributyrin-treated cells

After treated with indicated concentrations of tributyrin for 48 h, the expression of Bcl-2 protein was markedly decreased while that of Bax displayed an increased trend. PARP cleavage in the experimental cells appeared at 0.5 mmol· L^{-1} and was obvious at 2 mmol· L^{-1} of tributyrin treatment for 48 h (Figure 7).

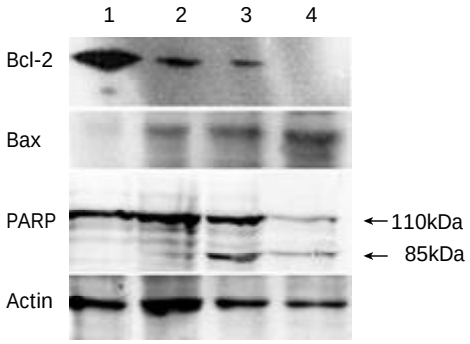

Figure 7 The expression of Bcl-2, Bax protein and PARP cleavage in tributyrin-treated SGC-7901 cells. (1) The control cells; (2)-(4) The experimental cells treated with tributyrin for 48 h at 0.5, 2 and 10 mmol·L^{-1}, respectively.

DISCUSSION

It has been reported tributyrin, a substance that naturally exists in some foods, was a potent agent against various malignancies, including colon and pancreas carcinomas, and that 1 mmol of tributyrin could result in an inhibitory effect comparable with 3 mmol of butyrate[32,33]. The high lipophilic property and the long duration in blood made tributyrin a promising anti-tumor agent. However, the effects of tributyrin on gastric cancer cells have not been reported.

The present study demonstrated that tributyrin could inhibit the growth of human gastric cancer SGC-7901 cells in a dose- and time-dependent manner, which might be caused by DNA synthesis arrest as shown in our experiment via preventing SGC-7901 cells from progressing into S-phase and ultimately blocking the cell proliferation. The inhibition of DNA synthesis was more than 90 % when SGC-7901 cells were treated with tributyrin at 2 mmol· L^{-1} for 48-72 h.

Besides DNA synthesis arrest, the induced cell death was another major reason for the cell growth inhibition. Apoptosis, also called programmed cell death, is a natural process of cell suicide which plays a critical role in the development and homeostasis of metazoans[34,35]. Our results that tributyrin could induce apoptosis in SGC-7901 cells revealed by the typical apoptotic alterations, including the morphological changes by electron microscopy, positive Hoechst-33258 staining, DNA fragmentation by TUNEL assay and apoptotic sub-G_1 peak by flow cytometry.

Apoptosis is a complex process regulated by a variety of factors[36-39]. The members of the Bcl-2 family are important regulators in the apoptotic pathway with individual members that can suppress (eg Bcl-2, Bcl-xl) or promote (eg Bax, Bad) apoptosis. As an oncogene-derived protein, Bcl-2 confers a negative control in the pathway of cellular suicide machinery, whereas Bax, a Bcl-2-homologous protein, promotes cell death by competing with Bcl-2. Introduction of Bcl-2 into most eukaryotic cells has been reported to be able to protect the recipient cell from a wide variety of stress applications that lead to cell death[40, 41]. In the present study, we observed that the expression of Bcl-2 was reduced and that of Bax was up-regulated, indicating the reduced ratio of Bcl-2/Bax might serve as a mechanism of SGC-7901 cells apoptosis induced by tributyrin. Its subsequent event might be the release of cytochrome c and caspase-3 activation. On the other hand, the cleavage of PARP, one of caspase-3 downstream target[42], was also observed in the experimental SGC-7901 cells with the increase of tributyrin concentrations. However, PARP could also be cleaved through a parallel caspase-3 independent pathway. Therefore, the exact mechanism underlying the apoptosis of SGC-7901 cells needed to be further investigated.

In summary, we have demonstrated that tributyrin, an oral analogue of butyrate, could induce DNA synthesis arrest and apoptosis in human gastric cancer SGC-7901 cells in vitro. The effect was dose- and time-dependent. The apoptotic mechanism of the SGC-7901 cells induced by tributyrin was at least via the reduction of Bcl-2/Bax ratio. These data suggested that further evaluation of tributyrin, a promising anti-tumor agent, for the treatment gastric cancer was warranted.

ACKNOWLEDGEMENT

We thank Dr. Rugang Zhang from Institute of Biochemistry and Cell Biology, Shanghai Institutes for Biological Sciences, Chinese Academy of Sciences, for his helpful suggestion.

REFERENCES

1 **Xue FB**, Xu YY, Wan Y, Pan BR, Ren J, Fan DM. Association of *H. pylori* Infection with gastric carcinoma: a Meta analysis. *World J Gastroenterol* 2001; **7**: 801-804

2 **Sugie S**, Okamoto K, Watanabe T, Tanaka T, Mori H. Suppressive effect of irsogladine maleate on N-methyl-N-nitro-N-nitrosoguanidine (MNNG)-initiated and glyoxal-promoted gastric carcinogenesis in rats. *Toxicology* 2001; **166**: 53-61

3 **Palli D**, Russo A, Saieva C, Salvini S, Amorosi A, Decarli A. Dietary and familial determinants of 10-year survival among patients with gastric carcinoma. *Cancer 2*000; **89**: 1205-1213

4 **Mathew A**, Gangadharan P, Varghese C, Nair MK. Diet and stomach cancer:a case-control study in South India. *Eur J Cancer Prev* 2000; **9**: 89-97

5 **Palli D**. Epidemiology of gastric cancer: an evaluation of available evidence. *J Gastroenterol* 2000; **35**(Suppl 12): 84-89

6 **Palli D**, Russo A, Ottini L, Masala G, Saieva C, Amorosi A, Cama A, D'Amico C, Falchetti M, Palmirotta R, Decarli A, Costantini RM, Fraumeni JF Jr. Red meat, family history, and increased risk of gastric cancer with microsatellite instability. *Cancer Res* 2001; **61**: 5415-5419

7 **Skoropad V**, Berdov B, Zagrebin V. Concentrated preoperative radiotherapy for resectable gastric cancer: 20-years follow-up of a randomized trial. *J Surg Oncol* 2002; **80**: 72-78

8 **Yao XX**, Yin L, Sun ZC. The expression of hTERT mRNA and cellular immunity in gastric cancer and precancerosis. *World J Gastroenterol* 2002; **8**: 586-590

9 **Fahey JW**, Haristoy X, Dolan PM, Kensler TW, Scholtus I, Stephenson KK, Talalay P, Lozniewski A. Sulforaphane inhibits extracellular, intracellular, and antibiotic-resistant strains of *Helicobacter pylori* and prevents benzo[a]pyrene-induced stomach tumors. *Proc Natl Acad Sci U S A* 2002; **99**: 7610-7615

10 **Martin RC 2nd**, Jaques DP, Brennan MF, Karpeh M. Extended

local resection for advanced gastric cancer: increased survival versus increased morbidity. *Ann Surg* 2002; **236**: 159-165
11 **Yu WL**, Huang ZH. Progress in studies on gene therapy for gastric cancer. *Shijie Huaren Xiaohua Zazhi* 1999; **7**: 887-889
12 **Chen GY**, Wang DR. The expression and clinical significance of CD44v in human gastric cancers. *World J Gastroenterol* 2000; **6**: 125-127
13 **Wang RQ**, Fang DC, Liu WW. MUC2 gene expression in gastric cancer and preneoplastic lesion tissues. *Shijie Huaren Xiaohua Zazhi* 2000; **8**: 285-288
14 **Guo YQ**, Zhu ZH, Li JF. Flow cytometric analysis of apoptosis and proliferation in gastric cancer and precancerous lesion. *Shijie Huaren Xiaohua Zazhi* 2000; **8**: 983-987
15 **Chen SY**, Wang JY, Ji Y, Zhang XD, Zhu CW. Effects of *Helicobacter pylori* and protein kinase C on gene mutation in gastric cancer and precancerous lesions. *Shijie Huaren Xiaohua Zazhi* 2001; **9**: 302-307
16 **Xu AG**, Li SG, Liu JH, Gan AH. Function of apoptosis and expression of the proteins Bcl-2, p53 and C-myc in the development of gastric cancer. *World J Gastroenterol* 2001; **7**: 403-406
17 **Zhou HP**, Wang X, Zhang NZ. Early apoptosis in intestinal and diffuse gastric carcinomas. *World J Gastroenterol* 2000; **6**: 898-901
18 **Zhang FX**, Zhang XY, Fan DM, Deng ZY, Yan Y, Wu HP, Fan JJ. Antisense telomerase RNA induced human gastric cancer cell apoptosis. *World J Gastroenterol* 2000; **6**: 430-432
19 **Gu QL**, Li NL, Zhu ZG, Yin HR, Lin YZ. A study on arsenic trioxide inducing *in vitro* apoptosis of gastric cancer cell lines. *World J Gastroenterol* 2000; **6**: 435-437
20 **Wu K**, Shan YJ, Zhao Y, Yu JW, Liu BH. Inhibitory effects of RRR-alpha-tocopheryl succinate on benzo(a)pyrene (B(a)P)a 2induced forestomach carcinogenesis in female mice. *World J Gastroenterol* 2001; **7**: 60-65
21 **Jung YD**, Mansfield PF, Akagi M, Takeda A, Liu W, Bucana CD, Hicklin DJ, Ellis LM. Effects of combination anti-vascular endothelial growth factor receptor and anti-epidermal growth factor receptor therapies on the growth of gastric cancer in a nude mouse model. *Eur J Cancer* 2002; **38**: 1133-1140
22 **Cui RT**, Cai G, Yin ZB, Cheng Y, Yang QH, Tian T. Transretinoic acid inhibits rats gastric epithelial dysplasia induced by N-methyl-N-nitro-N-nitrosoguanidine: influences on cell apoptosis and expression of its regulatory genes. *World J Gastroenterol* 2001; **7**: 394-398
23 **Gonzalez CA,** Sala N, Capella G. Genetic susceptibility and gastric cancer risk. *Int J Cancer* 2002; **100**: 249-260
24 **Morse MA**, Stoner GD. Cancer chemoprevention: Principles and prospects. *Carcinogenesis* 1993; **14**: 1737-1746
25 **Wattenberg LW**. Inhibition of carcinogenesis by minor dietary constituents. *Cancer Res* 1992; **52**(Suppl 7): S2024-S2029
26 **Bach A**, Metais P. Fats with short and medium chains. Physiological, biochemical, nutritional and therapeutic aspects. *Ann Nutr Alim* 1970; **24**: 75-144
27 **Heerdt BG**, Houston MA, Anthony GM, Augenlicht LH. Initiation of growth arrest and apoptosis of MCF-7 mammary carcinoma cells by tributyrin, a triglyceride analogue of the short-chain fatty acid butyrate, is associated with mitochondrial activity. *Cancer Res* 1999; **59**: 1584-1591
28 **Scheppach W**. Effects of short chain fatty acids on gut morphology and function. *Gut* 1994; **35**: S35-38
29 **Schroder C**, Eckert K, Maurer HR. Tributyrin induces growth inhibitory and differentiating effects on HT-29 colon cancer cells *in vitro*. *Int J Oncol* 1998; **13**: 1335-1340
30 **Maier S**, Reich E, Martin R, Bachem M, Altug V, Hautmann RE, Gschwend JE. Tributyrin induces differentiation, growth arrest and apoptosis in androgen-sensitive and androgen-resistant human prostate cancer cell lines. *Int J Cancer* 2000; **88**: 245-251
31 **Egorin MJ**, Yuan ZM, Sentz DL, Plaisance K, Eiseman JL. Plasma pharmacokinetics of butyrate after intravenous administration of sodium butyrate or oral administration of tributyrin or sodium butyrate to mice and rats. *Cancer Chemother Pharmacol* 1999; **43**: 445-453
32 **Ying H,** Yu Y, Xu Y. Cloning and characterization of F-LANa, upregulated in human liver cancer. *Biochem Biophys Res Comm* 2001; **286**: 394-400
33 **Clarke KO**, Feinman R, Harrison LE. Tributyrin, an oral butyrate analogue, induces apoptosis through the activation of caspase-3. *Cancer Lett* 2001; **171**: 57-65
34 **Green DR**, Reed JC. Mitochondria and apoptosis. *Science* 1998; **281**: 1309-1312
35 **Ashkenazi A**, Dixit VM. Apoptosis control by death and decoy receptors. *Curr Opin Cell Biol* 1999; **11**: 255-260
36 **Adams JM**, Cory S. The Bcl-2 protein family: arbiters of cell survival. *Science* 1998; **281**: 1322-1326
37 **Li HL**, Chen DD, Li XH, Zhang HW, Lu JH, Ren XD, Wang CC. JTE-522-induced apoptosis in human gastric adenocarcinoma [correction of adenocarinoma] cell line AGS cells by caspase activation accompanying cytochrome C release, membrane translocation of Bax and loss of mitochondrial membrane potential. *World J Gastroenterol* 2002; **8**: 217-223
38 **Fan XQ**, Guo YJ. Apoptosis in oncology. *Cell Res* 2001; **11**: 1-7
39 **Yuan RW**, Ding Q, Jiang HY, Qin XF, Zou SQ, Xia SS. Bcl-2, P53 protein expression and apoptosis in pancreatic cancer. *Shijie Huaren Xiaohua Zazhi* 1999; **7**: 851-854
40 **Basu A**, Haldar S. The relationship between Bcl2, Bax and p53: consequences for cell cycle progression and cell death. *Mol Hum Reprod* 1998; **4**: 1099-1109
41 **Chang YC**, Xu YH. Expression of Bcl-2 inhibited Fas-mediated apoptosis in human hepatocellular carcinoma BEL-7404 cells. *Cell Res* 2000; **10**: 233-242
42 **Tewari M**, Quan LT, O'Rourke K, Desnoyers S, Zeng Z, Beidler DR, Poirier GG, Salvesen GS, Dixit VM. Yama/CPP32b, a mammalian homolog of CED-3, is a CrmA-inhibitable protease that cleaves the death substrate poly(ADP-ribose) polymerase. *Cell* 1995; **81**: 801-809

Edited by Zhu L

P.O.Box 2345, Beijing 100023, China
Fax: +86-10-85381893
E-mail: wjg@wjgnet.com www.wjgnet.com

World J Gastroenterol 2003;9(4):665-669
World Journal of Gastroenterology
 ISSN 1007-9327

• GASTRIC CANCER •

Expression of estrogen receptor and estrogen receptor messenger RNA in gastric carcinoma tissues

Xin-Han Zhao, Shan-Zhi Gu, Shan-Xi Liu, Bo-Rong Pan

Xin-Han Zhao, Shan-Zhi Gu, Shan-Xi Liu, Department of Medical Oncology, First Hospital of Xi' an Jiaotong University, Xi' an 710061, Shaanxi Province, China
Bo-Rong Pan, Department of Oncology, Xijing Hospital, Fourth Military Medical University, Xi' an 710032, Shaanxi Province, China
Supported by the First Hospital Scientific Foundation of Xi'an Jiaotong University, No.95012
Correspondence to: Dr. Xin-Han Zhao, Department of Medical Oncology, First Hospital of Xi' an Jiaotong University, Xi' an 710061, Shaanxi Province, China. zhxinhan@pub.xaonline.com
Telephone: +86-29-5324136 **Fax:** +86-29-5275472
Received: 2002-12-22 **Accepted:** 2003-01-16

Abstract

AIM: To study estrogen receptor (ER) and estrogen receptor messenger RNA (ERmRNA) expression in gastric carcinoma tissues and to investigate their association with the pathologic types of gastric carcinoma.

METHODS: The expression of ER and ERmRNA in gastric carcinoma tissues (15 males and 15 females, 42-70 years old) was detected by immunohistochemistry and *in situ* hybridization, respectively.

RESULTS: The positive rate of ER (immunohistochemistry) was 33.3 % in males and 46.7 % in females. In Borrmann IV gastric carcinoma ER positive rate was greater than that in other pathologic types, and in poorly differentiated adenocarcinoma and signet ring cell carcinoma the positive rates were greater than those in other histological types of both males and females ($P<0.05$). The ER was more highly expressed in diffused gastric carcinoma than in non-diffused gastric carcinoma ($P<0.05$). The ER positive rate was also related to regional lymph nodes metastases ($P<0.05$), and was significantly higher in females above 55 years old, and higher in males under 55 years old ($P<0.05$). The ERmRNA (*in situ* hybridization) positive rate was 73.3 % in males and 86.7 % in females. The ERmRNA positive rates were almost the same in Borrmann I, II, III and IV gastric carcinoma ($P>0.05$). ERmRNA was expressed in all tubular adenocarcinoma, poorly differentiated adenocarcinoma and signet ring cell carcinoma ($P<0.05$). The ERmRNA positive rate was related to both regional lymph nodes metastases and gastric carcinoma growth patterns, and was higher in both sexes above 55 years old but without statistical significance ($P>0.05$). The positive rate of ERmRNA expression by *in situ* hybridization was higher than that of ER expression by immunohistochemistry ($P<0.05$).

CONCLUSION: ERmRNA expression is related to the pathological behaviors of gastric carcinoma, which might help to predict the prognosis and predict the effectiveness of endocrine therapy for gastric carcinoma.

Zhao XH, Gu SZ, Liu SX, Pan BR. Expression of estrogen receptor and estrogen receptor messenger RNA in gastric carcinoma tissues. *World J Gastroenterol* 2003; 9(4): 665-669
http://www.wjgnet.com/1007-9327/9/665.htm

INTRODUCTION

Gastric carcinoma is the most common cause of cancer mortality in China[1-6] and is responsible for approximately 160 000 deaths annually. During the last 10 years, there has been no improvement in survival after the diagnosis of gastric cancer with an overall 5-year survival rate of 20 %. Surgery remains the primary treatment of choice. However, the disease is often advanced at first presentation, and only 30-40 % of patients undergoing surgery will have a curative resection. The failure of surgery on the disease has led to the use of chemotherapy and radiotherapy as adjuvant or palliative means, but their value is limited because of toxicity and lack of efficacy[7-12]. Since Jensen discovered the existence of estrogen receptor (ER) in the cytoplasm of human mammary cancer cells in 1960, many researchers have also discovered the presence of ER in some gastric cancer cells, suggesting that these cells can be controlled and regulated by sex hormones. From this we can infer that some cases of gastric cancer are hormone-dependent tumor, and this has stimulated the use of the anti-estrogen compound in its treatment. In this study, the expression of ER, ERmRNA in gastric cancer tissues was examined by immunohistochemistry and *in situ* hybridization, respectively, and the association of their expression and clinical significance at molecular pathological level was also investigated.

MATERIALS AND METHODS

Specimens

Thirty specimens of gastric cancer tissue were collected from The General Surgical Department and The Tumor Surgical Department of the First hospital of Xi' an Jiaotong University. All the cases were pathologically proved to be gastric carcinoma. Of the patients, 15 were females and 15 males. Their age ranged from 42 to 70 and the average age was 58.4. Pathologically 2 cases were papillary adenocarcinoma, 12 tubular adenocarcinoma, 13 poorly differentiated adenocarcinoma, and 3 signet ring cell carcinoma. According to Borrmann classfication, 6 cases were type I, 8 type II, 8 type III and another 8 type IV.

ERmRNA in situ Hybridization

The slides were treated with 3-amino propyltri-ethoxy saline (APES) and with polylysine. The slides were deparaffinized, hydrated and treated with 30 mL/L H_2O_2 at room temperature for 10 minutes to eliminate the endogenous peroxidase. The slides were incubated with freshly diluted protease K (1:1 000 with 0.01 mol/L Tris buffer saline (TBS)) at 37 ℃ for 5 to 15 minutes. After being washed with distilled water three times, the slides were treated with 2 g/L glycine for 5 minutes, washed with PBS for 5 minutes, fixed with 40 g/L polymethanol for 30 minutes, and washed again with PBS for 5 minutes, dehydrated with gradient alcohol, and then washed with DEPC, treated with digoxin-labeled probe in 90-100 ℃ water for 5 to 10 minutes, and then taken out and immediately put in shattered ice for 5 minutes. After the slides became dry in the air, 10 μL *in situ* hybridization solution containing digoxin-labeled probe was added onto each slide,

and the hybridization was conducted in a humidified box for 20 hours. The slides were then washed twice with 2×SSC at 20-30 ℃ for 5 minutes and with 1×SSC at 37 ℃ for 10miutes, incubated with mouse anti-digoxin at 20-37 ℃ for 30 minutes and washed with 0.5 mol/L PBS three times, each for 2 minutes. The slides were then incubated with anti-mouse biotin IgG at 20-37 ℃ for 20 minutes, washed with 0.5 mol/L PBS three times, each for 2 minutes and again incubated with SABC at 20-37 ℃ for 20 minutes, washed with 0.5 mol/L PBS four times, each for 5 minutes. The color reaction was developed with the addition of DAB, and the slides were counter-stained with hematoxylin and sealed with xylene.

Negative control: No estrogen receptor probe in the hybridization solution. The slices showed color directly without any solution added. Hybridization solution was replaced by reserve hybridization solution containing no probe.

Positive control: The specimens from 3 women with mammary cancer and 3 with ovarian cancer, all under 45 years old, were collected and treated in the same way as in the gastric cancer specimens.

ER Immunohistochemistry

Consecutive 5 μm thick sections were stained with HE and by immunohistochemistry separately. The deparaffinized sections were washed with PBS three times, soaked in 30 mL/L hydrogen dioxide solution for 10 minutes to eliminate the endogenous peroxidase, washed with PBS three times, digested with 10 g/L trypsin for 15 minutes (37 ℃), washed with PBS three times, heated to 95 ℃ in pH 6.0 citric acid buffer solution for 10 minutes before cooled down to room temperature, and then washed three times with PBS, and then blocked with serum (45 ℃). The sections were then incubated with the first antibody (1:50) over night, washed three times with PBS, incubated with biotin-labeled secondary antibody and then washed with PBS. The sections were finally incubated with streptavidin biotin peroxidase complex, the color reaction was developed with the addition of DAB, and the sections were counter-stained with hematoxylin and sealed transparently.

Positive cells from *in situ* hybridization appeared yellow and the positive stain was mainly located in the nuclei and cytoplasm around the nuclei. Immunohistochemically positive cells appeared brown yellow and the positive stain was located in the cytoplasm. The average positive rate in every case was calculated in 5 high-power fields. When 10 % or more of the cancer cells were stained positive in a labeled slice, it was defined as ER or ERmRNA positive.

Statistical analysis

All data were analyzed with SPSS 8.0 statistical software (including the accurate four square table probability method and similar χ^2 test) and $P<0.05$ was considered to have statistical significance.

RESULTS

Immunohistochemically stained positive cells looked brown yellow in cytoplasm. The distribution of ER positive cells and the intensity of positive reaction were uneven (Figure 1). The smooth muscle cells and the lymphocytes in the interstice and the mucosa membrane beside the cancer tissue appeared negative. The positively expressed ERmRNA were mainly located in cytoplasm and nuclei of cancer cells, next to the interstice (Figure 2). The number of positive cells was different in different fields. It was greater in some fields, with 34 positive cells in a high power field, but in other fields, the positive cells were scarce or absent. There were weakly hybridized positive signals in interstitial smooth muscle cells and lymphocytes. The tissue beside the cancer appeared negative.

ER positive gastric cancer tissues both in men and women were more common in Borrmann type IV, histologically it was more common in poorly differentiated adenocarcinoma and signet ring cell carcinoma ($P<0.05$). ERmRNA positive cells were found in Borrmann type I, II, III and IV ($P>0.05$). ERmRNA expression was also found in tubular adenocarcinoma, poorly differentiated adenocarcinoma and signet ring cells ($P<0.05$, Table 1).

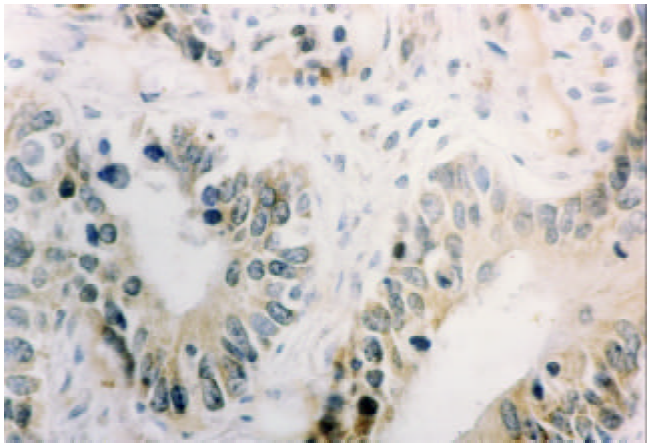

Figure 1 ER positive expression in gastric carcinoma tissue SABC×400.

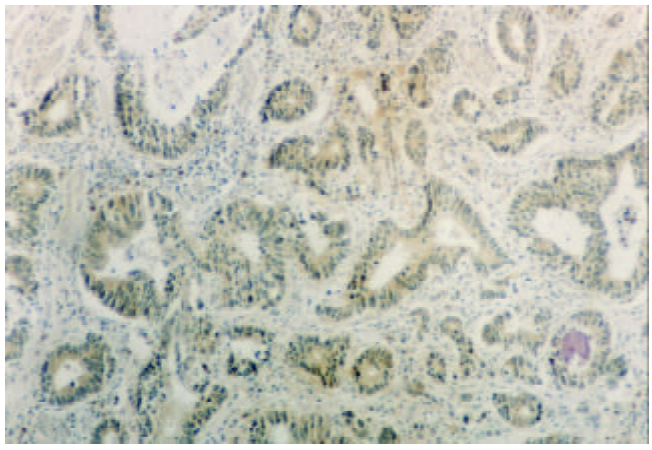

Figure 2 ER mRNA positive expression in gastric carcinoma tissue *in situ* hybridization ×100.

ER expression had a high positive rate in females above 55 years old and in males under 55 years old ($P<0.05$). And ERmRNA expression had a high positive rate in both males and females above 55 years old ($P>0.05$, Table 1).

Diffusely growing gastric cancer had a high ER positive rate ($P<0.05$). Both the diffusely and non-diffusely growing gastric cancers had a high positive expression rate of ERmRNA ($P>0.05$, Table 1). The increase of ER positive rate is associated with the increase of the involved regional lymph nodes including the upper and lower parts of pylorus, the greater and lesser curvatures of the stomach and the lymph nodes on both sides of cardia ($P<0.05$). There seemed to be a tendency that the increase of ERmRNA positive rate is associated with the increase of the number of the involved lymph nodes ($P>0.05$, Table 1).

To compare the immunohistochemistry results with *in situ* hybridization results, ER positive rate was 40.0 % (M/F: 33.3 % *vs* 46.7 %), and ERmRNA positive rate was 80.0 % (M/F: 73.3 % *vs* 86.7 %, $P<0.05$, Table 1).

Table 1 Relationship between ER, ERmRNA expression and pathology in gastric cancer

Pathology	Male					Female					Total				
	n	ER(+)	%	ERmRNA(+)	%	*n*	ER(+)	%	ERmRNA(+)	%	*n*	ER(+)	%	ERmRNA(+)	%
Borrmann I	3	1	33.3	1	33.3	3	0	0	2	66.7	6	1	16.7	3	50.0
II	4	1	25.0	3	75.0	4	2	50.0	3	75.0	8	3	37.5	6	75.0
III	4	1	25.0	3	75.0	4	2	50.0	4	100.0	8	3	37.5	7	87.5
IV	4	2	50.0	4	100.0	4	3	75.0	4	100.0	8	5	62.5	8	100.0
Papillary	1	0	0	0	0	1	0	0	0	0	2	0	0	0	0
Tubular	6	0	0	4	66.7	6	1	16.7	5	88.3	12	1	8.3	10	83.3
Poorly differentiated	7	4	57.1	6	85.7	6	4	66.7	6	100.0	13	8	61.5	11	84.6
Signet ring cell	1	1	100.0	1	100.0	2	2	100.0	2	100.0	3	3	100.0	3	100.0
Nondiffused	9	2	22.2	6	66.7	5	1	20.0	4	80.0	14	3	21.4	10	71.4
Diffused	6	3	50.0	5	83.3	10	6	60.0	9	90.0	16	9	56.3	14	87.5
Lymph node 0	3	0	0	1	33.3	4	0	0	3	75.0	7	0	0	4	57.1
Involvemen ≤3	4	1	25.0	3	75.0	5	3	60.0	4	80.0	9	4	44.4	7	77.8
4~6	6	2	33.3	5	83.3	5	3	60.0	5	100.0	11	5	45.5	10	90.9
>6	2	2	100.0	2	100.0	1	1	100.0	1	100.0	3	3	100.0	3	100.0
Age ≤55	6	3	50.0	4	66.7	9	3	33.3	7	77.8	15	6	40.0	11	73.3
>55	9	2	22.2	7	77.8	6	4	66.7	6	100.0	15	6	40.0	13	86.7
Total	15	5	33.3	11	73.3	15	7	46.7	13	86.7	30	12	40.0	24	80.0

DISCUSSION

In 1960 Jensen reported for the first time that after injecting a physiological dose of ^{3}H-E_2 into the hypoderm of a young mouse, the amount of ^{3}H-E_2 found in the tissues of uterus, vagina and other parts was far greater than that found in blood plasma. This proved for the first time that ER protein was present in the tissues of uterus and vagina. When estrogen enters target cells, it first combines with its receptor in cytoplasm, then forms a compound of receptor protein-estradiol which then enters cell nucleus, binds to the chromatin and affects the transcription of DNA. To sexual and non-sexual target organs, estrogen may be a hormone promoting splitting. There are proved documents that gastric cancer cells have sex hormone receptors and may be controlled and regulated by sex hormones, suggesting that gastric cancer in some cases is hormone-dependent tumor, but the molecular mechanisms underlying carcinogenesis are still largely unknown[13-17]. A lot of documents have proved that molecular biology plays an important role in the development and metastasis of some cancers, such as endometrial adenocarcinoma[18-20], lung cancer[21], breast cancer[22-37], apocrine carcinoma[38], leukemia[39] and prostate cancer[40,41]. But there are very few studies on the ERmRNA expression in gastric cancer tissues.

With ER examination on the specimens of ten primary gastric cancer patients (6 men and 4 women), Tokunaga discovered that 2 cases were ER(+) and the patients were women with histological undifferentiated cancer. Yanzuoshaner used the PAP method to analyze 140 specimens of primary gastric cancer after operation. The results showed that 23 cases were ER(+) (16.4 %), 6 cases were ER(±) (4.3 %), 111 cases were ER(-) (79.3 %). Recently, a new estrogen receptor, called estrogen receptor beta, has been found to be expressed in various tissues including normal gastrointestinal tract, the effect of estrogen in stomach cancer, as well as in normal stomach, might be mediated by ER beta, and the role of ER beta might differ by the subtype of stomach adenocarcinoma, specifically signet ring cell adenocarcinomas. But the conclusions needed more evidence to support[13]. Takano *et al* reported the expression of estrogen receptor-alpha and ER-beta mRNAs in human gastric cancers, and the results showed that the expression of estrogen receptor-alpha and ER-beta mRNAs were changed in 20 cases (49 %) and unchanged in 21cases (51 %). The incidences of lymph node metastasis and liver metastasis were significantly higher in changed cases than in unchanged cases[14]. One fourth gastric cancers were ER positive compared with breast cancers, and gastric cancer nuclear receptors were also smaller than that of breast cancers in number[22,23]. Of 95 cases of male patients with gastric cancers, 12 were ER(+) (12.6 %), of 45 cases of female patients 10 were ER(+) (22.2 %), 11.5 % of men under 50 years old were ER(+) and 14.5 % of men above 50 years old were ER (+). There was no marked difference between them, most of the ER(+) cases were Borrmann II, and most cases of the histological type were undifferentiated[15-16].

Our results of the present study showed that ER positive rate was 40.0 % and ER-mRNA positive rate was 80.0 % in gastric cancers. ER(+) was related to lymph node metastasis and gastric cancer growth patterns. Furthermore, we also discovered that the positive rates of gastric cancer ER, ERmRNA were higher in female than in male. Thus we can conclude that female gastric cancer patients are more easily affected by estrogen than male gastric cancer patients. Our results are similar to the results reported by other scholars.

Many foreign researchers think that compared with other methods in examining ER protein, the molecular hybridizations in examining ERmRNA has a higher sensitivity[13-17]. By using Northern hybridization method Hankin found that the ERmRNA positive rate of breast cancer was 87.0 %. But by using the ^{3}H-estradiol method to examine ER protein the positive rate was only 46.0 %. The two methods showed a marked difference. In our study, the immunohistochemical examination showed that the high expression of ER protein was most common in poorly differentiated adenocarcinoma and signet ring cell carcinoma. *In situ* hybridization showed

that ERmRNA had a high positive expression rate, which was also found in tubular adenocarcinoma and poorly differentiated adenocarcinoma of histological hype. What is more noteworthy is that in 13 cases of ER(-) gastric cancer tissues *in situ* hybridization examination showed that ERmRNA was (+). The reason may be that *in situ* hybridization probe could hybridize with mRNA which directs the synthesis of protein of irregular quality lacking function. The protein may lack the epitope that can be identified by the ER monoclonal antibody, and there may be defects present in ER protein synthesis after transcription. ERmRNA positive signal was also present in interstitial smooth muscle cells and lymphocytes, which suggests that estrogen can regulate not only epithelial cells but also interstitial cells.

We speculate that ERmRNA expression has greater value than ER protein expression in clinical application because of the high sensitivity of *in situ* hybridization and the strong ERmRNA expression in gastric cancer, which can be used to judge the prognosis of tumor and predict the effectiveness of endocrine therapy for gastric cancer.

REFERENCES

1 **Zhou Y,** Gao SS, Li YX, Fan ZM, Zhao X, Qi YJ, Wei JP, Zou JX, Liu G, Jiao LH, Bai YM, Wang LD. Tumor suppressor gene p16 and Rb expression in gastric cardia precancerous lesions from subjects at a high incidence area in northern China. *World J Gastroenterol* 2002; **8**: 423-425

2 **Cai L,** Yu SZ, Zhan ZF. Cytochrome p450 2El genetic polymorphism and gastric cancer in Changle, Fujian Province. *World J Gastroenterol* 2001; **7**: 792-795

3 **Su M,** Lu SM, Tian DP, Zhao H, Li XY, Li DR, Zheng ZC. Relationship between ABO blood groups and carcinoma of esophagus and cardia in Chaoshan inhabitants of China. *World J Gastroenterol* 2001; **7**: 657-661

4 **Cai L,** Yu SZ, Zhang ZF. Glutathione S-transferases M1, T1 genotypes and the risk of gastric cancer: a case-control study. *World J Gastroenterol* 2001; **7**: 506-509

5 **Xin Y,** Li XL, Wang YP, Zhang SM, Zheng HC, Wu DY, Zhang YC. Relationship between phenotypes of cell-function differentiation and pathobiological behavior of gastric carcinomas. *World J Gastroenterol* 2001; **7**: 53-59

6 **Wang RT,** Wang T, Chen K, Wang JY, Zhang JP, Lin SR, Zhu YM, Zhang WM, Cao YX, Zhu CW, Yu H, Cong YJ, Zheng S, Wu BQ. *Helicobacter pylori* infection and gastric cancer: evidence from a retrospective cohort study and nested case-control study in China. *World J Gastroenterol* 2002; **8**: 1103-1107

7 **Song ZJ,** Gong P, Wu YE. Relationship between the expression of iNOS, VEGF, tumor angiogenesis and gastric cancer. *World J Gastroenterol* 2002; **8**: 591-595

8 **Tao HQ,** Zou SC. Effect of preoperative regional artery chemotherapy on proliferation and apoptosis of gastric carcinoma cells. *World J Gastroenterol* 2002; **8**: 451-454

9 **Xao HB,** Co WX, Yin HR, Lin YZ, Ye SH. Influence of L-methionine-deprived total parenteral nutrition with 5-fluorouracil on gastric cancer and host metabolism. *World J Gastroenterol* 2001; **7**: 698-701

10 **Ma ZF,** Wang ZY, Zhang JR, Gong P, Chen HL. Carcinogenic potential of duodenal reflux juice from patients with long-standing postgastrectomy. *World J Gastroenterol* 2001; **7**: 376-380

11 **Miehlke S,** Kirsch C, Dragosics B, Gschwantler M, Oberhuber G, Antos D, Dite P, Lauter J, Labenz J, Leodolter A, Malfertheiner P, Neubauer A, Ehninger G, Stolte M, Bayerdorffer E. *Helicobacter pylori* and gastric cancer: current status of the Austrain Czech German gastric cancer prevention trial (PRISMA Study). *World J Gastroenterol* 2001; **7**: 243-247

12 **Wu K,** Shan YJ, Zhao Y, Yu JW, Liu BH. Inhibitory effects of RRR-alpha-tocophery1 succinate on benzo (a) pyrene (B(a)P)-induced forestomach carcinogenesis in female mice. *World J Gastroenterol* 2001; **7**: 60-65

13 **Matsuyama S,** Ohkura Y, Eguchi H, Kobayashi Y, Akagi K, Uchida K, Nakachi K, Gustafsson JA, Hayashi S. Estrogen receptor beta is expressed in human stomach adenocarcinoma. *J Cancer Res Clin Oncol* 2002; **128**: 319-324

14 **Takano N,** Iizuka N, Hazama S, Yoshino S, Tangoku A, Oka M. Expression of estrogen receptor-alpha and -beta mRNAs in human gastric cancer. *Cancer Lett* 2002; **176**: 129-135

15 **Tot T**. The role of cytokeratins 20 and 7 and estrogen receptor analysis in separation of metastatic lobular carcinoma of the breast and metastatic signet ring cell carcinoma of the gastrointestinal tract. *Apmis* 2000; **108**: 467-472

16 **Goldstein NS,** Long A, Kuan SF, Hart J. Colon signet ring cell adenocarcinoma: immunohistochemical characterization and comparison with gastric and typical colon adenocarcinomas. *Appl Immunohistochem Mol Morphol* 2000; **8**: 183-188

17 **Messa C,** Russo F, Pricci M, Di Leo A. Epidermal growth factor and 17beta-estradiol effects on proliferation of a human gastric cancer cell line (AGS). *Scand J Gastroenterol* 2000; **35**: 753-758

18 **Robertson JA,** Farnell Y, Lindahl LS, Ing NH. Estradiol up-regulates estrogen receptor messenger ribonucleic acid in endometrial carcinoma (Ishikawa)cells by stabilizing the message. *J Mol Endocrinol* 2002; **29**: 125-135

19 **Cobellis L,** Reis FM, Driul L, Vultaggio G, Ferretti I, Villa E, Petraglia F. Estrogen receptor alpha mRNA variant lacking exon 5 is coexpressed with the wild-type in endometrial adenocarcinoma. *Eur J Obstet Gynecol Reprod Biol* 2002; **102**: 92-95

20 **Horvath G,** Leser G, Hahlin M, Henriksson M. Exon deletions and variants of human estrogen receptor mRNA in endometrial hyperplasia and adenocarcinoma. *Int J Gynecol Cancer* 2000; **10**: 128-136

21 **Mollerup S,** Jorgensen K, Berge G, Haugen A. Expression of estrogen receptors alpha and beta in human lung tissue and cell lines. *Lung Cancer* 2002; **37**: 153-159

22 **Chearskul S,** Bhothisuwan K, Churintrapun M, Semprasert N, Onreabroi S. Estrogen receptor-alpha mRNA in primary breast cancer: relationship to estrogen and progesterone receptor proteins and other prognostic factors. *Asian Pac J Allergy Immunol* 2002; **20**: 13-21

23 **Zhao H,** Hart LL, Keller U, Holth LT, Davie JR. Characterization of stably transfected fusion protein GFP-estrogen receptor-alpha in MCF-7 human breast cancer cells. *J Cell Biochem* 2002; **86**: 365-375

24 **Bouras T,** Southey MC, Chang AC, Reddel RR, Willhite D, Glynne R, Henderson MA, Armes JE, Venter DJ. Stanniocalcin 2 is an estrogen-responsive gene coexpressed with the estrogen receptor in human breast cancer. *Cancer Res* 2002; **62**: 1289-1295

25 **Zheng WQ,** Lu J, Zheng JM, Hu FX, Ni CR. Variation of ER status between primary and metastatic breast cancer and relationship to p53 expression. *Steroids* 2001; **66**: 905-910

26 **Otto AM,** Schubert S, Netzker R. Changes in the expression and binding properties of the estrogen receptor in MCF-7 breast cancer cells during growth inhibition by tamoxifen and cisplatin. *Cancer Chemother Pharmacol* 2001; **48**: 305-311

27 **Yang X,** Phillips DL, Ferguson AT, Nelson WG, Herman JG, Davidson NE. Synergistic activation of functional estrogen receptor(ER)-alpha by DNA methyltransferase and histone deacetylase inhibition in human ER-alpha-negative breast cancer cells. *Cancer Res* 2001; **61**: 7025-7029

28 **Lacroix M,** Querton G, Hennebert P, Larsimont D, Leclercq G. Estrogen receptor analysis in primary breast tumors by ligand-binding assay, immunocytochemical assay, and northern blot: a comparison. *Breast Cancer Res Treat* 2001; **67**: 263-271

29 **Diel P,** Olff S, Schmidt S, Michna H. Molecular identification of potential selective estrogen receptor modulator(SERM) like properties of phytoestrogen in the human breast cancer cell line MCF-7. *Planta Med* 2001; **67**: 510-514

30 **Brouillet JP,** Dujardin MA, Chalbos D, Rey JM, Grenier J, Lamy PJ, Maudelonde T, Pujol P. Analysis of the potential contribution of estrogen receptor (ER) beta in ER cytosolic assay of breast cancer. *Int J Cancer* 2001; **95**: 205-208

31 **Fasco MJ,** Keyomarsi K, Arcaro KF, Gierthy JF. Expression of an estrogen receptor alpha variant protein in cell lines and tumors. *Mol Cell Endocrinol* 2000; **166**: 156-169

32 **Yang X,** Ferguson AT, Nass SJ, Phillips DL, Butash KA, Wang SM, Herman JG, Davidson NE. Transcriptional activation of estrogen receptor alpha in human breast cancer cells by histone deacetylase inhibition. *Cancer Res* 2000; **60**: 6890-6894

33 **Koduri S,** Poola I. Quantitation of alternatively spliced estrogen receptor alpha mRNAs as separate gene populations. *Steroids* 2001; **66**: 17-23

34 **Omoto Y,** Iwase H, Iwata H, Hara Y, Toyama T, Ando Y, Kobayashi S. Expression of estrogen receptor alpha exon 5 and 7 deletion variant in human breast cancers. *Breast Cancer* 2000; **7**: 27-31

35 **Anandappa SY,** Sibson R, Platt-Higgins A, Winstanley JH, Rudland PS, Barraclough R. Variant estrogen receptor alpha mRNAs in human breast cancer specimens. *Int J Cancer* 2000; **88**: 209-216

36 **Shao ZM,** Shen ZZ, Fontana JA, Barsky SH. Genistein's "ER-dependent and independent" actions are mediated through ER pathways in ER-positive breast carcinoma cell lines. *Anticancer Res* 2000; **20**: 2409-2416

37 **Koduri S,** Fuqua SA, Poola I. Alterations in the estrogen receptor alpha mRNA in the breast tumors of African American women. *J Cancer Res Clin Oncol* 2000; **126**: 291-297

38 **Bratthauer GL,** Lininger RA, Man YG, Tavassoli FA. Androgen and estrogen receptor mRNA status in apocrine carcinomas. *Diagn Mol Pathol* 2002; **11**: 113-118

39 **Cutolo M,** Carruba G, Villaggio B, Coviello DA, Dayer JM, Campisi I, Miele M, Stefano R, Castagnetta LA. Phorbol diester 12-O-tetradecanoylphorbol 13-acetate(TPA)up-regulates the expression of estropgen receptors in human THP-1 leukemia cells. *J Cell Biochem* 2001; **83**: 390-400

40 **Maruyama S,** Fujimoto N, Asano K, Ito A, Usui T. Expression of estrogen receptor alpha and beta mRNAs in prostate cancers treated with leuprorelin acetate. *Eur Urol* 2000; **38**: 635-639

41 **Li LC,** Chui R, Nakajima K, Oh BR, Au HC, Dahiya R. Frequent methylation of estrogen receptor in prostate cancer: correlation with tumor progression. *Cancer Res* 2000; **60**: 702-706

Edited by Pang LH

P.O.Box 2345, Beijing 100023, China
Fax: +86-10-85381893
E-mail: wjg@wjgnet.com www.wjgnet.com

World J Gastroenterol 2003;9(4):670-673
World Journal of Gastroenterology
 ISSN 1007-9327

• GASTRIC CANCER •

Effects of astragali radix on the growth of different cancer cell lines

Jiang Lin, Hui-Fang Dong, JJ Oppenheim, OM Howard

Jiang Lin, Department of Gastroenterology, Shuguang Hospital, Shanghai University of Traditional Chinese Medicine, Shanghai 200021, China
Hui-Fang Dong, JJ Oppenheim, OM Howard, Laboratory of Molecular Immunoregulation, National Cancer Institute, Frederick, MD 21702, USA
Correspondence to: Dr. Jiang Lin, Department of Gastroenterology, Shuguang Hospital, Shanghai University of Traditional Chinese Medicine, Shanghai, 200021, China. lin_jiang@hotmail.com
Telephone: +86-21-53821650-292
Received: 2002-04-12 **Accepted:** 2002-05-08

Abstract

AIM: To investigate the inhibitory effect of a Chinese herb medicine Astragali radix (AR) on growth of different cancer cell lines.

METHODS: To observe the in vitro effects of AR on tumor cell proliferation by trypan blue exclusion, MTS method and tritium thymidine incorporation assay. Apoptosis was detected by DNA ladder method.

RESULTS: The inhibition rates of AR on the cell respiration of AGS, KATOIII, HT29, MDA231, MEL7 and MEL14 were 68.25 %, 62.36 %, 22.8 %, 27.69 %, 2.85 % and 5.14 % respectively at the concentration of 100 ug/ml; it inhibited AGS DNA synthesis by 87.33 % at the concentration of 50 ug/ml. The inhibitory effect on AGS was time-and dose-dependent. AR did not induce apoptosis in AGS cells.

CONCLUSION: AR specifically inhibits gastric cancer cells growth in vitro and the mechanism is mainly cytostatic but not cytotoxic or inducing apoptosis.

Lin J, Dong HF, Oppenheim JJ, Howard OM. Effects of astragali radix on the growth of different cancer cell lines. *World J Gastroenterol* 2003; 9(4): 670-673
http://www.wjgnet.com/1007-9327/9/670.htm

INTRODUCTION

Astragali radix (AR) is the dried root of *Astragalus membranaceus Bge. Var. mongholicus* and is used as a tonic in the traditional Chinese medicine. It has been used extensively as an adjuvant[1,2] in cancer treatment and as a phytochemical immune modulator. Kurashige *et al*. reported that AR lowered the incidence of urinary bladder carcinoma in N-butyl-N' -butanolinitrosoamine treated mice by activating the cytotoxicity of lymphocytes and increasing the production of IL-2 and IFN-γ[3]. Lau' s study showed that it also restored the chemiluminescent oxidative burst activity of murine splenic macrophage suppressed by renal cell carcinoma[4]. Wang' s research suggested that an extract of AR had the synergetic effect with IL-2 in activating LAK cells, resulting in reducing the dosage of IL-2 and the associated toxicity[5]. In addition, AR also could promote the proliferation of B cell and the production of immunoglobulin[6] and has a bidirectional modulating effect on T cells. It was reported that it could reduce the suppressive activity of Ts in post-burn mice[7] and also increase Th cell activity in immunodepressed mice[8].

However, there was no report on whether AR affects tumor cells growth directly. In this paper, we studied the effect of an aqueous extract of AR on the growth of different cancer cell lines.

MATERIALS AND METHODS

Cell lines and culture conditions

Human gastric cancer cell lines AGS and KATO-III were purchased from the American Type Culture Collection. AGS is a cell line of moderately-poorly differentiated adenocarcinoma and KATO-III is a cell line of signet ring carcinoma. HT29 is a cell line of colon cancer and MDA231 is a breast cancer cell line, both of them were kindly provided by Dr. Bill Murphy. Mel7 and Mel14 are melanoma cell lines, which were gifted by Dr. D. Schadendorf. All the cells were cultured in RPMI1640 medium supplemented with 10 % FBS, 100 U/ml penicillin, 100 μg/ml streptomycin and Glutamine (GIBCO BRL, Life Technologies, Grand Island, NY, USA) in a humidified atmosphere of 95 % air with 5 % CO_2 at 37 ℃ as a monolayer.

Preparation of herbal extract

AR was purchased from Da Xing Chinese herbal medicines store in DC, USA. The aqueous extract was prepared by the Natural Product Branch of National Cancer Institute. 8 grams of aqueous extract was dissolved in 100 ml distilled water and centrifuged at 4 000 rpm for 20 min. The supernatant was passed through a 0.22 μm filter (Corning, Costar, NY, USA) and reached a final concentration of 80 mg/ml. The solution was aliquoted and stored at -20 ℃ for future use.

AR treatment

The herbal treatment was modified from the anti-cancer drug screening program of natural product branch in NCI[9]. Cells were harvested by trypsinization when they were confluenced. 1×10^4 and 3×10^5 cells were seeded in each of the 96-well and 6-well plates respectively and cultured in RPMI1640 medium supplemented with 5 % FBS for 24 hours. Then different concentrations of AR were added in each well to attain a series of different concentrations (1, 12.5, 25, 50 and 100 μg/ml) and incubated for 48 hours for further measurements.

MTS assay

Cell growth was measured by MTS assay. The Cell Titer 96 Aqueous Non-Radioactive Cell Proliferation Assay Kit was purchased from Promega, WI, USA. Briefly, MTS and PMS were mixed at the ratio of 20:1 immediately before being added to the samples. 20 μl of MTS/PMS solution was added to each of the 96-well plate and incubated at 37 ℃ in a humidified 5 % CO_2 atmosphere for 3 hours. The absorbance was read at 490 nm using Bio-Tek' s Power Wave x reader-assay system (BIO-TEK Instruments INC, VT, USA). Each sample was triplicated.

^{3}H-thymidine incorporation assay

Cell DNA synthesis was measured by ^{3}H-thymidine incorporation assay. At the end of herbal treatment, 1 μCi of ^{3}H-thymidine was added in each well of a 96-well plate. Then the plate was incubated at 37 ℃ in a humidified 5 % CO_2

atmosphere for 4 hours and stored at -70 ℃ overnight. On the second day, the frozen plate was thawed at 37 ℃ and the DNA was transferred to the filtermat using multi-channel cell collector. The filtermat was washed with distilled water thrice and 95 % alcohol once. 4.5 ml Betaplate Scint was added to the filtermat and read the filtermat with liquid scintillation and luminescence counter (Perkin Elmer Wallac Inc. MD, USA). Each sample was quadruplicated.

Cell viablility assay

Cells were cultured and treated in 6-well plate. At the end of the treatment, the cells were collected by trypsinization and counted with 1 % Trypan-blue. Each sample was triplicated.

DNA ladder analysis

DNA ladder was measured as described previously[10] with some modification. Briefly, 1×10^6 cells in 0.5 ml were lysed in 1 ml DNA lysis buffer containing 1 M Tris-HCl, 0.2 M EDTA, 4 M NaCl, 20 % SDS and 400 μg/ml proteinase K) and incubated at 37 ℃ overnight. DNA was extracted in Phase LockGel eppendorf (Eppendorf Scientific Inc. NY, USA) with an equal volume of phenol/choloroform/isoamyl alcohol (25:24:1) and precipitated with 2 volumes of ice-cold 100 % ethanol and 1/10 volume of 3 M sodium acetate at -70 ℃ for 1 hr. DNA was collected, washed with ice-cold 70 % ethanol once and dried in air. Then DNA was dissolved in TE buffer containing 10 μg/ml RNase I and incubated at 37 ℃ for 1 hr. Equal amounts of DNA (10 μg/well) were electrophoresed in 1.8 % agarose gels impregnated with ethidium bromide (0.1 μg/ml) for 2 hr at 70 V. DNA fragments were visualized by UV transillumination.

Statistical analysis

The inhibition rate was calculated by the following formula: inhibition rate (%)=(OD/CPMcontrol-OD/CPMtest)/OD/CPMcontrol×100 %. Student' s *t*-test was used to compare the results. All *P* values were described by two-tailed analysis. $P<0.05$ was considered statistically significant.

RESULTS

Growth inhibiting effect of AR on different cancer cell lines

Figure 1 illustrated the inhibiting effects of AR on the proliferation of 6 tumor cell lines, including AGS, KATOIII, HT29, MDA231, MEL7 and MEL14, measured by MTS method. It was found that after 48 hours incubation, 100 μg/ml of AR had greater inhibiting effect on gastric tumor cell lines of AGS and KATOIII than the other cancer cell lines. It inhibited the growth of AGS and KATOIII by 68.25 % and 62.36 % respectively, compared to only 22.8 %, 27.69 %, 2.85 % and 5.14 % reduction in cell growth of HT29, MDA231, MEL7 and MEL14. It appeared to be selectively inhibiting the growth of gastric cancer cell line.

Effect of AR on AGS viability

Whether the inhibitory effect of AR on AGS growth was cytotoxic was determined by the trypan blue measurement. Figure 2 showed the viable cell numbers of AGS treated with different concentrations of AR. In the range from 1 to 50 μg/ml, AR had a dose-dependent inhibiting effect on AGS growth and almost completely inhibited the AGS growth at the concentration of 50 μg/ml, of which the cell number of the test group was very close to the cell number seeded at the beginning of the test and few cells were stained blue. However, at the concentration of 100 μg/ml, AR showed cytotoxicity on AGS, of which the cell number was lower than the initial cell number.

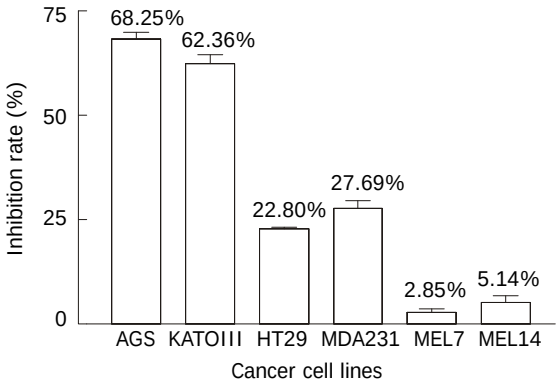

Figure 1 Effect of AR on the growth of 6 cancer cell lines. Cells were treated with AR at the concentration of 100 μg / ml for 48 hrs and cell growth was measured with MTS method.

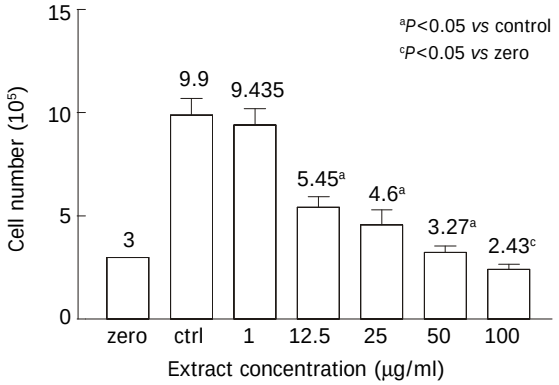

Figure 2 Effect of AR on AGS viability. AGS cells were treated with different concentrations of AR for 48 hrs and cell viability was measured with trypan blue. At or below the concentration of 50 μg / ml, AR was not cytotoxic to AGS cells. But at the concentration of 100 μg / ml, it showed cytotoxicity on AGS.

Dose-dependent and time-dependent effects of AR on AGS growth

The dose-dependent and time-dependent effects of AR on AGS growth were observed by MTS assay. AGS cells were treated with different concentrations of AR for 48 hours. Figure 3 showed that the inhibitory effect of AR on AGS was proportional to the extract concentrations. In the time-course experiment, AGS cells were treated with 50 μg/ml of AR and incubated for 6, 12, 24 and 48 hours respectively. In Figure 4, it was found that AR began to inhibit the cell growth significantly at the 12th hour and the effect was also improved linearly while prolonging the incubation time.

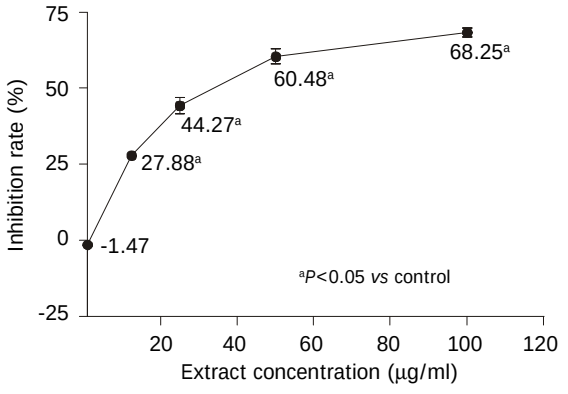

Figure 3 Dose-dependent effect of AR on AGS growth. AGS cells were treated with a serial of diluted concentrations (1, 12.5, 25, 50 and 100 μg / ml) of AR for 48 hrs and cell growth was measured with MTS method. The inhibition effect of AR was improved accompanied by increase of concentration.

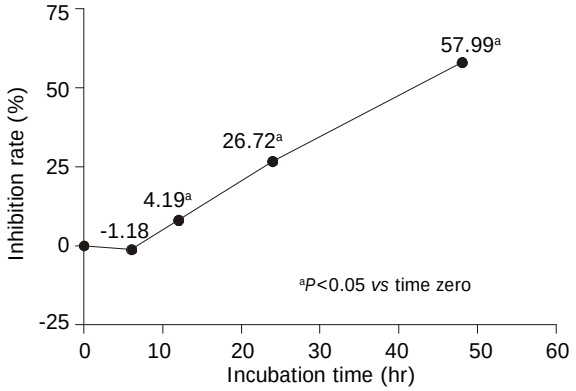

Figure 4 Time-dependent effect of AR on AGS growth. AGS cells were treated with 50 μg / ml of AR for 6, 12, 24 and 48 hrs. The cell growth was measured by MTS method. The inhibition effect of AR on AGS growth was enhanced with incubation time.

Effect of AR on AGS DNA synthesis

Tritium-labeled thymidine incorporation assay was used to evaluate the effect of AR on AGS DNA synthesis. AGS cells were treated with different concentrations of AR for 48 hours. Figure 5 demonstrated that AR could significantly inhibit the DNA synthesis of AGS. It was also observed that the inhibiting effect of AR increased sharply from the concentrations of 1 μg/ml to 25 μg/ml and it increased slowly from then on.

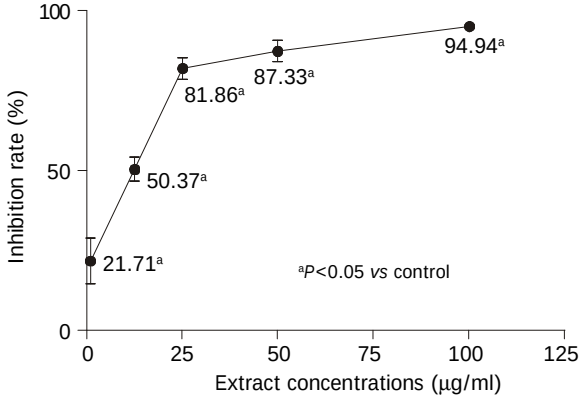

Figure 5 Effect of AR on DNA synthesis of AGS. AGS cells were treated with a serial of diluted concentrations (1, 12.5, 25, 50 and 100 μg / ml) of AR for 48 hrs and cell growth was measured with tritium labeled thymidine incorporation assay. AR started to inhibit the DNA synthesis of AGS at 1 μg / ml and the inhibiting effect was dose-dependent.

Effect of AR on AGS apoptosis

DNA fragmentation method was used to observe whether apoptosis was induced in AGS by AR. AGS cells were treated with different concentrations of AR for 48 hours. However, there was no DNA ladder appeared in the electropheresis gel. So the herbal extract had no effect on AGS apoptosis.

DISCUSSION

AR is a tonic herbal medicine which is used as an adjuvant extensively in the treatment of various cancers, such as lung cancer, digestive tract cancers, renal cancer, bladder cancer[1,2,11], melanoma and AIDS[12]. It had been reported that it could improve the host immune function suppressed by tumors and relieve the marrow suppression induced by chemotherapeutic agents so that it could make the patients more tolerant to chemotherapeutic therapy. Although there were some studies showing that AR could inhibit the tumor growth *in vivo*, the anti-cancer effect was testified through activating the activity of Th, LAK and macrophages and promoting the production of IL-2 and IFN-γ. However, whether it has direct inhibition effect on tumors cells has not been elucidated yet.

In this study, 6 different cancer cell lines were used to test the inhibitory effect of AR. After 48 hours incubation, AR inhibited the gastric cancer cell lines of AGS and KATOIII growth by 68.25 % and 62.36 %, compared to the inhibition rates of colon cancer cell line HT29, breast cancer cell line MDA231 and melanoma cell lines of Mel7 and Mel14 which were 22.8 %, 27.69 %, 2.85 % and 5.14 % respectively, suggesting that AR has anti-cancer effect on gastric cancer cell lines. To fully confirm this, many other kinds of cancer cell lines should be tested in order to determine the specificity of the effect. AGS and KATOIII are two different gastric cancer cell lines. AGS is a moderately-poorly differentiated adenocarcinoma cell line while KATOIII is a cell line of signet ring cell carcinoma, but AR has almost the same inhibitory effect on both cell lines.

Many herbal extracts can inhibit cell growth in vitro through their cytotoxic effect[13-16]. We determined whether the inhibitory effect of AR was due to cytotoxicitiy. In order to clarify this question, we measured the cell growth with trypan blue exclusion method. The initial cell number was 300 000/well and in the untreated wells the cell number reached 990 000/well after 48 hours incubation. The cell number in testing group treated with 1 μg/ml of AR was 943 500/well (P>0.05, *vs* control group). However, the cell numbers of the other testing groups treated with AR from the concentrations of 12.5 μg/ml to 100 μg/ml were significantly lower than that of the control group and but higher than the initial cell number except for the testing group treated with 100 μg/ml AR, whose cell number was only 243 000/well (P=0.017, compared to the initial cell number). Few cells stained trypan blue could be seen in the testing groups treated with AR at the concentration lower than 100 μg/ml. So the inhibition effect of AR at the concentrations of 50 μg/ml or below was not cytotoxic while AR is cytotoxic to AGS cell at the concentration of 100 μg/ml. Further studies showed that the inhibition effect of AR on AGS was dose- and time-dependent. The maximal concentration without cytotoxicity was around 50 μg/ml and the corresponding inhibition rate was 60.48 %. AR came into effect at the 12th hour and reached its peak at the 48th hour.

One characteristic of the tumor cells is that their rapid proliferations are accompanied by DNA synthesis and cellular replication. Tritium labeled thymidine incorporation assay reflects the cellular DNA synthesis. Our results showed that the DNA synthesis of AGS was significantly inhibited by AR. The inhibition rate increased sharply from 21.71 % to 81.86 % at the concentrations ranging from 1 μg/ml to 25 μg/ml, then it reached a plateau. So AR might suppress AGS cell growth through inhibition of DNA synthesis. The inhibition rates of AGS cell growth expressed by MTS method and tritium labeled thymidine incorporation assay were different. The latter was higher than the former. This maybe attributed to that MTS and tritium labeled thymidine incorporation assay were two different indirect measurements used in cell growth evaluation. MTS reflects the cell growth at the level of cell respiration while tritium labeled thymidine incorporation assay at the level of DNA synthesis. When the cellular DNA synthesis is suppressed, the cells might be in an inactive status in which the cells could still respire. So the inhibition rate of cell growth expressed by MTS is lower than that expressed by tritium labeled thymidine incorporation assay.

Apoptosis is a kind of programming cell death whose impairment may induce cell immortality and carcinogenesis[17]. Some agents such as aspirin, indomethacin and arsenic trioxide[10,18] and some herbs such as Anemarrhena asphodeloides Bunge, Albizzia Lucidior I. Nielsen and Paeoniae radix[19-21] were reported to have the ability of inducing apoptosis in gastric

cancer cells and inhibiting their growth. However, apoptosis could not be observed in AGS cells treated with AR. Combined with the results of trypan blue experiment that there were few cells, which were treated with AR, stained blue, the inhibition effect of AR on AGS is not through the mechanism of cytotoxic or apoptosis.

The aqueous and organic extracts of AR were used in this study. But the organic extract had no effect on AGS growth (data not shown). So the effective anti-cancer components are in the aqueous extract. Polysaccharide[22], astragaloside[23], and flavonoids[24] have been found in AR. Some studies showed that the polysaccharides and flavonoids from other herbs had the anti-tumor efficiency *in vitro* and *in vivo*[25-29]. But up to now, there has no evidence showing that these compounds from AR have anti-cancer activity *in vitro*. Hence, further studies are required. Selenium toxicity has been confirmed in the livestock consuming plants of the genus Astragalus and selenium was reported to have the carcinostatic activity in the animals[30,31]. So selenium might play a critical role in AR inhibiting AGS growth.

In conclusion, the inhibitory effect of AR on the growth of gastric cancer cell line of AGS is mainly cytostatic.

REFERENCES

1 **Cha RJ**, Zeng DW, Chang QS. Non-surgical treatment of small cell lung cancer with chemo-radio-immunotherapy and traditional Chinese medicine. *Zhonghua Neike Zazhi* 1994; **33**: 462-466

2 **Li NQ**. Clinical and experimental study on shen-qi injection with chemotherapy in the treatment of malignant tumor of digestive tract. *Zhongguo Zhongxiyi Jiehe Zazhi* 1992; **12**: 588-592

3 **Kurashige S**, Akuzawa Y, Endo F. Effects of astragali radix extract on carcinogenesis, cytokine production, and cytotoxicity in mice treated with a carcinogen, N-butly-N'-butanolnitrosoamine. *Cancer Invest* 1997; **17**: 30-35

4 **Lau BH**, Ruckle HC, Botolazzo T, Lui PD. Chinese medicinal herbs inhibit growth of murine renal cell carcinoma. *Cancer Biother* 1994; **9**: 153-161

5 **Wang Y**, Qian XJ, Hadley HR, Lau BH. Phytochemicals potentiate interleukin-2 generated lymphokine-activated killer cell cytotoxicity against murine renal cell carcinoma. *Mol Biother* 1992; **4:** 143-146

6 **Yoshida Y**, Wang MQ, Liu JN, Shan BE, Yamashita U. Immunomodulating activity of Chinese medicinal herbs and Oldenlandia diffusa in particular. *Int J Immunopharmacol* 1997; **19**: 359-370

7 **Liang H**, Zhang Y, Geng B. The effect of astragalus polysaccharides (APS) on cell mediated immunity (CMI) in burned mice. *Zhonghua Zhengxing Shaoshang Waike Zazhi* 1994; **10**: 138-141

8 **Zhao KS**, Mancini C, Doria G. Enhancement of the immune response in mice by Astragalus membranaceus extracts. *Immunopharmacology* 1990; **20**: 225-233

9 **Alley MC**, Scudiero DA, Monks PA, Hursey ML, Czenwinski MJ, Fine DL, Abbott BJ, Mayo JG, Shoemaker RH, Boyd MR. Feasibility of drug screening with panels of human tumor cell lines using a microculture tetrazolium assay. *Cancer Research* 1988; **48**: 589-601

10 **Jiang XH**, Wong BCY, Yuen ST, Jiang SH, Cho CH, La KC, Lin MCM, Kung HF, Lam SK. Arsenic trioxide induces apoptosis in human gastric cancer cells through up-regulation of p53 and activation of caspase-3. *Int J Cancer* 2001; **91**: 173-179

11 **Rittenhouse JR**, Lui PD, Lau BH. Chinese medicinal herbs reverse macrophage suppression induced by urological tumors. *J Urol* 1991; **146**: 486-490

12 **Chu DT**, Lin JR, Wong W. The in vitro potentioation of LAK cell cytotoxicity in cancer and AIDS patients induced by F3-a fractionated extract of Astragalus membranaceus. *Zhonghua Zhongliu Zazhi* 1994; **16**: 167-171

13 **Chen SB**, Gao GY, Li YS, Yu SC, Xiao PG. Cytotoxic constituents from Aquilegia ecalcarata. *Planta Med* 2002; **68**: 554-556

14 **Wang S**, Zhang YJ, Chen RY, Yu DQ. Goniolactones A-F, six new styrylpyrone derivatives from the roots of Goniothalamus cheliensis. *J Nat Prod* 2002; **65**: 835-841

15 **Fan CQ**, Sun HF, Chen SN, Yue JM, Lin ZW, Sun HD. Triterpene saponins from Graniotome furcata. *Nat Prod Lett* 2002; **16**: 161-166

16 **Li J**, Liang N, Mo L, Zhang X, He C. Comparison of the cytotoxicity of five constituents from Pteris semipinnata L. in vitro and the analysis of their structure-activity relationships. *Yaoxue Xuebao* 1998; **33**: 641-644

17 **Willie AH**, Bellamy CO, Bubb VJ, Clarke AR, Corbet S, Curtis L, Harrison DJ, Hooper ML, Toft N, Webb S, Bird CC. Apoptosis and carcinogenesis. *Br J Cancer* 1999; **80** (Suppl 1): 34-37

18 **Zhou XM**, Wong BCY, Fan XM, Zhang HB, Lin MCM, Kung HF, Fan DM, Lam SK. Non-steroidal anti-inflammatory drugs induce apoptosis in gastric cancer cells through up-regulation of bax and bak. *Carcinogenesis* 2001; **22**: 1393-1397

19 **Takeda Y**, Togashi H, Matsuo T, Shinzawa H, Takeda Y, Takahashi T. Growth inhibition and apoptosis of gastric cancer cell lines by Anemarrhena asphodeloides bunge. *J Gastroenterol* 2001; **36**: 79-90

20 **Cai B**, Zhang HF, Zhang DY, Cui CB, Li WX. Apoptosis-inducing activity of extract from Chinese herb, Albizzia Lucidior I. Nielsen. *Aizheng* 2002; **21**: 373-378

21 **Lee SM**, Li ML, Tse YC, Leung SC, Lee MM, Tsui SK, Fung KP, Lee CY, Waye MM. Paeoniae Radix, a Chinese herbal extract, inhibit hepatoma cells growth by inducing apoptosis in a p53 independent pathway. *Life Sci* 2002; **71**: 2267-2277

22 **Zheng Z**, Liu D, Song C, Cheng C, Hu Z. Studies on chemical constituents and immunological function activity of hairy root of Astragalus membranaceus. *Chin J Biotechnol* 1998; **14**: 93-97

23 **Hirotani M**, Zhou Y, Rui H, Furuya T. Cycloartane triterpene glycosides from the hairy root cultures of Astragalus membranaceus. *Phytochemistry* 1994; **37**: 1403-1407

24 **Lin LZ**, He XG, Lindenmairer M, Nolan G, Yang J, Cleary M, Qiu SX, Cordell GA. Liquid chromatography-electrospray ionization mass spectrometry study of the flavonoids of the roots of Astragalus mongholicus and A. membranaceus. *J Chromatogr A* 2000; **876**: 87-95

25 **Lu X**, Su M, Li Y, Zeng L, Liu X, Li J, Zheng B, Wang S. Effect of Acanthopanax giraldii Harms Var. Hispidus Hoo polysaccharides on the human gastric cancer cell line SGC-7901 and its possible mechanism. *Chin Med J (Engl)* 2002; **115**: 716-721

26 **Wang SY**, Hus ML, Hus HC, Tzeng CH, Lee SS, Shiao MS, Ho CK. The anti-tumor effect of Ganoderma lucidum is mediated by cytokines released from activiated macrophages and T lymphocytes. *Int J Cancer* 1997; **70**: 699-705

27 **Wang HB**, Zheng QY. Effects of phytolacca acinosa polysaccharides I with different schedules on its antitumor efficiency in tumor bearing mice and production of IL-1, IL-2, IL-6, TNF, CSF activity in normal mice. *Immunopharmacol Immunotoxicol* 1997; **19**: 197-213

28 **Chang WH**, Chen CH, Lu FJ. Different effects of baicalein, baicalin and wogonin on mitochondrial function, glutathione content and cell cycle progression in human hepatoma cell lines. *Planta Med* 2002; **68**: 128-132

29 **Zheng GQ**. Cytotoxic terpenoids and flavonoids from Artemisia annua. *Planta Med* 1994; **60**: 54-57

30 **Spallholz JE**. On the nature of selenium toxicity and carcinostatic activity. *Free Radic Bio Med* 1994; **17**: 45-64

31 **Harrison PR**, Lanfear J, Wu L, Fleming J, McGarry L, Blower L. Chemopreventive and growth inhibitory effects of selenium. *Biomed Environ Sci* 1997; **10**: 235-245

Edited by Wu XN

P.O.Box 2345, Beijing 100023, China
Fax: +86-10-85381893
E-mail: wjg@wjgnet.com www.wjgnet.com

World J Gastroenterol 2003;9(4):674-677
World Journal of Gastroenterology
 ISSN 1007-9327

• GASTRIC CANCER •

Correlation between expression of cyclooxygenase-2 and angiogenesis in human gastric adenocarcinoma

Hong-Xia Li, Xin-Ming Chang, Zheng-Jun Song, Shui-Xiang He

Hong-Xia Li, Xin-Ming Chang, Zheng-Jun Song, Shui-Xiang He, Department of gastroenterology, First Affiliated Hospital of Xi' an Jiaotong University, Xi' an 710061, Shaanxi Province, China
Correspondence to: Dr.Hong-Xia Li, Department of Gastroenterology, First Affiliated Hospital of Xi' an Jiaotong University, Xi' an 710061, Shaanxi Province, China. hx1105sina.com
Telephone: +86-29-5324101
Received: 2002-10-09 **Accepted:** 2002-11-09

Abstract

AIM: To evaluate the expression of cyclooxygenase (COX-2) and the relationship with tumor angiogenesis and advancement in gastric adenocarcinoma.

METHODS: Immunohistochemical stain was used for detecting the expression of COX-2 in 45 resected specimens of gastric adenocarcinoma; the monoclonal antibody against CD34 was used for displaying vascular endothelial cells, and microvascular density (MVD) was detected by counting of CD34-positive vascular endothelial cells. Paracancerous tissues were examined as control.

RESULTS: Immunohistological staining with COX-2-specific polyclonal antibody showed cytoplasmic staining in the cancer cells, some atypical hyperplasia and intestinal metaplasia, as well as angiogenic vasculature present within the tumors and prexisting vasculature adjacent to cancer lesions. The rate of expression of COX-2 and MVD index in gastric cancers were significantly increased, compared with those in the paracancerous tissues (77.78 *vs* 33.33 %, 58.13±19.99 *vs* 24.02±10.28, $P<0.01$, $P<0.05$, respectively). In 36 gastric carcinoma specimens with lymph node metastasis, the rate of COX-2 expression and MVD were higher than those in the specimens without metostasis (86.11 *vs* 44.44 %, 58.60±18.24 *vs* 43.54±15.05, $P<0.05$, $P<0.05$, respectively). The rate of COX-2 expression and MVD in the specimens with invasive serosa were significantly higher than those in the specimens without invasion to serosa (87.88 *vs* 50.0 %, 57.01±18.79 *vs* 42.35±14.65, $P<0.05$, $P<0.05$). Moreover, MVD in COX-2-positive specimens was higher than that in COX-2-negative specimens (61.29±14.31 *vs* 45.38±12.42, $P<0.05$). COX-2 expression was positively correlated with MVD ($r=0.63$, $P<0.05$).

CONCLUSION: COX-2 expression might correlate with the occurance and advancement of gastric carcinoma and is involved in tumor angiogenesis in gastric carcinoma. It is likely that COX-2 by inducing angiogenesis can be one of mechanisms which promotes invasion and metastasis of gastric carcinoma. It may become a new therapeutic target for anti-angiogenesis.

Li HX, Chang XM, Song ZJ, He SX. Correlation between expression of cyclooxygenase-2 and angiogenesis in human gastric adenocarcinoma. *World J Gastroenterol* 2003; 9(4): 674-677
http://www.wjgnet.com/1007-9327/9/674.htm

INTRODUCTION

COX is a key enzyme in the conversion of arachidonic acid to prostaglandin, and two isoforms of COX, namely COX-1 and COX-2, have been identified[1,2]. COX-1 is constitutively expressed in many tissues and is considered to be involved in various physiological functions, whereas COX-2 is induced by pathological stimuli, such as inflammation, various growth factors and cytokines produced by tumor cells[1-3].

Epidemiologic studies showed that nonsteroidal anti-inflammatory drugs (NSAIDs), known to inhibit COX, could reduce the incidence rate and mortality from digestive tract carcinomas[4-10]. In rodent models of FAP, a genetic disease leading to colonic carcinoma, blockade of COX-2, suppresses intestinal polyp formation[11]. Increased COX-2 expression has been reported in colorectal, pancreatic, hepatocellular and other cancers[12-20]. Taken together, these data provide strong evidence for the importance of COX-2 in oncogenesis.

It has been reported that tumor angiogenesis play an important role in tumor growth, invasion and metastasis[21-25]. We investigated the expression of COX-2, MVD in human gastric cancer. The aim of this study was to determine the relationship between COX-2 and tumor angiogenesis,and the development, progression of gastric cancer. The further understanding of oncogenesis might provide a new approach to tumor therapy.

MATERIALS AND METHODS

Materials

45 patients with gastric adenocarcinomas confirmed pathologically underwent gastrectomy in our hospital from January 2000 to October 2001. From these subjects, gastric tumor and paracancerous tissues (more than 5 cm away from the lesion) were obtained from resected specimen. Among them, 35 were male, and 10 female, with a mean age of 57.51±10.73 (33 to 78). Patients who had received radiotherapy or chemotherapy before gastrectomy were excluded.Histologically, they were classified by the WHO criteria, 5 were highly differentiated adenocarcinoma, 10 moderately-differentiated, 27 poorly-differentiated, 3 undifferentiated. As regards to the size of cancer, 20 were <5 cm, 25⩾5 cm. 33 tumors invaded to the serosa and 12 tumors not.36 cases had local lymph node metastasis.

Reagents and methods

Antibody against COX-2 was purchased from Santa Cruz Biotechnology. Inc; antiboby against CD34 and ready to use SP immunohistochemical reagent box were purchased from Fijian Maixin CO, Ltd. Formalin-fixed, paraffin-embedded surgical specimens from 45 cases of gastric carcinoma were available and sliced sequentially with a thickness of 4 μm. The slices carrying the detected antigen were dyed with SP immunohistochemical staining method, and those in the control group were dyed according to the above method, with the first antibody substituted by PBS.

Statistical methods

The data were presented as $\bar{x}\pm s$; numerical variable by χ^2 test;

enumeration data by *t* test; COX-2 relationship with MVD by spearman rank correlation test (depending on the quantitative index of COX-2 and MVD).

RESULTS

The cytoplasm of the gastric cancer cells stained with brown granules were identified to be COX-2 positive. Only nucleuses stained blue were identified to be COX-2 negative. COX-2 expression was scored semi-quantitatively according to the density and the percentage of positivity into score 0, 1, 2, 3. A minimum of 10 high power view were used to assess COX-2 expression level. If the sum of two scores was 1-3, the slice would be considered as low-expression of COX-2. If 4-6, it would be considered as high-expression of COX-2. Vascular endothelial cells were considered CD34-positive if their cytoplasm stained brown or brownish yellow. The microvessels were counted according to the number of single endothelial cell or endothelial cell clustor showing brownish yellow granules in the cytoplasm. The slices were observed first microscopically under the low power (×40),then selected the most dense area of microvessels was selected to be observed under high power (×200, the surface area of every visual field was 0.785 mm^2), and the number of microvessels in 3 visual field were counted and took the average as MVD of this specimen[26].

COX-2, MVD expression and distribution

77.78 % (35/45) cases of gastric carcinomas showed COX-2 positive expression while high-expression was detected in 22 cases, low-expression in 13. 33.33 % (15/45) cases of paracancerous tissues showed COX-2 positive expression while high-expression was only detected in 3 cases. The rate and density of COX-2 expression in cancerous tissues were significantly higher that in paracancerous tissues (χ^2=18, χ^2=6.09, P<0.005, P<0.05, respectively). The positive COX-2 staining was mainly diffusely located as brownish yellow stained granules in the cytoplasm. Immunohistological analysis revealed cytoplasmic staining in the neoplastic cells (Figure1), atypical hyperplasia and intestinal metaplasia. In addition, COX-2 was also detected in the angiogenic vasculature present within the tumors and preexisting vasculature adjacent to cancer lesions (Figure 2). In contrast, normal epithelium or stroma occasionally showed weak staining pattern or didn' t.

The mean MVD in gastric carcinoma was significantly higher than that in para-cancerous tissues (58.13±19.99, 24.02±10.28, t=10.18, P<0.001). The positive expression of CD34 was mainly presented as brownish yellow or brownish granules in the cytoplasm of vascular endothelial cell (Figure 3). New blood vessles in the cancerous lesions had no regular contour and were not evenly distributed.

The relationship between the rate of COX-2 expression and MVD

The result showed that MVD (61.29±14.31) in the COX-2-positive gastric cancerous tissues was higher than that (45.38±12.43) in the COX-2-negative one (t=5.64, P<0.001). The expression of COX-2 was positively correlated with MVD (r=0.63, P<0.05).

The relationship between the expression of COX-2, MVD and pathological features of gastric carcinoma

In Table 1, the associations between COX-2, MVD expression and the pathological features were shown. Both COX-2 and MVD were not correlated with tumor size, tumor histological type. However, there was correlation between COX-2, MVD and depth of invasion and lymph-node metastasis of gastric carcinoma respectively.

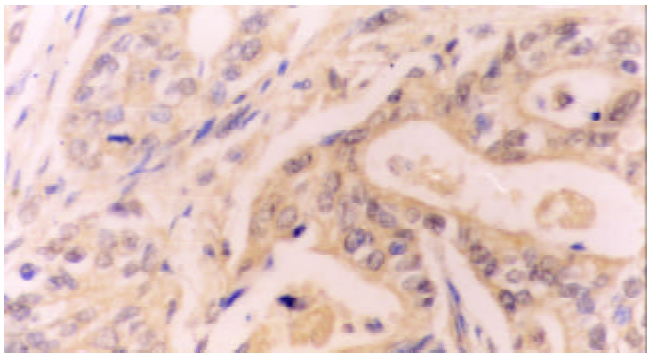

Figure 1 COX-2 expression in gastric adenocarcinoma.

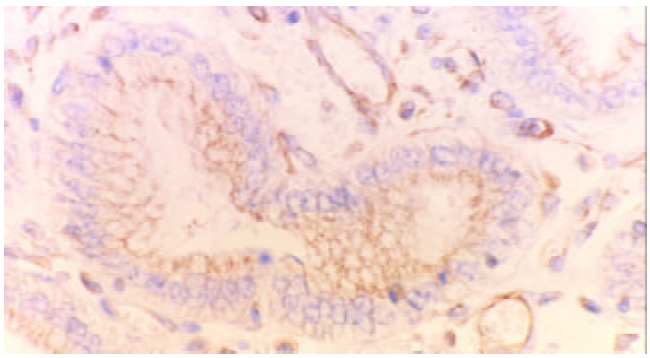

Figure 2 COX-2 expression was also detected in the vasculature within gastric adenocarcinoma.

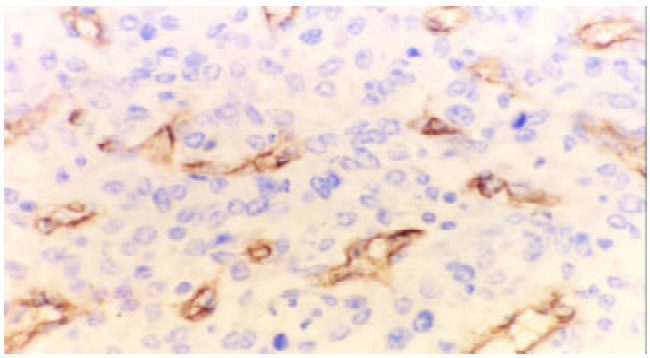

Figure 3 CD_{34} expression in the cytoplasm of vascular endothelial cell within gastric adenocarcinoma.

Table 1 The relationship between COX-2, MVD and pathological features of gastric carcinoma

Pathological characteristics	Positive COX-2(%)	MVD $\bar{x}$±s	Total
Tumor size			
<5 cm	15(75.0)	60.64±18.55	20
⩾5 cm	20(80.0)	55.68±17.98	25
Depth of invasion			
Invading serosa	29(87.88)[a]	57.01±18.79[c]	33
Noinvasion to serosa	6(50.0)	42.35±14.65	12
Degree of differentiation			
Well differentiated	12(80.0)	52.45±17.67	30
Poorly differentiated	23(76.67)	57.32±18.20	15
Lymph-node metastasis			
Positive	31(86.11)[b]	58.60±18.24[d]	36
negative	4(44.44)	43.54±15.05	9

Note: well differentiated cancer cells include highly and moderately differentiated ones: poorly differentiated cancer

cells include poorly differentidted and undifferediated ones. [a]$P<0.05$ ($\chi^2=5.23$), *vs* the rate of COX-2 expression in gastric carcinomas not invading serosa; [b]$P<0.05$ ($\chi^2=5.08$), *vs* the rate of COX-2 expression in gastric carcinoma without lymoph-node metastasis; [c]$P<0.05$ ($t=2.44$), *vs* MVD in gastric carcinomas not invading serosa; [d]$P<0.05$ ($t=2.28$), *vs* MVD in gastric carcinomas without lymph-node metastasis.

DISCUSSION

Human gastric mucosa normally expresses no detectable levels of COX-2 protein[27,28]. In the current study, we found that the rate of COX-2 expression in gastric cancer was significantly increased, compared with that in the paracancerous tissues, the expression of COX-2 showed cytoplasmic staining, not only in cancerous cells but also in precancerous lesion such as atypical hyperplasia and intestinal metaplasia. A similar pattern of COX-2 expression has previously been found in human gastric cancer[29-34]. The above data demonstrated that COX-2 was up-regulated in human gastric cancer, suggesting COX-2 may play an important role in occurrence of gastric cancer, being a relatively early event in the carcinogenesis of stomach.

Here, we also analyzed the relationship between COX-2 expression and clinical pathological features in gastric carcinoma. It was shown that the rate of COX-2 expression was correlated closely with the depth of tumor invasion, indicating COX-2 may contribute to invasive growth of gastric carcinoma. The rate of COX-2 expression of gastric carcinoma with lymph-node metastasis was higher than that without suggesting the increase of its expression in gastric cancer tissue can promote lymph-node metastasis. It seemed more likely that COX-2 probably heightened viability and increased infiltrative potential of gastric cancer. The mechanism was not clear. Tsujii concluded that overexpression of the COX-2 gene as a result of transfection promoted invasiveness in wild type human colon carcinoma cell lines through the induction of metalloproteinase-2 and membrane-type metalloproteinase[35]. Rat intestinal epithelial cells that overexpressed COX-2 protein were found to be resistant to butyrate-induced apoptosis and had elevated bcl-2 protein expression and decrease expression of both E-cadherin and the transforming growth factor-β receptor[36]. Each of these changes has been linked to enhanced tumorigenic potential and increased tumor invasiveness. Therefore, the above data further indicated that COX-2 might play an important role in gastric tumorigenesis and tumor progression.

Recently the relation of COX-2 and tumor angiogenesis is emphasized. One of the mechanisms by which PGE_2 supports tumor growth is by inducing the angiogenesis necessary to supply oxygen and nutrients to tumors >2 mm in diameter[37,38]. Masferrer[39] reported that SC-236, a COX-2-selective inhibitor, was effective in reducing angiogenesis driven by bFGF in the matriel rat model, whereas SC-560, a COX-1-selective inhibitor was ineffective. He also observed COX-2 expression in newly formed blood vessels within tumors grown in animals, whereas under normal physiological condibions the quiescent vasculature expressed only the COX-1 enzyme, indicating COX-2-derived prostaglandins contributed to tumor angiogenesis[40]. In our study, COX-2 expression was also detected in the angiogenic vasculature present within the tumors and preexisting vasculature adjacent to cancer lesions, suggesting COX-2 may induce newly formed blood vessels to sustain tumor cell viability and growth. COX-2 was also expressed within atypical hyperplasia, intestinal metaplasia and neovasculature in the paracancerous tissue, indicating COX-2 may promote precancerous lesion to cancer by new blood vessel formation.

MVD is a reliable index of tumor angiogenesis[41]. We found that the MVD in COX-2 positive tumors was significantly higher than that in COX-2 negative tumors, MVD in gastric carcinoma was higher than that in paracancerous tissues, suggesting its distribution was similar to the pattern of COX-2 in gastric carcinoma. A close correlation was present between MVD and COX-2 ($P<0.01$), indicating COX-2 was closely related to tumor angiogenesis further, and may be one of important factors involved in gastric carcinoma angiogenesis. In addition, MVD in the specimens with lymph node metastasis was significantly higher than that without and it was also correlated closely with the depth of tumor invasion,suggesting that tumor angiogenesis in gastric carcinomas might result in cancer cells entering blood circulation, and the lymph node metastasis could be promoted when the gastric cancer cells invade lymphatic vessels. Both COX-2 and MVD were associated with the depth of invasion and lymph-node metastasis, suggesting the effect of COX-2 on angiogenesis can promote metastatic protential as well as tumor invasiveness. Therefore, inducing tumor angiogenesis may be one of mechanisms which COX-2 promotes the development and metastasis of gastric cancer.

In conclusion, COX-2 expression in gastric adenocarcinoma was higher than that in the paracancerous tissues, and was related to lymph node metastasis and the depth of invasion, suggesting COX-2 might correlate with the occurance and advancement of gastric carcinoma; COX-2 expression in gastric carcinoma was closely related to MVD, suggesting COX-2 might be involved in tumor angiogenesis in gastric carcinoma, it is likely that COX-2 inducing angiogenesis may be one of mechanisms which COX-2 promotes the invasion, metastasis of tumor in gastric carcinoma. These findings suggest that COX-2 may be a new therapeutic target for anti-angiogenesis.

REFERENCES

1 **Williams CS**, DuBois RN. Prostaglandin endoperoxide synthase: why two isoforms? *Am J Physiol* 1996; **270**: G393-G400

2 **Eberhart CE**, DuboisRN. Eicosanoids and the gastrointestinal tract. *Gastroenterology* 1995; **109**: 285-301

3 **DuBois RN**, Awad J, Morrow J, Roberts LJ 2nd, Bishop P. Regulation of eicosanoid production and mitogenesis in rat intestinal epithelial cells by tranasforming growth factor-alpha and phorbol ester. *J Clin Inves*1994; **93**: 493-498

4 **Farrow DC**, Vaughan TL, Hansten PD, Stanford JL, Risch HA, Gammon MD, Chow WH, Dubrow R, Ahsan H, Mayne ST, Schoenberg JB, West AB, Rotterdam H, Fraumeni JF Jr, Blot WJ. Use of aspirin and other nonsteroidal antiinflammatory drugs and risk of esophageal and gastric cancer. *Cancer Epidemiol Biomarkers Prev* 1998; **7**: 97-102

5 **Garcia-Rodriguez LA**, Huerta-Alvarez C. Reduced risk of colorectal cancer among long-term users of aspirin and nonsteroidal antiinflammatory drugs. *Epidemiology* 2001; **12**: 88-93

6 **Morgan G**. Non-steroidal anti-inflammatory drugs and the chemoprevention of colorectal and nonaspirin oesophageal cancers. *Gut* 1996; **38**: 646-648

7 **Reeves MJ**, Newcomb PA, Trentham-Dietz A, Storer BE, Remington PL. Nonsteroidal anti-inflammatory drug use and protection against colorectal cancer in women. *Cancer Epidemiol Biomarkers Prev* 1996; **5**: 955-960

8 **Thun MJ**. NSAID use and decreased risk of gastrointestinal cancers. *Gastroenterol Clin North Amer*1996; **25**: 333-348

9 **Funkhouser EM**, Sharp GB. Aspirin and reduced risk of esophageal carcinoma. *Cancer* 1995; **76**: 1116-1119

10 **Zhuang ZH**, Wang LD. NSAID and digestive tract carcinomas. *Shijie Huaren Xiaohua Zazhi* 2001; **9**: 1050-1053

11 **Oshima M**, Dinchuk JE, Kargman SL, Oshima H, Hancock B, Kwong E, Trzaskos JM, Evans JF, Taketo MM. Suppression of intestinal polyposis in Apc deta716 knockout mice by inhibition of cyclooxygenase 2(COX-2). *Cell* 1996; **87**: 803-809

12 **Tsujii M**, Kawano S, DuBois RN. Cyclooxygenase-2 expression in human colon cancer cells increase metastatic potential. *Proc*

Natl Acad Sci USA 1997; **94**: 3336-3340

13 **Chan G**, Boyle JO, Yang EK, Zhang F, Sacks PG, Shah JP, Edelstein D, Soslow RA, Koki AT, Woerner BM, Masferrer JL, Dannenberg AJ. Cyclooxygenase-2 expression is up-regulated in squamous cell carcinome of the head and neck. *Cancer Res* 1999; **59**: 991-994

14 **Tucker ON**, Dannenberg AJ, Yang EK, Zhang F, Teng L, Daly JM, Soslow RA, Masferrer JL, Woerner BM, Koki AT, Fahey TJ. Cyclooxygenase-2 expression is up-regulated in human pancreatic cancer.*Cancer Res* 1999; **59**: 987-990

15 **Zimmermann KC**, Sarbia M, Weber AA, Borchard F, Gabbert HE, Schror K. Cyclooxygenase-2 expression in human esophageal carcinoma. *Cancer Res* 1999; **59**: 198-204

16 **Shiota G**, Okubo M, Noumi T, Noguchi N, Oyama K, Takano Y, Yashima K, Kishimoto Y, Kawasaki H. Cyclooxygenase-2 expression in hepatocellular carcinoma. *Hepatogastroenterology* 1999; **46**: 407-412

17 **Shirahama T**, Sakakura C. Overexpression of cyclooxygenase-2 in squamous cell carcinoma of the urinary bladder. *Clin Cancer Res* 2001; **7**: 558-561

18 **Soslow RA**, Dannenberg AJ, Rush D, Woerner BM, Khan KN, Masferrer J, Koki AT. COX-2 is expressed in human pulmonary, colonic,and mammary tumors. *Cancer* 2000; **89**: 2637-2645

19 **Wu QM**, Li SB, Wang Q, Wang DH, Li XB, Liu CZ. The expression of COX-2 in esophageal carcinoma and its relation to clinicoptahologic characteristics. *Shijie Huaren Xiaohua Zazhi* 2001; **9**: 11-14

20 **Qiu DK**, Ma X, Peng YS, Chen XY. Significance of cyclooxygenase-2 expression in human primary hepatocellular carcinoma. *World J Gastroenterol* 2002; **8**: 815-817

21 **Che X,** Hokita S, Natsugoe S, Tanabe G, Baba M, Takao S, Aikou T. Tumor angiogenesis related to growth pattern and lymph node metastasis in early gastric cancer. *Chin Med J* 1998; **111**: 1090-1093

22 **Shimoyama S**, Kaminishi M. Increased angiogenin expression in gastric cancer correlated with cancer progression. *J Cancer Res Clin Oncol* 2000; **126**: 468-474

23 **Yoshikawa T**, Yanoma S, Tsuburaya A, Kobayashi O, Sairenji M, Motohashi H, Noguchi Y. Angiogenesis inhibitor,TNP-470, suppresses growth of peritoneal disseminating foci. *Hepatogastroenterology* 2000; **47**: 298-302

24 **Xiangming C**, Hokita S, Natsugoe S, Tanabe G, Baba M, Takao S, Kuroshima K, Aikou T. Angiogenesis as an unfavorable factor related to lymph node metastasis in early gastric cancer. *Ann Surg Oncol* 1998; **5**: 585-589

25 **Maehara Y**, Hasuda S, Abe T, Oki E, Kakeji Y, Ohno S, Sugimachi K. Tumor angiogenesis and micrometastasis in bone marrow of patients with early gastric cancer.*Clin Cancer Res* 1998; **4**: 2129-2134

26 **Weidner N**, Folkman J, Pozza F, Bevilacqua P, Allred EN, Moore DH, Meli Gasparini G. Tumor anginogenesis:a new significant and independent prognostic indicator in early state breast carcinoma. *J Natl Cancer Inst* 1992; **84**: 1875-1887

27 **Mizuno H**, Sakamoto C, Matsuda K, Wada K, Uchida T, Noguchi H, Akamatsu T, Kasuga M. Induction of cyclooxygenase 2 in gastric mucosal lesions and its inhibition by the specific antagonigt delays healing in mice. *Gastroenterology* 1997; **112**: 389-397

28 **Kargman S**, Charleson S, Cartwright M, Frank J, Riendeau D, Mancini J, Evans J, O'Neill G. Characterization of prostaglandin G/H synthase 1 and 2 in rat, dog, monkey and human gastrointestinal tracts. *Gastroenterology* 1996; **111**: 445-454

29 **Uefujk K**, Ichikura T, Mochizuki H, Shinomiya N. Expression of cyclooxygenase-2 protein in gastric adenocarcinoma. *J Surg Oncol* 1998; **69**: 168-172

30 **Ratnasinghe D,** Tangrea JA, Roth MJ, Dawsey SM, Anver M, Kasprzak BA, Hu N, Wang QH, Taylor PR. Expression of cyclooxygenase-2 in human adenocarcinomas of the gastric cardia and corpus. *Oncel Rep* 1999; **6**: 965-968

31 **Lim HY**, Joo HJ, Choi JH, Yi JW, Yang MS, Cho DY, Kim H, Nam DK, Lee KB, Kim HC. Increased expression of cyclooxygenase-2 protein human gastric carcinoma. *Chin Cancer Res* 2000; **6**: 519-525

32 **van Rees BP**, Saukkonen K, Ristimaki A, Polkowski W, Tytgat GN, Drillenburg P, Offerhaus GJ. Cyclooxygenase-2 expression during carcinogenesis in the human stomach. *J Pathol* 2002; **196**: 171-179

33 **Ohon R**, Yoshinaga K, Fujita T, Hasegawa K, Iseki H, Tsunozaki H, Ichikawa W, Nihei Z, Sugihara K. Depth of invasion parallels increased cyclooxygenase-2 levels in patents with gastric carcinoma. *Cancer* 2001; **91**: 1876-1881

34 **Xue YW**, Zhang QF, Zhu ZB, Wang Q, Fu SB. Expression of cyclooxygenase-2 and clinicopathologic features in human gastric adenocarcinoma. *World J Gastroenterol* 2003; **9**: 250-253

35 **Murata H**, Kawano S, Tsuji S, Tsuji M, Sawaoka H, Kimura Y, Shiozaki H, Hori M. Cyclooxgenase-2 overexpressing enhances lymphatic invasion and metastasis in human gastric carcinoma. *Am J Gastroenterology* 1999; **94**: 451-455

36 **Tsujii M**, DuBois RN. Alterations in cellular adhesion and apoptosis in epithelial cells overexpressing prostaglandin endoperoxide synthase-2. *Cell* 1995; **83**: 493-501

37 **Form DM**, Auerbach R. PGE2 and angiogenesis. *Proc Soc Exp Biol Med* 1983; **172**: 214-218

38 **Hanahan D**, Folkman J. Patterns and emerging mechenisms of the angiogenic swithch during tumorigenesis. *Cell* 1996; **86**: 353-364

39 **Masferrer JL**, Koki A, Seibert K. COX-2 inhibitors.A new class of antiangiogentic agents. *Ann N Y Acad Sci* 1999; **889**: 84-86

40 **Masferrer JL**, Leahy KM, Koki AT, Zweifel BS, Settle SL, Woerner BM, Edwards DA, Flickinger AG, Moore RJ, Seibert K. Antiangiogenic and antitumor activities of cyclooxygenase-2 inhibitors. *Cancer Res* 2000; **60**: 1306-1311

41 **Fukumura D**, Jain RK. Role of nitric oxide in angiogenesis and microcirculation in tumors. *Cancer Metastasis Rev* 1998; **17**: 77-89

Edited by Xu JY

P.O.Box 2345, Beijing 100023, China
Fax: +86-10-85381893
E-mail: wjg@wjgnet.com www.wjgnet.com

World J Gastroenterol 2003;9(4):678-682
World Journal of Gastroenterology
 ISSN 1007-9327

• LIVER CANCER •

Expression, purification and serological analysis of hepatocellular carcinoma associated antigen HCA587 in insect cells

Bing Li, Hong-Yan Wu, Xiao-Ping Qian, Yan Li, Wei-Feng Chen

Bing Li, Hong-Yan Wu, Xiao-Ping Qian, Yan Li, Wei-Feng Chen, Immunology Department of Peking University Health Science Center, Beijing, 100083, China
Supported by National "973" foundation, No. G1999053904 and "863" foundation, No. 2001AA215411
Correspondence to: Dr. Wei-Feng Chen, Immunology Department of Peking University Health Science Center, 38 Xueyuan Road, Beijing, 100083, China. wfchen@public.bta.net.cn
Telephone: +86-10-62091155 **Fax**: +86-10-62091436
Received: 2002-12-08 **Accepted:** 2003-01-02

Abstract

AIM: In order to assess hepatocellular carcinoma associated antigen HCA587 as a potential target for immunotherapy, the Bac-to-Bac expression system was used to express recombinant protein HCA587 in insect cells.

METHODS: The cDNA encoding HCA587 gene was cloned into donor vector pFasBacHtb and recombinant pFasBac Htb-587 was transformed into competent cells DH10Bac. Recombinant Bacmid-587 was transfected into Sf9 insect cells using CELLFECTIN, Recombinant HCA587 protein was produced in Sf9 insect cells after infection with recombinant baculovirus, and was purified using Ni-NTA resin. Sera from HCC patients were also screened using recombinant protein HCA587.

RESULTS: The molecular weight of the recombinant protein HCA587 expressed in insect cells was approximately 43kd. Western blot results proved the recombinant protein HCA587 had the similar antigenicity with its native counterpart. Serological analysis told that the rate of seroreactivity to HCA587 was not high in HCC patients.

CONCLUSION: The recombinant protein HCA587 was successfully expressed and purified using Bac-to-Bac expression system. It paved the way for generation of specific antibody and investigation of immunohistochemical analysis and immune responses of HCC in the future.

Li B, Wu HY, Qian XP, Li Y, Chen WF. Expression, purification and serological analysis of hepatocellular carcinoma associated antigen HCA587 in insect cells. *World J Gastroenterol* 2003; 9 (4): 678-682
http://www.wjgnet.com/1007-9327/9/678.htm

INTRODUCTION

The recent developments in the molecular characterization of human tumors and a better understanding of tumor immunology have led to the identification of different kinds of tumor-associated antigens[1-5]. Of these antigens, Cancer/testis antigens (CT antigens) have played important roles as targets for cancer vaccine development because of their characteristic expression pattern in cancer and testis[6-9]. Many promising results have been achieved in tumor immunotherapy using peptides derived from CT antigens[10-13]. Identifying new CT antigens and evaluating their possible application in the clinic have become a hot spot in this field.

Since hepatocellular carcinoma (HCC) is one of the most pernicious cancers in China, we have adopted serological analysis of recombinant cDNA expression library (SEREX) method and successfully identified a number of novel HCC genes encoding immunogenic proteins. Of these, hepatocellular carcinoma associated antigen HCA587 was identified as one novel CT antigen which was predominantly expressed in HCC and other types of cancers, but not in normal tissues except testis[14]. Studies on HCA587 may play important roles in transformation, metastasis, diagnosis and immunotherapy of HCC.

The bac-to-bac baculovirus expression system is an eukaryotic gene expression system which allows the rapid and efficient generation of recombinant baculovirus DNAs by site-specific transposition in *E.coli*, rather than homologous recombinant in insect cells[15,16]. High level heterologous gene expression are often achieved compared to other eukaryotic expression systems, and most of the expressed proteins were shown to have the similar functions as their authentic counterparts. In the present studies, we utilized the Bac-to-Bac system to express the recombinant protein HCA587 in *Spodoptera frugiperda* (sf9) cell lines. The HCA587 protein was then purified using Ni-NTA resin, and the anti-HCA587 antibodies were screened in sera from 81 HCC patients.

MATERIALS AND METHODS

Expression system, insect cells and sera

The Gibco BRL BAC-TO-BAC Baculovirus expression system consists of the transposing vector pFasBacHTb, CELLFECTIN reagent and Max Efficiency DH10Bac competent cells which contain Bacmid (baculorivus shuttle vector plasmid) and helper plasmid to be used to generate recombinant Bacmids. *Sf9* insect cells were cultured at 27 ℃ in SF-900 SFM (Cell culture media and reagents were Gibco BRL brand). All sera of HCC were collected from Peking University teaching hospitals with the agreements of HCC patients.

Amplification and DNA sequencing of gene HCA587

The oligonucleotide primers specific for gene HCA587 were designed and synthesized by Sangon biotechnology company (P1: 5' ATCGGATCCCCTCCCGTTCCAGGCGT 3', P2: 5' ACTAAGCTTTCACTCAGAAAAGGAGAC 3'). The cDNA produced from normal testis was amplified as template. The PCR products were cloned into pGEM-T-easy vector and sequenced with T7 and SP6 primers by the dideoxy chain termination method using the BigDye Terminator cycle sequencing kit and an ABI PRISM automated DAN sequencer.

Construction of pFasBac HTb-587 plasmid

pFasBac HTb donor plasmid and pGEM-T-easy-587 were prepared by digesting with restriction enzymes BamHI and HindIII. The fragments of interests were purified and recovered from gel using clontech DNA purification system. After ligated

by T4 DNA ligase, the ligation mixture were transformed into DH5α competent cells. The recombinant plasmid pFasBac HTb-587 was identified by restriction endonuclease digestion.

Generation of recombinant bacmid DNA

Recombinant pFasBac HTb-587 plasmids were transformed into Max Efficiency DH10Bac competent cells, and the gene of interest was transposed into Bacmid through lacZ gene disruption. White clones, containing the recombinant Bacmids were selected on Luria agar plates with 50 μg/ml kanamycin, 7 μg/ml gentamicin, 10 μg/ml tetracycline, 100 μg/ml Bluogal, and 40 μg/ml IPTG. After 36 h incubation at 37 ℃, High-molecular-weight DNA was isolated from the overnight cultures as described in the manual. PCR analysis was used to verify successful transposition to the recombinant Bacmid with M13/pUC primes.

Transfection of Sf9 cells with recombinant bacmid-587

The minipreparations of recombinant Bacmid DNA were transfected into *Sf9* insect cells using CELLFECTIN reagent. For each transfection, 9×10^5 cells were seeded in a 6-well plate and allowed to attach for at least 1 h. The Lipid reagent and Bacmid DNA were diluted separately into 100 μl of SF-900 SFM without antibiotics, then combined to form lipid-DNA complexes. The lipid-DNA complexes were diluted to 1 ml with SFM and laid over the washed Sf9 cells. The cells were incubated for 5 h at 27 ℃, rinsed, and incubated for another 72 h. Recombinant baculovirus were harvested from supernatant and titrated by viral plaque assay. The expression of recombinant protein HCA587 was analyzed by western blot.

Expression and purification of HCA587 from Sf9 insect cells

The recombinant baculovirus were amplified from the suspension cultures of *Sf9* cells at MOI of 0.1. We analyzed the effects of several factors in various combinations on the level of protein expression, the factors were: adherent or suspension cultures in different densities; multiplicity of infection (MOI) and recombinant virus replication time. Since the expressed recombinant protein contained 6×histidine tag at N-terminal, it was purified using Ni-NTA resin conveniently according to the manufacturer' s instructions. SDS-PAGE was performed to analyze the purified protein from the infected cells.

Serological analysis of recombinant HCA587 protein

To analyze the anti-HCA587 antibody in sera of patients, Western blot method was used to screen the reactivity of recombinant HCA587 to sera from 81 HCC patients. The serum was diluted 1/250 as primary antibody, and rabbit-anti- human IgG, conjugated to AP, were used as secondary antibodies. In this assay, the negative control was the serum from healthy volunteers.

RESULTS

Identification of recombinant pFasBacHTb-587 and Bacmid-587

The fragments of gene HCA587 were amplified by PCR using specific primers (Figure 1) and sequenced to ensure the correctness of the ORF. Restriction endonuclease digestion was performed to verify the correct insertion of the gene HCA587 in the recombinant pFasBacHTb-587. The gel electrophoresis in 1 % agarose showed 1.2kb of HCA587 and 4.8kb of pFasBacHTb donor plasmid (Figure 2).

The Bacmid DNA is >135kb. Verification of the insertion of the gene HCA587 in recombinant Bacmid-587 is difficult using classical restriction endonuclease digestion analysis. So PCR was used to confirm the recombinant Bacmid-587. The pUC/M13 amplification primers are directed at sequences on either side of the mini-attTn7 site with the lacZ α-complemention region of the Bacmid. Amplification products from transposition of recombinant bacmid-587 generated a band of 3.5kb (lane1,2) while amplification of the non-recombinant Bacmid plasmid generated a 300bp band (lane3,4) (Figure 3).

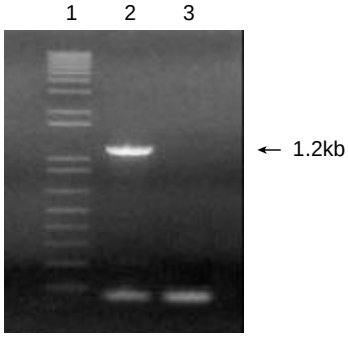

Figure 1 PCR amplified products of HCA587. (Lanes 1: 1 kb DNA marker; lane2: 1.2 kb fragment of HCA587; lane3: negative control).

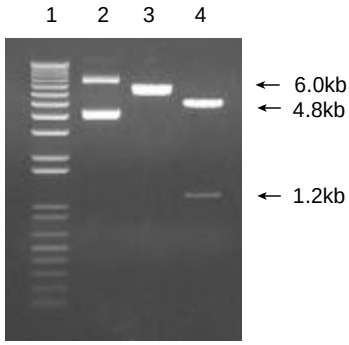

Figure 2 Recombinant pFasBac Htb-587 vector digested by BamHI and HindIII. (Lanes1: 1kb DNA marker; lane2: recombinant plasmid; lane3: digested by BamHI; lane4: digested by BamHI+HindIII).

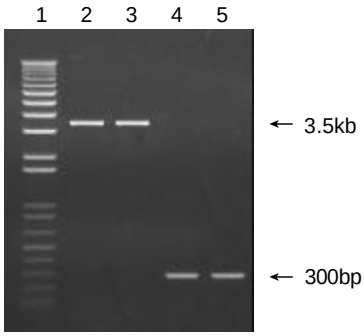

Figure 3 PCR identification of recombinant Bacmid-587. (lane 1: DNA marker; lane 2-3: recombinant Bacmid-587; lane 4-5: blank bacmid).

Transfection of Sf9 cells and amplification of recombinant virus

Recombinant Bacmid-587 was isolated from overnight cultures and transfected into insect cells sf9 with CELLFECTIN reagents. Infected and uninfected sf9 cells can be distinguished by morphology. Uninfected cells continued to divide and form a confluent monolayer while infected cells stopped dividing and enlarged (data not shown).

The Bacmid-587 transfected cells were collected and

analyzed for recombinant protein expression by western blot. Figure 4 showed a specific expressed protein band at 43kd as expected, while no specific band apperared in Sf9 cells without transfection (lane 3). Viral plaque assay showed the viral titer could reach 5×10^8 pfu/ml after amplifying the primary virus in *Sf9* suspension cell culture.

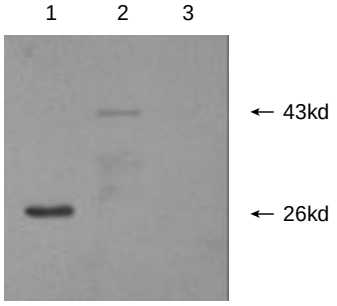

Figure 4 Western blot analysis of recombinant protein expression in sf9 insect cells after transfection. (lane 1: positive control; lane2: Sf9 cell transfected with bacmid-587; lane 3: blank Sf9 cells).

SDS-PAGE analysis of purified HCA587 protein

The optimal conditions varies to express different proteins. Recombinant HCA587 protein was expressed at the highest level when 1×10^6 *Sf9* cells/ml were infected with an MOI of 5 and harvested after 96 h of replication. After purification with chromatography using Ni-NTA resin, the purified protein, infected and uninfected *Sf9* cells were lysed directly in SDS-loading buffer and boiled for 5 min. All samples were cleared by centrifugation and analyzed on 12.5 % acrylamide gels, which was stained by Coomassie blue and scanned by a densitometer to visualize the purity of purified protein. Figure 5 showed that the recombinant protein with 43kd was more than 90 % purity.

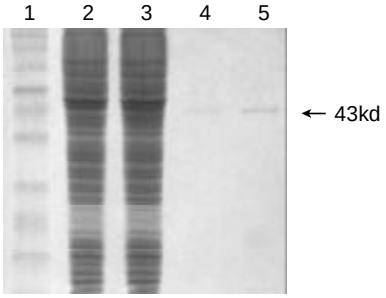

Figure 5 SDS-PAGE analysis of recombinant HCA587. (lane 1: protein marker; lane2: sf9 lysate; lane3: infected sf9 lysate; lane4-5: purified HCA587 protein).

Identification of antigenicity of the recombinant protein HCA587

In order to know if the recombinant protein HCA587 has the similar antigenicity with its native counterpart, the serum containing antibodies which recognize native HCA587 was used as primary antibody in western blot analysis. Figure 6 showed that the recombinant protein HCA587 was able to react with the specific antibody in serum (lane 2) while no reactivity was seen in negative control (lane 3), indicating it' s similar functions with natural counterpart.

Reactivity of allogeneic HCC sera to recombinant protein HCA587

To determine the anti-HCA587 antibody produced in HCC patients, Sera collected from 81 allogeneic HCC patients were screened to test their reactivities with the recombinant protein HCA587 expressed from *Sf9* insect cells. The positive frequency of antibody response in HCC patients was not high, with only 2 positive of 81 patients (Figure 7, negative results not shown). This low late of serological reactivities was also shown in other CT antigens[24].

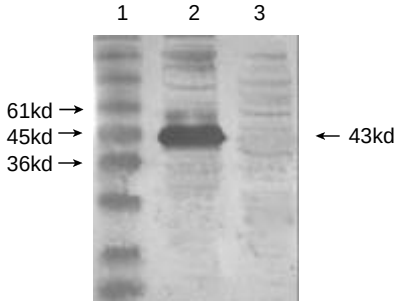

Figure 6 Western blot of recombinant HCA587 reacting with positive serum. (lane 1: protein marker; lane 2: positive serum of HCC; lane 3: negative control).

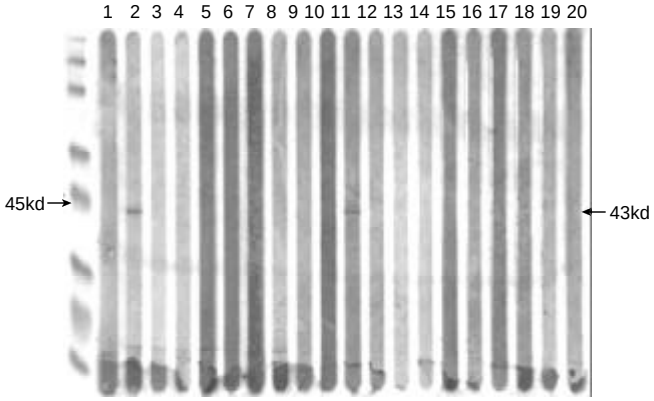

Figure 7 Serological analysis of HCC patients with recombinant protein HCA587. (lane 2 and 11: positive; others: negative; left: protein marker).

DISCUSSION

HCA587 was one of the SEREX-defined CT antigens identified from HCC patients[14]. The protein of HCA587 was immunogenic and capable of inducing an antibody response as it was cloned by serologic method from the sera of HCC patients. In view that the SEREX-defined NY-ESO-1 can induce a CTL response and CTL-defined MAGE-1 has also been identified by SEREX[17,18], this suggests that HCA587, as a CT antigen, may possibly contain both B and T epitopes and can elicit CTL responses. Because CTLs represent a major arm of the immune response against cancer, the elicitation of a specific CTL response against tumor Ags is one of the main aims of current immunotherapy trial. Therefore, it is crucial to define $CD8^+$ T cell epitopes in HCA587 protein, which may determine its potential vaccine candidates for HCC immunotherapy. In addition, the mRNA expression rate of CT antigens can reach 70 %(14/20) in liver cancer tissues from HCC patients but not in normal liver tissue or cirrhosis, indicating its potential functions in tumorigenesis[14]. Current knowledge about this expression pattern is mainly based on RT-PCR analysis, not based on protein levels[19-21], So immunohistochemical analysis of HCA587 antigen expression in HCC tissues is very necessary. Expression and purification of HCA587 protein makes both CTL-mediated responses and immunlohistochemical study become possible.

Bac-to-Bac baculovirus expression system was developed which allows rapid and efficient generation of recombinant baculovirus. With this system, recombinant virus DNA isolated from selected colonies is not mixed with parental virus which eliminate the need for multiple rounds of plaque purification. High-titer virus are produced from the initial transfection too. These features reduce the time to identify and purify recombinant virus from 4 to 6 weeks to 7 to 9 days. In the present study, The cDNAs of the HCA587 were subcloned into pFasBacHTb donor vector at the BamHI and HindIII sites. The recombinant bacmid-587 was constructed by transposing a mini-Tn7 element from a pFasBacHTb donor plasmid to the mini-*att*Tn7 attachment site on the bacmid when the Tn7 transposition functions are provided in *trans* by a helper plasmid in DH10Bac competent cells. After transfecting the recombinant bacmid-587 to Sf9 cells, we successfully expressed and purified the recombinant protein HCA587 which contained 333 amino acids with 6 his tags at its N-termianl, which makes the purification procedure more convenient with its high affinity to Ni-NTA resin[22,23].

Western blot analysis showed that the recombinant protein HCA587 has the similar immunological reactivity with its natural counterpart (Figure 6). It was used as antigen to screen the generation of anti-HCA587 antibody in serum from HCC patients. The results proved that HCC patients was able to develop humoral immune response to HCA587 antigen, but the frequency is not high (2/81). This low rate of seroreactivity to allogeneic sera is similar to some other CT antigens, either defined by a $CD8^+$ CTL response (MAGE-1)[24] or by SEREX (SSX-2)[25]. In a survey of humoral responses of cancer patients against recombinant tumor antigens, it was indeed shown that seroreactivity to MAGE gene products is uncommon, and sera from 234 cancer patients showed antibodies to MAGE-1 in 3, to MAGE-3 in 2, and to SSX-2 in 1 patient[24]. Since many members of MAGE family have been shown to be recognized by CTL from cancer patients[26-30], it would be important to investigate possible HCA587 epitopes recognized by $CD8^+$ and $CD4^+$ cells. In conclusion, our experiments pave the way for further study of HCA587 for the development of tumor vaccine and clinical tumor diagnosis.

REFERENCES

1 **Schultze JL**, Vonderheide RH. From cancer genomics to cancer immunotherapy: toward second-generation tumor antigens. *Trends in immunology* 2001; **22**: 516-523

2 **Krackhardt AM**, Witzens M, Harig S, Hodi FS, Zauls AJ, Chessia M, Barrett P, Gribben JG. Identification of tumor-associated antigens in chronic lymphocytic leukemia by SEREX. *Blood* 2002; **100**: 2123-2131

3 **Chomez P**, De Backer O, Bertrand M, De Plaen E, Boon T, Lucas S. An overview of the MAGE gene family with the identification of all human members of the family. *Cancer research* 2001; **61**: 5544-5551

4 **Offringa R**, van der Burg SH, Ossendorp F, Toes RE, Melief CJ. Design and evaluation of antigen-specific vaccination strategies against cancer. *Current opin Immunol* 2000; **12**: 576-582

5 **Perico ME**, Mezzanzanica D, Luison E, Alberti P, Panza L, Russo G, Canevari S. Development of a new vaccine formulation that enhances the immunogenicity of tumor-associated antigen CaMBr1. *Cancer Immunol Immunother* 2000; **49**: 296-304

6 **Jager D**, Jager E, Knuth A. Immune responses to tumor antigens: implications for antigen specific immunotherapy of cancer. *J Clin Pathol* 2001; **54**: 669-674

7 **Scanlan MJ**, Gure AO, Jungbluth AA, Old LJ, Chen YT. Cancer/testis antigens: an expanding family of targets for cancer immunotherapy. *Immunol Rev* 2002; **188**: 22-32

8 **Gure AO**, Stockert E, Arden KC, Boyer AD, Viars CS, Scanlan MJ, Old LJ, Chen YT. CT10: a new cancer testis(CT) antigen homologous to CT7 and the mage family, identified by RDA. *Int J Cancer* 2000; **85**: 726-732

9 **Tureci O**, Sahin U, Zwick C, Koslowski M, Seitz G, Pfreundschuh M. Identification of a meiosis-specific protein as a member of the class of cancer/testis antigens. *Proc Natl Acad Sci USA* 1998; **95**: 5211-5216

10 **Thurner B**, Haendle I, Roder C, Dieckmann D, Keikavoussi P, Jonuleit H, Bender A, Maczek C, Schreiner D, von den Driesch P, Brocker EB, Steinman RM, Enk A, Kampgen E, Schuler G. Vaccination with Mage-3A1 peptide-pulsed mature, monocyte-derived dendritic cells expands specific cytotoxic T cells and induceds regression of some metastases in advanced stage IV melanoma. *J EXP Med* 1999; **190**: 1669-1678

11 **Marchand M**, van Baren N, Weynants P, Brichard V, Dreno B, Tessier MH, Rankin E, Parmiani G, Arienti F, Humblet Y, Bourlond A, Vanwijck R, Lienard D, Beauduin M, Dietrich PY, Russo V, Kerger J, Masucci G, Jager E, De Greve J, Atzpodien J, Brasseur F, Coulie PG, van der Bruggen P, Boon T. Tumor regressions observed in patients with metastatic melanoma treated with an antigen peptide encoded by gene Mage-3 and presented by HLA-A1. *Int J Cancer* 1999; **80**: 219-230

12 **Fujie T**, Tahara K, Tanaka F, Mori M, Takesako K, Akiyoshi T. A mage-1-encoded HLA-A24-binding synthetic peptide induces specific anti-tumor cytotoxic T lymphocytes. *Int J Cancer* 1999; **80**: 169-172

13 **Ayyoub M**, Stevanovic S, Sahin U, Guillaume P, Servis C, Rimoldi D, Valmori D, Romero P, Cerottini JC, Rammensee HG, Pfreundschuh M, Speiser D, Levy F. Proteasome-assisted identification of a SSX-2-derived epitope recognized by tumor-reactive CTL infiltrating metastatic melanoma. *J Immunol* 2002; **168**: 1717-1722

14 **Wang Y**, Han KJ, Pang XW, Vaughan HA, Qu W, Dong XY, Peng JR, Zhao HT, Rui JA, Leng XS, Cebon J, Burgess AW, Chen WF. Large scale identification of human hepatocellular carcinoma-associated antigens by autoantibodies. *J Immunol* 2002; **169**: 1102-1109

15 **Schmidt M**, Olejnik AK, Stepien K, Olejnik AM, Butowska W, Grajek W, Warchol JB, Gozdzicka-Jozefiak A. Production of human papillomavirus type 16 early proteins in Bac-To-Bac Expression System (GibcoBRL). *Folia Histochem Cytobiol* 2001; **39**: 125-126

16 **Joshua MN**, Qi Y, Fu HY, Yong XH. Comparison of the biological activities of human immunodeficiency virus 1 P24 and GP41 expressed in Spodoptera frugiperda cells by use of bac-to-bac system. *Acta Virol* 2000; **44**: 125-130

17 **Jager E**, Nagata Y, Gnjatic S, Wada H, Stockert E, Karbach J, Dunbar PR, Lee SY, Jungbluth A, Jager D, Arand M, Ritter G, Cerundolo V, Dupont B, Chen YT, Old LJ, Knuth A. Monitoring CD8 T cell responses to NY-ESO-1: correlation of humoral and cellular immune responses. *PNAS* 2000; **97**: 4760-4765

18 **Chen YT**, Gure AO, Tsang S, Stockert E, Jager E, Knuth A, Old LJ. Identification of multiple cancer/testis antigens by allogenic antibody screening of a melanoma-cell line library. *PNAS* 1998; **95**: 6919-6923

19 **Scanlan MJ**, Gordon CM, Williamson B, Lee SY, Chen YT, Stockert E, Jungbluth A, Ritter G, Jager D, Jager E, Knuth A, Old LJ. Identification of cancer/testis genes by database mining and mRNA expression analysis. *Int J Cancer* 2002; **98**: 485-492

20 **Zendman AJ**, van Kraats AA, den Hollander AI, Weidle UH, Ruiter DJ, van Muijen GN. Characterization of XAGE-1b, a short major transcript of cancer/testis-associated gene XAGE-1, induced in melanoma metastasis. *Int J Cancer* 2002; **97**: 195-204

21 **Scanlan MJ**, Altorki NK, Gure AO, Williamson B, Jungbluth A, Chen YT, Old LJ. Expression of cancer-testis antigens in lung cancer: definition of bromodomain testis-specific gene (BRDT) as a new CT gene, CT9. *Cancer Let* 2000; **150**: 155-164

22 **Nakajima M**, Hirakata M, Nittoh T, Ishihara K, Ohuchi K. Expression and purification of recombinant rat eosinophil-associated ribonucleases, homologues of human eosinophil cationic protein and eosinophil-derived neurotoxin, and their characterization. *Int Arch Allergy Immunol* 2001; **125**: 241-249

23 **Jungbluth AA**, Chen YT, Busam KJ, Coplan K, Kolb D, Iversen K, Williamson B, Van Landeghem FK. CT7 (MAGE-C1) antigen expression in normal and neoplastic tissues. *Int J Cancer* 2002; **99**: 839-845

24 **Stockert E**, Jager E, Chen YT, Scanlan MJ, Gout I, Karbach J, Arand

M, Knuth A, Old LJ. A survey of the humoral immune response of cancer patients to a panel of human tumor antigens. *J Exp Med* 1998; **187**: 1349-1354

25 **Sahin U**, Tureci O, Pfreundschuh M. Serological identification of human tumor antigens. *Curr Opin Immunol* 1997; **9**: 709-716

26 **Oiso M**, Eura M, Katsura F, Takiguchi M, Sobao Y, Masuyama K, Nakashima M, Itoh K, Ishikawa T. A newly identified MAGE-3-derived epitope recognized by HLA-A24-restricted cytotoxic T lymphocytes. *Int J Cancer* 1999; **81**: 387-394

27 **Serrano A**, Lethe B, Delroisse JM, Lurquin C, De Plaen E, Brasseur F, Rimoldi D, Boon T. Quantitative evaluation of the expression of MAGE genes in tumors by limiting dilution of cDNA libraries. *Int J Cancer* 1999; **83**: 664-669

28 **Schultz ES**, Chapiro J, Lurquin C, Claverol S, Burlet-Schiltz O, Warnier G, Russo V, Morel S, Levy F, Boon T, Van den Eynde BJ, van der Bruggen P. The production of a new MAGE-3 peptide presented to cytolytic T lymphocytes by HLA-B40 requires the immunoproteasome. *J Exp Med* 2002; **195**: 391-399

29 **Chaux P**, Luiten R, Demotte N, Vantomme V, Stroobant V, Traversari C, Russo V, Schultz E, Cornelis GR, Boon T, Van der Bruggen P. Identification of five MAGE-A1 epitopes recognized by cytolytic T lymphocytes obtained by *in vitro* stimulation with dendritic cells transduced with MAGE-A1. *J Immunol* 1999; **163**: 2928-2936

30 **Graff-Dubois S**, Faure O, Gross DA, Alves P, Scardino A, Chouaib S, Lemonnier FA, Kosmatopoulos K. Generation of CTL recognizing an HLA-A*0201-restricted epitope shared by MAGE-A1, -A2, -A3, -A4, -A6, -A10, and -A12 tumor antigens: implication in a broad-spectrum tumor immunotherapy. *J Immunol* 2002; **169**: 575-580

Edited by Ren SY

P.O.Box 2345, Beijing 100023, China
Fax: +86-10-85381893
E-mail: wjg@wjgnet.com www.wjgnet.com

World J Gastroenterol 2003;9(4):683-687
World Journal of Gastroenterology
 ISSN 1007-9327

• LIVER CANCER •

Gene expression profiles of hepatoma cell line HLE

Lian-Xin Liu, Zhi-Hua Liu, Hong-Chi Jiang, Wei-Hui Zhang, Shu-Yi Qi, Jie Hu, Xiu-Qin Wang, Min Wu

Lian-Xin Liu, Hong-Chi Jiang, Wei-Hui Zhang, Department of Surgery, the First Clinical College, Harbin Medical University, Harbin 150001, Heilongjiang Province, China
Lian-Xin Liu, Zhi-Hua Liu, Xiu-Qin Wang, Min Wu, National Labortory of Molecular Oncology, Department of Cell Biology, Cancer Institute, Chinese Academy of Medical Science & Peking Union Medical College, Beijing 100021, China
Shu-Yi Qi, Jie Hu, Department of VIP, the First Clinical College, Harbin Medical University, Harbin 150001, Heilongjiang Province, China
Supported by China Key Program on Basic Research, No.Z-19-01-01-02; Chinese Climbing Project, No.18; Youth Natural Scientific Foundation of Heilongjiang Province and Harbin, No.QC01C11
Correspondence to: Dr. Lian-Xin Liu, Department of Surgery, the First Clinical College of Harbin Medical University, No.23 Youzheng Street, Nangang District, Harbin 150001, China. liulianxin@sohu.com
Telephone: +86-451-3668999 **Fax:** +86-451-3670428
Received: 2002-10-17 **Accepted:** 2002-12-16

Abstract

AIM: To investigate the global gene expression of cancer related genes in hepatoma cell line HLE using Atlas Human Cancer Array membranes with 588 well-characterized human genes related with cancer and tumor biology.

METHODS: Hybridization of cDNA blotting membrane was performed with ^{32}P-labeled cDNA probes synthesized from RNA isolated from Human hepatoma cell line HLE and non-cirrhotic normal liver which was liver transplantation donor. AtlasImage, a software specific to array, was used to analyze the result. The expression pattern of some genes identified by Atlas arrays hybridization was confirmed by reverse transcription polymerase chain reaction (RT-PCR) in 24 pairs of specimens and Northern blot of 4 pairs of specimens.

RESULTS: The differential expression of cell cycle/growth regulator in hepatocellular carcinoma (HCC) showed a stronger tendency toward cell proliferation with more than 1.5-fold up-regulation of Cyclin C, ERK5, ERK6, E2F-3, TFDP-2 and CK4. The anti-apoptotic factors such as Akt-1 were up-regulated, whereas the promotive genes of apoptosis such as ABL2 were down-regulated. Among oncogene/tumors suppressors, SKY was down-regulated. Some genes such as Integrin beta 8, Integrin beta 7, DNA-PK, CSPCP, byglycan, Tenacin and DNA Topo were up-regulated. A number of genes, including LAR, MEK1, eps15, TDGF1, ARHGDIA were down-regulated. In general, expression of the cancer progression genes was up-regulated, while expression of anti-cancer progression genes was down-regulated. These differentially expressed genes tested with RT-PCR were in consistent with cDNA array findings.

CONCLUSION: Investigation of these genes in HCC is helpful in disclosing molecular mechanism of pathogenesis and progression of HCC. For the first time few genes were discovered in HCC. Further study is required for the precise relationship between the altered genes and their correlation with the pathogenesis of HCC.

Liu LX, Liu ZH, Jiang HC, Zhang WH, Qi SY, Hu J, Wang XQ, Wu M. Gene expression profiles of hepatoma cell line HLE. *World J Gastroenterol* 2003; 9(4): 683-687
http://www.wjgnet.com/1007-9327/9/683.htm

INTRODUCTION

Hepatocellular carcinoma (HCC) is one of the most common malignant tumors and ranks the eighth in incidence of human cancer in Asia, Africa and South Europe, and causes an estimated 1 million deaths annually. The molecular mechanism underling HCC is currently unknown[1-15]. Tumor development and progression involves a cascade of genetic alterations. Techniques frequently used in study of gene expression, such as RT-PCR, differential display PCR and Northern blot analysis, have their limitations including requirement of large amounts of RNA, time-consuming, and limited number of genes being tested simultaneously. Hence, analysis of expression profiles of a large number of genes in hepatoma cell line is an essential step toward clarifying the detailed mechanisms of hepatocarcinogenesis and discovering target molecules for the development of novel therapeutic drugs.

DNA microarray enables investigators to study the gene expression profile and gene activation in thousands of genes and sequences[16-25]. In this study, we used cDNA expression microarray containing 588 genes related to carcinoma to analyze genes that are differentially expressed in human Hepatoma cell line HLE.

MATERIALS AND METHODS

Tissues and specimens

Four normal liver tissues without cirrhosis and 24 pairs of primary HCC and corresponding noncancerous liver tissues without cirrhosis were obtained with informed consent from patients who underwent liver transplantation and hepatectomy at the First Clinical College of Harbin Medical University. Histopathological identification was confirmed by the same pathologist. These specimens were immediately frozen in liquid nitrogen once obtained.

Cell culture

The HCC cell line HLE, epithelial-like cells, established from HCC patient in 1975 by Dr Dor was used in this study. HLE was cultured in RPMI1640 (Sigma, Saint Louis, USA) media containing 10 % fetal bovine serum, 1 % penicillin and streptomycin in a 37 ℃ incubator. Cells were harvested at 70-80 % confluence.

RNA isolation and purification

Total RNA of normal liver tissues was obtained by extracting frozen tissues in Trizol (Life Technologies Inc., Gaitherbur, MD) according to the manufacturer' s instructions. Normal liver were made in spices and homogenized in Trizol solution (1 ml/100 mg). Trizol was added into the bottles cultured with HLE, after washed with cold PBS. The concentration of RNA was assessed by absorbency at 260nm using a Nucleic Acid and Protein Analyzer (BECKMAN 470, USA).

cDNA microarray membrane

Atlas human cancer cDNA expression array (7742-1) was purchased from Clonech Laboratories Inc (Palo Alto, USA). The membrane contained 10 ng of each gene-specific cDNA from 588 known genes and 9 housekeeping genes. The cancer-related genes analyzed in this study were divided into six different groups according to its function.

cDNA synthesis, labeling and purification

Total RNA was reverse-transcribed into cDNA and labeled with α-^{32}P dCTP using Superscript™ Preamplification system for First Strand cDNA Synthesis Kit (Life Technologies, Gaithersburg, MD) following the manufacture' s instructions. The labeled first strand cDNA probes were purified by Spin 200 column (Clontech, Palo Alto, CA) to remove the unincorporated nucleotides.

Membrane hybridization and exposure

Different probes were added to tubes containing Atlas human cancer cDNA expression array, which were pre-hybridized at 68 ℃ for 2 hr, and hybridization was performed at 68 ℃ for 18 hr in rolling bottles. The membranes were washed strictly and exposed to X-ray films (Fuji Films, Tokyo, Japan) at -70 ℃ for 1-3 days.

Image and analysis

The images were scanned with Fluor-S MultiImager (Bio-Rad, Hercules, CA) and analyzed with AtlasImage analysis software Version 1.01a (Clontech, Palo Alto, CA). Human glyceraldehyde-3-phosphate dehydrogenase (*GAPDH*) was selected for normalization because its expression was constant in cancer array hybridization system. The normalized intensity of each spot representing a unique gene expression level was acquired. Genes were considered to be up-regulated when the intensity ratio was ≥1.5 or the difference was ≥10 000 between the expressions of HLE and normal liver tissues.

Semi-quantitative RT-PCR

To confirm the cDNA array results, semi-quantitative RT-PCR of 24 pairs of HCC tissues and normal liver tissues was performed for two genes (*TFDP2*, *E2F3*) displaying expression alterations. Twenty-five ml reaction mixture was performed under the following conditions: denaturation at 95 ℃ (3 min); 24 cycles of 94 ℃ (30 s), 60 ℃ (30 s) and 72 ℃ (45 s); then 72 ℃ extension (3 min). GAPDH were used as an internal reference in each PCR reaction. The 5 ml RT-PCR product was analyzed by electrophoresis on a 1.5% agarose gel.

Primer were as follows: GAPDH, forward primer 5' - ACCACAGTCCATGCCATCAC-3' and reverse primer 5' - TCCACCACCCTGTTGCTGTA-3' ; TFDP2, forward primer 5' - GGAGTCAGGCAAATGCTCTC-3' and reverse primer 5' - GCTAAGGCCACTTCTGCATC-3' ; E2F3, forward primer 5' - TTATGACTGCGTGAGCCTTAG-3' and reverse primer 5' - AGAGCCACAACAAAGAACAGA -3' .

Northern blot

RNAs of HCC and normal liver tissues were electrophoresed in a 1.5 % agarose gel containing 2.2M formaldehyde, and then transferred onto a nylon membrane (Zeta-Probe, Bio-Rad, USA) by capillary action. RNA was permanently attached to the membrane by UV illumination for 150 s (GS Gene Linker, Bio-Rad, USA). The hybridization probe was obtained by PCR. The primers were as follows: β-actin, forward primer 5' - CGTCTGGACCTGGCTGGCCGGGACC-3' and reverse primer 5' -CTAGAAGCATTTGCGGTGGACGATG-3' ; TFDP2, forward primer 5' - GGAGTCAGGCAAATGCTCTC -3' and reverse primer 5' - CTGCCCTCAGTATCCCTCAC-3' ; E2F3, forward primer 5' - AAGAGCAGGAGCAGAGAGATG-3' and reverse primer 5' - TTTGACAGGCCTTGACACTG-3' . α-^{32}P-labeled cDNA probes were synthesized using Primer-a-Gene random labeling Kit (Promega, USA). Hybridization was performed overnight in rolling bottles containing 8 ml of hybridization buffer. The membranes were washed and exposed to X-ray films (Fuji Films, Tokyo, Japan) at -70 ℃ for 24-48 h.

RESULTS

Atlas human cancer cDNA microarray expression profile

Using a cDNA expression microarray technique we established the expression profile of 588 genes selected from different areas in human hepatoma cell line HLE and normal liver tissues (Figure 1A, 1B). No signals were visible in the blank spots and negative control spots indicating that the Atlas human cancer array hybridization was highly specific. The intensity for housekeeping genes was similar at the same time indicating that the results were credible. GAPDH was used to normalize the intensities. The comparison results analyzed by AtlasImage software showed that there were 30 genes changed, 22 up-regulated and 8 down-regulated in Hepatoma cell line HLE versus normal liver tissues. In the test, the ratio one over the other ≥1.5 or the difference between two ≥10 000 was considered as up-regulated genes (Table 1).

Table 1 Genes differentially expressed between hepatoma cell line HLE and normal liver tissues generated by AtlasImage software (Version 1.01a)

Gene	Ratio	Difference	Protein / gene
F6k	0.361	-7908	TDGF1 + TDGF2 + TDGF3
B7g	0.412	-9606	SKY (DTK) (TYRO3) (RSE)
A5b	0.484	-8262	ERK activator kinase 1; MAPK / ERK kinase 1 (MEK1)
C5f	0.487	-8154	Epidermal growth factor receptor substrate (eps15)
E5b	0.504	-14946	Rho GDP-dissociation inhibitor 1
D6c	0.662	-10998	Semaphorin E
B7j	0.664	-12474	Tyrosine-protein kinase ABL2; tyrosine kinase ARG (ABLL)
F5l	0.732	-12132	Leukocyte interferon-inducible peptide
B2g	1.237	10252	TRAF-interacting protein (TRIP)
B3h	1.241	10508	Caspase-8 precursor; MACH; FLICE; (CAP4) (CASP8)
D5f	1.363	12000	CD9
C7l	1.381	14882	Retinoic acid receptor gamma
A3i	1.387	14088	CDK inhibitor p19INK4d
C7m	1.401	13224	Retinoid X receptor beta (RXR-beta)
C6n	1.444	11820	Sex gene
D3e	1.52	17176	Vitronectin precursor; serum spreading factor;
D4b	1.61	16212	Integrin alpha8
D2n	1.692	19718	TENASCIN-R
C1a	1.804	15096	DNA-dependent protein kinase (DNA-PK)
A4j	2.008	17856	Extracellular signal-regulated kinase 6 (ERK6) (ERK5)
D1b	2.038	20026	Byglycan
A7d	2.06	18522	Type II cytoskeletal 11 keratin; cytokeratin 1 (K1; CK 1);
A2k	2.061	18084	Cyclin C G1 / S-specific
D4j	2.178	27156	Integrin beta7
D4k	2.252	28122	Integrin beta8
A7g	2.257	13428	Type II cytoskeletal 4 keratin; cytokeratin 4 (K4; CK4)
D1a	2.31	29184	Cartilage-specific proteoglycan core protein (CSPCP); aggrecan1
A5i	2.418	10668	E2F-3
B4d	2.474	11814	Akt1; rac protein kinase alpha; protein kinase B; c-Akt
A5l	4.256	37824	DP2 dimerization partner of E2F

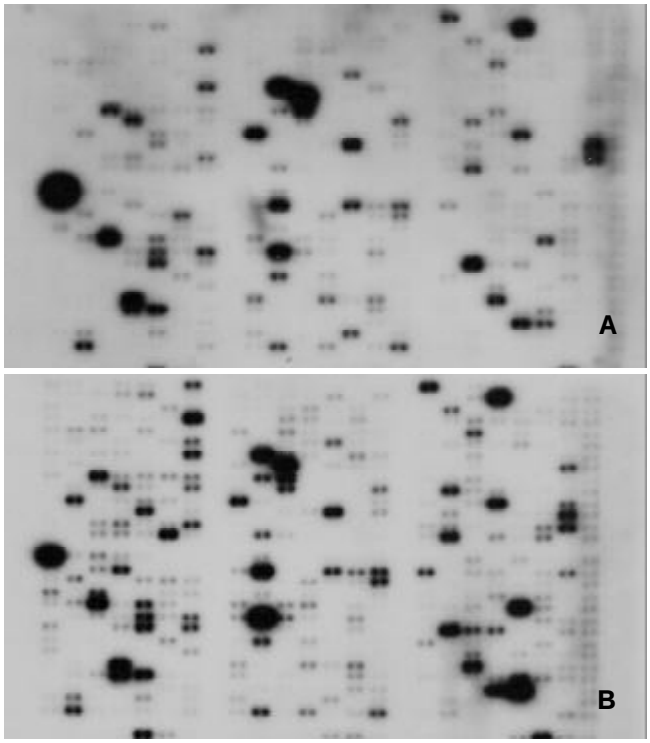

Figure 1 Parallel analyses of gene expression profiles in human hepatoma cell line HLE and normal liver tissues. Atlas human cancer cDNA expression array (Clontech, USA) was hybridized with ^{32}P-labeled cDNA probes in normal liver tissues (A) and human hepatoma cell line HLE (B).

Semi-quantitative RT-PCR

Twenty four paired tissues were performed for RT-PCR to verify accuracy and universality of the hybridization data. The RT-PCR results for 2 genes were consistent with hybridization data after normalization. Among the 24 paired tissues, the RT-PCR results of 2 genes were identical to the microarray results and the constituency was TFDP2 17/24, E2F3 16/24, respectively (Figure 2).

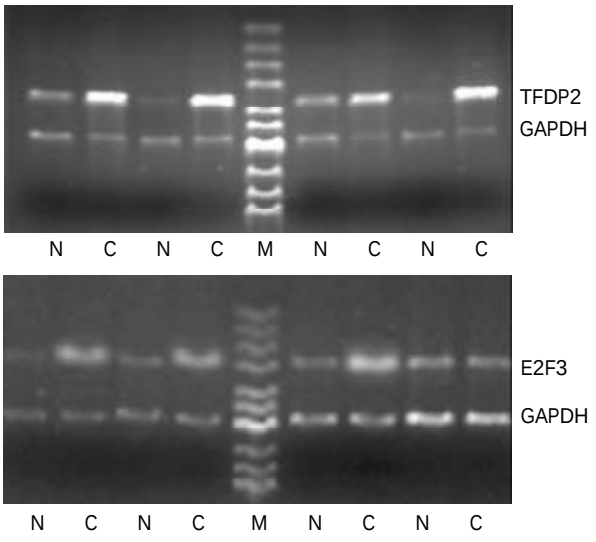

Figure 2 Partial semi-quantitative RT-PCR for 2 genes in 24 paired tissues. A total of 10 μl RT-PCR products were electrophoresed on 2 % agarose gel containing ethidium bromide. GAPDH was used as an internal control. (RT-PCR, reverse transcription polymerase chain reaction; N, adjacent normal liver tissue; C, human hepatocellular carcinoma tissue; GAPDH, glyceraldehyde-s-phosphate dehydrogenase; M, pUC Mix Maker).

Northern blot

Northern blot of four paired tissues were performed and verified the accuracy of the microarray. Among the 4 paired tissues, the northern blot results of 4 genes further meant that the Atlas human cancer cDNA microarray data were believable and comparable (Figure 3).

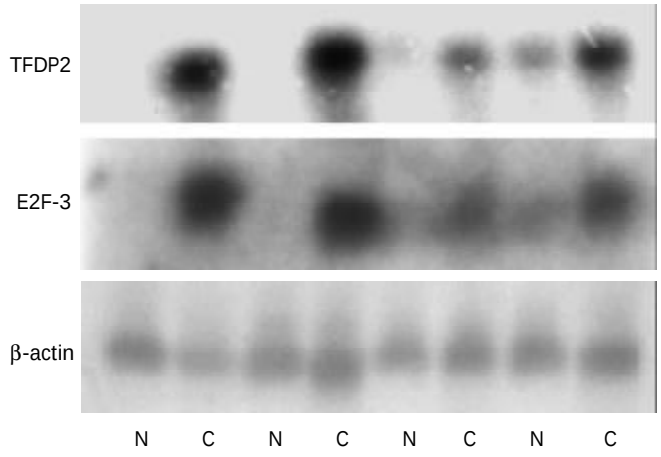

Figure 3 Northern blot analysis of 2 genes to confirm the Atlas human cancer cDNA expression array. Four paired cases were used to determine these genes expression patterns. Twenty μg RNA was analyzed on a 1.2 % denaturing agrose gel and transferred onto a nylon membrane. ^{32}P-labeled cDNA probes for these genes were hybridized to the RNA-blotted membranes. After stringent washes, membranes were exposed to X-ray film overnight at -70 ℃. The same membranes were rehybridized with human β-actin for an RNA loading control (N, adjacent normal liver tissue; C, human HCC tissue).

DISCUSSION

In this study, we explored the gene expression profiles in human hepatoma cell line HLE and normal liver tissues using Atlas human cancer array. cDNA array technology was used to examine simultaneously the expression of specific genes on a single hybridization. Although human genome projects have generated a large-scale sequence data for millions of genes, the biological functions of such genes remain to be deciphered. It is very important to define differential gene expression profiles of tumors and normal tissues before understanding the functional significance of specific gene products. Thus a systematic approach for examining large number of genes simultaneously is required. Microarray techniques have been developed in this conditions[23]. The gene expression profiles obtained from microarray technique was first reported in 1995[16]. It might be useful for tumor classification, elucidation of key factor in tumors, and identification of genes[24-27].

Several genes related to cell cycle regulators, growth regulators were abundantly up-regulated in our HCC samples. E2F-3 is a transcription factor that plays an important role during the cell cycle of proliferating cells, its products are rate limiting for initiation of DNA replication[28]. E2F-3 is able to activate transcription of E2F-responsive genes in a manner depending upon the presence of at least one functional E2F binding site[29,30]. TFDP2 gene is a member of the TFDP genes family of transcription factors. TFDP2 protein can form heterodimers with E2F family proteins in vivo. The E2F-TFDP transcription factors are major regulators of genes that are required for the progression of S-phase and they play a critical role in cell cycle regulation and differentiation[29]. TFDP2 may plays a major role in modulating the function of E2F in cell cycle regulation and oncogenesis. The retinoblastoma tumor suppressor protein has been shown to induce growth arrest by

binding to E2F-TFDP and repressing its activity[31]. The up-regulation of E2F-3 and TFDP2 may play an important role in HCC cell proliferation.

Protein kinase B (PKB)/Akt is a growth-factor-regulated serine/threonine kinase which contains a pleckstrin homology domain[32]. Activated PKB/Akt provides a survival signal that protects cells from apoptosis induced by various stresses, and also mediates a number of metabolic effects of insulin[33]. The up-regulation of Akt1 may have a great help for tumor cell to survive from apoptosis.

In our study, genes related to DNA repair and recombination was up-regulated in HLE, which indicates that the generative ability of tumor cell was stronger than that of normal hepatocytes. DNA-dependent protein kinase (DNA-PK) is a nuclear protein serine/threonine kinase that is activated by DNA double strand breaks (DSBs). It is a component of the DNA DSB repair apparatus, and cells deficient in DNA-PK are hypersensitive to ionizing radiation and radio-mimetic drugs[34]. DNA-PK may have roles in controlling transcription, apoptosis, and the length of telomeric chromosomal ends. The DNA-PK complex is regulated in a cell cycle-dependent manner, with peaks of activity found at the G_1/early S phase and again at the G_2 phase in wild-type cells[35].

Integrins are a major family of cell adhesion molecules involved in cell-cell and cell-extracellular matrix interactions. Integrins are suggested to be involved in many different biological processes such as growth, differentiation, migration, and cell death. The integrin alpha 8 beta 1 has been reported to bind to fibronectin, vitronectin, tenascin-C and osteopontin in cell adhesion or neurite outgrowth assays[36,37]. Integrins are heterodimeric cell adhesion proteins connecting the extracellular matrix to the cytoskeleton and transmitting signals in both directions[38]. The up-regulation of Integrin may play a role in HCC metastasis.

In conclusion, our study demonstrates the cDNA array is a powerful tool to explore gene expression profiles in cancer. The genes described in this study provide valuable resources not only for basic research, such as molecular mechanism of carcinogenesis, progression and prognosis, but also for clinical application, such as development of new diagnostic markers, identification of therapeutic intervention in human HCC.

REFERENCES

1 **Schafer DF,** Sorrell MF. Hepatocellular carcinoma. *Lancet* 1999; **353**: 1253-1257
2 **Qin LX,** Tang ZY. The prognostic molecular markers in hepatocellular carcinoma. *World J Gastroenterol* 2002; **8**: 385-392
3 **Wu W,** Lin XB, Qian JM, Ji ZL, Jiang Z. Ultrasonic aspiration hepatectomy for 136 patients with hepatocellular carcinoma. *World J Gastroenterol* 2002; **8**: 763-765
4 **Tang ZY,** Sun FX, Tian J, Ye SL, Liu YK, Liu KD, Xue Q, Chen J, Xia JL, Qin LX, Sun SL, Wang L, Zhou J, Li Y, Ma ZC, Zhou XD, Wu ZQ, Lin ZY, Yang BH. Metastatic human hepatocellular carcinoma models in nude mice and cell line with metastatic potential. *World J Gastroenterol* 2001; **7**: 597-601
5 **Liu LX,** Jiang HC, Piao DX. Radiofrequence ablation of liver cancers. *World J Gastroenterol* 2002; **8**: 393-399
6 **Rabe C,** Pilz T, Klostermann C, Berna M, Schild HH, Sauerbruch T, Caselmann WH. Clinical characteristics and outcome of a cohort of 101 patients with hepatocellular carcinoma. *World J Gastroenterol* 2001; **7**: 208-215
7 **Tang ZY**. Hepatocellular carcinoma-cause, treatment and metastasis. *World J Gastroenterol* 2001; **7**: 445-454
8 **Zhao WH,** Ma ZM, Zhou XR, Feng YZ, Fang BS. Prediction of recurrence and prognosis in patients with hepatocellular carcinoma after resection by use of CLIP score. *World J Gastroenterol* 2002; **8**: 237-242
9 **Jiang HC,** Liu LX, Piao DX, Xu J, Zheng M, Zhu AL, Qi SY, Zhang WH, Wu LF. Clinical short-term results of radiofrequency ablation in liver cancers. *World J Gastroenterol* 2002; **8**: 624-630
10 **Yip D,** Findlay M, Boyer M, Tattersall MH. Hepatocellular carcinoma in central Sydney: a 10-year review of patients seen in a medical oncology department. *World J Gastroenterol* 1999; **5**: 483-487
11 **Chen MS,** Li JQ, Zhang YQ, Lu LX, Zhang WZ, Yuan YF, Guo YP, Lin XJ, Li GH. High-dose iodized oil transcatheter arterial chemoembolization for patients with large hepatocellular carcinoma. *World J Gastroenterol* 2002; **8**: 74-78
12 **Zhang WH,** Zhu SN, Lu SL, Huang YL, Zhao P. Three-dimensional image of hepatocellular carcinoma under confocal laser scanning microscope. *World J Gastroenterol* 2000; **6**: 344-347
13 **Jiang YF,** Yang ZH, Hu JQ. Recurrence or metastasis of HCC: predictors, early detection and experimental antiangiogenic therapy. *World J Gastroenterol* 2000; **6**: 61-65
14 **Sithinamsuwan P,** Piratvisuth T, Tanomkiat W, Apakupakul N, Tongyoo S. Review of 336 patients with hepatocellular carcinoma at Songklanagarind Hospital. *World J Gastroenterol* 2000; **6**: 339-343
15 **Fan J,** Wu ZQ, Tang ZY, Zhou J, Qiu SJ, Ma ZC, Zhou XD, Ye SL. Multimodality treatment in hepatocellular carcinoma patients with tumor thrombi in portal vein. *World J Gastroenterol* 2001; **7**: 28-32
16 **Schena M,** Shalon D, Davis RW, Brown PO. Quantitative monitoring of gene expression patterns with a complementary DNA microarray. *Science* 1995; **270**: 467-470
17 **DeRisi J,** Penland L, Brown PO, Bittner ML, Meltzer PS, Ray M, Chen Y, Su YA, Trent JM. Use of a cDNA microarray to analyse gene expression patterns in human cancer. *Nat Genet* 1996; **14**: 457-460
18 **Liu LX,** Liu ZH, Jiang HC, Qu X, Zhang WH, Wu LF, Zhu AL, Wang XQ, Wu M. Profiling of differentially expressed genes in human Gastric carcinoma by cDNA expression array. *World J Gastroenterol* 2002; **8**: 580-585
19 **Wang K,** Gan L, Jeffery E, Gayle M, Gown AM, Skelly M, Nelson PS, Ng WV, Schummer M, Hood L, Mulligan J. Monitoring gene expression profile changes in ovarian carcinomas using cDNA microarray. *Gene* 1999; **229**: 101-108
20 **Ross DT,** Scherf U, Eisen MB, Perou CM, Rees C, Spellman P, Iyer V, Jeffrey SS, Van de Rijn M, Waltham M, Pergamenschikov A, Lee JC, Lashkari D, Shalon D, Myers TG, Weinstein JN, Botstein D, Brown PO. Systematic variation in gene expression patterns in human cancer cell lines. *Nat Genet* 2000; **24**: 227-235
21 **Khan J,** Simon R, Bittner M, Chen Y, Leighton SB, Pohida T, Smith PD, Jiang Y, Gooden GC, Trent JM, Meltzer PS. Gene expression profiling of alveolar rhabdomyosarcoma with cDNA microarrays. *Cancer Res* 1998; **58**: 5009-5013
22 **Lu J,** Liu Z, Xiong M, Wang Q, Wang X, Yang G, Zhao L, Qiu Z, Zhou C, Wu M. Gene expression profile changes in initiation and progression of squamous cell carcinoma of esophagus. *Int J Cancer* 2001; **91**: 288-294
23 **Kallioniemi OP**. Biochip technologies in cancer research. *Ann Med* 2001; **33**: 142-147
24 **Liu LX,** Jiang HC, Liu ZH, Zhou J, Zhang WH, Zhu AL, Wang XQ, Wu M. Intergrin gene expression profiles of human hepatocellular carcinoma. *World J Gastroenterol* 2002; **8**: 631-637
25 **Khan J,** Saal LH, Bittner ML, Chen Y, Trent JM, Meltzer PS. Expression profiling in cancer using cDNA microarrays. *Electrophoresis* 1999; **20**: 223-229
26 **Hu YC,** Lam KY, Law S, Wong J, Srivastava G. Identification of differentially expressed genes in esophageal squamous cellcarcinoma (ESCC) by cDNA expression array: overexpression of Fra-1, Neogenin, Id-1, and CDC25B genes in ESCC. *Clin Cancer Res* 2001; **7**: 2213-2221
27 **Selaru FM,** Zou T, Xu Y, Shustova V, Yin J, Mori Y, Sato F, Wang S, Olaru A, Shibata D, Greenwald BD, Krasna MJ, Abraham JM, Meltzer SJ. Global gene expression profiling in Barrett's esophagus and esophageal cancer: acomparative analysis using cDNA microarrays. *Oncogene* 2002; **21**: 475-478
28 **Leone G,** DeGregori J, Yan Z, Jakoi L, Ishida S, Williams RS, Nevins JR. E2F3 activity is regulated during the cell cycle and is required for the induction of S phase. *Genes Dev* 1998; **12**: 2120-2130
29 **Moberg K,** Starz MA, Lees JA. E2F-4 switches from p130 to p107

and pRB in response to cell cycle reentry. *Mol Cell Biol* 1996; **16**: 1436-1449

30 **Zhang Y,** Chellappan SP. Cloning and characterization of human DP2, a novel dimerization partner of E2F. *Oncogene* 1995; **10**: 2085-2093

31 **Zhang Y,** Venkatraj VS, Fischer SG, Warburton D, Chellappan SP. Genomic cloning and chromosomal assignment of the E2F dimerization partner TFDP gene family. *Genomics* 1997; **39**: 95-98

32 **Downward J.** Mechanisms and consequences of activation of protein kinase B / Akt. *Curr Opin Cell Biol* 1998; **10**: 10262-10267

33 **Alessi DR,** Cohen P. Mechanism of activation and function of protein kinase B. *Curr Opin Genet Dev* 1998; **8**: 55-62

34 **Jackson SP**. DNA-dependent protein kinase. *Int J Biochem Cell Biol* 1997; **29**: 935-938

35 **Lee SE,** Mitchell RA, Cheng A, Hendrickson EA. Evidence for DNA-PK-dependent and -independent DNA double-strand break repair pathways in mammalian cells as a function of the cell cycle. *Mol Cell Biol* 1997; **17**: 1425-1433

36 **Denda S,** Reichardt LF, Muller U. Identification of osteopontin as a novel ligand for the integrin alpha8 beta1 and potential roles for this integrin-ligand interaction in kidney morphogenesis. *Mol Biol Cell* 1998; **9**: 1425-1435

37 **Denda S,** Muller U, Crossin KL, Erickson HP, Reichardt LF. Utilization of a soluble integrin-alkaline phosphatase chimera to characterize integrin alpha 8 beta 1 receptor interactions with tenascin: murine alpha 8 beta 1 binds to the RGD site in tenascin-C fragments, but not to native tenascin-C. *Biochemistry* 1998; **37**: 5464-5474

38 **Fogerty FJ,** Akiyama SK, Yamada KM, Mosher DF. Inhibition of binding of fibronectin to matrix assembly sites by anti-integrin (alpha 5 beta 1) antibodies. *J Cell Biol* 1990; **111**: 699-708

Edited by Ren SY

P.O.Box 2345, Beijing 100023, China
Fax: +86-10-85381893
E-mail: wjg@wjgnet.com www.wjgnet.com

World J Gastroenterol 2003;9(4):688-691
World Journal of Gastroenterology
 ISSN 1007-9327

• LIVER CANCER •

Construction of a regulable gene therapy vector targeting for hepatocellular carcinoma

Shao-Ying Lu, Yan-Fang Sui, Zeng-Shan Li, Cheng-En Pan, Jing Ye, Wen-Yong Wang

Shao-Ying Lu, Cheng-En Pan, Department of General Surgery, First Hospital of Xi' an Jiaotong University, Xi' an 710061, Shaanxi Province, China
Yan-Fang Sui, Zeng-Shan Li, Cheng-En Pan, Jing Ye, Wen-Yong Wang, Department of Pathology, Fourth Military Medical University, Xi' an 710032, Shaanxi Province, China
Supported by Natural Scientific Foundation of China, No. 30271474
Correspondence to: Professor Yan-Fang Sui, Department of Pathology, Fourth Military Medical University, Xi' an 710032, China. suiyanf@fmmu.edu.cn
Telephone: +86-29-3374541-211 **Fax:** +86-29-3374597
Received: 2002-10-08 **Accepted:** 2002-12-07

Abstract

AIM: To construct a gene modified hepatocellular carcinoma (HCC) specific EGFP expression vector regulated by abbreviated cis-acting element of AFP gene.

METHODS: The minimal essential DNA segments of AFP gene enhancer and promoter were synthesized through PCR from Genome DNA of HepG2 cells. Gene fragments were then cloned into the multiple cloning site of non-promoter EGFP vector pEGFP-1. Recombinant plasmid was transferred into positive or negative AFP cell lines by means of lipofectamine. The expression of EGFP was tested by fluorescence microscope and flow cytometry. The effect of all-trans retinoic acid (ATRA) on the expression of EGFP was tested in different concentrations.

RESULTS: By the methods of restriction digestion and sequence analyses we confirmed that the length, position and orientation of inserted genes of cis-acting element of AFP were all correct. The transcription of EGFP was under the control of AFP cis-acting element. The expressing EGFP can only been detected in AFP producing hepatoma cells. The expression rate of EGFP in G418 screened cell line was 34.9±4.1 %. 48 h after adding 1×10^{-7}M retinoic acid, EGFP expression rate was 14.7±3.5 %. The activity of AFP gene promoter was significantly suppressed by addition of 1×10^{-7}M retinoic acid ($P<0.05$, $P=0.003$, $t=6.488$).

CONCLUSION: This recombinant expression vector can be used as a gene therapy vector for HCC. The expression of tumor killing gene will be confined within the site of tumor and the activity of which can be regulated by retinoic acid.

Lu SY, Sui YF, Li ZS, Pan CE, Ye J, Wang WY. Construction of a regulable gene therapy vector targeting for hepatocellular carcinoma. *World J Gastroenterol* 2003; 9(4): 688-691
http://www.wjgnet.com/1007-9327/9/688.htm

INTRODUCTION

Hepatocellular carcinoma (HCC) is one of the most common tumors worldwide, especially in several areas of Asia and Africa. It is the cause of death of around 1 000 000 people annually. Although many new methods appeared as palliative protocols in the past 30 years, patient survival after onset of symptoms remained dismal[1-3]. Surgical treatment such as resection or orthotopic liver transplantation is potentially curative only for patients with small and localized HCC[4]. Transfer of therapeutic genes to tumor mass or to the peritumoral tissues provides a promising new approach for cancer therapy[5-8]. Both viral and non-viral vectors were used to transfer genetic material to the interior of target cells[9]. Experiments demonstrate that tissue and transcriptional targeting expression of transgenes in tumor cells not only improves the outcome of treatment, but also reduces systemic toxicity[10]. This results in a much higher therapeutic index. Alpha-fetoprotein (AFP) is over expressed in about 70 % of HCC cases[11]. Several groups have used AFP promoter or/and enhancer to control foreign gene expression in different vectors [12, 13]. We constructed a gene modified AFP cis-acting element using the minimal essential DNA segments of AFP gene enhancer and promoter. Specific transcription activity of this element and it' s response to the addition of ATRA were tested using reporter gene vector pEGFP-1.

MATERIALS AND METHODS

Reagents

Reagents were obtained as follows: EX Taq DNA Polymerase, DNA Ligation Kit Ver.2, restriction endonuclease (TakaRa Biotechnology (Dalian) Co. Ltd.); DNA isolation and Purification kit (ShangHai ShunHua Biotechnology Ltd.); Lipofectamine™ 2000 (Invitrogen); IPTG, X-gal, DNA maker (Sino-American Biotechnology Company); Dulbecco' s Modified Eagle Media: high glucose, with L-glutamine (DMEM) and G418 (GibcoBRL); all-trans retinoic acid, ATRA (Sigma).

Plasmids

pBluescript II ks(+) vector was preserved in our laboratory. The reporter gene vector pEGFP-1 was purchased form Clontech. This vector encoded a red-shifted variant of wild-type green fluorescent protein (GFP), which had been optimized for brighter fluorescence and higher expression in mammalian cells. This vector was also a non-promoter EGFP vector which could be used to monitor transcription from different promoters and promoter/enhancer combinations inserted into the MCS located in upstream of the EGFP coding sequence.

Cell lines

HepG2 and SMMC-7721 are human hepatoma cell lines produce or do not produce AFP. Hela is human cervical cancer cell line, all Cell lines were cultured in Dulbecco' s modified Eagle' s medium, high glucose content, containing 10 % heat-inactivated fetal calf serum, 100 units/ml penicillin, 100 μg/ml streptomycin, 0.292 mg/ml glutamine. The cell lines were incubated in a humidified 5 % CO_2 and 95 % air incubator at 37 ℃.

Polymerase chain reaction (PCR)

The primer sequences used for PCR were used as reported[14, 15].

For PCR amplification, genomic DNA were extracted from 1×10^6 HepG2 cells and digested by *Eco*R I/*Xho* I. PCR was performed in a total volume of 50 μl consisting of 1 μM each primer, 200 μM each dNTP, 5 μL 10×polymerase reaction buffer, and 1.25U EX Taq DNA Polymerase with 1 μL digested DNA. The samples were heated to 94 ℃ for 5 min followed by amplification for 30 cycles of 30s at 94 ℃, 50s at 55 ℃, and 1 min at 72 ℃. After the last cycle, a final extension step was done at 72 ℃ for 7 min. Then 10 μl of each PCR product was analyzed by 1 % agarose gel (containing 0.5 μg/mL EB) electrophoresis. After which the amplified PCR products were purified from agarose gel according to DNA purification kit description. The abbreviated gene fragments of AFP enhancer (e) and promoter (p) were subcloned into pBluescript II ks(+). The positive clones were selected from the transfected DH5α and performed as described in reference[16]. The constructed plasmids (designated as ks-e, ks-p) were identified by restriction enzyme analysis. DNA sequences were verified by DNA Sequencing Core Facility in Bioasia (ShangHai) Biotechnology Company.

Construction and identification of expressing vector pEGFP-1-EP

Gene fragments of AFP enhancer (e) and promoter (p) were released by *Eco*R I-*Sal* I, and *Sal* I-*Bam*H I double digestions respectively, and inserted into the *Eco*R I- *Bam*H I sites of pEGFP-1. The Recombinant was identified by restriction endonuclease digestion. The restriction maps of pEGFP-1-EP were shown in Figure 1.

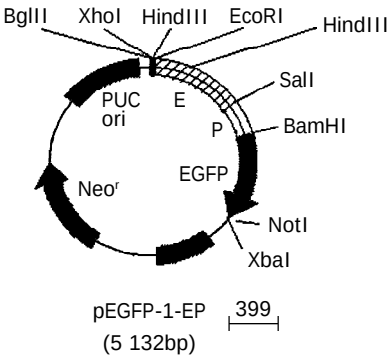

Figure 1 Gene map of pEGFP-1-EP.

Transient EGFP expression

18 hours before transfection, 2×10^5 HepG2, SMMC-7721 and Hela cells were plated into 12-well culture plates. At the bottom of each well, a sterilized coverslip was placed in advance. When the plated cells were 90 to 95 % confluence, transfection was performed with 1 μg of DNA (pEGFP-1 or pEGFP-1-EP) per dish, using Lipofectamine™ 2000 reagent according to the manufacturer' s instruction. 48 h after transfection, the cells were washed twice with cold PBS (0.01M) and fixed with 4 % paraformaldehyde for 30 min at room temperature. Coverslips were then mounted directly onto a glass slide with a tiny drop of 50 % glycerol in PBS (9.1 mM Na_2HPO_4/1.7 mM NaH_2PO_4 /50 mM NaCl, pH 7.4). Fluorescent images were captured at 490nm using a Nikon Eclipse E1000 microscope attached to a MicroMax camera (Princeton Instruments, Trenton, NJ).

Effect of all-trans retinoic acid (ATRA) on the expression of EGFP

A similar transfection procedure was perfomed to transfect vector pEGFP-1-EP for stable EGFP expression. After 48 h of transfection, the cells were passaged at a 1:4 dilution into fresh medium. The next day, selective medium (G418 400 μg/mL) was added to the cells for screening of stable lines of transfected cells. After culturing for an additional 2 weeks in G418, cells expressing EGFP fluorescence were selected using a fluorescence-activated cell sorter. The EGFP-positive cells were maintained in growth medium supplemented with 400 μg/mL G418. For RA regulation studies, stably transfected cells were plated on 12-well dishes at 1×10^5 cells/well in growth medium with G418, incubated overnight, then changed into the medium with or without all-trans retinoic acid (1×10^{-7}M, 2.5×10^{-7}M, 1×10^{-6}M ATRA) (without G418). The expression rate of EGFP fluorescence was measured by flow cytometry (ETITE ESP, COULTER Company) 48 h later. The green fluorescence was analyzed through a 530-nm/30-nm band pass filter after illumination with the 488-nm line of an argon ion laser.

Statistical analysis

All experiments were performed three times in triplicate, the data were presented as the mean ± SEM, and compared by Student' s *t* test.

RESULTS

PCR amplification and DNA sequencing of gene modified AFP enhancer and promoter

Electrophoretic result of PCR products showed that the size of amplified DNA fragments was consistent with design. Through PCR amplification of AFP promoter we obtained two gene fragments (0.3kb, 0.5kb). The 0.3kb fragment was what we expected, the 0.5kb one was nonspecific amplification (Figure 2). PCR products were subcloned into pBluescript II ks(+) vector. The DNA Sequencing results confirmed that DNA sequence of both fragments was correct.

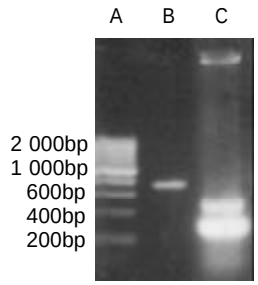

Figure 2 PCR result of gene segments. A. 200bp DNA marker; B. enhancer of AFP; C. promoter of AFP.

Gene modified AFP cis-acting element was successfully inserted into the MCS of pEGFP-1

Recombined AFP cis-acting element was 1 035 bp with *EcoR* I and *BamH* I restriction site on each side. The size of pEGFP-1 was 4.2 kb, which had *Bgl*II and *Hind* III sites in the 3' -side of MCS. The expressing vector pEGFP-1-EP was digested by *Bgl*II/*Sal* I/*Bam*H I, and *Xho* I/*Bam*H I, and *Hind* III respectively. 0.73 bp-0.31bp, and 1.03bp, and 0.27 bp DNA fragments appeared (Figure 3). This result meant that the size, direction of cis-acting element were correct and the construction of expressing vector was successful.

Specific expression of EGFP in AFP positive hepatoma

Three cell lines were transfected with plasmid pEGFP-1 and pEGFP-1-EP simultaneously. The expression of EGFP could only be detected in HepG2 cells (AFP positive) transfected with pEGFP-1-EP (Figure 4). The transient expression rate of EGFP in HepG2 was 16 %. Hela cell and SMMC-7721 cell (AFP negetive) did not express EGFP. The HepG2 cell transfected with pEGFP-1 also did not express EGFP. So we

could conclude that gene modified cis-acting element retained specific transcription activity in AFP positive cells.

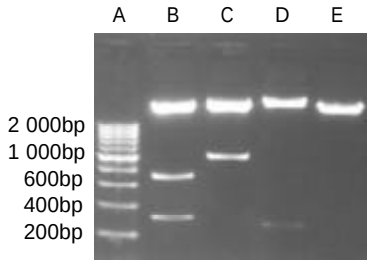

Figure 3 Enzyme digestion analysis of the recombinant expression vector. A. 200bp DNA marker; B. pEGFP-1-EP (*Bgl*II, Sal I, *Bam*H I); C. pEGFP-1-EP (*Xho* I, *Bam*H I); D. pEGFP-1-EP (*Hind* III); E. pEGFP-1(*Eco*R I, *Bam*H I).

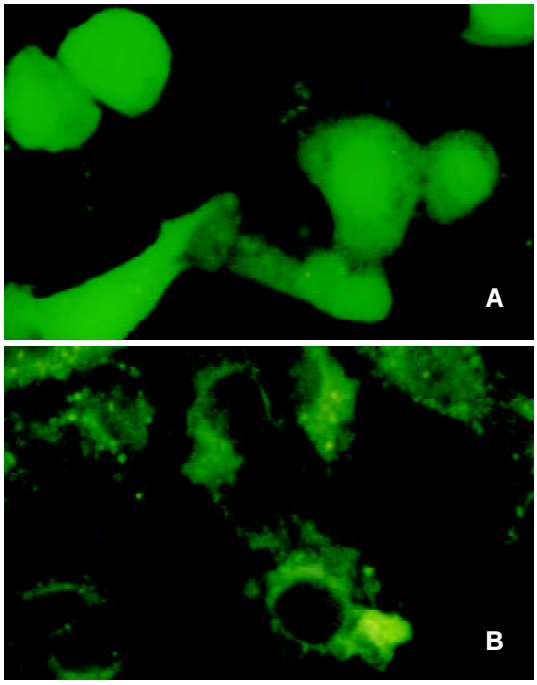

Figure 4 Transient expression of EGFP. A. EGFP expressing in HepG2; B. EGFP do not express in Hela cells.

The expressing of EGFP can be suppressed by the adding of ATRA

EGFP-expressing HepG2 cell line was obtained through two weeks screening by adding G418 into the culture medium. These cells were then cultured in the medium with or without retinoic acid for 48 h and measured by flow cytometry. The expression rate of EGFP was 34.9±4.1 % in cells without retinoic acid and 14.7±3.5 %, 13.5±2.7 %, 12.1±3.9 % in cells adding 1×10^{-7}M, 2.5×10^{-7}M, 1×10^{-6}M retinoic acid (Figure 5). Transcription activity of modified AFP cis-acting element was suppressed by adding either concentration of retinoic acid ($P<0.05$).

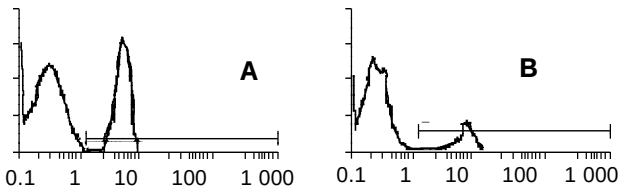

Figure 5 The expression of EGFP suppressed by ATRA. A. stable expression of EGFP in HepG2; B. expression of EGFP suppressed by 2.5×10^{-7}M ATRA.

DISCUSSION

There are numerous gene therapy strategies that have been applied to the treatment of HCC. They include gene replacement (e.g. tumor suppressor genes), antisense strategies, drug sensitization (suicide genes), genetic immunotherapy (cytokines, costimulatory molecules, polynucleotide vaccination), and interventions to interfere with the biology of the tumor growth (antiangiogenesis)[17-19]. But HCC frequently occurs in patients with liver cirrhosis, the potentially toxic effects of gene transfer may have marked deleterious consequences, so the targeted gene transfer or the specific expression of transfected genes to hepatoma cells is vital for gene therapy of HCC.

A practical system to ensure tumor-restricted expression of the transgenes is the use of tumor-specific promoters. Since elevated levels of AFP have been observed in about 70 % of hepatocellular carcinomas[20], using AFP transcriptional sequence to achieve hepatocellular carcinoma specific gene expression is an ideal way. Arbuthnot *et al*[21, 22]. demonstrated that retroviral and adenoviral vectors containing the lacZ reporter gene under the control of AFP regulatory sequences resulted in the specific expression of the lacZ gene only in HCC cells with AFP expression. Similar results were reported by Kanai *et al*[23]. who demonstrated that expression of the herpes simplex virus thymidine kinase (HSV-tk) gene by adenovirus from AFP promoter/enhancer induced the cells to be sensitive to ganciclovir (GCV) in the AFP-producing cells. But The AFP gene has a large and complex transcription control region which is located within a region from -7.6 kb to the transcription starting site. It contains the promoter, the enhancer, and the silencer that contain specific binding sequences for the transcription factors and provide precisely regulated AFP gene transcription[24, 25]. Most investigators have used human AFP 5' -flanking region that including the all the *trans*- and *cis*-acting elements from AFP 5' -flanking sequences [24, 26-29] as a hepatoma specific regulation element. Although this sequences can achieve sufficient cytotoxicity in AFP-producing hepatoma cells, but also induce a killing effect on hepatic stem cells that also express AFP and appear in the injured liver, thus resulting in damage of the hepatic reserve and a poor prognosis for patients with HCC. On the other hand, the package capacity of most gene therapy vectors is very small, which cannot accommodate the whole transcriptional sequence of AFP in the construct. The activity of promoter alone is too weak to be used in targeting gene therapy. In this study, we subcloned the minimal essential enhancer region (-4.0 to -3.3) and 0.3 kb minimal promoter of human AFP gene, and constructed abbreviated HCC specific cis-acting element. The expressing of the report gene (EGFP) was detected in AFP-producing hepatoma cells (HepG2), and none in non-AFP-producing hepatoma (SMMC-7721) and nonhepatoma cells (Hela). So this minimal cis-acting element well conserved the specific transcription characteristic of AFP 5' -flanking sequences. This element is very small (1.0 kb) and fits to the package capacity of most conventional gene therapy vectors.

The expression of AFP is under the control of retinoic acid which both activates and represses AFP expression in different cell lines[30, 31]. Within the AFP gene regulatory region three elements determining sensitivity for retinoic acid have been revealed. One of them is localized in promoter (-139/-127 bp) and overlaps with other transcription factor binding sites[31]. The influence of retinoic acid on AFP gene expression can be carried out both by means of HNF induction and through the hormone-receptor complex binding to the corresponding sites in AFP regulatory elements[32]. Activation of the AFP gene by RA had been reported in McA-RH8994 and F9 cell lines[30, 31], while AFP was down-regulated by RA in the human hepatoma cell line Hep3B. How can RA regulate the expression of AFP

in HepG2 human hepatoma cell line is rarelys reported. In this study we established an EGFP-expressing HepG2 cell line, the expressing of EGFP is under the control of modified cis-acting element of AFP. When treated with ATRA, we found that the transcription activity of AFP cis-acting element could be significantly suppressed by 1×10^{-7} M ATRA. So when we use this transcription element as a regulator of anti-tumor gene the cytotoxicity effects on target cell can be controlled by RA within the expected range. This is very important when a gene therapy vector is applied clinically.

There are restriction sites in the upstream or downstream of EGFP in the expressing vector pEGFP-1-EP, through which we can replace EGFP with any tumor-killing gene. So this vector can be used as a gene therapy vector targeting for hepatocellular carcinoma. The transcription activity of hepatocellular carcinoma specific promoter can be controlled by the adding of ATRA.

REFERENCES

1 **Badvie S**. Hepatocellular carcinoma. *Postgrad Med J* 2000; **76**: 4-11
2 **Llovet JM**, Mas X, Aponte JJ, Fuster J, Navasa M, Christensen E, Rodes J, Bruix J. Cost effectiveness of adjuvant therapy for hepatocellular carcinoma during the waiting list for liver transplantation. *Gut* 2002; **50**: 123-128
3 **Tang ZY**. Hepatocellular carcinoma-cause, treatment and metastasis. *World J Gastroenterol* 2001; **7**: 445-454
4 **Schöniger-Hekele M**, Müller C, Kutilek M, Oesterreicher C, Ferenci P, Gangl A. Hepatocellular carcinoma in Central Europe: prognostic features and survival. *Gut* 2001; **48**: 103-109
5 **Narvaiza I**, Mazzolini G, Barajas M, Duarte M, Zaratiegui M, Qian C, Melero I, Prieto J. Intratumoral coinjection of two adenoviruses, one encoding the chemokine IFN-gamma-inducible protein-10 and another encoding IL-12, results in marked antitumoral synergy. *J Immunol* 2000; **164**: 3112–3122
6 **Ruiz J**, Qian C, Drozdzik M, Prieto J. Gene therapy of viral hepatitis and hepatocellular carcinoma. *J Viral Hepat* 1999; **6**: 17–34
7 **Kuriyama S**, Nakatani T, Masui K, Sakamoto T, Tominaga K, Yoshikawa M, Fukui H, Ikenaka K, Tsujii T. Evaluation of prodrugs ability to induce effective ablation of cells transduced with viral thymidine kinase gene. *Anticancer Res* 1996; **16**: 2623–2628
8 **Schmitz V,** Qian C, Ruiz J, Sangro B, Melero I, Mazzolini G, Narvaiza I, Prieto J. Gene therapy for liver diseases: recent strategies for treatment of viral hepatitis and liver malignancies. *Gut* 2002; **50**: 130-135
9 **Qian C,** Idoate M, Bilbao R, Sangro B, Bruna O, Vazquez J, Prieto J. Gene transfer and therapy with adenoviral vector in rats with diethylnitrosamine-induced hepatocellular carcinoma. *Hum Gene Ther* 1997; **8**: 349–358
10 **Uto H**, Ido A, Hori T, Hirono S, Hayashi K, Tamaoki T, Tsubouchi H. Hepatoma-specific gene therapy through retrovirus-mediated and targeted gene transfer using an adenovirus carrying the ecotropic receptor gene. *Biochem Biophys Res Commun* 1999; **265**: 550-555
11 **Chen XP**, Zhao H, Zhao XP. Alternation of AFP-mRNA level detected in blood circulation during liver resection for HCC and its significance. *World J Gastroenterol* 2002; **8**: 818-821
12 **Dachs GU**, Dougherty GJ, Stratford IJ, Chaplin DJ. Targeting gene therapy to cancer: a review. *Oncol Res* 1997; **9**: 313-325
13 **Kanai F**. Transcriptional targeted gene therapy for hepatocellular carcinoma by adenovirus vector. *Mol Biotechnol* 2001; **18**: 243-250
14 **Su H**, Chang JC, Xu SM, Kan YW. Selective killing of AFP-positive hepatocellular carcinoma cells by adeno-associated virus transfer of the herpes simplex virus thymidine kinase gene. *Hum Gene Ther* 1996; **7**: 463-470
15 **Ido A,** Uto H, Moriuchi A, Nagata K, Onaga Y, Onaga M, Hori T, Hirono S, Hayashi K, Tamaoki T, Tsubouchi H. Gene therapy targeting for hepatocellular carcinoma: selective and enhanced suicide gene expression regulated by a hypoxia-inducible enhancer linked to a human alpha-fetoprotein promoter. *Cancer Res* 2001; **61**: 3016-3021
16 **Sambrook J**, Fritsch EF, Maniatis T. Molecular Cloning: A Laboratory Manual, 2nd ed. Cold Spring Harbor Laboratory Press, New York, 1989
17 **Ueki T**, Nakata K, Mawatari F, Tsuruta S, Ido A, Ishikawa H, Nakao K, Kato Y, Ishii N, Eguchi K. Retrovirus-mediated gene therapy for human hepatocellular carcinoma transplanted in athymic mice. *Int J Mol Med* 1998; **1**: 671-675
18 **Barajas M,** Mazzolini G, Genove G, Bilbao R, Narvaiza I, Schmitz V, Sangro B, Melero I, Qian C, Prieto J. Gene therapy of orthotopic hepatocellular carcinoma in rats using adenovirus coding for interleukin-12. *Hepatology* 2001; **33**: 52–61
19 **Brunda MJ,** Luistro L, Warrier RR, Wright RB, Hubbard BR, Murphy M, Wolf SF, Gately MK. Antitumor and antimetastatic activity of interleukin 12 against murine tumors. *J Exp Med* 1993; **178**: 1223–1230
20 **Sato Y**, Nakata K, Kato Y, Shima M, Ishii N, Koji T, Taketa K, Endo Y, Nagataki S. Early recognition of hepatocellular carcinoma based on altered profiles of á-fetoprotein. *N Engl J Med* 1993; **328**: 1802-1806
21 **Arbuthnot P**, Bralet MP, Thomassin H, Danan JL, Brechot C, Ferry N. Hepatoma cell-specific expression of a retrovirally transferred gene is achieved by alpha-fetoprotein but not insulin-like growth factor II regulatory sequences. *Hepatology* 1995; **22**: 1788–1796
22 **Arbuthnot PB**, Bralet MP, Le Jossic C, Dedieu JF, Perricaudet M, Brechot C, Ferry N. *In vitro* and *in vivo* hepatoma cell-specific expression of a gene transferred with an adenoviral vector. *Hum Gene Ther* 1996; **7**: 1503–1514
23 **Kanai F,** Shiratori Y, Yoshida Y, Wakimoto H, Hamada H, Kanegae Y, Saito I, Nakabayashi H, Tamaoki T, Tanaka T, Lan KH, Kato N, Shiina S, Omata M. Gene therapy for alpha-fetoprotein-producing human hepatoma cells by adenovirus-mediated transfer of the herpes simplex virus thymidine kinase gene. *Hepatology* 1996; **23**: 1359-1368
24 **Nakabayashi H**, Watanabe K, Saito A, Otsuru A, Sawadaishi K, Tamaoki T. Transcriptional regulation of alpha-fetoprotein expression by dexamethasone in human hepatoma cells. *J Biol Chem* 1989; **264**: 266-271
25 **Watanabe K**, Saito A, Tamaoki T. Cell-specific enhancer activity in a far upstream region of the human alpha-fetoprotein gene. *J Biol Chem* 1987; **262**: 4812-4818
26 **Ishikawa H**, Nakata K, Mawatari F, Ueki T, Tsuruta S, Ido A, Nakao K, Kato Y, Ishii N, Eguchi K. Retrovirus-mediated gene therapy for hepatocellular carcinoma with reversely oriented therapeutic gene expression regulated by alpha-fetoprotein enhancer/promoter. *Biochem Biophys Res Commun* 2001; **287**: 1034-1040
27 **Kaneko S**, Hallenbeck P, Kotani T, Nakabayashi H, McGarrity G, Tamaoki T, Anderson WF, Chiang YL. Adenovirus-mediated gene therapy of hepatocellular carcinoma using cancer-specific gene expression. *Cancer Res* 1995; **55**: 5283-5287
28 **Wills KN**, Huang WM, Harris MP, Machemer T, Maneval DC, Gregory RJ. Gene therapy for hepatocellular carcinoma: chemosensitivity conferred by adenovirus-mediated transfer of the HSV-1 thymidine kinase gene. *Cancer Gene Ther* 1995; **2**: 191-197
29 **Igarashi T**, Suzuki S, Takahashi M, Tamaoki T, Shimada T. A novel strategy of cell targeting based on tissue-specific expression of the ecotropic retrovirus receptor gene. *Hum Gene Ther* 1998; **9**: 2691-2698
30 **Li C**, Locker J, Wan YJ. RXR-mediated regulation of the alpha-fetoprotein gene through an upstream element. *DNA Cell Biol* 1996; **15**: 955-963
31 **Liu Y**, Chen H, Dong JM, Chiu JF. Cis-acting elements in 5'-flanking region of rat alpha-fetoprotein mediating retinoic acid responsiveness. *Biochem Biophys Res Commun* 1994; **205**: 700-705
32 **Magee TR**, Cai Y, El-Houseini ME, Locker J, Wan YJ. Retinoic acid mediates down-regulation of the alpha-fetoprotein gene through decreased expression of hepatocyte nuclear factors. *J Biol Chem* 1998; **273**: 30024-30032

Edited by Wu XN

P.O.Box 2345, Beijing 100023, China
Fax: +86-10-85381893
E-mail: wjg@wjgnet.com www.wjgnet.com

World J Gastroenterol 2003;9(4):692-695
World Journal of Gastroenterology
 ISSN 1007-9327

• LIVER CANCER •

Codon 249 mutation in exon 7 of p53 gene in plasma DNA: maybe a new early diagnostic marker of hepatocellular carcinoma in Qidong risk area, China

Xing-Hua Huang, Lu-Hong Sun, Dong-Dong Lu, Yan Sun, Li-Jie Ma, Xi-Ran Zhang, Jian Huang, Long Yu

Xing-Hua Huang, Li-Jie Ma, Long Yu, The State Key Laboratory of Genetic Engineering, Fudan University, 200433, Shanghai, China
Lu-Hong Sun, Dong-Dong Lu, Xi-Ran Zhang, School of life sciences, Nanjing Normal University, Nanjing 210097, Jiangsu Province, China
Xing-Hua Huang, Yan Sun, Jian Huang, Qidong Liver Cancer Institute, Qidong 226200, Jiangsu Province, China
Correspondence to: Long Yu, The State Key Laboratory of Genetic Engineering, Fudan University, 200433, Shanghai, China. longyu@fudan.edu.cn
Telephone: +86-21-65643954 **Fax:** +86-21-65643250
Received: 2002-08-02 **Accepted:** 2002-08-27

Abstract

AIM: One of the characteristics of hepatocellular carcinoma (HCC) in Qidong area is the selective mutation resulting in a serine substitution at codon 249 of the p53 gene (1, 20), and it has been identified as a "hotspot" mutation in heptocellular carcinomas occurring in populations exposed to aflatoxin and with high prevalence of hepatitis B virus carriers (2, 3, 9, 10, 16, 24). We evaluated in this paper whether this "hotspot" mutation could be detected in cell-free DNA circulating in plasma of patients with hepatocellular carcinoma and cirrhosis in Qidong, China, and tried to illustrate the significance of the detection of this molecular biomarker.

METHODS: We collected blood samples from 25 hepatocellular carcinoma patients, 20 cirrhotic patients and 30 healthy controls in Qidong area. DNA was extracted and purified from 200 μl of plasma from each sample. The 249^{Ser} p53 mutation was detected by restriction digestion analysis and direct sequencing of exon-7 PCR products.

RESULTS: We found in exon 7 of p53 gene G→T transversion at the third base of codon 249 resulting 249^{Arg}→249^{Ser} mutation in 10/25 (40 %) hepatocellular carcinoma cases, 4/20 (20 %) cirrhotics, and 2/30 (7 %) healthy controls. The adjusted odds ratio for having the mutation was 22.1 (95 % CI, 3.2~91.7) for HCC cases compared to controls.

CONCLUSION: These data show that the 249^{Ser} p53 mutation in plasma is strongly associated with hepatocellular carcinoma in Qidong patients. We found this mutation was also detected, although it was at a much lower frequency, in plasma DNA of Qidong cirrhotics and healthy controls; We consider that these findings, together with the usual method of HCC diagnosis, will give more information in early diagnosis of HCC, and 249^{Ser} p53 mutation should be developed to a new early diagnostic marker for HCC.

Huang XH, Sun LH, Lu DD, Sun Y, Ma LJ, Zhang XR, Huang J, Yu L. Codon 249 mutation in exon 7 of p53 gene in plasma DNA: maybe a new early diagnostic marker of hepatocellular carcinoma in Qidong risk area, China. *World J Gastroenterol* 2003; 9(4): 692-695
http://www.wjgnet.com/1007-9327/9/692.htm

INTRODUCTION

Qidong is a high risk area of hepatocellular carcinoma (HCC), chiefly due to chronic hepatitis B virus (HBV) infection, and exposure to AFB1[1, 2]. HCC is a major cause of cancer death in this area. Epidemiological and experimental evidence show that hepatitis B virus (HBV) and dietary exposure to aflatoxin B1 (AFB1) contribute to hepatocarcinogensis[3-9]. About 10-15 % of the Qidong populations are chronically infected with HBV (LU. PX *et al*, 1991). An analysis of individual biomarkers of aflatoxin exposure in Qidong (Daxing country) has shown 99 % (791/792) of individuals with detectable serum aflatoxin-albumin adducts (Zhu YR *et al*, 1999).

p53 mutations have been identified in several human cancers[10-12]. A selective G to T transversion mutation at codon 249 (AGG→AGT, arginine to serine) of the p53 gene has been identified as a "hotspot" mutation for HCC in Qidong area[13-16]. Data from Qidong Liver Cancer Institute have suggested that this mutation in HCC is strongly associated with exposure to AFB1[13]. Recent research in Gambia[17] has shown that in some human cancers, circulating tumor DNA can be successfully retrieved from plasma or serum and used as a surrogate material to analyze for genetic alterations present in the original tumor[18-20]. We adopted this approach to evaluate the presence of 249^{Ser} p53 mutation in plasma from HCC cases, cirrhotic patients and healthy controls, and this mutation could be regarded as a new biomarker in HCC earlier diagnosis.

MATERIALS AND METHODS

Subjects and specimens

Blood samples from 25 cases of HCC, 20 cirrhotic patients and 30 healthy controls were collected in Qidong Liver Cancer Institute. The definition for 25 cases of HCC included compatible clinical and ultrasonographic findings and serum AFP levels. The ultrasonographic data were most important. 20 Cirrhotic patients were included as an additional referent group for evaluation of factors associated with progression to HCC. The diagnosis of cirrhosis was also based on compatible clinical history and by ultrasonographic method. 30 cases of controls were recruited from the outpatient clinics among individuals with no history or clinical findings suggestive of liver disease, and have the same distributions of age, gender and recruitment site with the HCC and cirrhotic cases.

DNA extraction

Blood samples anticoagulated with EDTA were processed immediately after collection, plasma was transferred to a plain tube and stored at -70 ℃ at Qidong Liver Cancer Institute. AFP and HBV serological testing was performed using standard laboratory kits. A 500 μl aliquot of plasma was shipped in liquid nitrogen to the state key laboratory of genetic engineering, Fudan University (Shanghai), for 249 Ser testing. DNA was extracted from 200 μl of plasma using a QiAamp blood kit (Qiagen Company) according to the manufacturer' s protocol. The purified DNA was eluted from silica column with 50 μl of Nuclease-Free Water.

PCR

Primers used for PCR amplification synthesized by Sangon company (Shanghai) were as follows: p1 (up) (5' -ctt gcc aca ggt ctc ccc aa-3'), p2 (down) (5' -agg ggt cag cgg caa gca ga-3'). The expected size of the product was 254 bp, and this fragment was located in the exon 7 of p53 gene.

Using TaKaRa PCR kit, the 25 μl reaction included 18.3 μl ddH_2O, 2.5 μl 10×buffer, 1 μl dNTPs, 0.5 μl primer 1, 0.5 μl primer 2, 0.2 μl Taq DNA polymerase, 2 μl DNA templates. The thermo-cycling conditions were 94 ℃ for 5 min, and 40 cycles of 94 ℃ for 30 sec, 60 ℃ for 30 sec, 72 ℃ for 30 sec, and finally 72 ℃ for 10 min in a Peltier Thermal Cycler (PTC 200). The amplification products (254 bp) were visualized by staining with ethidium bromide, after electrophoresis on 2 % agarose gel.

Purification of PCR products

To obtain enough amounts of DNA fragments for further testing, 1 μl of PCR product of each sample was picked up as template to have another PCR reaction with the same amplifying condition. The PCR products were then purified with 3S PCR Product Purification Kit (Biocolor Biological Science & Technology Co., Ltd) to eliminate some impurities such as dNTPs, primers, polymerase, and mineral oil.

Mutation detection by restriction analysis

The 254 bp of purified DNA fragment, which is derived from exon 7 of p53 gene, was submitted to restriction enzyme *Hae III* (New England Biolabs Company) digestion. The restriction enzyme digestion reaction system was as follows: 1 μl *HaeIII*, 2 μl 10×buffer2, 5 μl DNA fragment, 12 μl ddH_2O (20 μl total volume). These reaction systems were submitted to 37 ℃ water incubation for 4 hours. Enzyme *Hae III* cleaves a GG/CC sequence at codons 249-250, generating 92bp, 66bp and several small fragments from the 254 bp purified DNA product of the PCR reaction. If there is a mutation at codon 249-250 resulting in an uncleaved, 158bp fragment, and this feature will be distinguished from that of normal samples on 2 % agarose gel stained with ethidium bromide. Absence of the band at 254 bp (full-length PCR products) provides a control for complete digestion of the PCR product. In our protocol, we also arrange positive (with 249 mutation) and negative (wild-type) controls. The presence of the uncleaved 158 bp fragment indicates that there are mutations in the corresponding samples, and DNA fragments of these special samples were analyzed by automated DNA sequencing (ABI 377) using BigDye Terminator Cycle Sequencing Ready Reaction Kit (PE company).

Statistical analysis

Pearson' s chi-square and Fisher' s exact test were used to assess statistical significance of frequency tables of independent variables and 249 Ser mutations as a dichotomous variable. Multivariable logistic regression analysis was performed to estimate odds ratios (OR) along with 95 % confidence intervals (CI) to estimate the risk of mutation among the different study groups considering age, gender, recruitment site, and hepatitis B surface antigen status as potential confounders.

RESULTS

The characteristics of the 75 subjects from Qidong were evaluated in the study (Table 1).

HCC cases, cirrhosis cases and controls from Qidong were of similar age and gender distribution. 84 % of HCC cases, 65 % of cirrhotics and 13 % of controls were positive for hepatitis B surface antigen (HBsAg), a marker of chronic infection with HBV (P<0.001 for difference between groups). 80 % of HCC cases, 70 % of cirrhotics and 0 % of controls were positive for serum alpha-fetoprotein positive (AFP>100 ng/ml).

Table 1 Characteristics of study participants from Qidong

	Hepatocellular carcinomas	Cirrhotics	Controls
	(25)	(20)	(30)
Age (average [range], in years)	49 (27-70)	39 (25-65)	45 (19-87)
Number of males (%)	20 (80)	17 (85)	25 (83)
Hepatitis B surface antigen positive (%)	21 (84)	13(65)	4 (13)
Serum alpha-fetoprotein positive (%)	20 (80)	14 (70)	0 (0)

The electrophoresis on 2 % agarose gel shows that the 254 bp specific DNA fragments amplified between p1 and p2 are at the appropriate location according to the DNA molecular weight markers (Figure 1).

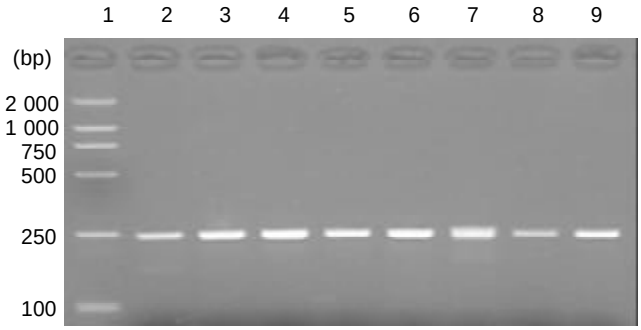

Figure 1 The electrophoresis map of PCR products. Lane 1: DNA Molecular weight markers. Lane 2-9: PCR products of partial samples.

DNA fragment from each sample was digested with restriction enzyme *HaeIII*. Presence of undigested 158 bp fragments on 2 % agarose gel indicates that there is a point mutation in the *Hae III r*ecognition site (Figure 2).

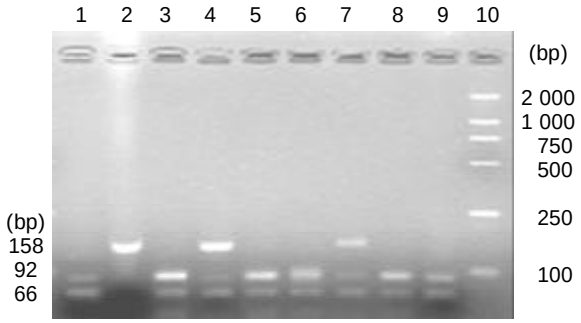

Figure 2 Mutation at coden 249 was identified by restriction digestion. Lane 1: negative control, Lane 2: positive control, Lane 3-9: HCC samples, Lane 10: DNA molecular weight markers.

p53 exon 7 fragments from normal controls (wild type) and mutation (identified by restriction digestion) HCC cases were sequenced (Figure 3).

We found in this paper 16 of 75 subjects from Qidong have 249^{ser} p53 mutation, including ten of 25 HCC cases, four of 20 cirrhotic patients, and two of 30 controls, giving a prevalence of 40 %, 20 % and 7 %, respectively (P<0.001 for difference between groups) (Table 2).

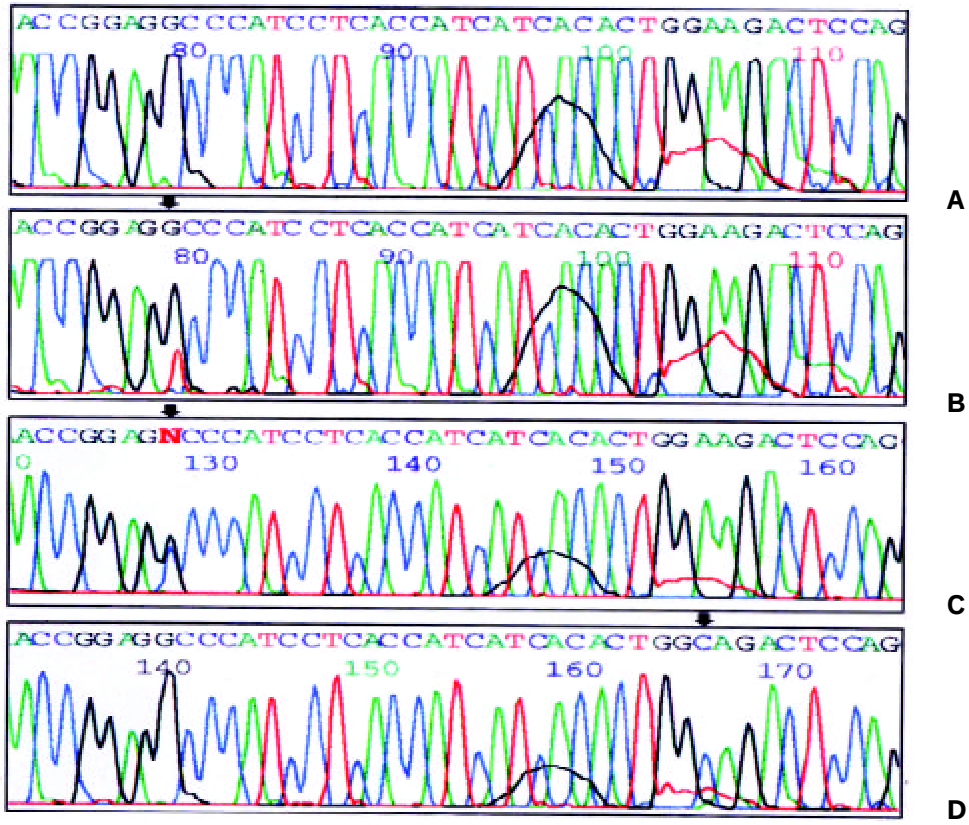

Figure 3 Sequencing results (partial electropherogram). A: Wild type sequence shows codon 249 AGG; B: Mutation sequence shows codon 249 AGG→AGT transversion; C: Mutation sequence shows codon 249 AGG→AGC transversion; D: A→C transversion at the second base of codon 258.

Table 2 Prevalence and adjusted odds ratios for plasma 249 ^{Ser} p53 mutations by subject groups from Qidong

	Controls[a]	Cirrhotics	Hepatocellular carcinomas
	(30)	(20)	(25)
No. positive (%)	2 (7)	4 (20)	10 (40)
OR (95% CI)	1.0	5 (0.6, 29.3)	22.1 (3.2,91.7)

[a]Estimated odds ratios (OR) and 95 % confidence intervals (CI) were adjusted for age, gender, recruitment site and hepatitis B surface antigen status, using controls as the referent group.

DISCUSSION

In the People' s Republic of China, HCC accounts for over 250 000 deaths annually with an incidence rate in some areas of the country approaching 150 cases/100 000/year. Mutations in the p53 tumor suppressor gene have been identified in a majority of human cancers[21], especially in HCC[2,22]. The most striking example of a specific mutation in the p53 gene is a G→T transversion in the third base of codon 249, which has been detected in 10-70 % of HCCs from area with a high exposure to AFB1[6,23-25], where this mutation is absent from HCC in regions with negligible exposure to AFB1[13,26,27].

Jackson *et al*. reported that a high percentage of the tumors from Qidong had G→T mutation at the third base of codon 249 of the p53 gene than tumors from Shanghai (46.7 % compared with 30 %)[10,28]. The mutation frequency corresponds to exposure to aflatoxins because these areas have high and intermediate exposure levels, respectively. A recent report by Kirk *et al*. reported for the first time the detection of codon 249 p53 mutation in the plasma of liver tumor patients from Gambia. DNA circulating in the serum or plasma can be successfully retrieved and used as surrogate material to analyze for genetic alterations present in the original tumor[10,29]. Although the mechanisms accounting the presence of this circulating DNA are uncertain, there is some evidence that the DNA, of up to 21 Kb, are released from the tumor as a glyconucleoprotein complex, and may protect the DNA from degradation by nucleases. Although we don' t understand the relationship between the release of tumor DNA into the plasma and necrosis of the tumor, apoptosis or other selective cellular processes, we considered from our experimental data that plasma or serum may be used as a source of tumor-specific DNA[30,31].

We reported the presence of 249^{Ser} p53 mutations in DNA circulating in the plasma of Qidong population at high risk for HCC, chronic HBV infection and exposure to the carcinogen AFB1. We found in this paper 16 of 75 subjects from Qidong had 249^{ser} p53 mutation, including ten of 25 HCC cases, four of 20 cirrhotic patients, and two of 30 controls (Table 2). It is interesting that we found in one HCC case a G→C transversion at the third base of codon 249 instead of G→T transversion, although both of AGC and AGT coded serine. The 249^{Ser} p53 "hotspot" mutation was detected in 40 % of HCC cases, and a much lower prevalence was observed in cirrhotic patients (20 %) and in controls (7 %) (P<0.001 for difference between groups). Additionally, we found in another HCC case A→C transversion at the second base of codon 258. We checked the exon 7 of p53 gene using NCBI Blast, and found none of the ESTs could support this point mutation. Is it a SNP or a point mutation associated with AFB1 exposure? It is to be studied. Although we didn' t check the 249^{Ser} p53 mutations in the corresponding tissues, we can draw a conclusion from these data that p53 mutation frequency of these different groups provided the strong relationship between cirrhosis and the future development of HCC[32]. This mutation may be regarded as an early detection marker or a prognostic molecular marker in HCC[33,34]. The detection of 249^{Ser} DNA may be useful as a

maker of neoplastic development, and the presence of the mutation in healthy subjects may reflect chronic exposure to high levels of AFB1[35].

Besides the detection of serum aflatoxin-albumin adducts, we can also use plasma 249^{Ser} p53 mutation as a marker of aflatoxin exposure in epidemiological studies. It is expected in Qidong area that the detection of p53 mutation in plasma DNA could be developed into a usual method to estimate the development of HCC, and this mutation could be regarded as an early diagnostic marker of hepatocellular carcinoma.

REFERENCES

1 **Jackson PE**, Groopman JD. Aflatoxin and liver cancer. *Baillieres Best Pract Res Clin Gastroenterol* 1999; **13**: 545-555
2 **Hsia CC**, Kleiner DE Jr, Axiotis CA, Di Bisceglie A, Nomura AM, Stemmermann GN, Tabor E. Mutations of p53 gene in hepatocellular carcinoma: roles of hepatitis B virus and aflatoxin contamination in the diet. *J Natl Cancer Inst* 1992; **84**: 1638-1641
3 **Lunn RM**, Zhang YJ, Wang LY, Chen CJ, Lee PH, Lee CS, Tsai WY, Santella RM. p53 mutations, chronic hepatitis B virus infection, and aflatoxin exposure in hepatocellular carcinoma in Taiwan. *Cancer Res* 1997; **57**: 3471-3477
4 **Park US**, Su JJ, Ban KC, Qin L, Lee EH, Lee YI. Mutations in the p53 tumor suppressor gene in tree shrew hepatocellular carcinoma associated with hepatitis B virus infection and intake of aflatoxin B1. *Gene* 2000; **251**: 73-80
5 **Lee YI**, Lee S, Das GC, Park US, Park SM, Lee YI. Activation of the insulin-like growth factor II transcription by aflatoxin B1 induced p53 mutant 249 is caused by activation of transcription complexes; implications for a gain-of-function during the formation of hepatocellular carcinoma. *Oncogene* 2000; **19**: 3717-3726
6 **Wang JS**, Huang T, Su J, Liang F, Wei Z, Liang Y, Luo H, Kuang SY, Qian GS, Sun G, He X, Kensler TW, Groopman JD. Hepatocellular carcinoma and aflatoxin exposure in Zhuqing Village, Fusui County, People's Republic of China. *Cancer Epidemiol Biomarkers Prev* 2001; **10**: 143-146
7 **Smela ME,** Hamm ML, Henderson PT, Harris CM, Harris TM, Essigmann JM. The aflatoxin B(1) formamidopyrimidine adduct plays a major role in causing the types of mutations observed in human hepatocellular carcinoma. *Proc Natl Acad Sci U S A* 2002; **99**: 6655-6660
8 **Zhang F,** Zhu Y, Sun Z. Universal presence of HBVx gene and its close association with hotspot mutation of p53 gene in hepatocellular carcinoma of prevalent area in China. *Zhonghua Zhongliu Zazhi* 1998; **20**: 18-21
9 **Zhu M**, Dai Y, Zhan R. HBxAg enhanced p53 protein accumulation in hepatoma cells. *Zhonghua Binglixue Zazhi* 1999; **28**: 31-34
10 **Jackson PE**, Qian GS, Friesen MD, Zhu YR, Lu P, Wang JB, Wu Y, Kensler TW, Vogelstein B, Groopman JD. Specific p53 mutations detected in plasma and tumors of hepatocellular carcinoma patients by electrospray ionization mass spectrometry. *Cancer Res* 2001; **61**: 33-35
11 **Pfeifer GP**, Denissenko MF, Olivier M, Tretyakova N, Hecht SS, Hainaut P. Tobacco smoke carcinogens, DNA damage and p53 mutations in smoking-associated cancers. *Oncogene* 2002; **21**: 7435-7451
12 **Niu ZS,** Li BK, Wang M. Expression of p53 and C-myc genes and its clinical relevance in the hepatocellular carcinomatous and pericarcinomatous tissues. *World J Gastroenterol* 2002; **8**: 822-826
13 **Hsu IC**, Metcalf RA, Sun T, Welsh JA, Wang NJ, Harris CC. Mutational hotspot in the p53 gene in human hepatocellular carcinoma. *Nature* 1991; **350**: 427-428
14 **Li D**, Cao Y, He L, Wang N J, Gu JR. Aberrations of p53 gene in human hepatocellular carcinoma from China. *Carcinogenesis* 1993; **14**: 169-173
15 **Fujimoto Y**, Hampton LL, Wirth PJ, Wang NJ, Xie JP, Thorgeirsson SS. Alterations of tumor suppressor genes and allelic losses in human hepatocellular carcinomas in China. *Cancer Res* 1994; **54**: 281-285
16 **Deng ZL**, Ma Y. Aflatoxin sufferer and p53 gene mutation in hepatocellular carcinoma. *World J Gastroenterol* 1998; **4**: 28-29
17 **Kirk GD**, Camus-Randon AM, Mendy M, Goedert JJ, Merle P, Trepo C, Brechot C, Hainaut P, Montesano R. 249 Ser- p53 mutations in plasm DNA of patients with hepatocellular carcinoma from the Gambia. *J Natl Cancer Inst* 2000; **92**: 148-153
18 **Wong IH**, Lo YM, Zhang J, Liew CT, Ng MH, Wong N, Lai PB, Lau WY, Hjelm NM, Johnson PJ. Detection of aberrant p16 methylation in the plasma and serum of liver cancer patients. *Cancer Res* 1999; **59**: 71-73
19 **Chen XQ**, Stroun M, Magnenat JL, Nicod LP, Kurt AM, Lyautey J,Lederrey C, Anker P. Microsatellite alterations in plasma DNA of small cell lung cancer patients. *Nat Med* 1996; **2**: 1033-1035
20 **Nawroz H**, Koch W, Anker P, Stroun M, Sidransky D. Microsatellite alterations in serum DNA of head and neck cancer patients. *Nat Med* 1996; **2**: 1035-1037
21 **Martins C**, Kedda MA, Kew MC. Characterization of six tumor suppressor genes and microsatellite instability in hepatocellular carcinoma in southern African blacks. *World J Gastroenterol* 1999; **5**: 470-476
22 **Jiang W**, Lu Q, Pan G. p53 gene mutation in hepatocellular carcinoma. *Zhonghua Waike Zazhi* 1998; **36**: 531-532
23 **Yang M**, Zhou H, Kong RY, Fong WF, Ren LQ, Liao XH, Wang Y, Zhuang W, Yang S. Mutations at codon 249 of p53 gene in human hepatocellular carcinomas from Tongan, China. *Mutat Res* 1997; **381**: 25-29
24 **Shimizu Y**, Zhu JJ, Han F, Ishikawa T, Oda H. Different frequencies of p53 codon-249 hot-spot mutations in hepatocellular carcinomas in Jiangsu province of China. *Int J Cancer* 1999; **82**: 187-190
25 **Ming L**, Yuan B, Thorgeirsson SS. Characteristics of high frequency 249 codon mutation of p53 gene in hepatocellular carcinoma in prevalent area of China. *Zhonghua Zhongliu Zazhi* 1999; **21**: 122-124
26 **Qian GS**, Ross RK, Yu MC, Yuan JM, Gao YT, Henderson BE, Wogan GN, Groopman JD. A follow-up study of urinary markers of aflatoxin exposure and liver cancer risk in Shanghai, People's Republic of China. *Cancer Epidemiol Biomark Prev* 1994; **3**: 3-10
27 **Liu H**, Wang Y, Zhou Q, Gui SY, Li X. The point mutation of p53 gene exon7 in hepatocellular carcinoma from Anhui Province, a non HCC prevalent area in China. *World J Gastroenterol* 2002; **8**: 480-482
28 **Qian GS,** Kuang SY, He X, Groopman JD, Jackson PE. Sensitivity of electrospray ionization mass spectrometry detection of codon 249 mutations in the p53 gene compared with RFLP. *Cancer Epidemiol Biomarkers Prev* 2002; **11**: 1126-1129
29 **Anker P**, Lefort F, Vasioukhin V, Lyautey J, Lederrey C, Chen XQ, Stroun M, Mulcahy HE, Farthing MJ. K-ras mutations are found in DNA extracted from the plasma of patients with colorectal cancer. *Gastroenterology* 1997; **112**: 1114-1120
30 **Stroun M**, Anker P, Beljanski M, Henri J, Lederrey C, Ojha M, Maurice PA. Presence of RNA in the nucleoprotein complex spontaneously released by human lymphocytes and frog auricles in culture. *Cancer Res* 1978; **38**: 3546-3554
31 **Goessl C**, Heicappell R, Munker R, Anker P, Stroun M, Krause H, Muller M, Miller K. Microsatellite analysis of plasma DNA from patients with clear cell renal carcinoma. *Cancer Res* 1998; **58**: 4728-4732
32 **Minouchi K**, Kaneko S, Kobayashi K. Mutation of p53 gene in regenerative nodules in cirrhotic liver. *J Hepatol* 2002; **37**: 231-239
33 **Qin LX**, Tang ZY. The prognostic molecular markers in hepatocellular carcinoma. *World J Gastroenterol* 2002; **8**: 385-392
34 **Qin LX**, Tang ZY, Ma ZC, Wu ZQ, Zhou XD, Ye QH, Ji Y, Huang LW, Jia HL, Sun HC, Wang L. P53 immunohistochemical scoring: an independent prognostic marker for patients after hepatocellular carcinoma resection. *World J Gastroenterol* 2002; **8**: 459-463
35 **Makarananda K,** Pengpan U, Srisakulthong M, Yoovathaworn K, Sriwatanakul K. Monitoring of aflatoxin exposure by biomarkers. *J Toxicol Sci* 1998; **23**: 155-159

Edited by Zhao M

P.O.Box 2345, Beijing 100023, China
Fax: +86-10-85381893
E-mail: wjg@wjgnet.com www.wjgnet.com

World J Gastroenterol 2003;9(4):696-700
World Journal of Gastroenterology
 ISSN 1007-9327

• LIVER CANCER •

Docetaxel inhibits SMMC-7721 human hepatocellular carcinoma cells growth and induces apoptosis

Chang-Xin Geng, Zhao-Chong Zeng, Ji-Yao Wang

Chang-Xin Geng, Ji-Yao Wang, Department of Gastroenterology, Zhongshan Hospital, Fudan University, Shanghai 200032, China
Zhao-Chong Zeng, Department of Radiation Oncology, Zhongshan Hospital, Fudan University, Shanghai 200032, China
Correspondence to: Prof. Ji-Yao Wang, Director of Department of Gastroenterology, Zhongshan Hospital, Fudan University, Shanghai 200032, China. jiyao_wang@hotmail.com
Telephone: +86-21-64041990-2420 **Fax:** +86-21-34160980
Received: 2002-08-06 **Accepted:** 2002-09-03

Abstract

AIM: To investigate the in vitro anti-hepatocellular carcinoma (HCC) activity of docetaxel against SMMC-7721 HCC cells and its possible mechanism.

METHODS: The HCC cells were given different concentrations of docetaxel and their growth was measured by colony forming assay. Cell cycle and apoptosis were analyzed by flow cytometry and fluorescence microscopy (acridine orange/ethidium bromide double staining, AO/EB), as well as electronic microscopy. The SMMC-7721 HCC cell reactive oxygen species (ROS) and glutathione (GSH) were measured after given docetaxel.

RESULTS: Docetaxel inhibited the hepatocellular carcinoma cells growth in a concentration dependent manner with $IC_{50}5\times10^{-10}$ M. Marked cell apoptosis and G2/M phase arrest were observed after treatment with docetaxel $\geqslant10^{-8}$M. Docetaxel promoted SMMC-7721 HCC cells ROS generation and GSH deletion.

CONCLUSION: Docetaxel suppressed the growth of SMMC-7721 HCC cells in vitro by causing apoptosis and G2/M phase arrest of the human hepatoma cells, and ROS and GSH may play a key role in the inhibition of growth and induction of apoptosis.

Geng CX, Zeng ZC, Wang JY. Docetaxel inhibits SMMC-7721 human hepatocellular carcinoma cells growth and induces apoptosis. *World J Gastroenterol* 2003; 9(4): 696-700
http://www.wjgnet.com/1007-9327/9/696.htm

INTRODUCTION

Decetaxel is a new taxoid structurally similar to paclitaxel, a semisynthetic product of a renewable resource, the needles of the European yew, Taxus baccata L. In comparison to paclitaxel, docetaxel is more potent as an inhibitor of microtubule depolymerization[1]. Docetaxel has shown an active effect against cancers[2-5]. Current studies have shown that docetaxel combined with other chemotherapeutic drugs has higher anticancer efficacy and reduced side effects in patients with breast, pancreatic, gastric, urothelial carcinomas[6-9]. But there is limited data about that in hepatocellular carcinoma and thus needs further investigation. Human hepatocellular carcinoma (HCC) is one of the major causes of death worldwide[10-12], and surgical resection is the only curative therapy[13]. However it has limitations for patients with multiple type or metastatic tumors. Searching for effective chemotherapeutic agents is important to improve the survival rate of patients with advanced or recurrent HCC after surgical treatment. HCC is usually insensitive to chemotherapeutic drugs currently used in clinical setting, and there is thus an urgent need for the evaluation of new active drugs against HCC. HCC is well known for its expression of multidrug resitance (MDR) gene and its poor response to chemotherapeutic agents, but it has been found that docetaxel is effective in treating mice bearing xenografts of MDR protein positive human tumors[14], also a low efflux of docetaxel from tumor cells being observed[15]. These results suggest that docetaxel may be effective in the treatment of HCC. But the related information is limited and the mechanism of docetaxel remains to be elucidated. This study is to investigate its growth inhibition and induction of apoptosis effect and the mechanism in human SMMC-7721 hepatocellular cell line, and to provide the theoretical basis for clinical application in patients with HCC.

MATERIALS AND METHODS

Reagents

Docetaxel (Rhone-Poulenc Rorer Pharmaceuticals Inc.) was stored as 100 μM stock solution in absolute ethanol at -80 ℃. This solution was further diluted in the medium and used in the cell culture immediately before each experiment.

Cell cultures

Human hepatocellular carcinoma SMMC-7721 cell line was obtained from Liver Cancer Institute of Fudan University. The cells were cultured in flasks with RPMI1640 (Gibco BRL, Grand Island, NY) medium supplemented with 100 IU/ml penicillin, 100 μg/ml streptomycin and 10 % new born bovine serum (Hyclone, Logan, UT) and maintained at 37 ℃ in humidified atmosphere containing 5 % CO_2.

Colony forming assay

Exponential growth phase SMMC-7721 cells were seeded in 60 mm culture plate (Corning, NY) at a density of 200 cells/plate, after 24hr, the media was discarded and replaced with equal volume of fresh media containing different doses of docetaxel (0, 10^{-11}, 10^{-10}, 10^{-9}, 10^{-8}, 10^{-7}, 10^{-6}M). 24hr later docetaxel containing media was again discarded and replaced by media without containing docetaxel. The cells were cultured continually for 9 days. The colonies were fixed with 95 % ethanol and stained with Giemsa, and manually counted. Colonies $\geqslant$50 cells were considered survivors. All experiments were conducted in triplicate.

Flow cytometric analysis of DNA content after docetaxel treatment

After exponential growth phase SMMC-7721 cells were treated with different doses of docetaxel (0, 10^{-11}, 10^{-10}, 10^{-9}, 10^{-8}, 10^{-7}, 10^{-6}M) for 24hr and harvested with 0.25 % trypsin and resuspended in RPMI1640 media. 1×10^{6} cells was centrifuged at 300 g for 5 minutes and then washed once with PBS .The cell pellets were added with 100 % precooled ethanol at 4 ℃

for 4hr, centrifuged at 300 g for 5 minutes and then washed once, resuspended with PBS (1×10^6cells/ml). The cells were added 500 u Rnase, incubated at 37 ℃ for 30 minutes, washed with PBS. 1×10^6cells were stained with 50 μg/ml PI for 20 minutes in the dark. The DNA content of each cell was measured using a Becton Dickinson FACSCalibur flow cytometer and analyzed with ModFit LT software (San Jose, CA).

Morphological study with fluorescence microscope

Exponential growth phase SMMC-7721 cells were treated with 10nM docetaxel for 24hr and 48hr and harvested with 0.25 % trypsin and resuspended in RPMI1640 medium. 1×10^6 cells were washed once and resuspended with PBS. 25 μl of the cells suspension was mixed with 1 μl of dye mixture containing AO 100 μg/ml and EB 100 μg/ml in PBS[16]. The cells were visualized immediately under a fluorescence microscope, the peak excitation wave length was 490 nm.

Transmission electron microscopic observation

After exponential growth phase SMMC-7721 cells treated with 10nM docetaxel for 24hr and 48hr, they were fixed in Karnovsky solution, followed by cacodylate buffer for ultrastructural examination. The cells were postfixed in 1 % osmium tetroxide and dehydrated for staining with uranyl acetate and lead citrate. Thin sections were observed under electron microscope.

ROS measurement

After exponential growth phase SMMC-7721 cells were treated with different doses of docetaxel (0.25 nM, 0.5 nM, 10 nM) for 24hr, the cells were incubated with 2', 7' -dichlorofluorescin diacetate (DCF/DA; 5 μM; Sigma) at 37 ℃ for 50 minutes to estimate the ROS level. The cells were harvested and detected immediately for fluorescence intensity detection on Becton Dickinson FACSCalibur flow cytometer and data were acquired and analyzed using FACS/CELLQuest software (San Jose, CA) on a Power Macintosh 7600/120 computer (Apple Computers, Cupertino, CA)[17], three independent experiments were repeated in each drug treated group and the control group was not given docetaxel but incubated with DCF/DA. All experiments were conducted in triplicate.

Determination of intracellular GSH content

The determination of intracellular GSH content was conducted according to Shen *et al*[18] with modification. Briefly after logarithmic growth phase SMMC-7721 cells ($\geqslant10^6$) were treated with different doses of docetaxel (0.25 nM, 0.5 nM, 10 nM) for 24hr, harvested by trypsination, washed, resuspended in PBS and counted under phase contrast microscope. The cells suspension was centrifuged at 300 g for 5 minutes, the cell pellets were added 0.75 ml distilled water and 0.25 ml thiosalicylic acid to precipitate the protein. After centrifugation at 12 000 g for 5 minutes at 4 ℃, the supernatant was used for GSH assay. The control group was not given docetaxel. All experiments were conducted in triplicate.

Statistical analysis

The intracellular GSH content was expressed as mean ±SD. Their differences between drug treated groups and the control group were analyzed with Student's *t*-test.

RESULTS

Effect of docetaxel on SMMC-7721 cells growth inhibition

The colony forming ability decreased gradually with increasing dose of docetaxel treatment, when the docetaxel concentration was increased to 10^{-8}M, the colony forming inhibition rate attained 100 % with IC_{50} 5×10^{-10} M (0.5 nM) (Figure 1).

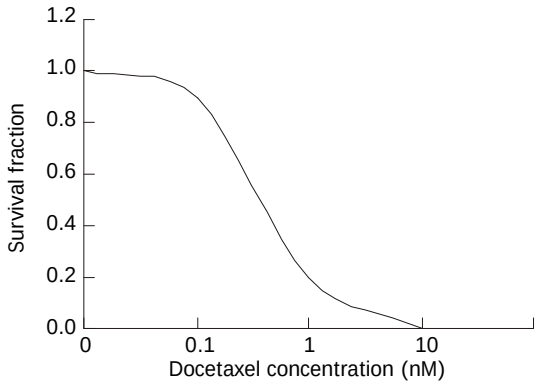

Figure 1 The survival fraction of SMMC-7721 cells treated with docetaxel for 24hr.

Effect on of docetaxel cell cycle and apoptosis of SMMC-7721 cells

As demonstrated in Figure 2, docetaxel induced a marked apoptosis at 10^{-8}M for 24hr, and caused cells G2/M phase arrest mainly at 10^{-7}M and 10^{-6}M, at 10^{-6}M the G2/M phase cells accounted for 96.1 %.

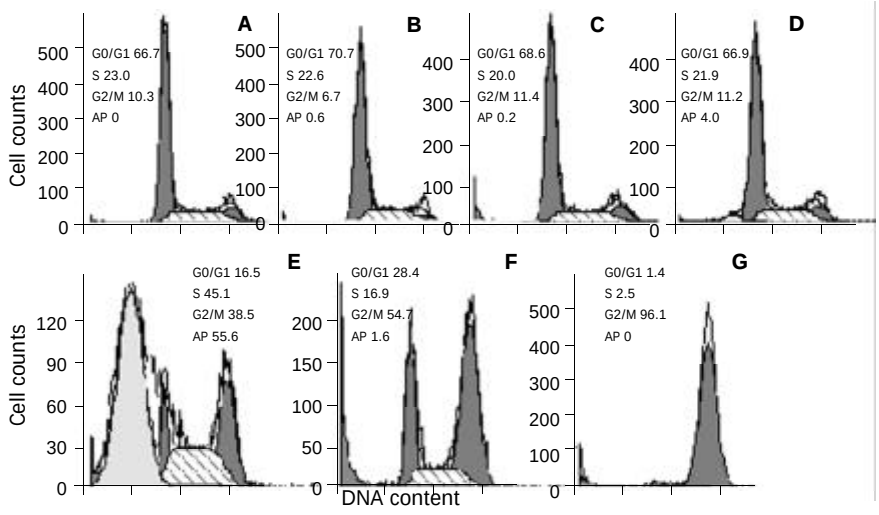

Figure 2 Cell cycle changes and apoptosis induction in SMMC-7721 cells treated with docetaxel for 24hr. Cells were treated with docetaxel at 0M(A), 10^{-11} M(B), 10^{-10} M(C), 10^{-9} M(D), 10^{-8} M(E), 10^{-7} M(F), 10^{-6}M(G). A marked apoptosis was induced at 10^{-8} M, and a peaked G2/M phase accumulation was caused at 10^{-6}M. Ap:apoptosis.

Morphological observation with fluorescence microscope

After the SMMC-7721 cells were given 10^{-8}M docetaxel for 24hr, the early apoptotic cells could be observed: because of their cells membrane integrity, the cells were stained green with AO, the nuclei exhibited bright condensed chromatin or fragmented, some cells blebbed. After the cells being treated for 48hr, some late apoptotic cells could be observed: Since their cell membrane lost integrity, they were stained red with EB, the apoptotic bodies could be seen clearly. On the contrary, the untreated cells did not show these apoptotic characteristics (Figure 3).

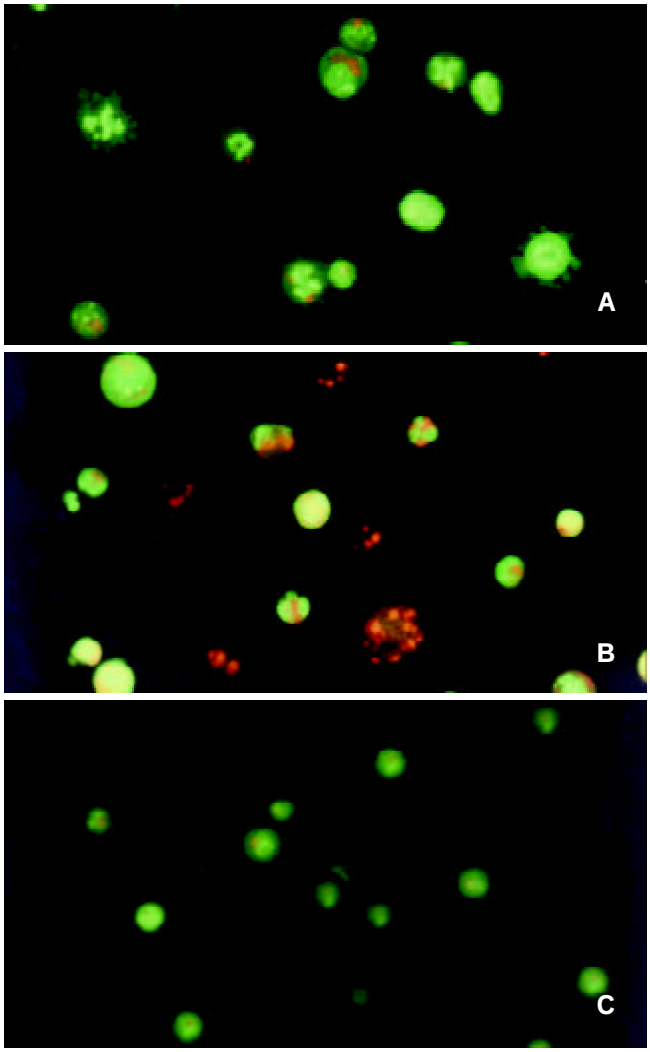

Figure 3 Morphological study with fluorescence microscope. After the SMMC-7721 cells were given 10^{-8}M docetaxel for 24hr (A), the cells were stained green with AO, the nuclei exhibited bright condensed chromatin or fragmented, some cells blebbed. After being treated for 48hr (B), cells were stained red with EB, the apoptotic bodies could be seen clearly. On the contrary, the untreated cells (C) did not show these apoptotic characteristics.

Transmission electron microscopic observation

After treatment with 10^{-8}M docetaxel for 24hr, the chromatin of some SMMC-7721 cells was located along the nuclear edges or formed irregularly shaped crescents at the nuclear edges, or became condensed or fragmented; Some cells nuclear membrane became irregular; The vacuole in some cytoplasma could be observed (Figure 4).

Effect of docetaxel on intracellular ROS

As demonstrated in Figure 5, The SMMC-7721 cells ROS level (corresponding to the fluorescence intensity) increased after treatment with 0.25 nM, 0.5 nM, 10 nM docetaxel. In comparison with the control group, the ROS level increased by 1.69, 1.78 and 1.80 times respectively.

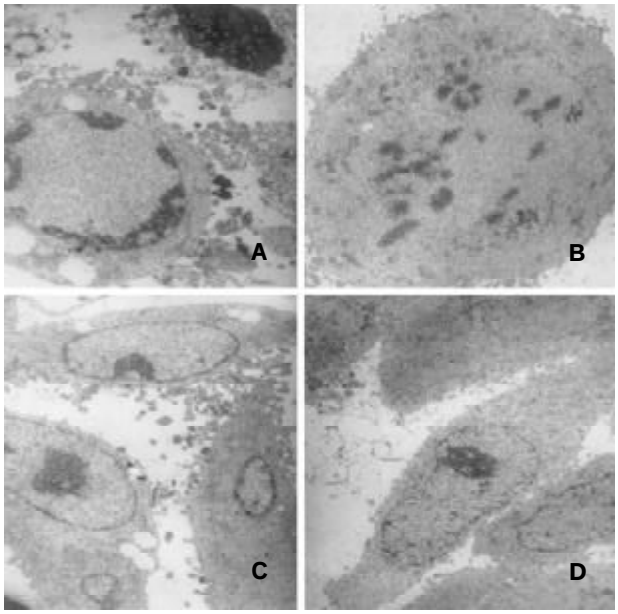

Figure 4 Transmission electron microscopic observation. After treatment with 10^{-8}M docetaxel for 24hr, the chromatin of some SMMC-7721 cells was located along the nuclear edges or formed irregularly shaped crescents at the nuclear edges (A, C),or became condensed or fragmented (A, B); The vacuole could be observed in some cytoplasm (A, C).

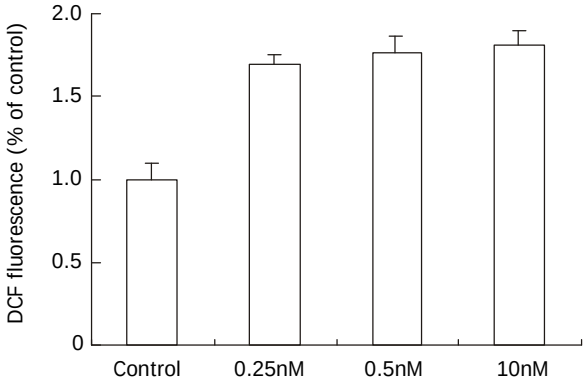

Figure 5 The effect of docetaxel on the formation of ROS in SMMC-7721 cells. Data are from three independent experiments.

Effect of docetaxel on intracellular GSH

The control group intracellular GSH content was 11.6±1.1 fmol/cell, after treatment with docetaxel 0.25 nM, 0.5 nM, 10 nM for 24hr, the SMMC-7721 cells GSH decreased to 4.7±0.7 fmol/cell, 3.0±0.5 fmol/cell, 1.0±0.1 fmol/cell respectively, there was a significant difference between the drug treated groups and the control group ($P<0.05$).

DISCUSSION

In the present study, we used colony forming assay to observe the effect of docetaxel on the growth of the human hepatocellular carcinoma SMMC-7721 cells in vitro, indicating that doctaxel can inhibit the SMMC-7721 cells growth and in concentration dependent manners, at 10^{-8}M the survival fraction decreased to 0 (Figure1). A previous study demonstrated that docetaxel showed cytotoxic effect on other human hepatoma cell lines[17], together with this report, our result suggests that

the growth-inhibiting effect of docetaxel may be a general phenomenon for human hepatocellular carcinoma cells. Also the flow cytometry showed that docetaxel causes SMMC-7721 cells apoptosis at a low dose (10^{-8}M), which was confirmed by fluorescence microscope, transmission electron microscope, and at 10^{-7}M, 10^{-6}M induced a marked G2/M phase arrest without apparent apoptosis, this phenomenon seems to suggest that docetaxel can induce apoptosis independent of G2/M phase arrest in SMMC-7721 cells.

In order to elucidate the mechanisms of the anti-hepatocellular carcinoma action of docetaxel, we examined its possible effect on cell cycle kinetics of SMMC-7721 cells. As demonstrated in Figure 2, following treatment with docetaxel for 24hr, the G2/M phase cells increased with docetaxel doses increasing from 10^{-8}M, at 10^{-6}M the G2/M phase cells accounted for 96.1 %. This result indicates that high dose of docetaxel blocks cell cycle at G2/M phase, disturbs mitosis and inhibits SMMC-7721 cells growth. In this clinical setting, such information may be useful for liver carcinoma therapy with docetaxel and other cytotoxic drugs which affect cell cycle progression.

According to Figure 1, docetaxel could inhibit SMMC-7721 cells at very low doses, the IC_{50} is 5×10^{-10}M. This dose of docetaxel had no significant effect on the cell apoptosis or cell cycle progression, which was confirmed by flow cytometry. In order to elucidate the mechanism underlying this phenomenon, the intracellular ROS and GSH were further investigated in this study. Our results indicated that docetaxel both at $1/2IC_{50}$, IC_{50} and apoptosis-inducing dose (10nM) could cause significantly increased ROS levels (Figure 5) and significantly decreased GSH, compared with those of the control.

It has been reported that tumor cells have persistently higher levels of ROS[19]. The relationship between ROS and apoptosis, cell growth inhibition has been broadly investigated. ROS has been found to regulate translocation of NF-κB[20] as well as translocation of p53 and the p53-mediated apoptosis pathway[21,22]. Also it has been found that induction of apoptosis was accompanied with the generation of intracellular ROS prior to the activation of caspase-3[23] and down-regulation of Bcl-2[24]. Simizu *et al*. reported that some anticancer agents, including vinblastin and camptothecin, induced cells apoptosis with the generation of ROS[25]. Recently it was reported that arsenic trioxide and l-S,R-buthionine sulfoximine (BSO) combination treatment enhanced hepatocellular carcinoma cells apoptosis through increased production of ROS[26], Also it was reported ROS played a mediatory role in the synergistic interaction between 1, 25-dihydroxyvitamin D (3) and anticancer cytokines[27], modulation of the ROS production intra and extracellularlly may influence the cell survival during oxidative insults[28].

Accordingly, we speculate that docetaxel-induced high level ROS may be involved in the growth inhibition and apoptosis of SMMC-7721 cells.

In order to confirm the SMMC-7721 cells redox status after docetaxel treatment, the intracellular GSH content was also investigated. Our result demonstrated that the intracellular GSH decreased significantly ($P<0.05$) after both $1/2IC_{50}$, IC_{50} and apoptosis-inducing dose docetaxel treatment, compared with that of the control group. This indicates that the decrease of GSH may be involved in the SMMC-7721 cells growth inhibition and apoptosis caused by docetaxel. Liu *et al*. found Salvia miltiorrhiza inhibited human hepatoma HepG2 cells growth and induced apoptosis involving in intracellular GSH deletion[29], early studies have also demonstrated that the onset of apoptosis was associated with a fall of intracellular GSH in different cellular systems[30]. And GSH could significantly reduce apoptosis mediated by a monoclonal antibody directed to Fas antigen, and apoptosis could be nearly completely prevented by GSH[31]. GSH is an important cellular thiol which is regarded as the major determinant of the intracellular redox potential, on the other hand, apoptosis may be regulated by the reodx status within the cells[32]. Loss of GSH was shown to be tightly coupled with a number of down-stream events in apoptosis, in caspase activation and events in chromatin[33], and GSH depletion may act as a link between oxidative stress and ceramide-mediated apoptosis[34]. Also it was found that decreased cells proliferation associated with decreased levels of intracellular GSH, and blockade of GSH synthesis enhanced ROS production and suppressed cells proliferation[35], cells with compromised cellular GSH were susceptible to redox imbalance-induced inhibition of proliferation[36].

In summary, the present study demonstrates that docetaxel has profound effects on SMMC-7721 hepatocellular carcinoma cells in vitro. It reduces the proliferation of these cells, causes changes in their morphology, and induces cell death by apoptosis. It leads to ROS generation and GSH deletion, subsequently results in redox imbalance in SMMC-7721 cells, and it is speculated that the redox imbalance caused by docetaxel may play an important role in the growth inhibition and induction of apoptosis of SMMC-7721 cells. As far as we know, there is few report concerning the redox imbalance and docetaxel. Our results not only provide the basis for further in vivo and clinical research in hepatocellular carcinoma, but also contribute to understanding of the pharmacology of docetaxel further.

REFERENCES

1 **Gueritte-Voegelein F**, Guenard D, Lavelle F, Le Goff MT, Mangatal L, Potier P. Relationships between the structure of taxol analogues and their antimitotic activity. *J Med Chem* 1991; **34**: 992-998

2 **Donnellan P**, Armstrong J, Rowan S, Fennelly D, Lynch V, McDonnell T, McDonnell T, McNicholas W, Crown J. New chemotherapy combination with docetaxel in the treatment of patients with non-small cell lung cancer. *Semin Oncol* 1998; **25**: 20-23

3 **Coleman RE**, Howell A, Eggleton SP, Maling SJ, Miles DW. Phase II study of docetaxel in patients with liver metastases from breast cancer. *Ann Oncol* 2000; **11**: 541-546

4 **Papakostas P**, Kouroussis C, Androulakis N, Samelis G, Aravantinos G, Kalbakis K, Sarra E, Souglakos J, Kakolyris S, Georgoulias V. First-line chemotherapy with docetaxel for unresectable or metastatic carcinoma of the biliary tract. A multicentre phase II study. *Eur J Cancer* 2001; **37**: 1833-1838

5 **Glisson BS**, Murphy BA, Frenette G, Khuri FR, Forastiere AA. Phase II Trial of docetaxel and cisplatin combination chemotherapy in patients with squamous cell carcinoma of the head and neck. *J Clin Oncol* 2002; **20**: 1593-1599

6 **Wenzel C**, Locker GJ, Schmidinger M, Rudas M, Taucher S, Gnant MF, Jakesz R, Steger GG. Combined analysis of two phase II trials in patients with primary and advanced breast cancer with epidoxorubicin and docetaxel plus granulocyte colony stimulating factor. *Anticancer Drugs* 2002; **13**: 67-74

7 **Cascinu S**, Graziano F, Barni S, Labianca R, Comella G, Casaretti R, Frontini L, Catalano V, Baldelli AM, Catalano G. A phase II study of sequential chemotherapy with docetaxel after the weekly PELF regimen in advanced gastric cancer. A report from the Italian group for the study of digestive tract cancer. *Br J Cancer* 2001; **84**: 470-474

8 **Ryan DP**, Kulke MH, Fuchs CS, Grossbard ML, Grossman SR, Morgan JA, Earle CC, Shivdasani R, Kim H, Mayer RJ, Clark JW. A Phase II study of gemcitabine and docetaxel in patients with metastatic pancreatic carcinoma. *Cancer* 2002; **94**: 97-103

9 **Sinibaldi VJ**, Carducci MA, Moore-Cooper S, Laufer M, Zahurak M, Eisenberger MA. Phase II evaluation of docetaxel plus one-day oral estramustine phosphate in the treatment of patients with androgen independent prostate carcinoma. *Cancer* 2002; **94**: 1457-1465

10 **Wu MC**. Clinical research advances in primary liver cancer. *World J Gastroenterol* 1998; **4**: 471-474

11 **Yip D**, Findlay M, Boyer M, Tattersall MH. Hepatocellular carcinoma in central Sydney:a 10-year review of patients seen in a medical oncology department. *World J Gastroenterol* 1999; **5**: 483-487

12 **Schmid R**. Prospect of gastroenterology and hepatology in the next century. *World J Gastroenterol* 1999; **5**: 185-190

13 **Qin LX**, Tang ZY. The prognostic significance of clinical and pathological features in hepatocellular carcinoma. *World J Gastroenterol* 2002; **8**: 193-199

14 **Vanhoefer U**, Cao S, Harstrick A, Seeber S, Rustum YM. Comparative antitumor efficacy of docetaxel and paclitaxel in nude mice bearing human tumor xenografts that overexpress the multidrug resistance protein (MRP). *Ann Oncol* 1997; **8**: 1221-1228

15 **Lavelle F**, Bissery MC, Combeau C, Riou JF, Vrignaud P, Andre S. Preclinical evaluation of docetaxel (Taxotere). *Semin Oncol* 1995; **22**: 3-16

16 **McGahon AJ**, Martin SJ, Bissonnette RP, Mahboubi A, Shi Y, Mogil RJ, Nishioka WK, Green DR. The end of the (cell) line: methods for the study of apoptosis *in vitro*. *Methods Cell Biol* 1995; **46**: 153-185

17 **Lin HL**, Liu TY, Chau GY, Lui WY, Chi CW. Comparison of 2-methoxyestrodiol-induced, docetaxel-induced, and paclitaxel-induced apoptosis in hepatoma cells and its correlation with reactive oxygen species. *Cancer* 2000; **89**: 983-994

18 **Shen HM**, Yang CF, Ong CN. Sodium selenite-induced oxidative stress and apoptosis in human hepatoma HepG2 cells. *Int J Cancer* 1999; **81**: 820-828

19 **Toyokuni S**, Okamoto K, Yodoi J, Hiai H. Persistent oxidative stress in cancer. *FEBS Lett* 1995; **358**: 1-3

20 **Kheradmand F**, Werner E, Tremble P, Symons M, Werb Z. Role of Rac1 and oxygen radicals in collagenase-1 expression induced by cell shape change. *Science* 1998; **280**: 898-902

21 **Takenaka K**, Moriguchi T, Nishida E. Activation of the protein kinase p38 in the spindle assembly checkpoint and mitotic arrest. *Science* 1998; **280**: 599-602

22 **Martinez JD,** Pennington ME, Craven MT, Warters RL, Cress AE. Free radicals generated by ionizing radiation signal nuclear translocation of p53. *Cell Growth Diff* 1997; **8**: 941-949

23 **Ueda S**, Nakamura H, Masutani H, Sasada T, Takabayashi A, Yamaoka Y, Yodoi J. Baicalin induces apoptosis via mitochondrial pathway as prooxidant. *Mol Immunol* 2002; **38**: 781-791

24 **Li HL**, Chen DD, Li XH, Zhang HW, Lu YQ, Ye CL, Ren XD. Changes of NF-κB, p53, Bcl-2 and caspase in apoptosis induced by JTE-522 in human gastric adenocarcinoma cell line AGS cells: role of reactive oxygen species. *World J Gastroenterol* 2002; **8**: 431-435

25 **Simizu S**, Takada M, Umezawa K, Imoto M. Requirement of caspase-3 (like) protease-mediated hydrogen peroxide production for apoptosis induced by various anticancer drugs. *J Biol Chem* 1998; **273**: 26900-26907

26 **Kito M**, Akao Y, Ohishi N, Yagi K, Nozawa Y. Arsenic trioxide-induced apoptosis and its enhancement by buthionine sulfoximine in hepatocellular carcinoma cell lines. *Biochem Biophys Res Commun* 2002; **291**: 861-867

27 **Koren R**, Rocker D, Kotestiano O, Liberman UA, Ravid A. Synergistic anticancer activity of 1, 25-dihydroxy vitamin D(3) and immune cytokines: the involvement of reactive oxygen species. *J Steroid Biochem Mol Biol* 2000; **73**: 105-112

28 **Teramoto S**, Tomita T, Matsui H, Ohga E, Matsuse T, Ouchi Y. Hydrogen peroxide-induced apoptosis and necrosis in human lung fibroblasts:protective roles of glutathione. *Jpn J Pharmacol* 1999; **79**: 33-40

29 **Liu J**, Shen HM, Ong CN. Salvia miltiorrhiza inhibits cell growth and induces apoptosis in human hepatoma HepG2 cells. *Cancer Letters* 2000; **153**: 85-93

30 **Hall AG**. The role of glutathione in the regulation of apoptosis. *Eur J Clin Invest* 1999; **29**: 238-245

31 **Wedi B**, Straede J, Wieland B, Kapp A. Eosinophil apoptosis is mediated by stimulators of cellular oxidative metabolisms and inhibited by antioxidants: involvement of a thiol-sensitive redox regulation in eosinophil cell death. *Blood* 1999; **94**: 2365-2373

32 **Watson RW**, Rotstein OD, Nathens AB, Dackiw AP, Marshall JC. Thiol–mediated redox regulation of neutrophil apoptosis. *Surgery* 1996; **120**: 150-157

33 **Van den Dobbelsteen DJ**, Nobel CS, Schlegel J, Cotgreave IA, Orrenius S, Slater AF. Rapid and specific efflux of reduced glutathione during apoptosis induced by anti-Fas/ APO-1 antibody. *J Biol Chem* 1996; **271**: 15420-15427

34 **Lavrentiadou SN**, Chan C, Kawcak T, Ravid T, Tsaba A, van der Vliet A, Rasooly R, Goldkorn T. Ceramide-mediated apoptosis in lung epithelial cells is regulated by glutathione. *Am J Respir Cell Mol Biol* 2001; **25**: 676-684

35 **Chang WK**, Yang KD, Shaio MF. Lymphocyte proliferation modulated by glutamine: involved in the endogenous redox reaction. *Clin Exp Immunol* 1999; **117**: 482-488

36 **Noda T**, Iwakiri R, Fujimoto K, Aw TY. Induction of mild intracellular redox imbalance inhibits proliferation of CaCo-2 cells. *FASEB J* 2001; **15**: 2131-2139

Edited by Wu XN

P.O.Box 2345, Beijing 100023, China
Fax: +86-10-85381893
E-mail: wjg@wjgnet.com www.wjgnet.com

World J Gastroenterol 2003;9(4):701-705
World Journal of Gastroenterology
 ISSN 1007-9327

• LIVER CANCER •

Experimental study on ultrasound-guided intratumoral injection of "Star-99" in treatment of hepatocellular carcinoma of nude mice

Li-Wu Lin, Xiao-Dong Lin, Yi-Mi He, Shang-Da Gao, En-Sheng Xue

Li-Wu Lin, Xiao-Dong Lin, Yi-Mi He, Shang-Da Gao, En-Sheng Xue, Department of Ultrasound, Union Hospital of Fujian Medical University, Fuzhou 350001, Fujian Province, China
Correspondence to: Dr. Li-Wu Lin, Department of Ultrasound, Union Hospital of Fujian Medical University, Fuzhou 350001, Fujian Province, China. lxdghl@163.net
Telephone: +86-591-3357896-8352
Received: 2002-08-06 **Accepted:** 2002-09-04

Abstract

AIM: To investigate the anti-cancer effect and the immunological mechanism of ultrasound-guided intratumoral injection of Chinese medicine "Star-99" in hepatocellular carcinoma (HCC) of nude mice.

METHODS: Twenty-eight human hepatocellular carcinoma SMMC-7721 transplanted nude mice, 14 of hypodermically implanted and 14 of orthotopic liver transplanted, were randomly divided into three groups of which 14 mice with Star-99, and 7 with ethanol and saline respectively. Ten days after the transplantation the medicines were injected into the tumors of all the nude mice once every 5 days. After 4 injections the nude mice were killed. The diameters of three dimension of the tumors were measured by high frequency ultrasound before and after the treatment and the tumor growth indexes* (TGI) were calculated. Radioimmunoassay was used to detect the serum levels of interleukin-2 (IL-2) and tumor necrosis factor (TNF)-alpha. The tumor tissues were sent for flow cytometry (FCM) DNA analysis. Apoptotic cells were visualized by TUNEL assay. All the experiments were carried out by double blind method.

RESULTS: The TGI of Star-99 group (0.076±0.024) was markedly lower than that of the saline group (4.654±1.283) (P<0.01). It also seemed to be lower than that of the ethanol group (0.082±0.028), but not significantly different (P>0.05). Serum levels of IL-2 and TNF-α were markedly higher than those of ethanol group and saline groups (P<0.05). The mean apoptotic index (AI: percentage of TUNEL signal positive cells) in Star-99 group (48.98±5.09 %) was significantly higher than that of the ethanol group (11.95±2.24 %) and the saline group (10.48±3.85 %) (P<0.01). FCM DNA analysis showed that the appearance rate of the apoptosis peak in Srar-99 group was 92.9 %, markedly higher than that of the ethanol group (14.3 %) and the saline group (0.0 %) (P<0.01). Correlation (r=0.499, P<0.05) was found between AI and serum level of TNF-α.

CONCLUSION: Star-99 has an effect on the elevation of the serum levels of IL-2 and TNF-α. It indicates that Star-99 has the function of enhancing the cellular immunity and inducing cancer cell apoptosis. The correlation between AI and serum level of TNF-α indicates that the elevation of the serum of TNF-α induced by Star-99 may be an important factor in the promotion of the hepatic cancer cell apoptosis. Star-99 has strong effects on the inhibition and destruction of cancer cells. Its curative effect is as good as ethanol. Its major mechanisms can be as follows: (1) it increases the serum levels of IL-2 and TNF-α and triggers cellular immunity. (2) It can induce cancer cells apoptosis, the effective mechanism of the Star-99 is different from that of the ethanol. The mechanisms of triggering the immunologic function of the organism and inducing cell apoptosis are, of particular significance. This study will provide a new pathway of drug administration and an experimental basis for the treatment of HCC with Chinese herbal, and the study of Star-99 in the treatment of tumor is of profound significance with good prospects.

Lin LW, Lin XD, He YM, Gao SD, Xue ES. Experimental study on ultrasound-guided intratumoral injection of "Star-99" in treatment of hepatocellular carcinoma of nude mice. *World J Gastroenterol* 2003; 9(4): 701-705
http://www.wjgnet.com/1007-9327/9/701.htm

INTRODUCTION

The ultrasound-guided percutaneous intratumoral injection with ethanol, in treatment of hepatocellular carcinoma (HCC), has been widely used in the clinic in recent years since the report by the Japanese scholars (1983)[1-3]. Yet there are certain limitations in this treatment that lead us to search for newer drug that we have been studied for many years. In 1999, we discovered that the compound Chinese medicine "Star-99" had anti-cancer effect. In order to probe the effective mechanism of the ultrasound-guided intratumoral injection of HCC with Star-99, we detected the serum levels of interleukin-2 (IL-2) and tumor necrosis factor (TNF)-alpha, and conducted FCM DNA analysis and TUNEL assay to observe the phenomenon of apoptosis and to appraise the biological effect of Star-99.

MATERIALS AND METHODS

Experimental animal

For the experiment, we used 28 BALB/CA nude mice, which were 5-8 weeks old, provided by the Medical Experimental Animal Unit of Anti-cancer Center of Xia Men University, China. The average weight of the nude mice was 18±2.1 grams. The mice were raised in the layer drift shelves under aseptic condition. The cages, cushion, drinking water and standard forage were provided by Shanghai Bikai Company periodically.

Animal model production of human HCC

Human HCC SMMC-7721 cellular cultural suspension was centrifuged and the supernatant was removed. Then the cellular cultural liquid was added to make up 5×10^7 cells per milliliter. Subcutaneous injection was taken in the back of a nude mouse with 0.2 ml liquid. When the tumor grew to 1 cm in diameter, part of it was taken out under the aseptic condition and cut into small pieces in the size of 0.2×0.2×0.2 cm, which were transplanted subcutaneously at the back of other nude mice with a canula needle and underwent passages from generation to generation. The nude mice, under general anesthesia with

sodium pentothal injected intraperitoneally. The process was as follows: The abdomen of the mouse was incised 1 cm in length deep to peritoneum on the linea alba below the xiphoid process. The liver was squeezed out, a piece of tumor was embedded into the liver with canula needle, the needle aperture was blocked with gelatin sponge to stop bleeding, then the liver was sent back into the abdomen, the peritoneum and skin were sutured and the process of orthotopic liver transplantation was completed.

Experimental method

Twenty-eight human HCC transplanted nude mice, including 14 implanted hypodermically and the other 14 with liver transplanted orthotopically, were randomly divided into three groups: the Star-99 group containing 14 nude mice, the ethanol group and the saline group containing 7 nude mice each. The three dimensional diameters of the tumor were measured by high frequency ultrasound (Aloka 5500 with 10MHz probe) after 10 days transplantation of HCC. Then 0.1 ml Star-99, ethanol and saline were respectively injected into the center of the tumor with No.5 needle. The nude mice were killed after being injected every 5 days for a total of 4 injections in each mouse. The three dimensional diameters of the tumor were measured again before the mice were killed. Mice blood was obtained from the eye socket, and the sera were separated by low velocity centrifugation. The Radioimmunoassay (RIA) kit was purchased from Beijing East Asian Institute of Immunology. Sn-682 Radioimmunoassay γ counting apparatus was used to detect the serum levels of IL-2 and TNF-α. The apoptotic cells were visualized by terminal deoxynucleotidyl transferase (TdT)-mediated dUTP nick end labelling (TUNEL). The TUNEL kit (POD) was purchased from Roche Molecular Biochemicals. The assay performance followed the technical manual and the references[4-7]. It was TUNEL positive when the nucleolus appeared evidently brown granule. Ten high power fields were observed in each slide and at least 1 000 positive cells were calculated at random. The cellular suspension made by fresh tumor tissues was analyzed by FCM DNA. The appearance rates of the heteroploidy peak and apoptosis peak were analyzed. Double blind method was applied in this experiment.

Observation indexes

The tumor growth index (TGI) was calculated by the formula: volume of tumor (after treatment-before treatment) / volume of tumor (before treatment). The serum levels of IL-2 and TNF-α were determined. The apoptotic index (AI: percentage of TUNEL signal positive cells) were calculated as the TUNEL-positive cells / the total number of cancer cells×100 %. The appearance rates of the heteroploidy peak and apoptosis peak of the tumor tissue were analyzed by FCM DNA. The correlation coefficient between AI and serum levels of TNF-α was calculated.

Statistics method

The results were expressed as the mean ±SD. The data were analyzed by one-way ANOVA with Student' s *t* test, chi-square test and liner regression analysis. Value of $P<0.05$ was considered significant.

RESULTS

The tumor growth index

Table 1 showed that the growth index of Star-99 group was markedly lower than that of the saline group ($P<0.01$). It was also lower than that of the ethanol group, but there was no significant difference between them ($P>0.05$).

Table 1 Comparison of the growth index of Star-99, ethanol and saline groups

Groups	*n*	$\bar{x}$	SD	*P*
Star-99 (A)	14	0.076	±0.024	A, B>0.05
Ethanol (B)	7	0.082	±0.028	B, C<0.01
Saline (C)	7	4.654	±1.283	A, C<0.01

The serum levels of IL-2 and TNF-α after treatment

Table 2 showed that the serum levels of IL-2 and TNF-α in the Star-99 group were 6.63±1.39 ng/ml and 3.98±1.05 ng/ml, markedly higher than those of the ethanol and the saline groups ($P<0.05$).

Table 2 Comparison of the serum levels of IL-2 and TNF-α after treatment in the three groups

Groups	*n*	IL-2 (ng/ml)	TNF-α (ng/ml)	*P*
Star-99 (A)	14	6.63±1.39	3.98 ±1.05	A:B <0.05
Ethanol (B)	7	4.22±1.23	2.95 ±1.01	A:C <0.05
Saline (C)	7	4.51±0.84	2.84± 1.05	B:C >0.05

The apoptotic index of Star-99, ethanol and saline groups after treatment

Table 3 showed that the AI in Star-99 group (48.98±5.09 %) was significantly higher than that of the ethanol group (11.95 ±2.24 %) and the saline group (10.48±3.85 %) ($P<0.01$), (Figure 1).

Table 3 Comparison of the apoptotic index of Star-99, ethanol and saline groups after treatment

Groups	*n*	AI (%)	*P*
Star-99 (A)	14	48.98±5.09	A:B<0.01
Ethanol (B)	7	11.95±2.24	B:C>0.05
Saline (C)	7	10.48±3.85	A:C<0.01

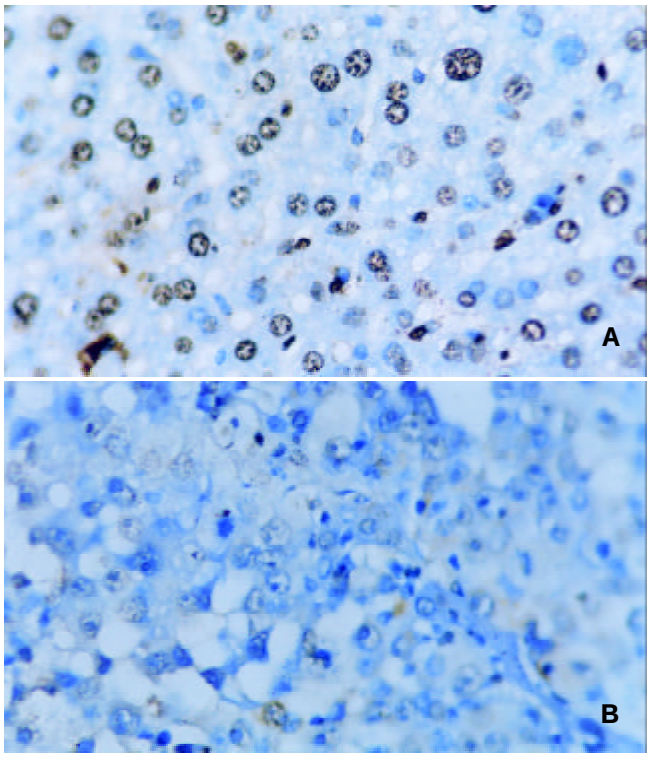

Figure 1 TUNEL marker (Nucleolus with brown granule indicated positive). A: Star-99 group; B: saline group; ×400.

FCM DNA analysis

Table 4 showed the results of FCM DNA analysis of the tumor tissues of the three groups. The appearance rate of the heteroploidy peak after the treatment was 57.1 % in the saline group (Figure 2), markedly higher than that of the ethanol group (0.0 %) and the Star-99 group (7.1 %) (P<0.01). Another remarkable characteristic was that 92.9 % of the Star-99 group appeared apoptosis peaks formed by the cells in the sub G_1 period (Figure 3), markedly higher than that of the ethanol group and the saline group, which were 14.3 % (1/7) and 0.0 (0/7), respectively (P<0.01).

Table 4 Comparison of the appearance rates of the hereroploidy and apoptosis peak after treatment in the three groups

Groups	*n*	Hereroploidy peak (%)	*P*	Apoptosis peak (%)	*P*
Star-99 (A)	14	7.1 (1/14)	A:B>0.05	92.9 (13/14)	A:B<0.01
Ethanol (B)	7	0. 0 (0/7)	B:C<0.05	14.3 (1/7)	B:C>0.05
Saline (C)	7	57.1 (4/7)	A:C<0.05	0.0 (0/7)	A:C<0.01

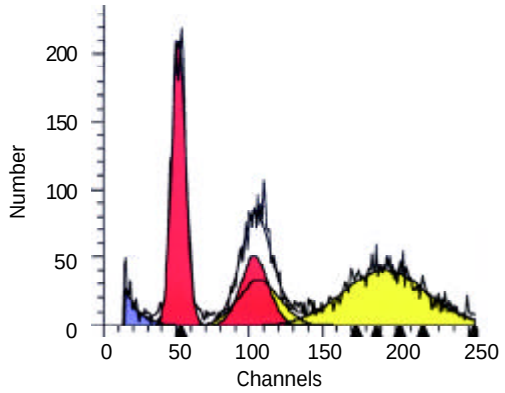

Figure 2 FCM DNA analysis showed the hereroploidy peak in the saline group. (Yellow peak).

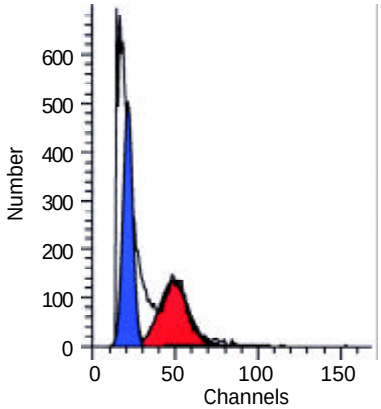

Figure 3 FCM DNA analysis showed the apoptosis peak in the Star-99 group. (Blue peak).

The relationship between HCC apoptosis and serum levels of TNF-α

There was close relationship between HCC apoptosis and serum level of TNF-α. Significant correlation (r=0.499, P<0.05) was found between AI and serum levels of TNF-α.

DISCUSSION

At present, many kinds of ultrasound-guided interventional therapy have been practiced by clinicians such as laser[8,9], microwave[10-13], radio frequency[14-19] and high energy focus ultrasound[20,21] since 1990s. The efficacy are as good as that of surgical resection[2, 22-24]. Early In 1985, the American National Cancer Institute considered biotherapy as the fourth modality in cancer treatment as it attacked the tumor cells directly; furthermore, it stimulates the immune system of the host. The present study provided a new avenue to combat the tumor from immunologic point of view. As shown in this experiment, the Star-99 has marked effect on the growth restraint of the tumor, the effectiveness is more or less equivalent to that of the ethanol.

The two important cytokines IL-2 and TNF-α can be used as biological response modifiers (BRM). IL-2 can enhance the activity of lymphocyte and the killing effect of CTL, NK and LAK cells, induce secretion of cytokine. The serum level of IL-2 reflects the host immunologic function to a certain degree[25]. In this experiment, the serum level of IL-2 in the Star-99 group was 6.63±1.39 ng/ml, markedly higher than those of ethanol and saline groups (P<0.05). In another experiment of this study, the electron microscopy showed many lymphocytes in the tumor tissues of the Star-99 group[26]. Figure 4 showed the microvilli on the surface of the lymphocytes attacked the cancer cells. The membrane of tumor cell in contact with the sensitized T lymphocyte became broken with the organelle and the nucleus dissolved and the vacuolation of the cytoplasm as well. This phenomenon further illustrate that the Star-99 could stimulate or induce the cellular immunity function of the organism. TNF-α is mainly produced by macrophage and activated T lymphocyte which can inhibit or destroy the cancer cells. It can also induce apoptosis by combining with TNF receptor and resulting in chain reactions[27,28]. In the Star-99 group, the serum level of TNF-α was 3.98±1.05 ng/ml, markedly higher than those of ethanol and saline groups. Significant correlation (r=0.499, P<0.05) was found between AI and serum levels of TNF-α. It indicated that the elevation of the serum TNF-α induced by Star-99 might be an important factor in the promotion of the HCC cells apoptosis.

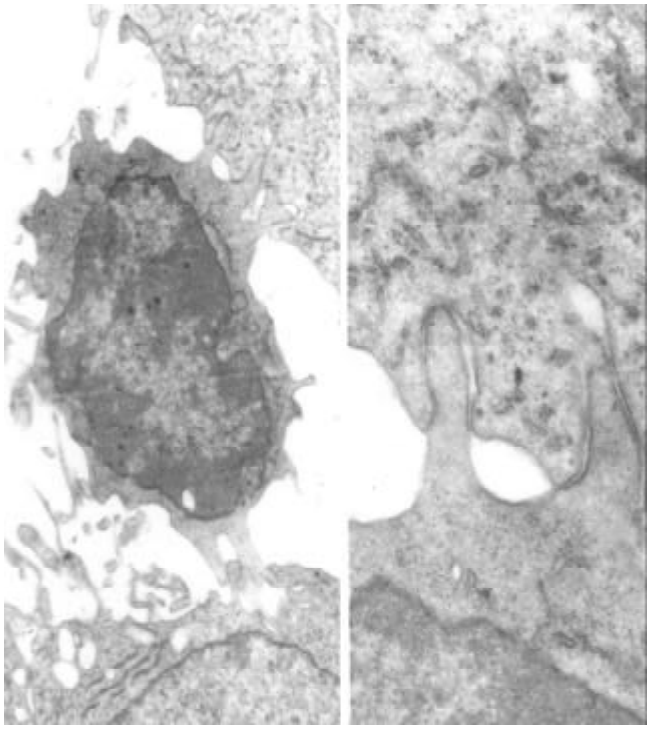

Figure 4 Many lymphocytes could be seen in the tumor tissues and the microvilli on the surface of the lymphocytes attacking the cancer cells in the Star-99 group (The right figure is a magnified image.).

Cancer growth not only depends on proliferation[29-35] but also on the reduced apoptosis[36-39]. At present time, cancer therapy is now focusing on promoting apoptosis[40,41]. The apoptotic cells could be identified by TUNEL assay[5, 42]. In this experiment, the apoptotic index in Star-99 group (48.98±5.09 %) was significantly higher than that in the ethanol group (11.95±2.24 %) and the saline group (10.48±3.85 %) (P<0.01), which was consistent with the result of FCM DNA analysis, the appearance rate of the apoptosis peak in Srar-99 group was 92.9 %, markedly higher than that of the ethanol group (14.3 %) and the saline group (0.0 %) (P<0.01). These results showed that although the cancer cells in ethanol group were destroyed which was different from that by means of apoptosis. In the Star-99 group it was mainly by induction of apoptosis.

The results of this study illustrated that the compound Chinese medicine Star-99 has the strong effect on the growth restraint of the tumor. Apart from its direct destruction of cancer cells, the mechanism of the efficacy may be due to: (1) It can increase the serum levels of IL-2 and TNF-α and trigger the cellular immunity. (2) It can induce apoptosis of the cancer cells. The anti-cancer effect of Star-99 is more or less equivalent to the ethanol, but by different mechanisms. Based on the above findings, Star-99 may have great significance and good prospects in the future treatment of HCC.

REFERENCES

1 **Lin LW**, Ye Z, Xue ES, Gao SD, He YM. A study of percutaneous hepatic quantified ethanol injection in treatment of hepatocarcinoma. *Zhongguo Chaosheng Yixue Zazhi* 2000; **16**: 514-516

2 **Arii S**, Yamaoka Y, Futagawa S, Inoue K, Kobayashi K, Kojiro M, Makuuchi M, Nakamura Y, Okita K, YAmada R. Results of surgical and nonsurgical treatment for small-sized hepatocellular carcinomas: A retrospective and nationwide survey in Japan. *Hepatology* 2000; **32**: 1224-1229

3 **Livraghi T**, Benedini V, Lazzaroni S, Meloni F, Torzilli G, Vettori C. Long term results of single session percutaneous ethanol injection in patients with large hepatocellular carcinoma. *Cancer* 1998; **83**: 48-57

4 **Tian G**, Yu JP, Luo HS, Yu BP, Yue H, Li JY, Mei Q. Effect of Nimesulide on proliferation and apoptosis of human hepatoma SMMC-7721 cells. *World J Gastroenterol* 2002; **8**: 483-487

5 **Li J**, Wang WL, Wang WY, Liu B, Wang BY. Apoptosis in human hepatocellular carcinoma by terminal deoxynucleotidyl transferase-mediate. *Huaren Xiaohua Zazhi* 1998; **6**: 491-494

6 **Wang LS**, Pan LJ, Li MS, Sun Y, Shi L, Zhang YL, Zhou DY. Apoptosis of large bowel carcinoma induced by complete peptide polyose. *Shijie Huaren Xiaohua Zazhi* 1999; **7**: 710

7 **Zhang Z**, Yuan Y, Gao H, Dong M, Wu HQ, Wang L, Wang MX. *In situ* observation of apoptosis and proliferation in gastric cancer and precanceration. *Shijie Huaren Xiaohua Zazhi* 1999; **7**: 802-803

8 **Pacella CM**, Bizzarri G, Magnolfi F, Cecconi P, Caspani B, Anelli V, Bianchini A, Valle D, Pacella S, Manenti G, Rossi Z. Laser thermal ablation in the treatment of small hepatocellular carcinoma: results in 74 patients. *Radiology* 2001; **221**: 712-720

9 **Pacella CM**, Bizzarri G, Magnolfi F, Cecconi P, Caspani B, Anelli V, Bianchini A, Valle D, Pacella S, Manenti G, Rossi Z. Hepatocellular carcinoma: long-term results of combined treatment with laser thermal ablation and transcatheter arterial chemoembolization. *Radiology* 2001; **219**: 669-678

10 **Lu MD**, Chen JW, Xie XY, Liu L, Huang XQ, Liang LJ, Huang JF. Hepatocellular carcinoma: us-guided percutaneous microwave coagulation therapy. *Radiology* 2001; **221**: 167-172

11 **Ishida T**, Murakami T, Shibata T, Inoue Y, Takamura M, Niinobu T, Sato T, Nakamura H. Percutaneous microwave tumor coagulation for hepatocellular carcinomas with interruption of segmental hepatic blood flow. *J Vasc Interv Radiol* 2002; **13**: 185-191

12 **Dick EA**, Taylor-Robinson SD, Thomas HC, Gedroyc WMW. Ablative therapy for liver tumours. *Gut* 2002; **50**: 733-739

13 **Matsuda M**, Fujii H, Kono H, Matsumoto Y. Surgical treatment of recurrent hepatocellular carcinoma based on the mode of recurrence: repeat hepatic resection or ablation are good choices for patients with recurrent multicentric cancer. *J Hepatobiliary Pancreat Surg* 2001; **8**: 353-359

14 **Gazelle GS**, Goldberg SN, Solbiati L, Livraghi T. Tumor ablation with radio-frequency energy. *Radiology* 2000; **217**: 633-646

15 **Ahmed M**, Lobo SM, Weinstein J, Kruskal JB, Gazelle GS, Halpern EF, Afzal SK, Lenkinski RE, Goldberg SN. Improved coagulation with saline solution pretreatment during radiofrequency tumor ablation in a canine model. *J Vasc Interv Radiol* 2002; **13**: 717-724

16 **Choi D**, Lim HK, Kim SH, Lee WJ, Jang HJ, Kim H, Lee SJ, Lim JH. Assessment of therapeutic response in hepatocellular carcinoma treated with percutaneous radio frequency ablation: comparison of multiphase helical computed tomography and power doppler ultrasonography with a microbubble contrast agent. *J Ultrasound Med* 2002; **21**: 391-401

17 **Giorgio A**, Francica G, Tarantino L, de Stefano G. Radio-frequency ablation of hepatocellular carcinoma lesions. *Radiology* 2001; **218**: 918-919

18 **Dupuy DE,** Goldberg SN. Image-guided radiofrequency tumor ablation: challenges and opportunities-part II. *J Vasc Interv Radiol* 2001; **12**: 1135-1148

19 **Livraghi T**, Goldberg SN, Lazzaroni S, Meloni F, Ierace T, Solbiati L, Gazelle GS. Hepatocellular carcinoma: radio-frequency ablation of medium and large lesions. *Radiology* 2000; **214**: 761-768

20 **Mc Dannold NJ, Jolesz FA, Hynynen KH**. Determination of the optimal delay between sonications during focused ultrasound surgery in rabbits by using MR imaging to monitor thermal buildup *in vivo*. *Radiology* 1999; **211**: 419-426

21 **Wu F**, Chen WZ, Bai J. Effect of high-intensity focused ultrasound on the patients with hepatocellular carcinoma:preliminary report. *Zhonghua Chaosheng Yingxiangxue Zazhi* 1999; **8**: 213-216

22 **Yamamoto J**, Okada S, Shimada K, Okusaka T, Yamasaki S, Ueno H, Kosuge T. Treatment strategy for small hepatocellular carcinoma: Comparison of long-term results after percutaneous ethanol injection therapy and surgical resection. *Hepatology* 2001; **34**: 707-713

23 **Bruix J**, Llovet JM. Prognostic prediction and treatment strategy in hepatocellular carcinoma. *Hepatology* 2002; **35**: 519-524

24 **Morimoto M**, Sugimori K, Shirato K, Kokawa A, Tomita N, Saito T, Tanaka N, Nozawa A, Hara M, Sekihara H, Shimada H, Imada T, Tanaka K. Treatment of hepatocellular carcinoma with radiofrequency ablation: Radiologic-histologic correlation during follow-up periods. *Hepatology* 2002; **35**: 1467-1475

25 **Parslow TG, Stites DP, Terr AI, Imboden JB**. Medical Immunology. *Beijing science Press* 2002: 154-156

26 **Lin LW**, He YM, Gao SD, Yan FD. Percutaneous intratumoral injection of chinese traditional medicine "Star-99" in treatment of hepatic carcinoma: an experimental study. *Zhonghua Chaosheng Yingxiangxue Zazhi* 2002; **11**: 45-48

27 **Kimura K**, Bowen C, Spiegel S, Gelmann EP. Tumor necrosis factor-alpha sensitizes prostate cancer cells to gamma-irradiation-induced apoptosis. *Cancer Res* 1999; **59**: 1606-1614

28 **Liang WJ**, Huang ZY, Ding YQ, Zhang WD. Lovo cell line apoptosis induced by cycloheximide combined with TNFα. *Shijie Huaren Xiaohua Zazhi* 1999; **7**: 326-328

29 **Shen YF**, Zhuang H, Shen JW, Chen SB. Cell apoptosis and neoplasms. *Shijie Huaren Xiaohua Zazhi* 1999; **7**: 267-268

30 **He SW**, Shen KQ, He YJ, Xie B, Zhao YM. Regulatory effect and mechanism of gastrin and its antagonists on colorectal carcinoma. *World J Gastroenterol* 1999; **5**: 408-416

31 **Huang PL**, Zhu SN, Lu SL, Dai SZ, Jin YL. Inhibitor of fatty acid synthase induced apoptosis in human colonic cancer cells. *World J Gastroenterol* 2000; **6**: 295-297

32 **Li J**, Wang WL, Liu B. Angiogenesis and apoptosis in human hepatocellular carcinoma. *Huaren Xiaohua Zazhi* 1998; **6**: 1057-1060

33 **Liu HF**, Liu WW, Fang DC, Yang SM, Wang RQ. Bax gene expression and its relationship with apoptosis in human gastric carcinoma and precancerous lesions. *Shijie Huaren Xiaohua Zazhi* 2000; **8**: 665-668

34 **Tu SP**, Jiang SH, Tan JH, Jiang XH, Qiao MM, Zhang YP, Wu YL, Wu YX. Proliferation inhibition and apoptosis induction by ar-

senic trioxide on gastric cancer cell SGC-7901. *Shijie Huaren Xiaohua Zazhi* 1999; **7**: 18-21

35 **Chen HY**, Liu WH, Qin SK. Induction of arsenic trioxide on apoptosis of hepatocarcinoma cell lines. *Shijie Huaren Xiaohua Zazhi* 2000; **8**: 532-535

36 **Liu HF**, Liu WW, Fang DC. Effect of combined anti-Fas mAb and IFN-γ on the induction of apoptosis in human gastric carcinoma cell line SGC-7901. *Shijie Huaren Xiaohua Zazhi* 2000; **8**: 1316-1364

37 **Sun BH**, Zhao XP, Wang BJ, Yang DL, Hao LJ. FADD and TRADD expression and apoptosis in primary human hepatocellular carcinoma. *World J Gastroenterol* 2000; **6**: 223-227

38 **Sun ZX**, Ma QW, Zhao TD, Wei YL, Wang GS, Li JS. Apoptosis induced by norcantharidin in human tumor cells. *World J Gastroenterol* 2000; **6**: 263-265

39 **Xue XC**, Fang GE, Hua JD. Gastric cancer and apoptosis. *Shijie Huaren Xiaohua Zazhi* 1999; **7**: 359-361

40 **Cheng J**, Huang HC. Programmed cell death and disease. *Peking Union Medical College Press* 1997: 1-8

41 **Brown JM**, Wouters BG. Apoptosis, p53, and tumor cell sensitivity to anticancer agents. *Cancer Res* 1999; **59**: 1391-1399

42 **Ikeda M**, Shomori K, Endo K, Makino T, Matsuura T, Ito H. Frequent occurrence of apoptosis is an early event in the oncogenesis of human gastric carcinoma. *Virchows Arch* 1998; **432**: 43-47

Edited by Wu XN

P.O.Box 2345, Beijing 100023, China
Fax: +86-10-85381893
E-mail: wjg@wjgnet.com www.wjgnet.com

World J Gastroenterol 2003;9(4):706-709
World Journal of Gastroenterology
 ISSN 1007-9327

• LIVER CANCER •

Right trisectionectomy for primary liver cancer

Jing-An Rui, Shao-Bin Wang, Shu-Guang Chen, Li Zhou

Jing-An Rui, Shao-Bin Wang, Shu-Guang Chen, Li Zhou, Department of General Surgery, Peking Union Medical College Hospital, Beijing 100032, China
Correspondence to: Prof. Jing-An Rui, Department of General Surgery, Peking Union Medical College Hospital, Beijing 100032, China. rlzhou@mail.bjmu.edu.cn
Telephone: +86-10-62091034 **Fax:** +86-10-62358270
Received: 2002-11-19 **Accepted:** 2003-01-02

Abstract

AIM: To evaluate the value of right trisectionectomy, previously named right trisegmentectomy, in the treatment of primary liver cancer by summarizing our 13-year experience for this procedure.

METHODS: Thirty three primary liver cancer patients undergoing right trisectionectomy from Apr. 1987 to Dec. 1999 were investigated retrospectively. The impacts in survival of patients by cancerous biological behavior, such as tumor thrombi and satellite nodules, were discussed respectively. All right trisectionectomies were performed under normothermic interruption of porta hepatis at single time. Ultrasonic dissector (CUSA system 200) was used in dissection of hepatic parenchyma from Nov. 1992, instead of finger fracture.

RESULTS: 1-, 3- and 5-year survival rates were 71.9 %, 40.6 % and 34.4 %, respectively. The longest survival term with free cancer was 150 months (alive). There were no significant differences in survival curves between cases with and without tumor thrombi (right branch of portal vein) and satellite nodules. Operative mortality was 3.0 % (1/33). Main surgical complications occurred in 5 cases.

CONCLUSION: Right trisectionectomy should be regarded as an effective and safe procedure for huge primary liver cancers and is worth using more widely.

Rui JA, Wang SB, Chen SG, Zhou L. Right trisectionectomy for primary liver cancer. *World J Gastroenterol* 2003; 9(4): 706-709
http://www.wjgnet.com/1007-9327/9/706.htm

INTRODUCTION

It has been documented that primary liver cancer has been the more common cancer killer worldwide, especially in the areas with high incidence, such as China[1]. Several methods has been developed for the therapy of the malignancy[2-11]. The outcomes have taken marked progress, but recurrence and metastasis rates remain high[12,13]. Up to now, the difficult point is still existing in treatment of large liver cancers, due to worse results and higher risk[14,15]. Since the middle of last century[16], right trisectionectomy (previous trisegmentectomy) has been used for huge hepatic neoplasms covering right and left medial section. In 1975, Starzl described and clearly defined in detail a safe technique of right trisectionectomy[17]. Then he reported on 30 cases of the operation in 1980, including malignant and benign hepatic lesion[18]. In the past two decades, some papers described the procedure in treatment of hepatic malignant neoplasm, such as liver infiltration of gallbladder cancer and metastatic and primary liver cancer[19-23]. Most reports demonstrated that right trisectionectomy was effective in extensive hepatic malignancy, based on some individuals with long-term survival[19, 20]. But the risk (morbidity and mortality) of liver resection remains high according to some authors[20, 22, 23], especially for primary liver cancer with cirrhosis. It is related to the fact that most primary liver cancer patients have a history of hepatitis and suffer a higher incidence of hepatic failure after major resection. Another reason perhaps, is occurrence of bleeding during the operation. Currently, we lack data about comprehensive evaluation of right trisectionectomy in treatment of primary liver cancer. In this study, we investigate 33 cases of right trisectionectomies retrospectively to explore the value of the procedure to deal with primary liver cancer patients.

MATERIALS AND METHODS

Patients

From April 1987 to December 1999, total of 459 primary liver cancer patients were hepatomized. Of them, 33 cases of right trisectionectomies were performed. There were 24 (72.7 %) males and 9 (27.3 %) females. Ages ranged from 15 to 69 years (mean ±SD, 45.9±16.7 years). Hepatitis B surface antigen (HBsAg): 28 (84.8 %) were positive and 5 (15.2 %) were negative. There were 8 (24.2 %) with slight cirrhosis and 25 (75.8 %) without. Child-Pugh's classification: 22 (66.7 %) were A grade and 11 (33.3 %) were B grade when the patients were hospitalized, but they were all A grade before surgical procedures through positive hepatic protective therapy. α-fetoprotein (AFP): 27 (81.8 %) were elevated and 6 (18.2 %) were normal. And the highest value of AFP was 20 000 ng/ml. Sizes of tumor ranged from 8 to 20 cm (mean ±SD, 13.9± 3.4 cm). Staging (TNM[24]) of Cancer: All tumors were stage IV_A ($T_4N_0M_0$). Pathology: 27 (81.8 %) were hepatocellular carcinoma, 2 (6.1 %) were cholangiocarcinoma and 4 (12.1 %) were mixed hepatocellular-cholangiocarcinoma. There were 17 cases (51.5 %) with tumor thrombi in the right branch of the portal vein. 19 macroscopic satellite nodules were found in 15 cases (45.5 %), and they didn't presented in left lateral section of the liver.

Evaluation for feasibility of surgery

The feasibility of right trisectionectomy for each patient was considered carefully according to the following standards: (1) Tumors (including satellite nodules no more than 2) were limited in right and left medial section of the liver. There weren't any evidence about cancer invasion in left lateral section. (2) Tumor masses had clear borders or psuedocapsule, and without tumor thrombus in trunk of portal vein and hepatic vein. (3) No evidence for distant metastasis. (4) Compensative enlargement of left lateral section. (5) Child-Pugh's classification of liver function was A and indocyanine green retention rate at 15 minutes (ICGR15)[25] was lower than 15 % before surgery. (6) Serum bilirubin smaller than 34 mmol· L^{-1}, serum albumin higher than 30 g· L^{-1} and serum prothrombin time larger than 60 % before surgery.

The situations of tumor were detected chiefly by image examinations, including B-type ultrasonography, computed tomography (CT), magnetic resonance imaging (MRI) and

angiography. To assess liver function reserve of these patients before operation, we adopted classical Child-Pugh's classification, ICGR test and some concrete parameters, as described in standards. 146 cases of huge primary liver cancer were eliminated from the indication according to above standards. Of them, 69 cases were due to advanced tumor and the rest 77 due to bad liver function reserve.

Surgical procedures

All of the right trisectionectomies were on standard style, i.e. the resection edges were along the falciform ligaments of the liver and removed blocks were Couinaud segments 4 to 8. From November 1992, the ultrasonic dissector (CUSA system 200) was adopted for dissecting hepatic parenchyma, instead of previous finger fracture technique, introduced by Lin *et al*[26]. The procedures were all performed under normothermic interruption of porta hepatis at single time. Interruption lasted 15 to 40 minutes (mean ±SD, 25.3±6.8 minutes). The total surgical time ranged from 165 to 312 minutes (mean ±SD, 236±63 minutes). The amount of bleeding ranged from 300 to 3 000 ml (mean ±SD, 1 240±560 ml). The quantities of transfused blood ranged from 0 to 2 200 ml (mean ±SD, 1 020±550 ml). There were 2 cases that did not require blood transfusion during right trisectionectomy. For dissection of the liver parenchyma, we used finger fracture in 9 cases (27.3 %) before November 1992 and ultrasonic dissector (CUSA System 200) in 24 cases (72.7 %) after the time. Net weight of specimens ranged from 1 500 to 3 100 g (mean ±SD, 2 330±520 g).

Adjuvant therapy and follow-up

All patients were covered in our strict follow-up after the procedure. AFP, B-type ultrosonography, computed tomography (CT) magnetic resonance imaging (MRI) and angiography were used as monitors of recurrence and metastasis. Moreover, follow-ups by mail, E-mail and telephone were taken for patients without reexaminations every year. Follow-up terms were 3 to 150 months. The latest follow-up was in November 2000 and survival terms of patients alive were calculated to October 2000. When the recurrences were found, they were treated by transcatheter arterial chemoembolization (TACE), percutaneous ethanol injection (PEI) etc. 11 patients underwent TACE, 5 patients underwent PEI and 7 patients underwent both.

Statistical analysis

Survival curves were analyzed by Kaplan-Meier and Log rank test. The χ^2 and Student *t* test were used to determine comparability of groups. Statistically significant *P* value was defined as <0.05.

RESULTS

Survival rates, recurrence and metastasis after right trisectionectomy

The postoperative survival rates at 1-, 2-, 3-, 4- and 5-years were 71.9 %, 50 %, 40.6 %, 37.5 % and 34.4 %, respectively (Kaplan-Meier method). Ten cases have survived from 13 to 150 months according to the November 2000 follow-up. Survival curve of all patients is shown in Figure 1. The longest tumor-free survival term was 150 months (alive). The clinicopathological features in cases with and without satellite nodules and tumor thrombi in the right branch of the portal vein are shown in Table 1, and their survival curves were presented in Figure 2 and 3, there were no significant differences (*P*>0.05, Log rank test). During follow-up term, recurrence and metastasis of cancer was found in 27 patients (81.8 %).

Operative mortality after right trisectionectomy

There was one patient who died of hepatic failure within one month after the operation. The operative mortality was 3.0 % (1/33).

Surgical complications after right trisectionectomy

There were 5 cases (15.2%) that developed main surgical complications after right trisectionectomies, including 2 cases of hepatic failure, 2 cases of bile leakage and 1 case of secondary bleeding. Four patients recovered by positive reoperation excluding 1 case of hepatic failure.

Table 1 Clinicopathological features of patients

Variables	TT present (17)	TT absent (16)	*P*	SN present (15)	SN absent (18)	*P*
Age	43.4(18.2)	47.6(16.5)	>0.05[b]	46.8(17.6)	45.1(15.7)	>0.05[b]
Sex			>0.05[a]			>0.05[a]
Male	14(82.4)	10(62.5)		13(86.7)	11(61.1)	
Female	3(17.6)	6(37.5)		2(13.3)	7(38.9)	
LC			>0.05[a]			>0.05[a]
Present	4(23.5)	4(25.0)		5(33.3)	3(16.7)	
Absent	13(76.5)	12(75.0)		10(66.7)	15(83.3)	
AFP			>0.05[a]			>0.05[a]
Elevated	15(88.2)	12(75.0)		13(86.7)	14(77.8)	
Normal	2(11.8)	4(25.0)		2(13.3)	4(22.2)	
TS (cm)	12.5(2.6)	16.7(5.8)	>0.05[b]	14.4(3.8)	13.2(3.1)	>0.05[b]
BL (ml)	1290(640)	1210(450)	>0.05[b]	1300(680)	1220(390)	>0.05[b]
BT (ml)	1100(720)	980(370)	>0.05[b]	1050(510)	990(570)	>0.05[b]
WS (g)	2280(490)	2350(530)	>0.05[b]	2380(570)	2300(460)	>0.05[b]
Pathology			>0.05[a]			>0.05[a]
HCC	13(76.5)	14(87.6)		12(80.0)	15(83.3)	
CC	1(5.9)	1(6.2)		1(6.7)	1(5.6)	
MHCC	3(17.6)	1(6.2)		2(13.3)	2(11.1)	

Values in parentheses are percentages or standard errors. TT, tumor thrombus; SN, satellite nodule; LC, liver cirrhosis; AFP, α-fetoprotein; TS, tumor size; BL, blood loss; BT, blood transfusion; WS, weight of specimen; HCC, hepatocellular carcinoma; CC, cholangiocarcinoma; MHCC, mixed hepatocellular-cholangiocarcinoma. [a]: χ^2 test, [b]: Student *t* test.

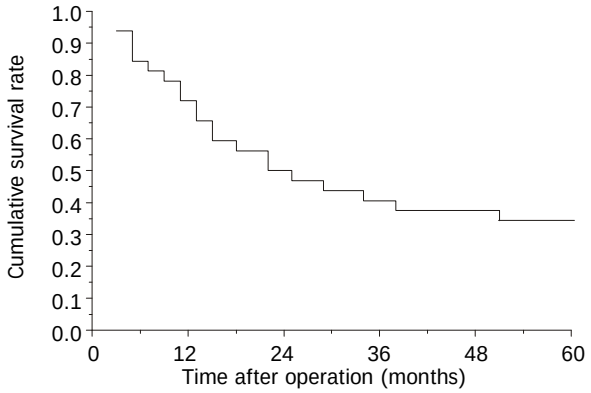

Figure 1 Survival curve of 32 patients underwent right trisectionectomy except 1 hospital death.

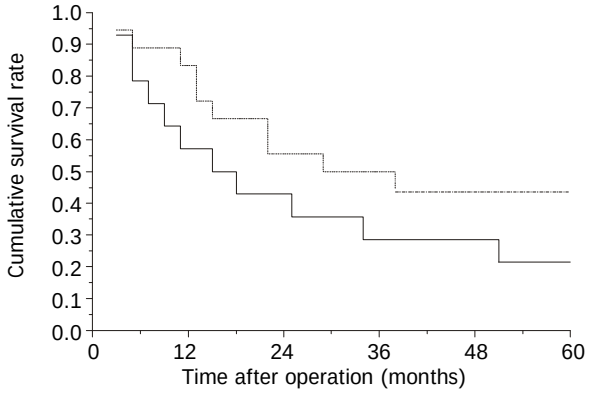

Figure 2 Survival curves of patients. ——, with satellite nodules (SN); ——, without satellite nodules. $P>0.05$, Log rank test.

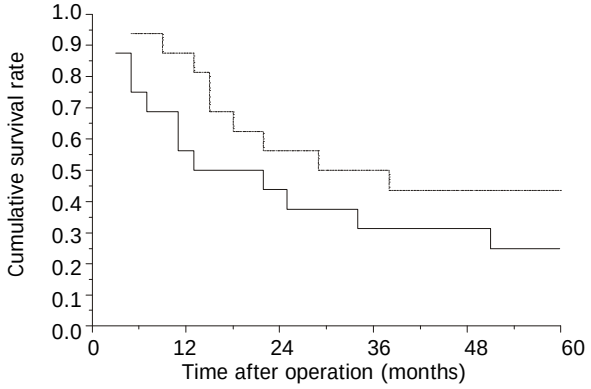

Figure 3 Survival curves of patients. ——, with tumor thrombus (TT); ——, without tumor thrombus. $P>0.05$, Log rank test.

DISCUSSION

In the therapy of primary liver malignancy, curative hepatic resection has been regarded as a primary method for radical treatment. But for hepatoma mainly in the right lobe and which invades the medial section of the left lobe, resection has always been difficult. Despite the fact that there has been research about right trisectionectomy, previous trisegmentectomy, mortality and morbidity remains high. There are few studies with large sample groups of primary liver cancer patients treated with right trisectionectomy. Starzl[18] reported on 19 cases of primary hepatic malignant tumors (14 primary liver cancers and 5 other types of tumors) treated by the procedure, The 1-year survival rate was more than 50 %. Holbrook *et al*[27] reported on 13-years of experience in resection of malignant primary liver tumors, including 9 right trisectionectomies. Overall 1-, 2-, 3-, and 5-year survival rates were 57 %, 52 %, 40 % and 33 %, respectively. Mortality was 7 % and complication incidence was 26 %. Kumada *et al*[28] reported on 11 cases of tri- and bi-sectionectomy for HCC, mean survival time was 16 months, mortality was 15.4 %. We had reported 4 right trisectionectomies to treat extensive primary liver cancers in 1991[29]. Three cases survived more than 1 year. From April 1987 to December 1999, we performed 33 right trisectionectomies for primary liver cancer patients, 1-, 2-, 3-, 4- and 5-year survival rates were 71.9 %, 50 %, 40.6 %, 37.5 % and 34.4 %, respectively. The longest term of survival with free cancer was 150 months. Mortality was 3.0 % and the surgical complication rate was 15.2 %. These results are related to new advances in liver surgery. To control severe intraoperative bleeding, we used normothermic interruption of the porta hepatis at single time. Previously, we reported on 20 cases of hemihepatectomy using this interruption method. Manipulation appeared simple and convenient. Mortality was 0 %[30]. These data suggested that normothermic interruption of the porta hepatis at single time should be regarded as an effective and safe method to limit bleeding in liver surgery. There were two patients in this study that were trisectionectomized without blood transfusion. Besides, the use of ultrasonic dissector in later period made the operative fields more clear. Thus, manipulations became more convenient and accurate. Meanwhile, the low incidence of complications and mortality were related to the accurate estimation of liver functional reserve prior to operation. We adopted the Child-Pugh' s classification, some detailed parameters and ICGR test. Child-Pugh' s classification was a classical method for estimating liver function. It could become more accurate if helped by other concrete markers, such as serum bilirubin, prothrombin time and albumin. Besides, ICGR test, a proven sensitive indicator of liver function reserve[25], also provided important information. Our experience is that the combination of these parameters could accurately predict liver function reserve.

In the present study, we analyzed the influence of some pathological features on outcome of right trisectionectomy for huge primary liver cancers. The clinicopathological features showed in Table 1 suggested the comparability between patients with and without tumor thrombi or satellite nodules (all $P>0.05$). And no significant differences could be found in their survival curves ($P>0.05$), in spite of some differences in these curves. These findings suggest that surgeons should use curative resection in therapy of huge tumors, even in those with a few satellite nodules and tumor thrombi, if the tumor thrombi are only in the right branch of the portal vein, a satisfactory effect could be expected.

In conclusion, right trisectionectomy is an effective and safe procedure and should become one of strategies, and surgical arts in the treatment of huge tumor of primary liver cancers.

REFERENCES

1 **Pisani P**, Parkin DM, Bray F, Ferlay J. Estimates of the world-wide mortality from 25 cancers in 1990. *Int J Cancer* 1999; **83**: 18-29
2 **Makuuchi M**, Takayama T, Kubota K, Kimura W, Midorikawa Y, Miyagawa S, Kawasaki S. Hepatic resection for hepatocellular carcinoma-Japanese experience. *Hepatogastroenterology* 1998; **45** (Suppl 3): 1267-1274
3 **Yamamoto J**, Iwatsuki S, Kosuge T, Dvorchik I, Shimada K, Marsh JW, Yamasaki S, Starzl TE. Should hepatomas be treated with hepatic resection or transplantation? *Cancer* 1999; **86**: 1151-1158
4 **Shen P**, Hoffman A, Howerton R, Loggie BW. Cryosurgery of close or positive margins after hepatic resection for primary and metastatic hepatobiliary malignancies. *Am Surg* 2002; **68**: 695-703
5 **Pelletier G**, Ducreux M, Gay F, Luboinski M, Hagege H, Dao T, Van Steenbergen W, Buffet C, Rougier P, Adler M, Pignon JP, Roche A. Treatment of unresectable hepatocellular carcinoma with lipiodol chemoembolization: a multicenter randomized trial. Groupe CHC. *J Hepatol* 1998; **29**: 129-134

6 **Livraghi T**, Benedini V, Lazzaroni S, Meloni F, Torzilli G, Vettori C. Long term results of single session percutaneous ethanol injection in patients with large hepatocellular carcinoma. *Cancer* 1998; **83**: 48-57

7 **Ohmoto K**, Tsuduki M, Shibata N, Takesue M, Kunieda T, Yamamoto S. Percutaneous microwave coagulation therapy for hepatocellular carcinoma located on the surface of the liver. *Am J Roentgenol* 1999; **173**: 1231-1233

8 **Livraghi T**, Goldberg SN, Lazzaroni S, Meloni F, Solbiati L, Gazelle GS. Small hepatocellular carcinoma: treatment with radiofrequency ablation versus ethanol injection. *Radiology* 1999; **210**: 655-661

9 **Cheng SH**, Lin YM, Chuang VP, Yang PS, Cheng JC, Huang AT, Sung JL. A pilot study of three-dimensional conformal radiotherapy in unresectable hepatocellular carcinoma. *J Gastroenterol Hepatol* 1999; **14**: 1025-1033

10 **Liu CL**, Fan ST, Ng IO, Lo CM, Poon RT, Wong J. Treatment of advanced hepato-cellular carcinoma with tamoxifen and the correlation with expression of hormone receptors: a prospective randomized study. *Am J Gastroenterol* 2000; **95**: 218-222

11 **Llovet JM**, Sala M, Castells L, Suarez Y, Vilana R, Bianchi L, Ayuso C, Vargas V, Rodes J, Bruix J. Randomized controlled trial of interferon treatment for advanced hepatocellular carcinoma. *Hepatology* 2000; **31**: 54-58

12 **Tang ZY**. Hepatocellular carcinoma-cause, treatment and metastasis. *World J Gastroenterol* 2001; **7**: 445-454

13 **Shuto T**, Hirohashi K, Kubo S, Tanaka H, Yamamoto T, Ikebe T, Kinoshita H. Efficacy of major hepatic resection for large hepatocellular carcinoma. *Hepatogastroenterology* 1999; **46**: 413-416

14 **Hanazaki K**, Kajikawa S, Shimozawa N, Shimada K, Hiraguri M, Koide N, Adachi W, Amano J. Hepatic resection for large hepatocellular carcinoma. *Am J Surg* 2001; **181**: 347-353

15 **Regimbeau JM**, Farges O, Shen BY, Sauvanet A, Belghiti J. Is surgery for large hepatocellular carcinoma justified? *J Hepatol* 1999; **31**: 1062-1068

16 **Quattlebaum JK**. Massive resection of the liver. *Ann Surg* 1953; **137**: 787-796

17 **Starzl TE**, Bell RH, Beart RW, Putnam CW. Hepatic trisegmentectomy and other liver resections. *Surg Gynecol Obstet* 1975; **141**: 429-437

18 **Starzl TE**, Koep LJ, Weil R 3rd, Lilly JR, Putnam CW, Aldrete JA. Right trisegmentectomy for hepatic neoplasms. *Surg Gynecol Obstet* 1980; **150**: 208-214

19 **Yamamoto M**, Miura K, Yoshioka M, Matsumoto Y. Disease-free survival for 9 years after liver resection for stage IV gallbladder cancer: report of a case. *Surg Today* 1995; **25**: 750-753

20 **Sugiura Y**, Nakamura S, Iida S, Hosoda Y, Ikeuchi S, Mori S, Sugioka A, Tsuzuki T. Extensive resection of the bile ducts combined with liver resection for cancer of the main hepatic duct junction: a cooperative study of the Keio Bile Duct Cancer Study Group. *Surgery* 1994; **115**: 445-451

21 **Chi DS**, Fong Y, Venkatraman ES, Barakat RR. Hepatic resection for metastatic gynecologic carcinomas. *Gynecol Oncol* 1997; **66**: 45-51

22 **Iwatsuki S**, Starzl TE. Experience with resection of primary hepatic malignancy. *Surg Clin North Am* 1989; **69**: 315-322

23 **Wakabayashi H**, Okada S, Maeba T, Maeta H. Effect of preoperative portal vein embolization on major hepatectomy for advanced-stage hepatocellular carcinomas in injured livers: a preliminary report. *Surg Today* 1997; **27**: 403-410

24 **Skeel RT**. Carcinomas of the pancreas, liver, gallbladder. In: Skeel RT, eds. Handbook of cancer chemotherapy (Fifth edition). *Philadelphia: Lippincott Williams & Wilkins* 1997: 249

25 **Lau H**, Man K, Fan ST, Yu WC, Lo CM, Wong J. Evaluation of preoperative hepatic function in patients with hepatocellular carcinoma undergoing hepatectomy. *Br J Surg* 1997; **84**: 1255-1259

26 **Lin TY**, Lee CS, Chen KM, Chen CC. Role of surgery in the treatment of primary carcinoma of the liver: a 31-year experience. *Br J Surg* 1987; **74**: 839-842

27 **Holbrook RF**, Koo K, Ryan JA. Resection of malignant primary liver tumors. *Am J Surg* 1996; **171**: 453-455

28 **Kumada K**, Ozawa K, Okamoto R, Takayasu T, Yamaguchi M, Yamamoto Y, Higashiyama H, Morikawa S, Sasaki H, Shimahara Y, Shimahara Y, Yamaoka Y, Takeuchi E. Hepatic resection for advanced hepatocellular carcinoma with removal of portal vein tumor thrombi. *Surgery* 1990; **108**: 821-827

29 **Rui JA**, Wang K, Su Y, Li ZW, Wang CF, Wu JX, Zhao P. Right trisegmentectomy for primary liver cancer-a report of 4 cases with review of literature. *Zhonghua Zhongliu Zazhi* 1991; **13**: 37-39

30 **Rui JA**, Qu JY, Su Y, Li ZW, Wang K, Zhu GJ, Wu JX, Chen GJ, Wang CF, Mao XW. Hemihepatectomy under hepato-portal interruption at normal temperature for liver malignancies: a report of 20 patients. *Zhonghua Zhongliu Zazhi* 1987; **9**: 221-223

Edited by Yuan HT

P.O.Box 2345, Beijing 100023, China
Fax: +86-10-85381893
E-mail: wjg@wjgnet.com www.wjgnet.com

World J Gastroenterol 2003;9(4):710-713
World Journal of Gastroenterology
 ISSN 1007-9327

• LIVER CANCER •

Glycylproline dipeptidyl aminopeptidase isoenzyme in diagnosis of primary hepatocellular carcinoma

Run-Zhou Ni, Jie-Fei Huang, Ming-Bing Xiao, Mei Li, Xian-Yong Meng

Run-Zhou Ni, Jie-Fei Huang, Ming-Bing Xiao, Mei Li, Xian-Yong Meng, Department of Gastroenterology, Affiliated Hospital of Nantong Medical College, Nantong 226001, Jiangsu Province, China
Correspondence to: Dr. Run-Zhou Ni, Department of Gastroenterology, Affiliated Hospital of Nantong Medical College, Nantong 226001, Jiangsu Province, China. nirz@public.nt.js.cn
Telephone: +86-513-5119461
Received: 2002-09-14 **Accepted:** 2002-10-17

Abstract

AIM: To investigate the role of glycylproline dipeptidyl aminopeptidase (GPDA) isoenzyme in the diagnosis of primary hepatocellular carcinoma (PHC), especially in patients with negative alpha-fetoprotein (AFP).

METHODS: A stage gradient polyacrylamide gel discontinuous electrophoresis system was developed to separate serum GPDA isoenzymes, which were determined in 102 patients with PHC, 45 cases with liver cirrhosis, 24 cases with chronic hepatitis, 35 cases with benign liver space-occupying lesions, 20 cases with metastatic liver cancer and 50 cases with extra-hepatic cancer, as well as 80 healthy subjects. The relationships between GPDA isoenzymes and AFP, the sizes of tumors, as well as alanine aminotransferase (ALT) were also analyzed.

RESULTS: Serum GPDA was separated into two isoenzymes, GPDA-S and GPDA-F. The former was positive in all subjects, while the latter was found mainly in majority of PHC (85.3 %) and a few cases with liver cirrhosis (11.1 %), chronic hepatitis (33.3 %), metastatic liver cancer (15.0 %) and non-hepatic cancer (16.0 %). GPDA-F was negative in all healthy subjects and patients with benign liver space-occupying lesions, including abscess, cysts and angioma. There was no correlation between GPDA-F and AFP concentration or tumor size. GPDA-F was consistently positive and not correlated with ALT in PHC, but GPDA-F often converted to negative as decline of ALT in benign liver diseases. The electrophoretic migration of GPDA-F became sluggish after the treatment of neuraminidase.

CONCLUSION: GPDA-F is a new useful serum marker for PHC. Measurement of serum GPDA-F is helpful in diagnosis of PHC, especially in patients with negative AFP. GPDA-F is one kind of glycoproteins rich in sialic acid.

Ni RZ, Huang JF, Xiao MB, Li M, Meng XY. Glycylproline dipeptidyl aminopeptidase isoenzyme in diagnosis of primary hepatocellular carcinoma. *World J Gastroenterol* 2003; 9(4): 710-713
http://www.wjgnet.com/1007-9327/9/710.htm

INTRODUCTION

Glycylproline dipeptidyl aminopeptidase (GPDA) was discovered by Hapsu-Hava and Glenner in 1966[1]. It is widely distributed in human and animal tissues and catalyzes the hydrolysis of N-terminal glycylproline from glycylprolyl-β-naphthylamide and glycylproline-β-nitroanilide. It was reported that serum GPDA activity increased in the patients with hepatobiliary diseases and in experimental hepatic cancer[2, 3]. Further studies demonstrated that GPDA activity was significantly higher in human hepatic cancer and embryonal tissues than in healthy adult liver tissues[4]. However, serum GPDA cannot be used as a marker for PHC due to its low sensitivity and specificity in diagnosis.

In order to improve the diagnostic value of GPDA for PHC, a stage gradient polyacrylamide gel discontinuous electrophoresis system was established to separate serum GPDA into two isoenzymes, and clinical significances of serum GPDA isoenzymes in diagnosis of PHC were studied.

MATERIALS AND METHODS

Patients and healthy subjects

The resources of all patients in this study were from Affiliated Hospital of Nantong Medical College. The diagnosis of PHC met the diagnostic criterion of Liver Cancer Branch Committee of Chinese Anti-cancer Association. The diagnosis in 35 patients was confirmed pathologically. The origins of 20 metastatic liver cancers were gastrointestinal tract cancer (16 cases), lung cancer (2 cases) and breast cancer (2 cases). The origins in 50 cases with extra-hepatic cancer were gastrointestinal tract (22 cases), pancreas (5 cases), bile duct (6 cases), ovary (8 cases), bladder (4 cases), lung (4 cases) and kidney (1 case). Thirty-five benign liver space-occupying lesions were composed of 8 liver abscess, 2 liver cysts and 25 liver angioma. The diagnoses of 45 cases with hepatic cirrhosis and 24 chronic hepatitis were based on clinical manifestations and liver biopsy. The control samples came from healthy blood donor.

Detection of GPDA isoenzymes

Separation of GPDA isoenzymes was performed on stage gradient polyacrylamide gel with a vertical slab electrophoresis apparatus. The gel consists of one layer of stack gel and two layers of separating gels. The following solutions were used for the preparation of gels: (1) Solution A: 30 % acrylamide containing 0.8 % bisacrylamide; (2) Solution B: 4.95 % Tris base containing 0.05 %TEMED, pH6.9; (3) Solution C: 0.14 % ammonium persulfate. A gel of dimensions of 12.0 cm×10.0 cm×0.15 cm was prepared and loaded with 20 μl of serum. The gel run at a constant voltage of 60 V for the first three hours and then at the voltage of 100 V for another 16 hours. After the electrophoresis, the gel was incubated at 37 ℃ for 30 min with a piece of acetate cellulose membrane of the gel size pre-soaked with a substrate solution, which consists of 15 mg of glycylproline-β-nitroanilide, 4.8 ml of 100 mmol· L^{-1} Tris-glycylglycine (pH 8.4), 0.1 ml of 100 ml· L^{-1} sodium nitrite and 0.1 ml of 50 g· L^{-1} N-(naphthyl)-ethylenediamine dihydrochloride. Finally red GPDA isoenzyme bands were visualized soon by immersing the acetate cellulose membrane into a solution composed of 100 ml· L^{-1} trichloracetic acid and 250 ml· L^{-1} glycerol.

Measurement of AFP and ALT

ALT was measured with the method recommended by International Federation of Clinical Chemistry[5] and AFP was determined with routine radioimmunoassay.

Treatment of serum with neuraminidase

Serum was incubated with 10 u/ml neuraminidase at 37 ℃ for 15 hr before electrophoresis.

Statistical analysis

Chi-square test and student *t* tests were used. $P<0.05$ was considered as statistically significant.

RESULTS

Serum GPDA isoenzyme in patients with PHC and other diseases

Serum GPDA was separated into two isoenzyme bands with the electrophoresis system (Figure 1). The band in the anode was called as GPDA-F (fast band) and the band in cathode as GPDA-S (slow band). GPDA-S was positive in all subjects, including healthy persons and patients, while positive rates of GPDA-F varied in different diseases. GPDA-F was found in most patients with PHC and a few patients with benign liver diseases and extra-hepatic cancer, but no GPDA-F was found in all healthy persons and the patients with benign liver space-occupying lesions (Table 1). In patients with PHC, positive GPDA-F was considered as true positive and negative GPDA-F as false negative, while in patients with other diseases positive GPDA-F was considered as false positive and negative GPDA-F as true negative. Therefore, the sensitivity, specificity and accuracy of GPDA-F in diagnosis of PHC were 85.3 %, 86.2 % and 85.9 % respectively (Table 1).

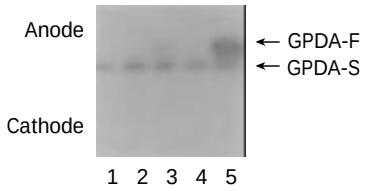

Figure 1 Serum GPDA isoenzymes separated with polyacrylamide electrophoresis. (Lane 1: healthy subject; lane 2: liver angioma; lane 3: chronic hepatitis; lane 4:liver cirrhosis; lane 5: PHC).

Table 1 Results of serum GPDA-F in patients and healthy subjects

	GPDA-F (+)		GPDA-F (-)	
	n	%	*n*	%
Healthy subjects	0	0	80	100.0
PHC	87[a]	85.3	15	14.7
Liver cirrhosis	5	11.1	40	88.9
Chronic hepatitis	8	33.3	16	66.7
Benign liver space-occupying lesions	0	0	35	100.0
Metastatic hepatic cancer	3	15.0	17	85.0
Extra-hepatic cancer	8	16.0	42	84.0

[a]$P<0.05$ *vs* other groups. True positive (TP)=87; False positive (FP)=24(5+8+0+3+8); False negative (FN)=15; True negative (TN)=150(40+16+35+17+42); Sensitivity=TP/(TP+FN)×100 %; Specificity=TN/(TN+FP)×100 %; Diagnostic accuracy=(TP+TN)/(TP+TN+FP+FN)×100 %.

The complementary value of GPDA-F and AFP for PHC

There was no correlation between positive rates of GPDA-F and AFP concentration (Table 2). GPDA-F was positive in 75.0 % PHC cases with negative AFP (<50 ng/ml). If positive GPDA-F and AFP≥50 ng/ml were set as diagnostic criterion of PHC, the sensitivity of AFP was 72.5 % and that of AFP with GPDA-F would reach up to 91.2 %. The diagnostic accuracy was also increased with the combination of AFP and GPDA-F (Table 3).

Table 2 Relationship between AFP and GPDA-F in sera of cases with PHC

AFP(ng/ml)	*n*	GPDA-F(+)
<50	28	21(75.0%)
-400	12	11(91.6%)
>400	62	55(88.7%)

Table 3 Diagnostic value of both AFP and GPDA-F in PHC

	Sensitivity (%)	Specificity (%)	Accuracy (%)
AFP alone	72.5	95.2	85.0
GPDA-F alone	85.3	87.1	86.3
AFP and GPDA-F	91.2	84.7	88.5

The relationship between GPDA-F and tumor size

One hundred and two cases with PHC were divided into two groups based on size of tumor, 23 cases were small liver cancer with tumor diameter ≤5 cm and 79 cases were advanced liver cancer with tumor diameter >5 cm. Positive rate of GPDA-F was 78.3 % (18/23) in small liver cancer, and 87.3 % (69/79) in advanced liver cancer. However, there was no statistical difference between the two groups ($P>0.05$).

Characteristics of GPDA-F in PHC and benign liver diseases

In order to know whether GPDA-F is associated with inflammation of hepatocytes, GPDA-F and ALT were measured simultaneously. There was no significant difference of ALT activities between positive and negative GPDA-F groups in PHC, but ALT activities in positive GPDA-F group were significantly higher than that in negative group in liver cirrhosis and chronic hepatitis (Table 4), suggesting that GPDA-F was associated with elevated ALT in benign liver diseases, but not in PHC. It was also found that GPDA-F often converted to negative with the decrease of ALT in benign liver diseases but no in PHC (data not shown).

Table 4 Relationship between GPDA-F and ALT in different liver diseases

	ALT ($\bar{x}$±s, u/L)		
	PHC	Hepatic cirrhosis	Chronic hepatitis
Negative GPDA-F	31.0±9.6	31.6±3.6[a]	67.3±13.2[a]
Positive GPDA-F	50.1±10.2	67.6±31.6	159.8±46.6

[a]$P<0.05$ *vs* positive GPDA-F group.

Effects of neuraminidase on GPDA-F

Serum was treated with neuraminidase before electrophoresis as mentioned in materials and methods. The migration rate of GPDA-F became slower than that of GPDA-S following treatment of neuraminidase, while GPDA-S was not obviously affected (Figure 2).

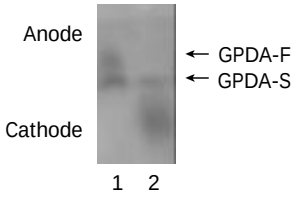

Figure 2 The effect of neuraminidase on migration of serum GPDA isoenzymes. (Lane 1: before treatment of neuraminidase; lane 2: after treatment of neuraminidase).

DISCUSSION

PHC is one of the most severe malignancies and ranks second mortality in malignant tumors in China[6,7]. The prognosis is poor due to its delayed diagnosis and low resectable rate. Thus early diagnosis is important to improve the prognosis. Tumor markers are very useful in diagnosis. AFP is the most widely used tumor marker for PHC with a positive rate from 60 % to 70 %[8-11]. AFP-L-3, one of the glycoforms of AFP, has higher specificity for PHC. However, it cannot increase the diagnostic sensitivity[12-16]. Many studies have focused on other tumor markers to improve the diagnostic sensitivity for PHC. It has been found that there are some tumor markers, which are complementary to AFP in diagnosis of PHC, such as des-gamma-carboxy prothrombin (PIVKA-II)[17-23], γ-glutamyltransferase isoenzyme[24-26], transforming growth factor-β1[27-29] and α-L-fucosidase[30-34] .

In present study, we have investigated the value of GPDA isoenzymes in diagnosis of PHC. With a stage gradient polyacrylamide gel electrophoresis system, serum GPDA has been separated into two isoenzymes, GPDA-F and GPDA-S. GPDA-F was often detected in sera of patients with PHC, with a much higher positive rate than in other liver diseases, including liver cirrhosis, chronic hepatitis, metastatic liver cancer and extra-hepatic tumors; while GPDA-F was negative in healthy subjects and patients with benign liver space-occupying lesions. The sensitivity and specificity of GPDA-F in diagnosis of PHC were 85.3 % and 86.2 %, respectively. These results indicate that GPDA-F may be a valuable serum marker for PHC.

Serum GPDA-F in patients with benign liver diseases possibly originates from the inflammatory hepatocytes because in such cases positive GPDA-F was often accompanied by elevated ALT and changed to negative with the decline of ALT. On the contrary, GPDA-F in PHC is persistently positive and not correlated with ALT. Therefore, simultaneous determination and follow-up of ALT may help to rule out the false positive GPDA-F in benign liver diseases. It is known that some serum hepatoma markers are of predictive and early diagnostic value for PHC, such as AFP, des-gamma-carboxy prothrombin and gamma-glutamyltransferase isoenzyme II[21-23, 26]. Whether persistent positive of GPDA-F in a few cases of liver cirrhosis is the precursor of hepatocarcinogenesis needs further investigation.

Although the diagnostic efficiency for PHC has been greatly improved in recent years with the use of many advanced image techniques, it is still difficult to make the diagnosis in some cases, especially for those at early stage or with negative AFP. Present study showed that GPDA-F and AFP were complementary for diagnosis of PHC. In these data, GPDA-F was positive in 75 % PHC cases of negative AFP but negative in all benign liver space-occupying lesions. Therefore, GPDA-F is of special value for the differential diagnosis of liver space-occupying lesions of unknown nature. Our data also showed that there was no correlation between tumor size and GPDA-F. In 23 cases of small liver cancer, the positive rate of GPDA-F was 78.3 %, suggesting that GPDA-F may be a good marker of PHC at early stage.

The exact mechanism by which GPDA-F appears in the sera of PHC cases is not clarified. It is possible that GPDA-F is produced by hepatoma tissues and then released into blood, since GPDA-F was only found in sera of those PHC cases in whose hepatoma tissues GPDA-F was positive (unpublished data). The electrophoretic migration of GPDA-F became slower than its isoenzyme GPDA-S after treatment with neuramidinase, indicating that GPDA-F is a kind of glycoprotein rich in sialic acids in its sugar chain. Therefore, the modification of the sugar chain after GPDA protein synthesis may be the main process of the production of GPDA-F. It has been known that several kinds of glycoproteins synthesized by hepatoma cells are different from those produced by hepatocytes. For example, AFP and alpha-1-antitrypsin have higher percentage of lens culinaris agglutinin-reactive species in hepatocellular carcinoma than in benign liver diseases. It is also clear that the fucosylation of the sugar chain at the innermost N-acetylglucosamine is the molecular basis of this variation[35, 36] Whether there is the difference of fucosylation of GPDA isoenzymes between hepatocellular carcinoma and benign liver diseases needs to be studied further.

REFERENCES

1 **Hopsu-Havu VK,** Glenner GG. A new dipeptide naphthylamidase hydrolyzing glycyl-prolyl-beta-naphthlamide. *Histochemie* 1966; **7**: 197-201

2 **Hutchinson DR**, Halliwell RP, Lockhart JD, Parke DV. Glycylprolyl-p-nitroanilidase in hepatobiliary disease. *Clin Chem Acta* 1981; **109**: 83-89

3 **Kojima J**, Kanatani M, Nakamura N, Kashiwagi T, Tohjoh F, Akiyama M. Serum and liver glycylproline dipeptidyl aminopeptidase activity in rats with experimental hepatic cancer. *Clin Chem Acta* 1980; **107**: 105-110

4 **Kojima J**, Ueno Y, Kasugai H, Okuda S, Akedo H. Glycylproline dipepdidyl aminopeptidase and gamma-glutamyl transpeptidase in human hepatic cancer and embryonal tissues. *Clin Chem Acta* 1987; **167**: 285-291

5 **Bergmeyer HU**, Horder M, Rej R. International federation of clinical chemistry (IFCC) scientific committee, analytical section: approved recommendation (1985) on IFCC methods for the measurement of catalytic concentration of enzymes. Part 3. IFCC method for alanine aminotransferase (L-alanine: 2-oxoglutarate aminotransferase, EC 2.6.1.2). *J Clin Chem Clin Biochem* 1986; **24**: 481-495

6 **Tang ZY**. Hepatocellular carcinoma-cause, treatment and metastasis. *World J Gastroenterol* 2001; **7**: 445-454

7 **Tang ZY.** Hepatocellular carcinoma. *J Gastroenterol Hepatol* 2000; **15** (Suppl): G1-7

8 **Rabe C**, Pilz T, Klostermann C, Berna M, Schild HH, Sauerbruch T, Caselmann WH. Clinical characteristics and outcome of a cohort of 101 patients with hepatocellular carcinoma. *World J Gastroenterol* 2001; **7**: 208-215

9 **Tangkijvanich P**, Anukulkarnkusol N, Suwangool P, Lertmaharit S, Hanvivatvong O, Kullavanijaya P, Poovorawa Y. Clinical characteristics and prognosis of hepatocellular carcinoma: analysis based on serum alpha-fetoprotein levels. *J Clin Gastroenterol* 2000; **31**: 302-308

10 **Yoshida S**, Kurokohchi K, Arima K, Masaki T, Hosomi N, Funaki T, Murota M, Kita Y, Watanabe S, Kuriyama S. Clinical significance of lens culinaris agglutini-reactive fraction of serum alpha-fetoprotein in patients with hepatocellular carcinoma. *Int J Oncol* 2002; **20**: 305-309

11 **Qin LX**, Tang ZY. The prognostic significance of clinical and pathologica l features in hepatocellular carcinoma. *World J Gastroenterol* 2002; **8**: 193-199

12 **Tamura A**, Oita T, Sakizono K, Nakajima T, Kasakura S. Clinical usefulness of lectin-reactive fraction of alpha-fetoprotein in hepatocellular carcinoma. *Rinsho Byori* 1998; **46**: 158-162

13 **Zaninotto M**, Ujka F, Lachin M, Bernardi D, Marafi C, Farinati F, Plebani M. Lectini-affinity electrophoresis for the detection of AFP microheterogeneities in patients with hepatocellular carcinoma. *Anticancer Res* 1996; **16**: 305-309

14 **Kumada T**, Nakano S, Takeda I, Kiriyama S, Sone Y, Hayashi K, Katoh H, Endoh T, Sassa T, Satomura S. Clinical utility of Lens culinaris agglutinin-reactive alpha-fetoprotein in small hepatocellular carcinoma: special reference to imaging diagnosis. *J Hepatol* 1999; **30**: 125-130

15 **Hayashi K**, Kumada T, Nakano S, Takeda I, Sugiyama K, Kiriyama S, Sone Y, Miyata A, Shimizu H, Satomura S. Usefulness of measurement of Lens culinaris agglutinin-reactive fraction of alpha-fetoprotein as a marker of prognosis and recurrence of small hepatocellular carcinoma. *Am J Gastroenterol* 1999; **94**: 3028-3033

16 **Li D**, Mallory T, Satomura S. AFP-L3: a new generation of tumor marker for hepatocellular carcinoma. *Clin Chim Acta* 2001; **313**: 15-19
17 **Sakon M**, Monden M, Gotoh M, Kanai T, Umeshita K, Nakano Y, Mori T, Sakurai M, Wakasa K. Relationship between pathologic prognostic factors and abnormal levels of des-gamma-carboxy prothrombin and alpha-fetoprotein in hepatocellular carcinoma. *Am J Surg* 1992; **163**: 251-256
18 **Lamerz R**, Runge M, Stieber P, Meissner E. Use of serum PIVKA-II (DCP) determination for differentiation between benign and malignant liver diseases. *Anticancer Res* 1999; **19**: 2489-2493
19 **Tanaka Y**, Kashiwagi T, Tsutsumi H, Nagasawa M, Toyama T, Ozaki S, Naito M, Ishibashi K, Azuma M. Sensitive measurement of serum abnormal prothrombin (PIVKA-II) as a marker of hepatocellular carcinoma. *Hepatogastroenterogy* 1999; **46**: 2464-2468
20 **Sassa T**, Kumada T, Nakano S, Uematsu T. Clinical utility of simultaneous measurement of serum high-sensitivity des-gamma-carboxy prothrombin and lens culinaris agglutinit A-reactive alpha-fetoprotein in patients with small hepatocellular carcinoma. *Eur J Gastroenterol Hepatol* 1999; **11**: 1387-1392
21 **Ishii M**, Gama H, Chida N, Ueno Y, Shinzawa H, Takagi T, Toyota T, Takahashi T, Kasukawa R. Simultaneous measurements of serum alpha-fetoprotein and protein induced by vitamin K absence for detecting hepatocellular carcinoma. South tohoku district study group. *Am J Gastroenterol* 2000; **95**: 1036-1040
22 **Ikoma J**, Kaito M, Ishihara T, Nakagawa N, Kamei A, Fujita N, Iwasa M, Tamaki S, Watanabe S, Adachi Y. Early diagnosis of hepatocellular carcinoma using sensitive assay for serum des-gamma-carboxy prothrombin: a prospective study. *Hepatogastroenterology* 2002; **49**: 235-238
23 **Fujiyama S**, Tanaka M, Maeda S, Ashihara H, Hirata R, Tomita K. Tumor markers in early diagnosis, follow-up and management of patients with hepatocellular carcinoma. *Oncology* 2002; **62**(Suppl 1): 57-63
24 **Okuyama K**. Separation and identification of serum gamma-glutamyl transpeptidase isoenzymes by wheat germ agglutinin affinity electrophoresis: a basic analysis and its clinical application to various liver diseases. *Keio J Med* 1993; **42**: 149-156
25 **Sacchetti L**, Castaldo G, Cimino L, Budillon G, Salvatore F. Diagnostic efficiency in discriminating liver malignancies from cirrhosis by serum gamma-glutamyl transferase isoforms. *Clin Chim Acta* 1988; **177**: 167-172
26 **Xu K**, Meng XY, Wu JW, Shen B, Shi YC, Wei Q. Diagnostic value of serum gamma-glutamyl transferase isoenzyme for hepatocellular carcinoma: a 10-year study. *Am J Gastroenterol* 1992; **87**: 991-995
27 **Tsai JF**, Chuang LY, Jeng JE, Yang ML, Chang WY, Hsieh MY, Lin ZY, Tsai JH. Clinical relevance of transforming growth factor-beta 1 in the urine of patients with hepatocellular carcinoma. *Medicine* 1997; **76**: 213-226
28 **Sacco R**, Leuci D, Tortorella C, Fiore G, Marinosci F, Schiraldi O, Antonaci S. Transforming growth factor beta1 and soluble Fas serum levels in hepatocellular carcinoma. *Cytokine* 2000; **12**: 811-814
29 **Song BC**, Chung YH, Kim JA, Choi WB, Suh DD, Pyo SI, Shin JW, Lee HC, Lee YS, Suh DJ. Transforming growth factor-beta 1 as a useful serological marker of small hepatocellular carcinoma. *Cancer* 2002; **94**: 175-180
30 **Giardina MG**, Matarazzo M, Varriale A, Morante R, Napoli A, Martino R. Serum alpha-L-fucosidase. A useful marker in the diagnosis of hepatocellular carcinoma. *Cancer* 1992; **70**: 1044-1048
31 **Takahashi H**, Saibara T, Iwamura S, Tomita A, Maeda T, Onishi S, Yamamoto Y, Enzan H. Serum alpha-L-fucosidase activity and tumor size in hepatocellular carcinoma. *Hepatology* 1994; **19**: 1414-1417
32 **Giardina MG**, Matarazzo M, Morante R, Lucariello A, Varriale A, Guardasole V, De Marco G. Serum alpha-L-fucosidase activity and early detection of hepatocellular carcinoma: a prospective study of patients with cirrhosis. *Cancer* 1998; **83**: 2468-2474
33 **Ishizuka H**, Nakayama T, Matsuoka S, Gotoh I, Ogawa M, Suzuki K, Tanaka N, Tsubaki K, Ohkubo H, Arakawa Y, Okano T. Prediction of the development of hepato-cellular-carcinoma in patients with liver cirrhosis by the serial determinations of serum alpha-L-fucosidase activity. *Intern Med* 1999; **38**: 927-931
34 **Tangkijvanich P**, Tosukhowong P, Bunyongyod P, Lertmaharit S, Hanvivatvong O, Kullavanijaya P, Poovorawan Y. Alpha-L-fucosidase as a serum marker of hepatocellular carcinoma in Thailand. *Southeast Asian J Trop Med Public Health* 1999; **30**: 110-114
35 **Naitoh A**, Aoyagi Y, Asakura H. Highly enhanced fucosylation of serum glycoprotein in patients with hepatocellular carcinoma. *J Gastroenterol Hepatol* 1999; **14**: 436-445
36 **Mita Y**, Aoyagi Y, Suda T, Asakura H. Plasma fucosyltransferase activity in patients with hepatocellular carcinoma, with special reference to correlation with fucosylated species of alpha-fetoprotein. *J Hepatol* 2000; **32**: 946-954

Edited by Ren SY

P.O.Box 2345, Beijing 100023, China
Fax: +86-10-85381893
E-mail: wjg@wjgnet.com www.wjgnet.com

World J Gastroenterol 2003;9(4):714-716
World Journal of Gastroenterology
 ISSN 1007-9327

• COLORECTAL CANCER •

Cloning and expression of ornithine decarboxylase gene from human colorectal carcinoma

Hai-Yan Hu, Xian-Xi Liu, Chun-Ying Jiang, Yan Zhang, Ji-Feng Bian, Yi Lu, Zhao Geng, Shi-Lian Liu, Chuan-Hua Liu, Xiao-Ming Wang, Wei Wang

Hai-Yan Hu, Xian-Xi Liu, Ji-Feng Bian, Yi Lu, Geng Zhao, Shi-Lian Liu, Chuan-Hua Liu, Xiao-Ming Wang, Yan Zhang, Wei Wang, Experimental Centre of Medical Molecular Biology, School of Medicine, Shandong University, Jinan 250012, Sandong Province, China
Chun-Ying Jiang, Department of colo-proctology, The affiliated Hospital of Shandong University of Tradition Chinese Medicine, Jinan 250012, Sandong Province, China
Supported by Scientific Research Fund of national Ministry of Health, No.98-1-173
Correspondence to: Xian-Xi Liu, Experimental Centre of Medical Molecular Biology, School of Medicine, Shandon University, Jinan 250012, Shandong Province, China. xianxi@sdu.edu.cn
Telephone: +86-531-8382346
Received: 2002-07-04 **Accepted:** 2002-10-31

Abstract

AIM: To construct and express ODC recombinant gene for further exploring its potential use in early diagnosis of colorectal carcinoma.

METHODS: Total RNA was extracted from colon cancer tissues and amplified by reverse-transcription PCR with two primers, which span the whole coding region of ODC. The synthesized ODC cDNA was cloned into vector pQE-30 at restriction sites BamH I and Sal I which constituted recombinant expression plasmid pQE30-ODC. The sequence of inserted fragment was confirmed by DNA sequencing, the fusion protein including 6His-tag was facilitated for purification by Ni-NTA chromatographic column.

RESULTS: ODC expression vector was constructed and confirmed with restriction enzyme digestion and subsequent DNA sequencing. The DNA sequence matching on NCBI Blast showed 99 % affinity. The vector was transformed into *E. coli* M15 and expressed. The expressed ODC protein was verified with Western blotting.

CONCLUSION: The ODC prokaryote expression vector is constructed and thus greatly facilitates to study the role of ODC in colorectal carcinoma.

Hu HY, Liu XX, Jiang CY, Zhang Y, Bian JF, Lu Y, Geng Z, Liu SL, Liu CH, Wang XM, Wang W. Cloning and expression of ornithine decarboxylase gene from human colorectal carcinoma. *World J Gastroenterol* 2003; 9(4): 714-716
http://www.wjgnet.com/1007-9327/9/714.htm

INTRODUCTION

Ornithine decarboxylase (ODC) is the first key enzyme of the biosynthesis of polyamine which catalyzes the decarboxylation of the amino acid ornithine to the diamine putrescine. Its activation regulates the metabolism of spermidine, spermine and their precursor putrescine. Activity of polyamine biosynthesis is closely associated with the proceeding of physiological cell growth, proliferation and regeneration[1] and pathological proliferation[2]. It is necessary for cell to progress into S phase, or polyamine depletion arrest cells in G1[3]. ODC activity and polyamine concentration in colorectal cancers are significantly elevated compared with that in normal adjacent and healthy control tissues on rodents[4-7] and human beings. ODC repressor (eg. Difluoromethylornithine) has been considered to be one of the molecular targeted interventions of colon cancer[8]. The changing of ODC activity is an early event during the expression of malignancy. In this study, an ODC expression vector expressing a 6His-tag fusion protein was successfully constructed. The 6His-tag enabled us to purify the fusion protein with high purity.

MATERIALS AND METHODS

Materials

Trizol, RNA extract reagent, were purchased from Life Technologies Inc. RT-PCR kit, T-A clone kit, DNA marker and all restrictive enzymes were purchased from TaKaRa Shuzo Co.Ltd. Primers were synthesized by Sangon. The QIAquick Gel Extraction Kit, and expression system were got from QIAGEN. Protein marker was purchased from Shanghai Lizhudongfeng biotechnologies Co.Ltd. Standard ODC was purchased from Sigma.

Tissues

Colorectal carcinoma and respective adjacent normal colorectal mucus were obtained during surgery. Once the specimens were removed during operation, the necrotic and ulcerated tumors were removed and the normal mucosa was dissociated from the muscle and connective tissue. All specimens were then kept in liquid nitrogen until further use.

Extraction of total RNA

The total cellular RNA was extracted from normal and cancer tissues, respectively. The method of RNA extraction was similar to the Trizol RNA extraction protocol (Life Technologies Inc.). The concentration of RNA extracted was determined at wavelength of 260nm using U-2000 spectrophotometer (HITACH Ltd, Tokyo, Japan).

Reverse transcription polymerase chain reaction (RT-PCR)

The sequence of ODC primers was as follows, up-stream primer: 5' - gca ggatcc acc atg aac aac ttt ggt aa; down-stream primer: 5' -gaa gtcgac cta cac att aat act agc cg. The 5' primer recognized the start codon of ODC in exon 3, and the 3' primer recognized the end-codon in exon 12. Restriction sites were BamH I and Sal I. The first strand of cDNA was synthesized at 55 ℃ for 30 min in the presence of AMV reverse transcriptase (0.5 unit/μl), RNase inhibitor 1 unit/ml, dNTP 1.0 mM, Mg^{2+} 2.5 mM. The PCR was processed through 35 cycles of denature (1 min at 95 ℃), annealing (1.5 min at 58 ℃), and extension (1 min at 72 ℃) (Perkin-Elmer2400 PCR apparatus).

Purification of PCR product and T-A cloning

The PCR products were separated in 1 % agarose gel, and the

band containing ODC cDNA was cut off and placed into the QIAquick spin column, the ODC cDNA was purified and linked to plasmid pMD-18 with a polyA linker. The recombinant was transformed into *E. coli*. DH5α and selected by selective culture medium containing ampicillin.

Construction of pQE30-ODC

The pMD-ODC and pQE30 were digested by restrictive enzymes BamH I and SalI. The inserted fragment of pMD-ODC was collected from electrophoretic gel, then it was ligated with the linearized pQE30 by T4 Ligase at 18 ℃ overnight. The recombinant was transformed into *E. coli* DH5α by $CaCl_2$ method and selected by agar plate containing ampicillin and confirmed by restriction enzyme mapping. The positive recombinant was transformed into *E. coli*. M15.The sequence of inserted fragment was confirmed by DNA sequencing (Shanghai Sangon Bioengineering Co.Ltd.).

The expression of ODC fusion protein

The ampicillin-resistant colony of *E. coli* cells transformed with plasmid were cultured in LB cultural medium containing 100 mg/L ampicillin and 25 mg/L Kanamycin, and induced by 1 mM IPTG. The cultured cells were harvested at 1, 2, 3, 4hr after culture, respectively. The optimum time of maximum expression of proteins was analyzed through SDS-PAGE. The expressed ODC protein was tested through Western blot with specific antiserum.

RESULTS

RT-PCR amplification of ODC encoding sequence

RT-PCR was done with total RNA template extracted from human colon cancer. The designed primers include encoding sequence of ODC. Electrophoresis of RT-PCR products confirmed the length of RT-PCR fragment (1 480 bp) (Figure 1).

The purified ODC cDNA was ligated to pMD-18 by T-A complimentary pairing. ODC cDNA was inserted into pQE30 at BamH I and Sal I sites (Figure 2).

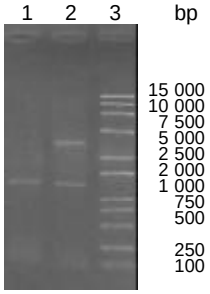

Figure 1 RT-PCR product on 1 % agarose gel. Lane 1: ODC RT-PCR product, 1 480 bp in length; Lane 2: pQE30-ODC plasmid digested by restriction enzyme BamHI and SalI.

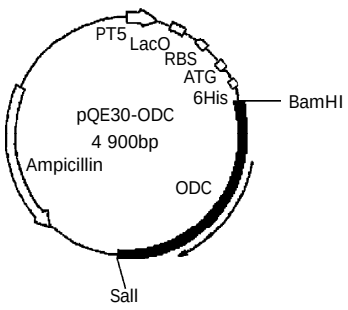

Figure 2 The pQE30-ODC expression vector including early promoter T5, Lac operator and 6His-Tag.

Sequence analysis

Sequence of inserted DNA was analyzed with automatic sequence analyzer and found to be about 1 500 bp in size and showed 99 % affinity in comparison with DNA sequence published on line [gi: 4505488].

SDS-PAGE and western blotting

Inserted ODC gene was expressed significantly in the prokaryotic expression system, and specific strip at 50kDa was demonstrated in Western blot. The optimum induction period is 4hr after administration of IPTG (Figure 3, 4).

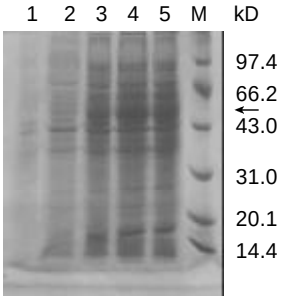

Figure 3 Expressed ODC protein on SDS-PAGE. Lane 1: M15 negative control; Lane 2-5: Expressed ODC proteins in M15 1 to 4 hour(s) after induction of IPTG; M: Protein marker; The arrow showed the expressed ODC protein.

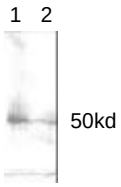

Figure 4 Western blot shows a strip of 50kD indicating the expression of ODC protein.

DISCUSSION

The polyamines are naturally occurring aliphatic polycations found in almost all living cells[9]. They are positively charged at neutral pH and the charge is distributed along the length of the molecule. This facilitates their interaction with anionic molecules such as DNA and RNA[9,10]. Polyamines have been shown to be essential for optimal rates of cell growth and differentiation, with high concentrations being found in rapidly growing cells and tissues[11].

Cancer cells always have a higher intracellular polyamine content than the equivalent normal tissue[12-15]. In addition to changes in polyamine content, ODC activity has also been found to be increased significantly in colon adenocarcinoma tissue compared to microscopically normal tissue from the same patients[13,16]. Similar findings were observed in human colonic surgical specimens with both ODC activity and polyamine content of the malignant tissue being increased[16,17]. Intratumour content of spermidine and spermine was increased in line with the increase in ODC activity.

Ornithine decarboxylase (ODC) is a rate-limiting enzyme in the biosynthesis of polyamines, and is induced in response to many growth stimuli such as hormones, growth factors, and tumor promoters, it has a rapid turnover rate with half-life at 15 minutes[18]. Numerous studies have demonstrated that regulation of ODC can occur at multiple levels, including the transcription of protooncogene c-myc[19-22], mRNA translation[10,23,24], protein turnover[10,25,26], and post-transcriptional interactions and modifications[27-30]. Recent studies focus intensely on ODC and

polyamine regulation as therapeutic targets. Inhibitors of ODC were found to suppress tunor formation in experimental models of bladder, breast, colon, and skin carcinogenesis[31-35].

Colorectal cancer is a major health problem in the western world and is associated with significant morbidity and mortality. First-line therapy is radical surgery with adjuvant chemotherapy commonly being treatment with antimetabolites such as 5-fluorouracil[30]. Although great clinical efforts have been made for the therapy of colorectal cancer with new technologies, such as CT or MRI colography[4,14], there is still much to be done on the early diagnosis and treatment. It is suggest that ODC activity and polyamine content may have interest in the diagnosis of malignancy and prognosis[15]. As the change of ODC activity is an early event in the development of the disease, it may be helpful for early screening and diagnosis of colon cancer.

We designed two primers from human ODC gene including the start codon (ATG) in exon 3 and the termination codon (TAG) so as to amplify the whole encoding sequence about 1 480 bp of ODC. The exons encode a protein is identical to the 461-amino acid sequence derived from human ODC.

The restriction fragment mapping of the recombinant, pQE 30-ODC, indicated that the inserted fragment was about 1.5kb, which was consistent with the encoding sequence of ODC. ODC activity in the lysate of transformed M15 was demonstrated through Western blot. The expressed fusion protein is about 50kDa, which is similar to the known ODC protein. The construction and expression of recombinant ODC provide a tool for ODC related further study.

REFERENCES

1 **Jeevanandam M**, Petersen SR. Clinical role of polyamine analysis: problem and promise. *Curr Opin Clin Nutr Metab Care* 2001; **4**: 385-390

2 **Auvinen M**. Cell transformation, invasion, and angiogenesis: a regulatory role for ornithine decarboxylase. *J Natl Cancer Inst* 1997; **85**: 533-537

3 **Bowlin TL**, McKown BJ, Davis GF, Sunkara PS. Effect of polyamine depletion *in vivo* by DL-alpha-difluoromethylornithine on functionally distinct populations of tumoricidal effector cells in normal and tumor-bearing mice. *Cancer Res* 1986; **46**: 5494-5498

4 **Umar A**, Viner JL, Hawk ET. The future of colon cancer prevention. *Ann N Y Acad Sci* 2001; **952**: 88-108

5 **Rozhin J**, Wilson PS, Bull AW, Nigro ND. Ornithine decarboxylase activity in the rat and human colon. *Cancer Res* 1984; **44:** 3226-3230

6 **Hixson LJ**, Garewal HS, McGee DL, Sloan D, Fennerty MB, Sampliner RE, Gerner EW. Ornithine decarboxylase and polyamines in colorectal neoplasia and mucosa. *Cancer Epidemiol Biomarkers Prev* 1993; **2**: 369-374

7 **Giardiello FM**, Hamilton SR, Hylind LM, Yang VW, Tamez P, Casero RA Jr. Ornithine decarboxylase and polyamines in familial adenomatous polyposis. *Cancer Res* 1997; **57:** 199-201

8 **Pegg AE**, Shantz LM, Coleman CS. Ornithine decarboxylase as a target for chemoprevention. *J Cell Biochem (Suppl.)* 1995; **22:** 132-138

9 **Thomas T,** Thomas TJ. Polyamines in cell growth and cell death: molecular mechanisms and therapeutic applications. *Cell Mol Life Sci* 2001; **58**: 244-258

10 **Wallon UM**, Persson L, Heby O. Regulation of ornithine decarboxylase during cell growth. Changes in the stability and translatability of the mRNA, and in the turnover of the protein. *Mol Cell Biochem* 1995; **146**: 39-44

11 **Seiler N**, Atanassov CL, Raul F. Polyamine metabolism as target for cancer chemoprevention (review). *Raul F Int J Oncol* 1998; **13**: 993-1006

12 **Kingsnorth AN**, Wallace HM. Elevation of monoacetylated polyamines in human breast cancers. *Eur J Cancer Clin Oncol* 1985; **21**: 1057-1062

13 **Wallace HM**, Caslake R. Polyamines and colon cancer. *Eur J Gastroenterol Hepatol* 2001; **13**: 1033-1039

14 **Faaland CA**, Thomas TJ, Balabhadrapathruni S, Langer T, Mian S, Shirahata A, Gallo MA, Thomas T. Molecular correlates of the action of bis(ethyl)polyamines in breast cancer cell growth inhibition and apoptosis. *Biochem Cell Biol* 2000; **78**: 415-426

15 **Canizares F**, Salinas J, de las Heras M, Diaz J, Tovar I, Martinez P, Penafiel R. Prognostic value of ornithine decarboxylase and polyamines in human breast cancer: correlation with clinicopathologic parameters. *Clin Cancer Res* 1999; **5**: 2035-2041

16 **Linsalata M**, Caruso MG, Leo S, Guerra V, D'Attoma B, Di Leo A. Prognostic value of tissue polyamine levels in human colorectal carcinoma. *Anticancer Res* 2002; **22**: 2465-2469

17 **Takami H**, Koudaira H, Kodaira S. Relationship of ornithine decarboxylase activity and human colon tumorigenesis. *Jpn J Clin Oncol* 1994; **24**: 141-143

18 **Pegg AE**. Recent advances in the biochemistry of polyamines in eukaryotes. *Biochem J* 1986; **234**: 249-262

19 **Evan GI**, Wyllie AH, Gilbert CS, Littlewood TD, Land H, Brooks M, Waters CM, Penn LZ, Hancock DC. Induction of apoptosis in fibroblasts by c-myc protein. *Cell* 1992; **69**: 119-128

20 **Bello-Fernandez C**, Packham G, Cleveland JL. The ornithine decarboxylase gene is a transcriptional target of c-Myc. *Proc Natl Acad Sci U S A* 1993; **90**: 7804-7808

21 **Packham G**, Cleveland JL. Ornithine decarboxylase is a mediator of c-Myc-induced apoptosis. *Mol Cell Biol* 1994; **14**: 5741-5747

22 **Iyengar RV**, Pawlik CA, Krull EJ, Phelps DA, Burger RA, Harris LC, Potter PM, Danks MK. Use of a modified ornithine decarboxylase promoter to achieve efficient c-MYC- or N-MYC-regulated protein expression. *Cancer Res* 2001; **61**: 3045-3052

23 **Kahana C,** Nathans D. Translational regulation of mammalian ornithine decarboxylase by polyamines. *J Biol Chem* 1985; **260**: 15390-15393

24 **Shantz LM**, Pegg AE. Translational regulation of ornithine decarboxylase and other enzymes of the polyamine pathway. *Int J Biochem Cell Biol* 1999; **31**: 107-122

25 **Lu L**, Stanley BA, Pegg AE. Identification of residues in ornithine decarboxylase essential for enzymic activity and for rapid protein turnover. *Biochem J* 1991; **277**: 671-675

26 **Dircks L**, Grens A, Slezynger TC, Scheffler IE. Post-transcriptional regulation of ornithine decarboxylase activity. *J Cell Physiol* 1986; **126**: 371-378

27 **Heller JS,** Fong WF, Canellakis ES. Induction of a protein inhibitor to ornithine decarboxylase by the end products of its reaction. *Proc Nat Acad Sci USA* 1976; **73**: 1858-1862

28 **Fogel-Petrovic M**, Vujcic S, Miller J, Porter CW. Differential post-transcriptional control of ornithine decarboxylase and spermidine-spermine N1-acetyltransferase by polyamines. *FEBS Lett* 1996; **391**: 89-94

29 **Ruhl KK**, Pomidor MM, Rhim JS, Tuan RS, Hickok NJ. Post-transcriptional suppression of human ornithine decarboxylase gene expression by phorbol esters in human keratinocytes. *J Invest Dermatol* 1994; **103**: 687-692

30 **Flamigni F**, Campana G, Carboni L, Rossoni C, Spampinato S. Post-transcriptional inhibition of ornithine decarboxylase induction by zinc in a difluoromethylornithine resistant cell line. *Biochim Biophys Acta* 1994; **1201**: 101-105

31 **Thompson HJ**, Ronan AM. Effect of D,L-2-difluoromethylornithine and endocrine manipulation on the induction of mammary carcinogenesis by 1-methyl-1-nitrosourea. *Carcinogenesis* 1986; **7**: 2003-2006

32 **Nigro ND**, Bull AW, Boyd ME. Inhibition of intestinal carcinogenesis in rats: effect of difluoromethylornithine with piroxicam or fish oil. *J Natl Cancer Inst* 1986; **77**: 1309-1313

33 **Loprinzi CL**, Messing EM, O'Fallon JR, Poon MA, Love RR, Quella SK, Trump DL, Morton RF, Novotny P. Toxicity evaluation of difluoromethylornithine: doses for chemoprevention trials. *Cancer Epidemiol Biomarkers Prev* 1996; **5**: 371-374

34 **Carbone PP**, Douglas JA, Larson PO, Verma AK, Blair IA, Pomplun M, Tutsch KD. Phase I chemoprevention study of piroxicam and alpha-difluoromethylornithine.*Cancer Epidemiol Biomarkers Prev* 1998; **7**: 907-912

35 **Love RR**, Carbone PP, Verma AK, Gilmore D, Carey P, Tutsch KD, Pomplun M, Wilding G. Randomized phase I chemoprevention dose-seeking study of alpha-difluoromethylornithine. *J Natl Cancer Inst* 1993; **85**: 732-737

Edited by Ren SY

P.O.Box 2345, Beijing 100023, China
Fax: +86-10-85381893
E-mail: wjg@wjgnet.com www.wjgnet.com

World J Gastroenterol 2003;9(4):717-720
World Journal of Gastroenterology
 ISSN 1007-9327

• COLORECTAL CANCER •

Pre-operative radiochemotherapy of locally advanced rectal cancer

Xiao-Nan Sun, Qi-Chu Yang, Jian-Bin Hu

Xiao-Nan Sun, Qi-Chu Yang, Jian-Bin Hu, Department of Radiation Oncology, Sir Run Run Shaw Hospital, College of Medicine, Zhejiang University, Hangzhou 310016, Zhejiang Province, China
Correspondence to: Dr. Xiao-Nan Sun, Department of Radiation Oncology, Sir Run Run Shaw Hospital, College of Medicine, Zhejiang University, Hangzhou 310016, Zhejiang Province, China. sunxiaonan@hotmail.com
Telephone: +86-571-86090073 **Fax:** +86-571-86044817
Received: 2002-08-01 **Accepted:** 2002-11-19

Abstract

AIM: To evaluate results of pre-operative radiochemotherapy followed by surgery for 15 patients with locally advanced un-resectable rectal cancer.

METHODS: 15 patients with advanced non-resectable rectal cancer were treated with pre-operative irriadiation of 40-46 Gy plus concomitant chemotherapy (5-FU+LV and 5'-DFuR) (RCS group). For comparison, 27 similar patients, treated by preoperative radiotherapy (40-50 Gy) plus surgery were served as control (RS group).

RESULTS: No radiochemotherapy or radiotherapy was interrupted and then was delayed because of toxicities in both groups. The radical resectability rate was 73.3 % in the RCS group and 37.0 % (P=0.024) in RS group. Sphincter preservation rates were 26.6 % and 3.7 % respectively (P=0.028). Sphincter preservation rates of lower rectal cancer were 27.3 % and 0.0 % respectively (P=0.014). Response rates of RCS and RS groups were 46.7 % and 18.5 % (P=0.053). The tumor downstage rates were 8 (53.3 %) and 9 (33.3 %) in these groups (P=0.206). The 3-year overall survival rates were 66.7 % and 55.6 % (P=0.485), and the disease free survival rates were 40.1 % and 33.2 % (P=0.663). The 3-year local recurrent rates were 26.7 % and 48.1 % (P=0.174). No obvious late effects were found in either groups.

CONCLUSION: High resectability is possible following pre-operative radiochemotherapy and can have more sphincters preserved. It is important to improve the quality of the patients' life even without increasing the survival or local control rates. Preoperative radiotherapy with concomitant full course chemotherapy (5-Fu+LV and 5'-DFuR) is effective and safe.

Sun XN, Yang QC, Hu JB. Pre-operative radiochemotherapy of locally advanced rectal cancer. *World J Gastroenterol* 2003; 9 (4): 717-720

http://www.wjgnet.com/1007-9327/9/717.htm

INTRODUCTION

Neoadjuvant treatment is delivered as radiotherapy (RT) or radiochemotherapy (RCT) prior to surgery with the aim to devitalize primary and metastatic tumor cells and to shrink the tumor so that resection is facilitated even in case of primarily nonresectable cases[1-6]. The trials of several "neoadjuvant" radiochemotherapy have generated clear evidence downstaging is possible, resectability rates are increased, local relapse rates decreased, and survival rates possibly improved. Preoperative radiochemotherapy has been regarded as 'standard' therapy[1,7].

The infusional chemotherapy protocol of 5-FU demonstrated a higher response rate and a marginal survival benefit in advanced colorectal cancer[8]. The toxicity was lower in the infusion protocol than that in bolus protocol[9]. In chemoradiotherapy with the infusion protocol, this advantage can still work and have a theoretically better chance of drug-radiation interaction as well[10]. However, i.v. chemotherapy, either by infusion or bolus, is still a major source of discomfort to the patients.

Oral administration enables sustained exposure to 5-FU, avoids the technical barrier of intravenous (IV) administration and allows significant flexibility in choice of the dosage regimens, provided that efficacy is not compromised[11,12]. Doxifluridine (5'-deoxy-5-fluorouridine, 5'-DFuR) is synthetic 5-deoxy-nucleoside derivative. In experimental murine tumor systems, doxifluridine has achieved a therapeutic index of 10-15 times greater than that of 5-FU or other fluoropyrimidines[13]. This drug has been shown to be an effective agent when administered orally[14]. The use of oral doxifluridine and leucovorin in chemoradiotherapy provides several advantages. Administration of the drug during the entire radiotherapy course offers more chances of interaction between the drug and radiation, similar to infusion chemoradiotherapy; i.v. infusion-associated complications can be avoided. The use of oral chemotherapy also provides convenience and a comfortable environment of drug administration to patients.

In our study, 15 patients received mean dose of 41.5 Gy of pelvic irradiation with concurrent chemotherapy of 5-FU+leucovorin (LV) was administered by bolus injection during d1-3 and d26-28 of RT. 5'-DFuR were given during d4-25 of RT (RCS group). 27 similar patients treated by preoperative radiotherapy (mean dose of 42.6 Gy) were served as control (RS group). The points of the study were to evaluate the toxicity, resectability rates and relative response rates of the treatment, 3-year survival rates and 3-year recurrent rates in the two groups.

MATERIALS AND METHODS

Patients

Patients with advanced non-resectable rectal cancer were considered elegible for radiochemotherapy plus surgery study (RCS group) if they fulfilled the following criteria: Below 72 years old, KPS of 60 or over, histologically confirmed adenocarcinoma of the rectum, advanced tethered and fixed primary tumor that were considered unresectable by surgeon. From December 1995 to January 1997, 15 patients were entered in the study. They were 12 men and 3 women and age ranging from 33 to 72 years (mean 50.6). For comparison, 27 similar patients, treated by preoperative radiotherapy (40-50 Gy) plus surgery served as control (RS group). They were 21 men and 6 women and age ranging from 18 to 71 (mean 58).

Table 1 summarized the main demography and baseline characteristics of all elegible patients.The two groups were well matched for all evaluated characteristics. All tumors of

two groups were middle and lower rectal cancers (5-11cm from anus). 11 and 20 lower rectal cancers in RCS group and RS group respectively. Before starting treatment all patients underwent a general examination and got CBC done. These examinations were repeated every week during the treatment period and before operation ultrasound and/or CT or MRI and digital examination were mandatory. Digital examination was done every week.

Table 1 Patient demography and disease charateristiscs at baseline

Parameter	RCS group	RS group
Male/female	12/3	21/6
Age(years):median(range)	56(33-72)	58(18-71)
Karnofsky performance status	70-90	70-90
Primary site		
Middle	4	7
lower	11	20
Degree of differentiation		
Well	1	2
Moderate	7	15
Poor	3	4
Not specified	4	6
TNM staging		
T3N0M0	5	14
T3N1M0	0	3
T4N0M0	6	3
T4N1M0	4	5
T4N2M0	0	2

Treatment

Radiation was delivered by linear accelerator (10 MV X-ray). Similar fields were used for treatment in both groups. The initial pelvic radiation therapy volume of AP/PA ports and two lateral fields treated to 4 000 cGy. The use of a boost field to the primary tumor bed and immediately adjacent lymph nodes were given in some patients.Total doses of 4 000cGy to 4 600 cGy (mean 4 150 cGy) were delivered in 4 to 5 weeks in RCS group. Total doses of 4 000cGy to 5 000cGy (mean 4 260 cGy) were delivered in 4 to 5 weeks in RS group. In RCS group, chemotherapy was given concomitantly and consisted of two courses of 5-FU at a dose of 500 mg/m^2/day plus leucovorin at a dose of 300 mg by intravenous injection for 3 days in week 1 and week 4, 5' -DFuR was administered orally at a dose of 200 mg three times daily concomitantly during radiotherapy between interval of the two courses of intravenous chemotherapy. All patients in two groups underwent subsequent surgery 4 to 5 weeks after the preoperative treatment. 4 to 6 courses adjuvant chemotherapy (5-FU based) were given after surgery in two groups.

Evaluation of patients

Assessments of tumor dimensions and involved sites were performed before the start of treatment and were scheduled after week 4. Tumor dimensions were assessed by use of computed tomography scans, x-rays, magnetic resonance imaging. Tumor response classification was based on standard World Health Organization criteria. Disappearance of all known disease at all involved sites was considered a complete response (CR). Partial reponse (PR) was defined as residual disease with a decrease=50 % in sum of the products greatest perpendicular diameters (SPD) of all indicator lesions. Progressive disease (PD) was defined as the appearance of a new lesion or an increase of 25 % in the SPD. Stable disease (SD) was defined as no change in SPD or a change not reaching to PR or PD. Total response rate was defined as CR plus PR. Surgical treatment results were summerized (the radical resectability rate, sphincter preservation rate and complication).

Patients were followed up every 3 months after the end of treatment with progression and survival of the disease recorded. The duration of follow-up ranged from 36-61 months (mean 43). Disease progression and survival time were analyzed according to Kaplan-Meier estimates and compared using the log-rank test. A one-sided chi-square test was used at an alpha level of 2.5 % to compare response data in two patient groups. The data of toxicity were scored retrospectively according to the World Health Organization (WHO) toxicity evaluation.

RESULTS

Tumor response

No radiochemotherapy or radiotherapy was interrupted and was then delayed because of toxicities in both groups. Obvious pain relief has been achieved in all patients of two groups presenting with buttock/sciatic/perineal pain, usually within days of commencing radiochemotherapy/radiotherapy. The median time of obvious pain relief was 7 days (range 5-10) in RCS group, 10 days (range 7-18) in RS group.

11 radical resection, 3 palliative surgery and 1 cytoreductive surgery were undertaken in RCS group.10 radical resection, 15 palliative surgery and 2 cytoreductive surgery were undertaken in RS group. Table 2 summarizes the radical resectability, sphincter preservation, lower rectal cancer sphincter preservation, response and tumor downstage rates of the two groups. Pathologic complete response (pCR) of the primary tumor was observed in two patients of RCS group.

Table 2 The radical resectability, sphincter preservation, lower rectal cancer sphincter preservation, response and tumor downstage rates in the two groups

Parameter	RCS group	RS group	*P*
Radical resectability rate	73.3%	37.0%	0.024
Sphincter preservation rate	26.6%	3.7%	0.028
Lower rectal cancer sphincter preservation rate	27.3%	0.0%	0.014
Response rate	46.7%	18.5%	0.053
Tumor downstage rate	53.3%	33.3%	0.206

Follow-up results

In Table 3 the 3-year overall survival rates, the disease free survival rates and the 3-year local recurrent rates are compared in the patients of two groups. Four patients of RCS group had good to excellent sphincter function.

Table 3 The 3-year overall survival, disease free survival and local recurrent rates of the patients of two groups

Parameter	RCS group	RS group	*P*
3-year overall survival rate	66.7%	55.6%	0.485
3-year disease free survival rate	40.1%	33.2%	0.663
3-year local recurrent rate	26.7%	48.1%	0.174

Toxicity

Patients were scored according to the WHO grading. A detailed description of acute toxicities was given in Table 4. The most relevant toxic reactions included rectal tenesmus, diarrhea and perianal area skin reaction. No toxic death was observed in

this study. No patient interrupted the radiochemotherapy and delayed the operation because of these acute toxicities. Total incidence of grade 3/4 toxicity were 73.3 % in RCS group, 44.4 % in RS group (P=0.071) respectively. No severe late toxicity was found in the two groups.

Table 4 WHO modified scale for acute toxicity

Site	Grading (RCS group)					Grading (RS group)				
	0	1	2	3	4	0	1	2	3	4
Hematologic:										
Neutropenia	8	2	4	1	0	19	3	5	0	0
Non-hematologic:										
Small bowl	4	3	7	3	0	6	9	10	2	0
Bladder	6	4	5	0	0	10	11	6	0	0
Skin	0	2	6	7	0	0	10	8	9	0

DISCUSSION

Preoperative radiotherapy (RT) (45 Gy) with continuous infusion of 5-FU for 5 days per week with or without CDDP were used by the M.D. Anderson group[15] in locally advanced tethered and fixed primary rectal cancer to downstage the tumors. It was concluded that preoperative radiochemotherapy decreased the local recurrence rate as compared to preoperative radiotherapy only, with no increase of surgical morbidity and late morbidity after a follow-up of 3 years. In this study, the acute toxicities of grade 3 in RCS group were more pronounced than that in RS group but without statistical differences and no patient had interrupted the radiochemotherapy and delayed the operation because of these acute toxicities. University of Uppsala study[16] proved that the volume of bowel under radiation, rather than the energy of the radiation influence postoperative mortality, and emphasize the importance of precise radiotherapy planning to minimize normal tissue toxic reactions.

Continuous infusion of 5-FU led to significantly higher response rates than bolus 5-FU, and a meta-analysis identified a statistically significant increase in overall survival[17]. However, this improvement was the only report, and other trials had failed to repeat the significant survival benefit. Continuous infusion 5-FU is not routinely practised, partly because of its inconvenience and cost and partly due to central venous access that might cause significant complications in 15 % to 20 % of patients[18], including infections, bleeding, thrombosis, and pneumothorax. Each of these complications has a negative impact on quality of life. Several of the new chemotherapy drugs used in colorectal cancer also appear to be radiosensitizers. Pilot and phase II trials incorporating irinotecan and oxaliplatin[19] into 5-FU-plus-radiation program are currently used, with encouraging results. Similarly, the oral 5-FU prodrugs[20,21] represent promising new agents to combine with radiation. The oral route not only makes these drugs convenient to the patient but also gives prolonged theraputic serum levels, simulating continuous venous infusion, which may be the preferable fluoropyrimidine schedule for radiosensitization.

5-FU as a radiosensitizer was given by continuous infusion. 5' -DFuR kills cancer cell through PyNPase transformation. The study by Watanabe *et al*[22] found that fifty three patients with advanced colorectal cancer when given single oral doses of 5' -DFuR, high 5-FU concentration and PyNPase activity were noted in tumor tissue and lymph nodes. Effective 5-FU concentration in tumor tissue was maintained even 24 hours after treatment. Effective lymph node concentration of 5-FU was maintained even 8 hours after treatment. PyNPase activity in tumor tissue was significantly higher than that in the normal intestinal mucosa (P<0.05). In this study, pre-operative radiochemotherapy was well tolerated. The relatively hight rate of curative resections indicates that 5-FU and Oral 5' -DFuR treatment as radiosensizers, maintaining highier concentrations of 5-FU during RT, are safe and effective. The aim of giving two courses of 5-FU intravenous injection was to relieve the local symptoms of the patients with local advanced rectal cancer and to improve systemic treatment efficacy. The appropriate dosage of oral 5' -DFuR as radiosensitizer during RT should be further studied.

Sphincter preservation rate and sphincter preservation rate of lower rectal cancer in RCS group were significantly higher than that of RS group. Therefore, this study at least demonstrates that sphincter preservation operation did not decrease local control and survival rates, although when local control and survival rates were analyzed, the RCS group had no significant advantage compared with RS group. But it is very important to meet the request of sphincter preservation by the rectal cancer patients and to improve their quality of life.

Local failure rates are high for locally irresectable primary or recurrent colorectal cancer, even when chemoradiation therapy is employed. A tumor-free surgical resection margins are paramount to achieve cure[23-25]. In this study, the radical resectability rate in the RCS group was significantly higher than that in RS group, but without significant decrease local relapse rate, and no significant improvement of survival rate. Therefore, further study of this modality of treatment should be continued[26-32].

REFERENCES

1 **Landry JC**, Koretz MJ, Wood WC, Bahri S, Smith RG, Costa M, Daneker GW, York MR, Sarma PR, Lynn M. Preoperative irradiation and fluorouracil chemotherapy for locally advanced rectosigmoid carcinoma: Phase I-II study. *Radiology* 1993; **188**: 423-426

2 **Chan A**, Wong A, Langevin J, Khoo R. Preoperative concurrent 5-fluruorouracil infusion, mitomycin-c and pelvic radiation therapy in tethered and fixed rectal carcinoma. *Int J Radiat Oncol Biol Phys* 1993; **25:** 791-799

3 **Rich TA**, Skibber JM, Ajani JA, Buchholz DJ, Gleary KR, Dubrow RA, Levin B, Lynch PM, Meterissian SH, Roubein LD. Preoperative infusional chemoradiation therapy for stage T_3 rectal cancer. *Int J Radiat Oncol Biol Phys* 1995; **32:** 1025-1029

4 **Chen ET**, Mohiuddin M, Brodovsky H, Fishbein G, Marks G. Downstaging of advanced rectal cancer following combined preoperative chemotherapy and high dose radiation. *Int J Radiat Oncol Biol Phys* 1994; **30:** 169-175

5 **Minsky B**, Cohen A, Enker W, Kelsen D, Kemeng N, Ilson D, Guillem J, Saltz L, Frankel, Conti J. Preoperative 5-FU, low dose leucovorin and concurrent radiation therapy for rectal cancer. *Cancer* 1994; **73:** 273-280

6 **Yuan HY**, Li Y, Yang GL, Bei DJ, Wang K. Study on the causes of local recurrence of rectal cancer after curative resection: analysis of 213 cases. *World J Gastroenterol* 1998; **4:** 527-529

7 **Gunderson LL**. Indications for and results of combined modality treatment of colorectal cancer. *Acta Oncol* 1999; **38:** 7-21

8 **Rougier P**, Paillot B, La Planche A, Morvan F, Seits JF, Rekacewicz C, Laplaige P, Jacob J, Grandjouan S, Tigaud JW, Fabri MC, Luboinski M, Ducreux M. 5-Fluorouracil (5-FU) continuous intravenous infusion compared with bolus administration. Final results of a randomized trial in metastatic colorectal cancer. *Eur J Cancer* 1997; **33:** 1789-1793

9 **Rodel C**. Efficacy and toxicity spectrum of continuous infusion of 5-fluorouracil compared with bolus administration in advanced colorectal tumors. *Strahlenther Onkol* 1999; **175:** 294-295

10 **Byfield JE**, Frankel SS, Hombeck CL, Sharp TR, Callipari FB. Phase I and pharmacologic study of 72-hour infused 5-fluorouracil and hyperfractionated cyclical radiation. *Int J Radiatoncol Biol Phys* 1985; **11:** 791-800

11 **Payne SA**. A study of quality of life in cancer patients receiving palliative chemotherapy. *Soc Sci Med* 1992; **35:** 1505-1509

12 **Liu G**, Franssen E, Fitch MI, Warner E. Patient preferences for

oral versus intravenous palliative chemotherapy. *J Clin Oncol* 1997; **15:** 110-115

13 **Bollag W**, Hartmann HR. Tumor inhibitory effects of a new fluorouracil derivative: 5'-Deoxy-5-fluorouracil. *Eur J Cancer* 1980; **16:** 427-432

14 **Heintz RC**, Guentert TW, Ssutter C. Pharmacokinetic profile of doxifluridine (5'dFUR, furtulon), 5-fluorouracil (5-FU) prodrug. *Proc Am Assoc Cancer Res* 1986; **27:** 207

15 **Weinstein GD**, Rich TA, Shumate CR, Skibber JM, Cleary KR, Ajani JA, Ota DM. Preoperative infusional chemoradiation and surgery with or without an electron beam introoperative boost for advanced primary rectal cancer. *Int J Radiat Oncol Biol Phys* 1995; **32:** 197-204

16 **Frykholm GJ**, Isacsson U, Nygard K, Montelius A, Jung B, Pahlman L, Glimelius B. Preoperative radiotherapy in rectal carcinoma: aspects of acute adverse effects and radiation technique. *Int J Radiat Oncol Biol Phys* 1996; **35:** 1039-1048

17 **Tsuji A**, Morita S, Horimi T, Takasaki M, Takahashi I, Shirasaka T. Combination chemotherapy of continuous 5-FU infusion and low-dose cisplatin infusion for the treatment of advanced and recurrent gastric and colorectal adenocarcinomas. *Gan To Kagaku Ryoho* 2000; **27**(Suppl 2)**:** 528-534

18 **Grem JL**. Systemic treatment options in advanced colorectal cancer: Perspectives on combination 5-fluorouracil plus leucovorin. *Semin Oncol* 1997; **24**(Suppl 18)**:** S8-S18

19 **Uzcudun AE**, Batlle JF, Velasco JC, Sanchez Santos ME, Carpeno Jde C, Grande AG, Juberias AM, Pineiro EH, Olivar LM, Garcia AG. Efficacy of preoperative radiation therapy for resectable rectal adenocarcinoma when combined with oral tegafur-uracil modulated with leucovorin: results from a phase II study. *Dis colon rectum* 2002; **45:** 1349-1358

20 **Janjan NA**, Crane C, Feig BW, Cleary K, Dubrow R, Curley S, Vauthey JN, Lynch P, Ellis LM, Wolff R, Lenzi R, Abbruzzese J, Pazdur R, Hoff PM, Allen P, Brown T, Skibber J. Improved overall survival among reponders to preoperative chemoradiation for locally advanced rectal cancer. *Am J Clin Oncol* 2001; **24:** 107-112

21 **Van Cutsem E**, Peeters M, Verslype C, Filez L, Haustermans K, Janssens J. The medical treatment of colorectal cancer: actual status and new developments. *Hepatogastroenterology* 1999; **46:** 709-716

22 **Mori K**, Hasegawa M, Nishida M, Toma H, Fukuda M, Kobota T, Nagasue N, Yamana H, Hirakawa-YS Chung K, Ikeda T, Takasaki K, Oka M, Kameyama M, Toi M, Fujii H, Kitamura M, Murai M, Sasaki H, Ozono S, Makuuchi H, Shimada Y, Onishi Y, Aoyagi S, Mizutani K, Ogawa M, Nakao A, Kinoshita H, Tono T, Imamoto H, Nakashima Y, Manabe T. Expression levels of thymidine phosphorylase and dihydropyrimidine dehydrogenase in various human tumor tissues. *Int J oncol* 2000; **17:** 33-38

23 **Farouk R**, Nelson H, Gunderson LL. Aggressive multimodility treatment for locally advanced irresectable rectal cancer. *Br J Surg* 1997; **84:** 741-749

24 **Farouk R**, Nelson H, Radice E, Mercill S, Gunderson L. Accuracy of computed tomography in determining respectability for locally advanced primary or recurrent colorectal cancers. *Am J Surg* 1998; **175:** 283-287

25 **Holm T**, Cedermark B, Rutqvist LE. Local recurrence of rectal adenocarcinoma after "curative" surgery with and without preoperative radiotherapy. *Br J Surg* 1994; **81:** 452-455

26 **Makin GB**, Breen DJ, Monson JR. The impact of new technology on surgery for colorectal cancer. *World J Gastroenterol* 2001; **7:** 612-621

27 **Shen LZ**, Wu WX, Xu DH, Zheng ZC, Liu XY, Ding Q, Hua YB, Yao K. Specific CEA-producing colorectal carcinoma cell killing with recombination adenoviral vect or containing cytosine deaminase gene. *World J Gastroenterol* 2002; **8:** 270-275

28 **Xiong B**, Gong LL, Zhang F, Hu MB, Yuan HY. TGF beta$_1$ expression and angiogenesis in colorectal cancer tissue. *World J Gastroenterol* 2002; **8:** 496-498

29 **Jiang Q**, Ge K, Xu DH, Sun LY, Zheng ZC, Liu XY. Expression of cytosine deaminase gene in human colon carcinoma cells by recombinant retrovral vector. *Shengwu Huaxue Yu Shengwu Wuli Xuebao(Shanghai)* 1997; **29:** 135-141

30 **Jiang Q**, Ge K, Xu DH, Sun LY, Zheng ZC, Liu XY. Use of carcinoebryonic antigen gene promoter in colorectal carcinoma-specific suicidal gene therapy. *Shengwu Huaxue Yu Shengwu Wuli Xuebao(Shanghai)* 1998; **30:** 1-8

31 **Pederson LC**, Buchsbaum DJ, Vickers SM, Kancharla SR, Mayo MS, Curiel DT, Stackhouse MA. Molecular chemotherapy combined with radiation therapy enhances killing of cholangiocarcinoma cells *in vitro* and *in vivo*. *Cancer Res* 1997; **57:** 4325-4332

32 **Chen G**, Li S, Yu B, An P, Cai H, Guo W. X-ray combined with cytosine deaminase suicide gene therapy enhances killing of colorectal carcinoma cells *in vitro*. *Zhonghua Waike Zazhi* 2002; **40:** 136-138

Edited by Xu JY

P.O.Box 2345, Beijing 100023, China
Fax: +86-10-85381893
E-mail: wjg@wjgnet.com www.wjgnet.com

World J Gastroenterol 2003;9(4):721-725
World Journal of Gastroenterology
 ISSN 1007-9327

• COLORECTAL CANCER •

Racial differences in the anatomical distribution of colorectal cancer: a study of differences between American and Chinese patients

San-Hua Qing, Kai-Yun Rao, Hui-Yong Jiang, Steven D. Wexner

San-Hua Qing, Kai-Yun Rao, Hui-Yong Jiang, Nan Fang Hospital, First Military Medical University, Guangzhou, 510515, Guangdong Province, China
Steven D. Wexner, Department of Colorectal Surgery, Cleveland Clinic Florida, Weston, Florida 33308, USA
Correspondence to: Dr. San-Hua Qing, Nan Fang Hospital, First Military Medical University, Guangzhou, 510515, Guangdong Province, China. sanhuaq@yahoo.com
Telephone: +86-20-61641696 **Fax:** +86-20-87280340
Received: 2002-07-08 **Accepted:** 2002-08-02

Abstract

AIM: To compare the racial differences of anatomical distribution of colorectal cancer (CRC) and determine the association of age, gender and time with anatomical distribution between patients from America (white) and China (oriental).

METHODS: Data was collected from 690 consecutive patients in Cleveland Clinic Florida, U.S.A. and 870 consecutive patients in Nan Fang Hospital affiliated to the First Military Medical University, China over the past 11 years from 1990 to 2000. All patients had colorectal adenocarcinoma diagnosed by histology and underwent surgery.

RESULTS: The anatomical subsite distribution of tumor, age and gender were significantly different between white and oriental patients. Lesions in the proximal colon ($P<0.001$) were found in 36.3 % of white *vs* 26.0 % of oriental patients and cancers located in the distal colon and rectum in 63.7 % of white and 74 % of oriental patients ($P<0.001$). There was a trend towards the redistribution from distal colon and rectum to proximal colon in white males over time, especially in older patients (>80 years). No significant change of anatomical distribution occurred in white women and Oriental patients. The mean age at diagnosis was 69.0 years in white patients and 48.3 years in Oriental patients ($P<0.001$).

CONCLUSION: This is the first study comparing the anatomical distribution of colorectal cancers in whites and Chinese patients. White Americans have a higher risk of proximal CRC and this risk increased with time. The proportion of white males with CRC also increased with time. Chinese patients were more likely to have distal CRC and developed the disease at a significantly earlier age than white patients. These findings have enhanced our understanding of the disease process of colorectal cancer in these two races.

Qing SH, Rao KY, Jiang HY, Wexner SD. Racial differences in the anatomical distribution of colorectal cancer: a study of differences between American and Chinese patients. *World J Gastroenterol* 2003; 9(4): 721-725
http://www.wjgnet.com/1007-9327/9/721.htm

INTRODUCTION

Colorectal cancer (CRC) is one of the most common cancers in the world and the second leading cause of cancer death in the United States[1, 2]. It is estimated that 552 000 Americans died of cancer in the year 2000; about 55 000 of these cancer deaths were attributed to CRC. In recent years, the incidence of CRC has increased rapidly in China making it the fourth leading cause of cancer mortality in China[3]. In general, majority of these cancers are distally located. During the last two decades many investigators have noted that the incidence rate of CRC vary widely by race and gender and the location also has changed with time[4-15], with a trend towards redistribution of primary CRC from left to right[16, 17]. Proximal cancers have a tendency to present at a more advanced stage and are associated with a poor prognosis. Increasing age, female gender, black, non-Hispanic race and the presence of comorbid illnesses were factors associated with a greater likelihood of developing colorectal cancer in a proximal location. Black patients with colon cancer are more likely to have a poorer survival than white patients[13, 18-21]. However, it is not clear whether there are any differences in anatomical distribution of primary colorectal cancer between American (white) and Chinese (oriental) patients.

We hypothesized that there are significant differences of anatomical distribution of primary colorectal cancers between the white (American) and oriental (Chinese) patients. The purpose of this study is to compare the differences in anatomical distribution of colorectal cancers and to describe any association of age, gender and time with primary CRC in white and oriental patients.

MATERIALS AND METHODS

A retrospective study was undertaken. Data was collected from 690 consecutive white patients in Cleveland Clinic Florida U. S.A. and 870 consecutive Chinese patients in Nan Fang Hospital affiliated to the First Military Medical University in southern China over the past 11 years from 1990 to 2000. All the patients with CRC were diagnosed by histology and underwent surgery. Anatomical location of primary colorectal adenocarcinoma, race, age at diagnosis, gender and year of diagnosis were noted. Descriptive data on the type of treatment, patterns of recurrence and metastasis, survival, and the coexistence of disease were not the focus of our analysis. The Z-test and Fisher' s Exact Test were performed to detect statistically significant differences in anatomical site distribution, age and gender over time between the white and oriental groups. In this study "proximal colon" includes the cecum, ascending colon, hepatic flexure, transverse colon and splenic flexure; "distal colon" includes the descending colon, sigmoid colon and rectum[22]

RESULTS

664 Consecutive white patients in Cleveland Clinic Florida and 816 consecutive oriental patients in Nan Fang Hospital in China had documented histological diagnosis of colorectal

adenocarcinomas (Table 1). Patients with a diagnosis of adenocarcinoma only were included in this study.

Table 1 Histological diagnosis of patients with colorectal cancer

	No of patients (%)	
	White	Oriental
Adenocarcinoma	664 (96.2)	816 (93.8)
Nonadenocarcinoma	26 (3.8)	54 (6.2)
Total	690 (100.0)	870 (100.0)

Anatomical subsite distribution

Data on the anatomical distribution, race and gender in the two groups are shown in Table 2. The anatomical distribution of the lesions was markedly different between the two races. Comparision showed that 36.3 % of whites *vs* 26.0 % of oriental patients ($P<0.001$) had lesions in the proximal colon and 63.7 % of whites *vs* 74 % of orientals ($P<0.001$) had cancers located in the distal colon. The proportions of cancers located in the cecum, ascending and descending colon in white patients were higher than those in the orientals ($P<0.01$). Rectal and hepatic flexure tumors were less frequent in whites than in the orientals ($P<0.001$). There was no significant difference between cancers located in the transverse colon, splenic flexure and sigmoid colon.

Gender

Analysis by gender conforms to the overall racial differences. The proportions of cecal tumors was higher in the white men ($P<0.001$) and women ($P<0.001$) compared with their Oriental counterparts. Ascending and descending colon cancers were also significantly more common in white men ($P<0.05$) but not in women ($P>0.05$). Rectal cancers were significantly more common in oriental men ($P<0.001$) and women ($P<0.001$). Oriental patients also had significantly more hepatic flexure cancers among men ($P<0.001$) and women ($P<0.001$). There was no significant difference in the rates of transverse colon, splenic flexure or sigmoid colon cancers.

There was a significant gender difference beteen the races (Table 3). The male: female ratio was slightly higher in whites (1.49:1) as compared with oriental patients (1.22:1). The gender ratio (m:f) in whites was 1.43:1 for proximal tumors and 1.52:1 for distal tumors; in oriental patients the ratio was 1.06:1 for proximal tumors and 1.29:1 for distal tumors.

Age

The mean age at diagnosis was 69.8 years (range 20-91) in white patients *vs* 48.3 years (range 13-84) years in oriental patients; oriental patients were therefore younger by twenty-one years ($P<0.001$). Incidence of CRC generally increased with age; it peaked between 70-79 years in white patients, whereas the highest incidence in oriental patients was observed between 50-59 years ($P<0.001$) (Figure 1).

We have further analyzed the age related distribution of proximal and distal tumors in the two racial groups (Figure 2). In white patients, the incidence of proximal tumors had an early peak by the age of 29 years; the incidence then declined significantly so that the lowest rates of proximal lesions were found in the 30-59 years; the incidence of proximal tumors then gradually rose to a peak at 70-79 years. There was a significant difference in the proportions of proximal tumors

Table 2 Anatomic subsite distribution of colorectal cancer by race

	Men				Women				Total			
	White		Oriental		White		Oriental		White		Oriental	
	n	%	*n*	%	*n*	%	*n*	%	*n*	%	*n*	%
Cecum	57	8.6	14	1.7[c]	50	7.5	16	2.0[c]	107	16.1	30	3.7[c]
Ascending	45	6.8	31	3.8[a]	32	4.8	29	3.6	77	11.6	60	7.4[b]
Hepatic flexure	5	0.8	27	3.3[c]	2	0.3	26	3.2[c]	7	1.1	53	6.5[c]
Transverse	27	4.1	20	2.5	13	1.9	25	3.0	40	6.0	45	5.5
Splenic flexure	8	1.2	17	2.1	2	0.3	7	0.8	10	1.5	24	2.9
Descending	20	3.0	9	1.1[a]	11	1.7	7	0.9	31	4.7	16	2.0[b]
Sigmoid	63	9.5	82	10.0	54	8.1	64	7.9	117	17.6	146	17.9
Rectum	172	25.9	249	30.5[c]	103	15.5	193	23.7[c]	275	41.4	442	54.2[c]
Proximal	142	21.4	109	13.6[c]	99	14.9	103	12.6[a]	241	36.3	212	26.0[c]
Distal	255	38.4	340	41.7[c]	168	25.3	264	32.3[a]	423	63.7	604	74.0[c]
Total	397	59.8	449	55.0	267	44.2	367	45.0	664	100.0	816	100.0

[a]$P<0.05$, [b]$P<0.01$, [c]$P<0.001$.

Table 3 Anatomic subsite distribution of colorectal cancer by race and time

		Proximal			Distal			Total		
Time		Man	Woman	Ratio	Man	Woman	Ratio	Man	Woman	Ratio
1990-1995	White	51	43	1.19	106	72	1.47	157	115	1.37
	Yellow	55	49	1.12	163[b]	128[a]	1.27	218[b]	177	1.23
1996-2000	White	91	56	1.63	149	96	1.55	240	152	1.58
	Yellow	54[c]	54[a]	1.00	177	136	1.30	231[b]	190	1.22
Total	White	142	99	1.43	255	168	1.52	397	267	1.49
	Yellow	109[c]	103[a]	1.06	340[c]	264[a]	1.29	449	367	1.22

[a]$P<0.05$, [b]$P<0.01$, [c]$P<0.001$.

between various age groups: 0-29 years *vs* 30-59 years as well as 30-59 years vs. 60 years and older (P<0.001). In oriental patients, the curve for incidence of proximal lesions was relatively flat. Young patients between 0-29 years had the lowest rate which was significantly lower than patients above 30 years (P<0.001). The curves for proximal cancers in White and Oriental patients diverge at the extremes of age and there were significant differences between the two races at 0-29 years as well as above 70 years (P<0.01). In White patients, there was a marked increase in the rates of proximal tumors whereas the frequency of distal tumors decreased with age. This trend was not observed in Oriental patients (Figure 2).

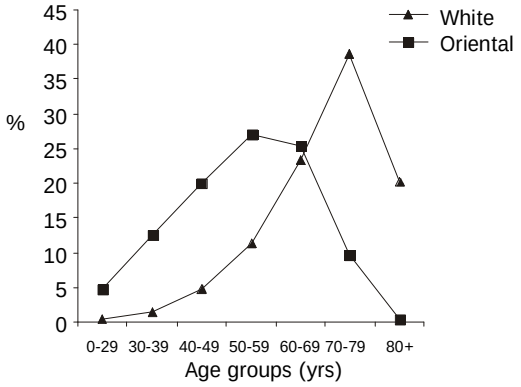

Figure 1 Age related incidence of colorectal cancers in two races.

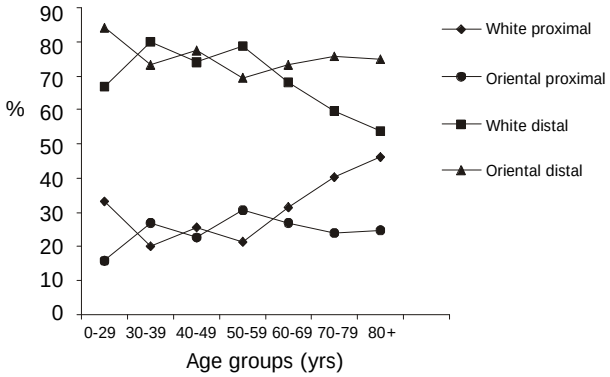

Figure 2 Age-related distribution of cancers.

Time

Generally, there was an increase in the proportion of white men with colorectal cancer from 1.37:1 during 90-95 to 1.58: 1 during 96-2000 (P<0.05) (Table 3). This increase was especially seen in proximal cancers of whites which increased from 1.19:1 in 90-95 to 1.63:1 in 96-2000 (P<0.01); the gender ratio among whites for distal cancers changed from 1.47:1 in 90-95 to 1.55:1 in 96-2000 (P>0.05). There was no significant change in the gender distribution of oriental patients (P>0.05) between these two time periods.

Table 3 shows that in whites the proportion of proximal cancers increased from 34.6 % in 1990-1995 to 37.5 % between 1996-2000 and distal cancers decreased from 65.4 % to 62.5 % of all cancers between the same periods of time. There was a trend towards a redistribution of primary colorectal cancers from distal to proximal colon, but the difference was not significant. When we further compared the relationshiPbetween anatomical distribution and gender, a marked trend was found towards the redistribution of primary colorectal cancers from distal colorectum to proximal colon in white men with time, especially in the 80-99 years group, but this change was not significant (P>0.05) (Figure 3). No significant change of anatomical distribution of tumor occurred in Oriental patients over time (P>0.05); in whom the proportion of cancers on the proximal side remained significantly higher. In addition, the proportion of proximal tumors remained significantly lower in white than in oriental patients.

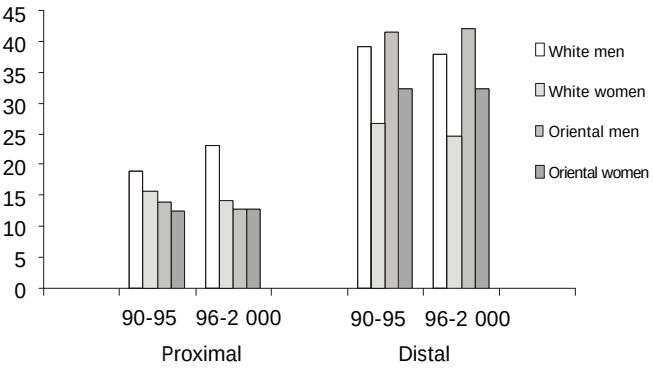

Figure 3 Gender and time based distribution of colorectal adenocarcinomas. The Y-axis shows percentage of tumors.

DISCUSSION

An important aspect of colorectal cancer is its anatomical site of origin, the majority of these cancers being diagnosed in the distal colon and rectum. Epidemiological characteristics of colorectal cancer differ by anatomical subsite, which suggests that other underlying subsite-specific differences may be present. There is evidence of a steady migration of colorectal cancer from distal to more proximal sites[17], although a decrease in proximal cancerswas reported[22]. This is the first study comparing the anatomical distribution of colorectal cancers in these two large racial groups - American and Chinese. The study demonstrates that the most frequent anatomical subsite of origin of primary colorectal adenocarcinomas is the same - the rectum and sigmoid colon, in American and Chinese patients. The proportion of cancers located in the cecum and ascending colon in whites are significantly higher than those in the oriental patients; the latter did have significantly more tumors in the rectum. The proportion of cancers located in the transverse and sigmoid colon was similar in the two groups. Overall, the frequency of lesions in the proximal colon of white patients (36.3 %) was markedly higher than that of oriental patients (26.0 %). Likewise, the proportion of tumors located in the distal colon of oriental patients (74 %) was significantly higher than that of whites (63.7 %). CRC is considerd a disease of western developed countries, which has an approximately 10 times greater incidence than developing countries of Africa[23]. In general, the developed countries have a predominance of left-sided cancers, whereas low-risk communities have a higher proportion of right-sided cancers[24]. Compared with America, China is a low risk community. The reasons for the significantly higher incidence of right-sided CRC in white patients are still not clear.

Many hypotheses have been developed based on histological differences between the left and right colon, differences in their functions, sex hormones, diet, and genetics. Proximal and distal sections of the colon also have different embryologic origins and morphology. The proximal colon is primarily involved with water absorption and solidification of fecal contents for storage. It is likely that there are differences in sensitivity and exposure to carcinogens for the proximal and distal sections of colon. There might even be differences in the etiologic agent between right-sided and left sided colorectal cancers; a study showed that different carcinogens produced cancers in different parts of the large bowel in experimental animals[20].

No specific carcinogen has been found to cause CRC in humans, but the differences in the epidemiological patterns of CRC among various populations suggest the role of an environmental or dietary etiologic agent[25]. The higher consumption of refined carbohydrates and fat and less dietary fiber may contribute to the increased incidence of colorectal cancers in the western countries[16, 26]. Increased dietary fat resulted in increased bile acids in the intestine, a possible mechanism for carcinogenesis[27]. High concentrations of fecal bile acids have been observed in people who eat a high fat diet. Bile acids in turn caused colonic bacteria to produce increased amounts of secondary bile acids and other metabolic by products, compounds that may be associated with the high risk of large bowel cancer[9, 28-30].

Dietary fiber may play an important protective role against colorectal cancer by diluting the fecal concentration of mutagens and bile acids, and by altering the colonic luminal environment[31]. Even the type of dietary fiber may be important in reducing the fecal mutagenic activity[31]. It is said that, it is imperative to point out that the evidence linking fiber and colorectal cancer is not conclusive. Dietary fiber probably protects against carcinogenesis, if it is present in the diet from an early age[32].

Another possible factor increasing the risk of rectal cancer is consumption of large amounts of alcoholic beverages, particularly beer. For example, alcohol has been shown to increase the relative risk for colon cancer by 1.71 when prospective study is made in black and white patients. In contrast, increased amount of vitamin C intake may be protective against rectal cancer[22, 24, 33-34].

We have observed a trend toward a redistribution of CRC from distal to proximal in white men, especially in the older men, a finding that is similar to others in the literature which showed a trend towards the redistribution of primary CRC from left to right with increasing time[35]. We found no significant change in the anatomical distribution of colorectal cancer in white women and oriental patients, the distribution remaining fairly stable in these two groups.

In recent years, the male**:** female ratio for CRC rose in many published reports[4, 36]. This study showed that overall rates of colorectal cancers were higher among men than women in both races, but the proportion of white men was greater than that of oriental men, especially for proximal cancers. Between the periods 1990-95 and 1996-2000, we found the male-female ratio in whites rose from 1.19:1 to 1.68:1 for proximal colon cancers and 1.47:1 to 1.55:1 for distal colon cancers; over the same periods, in Oriental patients, the male-female ratio declined from 1.12:1 to 1:1 for proximal and rose from 1.27:1 to 1.30:1 for distal cancers (Table 3). There was no significant change in the oriental race, a finding in agreement with others[9].

This gender-based disparity is largely unexplained. Recently it has been suggested that hormone replacement therapy may decrease the incidence of colorectal cancer in females. Female sex hormones are known to affect cholesterol metabolism which in turn affects bile acid production, a pathway linked to the development of colorectal cancer. Differences in bile acid metabolism between the proximal and distal colon may contribute to the gender-based disparity in colorectal cancer risk[24].

Age at diagnosis was significantly different between the races. The mean age was 69.8 years in whites and 48.3 years in oriental patients; oriental patients being diagnosed about twenty-one years earlier. The whites presented most commonly between 70-79 years, but the oriental patients had the highest rate of presentation between 50-59 years. The greater proportion of proximal tumors with increasing age in older white patients has also been noted by others[15,37-40]. This trend was not observed in oriental patients. There was a higher incidence of CRC in younger oriental patients of both sexes, the reasons for which are unknown.

The explanation for differences among racial or ethnic groups may lie in host, environmental, or behavioral factors that act alone or in combination. Heredity plays only a small role. As for colorectal adenocarcinoma, patients in China share the epidemiological characteristics of developing countries. It seems that behavioral factors, such as the dietary habits of Americans and Chinese are more likely to contribute to the difference.

We found that white Americans have a higher risk of proximal CRC and this risk increased with time. The proportion of white males with CRC also increased with time. Chinese patients were more likely to have distal CRC and developed the disease at a significantly earlier age than white patients. As colorectal cancer is one of the most common cancers in the world, it is important to conduct further study to explain subsite differences between the races and sexes. Evaluation of such differences will improve our understanding of colorectal carcinogenesis and may help formulate preventive strategies and perhaps guide research on therapy.

REFERENCES

1 **Ries LA**, Wingo PA, Miller DS, Howe HL, Weir HK, Rosenberg HM, Vernon SW, Cronin K, Edwards BK. The annual report to the nation on the status of cancer, 1973-1997, with a special section on colorectal cancer. *Cancer* 2000; **88**: 2398-2424

2 **Greenlee RT**, Murray T, Bolden S, Wingo PA. Cancer statistics, 2000. *CA Cancer J Clin* 2000; **50**: 7-33

3 **Shu Z**. Colorectal Cancer. Gastrointestinal Surgery. Ed Jiefu Wang, Beijin,People·s Medical Publishing House, 2000: 920-923

4 **Coates RJ**, Greenberg RS, Liu MT, Correa P, Harlan LC, Reynolds P, Fenoglio-Preiser CM, Haynes MA, Hankey BF, Hunter CP. Anatomic site distribution of colon cancer by race and other colon cancer risk factors. *Dis Colon Rectum* 1995; **38**: 42-50

5 **Thomas CR** Jr, Jarosz R, Evans N. Racial differences in the anatomical distribution of colon cancer. *Arch Surg* 1992; **127**: 1241-1245

6 **Chattar-Cora D**, Onime GD, Coppa GF, Valentine IS, Rivera L. Anatomic, age, and sex distribution of colorectal cancer in a new york city hispanic population. *J Natl Med Assoc* 1998; **90**: 19-24

7 **Devesa SS,** Chow WH. Variation in colorectal cancer incidence in the United States by subsite of origin. *Cancer* 1993; **71**: 3819-3826

8 **Griffin PM**, Liff JM, Greenberg RS, Clark WS. Adenocarcinomas of the colon and rectum in persons under 40 years old. A population-based study. *Gastroenterology* 1991; **100**: 1033-1040

9 **Ji BT**, Devesa SS, Chow WH, Jin F, Gao YT. Colorectal cancer incidence trends by subsite in urban Shanghai, 1972- 1994. *Cancer Epidemiol Biomarkers Prev* 1998; **7**: 661-666

10 **Yoichi I**, Nobuhiro K, Masaki M, Minagawa S, Toyomasu T, Ezaki T, Tateishi H, Sugimachi K. Tumor stage in the proximal colon under conditions of a proximal shift of colorectal cancer with age. *Hepato-Gastroenterology* 1998; **45**: 1535-1538

11 **Chattar-Cora D**, Onime GD, Valentine IS, Rivera-Cora L. The anatomic distribution of colorectal cancer in a new york city puerto rican group. *Bol Asoc Med PR* 1998; **90**: 126-129

12 **Loffeld R**, Putten A, Balk A. Changes in the localization of colorectal cancer: implications for clinical practice. *J Gastroenterol Hepatol* 1996; **11**: 47-50

13 **Mayberry RM**, Coates RJ, Hill HA, Click LA, Chen VW, Austin DF, Redmond CK, Fenoglio-Preiser CM, Hunter CP, Haynes MA. Determinants of black / white differences in colon cancer survival. *J Natl Cancer Inst* 1995; **87**: 1686-1693

14 **Nelson RL**, Dollear T, Freels S, Persky V. The relation of age, race, and gender to the subsite location of colorectal carcinoma. *Cancer* 1997; **80**: 193-197

15 **Sharma VK**, Vasudeva R, Howden CW. Changes in colorectal cancer over a 15-year period in a single united states city. *Am J Gastroenterol* 2000; **95**: 3615-3619

16 **Wan J**, Zhang ZQ, Zhu C, Wang MW, Zhao DH, Fu YH, Zhang

JP, Wang YH, Wu BY. Colonoscopic screening and follow-upfor colorectal cancer in the elderly. *World J Gastroenterol* 2002; **8**: 267-269
17 **Gonzalez EC**, Roetzheim RG, Ferrante JM, Campbell R. Predictors of proximal *vs* distal colorectal cancers. *Dis Colon Rectum* 2001; **44**: 251-258
18 **Fireman Z**, Sandler E, Kopelman Y, Segal A, Sternberg A. Ethnic difference in colorectal cancer among arab and jewish neighbor isral. *Am J Gastroenterol* 2001; **96**: 204-207
19 **Chattar-Cora D**, Onime GD, Valentine IS, Cudjoe E, Rivera L. Colorecat cancer in a multi-ethnic urban group:its anatomical and age profile. *Int Surg* 2000; **85**: 137-142
20 **Nelson RL**, Dollear T, Freels S, Persky V. The relation of age, race,and gender to the subsites location of colonrectal carcinoma. *Cancer* 1997; **80**: 193-197
21 **Reddy BS**, Simi B, Engle A. Biochemical epidemiology of colon cancer: effect of types of dietary fiber on colonic diacylglycerols in women. *Gastroenterology* 1994; **106**: 883-889
22 **Holt PR**. Dairy foods and prevention of colon cancer: human studies. *J Am Coll Nutr* 1999; **18**(Suppl 5): 379S-391S
23 **Kim D,** Wong WD, Bleday R. Rectal Carcinoma: Etiology and evaluation. Beck DE, Wexner SD, eds. In fundamentals of. *Anorectal Surgery* 1998: 278-300
24 **Rudy DR**, Zdon MJ. Update on colorectal cancer. *Am Fam Physician* 2000; **61**: 1759-1770
25 **Chattar-Cora D**, Onime GD, Valentine IS, Cudjoe E, Rivera L. Colorectal cancer in a multi-ethnic urban group:its anatomical and age profile. *Int Surg* 2000; **85**: 137-142
26 **Marchand LL**. Combined influence of genetic and dietary factors on colorectal cancer incidence in Japanese Americans. *J Natl Cancer Inst Monogr* 1999; **26**: 101-105
27 **Cooper GS**, Yuan Z, Rimm AA. Radical disparity in the incidence and case-fatality of olorectal cancer:analysis of 329 United States countries. *Cancer Epidemiol Biomarkers Pre* 1997; **6**: 283-285
28 **Baquet CR**, Commiskey P. Colorectal cancer epidemiology in minorities: a review. *J Assoc Acad Minor Phys* 1999; **10**: 51-58
29 **Flood DM**, Weiss NS, Cook LS, Emerson JC, Schwartz SM, Potter JD. Colorectal cancer incidence in Asian migrants to the United States and their descendants. *Cancer Causes Control* 2000; **11**: 403-411
30 **Chattar-Cora D,** Onime GD, Coppa GF, Valentine IS, Rivera L. Anatomic, age, and sex distribution of colorectal cancer in a New York City Hispanic population. *J Natl Med Assoc* 1998; **90**: 19-24
31 **Jass JR**, Young J, Leggett BA. Evolution of colorectal cancer: change of pace and change of direction. *J Gastroenterol Hepatol* 2002; **17**: 17-26
32 **Sengupta S**, Tjandra JJ, Gibson PR. Dietary fiber and colorectal neoplasia. *Dis Colon Rectum* 2001; **44**: 1016-1033
33 **Taylor RH**, Moffet FJ. Profile of colorectal cancer at a community hospital with a multiethnic population. *Am J Surg* 1994; **167**: 509-512
34 **Zhang X**, Zhang B, Li X, Wang X, Nakama H. Relative risk of dietary components and colorectal cancer. *Eur J Med Res* 2000; **5**: 451-454
35 **Miller A,** Gorska M, Bassett M. Proximal shift of colorectal cancer in the australian capital territory over 20 years. *Aust N Z J Med* 2000; **30**: 221-225
36 **Ikeda Y**, Akagi K, Kinoshita J, Abe T, Miyazaki M, Mori M, Sugimachi K. Different distribution of Dukes' stage between proximal and distal colorectal cancer. *Hepatogastroenterology* 2002; **49**: 1535-1537
37 **Rodriguez-Bigas MA**, Mahoney MC, Weber TK, Petrelli NJ. Colorectal cancer in patients aged 30 years or younger. *Surg Oncol* 1996; **5**: 189-194
38 **Paraf F**, Jothy S. Colorectal cancer before the age of 40:a case-control study. *Dis Colon Rectem* 2000; **43**: 1222-1226
39 **Sahraoui S**, Acharki A, Tawfiq N, Jouhadi H, Bouras N, Benider A, Kahlain A. Colorectal cancer in patients younger than 40years of age. *Cancer Radiother* 2000; **4**: 428-432
40 **Parramore JB**, Wei JP, Yeh KA. Colorectal cancer in patients under forty: presention and outcome. *Am Surg* 1998; **64**: 563-567

Edited by Ma JY

P.O.Box 2345, Beijing 100023, China
Fax: +86-10-85381893
E-mail: wjg@wjgnet.com www.wjgnet.com

World J Gastroenterol 2003;9(4):726-730
World Journal of Gastroenterology
 ISSN 1007-9327

• COLORECTAL CANCER •

Construction, expression and tumor targeting of a single-chain Fv against human colorectal carcinoma

Jin Fang, Hong-Bin Jin, Jin-Dan Song

Jin Fang, Hong-Bin Jin, Jin-Dan Song, Key Lab of Cell Biology, Ministry of Public Health of China, China Medical University, Shenyang 110001, Liaoning Province, China
Supported by the Natural Science Foundation of China, No.85-722-18-02
Correspondence to: Prof. Jin-Dan Song, Key Lab of Cell Biology, Ministry of Public Health of China, China Medical University, 92 Beier Road, Heping District, Shenyang 110001, Liaoning Province, China. jdsong@mail.cmu.edu.cn
Telephone: +86-24-23256666-5349
Received: 2002-11-26 **Accepted:** 2003-01-02

Abstract

AIM: A single-chain antibody fragment, ND-1scFv, against human colorectal carcinoma was constructed and expressed in *E.coli*, and its biodistribution and pharmacokinetic properties were studied in mice bearing tumor.

METHODS: V_H and V_L genes were amplified from hybridoma cell IC-2, secreting monoclonal antibody ND-1, by RT-PCR, and connected by linker $(Gly_4Ser)_3$ to form scFv gene, which was cloned into expression vector pET 28a(+) and finally expressed in *E.coli*. The expressed product ND-1scFv was purified by metal affinity chromatography using Ni-NTA, its purity and biological activity were determined using SDS-PAGE and ELISA. ND-1scFv was labeled with ^{99m}Tc, and then injected into mice bearing colorectal carcinoma xenograft for phamacokinetic study *in vivo*.

RESULTS: SDS-PAGE analysis showed that the relative molecular weight of recombinant protein was 30kDa with purity of 94 %. ELIAS assay revealed that ND-1scFv retained the immunoactivity of parent mAb, being capable of binding specifically to human colorectal carcinoma cell line expressing associated antigen. Radiolabeled ND-1scFv exhibited rapid tumor targeting, with specific distribution in mice bearing colorectal carcinoma xenograft observed as early as 1 h following injection. *In vivo* pharmacokinetic studies also demonstrated that ND-1scFv had very rapid plasma clearance ($T_{1/2}\alpha$ of 5.7 min, $T_{1/2}\beta$ of 2.6 h).

CONCLUSION: ND-1scFv shows significant immunoactivity, and better pharmacokinetic and biodistribution characteristics compared with intact mAbs, demonstrating the possibility as a carrier for tumor-imaging.

Fang J, Jin HB, Song JD. Construction, expression and tumor targeting of a single-chain Fv against human colorectal carcinoma. *World J Gastroenterol* 2003; 9(4): 726-730
http://www.wjgnet.com/1007-9327/9/726.htm

INTRODUCTION

Colorectal carcinoma is one of the common malignant tumors with relatively high incidence, occupying the fourth rate of mortality in China. Therefore, efficient diagnosis and therapeutic approaches are important for colorectal carcinoma research. Although in recent years some progress has been made in respect to application of monoclonal antibodies for the therapy and diagnosis of colorectal carcinoma, most mAbs are of murine origin, so that repeated administration can induce human anti- mouse antibodies (HAMA), moreover, intact mAbs are generally too large (Mt 150 000) to penetrate tumor masses, which can severely limit the efficacy of antibody in clinical utilization[1]. To overcome such deficiencies, gene engineering antibody, including human origin antibodies, single chain Fv (scFv), human-murine chimed antibodies are developed to improve murine origin mAbs[2-9]. ScFv, which is comprised of immunoglobulin heavy- and light-chain variable regions that are connected by a short peptide linker, is the gene engineered antibody employed most widely at present. The main advantages of scFv over intact mAbs and Fab fragment are their small size (M_r 30 000, amounting to one sixth of intact mAbs), making them penetrate a solid tumor mass rapidly and evenly. In addition, the lack of Fc domains makes them less immunogenic responsive and less capable of binding to Fc receptors distributed on normal cells. These characteristics make scFv potentially useful in tumor diagnosis and therapy as a carrier[10,11].

ND-1 is a murine monoclonal antibody against tumor-associated antigen LEA , mainly expressed in human colorectal carcinoma, developed by Jindan Song in 1986, which was obtained by immunizing Balb/c mouse with CCL-187 human colorectal carcinoma cell line. The histochemical determination of one thousand pathologic samples showed that ND-1 binded specifically to well differentiated and moderately differentiated colorectal carcinoma tissues and its specificity is superior to mAbs against CEA. ^{131}I labeled ND-1 also exhibited excellent imaging of tumor tissue in mice bearing colorectal carcinoma xenograft. We constructed a scFv by gene engineering technology from the V_L and V_H of ND-1, a monoclonal antibody against human colorectal carcinoma, and determined the biological properties of ND-1 scFv *in vivo* and *in vitro*.

MATERIALS AND METHODS

Materials

IC-2 is murine hybridoma cell that secrets monoclonal antibody ND-1against human colorectal carcinoma. Both IC-2 and HeLa human cervical carcinoma cell line were from our group. pET28a(+) expression vector and *E. coli* BL21 were kindly provided by Dr. YH. Chen. CCL-187 human colorectal carcinoma cell line was kindly provided by Tumor Research Institution of Medical College of Harvard University. pMD18-T vector, *E.coli* JM109 component cell, DNA polymerase, restriction enzyme, and DNA recovery kit were purchased from TarkaRa Biotechnology (Dalian, China). mRNA purification kit and T4 DNA ligase were bought from Pharmacia Biotech. Anti-His6 tag antibody was from Invitrogen. Ni-NTA resin was provided by Qaigen company. MDP and ^{99m}Tc were kindly provided by Department of Nuclear Medicine at China Medical University. Heavy chain primer 1 and 2, light chain primer mix, linker primer mix, and RS primer mix was purchased from Pharmacia Biotech.

Genetic construction of ND-1scFv

ND-1scFv gene was constructed as previously described. Briefly, mRNA was extracted from 5×10^6 hybridoma cells IC-2 and cDNA was synthesized by reverse transcription using random primer. V_H and V_L gene were separately amplified from the cDNA by PCR using heavy chain primer and light primer mix. The V_H and V_L gene fragments were recovered and mixed in equimolar ratios for two PCR reactions, the first one using linker primer mix for 7 cycles, followed by the second one using RS primer mix for 30 cycles. As a result, V_H and V_L gene fragments were connected to form scFv gene by extension overlap splicing PCR, and then, obtained ND-1 scFv gene was cloned into pMD18-T, and transformed into *E. coli* JM109, positive clones were identified by colony PCR and DNA sequencing.

Oligonucleotide primers S1 and S2 were designed to add *Eco*RI site at the 5' end of ND-1scFv, and *Hind* III site, *Sal*Isite at the 3' end. S1: 5' ACTGAATTCATGGCCCAGGT GCAGCTGCAGC 3' , S2: 5' CGCAAGCTTCTAGTCGAC TTTCCAGCTTGGTC 3' . pMD18-T-ND-1scFv was used as template for a PCR by primer S1 and S2, and the product was cloned into the vector pET28a(+) after digestion with *Eco*RI and *Hind*III, and then transformed into competent *E.coli* BL21cells for protein expression.

DNA sequencing

ND-1scFv genes cloned into pMD18T and pET28a(+) were sequenced by the dideoxy chain termination method with M13 primer, T7 promoter primer and T7 terminator primer.

Expression and purification of ND-1scFv

E.coli BL21 cells containing pET28a(+)-ND-1scFv plasmid were grown in 100 ml LB broth with 50 μg/ml kanamycin at 37 ℃, when $O.D_{600}$ of the culture attained about 0.6, IPTG was added in a final concentration of 1 mmol, and cells were shaken at 37 ℃, after 3.5 h, the culture was centrifuged at 5 000 rpm for 10 min, the cell pellet was treated with lyses solution. After sonication and centrifugation, inclusion body containing scFv protein was solubilized and denatured in the presence of 6 mol/L Guanidine hydrochloride. Affinity chromatography on Ni-NTA resin was performed to purify scFv, the column was eluted with 8 mol /L urea at pH8.0, pH6.5 and pH4.2, and the component of pH4.2, containing scFv, was collected, following renaturing by dialysis. Purity and concentration of protein were determined with Bradford assay.

ELISA assay for activity of ND-1scFv

CCL-187 cells and HeLa cells (5×10^4) were grown in 96- well microtiter plates at 37 ℃ for 24 h, then fixed with 2.5 % glutaradehyde and blocked with 1 % BSA, followed by incubation with ND-1IgG or ND-1scFv at 37 ℃ for 2 h; after washing 3 times with PBS, anti-His6 antibody was added into wells with ND-1scFv and incubated as above, the plate was washed and HRP-labeled goat anti-mouse IgG was added into both ND-IgG and ND-1scFv wells, incubating at 37 ℃ for 2 h, substrate TMB was added, incubated in darkness for 30 min, the reaction was terminated with1N H_2SO_4; PBS was used as a negative control.

Tumor model

Human colorectal carcinoma cells (1×10^6) were injected s.c. into the back of athymic mice (nu/nu)(4-6 weeks old). When a tumor developed at 0.5-1.5 cm in diameter, biodistribution and pharmacokinetics were studied.

Biodistribution and pharmacokinetics studies

ND-1scFv and ND-1IgG were labeled with ^{99m}Tc using MDP. Excess β-mercaptoethanol was added to the solution containing ND-1scFv and ND-1IgG, reduced product (1 mg) was mixed with 40 μl MDP (2.5 mg/ml) and 370MBq ^{99m}Tc. Biodistribution study was performed using tumor-bearing mice injected i.p. with 0.2 ml ^{99m}Tc-ND-1scFv, the mice were killed at different periods. Blood, tumor and all the main organs were collected and weighed. The radioactivity was counted in a gamma scintillation counter. The T/NT value for each organ was calculated.

Pharmacokinetic study was performed by the tumor- bearing mice injected via the tail vein with 0.1 ml ^{99m}Tc-ND-1scFv and ^{99m}Tc-ND-1 IgG. Blood samples were obtained via tail bleeds at 0, 5, 10, 15, 30, 60, 120, 180 min and 24 h after injection, the radioactivity was counted in a gamma scintillation counter, and pharmacokinetic parameters were calculated.

RESULTS

Clone of ND-1scFv gene

V_H and V_L gene were amplified from hybridoma cell IC-2 that secreted monoclonal antibody against human colorectal carcinoma, and then were connected by a linker $(Gly_3Ser)_4$ using extension overlap splicing PCR to construct scFv gene, which had *Eco*RI site at 5' end and *Hind*III site at 3' end. scFv gene was cloned into the vector pET28a(+) and expressed in *E.coli* BL21. Restriction enzyme digestion analysis showed scFv gene had been accurately inserted into vector pET28a (+). Sequence analysis revealed that scFv gene consisted of 732bp, encoding 243 amino acids. Of which, 354bp for heavy chain gene, was located upstream of scFv gene, and 330bp for the light chain gene, was located downstream. They were connected by a 45bp linker sequence. The deduced protein sequence of ND-1scFv was showed in Figure 1.

M A Q V Q L Q Q S G P G L V A P S Q S L
S I T CT V S G F S L T T D V H W V R Q P
P R K G L E W L G L V W A N G R T N C T
S A L M S R I S I T R D T S K N Q V F L T
M N S L Q T D D T A M Y Y C A R G S Y
G A V D F W G Q G T T V T V S S G G G G
S G G G G S G G G G S D I E L T Q S P A
linker
S L A V S L G Q R A T I S Y R A S K S V S
T S G Y S Y M H W N Q Q K P G Q P P R L
L I Y L V S N L E S G V P A R F S G S G S
G T D F TL N I H P V E E E DA A T Y Y C
Q H I R E L T R S E G G P S W K

Figure 1 Amino acid sequences of ND-1scFv deduced from nucleotide sequences.

Expression and purification of ND-1scFv

Plasmid ND-1scFv-pET28a(+) was transformed into *E.coli* BL21, the protein was expressed with induction of IPTG. SDS-PAGE analysis showed that the lysates of BL21 cell expressing scFv protein exhibited a new protein band with molecular weight at 30kDa (Figure 2). Because a sequence encoding a short peptide His-tag exists at the upstream of multi-clone site (MCS) of vector pET28a(+), ND-1scFv was expressed as a recombinant fusion protein with His tag, consisting of 26kDa for scFv and 4kDa for His-tag and its upstream sequence, which was consistent with the theoretically predicted value. SDS-PAGE analysis also showed that no new protein component was found in the supernatant of cell lysate of *E.coli* BL21induced by IPTG, which indicated scFv protein was expressed in the form of inclusion body. Inclusion body protein was purified by metal affinity chromatography using Ni-NTA resin which could bind to the His-tag protein marker located on the N terminal end of scFv specifically, purity of purified scFv was 94 % purity.

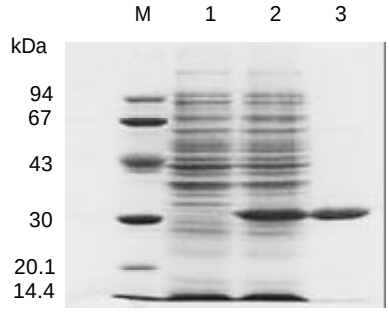

Figure 2 Expressed ND-1scFv. M: Protein marker; 1: Expression of pET28a(+)-ND-1scFv without induction; 2: Expression of pET28a(+)-ND-1scFv with induction of IPTG; 3: purified ND-1scFv protein.

Determination of immunoactivity of ND-1scFv

The immunoreactivity of purified ND-1scFv was determined by ELISA, the result revealed that scFv exhibited an immunoreactivity similar to the parent ND-1 antibody, and showed strong binding to CCL-187 cells expressing colorectal carcinoma associated antigen LEA, and weak binding to LEA-negative HeLa cells. This suggested that scFv had excellent specificity and still retained higher activity after undergoing refolding and purifying procedures.

Table 1 Immune activity of ND-1scFv determined by ELISA

Sample	OD_{450nm} ($\bar{x}\pm s$)	
	CCL-187	HeLa
ND-1IgG	1.92±0.28	0.20±0.06
ND-1scFv	0.87±0.17	0.19±0.03
PBS	0.14±0.03	0.13±0.01

In vivo distribution studies

ND-1scFv was labeled with ^{99m}Tc. ^{99m}Tc-ND-1scFv was injected into mice bearing the CCL-187 xenograft for biodistribution studies. Radioactivity in blood, tumor and normal tissue was determined at 1 and 3 h following injection, and the ratios of radioactivity between tumor tissue and normal tissue (T/NT) were evaluated. The result showed that labeled scFv displayed rapid localization in tumors, accumulation was found in tumors in high concentrations 1 hour after injection, and scFv uptake in tumor was significantly higher than that in other normal tissues (Table 2).

Table 2 Distribution of ^{99m}Tc- labeled ND-1scFv in mice-bearing tumor ($\bar{x}\pm s$)

Tissue	T/NT value	
	1 h	3 h
Blood	2.61±0.97	2.16±1.05
Liver	1.20±0.40	1.75±1.10
Spleen	2.72±0.10	1.23±0.65
Kidney	0.07±0.05	0.26±0.01
Heart	1.75±0.51	1.90±0.60
Lung	0.83±0.31	0.62±0.16

Pharmocokinetic studies

Studies were conducted to define the pharmocokinetic properties of plasma clearance of ^{99m}Tc labeled ND-1scFv in mice bearing tumor (Table 3). Compared with intact ND-1 IgG, ^{99m}Tc-ND-1scFv exhibited an extremely rapid clearance from the plasma, 80 % of the scFv was cleared out of the plasma pool at 15 min following injection, $T_{1/2}\alpha$ phase for the scFv was 5.7 min, $T_{1/2}\beta$ phase was 2.6 h, while $T_{1/2}\alpha$ and $T_{1/2}\beta$ for the ND-1 were 60 min and 18 h, respectively.

Table 3 Pharmacokinetic parameter of ^{99m}Tc-labeled ND-1scFv in mice-bearing tumor

	ND-1IgG	ND-1scFv
Alpha half-life (min)	5.7	60
Beta half-life (h)	2.6	18

DISCUSSION

The critical issue in application of mAbs is its high specificity and good *in vivo* biological features. In this study, single chain Fv ND-1scFv against human colorectal carcinoma was constructed by fusing gene of variable region of heavy chain with gene of variable region of light chain, and the ND-1scFv protein was functionally expressed in *E.coli*. ELISA analysis showed that ND-1scFv had an immunoactivity similar to the parent ND-1 mAbs, and binded specifically to the CCL-187 human colorectal carcinoma cell that expressed associated antigen LEA. This suggests that ND-1 mAb with only a Fv segment still retained its immunoactivity of binding to corresponding antigens, which is consistent to the previous reports. In addition, ND-1scFv also exhibited excellent specific distribution and pharmacokinetic characteristic in tumor-bearing mice.

A linker sequence was required to connect V_H and V_L for the construction of scFv, the linker widely used at present was a 15-amino acid sequence consisting of repetition of four Gly and one Ser (GGGGS)[12-15]. In this study, the $(Gly_4Ser)_3$ sequence was used, and the fusion molecule was constructed in V_H-linker-V_L order, the expressed ND-1scFv protein retained favorable stability during the renaturing and dialyzing, and retained biological activity similar to the parent antibody. In addition, a *Sal*I site was provided at scFv 3' end except for adding a *Hind*III site for ligasing the vector. In another experiment, we have already constructed a fusion protein of ND-1scFv and yeast cytosine deaminase using the same restriction site.

E.coli gene expression system is known as the earliest developed and most widely applied system for gene engineering. Although expressed proteins are usually lack of the effective modification such as glycosylation, there are some evidences suggesting that a variety of antibody fragments expressed in *E.coli* were able to fold and assemble correctly into bioactive products without the processing[16-20], which was also confirmed in own studies. pET vector which belongs to the T7 expression system propagating in *E.coli* was used to express of ND-1scFv. This vector contains T7 promoter, which can achieve high level controlled gene transcription in the presence of T7 RNA polymerase[19, 21-24]. ND-1scFv protein was intensively expressed to 17 % of the total bacterial protein. In addition, a 6×His tag sequence exists at the upstream of clone site in the pET vector, which was expressed in the form of fusion protein with the downstream scFv. Since it did not influence the bioactivity of expressed products, no enzyme hydrolysis process was required to remove it from the final products. This simplified the whole expression procedure. It was even more worth noticing that this sequence could be used as a protein marker for the determination and purification of expressed proteins[25-27]. ND-1scFv protein was purified by metal affinity chromatography using Ni-NTA resin which can bind to His tag specifically located on -NH_3 of scFv. SDS-PAGE analysis showed that the purity of ND-1scFv was as

high as 94 %, and the concentration was 1.5 mg/ml, demonstrating its potential usefulness in clinical application.

After being reconstructed into small molecules, the molecular weight of mAbs usually reduced to as 1/3 or 1/6 of intact mAbs, which significantly increased their penetrability to tumor tissue. Related experimental observation revealed that intact mAbs mainly concentrated nearby the blood vessel, while scFv seemed to be distributed uniformly within the tumor tissue and performing targeting function with high efficiency[28,29]. Furthermore, scFv exhibited two- phase pharmacokinetic characteristic *in vivo*, its $T_{1/2}\alpha$ (equilibrium phase) is much shorter than that of intact mAbs, implying that the *in vivo* equilibrated distribution of scFv may be reached rapidly, and its penetration into the interior of solid tumor could be achieved in a short time. In our experiment, ^{99m}Tc labeled ND-1scFv accumulated in tumor tissue in high concentration rapidly only 1 h after being injected into mice bearing xenograft. The radioactivity was significantly higher than that in most of normal tissues, while intact ND-1 required 20-24 h to obtain similar accumulation. Plasma pharmacokinetic studies in mice bearing tumor also showed a rapid plasma clearance of ND-1scFv superior to intact ND-1. Strong penetrability, rapid localization and elimination are the main biological behavior of scFv *in vivo*, making it an ideal localizing diagnostic agent for clinical applications. These were further validated by the immunoimaging experiments in mice bearing tumor using a various of scFvs against different tumor antigen[30-32]. Hitherto, the superiority of ND-1 developed by our group over the commercial product, mAb *vs* CEA, both in specificity and affinity, has been demonstrated in a number *in vivo* and *in vitro* experiments. Thus ND-1scFv, constructed from V_H and V_L of ND-1, may provide a new approach for clinical diagnosis and treatment of human colorectal carcinoma.

In this study, we observed that labeled scFv simultaneously accumulated intensively in kidney and in tumors of mice bearing xenograft, which also has been reported by other researchers[30]. On one hand, relative small size of scFv promotes its rapid uptake by kidney, so that the accumulation in kidney occurs shortly after injection, on the other hand, the half life of ^{99m}Tc is shorter, which, although beneficial for *in vivo* fast imaging, also increases the uptake of labeled scFv by kidney[28]. Recently, Goel *et al*[33,34] constructed divalent $[sc(Fv)_2]$ and tetravalent $\{[sc(Fv)_2]_2\}$ by covalent interaction, which increased the valence of scFvs and improved their affinity. Compared to the monovalent scFv, the divalent scFvs showed approximately 20-fold higher affinities. Furthermore, the molecular weight of multivalent scFvs was larger than scFv, but still smaller than intact IgG, so the in vivo pharmacokinetic behavior would be more promising[35-40]. Some researchers suggested that this uptake also may be related to the IP of the scFv, thus, there exists the possibility of directly modifying the isoelectric point of the scFv by introducing mutation in framework regions. A lower IP may reduce non-specific uptake into tissues such as the kidney[31]. The ND-1scFv constructed in this study retained the immunoactivity of parent mAbs and the clinical application are demonstrated preliminarily in radiolabling experiment with mice bearing tumor. With further development, it may become a promising targeting carrier for clinical diagnosis.

REFERENCES

1 **Borsi L**, Balza E, Bestagno M, Castellani P, Carnemolla B, Biro A, Leprini A, Sepulveda J, Burrone O, Neri D, Zardi L. Selective targeting of tumoral vasculature: Comparison of different formats of an antibody (L19) to the ED-B domain of fibronectin. *Int J Cancer* 2002; **102**: 75-85

2 **He FT**, Nie YZ, Chen BJ, Qiao TD, Fan DM, Li RF, Kang YS, Zhang Y. Expression and identification of recombinant soluble single-chain variable fragment of monoclonal antibody MC3. *World J Gastroenterol* 2002; **8**: 258-262

3 **Yu ZC**, Ding J, Nie YZ, Fan DM, Zhang XY. Preparation of single chain variable fragment of MG(7) mAb by phage display technology. *World J Gastroenterol* 2001; **7**: 510-514

4 **Kim SH**, Chun JH, Park SY. Characterization of monoclonal antibodies against carcinoembryonic antigen (CEA)and expression in *E. coli*. *Hybridoma* 2001; **20**: 265-272

5 **Pavlinkova G,** Colcher D, Booth BJ, Goel A, Batra SK. Pharmacokinetics and biodistribution of a light-chain-shuffled CC49 single-chain Fv antibody construct. *Cancer Immunol Immunother* 2000; **49**: 267-275

6 **Arakawa F**, Yamamoto T, Kanda H, Watanabe T, Kuroki M. cDNA sequence analysis of monoclonal antibody FU-MK-1 specific for a transmembrane carcinoma-associated antigen, and construction of a mouse / human chimeric antibody. *Hybridoma* 1999; **18**: 131-138

7 **De Kleijn EM**, Punt CJ. Biological therapy of colorectal cancer. *Eur J Cancer* 2002; **38**: 1016-1022

8 **Allison DE**, Gourlay SG, Koren E, Miller RM, Fox JA. Pharmacokinetics of rhuMAb CD18, a recombinant humanised monoclonal antibody fragment to CD18, in normal healthy human volunteers. *Bio Drugs* 2002; **16**: 63-70

9 **Al-Yasi AR**, Carroll MJ, Ellison D, Granowska M, Mather SJ, Wells CA, Carpenter R, Britton KE. Axillary node status in breast cancer patients prior to surgery by imaging with Tc-99m humanised anti-PEM monoclonal antibody, hHMFG1. *Br J Cancer* 2002; **86**: 870-878

10 **Pavlinkova G**, Beresford GW, Booth BJ, Batra SK, Colcher D. Pharmacokinetics and biodistribution of engineered single-chain antibody constructs of MAb CC49 in colon carcinoma xenografts. *J Nucl Med* 1999; **40**: 1536-1546

11 **Kim DJ**, Chung JH, Ryu YS, Rhim JH, Kim CW, Suh Y, Chung HK. Production and characterisation of a recombinant scFv reactive with human gastrointestinal carcinomas. *Br J Cancer* 2002; **87**: 405-413

12 **Kobayashi N**, Shibahara K, Ikegashira K, Shibusawa K, Goto J. Single-chain Fv fragments derived from an anti-11-deoxycortisol antibody.Affinity, specificity, and idiotype analysis. *Steroids* 2002; **67**: 733-742

13 **Ren X,** Gao H, Su K, Chen W, Yang A, Yu Z. Construction and nucleotide sequence assay of human anti-HBs variable region single-chain antibody gene. *Shengwu Yixue Gongchengxue Zazhi* 2000; **17**: 484-486

14 **Nakayashiki N**, Yoshikawa K, Nakamura K, Hanai N, Okamoto K, Okamoto S, Mizuno M, Wakabayashi T, Saga S, Yoshida J, Takahashi T. Production of a single-chain variable fragment antibody recognizing type III mutant epidermal growth factor receptor. *Jpn J Cancer Res* 2000; **91**: 1035-1043

15 **Hashimoto Y**, Ikenaga T, Tanigawa K, Ueda T, Ezak I, Imoto T. Expression and characterization of human rheumatoid factor single-chain Fv. *Biol Pharm Bull* 2000; **23**: 941-945

16 **Luo YM,** Mu Y, Wei JY, Yan GL, Luo GM. Studies on the optimal expression condition, purification and its characterization of ScFv-2F3. *Shengwu Gongcheng Xuebao* 2002; **18**: 74-78

17 **Norton EJ,** Diekman AB, Westbrook VA, Flickinger CJ, Herr JC. RASA, a recombinant single-chain variable fragment (scFv) antibody directed against the human sperm surface: implications for novel contraceptives. *Hum Reprod* 2001; **16**: 1854-1860

18 **Zeng JZ**, Zhou ZY, Wu YQ, Liu ZP, Wang WX, Huang HL, Cai ZN, Yu JL. Expression of single-chain Fv antibody for anti-beet necrotic yellow vein virus in Escherichia coli. *Yichuan Xuebao* 2000; **27**: 1006-1011

19 **He HJ**, Yang WD, Chang YN, Shi HJ, Yang GZ, Wu XF, Yuan QS. Fusion and expression of the gene encoding human Mn-SOD to anti-CEA single-chain antibody in Escherichia coli. *Shengwu Gongcheng Xuebao* 2000; **16**: 566-569

20 **Fernandez LA**, Sola I, Enjuanes L, de Lorenzo V. Specific secretion of active single-chain Fv antibodies into the supernatants of Escherichia coli cultures by use of the hemolysin system. *Appl Environ Microbiol* 2000; **66**: 5024-5029

21 **Lee MH**, Park TI, Park YB, Kwak JW. Bacterial expression and *in vitro* refolding of a single-chain fv antibody specific for human plasma apolipoprotein B-100.*Protein Expr Purif* 2002; **25**: 166-173

22 **Song LX**, Yu WY. Construction and expression of anticolonic cancer scFv fragment. *Shengwu Gongcheng Xuebao* 2000; **16**: 82-85

23 **Cho WK**, Sohn U, Kwak JW. Production and *in vitro* refolding of a single-chain antibody specific for human plasma apolipoprotein A-I. *J Biotechnol* 2000; **77**: 169-178

24 **Guo L**, Yan X, Qian S, Meng G. Selecting and expressing protective single-chain Fv fragment to stabilize L-asparaginase against inactivation by trypsin. *Biotechnol Appl Biochem* 2000; **31**: 21-27

25 **Sandee D**, Tungpradabkul S, Tsukio M, Imanaka T, Takagi M. Construction and high cytoplasmic expression of a tumoricidal single-chain antibody against hepatocellular carcinoma. *BMC Biotechnol* 2002; **2**: 16

26 **Goel A**, Beresford GW, Colcher D, Pavlinkova G, Booth BJ, Baranowska-Kortylewicz J, Batra SK. Divalent forms of CC49 single-chain antibody constructs in Pichia pastoris:expression, purification, and characterization. *J Biochem (Tokyo)* 2000; **127**: 829-836

27 **Hashimoto Y**, Tanigawa K, Nakashima M, Sonoda K, Ueda T, Watanabe T, Imoto T. Construction of the single-chain Fv from 196-14 antibody toward ovarian cancer-associated antigen CA125. *Biol Pharm Bull* 1999; **22**: 1068-1072

28 **Kang N**, Hamilton S, Odili J, Wilson G, Kupsch J. *In vivo* targeting of malignant melanoma by 125Iodine- and 99mTechnetium-labeled single-chain Fv fragments against high molecular weight melanoma-associated antigen. *Clin Cancer Res* 2000; **6**: 4921-4931

29 **Kang NV**, Hamilton S, Sanders R, Wilson GD, Kupsch JM. Efficient *in vivo* targeting of malignant melanoma by single-chain Fv antibody fragments. *Melanoma Res* 1999; **9**: 545-556

30 **Reilly RM**, Maiti PK, Kiarash R, Prashar AK, Fast DG, Entwistle J, Dan T, Narang SA, Foote S, Kaplan HA. Rapid imaging of human melanoma xenografts using an scFv fragment of the human monoclonal antibody H11 labelled with 111In. *Nucl Med Commun* 2001; **22**: 587-595

31 **Turatti F**, Mezzanzanica D, Nardini E, Luison E, Maffioli L, Bambardieri E, de Lalla C, Canevari S, Figini M. Production and validation of the pharmacokinetics of a single-chain Fv fragment of the MGR6 antibody for targeting of tumors expressing HER-2. *Cancer Immunol Immunother* 2001; **49**: 679-686

32 **Mayer A**, Tsiompanou E, O'Malley D, Boxer GM, Bhatia J, Flynn AA, Chester KA, Davidson BR, Lewis AA, Winslet MC, Dhillon AP, Hilson AJ, Begent RH. Radioimmunoguided surgery in colorectal cancer using a genetically engineered anti-CEA single-chain Fv antibody. *Clin Cancer Res* 2000; **6**: 1711-1719

33 **Goel A**, Augustine S, Baranowska-Kortylewicz J, Colcher D, Booth BJ, Pavlinkova G, Tempero M, Batra SK. Single-Dose versus fractionated radioimmunotherapy of human colon carcinoma xenografts using 131I-labeled multivalent CC49 single-chain fvs. *Clin Cancer Res* 2001; **7**: 175-184

34 **Goel A**, Colcher D, Baranowska-Kortylewicz J, Augustine S, Booth BJ, Pavlinkova G, Batra SK. Genetically engineered tetravalent single-chain Fv of the pancarcinoma monoclonal antibody CC49: improved biodistribution and potential for therapeutic application. *Cancer Res* 2000; **60**: 6964-6971

35 **Power BE**, Caine JM, Burns JE, Shapira DR, Hattarki MK, Tahtis K, Lee FT, Smyth FE, Scott AM, Kortt AA, Hudson PJ. Construction, expression and characterisation of a single-chain diabody derived from a humanised anti-Lewis Y cancer targeting antibody using a heat-inducible bacterial secretion vector. *Cancer Immunol Immunother* 2001; **50**: 241-250

36 **Wang F**, Ma QJ. Cloning and expressing of an anti-CD5 single chain antibody. *Shengwu Gongcheng Xuebao* 2001; **17**: 131-134

37 **Yazaki PJ**, Shively L, Clark C, Cheung CW, Le W, Szpikowska B, Shively JE, Raubitschek AA, Wu AM. Mammalian expression and hollow fiber bioreactor production of recombinant anti-CEA diabody and minibody for clinical applications. *J Immunol Methods* 2001; **253**: 195-208

38 **Yazaki PJ**, Wu AM, Tsai SW, Williams LE, Ikler DN, Wong JY, Shively JE, Raubitschek AA. Tumor targeting of radiometal labeled anti-CEA recombinant T84.66 diabody and t84.66 minibody: comparison to radioiodinated fragments. *Bioconjug Chem* 2001; **12**: 220-228

39 **Wu AM**, Yazaki PJ. Designer genes: recombinant antibody fragments for biological imaging. *Q J Nucl Med* 2000; **44**: 268-283

40 **Power BE**, Hudson PJ. Synthesis of high avidity antibody fragments (scFv multimers) for cancer imaging. *J Immunol Methods* 2000; **242**: 193-204

Edited by Ren SY

P.O.Box 2345, Beijing 100023, China
Fax: +86-10-85381893
E-mail: wjg@wjgnet.com www.wjgnet.com

World J Gastroenterol 2003;9(4):731-735
World Journal of Gastroenterology
 ISSN 1007-9327

• VIRAL HEPATITIS •

Follow up of infection of chacma baboons with inoculum containing a and non-a genotypes of hepatitis B virus

Marina Baptista, Anna Kramvis, Saffie Jammeh, Jocelyn Naicker, Jacqueline S. Galpin, Michael C. Kew

Marina Baptista, Anna Kramvis, Saffie Jammeh, Jocelyn Naicker, Michael C. Kew, University Molecular Hepatology Research Unit, Department of Medicine, University of the Witwatersrand, Johannesburg, South Africa
Jacqueline S. Galpin, School of Statistics and Actuarial Sciences, University of the Witwatersrand, Johannesburg, South Africa
Correspondence to: Professor Michael C. Kew, Department of Medicine, Witwatersrand University Medical School, 7 York Road, Parktown, 2193, Johannesburg, South Africa. kewmc@medicine.wits.ac.za
Telephone: +27-11-4883628 **Fax:** +27-11-6434318
Received: 2002-12-05 **Accepted:** 2002-12-22

Abstract

AIM: To determine whether one genotype (A or non-A genotypes of HBV) predominated over the other during the course of HBV infection.

METHODS: Four baboons were inoculated with HBV. DNA was extracted from serum obtained at monthly intervals post-inoculation for 52 weeks and HBV DNA was amplified using primers specific for the core region containing an insert characteristic of genotype A (nt 2 354-2 359, numbering from the *EcoRI* site). The amplicons were cloned into PCR-Script™ and a minimum of 15 clones per time point were sequenced in both directions.

RESULTS: Both genotypes persisted for the entire follow-up period of 52 weeks. Genotype non-A predominated in two baboons and genotype A in one baboon. Neither genotype predominated in the fourth baboon, as shown at a 5 % level of testing.

CONCLUSION: No conclusions concerning the dominance of either genotype or the natural progression or replication rates of HBV could be drawn because the pattern of the genotypes found may have been caused by sampling fluctuations at the time of DNA extraction and cloning as a result of the very low viral loads in the baboon sera.

Baptista M, Kramvis A, Jammeh S, Naicker J, Galpin JS, Kew MC. Follow up of infection of chacma baboons with inoculum containing a and non-a genotypes of hepatitis B virus. *World J Gastroenterol* 2003; 9(4): 731-735
http://www.wjgnet.com/1007-9327/9/731.htm

INTRODUCTION

Xenografts from closely related non-human primates or pigs have been suggested as one way to alleviate the chronic shortage of donor organs for human liver transplantation. Baboons (*Papio* species) which are phylogenetically close to humans, have reasonably large livers, and are not endangered. They have already been the source of xenografts for two humans undergoing liver transplantation[1-3] (as well as for a few patients receiving kidney or heart transplants[2, 4-6]). The use of liver xenografts would, however, be precluded if they were infected by zoonotic pathogens. In addition, because chronic hepatitis C and B virus infections are now the most frequent causes of end-stage liver disease requiring transplantation in humans[7], the donor livers should be resistant to infection with these viruses. Our study has previously shown that Chacma baboons (*Papio ursinus orientalis*) are resistant to infection of hepatitis C virus[8] but are susceptible to infection of hepatitis B virus (HBV)[9].

In the latter study[9], pooled serum from three patients with acute hepatitis B (the serum of all three was HBV surface (HBsAg)- and e antigen (HBeAg)-positive and had high titers of HBV DNA) had been injected into the baboons. Direct sequencing of HBV DNA amplified at various times post-inoculation indicated that the baboons had been inoculated with a mixed population of HBV. Cloning of the HBV DNA amplified from the inoculum revealed that it fortuitously contained approximately equal proportions of A and non-A genotypes of HBV. HBV has been classified into genotypes A-H, with an intergenotypic diversity of at least 8 %[10-13]. Genotype A accounts for 80 % and genotype D for 10 % of the genotypes found in southern Africa, with the other genotypes being either absent or present in very few isolates[14]. HBV genotypes have a characteristic geographical distribution[15], which help in tracing the route of HBV infection[16], and may influence the severity and outcome of infection with this virus[17]. However, little is known about the natural progression and severity of the infection when more than one genotype is present[18].

Co-infection with two or more genotypes may be the consequence of multiple exposures to infection at an early age when immune responses are immature or in older individuals with immune disorders[19], or the result from genotype changes during seroconversion from e antigen positivity to negativity[20]. Documented cases of co-infection with more than one genotype of HBV were rare[18,19,21,22], and the natural progression of HBV infection in this circumstance has not been thoroughly evaluated. In one patient studied recently, infection with genotypes D and A (with D predominant) was serologically "silent" (HBsAg-negative but HBV DNA-positive), although with pathological consequences because the patient was cirrhotic and died of liver failure[18]. This patient may be of particular interest in view of our failure to detect HBsAg in the serum of our HBV DNA-positive inoculated baboons[9]. Therefore, the opportunity was taken in the present study to monitor the changes over time in the relative proportions of genotypes A and non-A in the inoculated baboons and to ascertain if the two genotypes differed in their rate of replication or in their ability to persist in the inoculated baboons.

MATERIALS AND METHODS

Samples

For this study, serum samples which were collected at 4-weekly intervals from 4 baboons infected by inoculated HBV[9] were analyzed which was started at week 8,. Because the initial phases of the study included the housing and inoculation of the baboons, the collection of serum samples were carried out at the Medical University of Southern Africa, this study was

undertook with the permission given by the Animal Ethics Committee of that institution. The Committee approved the procedures, and the care of the baboons according to its guidelines and those of the South African Medical Research Council. Each of the baboons had received intravenous injection of 1 ml pooled serum obtained from 3 HBV surface antigen (HBsAg) and HBV e antigen (HBeAg)-positive patients with clinically-overt acute hepatitis B. The concentration of HBV DNA in the pooled sera was 2 133 pg/ml (which was 2 982 pg/ml in another laboratory) using the Digene Hybrid Capture System (Digene Diagnosis Inc., Beltsville, MD, USA); the values in the individual isolates were 2 870 pg/ml, 6 660 pg/ml and 692 pg/ml, respectively. Using methods of amplification and cloning (see below), the HBV DNA amplfied from the pooled inoculum was shown to contain equal proportions of genotype A and non-A of HBV. All of the baboon sera were tested for HBsAg, anti-HBc, and anti-HBs using commercially available assays (Abbott Laboratories, Chicago, IL, USA). All serum samples were stored at -20 ℃.

PCR assay of HBV

HBV DNA levels were assessed with a quantitative PCR assay (Amplicor™ HBV monitor test, Roche Diagnostics). Briefly, 50 μl of serum were prepared with pre-treatment with polyethylene glycol, alkaline lysis of the pelleted viral particles, and neutralization of the lysate. After adding a fixed amount of internal standard and a PCR mix, 30 cycles of PCR amplification were performed according to the manufacturer' s instructions. Biotinylated amplicons were captured on strepavidin-coated microwells and hybridized with specific dinitrophenyl-labelled oligonucleotide probes. It was incubated with alkaline phosphatase conjugated anti-DNP antibodies and a colorimetric substrate, then a kinetic of O.D. determination of HBV DNA levels was performed. The limit of detection of this PCR assay was 400 copies of viral genome per ml, and quantitation was linear up to 4×10^7 copies per ml[23,24].

DNA extraction

DNA was extracted from serum using the QIAamp blood kit (Qiagen Inc., Hilden Germany), according to the manufacturer' s instructions and as previously described[25]. Known positive and negative sera, as well as best quality water were used as controls for the extraction procedure.

PCR of HBV DNA

HBV DNA in the core region was amplified using primers designed to amplify all the HBV genotypes (Table 1A and 1B). PCR was performed in 25 μL and 50 μL final reaction volumes for the first and second rounds, respectively. The reaction for the first round of the PCR consisted of 0.02 U/μL Dynazyme™ Taq DNA polymerase (version 2.0, Finnzymes OY, Espoo, Finland), 200 μmol/L of each of the nucleotide triphosphates, 1 μmol/L of each of the primers, 4 mmol/L $MgCl_2$ and 10 mmol/L Tris-HCl (pH 8.8 at 25 ℃), 50 mmol/L KCl, and 0.1 % Triton® X-100. The reaction mixture for the second round of the PCR was the same as for the first round except that 1.5 mmol/L $MgCl_2$ was used. A third round of PCR was used on the serum from those time points that were negative after 2 rounds of PCR. The reaction mixture was the same as for the second round of PCR except that concentrations of $MgCl_2$ of 1.0 mmol/L, 1.5 mmol/L, and 1.5 mmol/L, were used for the first, second, and third rounds of PCR, respectively. All PCR assays were performed in a programmable thermal cycler (Perkin Elmer, Norwalk, CT, USA) with the 3-step cycling profile shown in Table 1B. Sera positive for HBsAg, HBeAg, and HBV DNA detected by slot-blot hybridization were used as positive controls and best quality water instead of DNA as negative controls. To avoid cross-contamination and false-positive results, the precautions and procedures recommended by Kwok and Higuchi[26] were strictly adhered to DNA extraction, the various stages of PCR amplification, and gel electrophoresis were performed in physically separate venues.

Table 1A Oligonucleotide primers

		Primer	Position[a]	Sequence
		1687(+)	1687-1706	5' CGA CCG ACC TTG AGG CAT AC 3'
Double-	PCR1	2498(-)	2498-2477	5' AAG CCC AGT AAA GTT TCC CAC C 3'
round		2267(+)	2267-2284	5' GGA GTG TGG ATT CGC ACT 3'
PCR	PCR2	2436(-)	2436-2419	5' TGA GAT CTT CTG CGA CGC 3'
		1687(+)	1687-1706	5' CGA CCG ACC TTG AGG CAT AC 3'
Triple-	PCR1	2498(-)	2498-2477	5' AAG CCC AGT AAA GTT TCC CAC C 3'
round		1795(+)	1795-1812	5' TGG TCT GTC GAC CAG CAC 3'
PCR	PCR2	2436(-)	2436-2419	5' TGA GAT CTT CTG CGA CGC 3'
		2267(+)	2267-2284	5' GGA GTG TGG ATT CGC ACT 3'
	PCR3	2400(-)	2400-2382	5' CTG CGA GGC GAG GGA GTT 3'

Table 1B Polymerase chain reaction cycling profiles

		Amplification conditions			Size[b]
		Denaturation	Annealing	Extension	
Double-round PCR	PCR1	94°C 30 sec	62°C 40 sec	72°C 80 sec	812bp
	PCR2	94°C 30 sec	57°C 50 sec	72°C 50 sec	170bp
Triple-round PCR	PCR1	94°C 30 sec	62°C 40 sec	72°C 80 sec	812bp
	PCR2	94°C 30 sec	48°C 60 sec	72°C 50 sec	642bp
	PCR3	94°C 30 sec	50°C 60 sec	72°C 50 sec	134bp

Notes: PCR1: the first round polymerase chain reaction; PCR2: the second round polymerase chain reaction; PCR3: the triple round polymerase chain reaction. (+) sense; (-) anti-sense. [a]Denotes the nucleotide position of hepatitis B virus *adw* genome (GenBank accession #V00866) where the *EcoRI* cleavage site is position 1. [b]Size of the amplicons in base pairs.

Detection of amplified products

A 5 μl aliquot of the amplified PCR product was electrophoresed in a 2 % agarose gel. Bands of the appropriate size (Table 1A and 1B) were visualised under ultraviolet light after ethidium bromide staining.

Cloning and nucleotide sequencing

Following the double or triple round PCR, amplicons were cloned using PCR-Script (Stratagene, La Jolla, CA, USA). Plasmid DNA was extracted using the QIAprep spin miniprep kit (Qiagen Inc., Hilden, Germany) and restricted with *Pvu II* to confirm the presence of the correct insert (Table 1A and 1B). Sequencing of positive clones was performed using the T7 Sequenase Version 2.0 DNA sequencing kit (Amersham Life Science Inc., Cleveland, OH, USA). Sequences were analyzed in both forward and reverse directions with primers T3 and T7 on 8 % glycerol-tolerant acrylamide gels and autoradiographed. The number of clones of A and non-A genotypes obtained at each time point was used as a measure of the relative proportions of the two genotypes in the serum at that time.

Statistical analysis

Fisher' s Exact test and the Chi-squared tests were used for statistical analysis, where appropriate.

RESULTS

HBV DNA was detected in the serum using either double or triple round PCR in the four inoculated baboons at various time points during the 52-week follow up period. For baboons 1 and 13 HBV DNA concentration was determined at various time of post-inoculation using the Amplicor HBV Monitor™ Test (Table 2). When serum was available for further analysis and HBV DNA was successfully amplified, the amplicons were cloned and sequenced. Genotype A was distinguished from the other genotypes by the sequence 5' CGGGAC3' (nt 2 354 -nt 2 359, numbering from the Eco R1 site) that is specific to this genotype (Figure 1). Depletion of inoculum serum prevented us from amplifying the S region and carrying out restriction fragment length polymorphisms in order to assign the non-A genotype to one of genotypes B to H. Although we could not preclude the possibility that the non-A isolates were comprised of more than one genotype, the most likely genotype would be genotype D, the genotype besides A commonly found in South Africa[14].

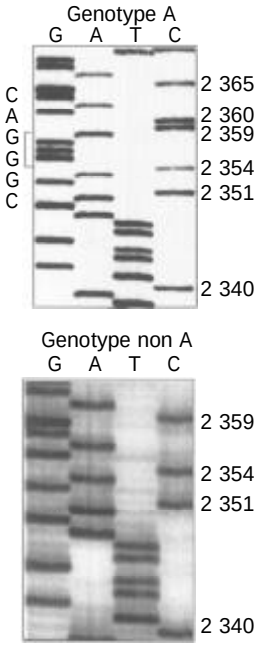

Figure 1 Sequence profiles of the core region (nucleotides 2 340-2 368 numbering from the *EcoRI* site) showing the insertion of 5'CGGGAC3' (nucleotide 2 354-2 359) found in genotype A and its absence in genotypes non-A. Tracks G, A, T and C are labelled.

Table 2 HBV DNA levels measured by the amplicor HBV monitor test

Time of post-inoculation (months)	HBV DNA Levels (genomes / ml)									
	2	3	4	5	6	7	8	9	10	10
Baboon 1	<400	<400	4 338	3 711	ns	ns	<400	ns	<400	<400
Baboon 13	<400	ns	ns	ns	ns	ns	2 6216	1 003	ns	ns

Notes: ns: no serum available.

Figure 2 showed the relative concentration of genotypes A and non-A at the various time points represented as a percentage of the total number of clones obtained and sequenced at that time point. The hypothesis of equal proportions of the genotypes over time was rejected for all four baboons (P<0.002 in each instance). For each specific time/baboon combination, the hypothesis that the proportions of genotype A and non-A were equal was rejected in all but 4 cases, namely, at 10 months for baboons 2 and 12, and at 11 months for baboons 1 and 13.

Genotype non-A predominated in two baboons (baboon 2 and 13) and genotype A in one baboon (baboon 1); neither genotype predominated in the fourth baboon (baboon 12), as shown at a 5 % level of testing. In the three baboons in which one or other genotype predominated, there was at least one time-point at which the non-dominant genotype was present in the highest concentration at a proportion significantly different from zero.

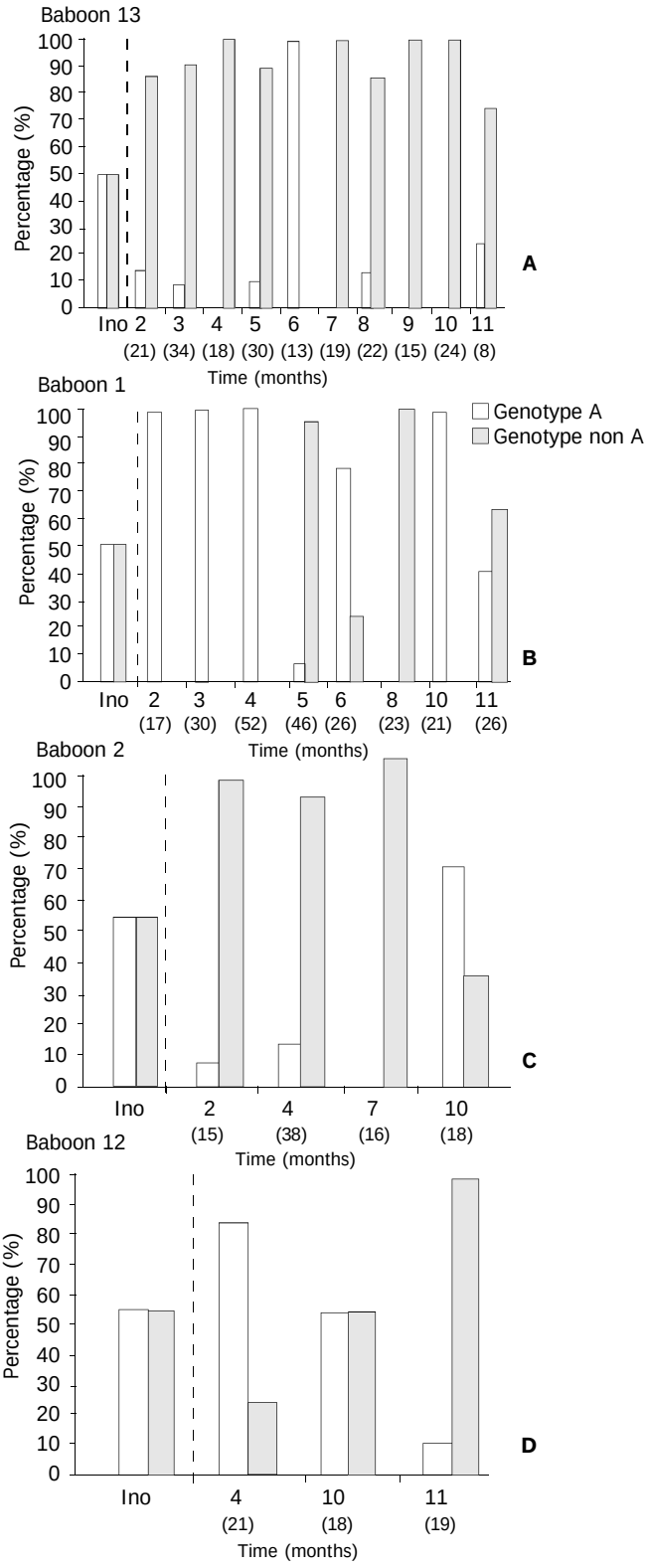

Figure 2 The change of genotype of hepatitis B virus at various time of post-infection which was represented as a percentage. The number of clones sequenced at each time point was showed in brackets. *ino: inoculum.

DISCUSSION

Neither HBsAg nor antibody to HBsAg (anti-HBs) was detected by conventional tests in the serum of the four inoculated baboons at any time during the 52 weeks they were monitored[9]. HBV DNA identical to either the A or non-A HBV genotypes inoculated was, however, detected in each baboon throughout the follow-up period, and the presence of anti-HBc and Dane particles, small spherical particles and tubular particles was demonstrated in the serum at 16 weeks[9]. The viral titers in the baboons were low (Table 2), as shown by the need to use nested PCR amplification to detect HBV DNA at all time points and three rounds of amplification at some time-points. No biochemical evidence of liver injury was evident at any stage and liver histology was normal at 52 weeks. These findings together suggested that the animals had become chronic asymptomatic carriers of the virus.

We had hoped that a clear pattern of different rates of replication of the two genotypes would be evident. However, no uniform pattern could be discerned in the relative concentration of genotypes A and non-A during the 52 weeks (Figure 2). Other explanations of a technical nature for the varying concentrations of the genotypes were needed therefore to be considered. One possibility was that the number of clones sampled at each time-point was too small to accurately assess the relative proportions of the genotypes in the serum at that time. This explanation was not supported by statistical analysis of the numbers of clones involved at each time point. A more likely explanation was that the low copy number of the genotypes resulted in sampling error at the time of HBV DNA extraction and cloning. This explanation was particularly apposite for the genotype pattern in baboon 13, in which genotype A alone was found in a single sample, whereas at all other time-points on either side of this sample, genotype non-A either predominated or was the sole genotype cloned (Figure 2A). It was also relevant that the conditions created in the study were artificial on two counts: the approximately equal concentrations of the two genotypes inoculated into the baboons resulted from the pooling of three serum samples from different patients, and we were assessing the effects of a human virus injected into a non-human primate.

Jeantet and co-workers were able to clone and sequence entire HBV genomes and found a number of mutations in the surface, precore and other regions affecting expression of the surface gene in both genotypes[18]. The A genotype was fully replication competent, although, surprisingly, this was not true of the predominant D genotype. Sequencing of the subgenomic amplicons of HBV from our infected baboons did not reveal any mutations in the core region of the HBV isolates. Full genome analysis was impossible in our study because the study was carried out retrospectively. Either the serum samples were depleted or when serum was available full genome amplification did not work, possibly because of the low viral load.

The very low concentrations of HBV in the serum of the infected baboons (Table 2) and the resulting likelihood of sampling error during viral DNA extraction and cloning prevented us from drawing firm conclusions about the natural progression over time of genotypes A and non-A replication in baboons. The study did however show that both genotypes persisted for the entire period of 52-week of follow-up.

ACKNOWLEDGEMENTS

The authors thank Professor F. Chisari, The Scripps Research Institute for his helpful comments. The H.E. Griffin Cancer Trust supported this work.

REFERENCES

1 **Lanford RE**, Michaels MG, Chavez D, Brasky K, Fung J, Starzl TE. Persistence of extrahepatic hepatitis B virus DNA in the absence of detectable hepatic replication in patients with baboon liver transplants. *J Med Virol* 1995; **46**: 207-212
2 **Starzl TE**, Machioro TL, Peter GNH. Renal heterotransplantion from baboons to man: experience with 6 cases. *Transplantation* 1964; **2**: 752-756
3 **Starzl TE**, Fung J, Tzakis A, Todo S, Demetris AJ, Marino IR, Doyle H, Zeevi A, Warty V, Michaels M, Kusne S, Rudert WA, Trucco M. Baboon-to-human liver transplantation. *Lancet* 1993; **341**: 65-71
4 **Bailey LL**, Nehlsen-Cannarella SL, Concepcion W, Jolley WB. Baboon-to-human cardiac xenotransplantation in a neonate. *JAMA* 1985; **254**: 3321-3329
5 **Barnard CN**, Wolpowitz A, Losman JG. Heterotopic cardiac transplantation with a xenograft for assistance of the left heart in cardiogenic shock after cardiopulmonary bypass. *S Afr Med J* 1977; **52**: 1035-1038
6 **Hitchcock CR**, Kiser JC, Telander RL, Seljeskog EL. Baboon renal grafts. *J Am Med Assoc* 1964; **189**: 934-937
7 **Sheiner PA**. Hepatitis C after liver transplantation. *Semin Liver Dis* 2000; **20**: 201-209
8 **Sithebe NP**, Kew MC, Mphahlele MJ, Paterson AC, Lecatsas G, Kramvis A, de Klerk W. Lack of susceptibility of Chacma baboons (Papio ursinus orientalis) to hepatitis C virus infection. *J Med Virol* 2002; **66**: 468-471
9 **Kedda MA**, Kramvis A, Kew MC, Lecatsas G, Paterson AC, Aspinall S, Stark JH, De Klerk WA, Gridelli B. Susceptibility of chacma baboons (Papio ursinus orientalis) to infection by hepatitis B virus. *Transplantation* 2000; **69**: 1429-1434
10 **Norder H**, Courouce AM, Magnius LO. Complete genomes, phylogenetic relatedness, and structural proteins of six strains of the hepatitis B virus, four of which represent two new genotypes. *Virology* 1994; **198**: 489-503
11 **Okamoto H**, Tsuda F, Sakugawa H, Sastrosoewignjo RI, Imai M, Miyakawa Y, Mayumi M. Typing hepatitis B virus by homology in nucleotide sequence: comparison of surface antigen subtypes. *J Gen Virol* 1988; **69** (Pt 10): 2575-2583
12 **Stuyver L**, De Gendt S, Van Geyt C, Zoulim F, Fried M, Schinazi RF, Rossau R. A new genotype of hepatitis B virus: complete genome and phylogenetic relatedness. *J Gen Virol* 2000; **81**: 67-74
13 **Arauz-Ruiz P**, Norder H, Robertson BH, Magnius LO. Genotype H: a new Amerindian genotype of hepatitis B virus revealed in Central America. *J Gen Virol* 2002; **83**: 2059-2073
14 **Bowyer SM**, van Staden L, Kew MC, Sim JG. A unique segment of the hepatitis B virus group A genotype identified in isolates from South Africa. *J Gen Virol* 1997; **78** (Pt 7): 1719-1729
15 **Courouce-Pauty AM**, Plancon A, Soulier JP. Distribution of HBsAg subtypes in the world. *Vox Sang* 1983; **44**: 197-211
16 **Yamishita Y**, Kurashina S, Miyakawa Y, Mayumi M. South-to-north gradient in distribution of the r determinant of hepatitis B surface antigen in Japan. *J Infect Dis* 1975; **131**: 567-569
17 **Mayerat C**, Mantegani A, Frei PC. Does hepatitis B virus (HBV) genotype influence the clinical outcome of HBV infection? *J Viral Hepat* 1999; **6**: 299-304
18 **Jeantet D**, Chemin I, Mandrand B, Zoulim F, Trepo C, Kay A. Characterization of two hepatitis B virus populations isolated from a hepatitis B surface antigen-negative patient. *Hepatology* 2002; **35**: 1215-1224
19 **Yamanaka T**, Akahane Y, Suzuki H, Okamoto H, Tsuda F, Miyakawa Y, Mayumi M. Hepatitis B surface antigen particles with all four subtypic determinants: point mutations of hepatitis B virus DNA inducing phenotypic changes or double infection with viruses of different subtypes. *Mol Immunol* 1990; **27**: 443-449
20 **Gerner PR**, Friedt M, Oettinger R, Lausch E, Wirth S. The hepatitis B virus seroconversion to anti-HBe is frequently associated with HBV genotype changes and selection of preS2-defective particles in chronically infected children. *Virology* 1998; **245**: 163-172
21 **Okamoto H**, Imai M, Tsuda F, Tanaka T, Miyakawa Y, Mayumi M. Point mutation in the S gene of hepatitis B virus for a d/y or w/r subtypic change in two blood donors carrying a surface antigen of compound subtype adyr or adwr. *J Virol* 1987; **61**: 3030-3034
22 **Paul DA**, Purcell RH, Peterson DL. Use of monoclonal antibod-

ies to determine if HBsAg of mixed subtype is one particle or two. *J Virol Methods* 1986; **13**: 43-53

23 **Gerken G**, Gomes J, Lampertico P, Colombo M, Rothaar T, Trippler M, Colucci G. Clinical evaluation and applications of the Amplicor HBV Monitor test, a quantitative HBV DNA PCR assay. *J Virol Methods* 1998; **74**: 155-165

24 **Kessler HH**, Pierer K, Dragon E, Lackner H, Santner B, Stunzner D, Stelzl E, Waitzl B, Marth E. Evaluation of a new assay for HBV DNA quantitation in patients with chronic hepatitis B. *Clin Diagn Virol* 1998; **9**: 37-43

25 **Kramvis A**, Bukofzer S, Kew MC, Song E. Nucleic acid sequence analysis of the precore region of hepatitis B virus from sera of southern African black adult carriers of the virus. *Hepatology* 1997; **25**: 235-240

26 **Kwok S**, Higuchi R. Avoiding false positives with PCR. *Nature* 1989; **339**: 237-238

Edited by Xu XQ

P.O.Box 2345, Beijing 100023, China
Fax: +86-10-85381893
E-mail: wjg@wjgnet.com www.wjgnet.com

World J Gastroenterol 2003;9(4):736-740
World Journal of Gastroenterology
 ISSN 1007-9327

• VIRAL HEPATITIS •

Effects of hepatitis B virus infection on human sperm chromosomes

Jian-Min Huang, Tian-Hua Huang, Huan-Ying Qiu, Xiao-Wu Fang, Tian-Gang Zhuang, Hong-Xi Liu, Yong-Hua Wang, Li-Zhi Deng, Jie-Wen Qiu

Jian-Min Huang, Tian-Hua Huang, Xiao-Wu Fang, Tian-Gang Zhuang, Hong-Xi Liu, Department of Cell Biology and Medical Genetics, Shantou University Medical College, Shantou 515031, Guangdong Province, China
Huan-Ying Qiu, Yong-Hua Wang, Shantou University Hospital, Shantou 515063, Guangdong Province, China
Li-Zhi Deng, Jie-Wen Qiu, Department of Internal Medicine, Second Affiliated Hospital, Shantou University Medical College, Shantou 515041, Guangdong Province, China
Jian-Min Huang, Allergy and Inflammation Institute, Shantou University Medical College, Shantou 515031, Guangdong Province, China
Supported by the Natural Science Foundation of Guangdong Province, No. 940567; and by the National Natural Science Foundation of China, No. 39970374
Correspondence to: Dr. Tian-Hua Huang, Department of Cell Biology and Medical Genetics, Shantou University Medical College, Shantou 515031, Guangdong Province, China. thhuang@stu.edu.cn
Telephone: +86-754-8900497 **Fax:** +86-754-8557562
Received: 2002-08-06 **Accepted:** 2002-08-29

Abstract

AIM: To evaluate the level of sperm chromosome aberrations in male patients with hepatitis B, and to directly detect whether there are HBV DNA integrations in sperm chromosomes of hepatitis B patients.

METHODS: Sperm chromosomes of 14 tested subjects (5 healthy controls, 9 patients with HBV infection, including 1 with acute hepatitis B, 2 with chronic active hepatitis B, 4 with chronic persistent hepatitis B, 2 chronic HBsAg carriers with no clinical symptoms) were prepared using interspecific *in vitro* fertilization between zona-free golden hamster ova and human spermatozoa, and the frequencies of aberration spermatozoa were compared between subjects of HBV infection and controls. Fluorescence *in situ* hybridization (FISH) to sperm chromosome spreads was carried out with biotin-labeled full length HBV DNA probe to detect the specific HBV DNA sequences in the sperm chromosomes.

RESULTS: The total frequency of sperm chromosome aberrations in HBV infection group (14.8 %, 33/223) was significantly higher than that in the control group (4.3 %, 5/116). Moreover, the sperm chromosomes in HBV infection patients commonly presented stickiness, clumping, failure to staining, etc, which would affect the analysis of sperm chromosomes. Specific fluorescent signal spots for HBV DNA were seen in sperm chromosomes of one patient with chronic persistent hepatitis. In 9 (9/42) sperm chromosome complements containing fluorescent signal spots, one presented 5 obvious FISH spots, others presented 2 to 4 signals. There was significant difference of fluorescence intensity among the signal spots. The distribution of signal sites among chromosomes was random.

CONCLUSION: HBV infection can bring about mutagenic effects on sperm chromosomes. Integrations of viral DNA into sperm chromosomes which are multisites and nonspecific, can further increase the instability of sperm chromosomes. This study suggested that HBV infection can create extensively hereditary effects by alteration genetic constituent and/or induction chromosome aberrations, as well as the possibility of vertical transmission of HBV via the germ line to the next generation.

Huang JM, Huang TH, Qiu HY, Fang XW, Zhuang TG, Liu HX, Wang YH, Deng LZ, Qiu JW. Effects of hepatitis B virus infection on human sperm chromosomes. *World J Gastroenterol* 2003; 9(4): 736-740
http://www.wjgnet.com/1007-9327/9/736.htm

INTRODUCTION

Hepatitis B virus (HBV) infection is a serious public health problem worldwide[1-3], especially in Far-East Asia such as China. During HBV infection, HBV can be found in saliva, vaginal secretions, semen and other tissues beyond the liver and blood[4-6]. It is well established that HBV DNA could integrate not only into the host hepatocytes but also into sperm cells[7-19]. Extensive studies have confirmed that HBV DNA integrated into the hepatocytes will increase chromosome instability and cause genetic recombination and hepatocarcinogenesis[7-17]. In this study, in order to clarify the inheritable influence of HBV on sperm chromosomes, we used interspecific *in vitro* fertilization with zona-free hamster eggs to prepare sperm chromosomes and compared the aberration frequencies of sperm chromosomes between patients with hepatitis B and the controls. In addition, FISH technique with HBV DNA as a probe was used to detect HBV sequences in sperm chromosomes and to analyze features of sperm chromosomes integrated HBV DNA. The genetic significance of the results from this investigation was discussed.

MATERIALS AND METHODS

Subjects

Nine men with HBV infection, including 1 subject with acute hepatitis, 6 with chronic hepatitis (2 with chronic active hepatitis, 4 with chronic persistent hepatitis), 2 chronic HBsAg carriers with no clinical symptoms, and 5 healthy men as controls were studied. The age range was from 22 to 38 years old (mean 27), without the history of exposure of radiation and use of mutagenic agent. The status of the markers of HBV infection of the subjects tested was listed in Table 1.

Preparation of sperm chromosomes

The technique of interspecific *in vitro* fertilization of zona-free golden hamster was used to prepare the sperm chromosomes. Those procedures included the treatment of semen samples from the tested subjects, superovulation of golden hamsters and egg processing, insemination and postinsemination culture and preparation of chromosome slides[20,21].

Analysis of aberrations of sperm chromosome

Sperm chromosome slides were stained with 10-fold diluted

Giemsa in 50 ml Sorensen' s buffer, pH6.8, for 20-30 min and observed under the light microscope. After the observation, the slides were stored at -70 ℃ for FISH test. Frequency distributions of spermatozoa with chromosome aberrations were evaluated by using Chi-square test.

Fluorescence in situ hybridization of sperm chromosomes

Labeling HBV DNA probe with biotin Recombinant plasmid, pHBV-1 containing 3.2kb HBV genomic DNA, was taken to amplify according to the routine method[22]. The 3.2kb HBV DNA probe with its vector (altogether 6.2kb) was labeled with biotin-14-dATP by nick translation (GIBCOBRL No. 18247-015). Unincorporated nucleotides were separated by cold ethanol precipitation method.

***In situ* hybridization** Sperm chromosome slides were orderly treated with RNase (Sigma) at 100 mg/L for 60 min at 37 ℃, then at 50 mg/L pepsin (Sigma) in 0.01N HCl for 10 min at 37 ℃, at last at 1 % polyformaldehyde in PBS for 10 min at room temperature. Chromosomes were denatured at 75 ℃ for 4 min in 70 % formamide in 2×SSC. *In situ* hybridization with denatured DNA probe mentioned above was performed with a modification of the procedure described by our previous paper[23]. Briefly, 10 μl hybridization buffer (50 % deionized formamide, 10 % dextran sulfate, and 2×SSC) containing 40 ng/μl biotin-labeled HBV DNA probe, 500 ng/μl sheared salmon sperm DNA was placed on each slide. A coverslip (18×18 mm) was then applied and sealed with rubber cement, followed by overnight incubation in a humidified chamber at 37 ℃.

Detection of hybridization signals Post-hybridization washing was carried out, referring to Korenberg' s methods for mapping small DNA probes[24], once in 40 % formamide, 2×SSC for 10 min at 40 ℃, then twice, each for 5 min, in 2×SSC at room temperature. Hybridization signals were detected with FITC-conjugated avidin and amplified with goat biotinylated anti-avidin antibody followed by another layer of FITC-avdin (avidin and anti-avidin, Vector Laboratories). To increase the intensity of the hybridization signal, a second round of amplification was applied by sandwich method as above. In order to reduce the nonspecific binding, the slides were preincubated in 4×SSC with 15 % nonfat dry milk for 10 min at 37 ℃ prior to each step of immunological reactions. The chromosomes were counterstained with propidium iodide (PI, Sigma) and 4, 6-diamidino-2-phenylindole (DAPI, Sigma), 2 μg/ml each in PBS/glycerol (1:9, v/v) containing 0.2 % (1,4)-diazobicyclo-(2, 2, 2) octane (DABCO, Sigma) as an anti-fade agent. Photograghy was taken under a fluorescence microscope (BH-2, Olympus) with the G excitation filter, EY-455 help excitation filter and Y-475 barrier filter, using Fuji ASA 400 color film.

RESULTS

Analysis of chromosomal quality

Under the same conditions of the experiment, sperm of the subjects with HBV infection as well as healthy controls appeared to be able to penetrate into zona-free hamster oocytes and to develop to the first-cleavage metaphase. However, the quality of metaphase spreads of sperm chromosomes had significant difference between the above two groups ($P<0.005$, χ^2-test). The quality of a number of sperm chromosome plates of the subjects with HBV infection was low, showing generally hard to be stained, stickiness of chromosome, clumping, tortuosity and so on, making the analyzable metaphase spreads greatly decreased. Whereas, few of these phenomena occurred in the controls although a small proportion of sperm chromosome plates of the controls could not be analyzed because of poor separation of chromosomes (Table 2).

Incidence of chromosome aberrations

Among the analyzable metaphase spreads, chromosome aberrations observed included numerical anomaly (aneuploidy), gap, ring chromosome, triradial, dicentric chromosome, pulverization, acentric fragment and deletion, orderly. Of the 233 analyzable sperm metaphase spreads in the hepatitis group, 33 (14.8 %) complements contained chromosome aberrations, being significantly higher than 5 (4.3 %) chromosome aberrations in the control group ($P<0.005$, χ^2-test).

Signals of in situ hybridization

Using specific whole length HBV DNA as probe to perform *in situ* hibridization on sperm chromosome slides, the sperm metaphases of one patient with chronic persistent hepatitis (subject 6) presented positive signals, all other tested subjects' spermatozoa (50 per subject), as well as all hamster oocytes (more than 200) did not have FISH signal (Table 1). Of 42 chromosome complements of subject 6 with chronic persistent hepatitis, 9 complements showed clearly twin yellow spots on some chromosomes. In 9 sperm metaphase spreads with positive signals, one had 5 signals on different chromosomes, the rest ranged from 2 to 4 spots involving unrelated

Table 1 Markers of HBV infection of the tested subjects

Subjects	Age	Serum						Seminal fluid	
		HBsAg	Anti-HBc	HBeAg	Anti-HBs	Anti-HBe	HBV-DNA	HBsAg	HBV-DNA
Hepatitis[a]									
1	38	+	+	-	-	-	+	+	-
2	32	+	+	+	-	-	+	-	+
3	25	+	+	-	-	+	+	-	-
4	22	+	+	+	-	-	-	+	+
5	26	+	+	-	-	+	-	+	+
6	23	+	+	-	-	+	-	-	+
7	27	+	+	+	-	-	+	+	-
8	22	+	+	-	-	+	-	-	-
9	25	+	+	-	-	-	+	-	+
Controls									
1	32	-	-	-	-	-	-	-	-
2	29	-	-	-	-	-	-	-	-
3	23	-	-	-	-	-	-	-	-
4	25	-	-	-	-	-	-	-	-
5	26	-	-	-	-	-	-	-	-

[a]1: acute hepatitis; 2, 3: chronic active hepatitis; 4, 5, 6, 7: chronic persistent hepatitis; 8, 9: chronic HBsAg carriers.

Table 2 Analytical results of sperm chromosomes of the tested subjects

Sub-jects	Number of metaphase spreads observed	Number (%) of analyzable metaphase spreads	Number(%) of normal sperm karyotypes	Number of abnormal sperm								Rates (%) of anormal sperm	FISH Re -sults
				With aneu -ploidy	With structural aberrations								
					g	r	tr	dic	pul	ace	del		
Hepatitis													
1	73	23(31.5)	20(87.0)	1	0	0	0	1	0	1	0	13.0	-
2	69	20(29.0)	15(75.0)	1	1	0	2	0	0	0	1	25.0	-
3	72	24(33.3)	22(91.7)	0	1	0	0	0	1	0	0	8.3	-
4	68	29(42.6)	25(86.2)	0	0	1	0	2	0	1	0	13.8	-
5	86	30(34.9)	28(93.3)	1(1)[a]	0	1	1[a]	0	0	0	0	6.7	-
6	113	43(38.1)	30(69.8)	5(2)[a]	4(1)[b]	2(1)[a]	2(1)[a]	0	2	1[b]	0	30.2	+
7	82	19(23.2)	19(100)	0	0	0	0	0	0	0	0	0.0	-
8	61	23(37.7)	20(87.0)	0	0	1	0	1	1	0	0	13.0	-
9	48	12(25.0)	11(91.7)	1	0	0	0	0	0	0	0	8.3	-
Total	672	223(33.2)	190(85.2)	9(3)[a]	6(1)[b]	5	5	4	4	3	1	14.8	-
Controls													
1	57	31(54.3)	29(93.5)	0	0	1	0	0	0	1	0	6.5	-
2	61	21(34.4)	21(100)	0	0	0	0	0	0	0	0	0.0	-
3	50	19(38.0)	19(100)	0	0	0	0	0	0	0	0	0.0	-
4	36	17(47.2)	16(94.1)	1	0	0	0	0	0	0	0	5.9	-
5	42	28(66.7)	26(92.9)	0	1	0	0	1	0	0	0	7.1	-
Total	246	116(47.2)	111(95.7)	1	1	1	0	1	0	1	0	4.3	-

g=Gap; r=Ring; tr=Triradial; dic=Dicentric chromosome; pul=Pulverization; ace=Acentric fragment; del=Deletion
[a]For containing both numerically and structurally chromosomal aberrations simultaneously
[b]For containing gap and acentric fragment chromosome aberrations simultaneously

chromosomes. The intensity of signal presented distinct difference among the spots. Positive signals detected were not identical in the chromosomes and in distribution (Figure1).

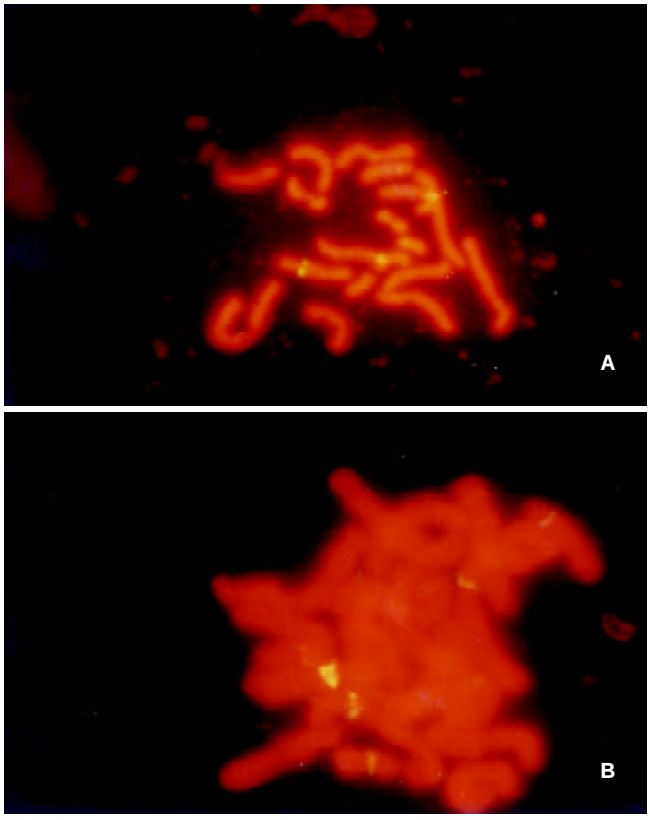

Figure 1 Detection of HBV DNA sequences in sperm chromosomes by FISH with biotinylated whole length HBV DNA probe: (A) a well separated chromosome plate from one patient (subject 6) with chronic persistent hepatitis, with three fluorescent signals on different chromosomes; (B) a poorly separated chromosome plate from the same patient with five fluorescent signals.

DISCUSSION

Our studies showed that the frequency of sperm chromosomal aberrations was greatly elevated after the infection of hepatitis B virus, and FISH could directly visualize the integration of HBV DNA sequences into sperm chromosomes. These results suggested that HBV infection could produce inheritable biological effects by carrying genetic materials damaged by virus or carrying altered genetic constituent due to the insertions of virus DNA in germ cells. As we know, this is the first report about the influence of biological factors on human sperm chromosomes.

In our study, we unexpectedly found that the sperm chromosomes frequently presented stickiness, faint stain and extreme tortuosity in the tested subjects with HBV infection and analyzable metaphases were low. Nevertheless, these changes were not found in the healthy controls under the strictly identical conditions. A previous report demonstrated that this manifestation had occurred in the chromosomes of somatic cells of HB patients with positive HBsAg[25]. The reasons of causing chromosomal stickiness in the HBV infection patients were unclear. The possibilities we considered might include the following events: First, antigen components of HBV such as core protein might interfere with the assembly of chromosome from chromatin due to its interaction with histones, it was confirmed that the core protein of HBV had participated in the organization of nucleosomes with histones in the hepatitis B virus minichromosome[26,27], so the condensation degree of chromosome was decreased and staining of chromosome became more difficult. Second, local despiralizations in the chromosomes occurred due to virus or its components. Third, premature chromosome condensation (PCC) might be induced by HBV, because virus-induced PCC was a common phenomenon[28]. Chromosome stickiness itself may be a manifestation of chromosomal pulverizations.

Previous reports have indicated that HBV infection can induce genetic alterations in somatic cells including hepatocytes and blood cells etc, showing increase of the rate of chromosomal aberrations or SCEs[29-35]. It was reported that influenza in spermatocytes of mice could greatly induce the

increase of chromosomal anomalies[36]. Our studies revealed that the incidence of chromosomal aberrations in the HBV infection group was significantly higher than that in the controls. Although in the present study the individual sample sizes and analyzable chromosome numbers were not large enough and it was difficult to compare the differences of rates and types of aberrations among the different clinical and serological states of HBV infection, there were some features worthy to be considered: First, the incidence of chromosome aberrations did not appear to be closely correlated with the seminal fluid status of HBV infection; Second, the chromosome pulverizations were not observed in the controls but were present in 4 sperm cells in the HBV infection group; Third, subject 6 with proven HBV integrations in the sperm chromosomes had prominently higher level of chromosomal aberration than the other HBV infection subjects; Fourth, the chromosome breakages were more frequent in the HBV infection group than that in the controls.

FISH onto sperm chromosomes by specific HBV DNA as a probe had showed positive signals in an HBV patient. The results directly indicated that HBV could penetrate blood-testis barrier and enter male germ line and integrate into their genome. So the possibility of vertical transmission of HBV via the germ cells was further confirmed[18,19]. Our preliminary observations showed that HBV integrations into sperm chromosomes had the feature of multi-site integrations and that the predilection site of HBV insertion into chromosomes seemed to be unlikely present. These results were similar with other previous reports about HBV-related hepatocellular carcinoma either in HCC-derived cell lines or in liver tumor samples[7-17,32,33]. During spermatogeneis, the stem cells sequentially undergo proliferation by mitosis and differentiation into spermatocytes and formation into spermatozoa by meiosis. The occurred important events of meiosis were the pairing and recombination of chromosomes during the prophase of meiosis I[37]. Thus it was possible that relocation of viral sequences and multi-site integrations could occur via genetic recombination when HBV was inserted into male reproductive cells, but the genetic effect of initial HBV insertion into various spermatogenic stages must have been greatly various. If the insertion occurred in stem cells, their all daughter cells would carry the integrated form of viral DNA and the effects would be long-term. In our studies, we were surprised by the fact that FISH showed strong signals in a patient using single small DNA probe. The reasonable explanations for this result included that the copies of HBV strand-invasion may be multiple, HBV sequence generated duplications *in situ* after the invasion into host genome, during the processes of making spermatozoa, unequal cross-over or DNA rearrangements occurred repeatedly due to HBV insertion into DNA of stem cells. According to the sperm chromosome aberration analysis (Table 2), such a subject with HBV integrations had relatively higher incidence of sperm chromosome aberration than that in other subjects without HBV integration. This correlation implied that viral DNA integrations into germ line significantly increased the instability of gametic genome. Thus, HBV integration into sperm cells would create extensively inheritable effects including offspring from such sperm fusion with ovum presenting HBV infection status in newborn infant and producing congenital or hereditary disease (for example, embryonal tumor) by altering genetic constituent and/or inducing mutations[38-40].

We conclude that H BV infection can bring about mutagenic effects on sperm chromosomes which show that the incidence of sperm chromosome aberrations is significantly elevated after the infection of HBV. Integrations of viral DNA into sperm chromosomes with feature of multisites and nonspecific can further increase the instability of sperm chromosomes. Our study suggests that HBV infection can create extensively inheritable effects not only by altering genetic constituent and/or inducing mutations but also possibly by vertical transmission of HBV via the germ line to the next generation.

REFERENCES

1 **Fang JN**, Jin CJ, Cui LH, Quan ZY, Choi BY, Ki M, Park HB. A comparative study on serologic profiles of virus hepatitis B. *World J Gastroenterol* 2001; **7**: 107-110

2 **Yan JC**, Ma JY, Pan BR, Ma LS. Studies on viral hepatitis B in China. *Shijie Huaren Xiaohua Zazhi* 2001; **9**: 611-616

3 **Rabe C**, Pilz T, Klostermann C, Berna M, Schild HH, Sauerbruch T, Caselmann WH. Clinical characteristics and outcome of a cohort of 101 patients with hepatocellular carcinoma. *World J Gastroenterol* 2001; **7**: 208-215

4 **Heathcote J**, Cameron CH, Dane DS. Hepatitis B antigen in saliva and semen. *Lancet* 1974; **1**: 71-73

5 **Darani M**, Gerber M. Letter: Hepatitis B antigen in vaginal secretions. *Lancet* 1974; **2**: 1008

6 **Dejean A**, Lugassy C, Zafrani S, Tiollais P, Brechot C. Detection of hepatitis B virus DNA in pancreas, kidney and skin of two human carriers of the virus. *J Gen Virol* 1984; **65**: 651-655

7 **Rogler CE**, Sherman M, Su CY, Shafritz DA, Summers J, Shows TB, Henderson A, Kew M. Deletion in chromosome 11p associated with a hepatitis B integration site in hepatocellular carcinoma. *Science* 1985; **230**: 319-322

8 **Hino O**, Shows TB, Rogler CE. Hepatitis B virus integration site in hepatocellular carcinoma at chromosome 17;18 translocation. *Proc Natl Acad Sci USA* 1986; **83**: 8338-8342

9 **Tokino T**, Fukushige S, Nakamura T, Nagaya T, Murotsu T, Shiga K, Aoki N, Matsubara K. Chromosomal translocation and inverted duplication associated with integrated hepatitis B virus in hepatocellular carcinoma. *J Virol* 1987; **61**: 3848-3854

10 **Zhou YZ**, Slagle BL, Donehower LA, vanTuinen P, Ledbetter DH, Butel JS. Structural analysis of a hepatitis B virus genome integrated into chromosome 17p of a human hepatocellular carcinoma. *J Virol* 1988; **62**: 4224-4231

11 **Urashima T**, Saigo K, Kobayashi S, Imaseki H, Matsubara H, Koide Y, Asano T, Kondo Y, Koike K, Isono K. Identification of hepatitis B virus integration in hepatitis C virus-infected hepatocellular carcinoma tissues. *J Hepatol* 1997; **26**: 771-778

12 **Pineau P**, Marchio A, Terris B, Mattei MG, Tu ZX, Tiollais P, Dejean A. At(3;8) chromosomal translocation associated with hepatitis B virus integration involves the carboxypeptidase N locus. *J Virol* 1996; **70**: 7280-7284

13 **Hino O**, Tabata S, Hotta Y. Evidence for increased in vitro recombination with insertion of human hepatitis B virus DNA. *Proc Natl Acad Sci USA* 1991; **88**: 9248-9252

14 **Hino O**, Ohtake K, Rogler CE. Features of two hepatitis B virus (HBV) DNA integrations suggest mechanisms of HBV integration. *J Virol* 1989; **63**: 2638-2643

15 **Tokino T**, Matsubara K. Chromosomal sites for hepatitis B virus integration in human hepatocellular carcinoma. *J Virol* 1991; **65**: 6761-6764

16 **Su TS**, Hwang WL, Yauk YK. Characterization of hepatitis B virus integrant that results in chromosomal rearrangement. *DNA Cell Biol* 1998; **17**: 415-425

17 **Shamay M**, Agami R, Shaul Y. HBV integrants of hepatocellular carcinoma cell lines contain an active enhancer. *Oncogene* 2001; **20**: 6811-6819

18 **Hadchouel M**, Scotto J, Huret JL, Molinie C, Villa E, Degos F, Brechot C. Presence of HBV DNA in spermatozoa: a possible vertical transmission of HBV via the germ line. *J Med Virol* 1985; **16**: 61-66

19 **Peng HW**, Su TS, Han SH, Ho CK, Ho CH, Ching KN, Chiang BN. Assessment of HBV persistent infection in an adult population in Taiwan. *J Med Virol* 1988; **24**: 405-412

20 **Huang TH**, Liu HX, Cai M, Huang JM. Chromosomal aberrations induced in human spermatozoa by mitomycin C. *Yichuan Xuebao* 1997; **24**: 291-295

21 **Kamiguchi Y**, Mikamo K. An improved, efficient method for analyzing human sperm chromosomes using zona-free hamster ova. *Am J Hum Genet* 1986; **38**: 724-740

22 **Sambrook J**, Fritsch EF, Maniatis. Molecular cloning-a laboratory manual. 3rd edition, *New york: Clod Spring Habor Laboratory Press* 2001: 1.21-1.83
23 **Huang JM**, Huang TH, Fang XW, Zhuang TG, Liu HX. Detection of aneuploidy in human sperm by FISH. *Zhonghua Yixue Yichuanxue Zazhi* 1997; **14**: 248-249
24 **Korenberg JR**, Chen XN. Human cDNA mapping using a high-resolution R-banding technique and fluorescence *in situ* hybridization. *Cytogenet Cell Genet* 1995; **69**: 196-200
25 **Vianello MG**, Fasce LC, Mura MS, Andreoni G, Scalise G. Cytogenic analysis in HBsAg positive subjects, healthy carriers and patients with acute-phase hepatitis. *Boll Ist Sieroter Milan* 1979; **58**: 266-272
26 **Bock CT**, Schranz P, Schroder CH, Zentgraf H. Hepatitis B virus genome is organized into nucleosomes in the nucleus of the infected cell. *Virus Genes* 1994; **8**: 215-229
27 **Bock CT**, Schwinn S, Locarnini S, Fyfe J, Manns MP, Trautwein C, Zentgraf H. Structural organization of the hepatitis B virus minichromosome. *J Mol Biol* 2001; **307**: 183-196
28 **Aula P**. Virus-induced premature chromosome condensation (PCC) in single cells and G-bands of PCC-chromatin. *Hereditas* 1973; **74**: 81-87
29 **Chen HL**, Chiu TS, Chen PJ, Chen DS. Cytogenetic studies on human liver cancer cell lines. *Cancer Genet Cytogenet* 1993; **65**: 161-166
30 **Marchio A**, Meddeb M, Pineau P, Danglot G, Tiollais P, Bernheim A, Dejean A. Recurrent chromosomal abnormalities in hepatocellular carcinoma detected by comparative genomic hybridization. *Genes Chromosomes Cancer* 1997; **18**: 59-65
31 **Pang E**, Wong N, Lai PB, To KF, Lau JW, Johnson PJ. A comprehensive karyotypic analysis on a newly developed hepatocellular carcinoma cell line, HKCI-1, by spectral karyotyping and comparative genomic hybridization. *Cancer Genet cytogenet* 2000; **121**: 9-16
32 **Livezey KW**, Negorev D, Simon D. Hepatitis B virus-transfected Hep G2 cells demonstrate genetic alterations and de novo viral integration in cells replicating HBV. *Mutat Res* 2000; **452**: 163-178
33 **Livezey KW**, Negorev D, Simon D. Increased chromosomal alterations and micronuclei formation in human hepatoma HepG2 cells transfected with the hepatitis B virus HBX gene. *Mutat Res* 2002; **505**: 63-74
34 **Wang PL**, Liu SF, Shen SL, Dong XY. A study of sister-chromatid exchange in peripheral lymphocytes of hepatitis B patients with HBsAg positive and their children. *Mutat Res* 1986; **175**: 249-254
35 **Chatterjee B**, Ghosh PK. Constitutive heterochromatin polymorphism and chromosome damage in viral hepatitis. *Mutat Res* 1989; **210**: 49-57
36 **Sharma G**, Polasa H. Cytogenetic effects of influenza virus infection on male germ cells of mice. *Hum Genet* 1978; **45**: 179-187
37 **Hecht NB**. The making of a spermatozoon: a molecular perspective. *Dev Gen* 1995; **16**: 95-103
38 **Naumova AK**, Kisselev LL. Biological consequences of interactions between hepatitis B virus and human nonhepatic cellular genomes. *Biomed Sci* 1990; **1**: 233-238
39 **Kim H**, Lee MJ, Kim MR, Chung IP, Kim YM, Lee JY, Jang JJ. Expression of cyclin D1, cyclin E, cdk4 and loss of heterozygosity of 8p, 13q, 17p in hepatocellular carcinoma: comparison study of childhood and adult hepatocellular carcinoma. *Liver* 2000; **20**: 173-178
40 **Tanaka T**, Miyamoto H, Hino O, Kitagawa T, Koike M, Iizuka T, Sakamoto H. Primary hepatocellular carcinoma with hepatitis B virus-DNA integration in a 4-year-old boy. *Hum Pathol* 1986;**17**: 202-204

Edited by Xu XQ and Wu XN

P.O.Box 2345, Beijing 100023, China
Fax: +86-10-85381893
E-mail: wjg@wjgnet.com www.wjgnet.com

World J Gastroenterol 2003;9(4):741-744
World Journal of Gastroenterology
 ISSN 1007-9327

• VIRAL HEPATITIS •

TT virus and hepatitis G virus infections in Korean blood donors and patients with chronic liver disease

Mee Juhng Jeon, Jong Hee Shin, Soon Pal Suh, Young Chai Lim, Dong Wook Ryang

Mee Juhng Jeon, Division of Medical Research, Kwangju-Chonnam Red Cross Blood Center, Chonnam National University, Kwangju, Republic of Korea
Jong Hee Shin, Soon Pal Suh, Dong Wook Ryang, Department of Clinical Pathology, Chonnam National University, Kwangju, Republic of Korea
Young Chai Lim, Department of Pharmacology, Medical School, Chonnam National University, Kwangju, Republic of Korea
Jong Hee Shin, Soon Pal Suh, Young Chai Lim, Dong Wook Ryang, Research Institute of Medical Sciences, Chonnam National University, Kwangju, Republic of Korea
Correspondence to: Dong Wook Ryang M.D., Ph.D., Department of Clinical Pathology, Chonnam National University Medical School 8 Hak 1 dong, Dong-Ku, Kwangju, Korea. ryang@hitel.net
Telephone: +82-62-220-5353 **Fax:** +82-62-224-2518
Received: 2002-07-02 **Accepted:** 2002-07-27

Abstract

AIM: To determine the prevalences of TTV and HGV infections among blood donors and patients with chronic liver disease in Korea, to investigate the association of TTV and HGV infections with blood transfusion, and to assess the correlation between TTV and HGV viremia and hepatic damage.

METHODS: A total of 391 serum samples were examined in this study. Samples were obtained from healthy blood donors (n=110), hepatitis B surface antigen (HBsAg)-positive donors (n=112), anti-hepatitis C virus (anti-HCV)-positive donors (n=69), patients with type B chronic liver disease (n=81), and patients with type C chronic liver disease (n=19). TTV DNA was detected using the hemi-nested PCR. HGV RNA was tested using RT-PCR. A history of blood transfusion and serum levels of alanine aminotransferase (ALT) and aspartate aminotransferase (AST) were also determined.

RESULTS: TTV DNA was detected in 8.2 % of healthy blood donors, 16.1 % of HBsAg-positive donors, 20.3 % of anti-HCV-positive donors, 21.0 % of patients with type B chronic liver disease, and 21.1 % of patients with type C chronic liver disease. HGV RNA was detected in 1.8 % of healthy blood donors, 1.8 % of HBsAg-positive donors, 17.4 % of anti-HCV-positive donors, 13.6 % of patients with type B chronic liver disease, and 10.5 % of patients with type C chronic liver disease. The prevalence of TTV and HGV infections in HBV- or HCV-positive donors and patients was significantly higher than in healthy blood donors (P<0.05), except for the detection rate of HGV in HBsAg-positive donors which was the same as for healthy donors. There was a history of transfusion in 66.7 % of TTV DNA-positive patients and 76.9 % of HGV RNA-positive patients (P<0.05). No significant increase in serum ALT and AST was detected in the TTV- or HGV-positive donors and patients.

CONCLUSION: TTV and HGV infections are more frequently found in donors and patients infected with HBV or HCV than in healthy blood donors. However, there is no significant association between TTV or HGV infections and liver injury.

Jeon MJ, Shin JH, Suh SP, Lim YC, Ryang DW. TT virus and hepatitis G virus infections in Korean blood donors and patients with chronic liver disease. *World J Gastroenterol* 2003; 9(4): 741-744
http://www.wjgnet.com/1007-9327/9/741.htm

INTRODUCTION

A novel human DNA virus, TT virus (TTV), was first discovered in the sera of three Japanese patients with post-transfusion hepatitis in 1997[1]. TTV is a non-enveloped, single-stranded virus related to the Circoviridae family[2, 3]. Hepatitis G virus (HGV) is an enveloped RNA virus member of the Flaviviridae family[4]. TTV and HGV infections in healthy blood donors as well as in patients with liver disease have been recently reported in many areas of the world[3-22]. However, the role of these viruses in disease remains uncertain. Information regarding TTV and HGV infections in the Korean population is limited. Hepatitis B virus (HBV) and hepatitis C virus (HCV) are the viral agents most readily implicated in causing a liver disease in Korea[23, 24]. The aims of this study were to determine the prevalence of TTV and HGV in Korean blood donors and patients with type B or C chronic liver disease, to investigate the association between blood transfusion and TTV and HGV infections, and to assess the correlation between TTV and HGV viremia and hepatic damage.

MATERIALS AND METHODS

Materials

A total of 291 blood samples, derived from 110 healthy donors, 112 hepatitis B surface antigen (HBsAg)-positive donors, and 69 anti-hepatitis C virus antibody (anti-HCV Ab)-positive donors, were collected at the Kwangju-Chonnam Red Cross Blood Center. A total of 100 blood samples were obtained from 81 patients with type B chronic liver disease (46 chronic hepatitis, 15 liver cirrhosis, and 20 hepatocellular carcinoma) and 19 patients with type C chronic liver disease (10 chronic hepatitis and 9 hepatocellular carcinoma) at the Chonnam National University Hospital.

Serological and chemical studies

Blood samples were centrifuged and stored at -70 ℃ within hours of collection. HBsAg and anti-HCV Ab were tested with enzyme immunoassay (Axsym, Abbott Laboratories, USA). Immunoblot assay (ProfiBlot IIN, SLT Lab Instruments, Austria) was used to confirm anti-HCV. Serum levels of alanine aminotransferase (ALT) and aspartate aminotransferase (AST) were also measured using an autoanalyzer (Hitachi 747, Hitachi, Japan).

DNA extraction and TTV PCR

DNA was extracted from 250 μL of sera using a kit (DNAzol, Molecular Research Center, USA) according to the manufacturer' s guidelines. Nucleic acids were dissolved in 50 μL of NaOH (8 mM). A 7 μL volume was then removed and used for amplification of TTV DNA. The PCR reaction was performed in a volume of 50 μL containing 10 mM Tris-HCl

(pH 8.3), 50 mM KCl, 1.5 mM MgCl2, 200 μM dNTPs, 0.5 μM of NG059 (5'-ACAGACAGAGGAGAAGGCAACATG-3') as the sense primer, 0.5 μM of NG063 (5'-CTGGCATTTTACCATTTCCAAAGTT-3') as the antisense primer, and 2 U of Taq polymerase to amplify a 286-bp product. The second-round PCR was done under identical conditions, except that the template was 5 μL product from the first-round PCR, and the sense primer was 0.5 μM of NG061 (5'-GGCAACATGTTATG GATAGACTGG-3'). The size of the second-round PCR product was 271 bp. Each PCR was performed in a programmable thermal cycler (GeneAmp PCR System 9 600, Perkin-Elmer Cetus, USA). The PCR program consisted of 35 cycles of denaturation for 15 seconds at 95 ℃, annealing for 30 seconds at 58 ℃, and extension for 30 seconds at 72 ℃, followed by a final extension for 10 minutes at 72 ℃. The amplification products were separated by 2 % agarose gel electrophoresis, stained with ethidium bromide, and photographed under UV light.

Nucleotide sequencing

To ascertain the specificity of the PCR products, DNA sequences of the amplified product were determined. The PCR product was purified with a PCR purification kit (Boehringer Mannheim, Mannheim, Germany). Nucleotide sequences of the amplicon were directly determined using an AccuPower DNA sequencing kit (Bioneer, Korea). The sequence homology between the PCR products and published TTV DNA was examined. Two randomly selected PCR products were sequenced, both of which were positive for TTV DNA. Sequence comparison with databases confirmed the specific amplification of TTV genomic DNA.

RNA extraction and HGV RT-PCR

To detect HGV RNA in a sample, nucleic acids were isolated from 250 μL of serum using Trizol LS Reagent (GIBCO, USA) and a reverse-transcription PCR (RT-PCR) was performed. A total of 35 cycles of PCR (94 ℃ for 30 seconds, 50 ℃ for 30 seconds, and 72 ℃ for 60 seconds for each cycle) were completed in a programmable thermal cycler (GeneAmp PCR System 9 600, Perkin-Elmer Cetus, USA). The size of the PCR product was 234 bp. The amplification products were separated by 2 % agarose gel electrophoresis, stained with ethidium bromide, and photographed under UV light.

Transfusion history

To examine the association of TTV and HGV infections with blood transfusion, previous transfusion history was investigated in both patients with chronic liver disease and blood donors, by examining their medical records or via telephone interviews.

Statistical analysis

Statistical analysis was conducted using the Chi-square test and analysis of variance (ANOVA). Statistical significance was set when $P<0.05$.

RESULTS

Prevalences of TTV DNA and HGV RNA

The prevalences of TTV and HGV infections in blood donors and patients with chronic liver disease were shown in Table 1. TTV DNA was detected in 8.2 % (9/110) of healthy blood donors, 16.1 % (18/112) of HBsAg-positive donors, 20.3 % (14/69) of anti-HCV-positive donors, 21.0 % (17/81) of patients with type B chronic liver disease, and 21.1 % (4/19) of patients with type C chronic liver disease. The TTV prevalence was significantly higher both in HBsAg-positive or anti-HCV-positive donors and in patients with chronic liver disease than in healthy blood donors ($P<0.05$). HGV RNA was detected in 1.8 % (2/110) of healthy blood donors, 1.8 % (2/112) of HBsAg-positive donors, 17.4 % (12/69) of anti-HCV-positive donors, 13.6 % (11/81) of patients with type B chronic liver disease, and 10.5 % (2/19) of patients with type C chronic liver disease. The HGV prevalence was significantly lower in healthy blood donors or HBsAg-positive donors than in patients with chronic liver disease and anti-HCV-positive donors ($P<0.05$). The detection rates for TTV or HGV were not significantly different between the three types of chronic liver disease. The TTV prevalence was about 4.6 times higher than the HGV prevalence in healthy blood donors. Co-infection of TTV and HGV was also observed in ten cases of HBV- or HCV-infected patients and donors.

Table 1 The prevalence of TTV and HGV infections in blood donors and patients with chronic liver disease from Korea

Subject	*n*	TTV (%)	HGV (%)	TTV & HGV (%)
Healthy blood donors	110	9 (8.2)	2 (1.8)	0 (0.0)
HBsAg(+) donors	112	18 (16.1)[a]	2 (1.8)	0 (0.0)
Anti-HCV(+) donors	69	14 (20.3)[a]	12 (17.4)[b]	3 (4.3)
Patients with type B chronic liver disease	81	17 (21.0)[a]	11 (13.6)[b]	6 (7.4)
Chronic hepatitis	6	10(21.7)	5 (10.9)	3 (6.5)
Liver cirrhosis	15	3 (20.0)	3 (20.0)	2 (13.3)
Hepatocellular carcinoma	20	4(20.0)	3 (20.0)	1 (5.0)
Patients with type C chronic liver disease	19	4 (21.1)[a]	2 (10.5)[b]	1 (5.3)
Chronic hepatitis	10	2 (20.0)	1 (10.0)	0 (0.0)
Hepatocellular carcinoma	9	2 (22.2)	1 (11.1)	1 (11.1)
Total	391	62 (15.9)	29 (7.4)	10 (2.6)

[a]$P<0.05$ *vs* healthy blood donors, [b]$P<0.05$ *vs* healthy blood donors or HBsAg-positive donors.

Association of TTV and HGV infections with blood transfusion

To investigate the association of TTV and HGV infections with blood transfusion, the medical records for the previous transfusion history were reviewed in patients with chronic liver disease. The rate of transfusion history was higher in TTV- or HGV-positive patients than in TTV- or HGV-negative patients ($P<0.05$) (Table 2).

Table 2 Transfusion history according to the detection of TTV and HGV in patients with chronic liver disease

Group		*n*	Transfusion history	
			Yes (%)	No (%)
TTV	Positive	21	14 (66.7)[a]	7 (33.3)
	Negative	77	33 (42.9)	44 (57.1)
HGV	Positive	13	10 (76.9)	3 (23.1)
	Negative	85	37 (43.5)	48 (56.5)
Total		98	47 (48.0)	51 (52.0)

[a]$P<0.05$ *vs* TTV-or HGV-negative patients.

Correlation between TTV or HGV viremia and hepatic damage

To evaluate the correlation between TTV or HGV infections and hepatic damage, the serum levels of ALT and AST were measured in all subjects (data not shown). No significant increase in serum ALT and AST was observed in TTV- or HGV-positive blood donors, compared with TTV- or HGV-negative donors. In addition, TTV or HGV co-infection did

not elicit any further significant increase in ALT and AST levels in patients with chronic liver disease. Furthermore, no increase in ALT and AST was observed in HBV- or HCV-positive patients or donors infected with both TTV and HGV. These observations suggested that there is no significant association between TTV or HGV infections and hepatic injury.

DISCUSSION

TTV was detected in 8.2 % of healthy blood donors from Korea. The prevalence of TTV infection among blood donors in other countries is 1.9 % in the United Kingdom[5], 3.2 % in Germany[6], 7.5-10 % in the United States[7, 8], 12 % in Japan[3], 29.4 % in Egypt[9], 36 % in Thailand[10], and 62 % in Brazil[11]. These differences in prevalence between countries could be due to the different geographical distribution of TTV infections, and the heterogeneity and variability of TTV isolates[3, 5]. Variation could also arise due to different experimental methods to determine TTV infection, such as the primers used, and the sensitivity of the PCR methods employed[8, 25]. The primer used in our study was identical to that used in the aforementioned countries, suggesting that the discrepancies of TTV prevalence between countries were not due to variation in the primer used. The detection rate of HGV RNA in blood donors from many other countries ranged from 0.5 to 7.4 %[19-22]. In healthy Korean blood donors, the detection rate of HGV was 1.8 %, and the prevalence of TTV was higher (about 4.6 times) than that of HGV.

We observed TTV and HGV co-infection in subjects with HBV or HCV findings that had also been reported elsewhere[12-18]. The co-infection rate of TTV in HBV- and HCV-infected subjects was similar, a finding also reported by others[10, 12]. However, there was some difference in the co-infection rate of HGV between HBV and HCV. The prevalence of HGV in HBsAg-positive donors was lower than in patients with chronic liver disease and also anti-HCV-positive donors. Giulivi *et al*. have reported similar findings[26]. The discrepancy in the co-infection rate of HGV between HBV- and HCV-positive donors may have clinical significance. With the exception of HGV co-infection in HBV-positive donors, both HBV- and HCV-infected subjects had a higher detection rate of TTV or HGV than healthy donors. This suggested that HBV- or HCV-infected subjects had a greater exposure to a risk factor for viral infections. These viruses may also share a common route of transmission.

A total of 66.7 % of TTV DNA-positive patients and 76.9 % of HGV RNA-positive patients had a history of blood transfusion. This suggests the possibility of viral transmission via blood transfusion. TTV and HGV are prevalent in the sera of persons with hemophilia, intravenous drug users, and hemodialysis patients[3, 8, 21, 27]. However, our results indicate that TTV and HGV were observed in donors and patients without a transfusion history, which suggests a non-parenteral route of transmission. TTV and HGV have reportedly been detected in urine, feces, and breast milk[6, 28, 29]. Thus, TTV and HGV might be transmitted via several parenteral and non-parenteral routes.

No significant increase in ALT or AST was observed in healthy donors or liver disease patients infected with either TTV or HGV, compared to subjects without these viral infections. Kao *et al*. reported that TTV infection does not affect the disease process of type B or C hepatitis, or the response to interferon treatment[15]. Oguchi *et al*. demonstrated that a TTV carrier state was maintained without hepatitis in hemodialysis patients over a 5-year follow-up period[30]. Alter *et al*. showed that HGV infection was not associated with hepatitis and did not worsen the course of concurrent HCV infection[31]. Considering all these results, TTV or HGV infection seems not to be related to the initiation or potentiation of hepatic damage, which therefore suggests that the routine screening test for TTV and HGV on donated blood is not necessary. At present there also is no country that conducts the screening test for these viral infections.

REFERENCES

1 **Nishizawa T**, Okamoto H, Konishi K, Yoshizawa H, Miyakawa Y, Mayumi M. A novel DNA virus (TTV) associated with elevated transaminase levels in posttransfusion hepatitis of unknown etiology. *Biochem Biophys Res Comm* 1997; **241**: 92-97

2 **Mushahwar IS**, Erker JC, Muerhoff AS, Leary TP, Simons JN, Birkenmeyer LG, Chalmers ML, Piolt-Matias TJ, Dexai SM. Molecular and biophysical characterization of TT virus: evidence for a new virus family infecting humans. *Proc Natl Acad Sci USA* 1999; **96**: 3177-3182

3 **Okamoto H**, Nishizawa T, Kato N, Ukita M, Ikeda H, Iizuka H, Miyakawa Y, Mayumi M. Molecular cloning and characterisation of a novel DNA virus (TTV) associated with posttransfusion hepatitis of unknown etiology. *Hepatol Res* 1998; **10**: 1-16

4 **Simons JN**, Pilot-Mathias TJ, Leary TP. Identification of two flavivirus-like genomes in the GB hepatitis agent. *Proc Natl Acad Sci* 1995; **92**: 3401-3405

5 **Simmonds P**, Davidson F, Lycett C, Prescott LE, MacDonald DM, Ellender J, Yap PL, Ludlam CA, Haydon GH, Gillon J, Jarvis LM. Detection of a novel DNA virus (TTV) in blood donors and blood products. *Lancet* 1998; **352**: 191-194

6 **Wolff C**, Diekmann A, Boomgaarden M, Korner MM, Kleesiek K. Viremia and excretion of TT virus in immunosuppressed heart transplant recipients and in immunocompetent individuals. *Transplantation* 2000; **69**: 351-356

7 **Charlton M**, Adjei P, Poterucha J, Zein N, Moore B, Therneau T, Krom R, Wiesner R. TT-virus infection in north American blood donors, patients with fulminant hepatic failure, and cryptogenic cirrhosis. *Hepatology* 1998; **28**: 839-842

8 **Desai SM**, Muerhoff AS, Leary TP, Erker JC, Simons JN, Chalmers ML, Birkenmeyer LG, Pilot-Matias TJ, Mushahwar IK. Prevalence of TT virus infection in US blood donors and populations at risk for acquiring parenterally transmitted viruses. *J Infec Disease* 1999; **179**: 1242-1244

9 **Gad A**, Tanaka E, Orii K, Kafumi T, Serwah AE, El-Sherif A, Nooman Z, Kiyosawa K. Clinical significance of TT virus infection in patients with chronic liver disease and volunteer blood donors in Egypt. *J Med Virol* 2000; **60**: 177-181

10 **Tanaka H**, Okamoto H, Luengrojanakul P, Chainuvata T, Tsuda F, Tanaka T, Miyakawa Y, Mayumi M. Infection with an unenveloped DNA virus (TTV) associated with posttransfusion non-A-G hepatitis in hepatitis patients and healthy blood donors in Thailand. *J Med Virol* 1998; **56**: 234-238

11 **Niel C**, de Oliveira JM, Ross RS, Gomes SA, Roggendorf M, Viazov S. High prevalence of TT virus infection in Brazilian blood donors. *J Med Virol* 1999; **57**: 259-263

12 **Naoumov NV**, Petrova EP, Thomas MG, Villians R. Presence of a newly described human DNA virus (TTV) in patients with liver disease. *Lancet* 1998; **352**: 195-197

13 **Orii K**, Tanaka E, Umemura T, Rokuhara A, Iijima A, Yoshisawa K, Imai H, Kiyosawa K. Prevalence and disease association of TT virus infection in Japanese patients with viral hepatitis. *Hepatol Res* 1999; **14**: 161-170

14 **Berg T**, Schreier E, Heuft HG, Hohne M, Bechstein WO, Leder K, Hopf U, Neuhaus P, Wiedenmann B. Occurrence of a novel DNA virus (TTV) infection in patients with liver diseases and its frequency in blood donors. *J Med Virol* 1999; **59**: 117-121

15 **Kao JH**, Chen W, Chen PJ, Lai MY, Chen DS. TT virus infection in patients with chronic hepatitis B or C: influence on clinical, histological and virological features. *J Med Virol* 2000; **60**: 387-392

16 **Schleicher S**, Chaves RL, Dehmer T, Gregor M, Hess G, Flehming B. Identification of GBV-C hepatitis G RNA in chronic hepatitis C patients. *J Med Virol* 1996; **50**: 71-74

17 **Bralet MP**, Thorabla FR, Pawlotsky JM, Bastie A, Nhieu JTV, Duval J. Histopathologic impact of GB virus C infection on chronic hepatitis C. *Gastroenterology* 1997; **112**: 188-192

18 **Alter MJ**, Gallagher M, Morris T, Moyer LA, Meeks EL, Krawczynski K. Acute non-A-E hepatitis in the United States and the role of hepatitis G virus infection. *N Engl J Med* 1997; **336**: 741-746
19 **Simons JN**, Leary TP, Dawson GJ, Piolot-Matias TJ, Muerhofff AS, Schlauder GG, Desai SM, Mushahwar IK. Isolation of novel virus-like sequences associated with human hepatitis. *Nat Med* 1995; **1**: 564-569
20 **Buorkman P**, Sundstrom G, Widell A. Hepatitis C virus and GB virus C / hepatitis G virus viremia in Swedish blood donors with different alanine aminotransferase levels. *Transfusion* 1998; **38**: 378-384
21 **Hadlock KG**, Joung KH. GBV-C / HGV: a new virus within the Flaviviridae and its clinical implication. *Transfus Med Rev* 1998; **12**: 94-108
22 **Cheung RC**, Keeffe EB, Greenberg HB. Hepatitis G virus: Is it a hepatitis virus? *West J Med* 1997; **167**: 23-33
23 **Lee HS**, Han CJ, Kim CY. Predominant etiologic association of hepatitis C virus with hepatocellular carcinoma compared with hepatitis B virus in elderly patients in a hepatitis B-endemic area. *Cancer* 1993; **72**: 2564-2567
24 **Park BC**, Han BH, Ahn SY, Lee SW, Lee DH, Lee YN, Seo JH, Kim KW. Prevalence of hepatitis C antibody in patients with chronic liver disease and hepatocellular carcinoma in Korea. *J Viral Hepat* 1995; **2**: 195-202
25 **Mizokami M**, Albrecht JK, Kato T, Orito E, Lai VC, Goodman Z, Hong Z, Lau JY. TT virus infection in patients with chronic hepatitis C virus infection - effect of primers, prevalence, and clinical significance. Hepatitis Interventional Therapy Group. *J Hepatol* 2000; **32**: 339-343
26 **Giulivi A**, Slinger R, Tepper M, Sher G, Scalia V, Kessler G, Gill P. Prevalence of GBV-C / hepatitis G virus viremia and anti-E2 in Canadian blood donors. *Vox Sang* 2000; **79**: 201-205
27 **Aikawa T**, Sugai Y, Okamoto H. Hepatitis G infection in drug abusers with chronic hepatitis C. *N Eng J Med* 1996; **334**: 195-196
28 **Schröter M**, Polywka S, Zöllner B, Schäfer P, Laufs R, Feucht HH. Detection of TT virus DNA and GB virus type C / Hepatitis G virus RNA in serum and breast milk: Determination of mother-to-child transmission. *J Clin Microbiol* 2000; **38**: 745-747
29 **Okamoto H**, Akahane Y, Ukita M, Fukuda M, Tsuda F, Miyakawa Y, Mayumi M. Fecal excretion of a nonenveloped DNA virus (TTV) associated with posttransfusion non-A-G hepatitis. *J Med Virol* 1998; **56**: 128-132
30 **Oguchi T**, Tanaka E, Orii K, Kobayashi M, Hora K, Kiyosawa K. Transmission of and liver injury by TT virus in patients on maintenance hemodialysis. *J Gastroenterol* 1999; **34**: 234-240
31 **Alter HJ**, Nakatsuji Y, Melpolder J, Wages J, Wesley R, Shih WK, Kim JP. The incidence of transfusion-associated hepatitis G virus infection and its relation to liver disease. *N Engl J Med* 1997; **336**: 747-754

Edited by Ma JY and Xu XQ

P.O.Box 2345, Beijing 100023, China
Fax: +86-10-85381893
E-mail: wjg@wjgnet.com www.wjgnet.com

World J Gastroenterol 2003;9(4):745-750
World Journal of Gastroenterology
 ISSN 1007-9327

• VIRAL HEPATITIS •

Is laparoscopy an advantage in the diagnosis of cirrhosis in chronic hepatitis C virus infection?

Perdita Wietzke-Braun, Felix Braun, Peter Schott, Giuliano Ramadori

Perdita Wietzke-Braun, Felix Braun, Peter Schott, Giuliano Ramadori, Department of Internal Medicine, Division of Gastroenterology and Endocrinology, University of Goettingen, Germany
Correspondence to: Prof. Giuliano Ramadori, Medizinische Universitätsklinik, Abteilung Gastroenterologie, Robert-Koch-Straβe 40, 37075 Goettingen, Germany. gramado@med.uni-goettingen.de
Telephone: +49-551-396301 **Fax:** +49-551-398596
Received: 2002-10-08 **Accepted:** 2002-11-04

Abstract

AIM: To evaluate the potential of laparoscopy in the diagnosis of cirrhosis and outcome of interferon treatment in HCV-infected patients.

METHODS: In this retrospective study, diagnostic laparoscopy with laparoscopic liver biopsy was performed in 72 consecutive patients with chronic HCV infection. The presence or absence of cirrhosis was analyzed macroscopically by laparoscopy and microscopically by liver biopsy specimens. Clinical and laboratory data and outcome of interferon-alfa treatment were compared between cirrhotic and noncirrhotic patients.

RESULTS: Laparoscopically, cirrhosis was seen in 29.2 % (21/72) and non-cirrhosis in 70.8 % (51/72) of patients. Cirrhotic patients were significantly older with a significant longer duration of HCV infection than noncirrhotic patients. Laboratory parameters (AST, y-GT, y-globulin fraction) were measured significantly higher as well as significantly lower (prothrombin index, platelet count) in cirrhotic patients than in non-cirrhotic patients. Histologically, cirrhosis was confirmed in 11.1 % (8/72) and non cirrhosis in 88.9 % (64/72). Patients with macroscopically confirmed cirrhosis (n=21) showed histologically cirrhosis in 38.1 % (8/21) and histologically non-cirrhosis in 61.9 % (13/21). In contrast, patients with macroscopically non-cirrhosis (n=51) showed histologically non cirrhosis in all cases (51/51). Thirty-nine of 72 patients were treated with interferon-alfa, resulting in 35.9 % (14/39) patients with sustained response and 64.1 % (25/39) with non response. Non-responders showed significantly more macroscopically cirrhosis than sustained responders. In contrast, there were no significant histological differences between non-responders and sustained responders.

CONCLUSION: Diagnostic laparoscopy is more accurate than liver biopsy in recognizing cirrhosis in patients with chronic HCV infection.Liver biopsy is the best way to assess inflammatory grade and fibrotic stage. The invasive marker for staging, prognosis and management, and treatment outcome of chronic HCV-infected patients need further research and clinical trials. Laparoscopy should be performed for recognition of cirrhosis if this parameter is found to be of prognostic and therapeutic relevance in patients with chronic HCV infection.

Wietzke-Braun P, Braun F, Schott P, Ramadori G. Is laparoscopy an advantage in the diagnosis of cirrhosis in chronic hepatitis C virus infection? *World J Gastroenterol* 2003; 9(4): 745-750
http://www.wjgnet.com/1007-9327/9/745.htm

INTRODUCTION

Hepatitis C virus (HCV) infection is the leading cause of chronic liver disease. Up to 85 % of HCV-infected patients develop chronic liver disease without elimination of the virus[1-3]. Chronic HCV infected patients develop cirrhosis in 7 % and 20 % after 20 and 40 years of infection[4], while symptoms and alarming biochemical markers appear late[5,6]. Patients with cirrhosis secondary to chronic HCV infection also have an increased risks for development of hepatocellular carcinoma (HCC), estimated to be between 1-4 % per year[7].

The diagnostic spectrum for chronic hepatitis C includes biochemical parameters, antibodies against HCV, qualitative and quantitative HCV RNA with genotyping, abdominal ultrasound and liver histology. Random core biopsy analysis can reveal information about the inflammatory grade and fibrotic stage of chronic HCV infection[8]. Diagnosis of compensated liver cirrhosis can be made with a high accuracy neither by percutaneous liver biopsy nor by ultrasound[9]. In comparison with percutaneous liver biopsy, laparoscopy allows macroscopic inspection of both liver lobes that might variate during progression of liver disease[10]. Percutaneous liver biopsy only allows the interpretation of a small biopsy. It has been reported that histological analysis fail with error ranges above 25 % in the diagnosis of cirrhosis in chronic liver disease[11,12], especially during the early phase of cirrhosis (Child A) and macronodular cirrhosis[13]. In a retrospective study, Poniachik *et al.* compared the presence of cirrhosis in 434 patients by liver biopsy and laparoscopy. Cirrhosis was seen laparoscopically in 169 patients and was confirmed in 115 patients histologically. In contrast, only 2 of 265 histologically confirmed cirrhotic livers were macroscopically without cirrhosis[14]. Ultrasound guided liver biopsy can result in a false negative histology due to the puncture of a regenerative nodule[15]. Cardi *et al.* showed superiority of laparoscopy over ultrasonography in diagnosis of widespread liver diseases[16]. Oberti *et al.* reported that only prothrombin index and serum hyalorunate were sensitive parameters for screening cirrhosis[17]. Early cirrhosis may often be missed due to clinical inappearance especially in patients with chronic HCV infection and accurate noninvasive markers of disease activity and fibrosis are not available[18]. The absence of early cirrhosis in chronic HCV infected patients might be a potential field for diagnostic laparoscopy that is not performed routinely and patients with early cirrhosis can be enrolled in the screening programs for HCC, too.

In the treatment of chronic HCV infection has proved beneficial interferon-alfa in the last two decades[19-23]. Old age, high level of viraemia, HCV genotype II (1b), long duration of disease, high levels of hepatic iron store, especially the advanced liver damage represented by dimension of fibrosis were considered to be negative predictive factors in the outcome of interferon treatment[22,24-34]. Two studies focused exclusively on interferon treatment in patients with HCV related cirrhosis[35,36]. After introduction of pegylated interferon given only once a week, HCV-infected patients with cirrhosis or bridging fibrosis were treated in a clinical trial[37]. These data implicated that HCV infected patients with liver cirrhosis need different therapeutic schedules with longer duration and higher dose of interferon.

Since cirrhosis is a negative predictor for antiviral therapy in chronic HCV-infected patients and liver histology might underestimate the frequency of cirrhosis, the aim of this retrospective study was to evaluate the potential of laparoscopy in the diagnosis of cirrhosis and outcome of interferon treatment in this particular group of patients.

MATERIALS AND METHODS

Patients

Laparoscopy and laparoscopic liver biopsy were performed in 72 chronic HCV-infected patients. Diagnosis of chronic HCV infection was based on elevated liver enzymes for at least 6 months, detection of anti-HCV antibodies in ELISA (2nd generation) and HCV RNA by RT/PCR. Patients with active viral coinfections (HBV, HIV, CMV, EBV), evidence for autoimmune hepatitis with positive serologic constellation of specific autoantibodies (ANA, AMA, anti-SLA, SMA, anti-LKM), alcohol and/or i.v. drug abusers and patients with signs of liver cirrhosis and/or hepatic decompensation (e.g. ascites, gastrointestinal bleeding, etc.) were excluded. Each patient was asked to sign a written informing consent for diagnostic laparoscopy and liver biospy.

Biochemical and serological analysis

Serum levels of ALT, AST, γ-GT, AP and CHE, as well as concentrations of serum bilirubin, prothrombin index, γ-globuline fraction and platelet count were measured by established routine methods before laparoscopy, during and after interferon treatment. Anti-HCV antibodies were analyzed using an ELISA (2nd generation, Ortho Diagnostic Systems, Raritan, NJ, USA) according to the instructions of the manufacturer.

Detection of HCV RNA and determination of HCV genotypes

According to Okamoto *et al.* and Simmonds *et al.*[38,39] determination of serum HCV RNA by a nested RT/PCR technique and determination of genotypes by a restriction enzyme analysis were carried out as described previously[40].

Laparoscopy

Abdominal ultrasound, electrocardiogram and, in patients older than 60 years, a chest X-ray were performed before laparoscopy. The evening before laparoscopy, each patient received 75 mg promethazin orally. Two hours before examination, 50 mg promethazin and 30 minutes before exploration 50 mg pethidin and 0.5 mg atropine were injected intramascularly. If necessary, patients received sedativa or analgetics during the laparoscopic intervention. During laparoscopy, each patient was given continuously an isotonic electrolyte solution intravenously. Patients were monitored by pulsoxymetry. After local anesthesia, the pneumoperitoneum was installed by puncturing at Monros' point with the Verres needle followed by insufflation of 2-3 L nitrous oxide. After insertion of the laparoscope in a trocar with a safety shield at Kalks' point, macroscopic exploration of liver, spleen and peritoneum followed. Liver biopsies were taken generally from an area on the anterior surface of the left lobe of the liver or of macroscopic suspect areas using a Menghini needle, at least 2 cm from the liver edge, containing at least five portal areas. Macroscopic diagnosis of cirrhosis was made based on the following criteria: (1) diffuse nodules on the liver surface, or (2) shallow nodules (i.e., nodules usually of large diameter, slightly protruding from the liver surface) if the liver was hard on palpation and rigid on lifting with a blunt probe and if clearcut features of portal hypertension were observed[41,42].

Histopathological evaluation

Formalin-fixed and paraffin-embedded liver biopsies were stained with hematoxylin-eosin, trichrome and by applying the Prussian blue reaction as described previously[43]. One pathologist examined samples unblindedly. A modified "Histology Activity Index" (HAI) on the basis of reported staging scores served to assess the stage of fibrosis[44-46]. Absent portal fibrosis was staged as fibrosis score I (HAI^b=0, no fibrosis), mild to moderate fibrosis as stage II (HAI^b=1, fibrotic portal expansion), marked fibrosis as stage III (HAI^b=3, bridging fibrosis) and complete fibrosis as cirrhosis (HAI^b=4).

Interferon treatment

Patients received recombinant interferon-alfa 2a (Roferon A, Hoffmann-La Roche, Basel, Switzerland) for initial treatment of chronic HCV infection. In our retrospective study, a dose of 6 MU three times a week was administered for 12 months according to Chemello *et al*[47]. Patients were classified as sustained responders if serum transaminases normalized (biochemical response) and serum HCV RNA became undetectable (virological response) during the treatment and at 6 months after the end of treatment (follow-up). During the follow-up, the re-emergence of both parameters after the end of treatment was defined as relapse. Patients with no improvement of biochemical or virological parameters within the first 3 months of treatment were classified as non-responders and treatment was stopped. For statistical analysis patients with relapse and non-response were classified as non-responders and compared with sustained responders. Patients who finished their course of treatment and 6 months of follow-up after the end of treatment were analysed.

Statistical analysis

Significant levels of differences between values were analyzed using the Chi-square test, Mann-Whitney test and student' s *t*-test as indicated.

RESULTS

Mean (M±SD) age of the 72 patients (49 % female, 51 % male) with chronic HCV infection was 46.8±12.1 years with a range of 27-72 years. Route and date of HCV infection were identified in 44 patients. The duration of HCV infection was 15.4±9.7 years and route of viral transmission was blood transfusion in 23 %, intravenous drug abuse in 18 % and anti-D prophylaxis in 3 %.

Laparoscopy found no severe complications. Liver biopsy caused mild bleeding in 6 (8 %) patients which was controlled during laparoscopy by local compression. None of the patients required blood transfusion. One patient developed a mesenteric emphysema after insufflation of nitrous oxide.

Cirrhosis was found by laparoscopy in 21/72 (29.2 %) patients and by histology in 8/72 (11.1 %) patients. According to HAI, patients with macroscopic cirrhosis by laparoscopy (n=21) showed histologically fibrosis stage I in 14.3 % (3/21), fibrosis stage II in 19 % (4/21), fibrosis stage III in 28.6 % (6/21) and cirrhosis in 38,1 % (8/21) (Table 1). Therefore 13/21 (61.9 %) macroscopic cirrhosis was not identified histologically. No cirrhosis was detected by laparoscopy in 51/72 (70.8 %) patients. According to HAI, patients without macroscopic cirrhosis (n=51) showed histologically fibrosis stage I in 58.8 % (30/51), fibrosis stage II in 31.4 % (16/51), fibrosis stage III in 9.8 % (5/51) and cirrhosis in 0 (0/51).

For statistical analysis, patients were divided into two groups. Group A represented patients with macroscopic cirrhosis (n=21) and group B patients without macroscopic cirrhosis (n=51) diagnosed by laparoscopic criteria. The mean (M±SD) age of patients in group A was 56.4±9.4 years, being significantly higher than in group B aged 41.7±11.2 years (P<0.02). There were 10 men and 11 women in group A and 27 men and 24 women in group B (n.s.). Mean (M±SD)

duration of chronic HCV infection in 44 patients of group A was 23.2±8.3 years, being significantly longer than in patients without macroscopic cirrhosis (group B) aged 10.4±5.7 years (P<0.02) (Table 2). In blood chemistry, patients of group A had significantly higher AST, γ-GT and γ-globulin fraction in serum electrophoresis as well as significant lower prothrombin index and platelet count than patients of group B. No significant differences were found for ALT, AP, bilirubin and cholinesterasis in both groups (Table 3). According to the Child-Pugh-Turcotte classification, 18 of the 21 patients with macroscopic cirrhosis were classified as Child A, 3 Child B and none Child C. In comparison of histological cirrhosis (8/21) and histologic non cirrhosis (13/21) of group A with macroscopic cirrhosis (n=21), significant differences were only found in AST and y-GT (Table 4). Differences were not significant in prothrombin index, y-globuline fraction and platelet count between cirrhosis (8/21) and histologic non-cirrhosis (13/21) of group A with macroscopic cirrhosis (n=21) (Table 4).

Table 1 Outcome of macroscopic laparoscopic exploration and histological analysis in 72 patients with chronic HCV infection

Histology (fibrosis stage score)	Laparoscopy	
	Patients without signs of cirrhosis (n=51)	Patients with signs of cirrhosis (n=21)
Fibrosis I	30	3
Fibrosis II	16	4
Fibrosis III	5	6
Cirrhosis	0	8

Absent portal fibrosis was judged as fibrosis score I (HAI[b]=0, no fibrosis), mild to moderate fibrosis as stage II (HAI[b]=1, fibros portal expansion), marked fibrosis as stage III (HAI[b]=3, bridging fibrosis), and complete fibrosis as cirrhosis (HAI[b]=4).

Table 2 Demographic and clinical data of patients with and without laparoscopically diagnosed cirrhosis

	Laparoscopy		P
	Patients with signs of Cirrhosis (n=21)	Patients without signs of Cirrhosis (n=51)	
Age (years)	56.36±9.42	41.7±11.2	<0.02[a]
Duration of disease (years) (n=44)	23.2±8.3	10.4±5.68	<0.02[a]
Sex ratio (m / f)	10 / 11	27 / 24	ns

[a]Student's t-test (unpaired); ns=not significant, years were showed as mean ± standard deviation. Duration of disease could be evaluated in 44 cases by patients' history.

Table 3 Laboratory data of patients with and without laparoscopic macroscopic evidence of cirrhosis

Laboratory data	Laparoscopy		P
	Patients with evidence of cirrhosis (n=21)	Patients without evidence of cirrhosis (n=51)	
AST (U / l)	59.7±54.2	29.3±19.6	< 0.02
ALT (U / l)	82.5±70.3	72.6±47.2	ns
γ-GT (U / l)	72.6±78.4	34.1±38.2	< 0.02
AP (U / l)	129.8±48.9	137.5±49.6	ns
Bilirubin (mg / dl)	1.1±0.93	1.86±6.23	ns
CHE (U / l)	5114±1331	5910±1001	ns
Prothrombin index (%)	93.8±12.6	102.2±6.3	<0.02
γ-globuline fraction (%)	19.9±6.5	13.7±2.9	<0.02
Platelet count (cell / µl)	172 940±65068	253 230±57096	<0.02

All data were showed as mean ± standard deviation. Statistical analysis was performed by applying Mann-Whitney test. ns=not significant.

Table 4 Comparing laboratory data of patients with macroscopic laparoscopic signs of cirrhosis

Laboratory data	Histological analysis		P
	No cirrhosis (n=13)	Cirrhosis (n=8)	
AST (U / l)	35.9±24.9	87.7±67.8	<0.02
ALT (U / l)	64.9±72.2	97.0±66.34	ns
γ-GT (U / l)	51.64±39.78	103.0±104.6	<0.02
AP (U / l)	126.3±54.6	144.6±39.6	ns
Bilirubin (mg / dl)	0.36±0.5	1.4±3.438	ns
CHE (U / l)	5129±1861	4685±1773	ns
Prothrombin index (%)	95.8±10.6	90.7±14.3	ns
γ-globuline fraction (%)	16.3±3.2	19.6±10.6	ns
Platelet count (cells / µl)	180 700±56 240	167 000±77 110	ns

All data were showed as mean ± standard deviation, statistical analysis were performed by Mann-Whitney test. ns=not significant.

Thirty-nine patients were treated with interferon-alfa 2a and followed up for 6 months after the end of treatment. HCV genotyping was performed in all 39 patients before start of therapy. HCV genotype II (1b) was the predominat genotype. The HCV genotypes of the 39 patients were 23 II (1b), 5 I (1a), 3 IV (2b), 5 V (3a) and 3 I (1a) combined with II (1b). Patients with macroscopic cirrhosis showed no significant difference of genotype distribution as compared with patients without cirrhosis. Interferon treatment resulted in 14/39 (35.9 %) sustained responders and 25/39 (64.1 %) non-responders including 2 relapsers. According to HCV genotype distribution, a significant higher rate of genotype II (1b) was observed in non-responders than sustained responders (P<0.02). Non-responders had a higher rate of macroscopic cirrhosis than sustained responders (P<0.02) (Table 5).

Table 5 Comparisons in pretreatment parameters between patients with sustained response and patients with non-response to interferon treatment (n=39)

	Sustained-responders	Non-responders	P
Number (%)	14 (35.9 %)	25 (64.1 %)	
Age (years)	50.6±13.9	47.2±10.6	ns
Genotype 1b (%)	5 (35.7 %)	18 (72 %)	<0.02[a]
Fibrosis staging score (%)			
I	7 (50.0 %)	9 (36.0 %)	
II	3 (21.4 %)	8 (32.0 %)	
III	3 (21.4 %)	3 (12.0 %)	
Cirrhosis	1 (7.0 %)	5 (20.0 %)	ns
Laparoscopic evidence of cirrhosis (%)	2 (14.2 %)	9 (36.0 %)	<0.02[a]

Data of age were showed as mean ± standard deviation; [a]Chi-square test, ns=not significant.

DISCUSSION

Diagnostic laparoscopy is recommended in the diagnosis of peritoneal diseases, evaluation of ascites of unknown origin, staging of abdominal cancer and chronic and focal liver disease[48]. Laparoscopy is commonly not performed for the diagnosis of cirrhosis in patients with chronic HCV. The availability of percutaneous liver biospy guided by ultrasound, CT- or MRI-scan offers selected biopsy of an suspicious area in the liver. The rate of laparoscopic liver biopsies in gastroenterology declined and also the number of training programs for this procedure[49]. However, all imaging procedures do not allow a direct viewing of the liver. The direct

visual inspection of the liver and the abdomen is the privilege of laparoscopy.

In this study, more chronic HCV infected patients had been diagnosed of cirrhosis macroscopically by laparoscopic inspection of the liver than histologically by using the Menghini needle for laparoscopic liver biopsy. All patients with histological cirrhosis also had cirrhosis macroscopically, but 13/21 patients with macroscopic cirrhosis had no cirrhosis histologically. This discrepancy implicates an underestimation of cirrhosis in chronic HCV-infected patients, if diagnosis of cirrhosis is based only on liver biopsy using the Menghini needle. Poniachik *et al.* investigated the role of laparoscopy and laparoscopic liver biopsy in the diagnosis of cirrhosis in 434 patients with chronic liver disease including 169 patients with laparoscopic evidence of cirrhosis. The histological sampling error was 32 % among patients documented to have cirrhosis by laparoscopy[14]. The selection of a suction or cutting needle for liver biopsy has a major impact at the stage of cirrhosis. The use of a cutting needle like Vim-Silverman or Tru-Cut is reported to give a more representive histology than suction needles like Menghini, Klatskin or Jamshidi, because fibrotic tissue tends to fragment with the use of suction needle[49,50]. In a randomized study on 1192 patients with diffuse liver disease, Colombo *et al* investigated percutaneous liver biopsies comparing the Tru-Cut and the Menghini needle. For diagnosing cirrhosis accuracy of the Tru-Cut needle is significantly better (89.5 %) than the Menghini needle (65.5 %). Complication rates were very low with both needles[51].

Comparing laparoscopy and laparoscopic biopsy for diagnosis of cirrhosis, laparoscopic diagnosis of macroscopic cirrhosis was of higher value than histological diagnosis of microscopic cirrhosis regarding blood chemistry and the response to interferon therapy. The rate of non-response to interferon therapy was 64.1 % in our study. Significant parameters for non-response were genotype II (1b) and laparoscopic evidence of cirrhosis, but not histological diagnosis of cirrhosis. Nowadays, new therapeutic regimes have replaced interferon monotherapy. The combination of interferon-alfa with ribavirin improved sustained response rate for chronic HCV-infected patients[52] and for relapsers and non-responders after initially interferon monotherapy[53-55]. Increased efficacy was shown with pegylated interferon as compared with standard interferons in cirrhotic and noncirrhotic patients with chronic hepatitis C[37,56,57] and currently standard therapy is pegylated interferon in combination with ribavirin[8]. In this treatment situation, the role of liver biopsy has increasingly been discussed[58]. If patients with positive predictors of virological response, such as low viral load and infection with genotype 2 or 3, can be treated and have very high chances of response, a biopsy that reveals mild histologic changes may do little to dissuade the clinician and patients from immediate treatment[8]. Liver biopsy may become recommended only in those patients whose pretreatment characteristics predict the lowest success rate[8]. Paired liver biopsy specimens enable staging of inflammation and fibrosis before and after treatment to define histological response in those patients. Compaired with our data, the rate of cirrhosis before treatment will be underestimated without performing laparoscopy in those patients. Both procedures, liver biopsy and laparoscopy, are invasive, but accurate noninvasive markers for staging disease activity, fibrosis and cirrhosis are not available[18]. Our rate of complications related to laparoscopy and laparoscopic liver biopsy was 10 % and no severe complication was observed. These data are in accordance with other reports[11,42,59-62]. The rate of severe complications using blind percutaneous liver biopsy is reported to be 0.3-1.5 % and is almost comparable with laparoscopic liver biopsy[41,63-67]. Diagnostic laparoscopy and laparoscopic liver biopsy are a safe and invasive procedure in patients with compensated liver disease. Minilaparoscopy has increasingly emerged as a less invasive diagnostic method in this field[68].

Based on our data, diagnostic laparoscopy is indicated for recognition of early cirrhosis in patients with chronic HCV infection. In fact, as early diagnosis of cirrhosis affects management of chronic HCV infected patients, it should be the key factor in the decision-making process.

REFERENCES

1 **Alter MJ**, Margolis HS, Krawczynski K, Judson FN, Mares A, Alexander WJ, Hu PY, Miller JK, Gerber MA, Sampliner RE. The natural history of community-acquired hepatitis C in the united states. the sentinel counties chronic non-A, non-B hepatitis study team. *N Engl J Med* 1992; **327**: 1899-1905

2 **Hoofnagle JH**. Hepatitis C: the clinical spectrum of disease. *Hepatology* 1997; **26**: 15S-20S

3 **Ramadori G**, Meier V. Hepatitis C virus infection: 10 years after the discovery of the virus. *Eur J Gastroenterol Hepatol* 2001; **13**: 465-471

4 **Dore GJ**, Freeman AJ, Law M, Kaldor JM. Is severe liver disease a common outcome for people with chronic hepatitis C? *J Gastroenterol Hepatol* 2002; **17**: 423-430

5 **Di Bisceglie AM**, Goodman ZD, Ishak KG, Hoofnagle JH, Melpolder JJ, Alter HJ. Long-term clinical and histopathological follow-up of chronic posttransfusion hepatitis. *Hepatology* 1991; **14**: 969-974

6 **Zeuzem S**, Roth WK, Herrmann G. Viral hepatitis C. *Z Gastroenterol* 1995; **33**: 117-132

7 **Di Bisceglie AM**. Hepatitis C and hepatocellular carcinoma. *Hepatology* 1997; **26**: 34S-38S

8 **Herrine SK**. Approach to the patient with chronic hepatitis C virus infection. *Ann Intern Med* 2002; **136**: 747-757

9 **Gaiani S**, Gramantieri L, Venturoli N, Piscaglia F, Siringo S, D'Errico A, Zironi G, Grigioni W, Bolondi L. What is the criterion for differentiating chronic hepatitis from compensated cirrhosis? A prospective study comparing ultrasonography and percutaneous liver biopsy. *J Hepatol* 1997; **27**: 979-985

10 **Regev A**, Berho M, Jeffers LJ, Milikowski C, Molina EG, Pyrsopoulos NT, Feng ZZ, Reddy KR, Schiff ER. Sampling error and intraobserver variation in liver biopsy in patients with chronic HCV infection. *Am J Gastroenterol* 2002; **97**: 2614-2618

11 **Jalan R**, Harrison DJ, Dillon JF, Elton RA, Finlayson ND, Hayes PC. Laparoscopy and histology in the diagnosis of chronic liver disease. *QJ Med* 1995; **88**: 559-564

12 **Nord HJ**. Biopsy diagnosis of cirrhosis: blind percutaneous versus guided direct vision techniques-a review. *Gastrointest Endosc* 1982; **28**: 102-104

13 **Vido I**, Wildhirt E. Correlation of the laparoscopic and histological findings in chronic hepatitis and liver cirrhosis. *Dtsch Med Wochenschr* 1969; **94**: 1633-1637

14 **Poniachik J**, Bernstein DE, Reddy KR, Jeffers LJ, Coelho-Little ME, Civantos F, Schiff ER. The role of laparoscopy in the diagnosis of cirrhosis. *Gastrointest Endosc* 1996; **43**: 568-571

15 **Mossner J**. Laparoscopy in differential internal medicine diagnosis. *Z Gastroenterol* 2001; **39**: 1-6

16 **Cardi M**, Muttillo IA, Amadori L, Petroni R, Mingazzini P, Barillari P, Lisi D, Bolognese A. Superiority of laparoscopy compared to ultrasonography in diagnosis of widespread liver diseases. *Dig Dis Sci* 1997; **42**: 546-548

17 **Oberti F**, Valsesia E, Pilette C, Rousselet MC, Bedossa P, Aube C, Gallois Y, Rifflet H, Maiga MY, Penneau-Fontbonne D, Cales P. Noninvasive diagnosis of hepatic fibrosis or cirrhosis. *Gastroenterology* 1997; **113**: 1609-1616

18 **Saadeh S**, Cammell G, Carey WD, Younossi Z, Barnes D, Easley K. The role of liver biopsy in chronic hepatitis C. *Hepatology* 2001; **33**: 196-200

19 **Davis GL**, Balart LA, Schiff ER, Lindsay K, Bodenheimer HC Jr, Perrillo RP, Carey W, Jacobson IM, Payne J, Dienstag JL. Treatment of chronic hepatitis C with recombinant interferon alfa. A multicenter randomized, controlled trial. Hepatitis Interventional Therapy Group. *N Engl J Med* 1989; **321**: 1501-1506

20 **Di Bisceglie AM**, Martin P, Kassianides C, Lisker-Melman M, Murray L, Waggoner J, Goodman Z, Banks SM, Hoofnagle JH. Recombinant interferon alfa therapy for chronic hepatitis C. A randomized, double-blind, placebo-controlled trial. *N Engl J Med* 1989; **321**: 1506-1510

21 **Poynard T**, Leroy V, Cohard M, Thevenot T, Mathurin P, Opolon P, Zarski JP. Meta-analysis of interferon randomized trials in the treatment of viral hepatitis C: effects of dose and duration. *Hepatology* 1996; **24**: 778-789

22 **Hoofnagle JH**, di Bisceglie AM. The treatment of chronic viral hepatitis. *N Engl J Med* 1997; **336**: 347-356

23 **Saracco G**, Borghesio E, Mesina P, Solinas A, Spezia C, Macor F, Gallo V, Chiandussi L, Donada C, Donadon V, Spirito F, Mangia A, Andriulli A, Verme G, Rizzetto M. Prolonged treatment (2 years) with different doses (3 versus 6 MU) of interferon alpha-2b for chronic hepatitis type C. Results of a multicenter randomized trial. *J Hepatol* 1997; **27**: 56-62

24 **Mizokami M**, Orito E, Gibo Y, Suzuki K, Ohba K, Ohno T, Lau JY. Genotype, serum level of hepatitis C virus RNA and liver histology as predictors of response to interferon-alpha 2a therapy in Japanese patients with chronic hepatitis C. *Liver* 1996; **16**: 23-27

25 **Rumi M**, Del Ninno E, Parravicini ML, Romeo R, Soffredini R, Donato MF, Wilber J, Russo A, Colombo M. A prospective, randomized trial comparing lymphoblastoid to recombinant interferon alfa 2a as therapy for chronic hepatitis C. *Hepatology* 1996; **24**: 1366-1370

26 **Jouet P**, Roudot-Thoraval F, Dhumeaux D, Metreau JM. Comparative efficacy of interferon alfa in cirrhotic and noncirrhotic patients with non-A, non-B, C hepatitis. Le Groupe Francais pour l'Etude du Traitement des Hepatites Chroniques NANB/C. *Gastroenterology* 1994; **106**: 686-690

27 **Pagliaro L**, Craxi A, Cammaa C, Tine F, Di Marco V, Lo Iacono O, Almasio P. Interferon-alpha for chronic hepatitis C: an analysis of pretreatment clinical predictors of response. *Hepatology* 1994; **19**: 820-828

28 **Tsubota A**, Chayama K, Ikeda K, Yasuji A, Koida I, Saitoh S, Hashimoto M, Iwasaki S, Kobayashi M, Hiromitsu K. Factors predictive of response to interferon-alpha therapy in hepatitis C virus infection. *Hepatology* 1994; **19**: 1088-1094

29 **Martinot-Peignoux M**, Marcellin P, Pouteau M, Castelnau C, Boyer N, Poliquin M, Degott C, Descombes I, Le Breton V, Milotova V. Pretreatment serum hepatitis C virus RNA levels and hepatitis C virus genotype are the main and independent prognostic factors of sustained response to interferon alfa therapy in chronic hepatitis C. *Hepatology* 1995; **22** (4 Pt 1): 1050-1056

30 **Nousbaum JB**, Pol S, Nalpas B, Landais P, Berthelot P, Brechot C. Hepatitis C virus type 1b (II) infection in France and Italy. Collaborative Study Group. *Ann Intern Med* 1995; **122**: 161-168

31 **Kanazawa Y**, Hayashi N, Mita E, Li T, Hagiwara H, Kasahara A, Fusamoto H, Kamada T. Influence of viral quasispecies on effectiveness of interferon therapy in chronic hepatitis C patients. *Hepatology* 1994; **20**: 1121-1130

32 **Enomoto N**, Sakuma I, Asahina Y, Kurosaki M, Murakami T, Yamamoto C, Izumi N, Marumo F, Sato C. Comparison of full-length sequences of interferon-sensitive and resistant hepatitis C virus 1b. Sensitivity to interferon is conferred by amino acid substitutions in the NS5A region. *J Clin Invest* 1995; **96**: 224-230

33 **Van Thiel DH**, Friedlander L, Fagiuoli S, Wright HI, Irish W, Gavaler JS. Response to interferon alpha therapy is influenced by the iron content of the liver. *J Hepatol* 1994; **20**: 410-415

34 **Shindo M**, Arai K, Okuno T. The clinical value of grading and staging scores for predicting a long-term response and evaluating the efficacy of interferon therapy in chronic hepatitis C. *J Hepatol* 1997; **26**: 492-497

35 **Valla DC**, Chevallier M, Marcellin P, Payen JL, Trepo C, Fonck M, Bourliere M, Boucher E, Miguet JP, Parlier D, Lemonnier C, Opolon P. Treatment of hepatitis C virus-related cirrhosis: a randomized, controlled trial of interferon alfa-2b versus no treatment. *Hepatology* 1999; **29**: 1870-1875

36 **Shiratori Y**, Yokosuka O, Nakata R, Ihori M, Hirota K, Katamoto T, Unuma T, Okano K, Ikeda Y, Hirano M, Kawase T, Takano S, Matsumoto K, Ohashi Y, Omata M. Prospective study of interferon therapy for compensated cirrhotic patients with chronic hepatitis C by monitoring serum hepatitis C RNA. *Hepatology* 1999; **29**: 1573-1580

37 **Heathcote EJ**, Shiffman ML, Cooksley WG, Dusheiko GM, Lee SS, Balart L, Reindollar R, Reddy RK, Wright TL, Lin A, Hoffman J, De Pamphilis J. Peginterferon alfa-2a in patients with chronic hepatitis C and cirrhosis. *N Engl J Med* 2000; **343**: 1673-1680

38 **Okamoto H**, Sugiyama Y, Okada S, Kurai K, Akahane Y, Sugai Y, Tanaka T, Sato K, Tsuda F, Miyakawa Y. Typing hepatitis C virus by polymerase chain reaction with type-specific primers: application to clinical surveys and tracing infectious sources. *J Gen Virol* 1992; **73**: 673-679

39 **Simmonds P**, McOmish F, Yap PL, Chan SW, Lin CK, Dusheiko G, Saeed AA, Holmes EC. Sequence variability in the 5'non-coding region of hepatitis C virus: identification of a new virus type and restrictions on sequence diversity. *J Gen Virol* 1993; **74** (Pt 4): 661-668

40 **Polzien F**, Schott P, Mihm S, Ramadori G, Hartmann H. Interferon-alpha treatment of hepatitis C virus-associated mixed cryoglobulinemia. *J Hepatol* 1997; **27**: 63-71

41 **Pagliaro L**, Rinaldi F, Craxi A, Di Piazza S, Filippazzo G, Gatto G, Genova G, Magrin S, Maringhini A, Orsini S, Palazzo U, Spinello M, Vinci M. Percutaneous blind biopsy versus laparoscopy with guided biopsy in diagnosis of cirrhosis. A prospective, randomized trial. *Dig Dis Sci* 1983; **28**: 39-43

42 **Henning H**, Look D. Laparoskopie: Atlas und Lehrbuch. *Stuttgart Thieme* 1985: 32-46

43 **Mihm S**, Fayyazi A, Hartmann H, Ramadori G. Analysis of histopathological manifestations of chronic hepatitis C virus infection with respect to virus genotype. *Hepatology* 1997; **25**: 735-759

44 **Knodell RG**, Ishak KG, Black WC, Chen TS, Craig R, Kaplowitz N, Kiernan TW, Wollman J. Formulation and application of a numerical scoring system for assessing histological activity in asymptomatic chronic active hepatitis. *Hepatology* 1981; **1**: 431-435

45 **Desmet VJ**, Gerber M, Hoofnagle JH, Manns M, Scheuer PJ. Classification of chronic hepatitis: diagnosis, grading and staging. *Hepatology* 1994; **19**: 1513-1520

46 **Ishak K**, Baptista A, Bianchi L, Callea F, De Groote J, Gudat F, Denk H, Desmet V, Korb G, MacSween RN. Histological grading and staging of chronic hepatitis. *J Hepatol* 1995; **22**: 696-699

47 **Chemello L**, Bonetti P, Cavalletto L, Talato F, Donadon V, Casarin P, Belussi F, Frezza M, Noventa F, Pontisso P. Randomized trial comparing three different regimens of alpha-2a-interferon in chronic hepatitis C. The TriVeneto Viral Hepatitis Group. *Hepatology* 1995; **22:** 700-706

48 **Nord HJ**. What is the future of laparoscopy and can we do without it? *Z Gastroenterol* 2001; **39**: 41-44

49 **Bravo AA**, Sheth SG, Chopra S. Liver biopsy. *N Engl J Med* 2001; **344**: 495-500

50 **Goldner F**. Comparison of the Menghini, Klatskin and Tru-Cut needles in diagnosing cirrhosis. *J Clin Gastroenterol* 1979; **1**: 229-231

51 **Colombo M**, Del Ninno E, de Franchis R, De Fazio C, Festorazzi S, Ronchi G, Tommasini MA. Ultrasound-assisted percutaneous liver biopsy: superiority of the Tru-Cut over the Menghini needle for diagnosis of cirrhosis. *Gastroenterology* 1988; **95**: 487-489

52 **McHutchison JG**, Gordon SC, Schiff ER, Shiffman ML, Lee WM, Rustgi VK, Goodman ZD, Ling MH, Cort S, Albrecht JK. Interferon alfa-2b alone or in combination with ribavirin as initial treatment for chronic hepatitis C. hepatitis interventional therapy group. *N Engl J Med* 1998; **339**: 1485-1492

53 **Davis GL**, Esteban-Mur R, Rustgi V, Hoefs J, Gordon SC, Trepo C, Shiffman ML, Zeuzem S, Craxi A, Ling MH, Albrecht J. Interferon alfa-2b alone or in combination with ribavirin for the treatment of relapse of chronic hepatitis C. International Hepatitis Interventional Therapy Group. *N Engl J Med* 1998; **339**: 1493-1499

54 **Cheng SJ**, Bonis PA, Lau J, Pham NQ, Wong JB. Interferon and ribavirin for patients with chronic hepatitis C who did not respond to previous interferon therapy: a meta-analysis of controlled and uncontrolled trials. *Hepatology* 2001; **33**: 231-240

55 **Wietzke-Braun P**, Meier V, Braun F, Ramadori G. Combination of "low-dose" ribavirin and interferon alfa-2a therapy followed by interferon alfa-2a monotherapy in chronic HCV-infected non-responders and relapsers after interferon alfa-2a monotherapy.

World J Gastroenterol 2001; **7**: 222-227

56 **Zeuzem S**, Feinman SV, Rasenack J, Heathcote EJ, Lai MY, Gane E, O'Grady J, Reichen J, Diago M, Lin A, Hoffman J, Brunda MJ. Peginterferon alfa-2a in patients with chronic hepatitis C. *N Engl J Med* 2000; **343**: 1666-1672

57 **Reddy KR**, Wright TL, Pockros PJ, Shiffman M, Everson G, Reindollar R, Fried MW, Purdum PP 3rd, Jensen D, Smith C, Lee WM, Boyer TD, Lin A, Pedder S, DePamphilis J. Efficacy and safety of pegylated (40-kd) interferon alpha-2a compared with interferon alpha-2a in noncirrhotic patients with chronic hepatitis C. *Hepatology* 2001; **33**: 433-438

58 **Griffiths A**, Viiala CH, Olynyk JK. Liver biopsy in the 21st century: where and why? *Med J Aust* 2002; **176**: 52-53

59 **Phillips RS**, Reddy KR, Jeffers LJ, Schiff ER. Experience with diagnostic laparoscopy in a hepatology training program. *Gastrointest Endosc* 1987; **33**: 417-420

60 **Adamek HE**, Maier M, Benz C, Huber T, Schilling D, Riemann JF. Severe complications in diagnostic laparoscopy. 9 years experience in 747 examinations. *Med Klin* 1996; **91**: 694-697

61 **Bruhl W**. Incidents and complications in laparoscopy and directed liver puncture. Result of a survey. *Dtsch Med Wochenschr* 1966; **91**: 2297-2299

62 **Leinweber B**, Korte M, Kratz F, Gerhardt H, Matthes KJ. Laparoscopy. Results and experiences. *Med Welt* 1975; **26**: 1762-1765

63 **Terry R**. Risk of needle biopsy of the liver. *Br Med J* 1952; **1**: 1102-1105

64 **Sherlock S**, Dick R, Van Leeuwen DJ. Liver biopsy today. the royal free hospital experience. *J Hepatol* 1985; **1**: 75-85

65 **Piccinino F**, Sagnelli E, Pasquale G, Giusti G. Complications following percutaneous liver biopsy. A multicentre retrospective study on 68,276 biopsies. *J Hepatol* 1986; **2**: 165-173

66 **Perrault J**, McGill DB, Ott BJ, Taylor WF. Liver biopsy: complications in 1000 inpatients and outpatients. *Gastroenterology* 1978; **74**: 103-106

67 **Knauer CM**. Percutaneous biopsy of the liver as a procedure for outpatients. *Gastroenterology* 1978; **74**: 101-102

68 **Helmreich-Becker I**, Meyer zum Buschenfelde KH, Lohse AW. Safety and feasibility of a new minimally invasive diagnostic laparoscopy technique. *Endoscopy* 1998; **30**: 756-762

Edited by Ma JY and Xu XQ

P.O.Box 2345, Beijing 100023, China
Fax: +86-10-85381893
E-mail: wjg@wjgnet.com www.wjgnet.com

World J Gastroenterol 2003;9(4):751-754
World Journal of Gastroenterology
 ISSN 1007-9327

• VIRAL HEPATITIS •

Effect of alpha 2b interferon on inducement of mIL-2R and treatment of HCV in PBMC from patients with chronic viral hepatitis C

Jian Wang, Gui-Ju Xiang, Bing-Xiang Liu

Jian Wang, Department of Aetiology and Immunology, Anhui University of Science and Technology, Huainan 232001, Anhui Province, China
Gui-Ju Xiang, Department of Infectious Diseases, the Second Miner Hospital of Huainan, Huainan 232001, Anhui Province, China
Bing-Xiang Liu, Department of Infectious Diseases, Shibei Hospital of Shanghai, Shanghai 200435, China
Supported by the grants from Science Foundation of the Ministry of Coal Industry of China, No. 96-072
Correspondence to: Jian Wang, Department of Aetiology and Immunology, Anhui University of Science and Technology, Huainan 232001, Anhui Province, China. wangjian8237@sina.com
Telephone: +86-0554-6659942
Received: 2002-07-31 **Accepted:** 2002-08-23

Abstract

AIM: To study the level of membrane interleukin-2 receptor (mIL-2R) on surface of peripheral blood mononuclear cells (PBMC) and the therapeutic efficacy of alpha 2b interferon on the treatment of HCV-RNA in PBMC of patients with chronic hepatitis C and to compare the negative rates of HCV-RNA in PBMC, HCV-RNA and anti-HCV in serum.

METHODS: Before and after treatment of alpha 2b interferon, the level of mIL-2R of patients with chronic hepatitis C was detected by biotin-streptavidin (BSA). The therapeutic group (26 cases) was treated with alpha 2b interferon (3 MU/d) and control therapeutic group (22 cases) was treated with routine drugs (VitC, aspartic acid). The total course of treatment with alpha 2b interferon and routine drug was six months and per course of the treatment was three months. The levels of HCV-RNA in PBMC, HCV-RNA and anti-HCV in serum were detected before and after a course of the treatment.

RESULTS: Before and after treatment of alpha 2b interferon and routine drugs, the levels of mIL-2R in silence stage were (3.44±0.77) % and (2.95±0.72) %, the levels of mIL-2R in inducement stage were (33.62±3.95) % and (30.04±3.73) %. There was a significant difference between two groups ($P<0.01$-$P<0.05$). After treatment of alpha 2b interferon with 3 MU/d for two courses of the treatment, the total negative rates of HCV-RNA in the PBMC and HCV-RNA, anti-HCV in serum were 42.31 % (11/26), 57.69 % (15/26), 65.38 %(17/26) respectively. After the treatment of routine drug, the negative rates of HCV-RNA in PBMC and HCV-RNA, anti-HCV in serum were 13.64 % (3/22), 22.73 % (5/22), 27.27 % (6/22) respectively. There was high significant difference in the group treated with alpha 2b interferon and the group treated with routine drugs ($P<0.01$-$P<0.05$).

CONCLUSION: The mIL-2R can be induced by alpha 2b interferon during the treatment. The alpha 2b interferon has a definite effect on the treatment of HCV-RNA in PBMC. The curative effect of alpha 2b interferon is better than that of the routine drugs.

Wang J, Xiang GJ, Liu BX. Effect of alpha 2b interferon on inducement of mIL-2R and treatment of HCV in PBMC from patients with chronic viral hepatitis C. *World J Gastroenterol* 2003; 9(4): 751-754
http://www.wjgnet.com/1007-9327/9/751.htm

INTRODUCTION

Treatment of interferon on the chronic viral hepatitis C has been shown to have a good curative effect on inhibition of HCV replication, reduction in transmission level in serum and liver cells[1-8], but the improvement in clinical condition was not obvious and its effective rate was only 50 %[9-17]. The curative effect of interferon was based on virostatic replication of HCV in serum and some improvement of liver function. The literatures show that the peripheral blood mononuclear cells (PBMC) have large different active immune cells and membrane interleukin-2 receptor (mIL-2R) is an important symbol of active T cells, and the immune function of PBMC will be inhibited after being infected by HCV and the scavenging effect limited[18,19]. In order to study the effect of interferon on treatment of HCV in PBMC and the effect of interferon on inducement to mIL-2R, forty-eight patients with typical chronic hepatitis C were observed.

MATERIALS AND METHODS

Clinical data

Forty-eight patients with chronic viral hepatitis C were selected from the Second Miner Hospital of Huainan and our teaching hospital during 1997/03-2000/05. The total number of patients was 48 (male 27, female 21) and range of age was from 18 to 57 years old (average 37.3). The clinical diagnosis was based on the modified diagnosis criterion being affirmed on the Chinese viral hepatitis conference in Xian (2000). The patients all needed the following qualifications: (1) The positivity of anti-HCV in serum for more than six months. (2) The HCV-RNA in peripheral blood mononuclear cells and serum were positive. (3) The patients had been eliminated the infection of hepatitis A, B, D, E and G viruses. (4) There were no any systemic treatment of antiviral medicine, immunomodulator, cortical hormone for the patients. The normal control was 20 healthy students (male 12, female 8) with range age from 20 to 23 years old (average 22.5).

Treatment medicine

The alpha 2b interferon was produced by High Science and Technology of Anke Biology in Anhui Province.

Treatment methods

The patients with chronic hepatitis C were divided into two groups with treatment of alpha 2b interferon 3MU (26 cases)

and routine medicine (22 cases) respectively. The total course of treatment lasted sixty months, and per course was three months. Alpha 2b interferon was given intramuscularly injection (im) qd for two weeks and then alt dieb for two courses of treatment. The routine treatment group (22 cases) was given with Vit C, Aspactic acid, etc for six months.

Reagents

The diagnostic reagent of anti-HCV was purchased from Huamei Bioengineering Company of Shanghai, No:980811. The diagnostic reagent of HCV-RNA with RT-PCR was purchased from Shanghai Zhongya Gene Institute, No: 980805. The diagnostic reagent of mIL-2R was purchased from Immunology Institute of Shanghai. The lymphocytes separation medium was purchased from the Second Reagent Factory of Shanghai, No:970505. The reagent of PRMI 1640 culture was produced by Sigma (USA).

Instruments

The analysis instrument of Spector-I was made in USA; MDF-135 CO_2 incubator was made in Japan; The instrument for gene amplification (Hema-8000) was made in Hema Company of China.

Methods

The total volume of 5 ml peripheral venous blood from patients with hepatitis C before breakfast was taken before and after treatment, and distributed a sterile Eppendorf tube and an anticoagulant tube (heparin) respectively. For detection of anti-HCV, the process was performed strictly according to the direction, and with two blank, two negative and two positive pores as controls in each test. The average titer was examined by the analyser Spector-I. The average OD titer of test sample $\geqslant$2.1 times of average OD titer in negative control was considered to be positive. Detection of HCV-RNA in PBMC with RT-nested-PCR: After the heparin anticoagulant blood mixed with the equal volume Hank' s liquid without Ca^{2+} and Mg^{2+}, lymphocytes separation medium was used to separate the PBMC. The cells were washed twice with Hank' s liquid without Ca^{2+}, Mg^{2+} and diluted to (1-3)×10^6/ml before detection of HCV-RNA. A positive and a negative control were set up at the same time for comparison in each test. The RT-nested-PCR was made by reverse transcription and primer selected from non-coded region and part of C region of HCV. The specific amplificated fragment length was 248 bp. The synthesis parameters for cDNA were 94 ℃ 40 s, 55 ℃ 40 s, 72 ℃ 1 min, for 30 circles. The amplification parameters for cDNA were 94 ℃ 50 s, 55 ℃ 40 s and 72 ℃ 90 s, 35 circles, including initial denaturation for 4 min at 94 ℃ and last extension for 5 min at 72 ℃. The amplification product was run for electrophoresis on gel with 2 % EB. The result that was uniform to the positive control was considered to be positive. The detection of mIL-2R in silence and inducement stages: 10 μl suspension of the PBMC was smeared on the slide and left dry naturally and fixed with acetone for fifteen minutes or twenty minutes. The 10 μl anti-Tac antibody was mixed with the membrane of smears. The cells were grown in continuous culture (37 ℃, 50 ml· L^{-1} CO_2 in atmosphere) for thirty minutes. The immune sheet glass pores were measured after staining with the color-developing agent and several washings with Tris Buffer Solution (TBS). Of the PBMC suspension, 0.5 ml was mixed with RPMI 1640 culture liquid, which had PHA 200 mg· L^{-1}. The cells were grown in continuous culture (37 ℃,50 ml· L^{-1} CO_2 in atmosphere) 72 h and its mIL-2R induced by PHA could be measured by the antibodies against membrane of T cells. The Tac with biotin and SA-HRP were smeared on different sheet glasses. The immune sheet glass pores were measured after staining with the color-developing agent and several washings with TBS. The total number of 200 PBMC was counted and its positive cells were statistically analyzed with the help of high power lens. The positive criterion was that the color of cytoplasm or cell membrane was brown.

Statistical analysis

Statistical analysis included analysis of Chi-square (χ^2) and *t* test.

RESULTS

The forty-eight patients with chronic hepatitis C were divided into two groups and treated with alpha 2b interferon (26 cases) and routine drugs (22 cases) respectively. The results had been shown that the high negative rates of anti-HCV and HCV-RNA in serum were in the group with treatment of alpha 2b interferon. There was very significant difference before and after treatment of alpha 2b interferon (P<0.01-P<0.05, Table 1). The negative rate of HCV-RNA between in PBMC and in serum was similar (P>0.05, Table 2). The level of mIL-2R in situation of silence and inducement stages after treatment with alpha 2b interferon was higher than that after treatment with routine drugs (P<0.05, Table 3).

Table 1 The detective results of HCV-RNA in serum and PBMC after treatment with alpha 2b interferon (*n*, %)

Group	*n*	HCV-RNA in PBMC		HCV-RNA in serum		Anti-HCV	
		Negative	Negative rate	Negative	Negative rate	Negative	Negative rate
Interferon treatment	26	11	42.31[a]	15	57.69[a]	17	65.38[b]
Routin treatment	22	3	13.64	5	22.73	6	27.27

[a]P<0.05, [b]P<0.01 *vs* interferon treatment.

Table 2 The results of negative rate of HCV-RNA in serum and PBMC

HCV-RNA in serum	HCV-RNA in PBMC		Total	χ^2	*P*
	+	-			
+	7	4	11		
-	8	7	15	0.75	>0.05
Total	15	11	26		

Table 3 The level of mIL-2R before and after treatment of interferon (*n*, $\bar{x}$±s, %)

Group	*n*	mIL-2R (in silence)		mIL-2R (inducement)	
		Before treatment	After treatment	Before treatment	After treatment
Interferon treatment	26	2.63±0.70	3.44±0.77[bcd]	30.34±3.55	33.62±3.95[cd]
Routin treatment	22	2.43±0.78	2.95±0.72[ad]	30.07±3.87	30.04±3.73[d]
Normal control	20	4.54±1.48		37.42±4.10	

[a]P<0.05, [b]P<0.01 *vs* before and after treatment, [c]P<0.05, [d]P<0.01 *vs* interferon treatment.

DISCUSSION

There are three kinds of interferon, α, β, γ. Interferon alpha is the most active one. Alpha 2b interferon can not enter into the host cells and kill the virus directly, but can induce the production of protein kinase (2' , 5' AS) in the infected cells.

The protein kinase and 2' , 5' AS can be produced after being infected by virus in cells. The degradation of virus-RNA can be made by endogenous ednonuclease induced with activated 2' , 5' AS so that the necessary enzyme activity for synthesis of ribose is killed, the synthetic protein of virus can be decreased, the growth of hepatitis virus C is inhibited[20-30].

The reports have been shown that interferon has definite curative effect of the treatment of chronic hepatitis C and elimination of HCV-RNA, anti-HCV in serum. Therefore, HCV-RNA is an important index to evaluate condition of the patient' s[4]. HCV-RNA in PBMC is a direct evidence of the existence of extrahepatic or latent infection, and is one of important reasons causing the chronicity of viral hepatitis C[28-31]. The results of Table 1 had shown that the rate of change HCV-RNA into negative in PBMC and serum after treatment of alpha 2b interferon was similar between two groups (P>0.05). The curative effect was higher in the treatment group with alpha 2b interferon than that with routine treatment (P<0.05-P<0.01). This result had showed that the inducing capability of alpha 2b interferon in lymphocytes of the patients was strong, and the high effect against HCV would be taken by activated lymphocytes obviously. Although the negative rate of HCV-RNA in PBMC was lower than that in serum, there was no significant difference (P>0.05). The results had shown that alpha 2b interferon had high effect on HCV-RNA both in PBMC and in serum. There were four cases of chronic hepatitis C with negative in serum and positive in PBMC. It indicated that with the T lymphocytes activation, multiple cell factors were released, that inhibited the replication of free HCV-RNA in serum, but not the HCV-RNA in PBMC. The cellular immune function was disorder in different extent in patients with chronic hepatitis C and so was their response to interferon and anti-HCV[32-37]. Otherwise, the low level of membrane interleukin-2 receptor (mIL-2R) on the surface of PBMC decreased the activity in chronic hepatitis C, which limited the inducement of protein kinase and the activity of 2' , 5' AS to eliminate HCV-RNA[38].

Anti-HCV is an important index for the diagnosis of HCV and is one of the evidences for evaluating the curative effect on the treatment of hepatitis C. The anti-HCV diagnostic kits of the second generation were used in our laboratory testing for core antigen, NS_3, NS_4 and had high specificity and sensitivity[39,40]. The rate of negative change of HCV-RNA was higher in alpha 2b interferon treatment group than that in routine treatment group (P<0.01). Among the twenty-six cases, there were six cases with anti-HCV(-) in serum and HCV-RNA (+) in PBMC, two cases with anti-HCV(-) in serum and HCV-RNA(+) in serum. This result showed that even the anti-HCV in serum became negative, HCV-RNA not stopping replication completely, some HCV-RNA could still be detected in some patients[6]. The probable reasons were: (1) After being treatment of alpha 2b interferon, the level of anti-HCV in serum decreased obviously and could not be detected by routine test. (2) The degree of variation of HCV is high, the hydrophilic peptid chain on core protein is subjective to escape the attack of CTL and keep the infection persist in chronic state. (3) The variant antigen of HCV can not match the antibody produced.

mIL-2R is an important symbol of active T cells and plays key role on biologic effect of IL-2 and its level can reflect the course of activity of T cells and immune state[38-41]. The levels of mIL-2R in silence stage detected by BSA were lower in patients with hepatitis C than those in normal controls (P<0.01). The probable reasons are: (1) The mIL-2R on surface of some T cells can be restrained by HCV. (2) The degree of variation of HCV is high, the hydrophilic peptid chain on core protein is subjective to escape the attack of CTL and keep the infection persist in chronic state. (3) The variant antigen of HCV can not match the antibody produced. A lot of soluble interleukin-2 receptor (sIL-2R) can be released after replication of HCV-RNA in PBMC so that the expression of mIL-2R was restrained. It is not only a kind of manifestation of disorder and low cellular immune to HCV but also one of reasons of chronic hepatitis C. Some T cells receptor (TCR) on surface of some Tc cells can combine with the complement (HCV-MHC-I) and some perforation proteins can be released so that many liver cells will be injured. The sIL-2R, a kind of restrained factor, as well as mIL-2R all can combine with IL-2 competitively and induce infection of HCV from activity to chronicity. With the inducement of PHA, the level of mIL-2R in silence and inducement stages was obviously increased. This result showed that the mIL-2R could be induced by PHA and had strong compete ability against sIL-2R in serum.

After inducement of PHA, the level of mIL-2R of patients in inducement stage was higher than that in silence stage, and lower than that in normal controls (P<0.01). The results of our study showed that the effect of PHA was infirm for patients with hepatitis C and was similar to the reports published. The level of mIL-2R in silence and inducement stages were higher after treatment of alpha 2b interferon than that before treatment of alpha 2b interferon (P<0.01). The active T cells and high level of mIL-2R can be induced by alpha 2b interferon during the treatment. The results showed that alpha 2b interferon not only can induce the protein kinase and 2' , 5' AS but also stimulate T cells and induce the effect of Tc cells against infected cells.

In conclusion, some active T cells and mIL-2R can be induced during the treatment of alpha 2b interferon. The patients with viremia are sensitive to treatment of alpha 2b interferon that have good effect on negative change of HCV-RNA in PBMC and serum and anti-HCV in serum. If the treatment time of alpha 2b interferon prolongs, the negative rate of anti-HCV and HCV-RNA will increase simultaneously. In treatment of HCV with alpha 2b interferon, the value of negative change of HCV-RNA in serum alone is limited. In well equipped hospital both HCV-RNA in serum and PBMC can be examined at the same time.

REFERENCES

1 **Piekarska A,** Sidorkiewicz M, Lewandowska U, Kuydowicz J. Evaluation of persistence of IFN-alpha treatment response in chronic hepatitis C patients according with HCV-RNA presence in PBMC. *Pol Arch Med Wewn* 2001; **106**: 939-944

2 **Piekarska A,** Kuydowicz J, Omulecka A. Interferon alpha-treatment predictive response factors in group of adults patients with chronic hepatitis C. *Pol Arch Med Wewn* 2001; **106**: 927-937

3 **Patel K,** McHutchison J. Peginterferon alpha-2b: a new approach to improving response in hepatitis C patients. *Expert Opin Pharmacother* 2001; **2**: 1307-1315

4 **Iwabuchi S,** Takatsuka K. Dynamics of serum HCV RNA levels during IFN therapy in patients with chronic hepatitis C for prediction of outcome of IFN therapy and beneficial dosing. *Nippon Rinsho* 2001; **59**: 1363-1368

5 **Fornai C,** Maggi F, Favilli F, Vatteroni ML, Pistello M, Marchi S, Ciccorossi P, Antonelli G, Bendinelli M. Rapid changes in hepatitis C virus quasispecies produced by a single dose of IFN-alpha in chronically infected patients. *J Interferon Cytokine Res* 2001; **21**: 417-422

6 **Malaguarnera M,** Di Fazio I, Trovato BA, Pistone G, Mazzoleni G. Alpha-interferon (IFN-alpha) treatment of chronic hepatitis C: analysis of some predictive factors for the response. *Int J Clin Pharmacol Ther* 2001; **39**: 239-245

7 **Malaguarnera M,** Laurino A, Di Fazio I, Pistone G, Castorina M, Guccione N, Rampello L. Neuropsychiatric effects and type of IFN-alpha in chronic hepatitis C. *J Interferon Cytokine Res* 2001; **21**: 273-278

8 **Reddy KR,** Wright TL, Pockros PJ, Shiffman M, Everson G, Reindollar R, Fried MW, Purdum PP, Jensen D, Smith C, Lee WM, Boyer TD, Lin A, Pedder S, DePamphilis J. Efficacy and safety of pegylated (40-kd) interferon alpha-2a compared with

interferon alpha-2a in noncirrhotic patients with chronic hepatitis C. *Hepatology* 2001; **33**: 433-438

9 **Kraus MR,** Schafer A, Csef H, Faller H, Mork H, Scheurlen M. Compliance with therapy in patients with chronic hepatitis C: associations with psychiatric symptoms, interpersonal problems, and mode of acquisition. *Dig Dis Sci* 2001; **46**: 2060-2065

10 **Suzuki T,** Yonemura K, Miyaji T, Suzuki H, Takahira R, Fujigaki Y, Fujimoto T, Hishida A. Progressive renal failure and blindness due to retinal hemorrhage after interferon therapy for hepatitis C virus-associated membranoproliferative glomerulonephritis. *Intern Med* 2001; **40**: 708-712

11 **Nishiguchi S,** Shiomi S, Enomoto M, Lee C, Jomura H, Tamori A, Habu D, Takeda T, Yanagihara N, Shiraki K. Does ascorbic acid prevent retinopathy during interferon therapy in patients with chronic hepatitis C? *J Gastroenterol* 2001; **36**: 486-891

12 **Ho SB,** Nguyen H, Tetrick LL, Opitz GA, Basara ML, Dieperink E. Influence of psychiatric diagnoses on interferon-alpha treatment for chronic hepatitis C in a veteran population. *Am J Gastroenterol* 2001; **96**: 157-164

13 **Garcia-Suarez J,** Burgaleta C, Hernanz N, Albarran F, Tobaruela P, Alvarez-Mon M. HCV-associated thrombocytopenia: clinical characteristics and platelet response after recombinant alpha2b-interferon therapy. *Br J Haematol* 2000; **110**: 98-103

14 **Hsieh MC,** Yu ML, Chuang WL, Shin SJ, Dai CY, Chen SC, Lin ZY, Hsieh MY, Liu JF, Wang LY, Chang WY. Virologic factors related to interferon-alpha-induced thyroid dysfunction in patients with chronic hepatitis C. *Eur J Endocrinol* 2000; **142**: 431-437

15 **Hino K,** Yamaguchi Y, Fujiwara D, Katoh Y, Korenaga M, Okazaki M, Okuda M, Okita K. Hepatitis C virus quasispecies and response to interferon therapy in patients with chronic hepatitis C: a prospective study. *J Viral Hepat* 2000; **7**: 36-42

16 **Sandres K,** Dubois M, Pasquier C, Payen JL, Alric L, Duffaut M, Vinel JP, Pascal JP, Puel J, Izopet J. Genetic heterogeneity of hypervariable region 1 of the hepatitis C virus (HCV) genome and sensitivity of HCV to alpha interferon therapy. *J Virol* 2000; **74**: 661-668

17 **Poynard T,** Daurat V, Chevret S, Moussalli J, Degos F, Bailly F, Borotto E, Buffet C, Bartolomei-Portal I, Richardet JP, Riachi G, Calmus Y, Brechot C, Vidaud M, Olivi M, Bedossa P, Riffaud PC, Chastang C. A short induction regimen of interferon-alpha is not effective for treatment of relapse in chronic hepatitis C: a randomized trial. For the multicentre GER-CYT-01 group. *J Viral Hepat* 1999; **6**: 381-386

18 **Weiss G,** Umlauft F, Urbanek M, Herold M, Lovevsky M, Offner F, Gordeuk VR. Associations between cellular immune effector function, iron metabolism, and disease activity in patients with chronic hepatitis C virus infection. *J Infect Dis* 1999; **180**: 1452-1458

19 **Vertuani S,** Bazzaro M, Gualandi G, Micheletti F, Marastoni M, Fortini C, Canella A, Marino M, Tomatis R, Traniello S, Gavioli R. Effect of interferon-alpha therapy on epitope-specific cytotoxic T lymphocyte responses in hepatitis C virus-infected individuals. *Eur J Immunol* 2002; **32**: 144-154

20 **Fujiwara T,** Kiura K, Ochi K, Matsubara H, Yamanari H, Shimomura H, Harada M. Giant negative T waves during interferon therapy in a patient with chronic hepatitis C. *Intern Med* 2001; **40**: 105-109

21 **Fukuda A,** Kobayashi H, Teramura K, Yoshimoto S, Ohsawa N. Effects of interferon-alpha on peripheral neutrophil counts and serum granulocyte colony-stimulating factor levels in chronic hepatitis C patients. *Cytokines Cell Mol Ther* 2000; **6**: 149-154

22 **Kakizaki S,** Takagi H, Yamada T, Ichikawa T, Abe T, Sohara N, Kosone T, Kaneko M, Takezawa J, Takayama H, Nagamine T, Mori M. Evaluation of twice-daily administration of interferon-beta for chronic hepatitis C. *J Viral Hepat* 1999; **6**: 315-319

23 **Jensen DM,** Krawitt EL, Keeffe EB, Hollinger FB, James SP, Mullen K, Everson GT, Hoefs JC, Fromm H, Black M, Foust RT, Pimstone NR, Heathcote EJ, Albert D. Biochemical and viral response to consensus interferon (CIFN) therapy in chronic hepatitis C patients: effect of baseline viral concentration. Consensus Interferon Study Group. *Am J Gastroenterol* 1999; **94**: 3583-3588

24 **Willson RA,** Fischer SH, Ochs HD. Long-term interferon alpha maintenance therapy for chronic hepatitis C infection in a patient with common variable immune deficiency. *J Clin Gastroenterol* 1999; **29**: 203-206

25 **Fabris C,** Del Forno M, Falleti E, Toniutto P, Pirisi M. Kinetics of serum soluble tumour necrosis factor receptor (TNF-R) type-I and type-II after a single interferon-alpha (IFN-alpha) injection in chronic hepatitis C. *Clin Exp Immunol* 1999; **117**: 556-560

26 **Begemann F,** Jablonowski H. Enhancing the response to interferon-alpha. *J Clin Virol* 1999; **13**: 1-7

27 **Huraib S,** Tanimu D, Romeh SA, Quadri K, Al Ghamdi G, Iqbal A, Abdulla A. Interferon-alpha in chronic hepatitis C infection in dialysis patients. *Am J Kidney Dis* 1999; **34**: 55-60

28 **Yagura M,** Murai S, Kojima H, Tokita H, Kamitsukasa H, Harada H. Interferon treatment in patients with chronic hepatitis C with normal alanine-aminotransferase activity. *Hepatogastroenterology* 1999; **46**: 1094-1099

29 **Seifarth C,** Benninger J, Bohm BO, Wiest-Ladenburger U, Hahn EG, Hensen J. Augmentation of the immune response to islet cell antigens with development of diabetes mellitus caused by interferon-alpha therapy in chronic hepatitis C. *Z Gastroenterol* 1999; **37**: 235-2239

30 **Boran M,** Cetin S. The role of alpha-glutathione S-transferase in the monitoring of hemodialysis patients with hepatitis C virus infection undergoing high-dose interferon-alpha-2b therapy. *Nephron* 1999; **82**: 22-26

31 **Woitas RP,** Petersen U, Moshage D, Brackmann HH, Matz B, Sauerbruch T, Spengler U. HCV-specific cytokine induction in monocytes of patients with different outcomes of hepatitis C. *World J Gastroenterol* 2002; **8**: 562-566

32 **Zeuzem S**. The kinetics of hepatitis C virus infection. *Clin Liver Dis* 2001; **5**: 917-930

33 **Cramp ME,** Rossol S, Chokshi S, Carucci P, Williams R, Naoumov NV. Hepatitis C virus-specific T-cell reactivity during interferon and ribavirin treatment in chronic hepatitis C. *Gastroenterology* 2000; **118**: 346-355

34 **Kawamura C,** Nakajima S, Kuroki T, Monna T. Two-dimensional analysis of production of IL-6 and TNF-alpha can predict the efficacy of IFN-alpha therapy. *Hepatogastroenterology* 1999; **46**: 2941-2945

35 **Song ZQ,** Hao F, Min F, Ma QY, Liu GD. Hepatitis C virus infection of human hepatoma cell line 7721 *in vitro*. *World J Gastroenterol* 2001; **7**: 685-689

36 **Fukutomi T,** Fukutomi M, Iwao M, Watanabe H, Tanabe Y, Hiroshige K, Kinukawa N, Nakamuta M, Nawata H. Predictors of the efficacy of intravenous natural interferon-beta treatment in chronic hepatitis C. *Med Sci Monit* 2000; **6**: 692-698

37 **Xu JZ,** Yang ZG, Le MZ, Wang MR, He CL, Sui YH. A study on patogenicity of hepatitis G virus. *World J Gastroenterol* 2001; **7**: 547-550

38 **Li CP,** Wang KX, Wang J, Pan BR. mIL-2R, T cell subsets and hepatitis C. *World J Gastroenterol* 2002; **8**: 298-300

39 **Jimenez-Saenz M,** Rojas M, Pinar A, Salas E, Rebollo J, Carmona I, Herrerias-Esteban JM, Herrerias-Gutierrez JM. Sustained response to combination therapy in a patient with chronic hepatitis C and thrombocytopenia secondary to alpha-interferon. *J Gastroenterol Hepatol* 2000; **15**: 567-569

40 **Yan FM,** Chen AS, Hao F, Zhao XP, Gu CH, Zhao LB, Yang DL, Hao LJ. Hepatitis C virus may infect extrahepatic tissues in patients with hepatitis C. *World J Gastroenterol* 2000; **6**: 805-811

41 **Oketani M,** Higashi T, Yamasaki N, Shinmyozu K, Osame M, Arima T. Complete response to twice-a-day interferon-beta with standard interferon-alpha therapy in acute hepatitis C after a needle-stick. *J Clin Gastroenterol* 1999; **28**: 49-51

Edited by Zhang JZ

P.O.Box 2345, Beijing 100023, China
Fax: +86-10-85381893
E-mail: wjg@wjgnet.com www.wjgnet.com

World J Gastroenterol 2003;9(4):755-758
World Journal of Gastroenterology
 ISSN 1007-9327

Anti-*Helicobacter pylori* immunoglobulin G (IgG) and IgA antibody responses and the value of clinical presentations in diagnosis of *H. pylori* infection in patients with precancerous lesions

Shao Li, Ai-Ping Lu, Lian Zhang, Yan-Da Li

Shao Li, Yan-Da Li, The Key Laboratory of Bioinformatics of Ministry of Education, Institute of Bioinformatics, Tsinghua University, Beijing 100084, China
Ai-Ping Lu, Institute of Basic Theory, China Academy of Traditional Chinese Medicine, Beijing 100700, China
Lian Zhang, Beijing Institute for Cancer Research, Beijing 100034, China
Supported by National Natural Science Foundation of China, No. 30200365
Correspondence to: Dr. Ai-Ping Lu, Institute of Basic Theory, China Academy of Traditional Chinese Medicine, Dongzhimen, Beijing 100700, China. catcm@public.bta.net.cn
Telephone: +86-10-64014411-2564 **Fax:** +86-10-64013896
Received: 2002-11-19 **Accepted:** 2002-12-18

Abstract

AIM: To determine the prevalence of *Helicobacter pylori* (*H. pylori*) infection, the serum anti-*H. pylori* immunoglobulin G (IgG) and IgA antibody responses, and the value of clinical presentations in diagnosis of *H. pylori* infection in patients with gastric atrophy, intestinal metaplasia and dysplasia.

METHODS: *H. pylori* infection was detected by histology in 209 patients with mild chronic atrophic gastritis (CAG, n=76), severe CAG (n=22), mild intestinal metaplasia (IM, n=22), severe IM (n=58), or dysplasia (DYS, n=31). Serum anti-*H. pylori* IgG and IgA were double sampled and evaluated by enzyme-linked immunoadsordent assays. 35 clinical presentations were observed and their relationship with *H. pylori* infection was analyzed by the *k*-means cluster method.

RESULTS: Both IgG and IgA levels in *H. pylori* positive patients were significantly higher than those negative for *H. pylori* (P<0.001-0.01). The prevalence of *H. pylori* was highest in severe IM (84.5 %), and lowest in mild CAG (51.3 %) (P<0.01). They were similar in severe CAG (68.2 %), mild IM (72.7 %), and DYS (67.7 %). In *H. pylori* positive patients, the IgG levels in severe CAG were significantly higher than those in mild CAG (P<0.01). In *H. pylori* negative patients, both IgG and IgA levels increased remarkably in severe IM, compared to those in mild IM (P<0.01-0.05). *H. pylori* infection exhibited no association with patient's gender (62.1 % in males; 71.7 % in females) and age (r=0.0814, P=0.241). The diagnostic accuracy based on 35 clinical presentations was 65.7 %. It could be improved by 5.7 % when only the assemblage of digestive symptoms were engaged, or by 8.6 % when the pathogenic factors, general status and grossoscopy were combined. The diagnostic accuracy could be decreased when only the general symptoms were engaged, or when the pathogenic factors were accompanied with some common digestive symptoms.

CONCLUSION: *H. pylori* infection is a major risk factor for the process from atrophy, IM to DYS of gastric mucosa. Serum IgG and IgA are good indicators to evaluate this progress with a certain arrearage. Investigation on the effective assemblages of clinical presentations may provide a better understanding in the pathogenesis, diagnosis and treatment for *H. pylori* infection.

Li S, Lu AP, Zhang L, Li YD. Anti-*Helicobacter pylori* immunoglobulin G (IgG) and IgA antibody responses and the value of clinical presentations in diagnosis of *H. pylori* infection in patients with precancerous lesions. *World J Gastroenterol* 2003; 9(4): 755-758
http://www.wjgnet.com/1007-9327/9/755.htm

INTRODUCTION

The persistence or repeated infection of pathogenic factors in the stomach may result in the chronic process of gastritis with glandular atrophy (AT), intestinal metaplasia (IM), dysplasia (DYS) and so on at different stages, which indicates diversiform prognosis. The roles of immune reactions in *Helicobacter pylori* (*H. pylori*) pathogenesis and chronic gastritis (CG) are research areas of rapid progress[1-4]. It is now recognized that the clinical detection of serum antibody is effective in monitoring the *H. pylori* infection[5,6]. However, *H. pylori* infection and the levels of serum anti-*H. pylori* immunoglobulin antibodies at different stages of CG are not fully investigated. Moreover, the complex clinical manifestations of *H. pylori* infection and associated CG leads to a diagnostic and therapeutic dilemma for CG[7].

To determine the prevalence of *H. pylori* infection, the serum anti-*H. pylori* immunoglobulin G (IgG) and IgA antibody responses, and the value of clinical presentations in diagnosis of *H. pylori* infection in patients with gastric atrophy, intestinal metaplasia and dysplasia a population-based investigation was designed and a novel analytic method was proposed in this work. The study also took a different perspective in assessing the association between *H. pylori* infection and clinical presentations.

MATERIALS AND METHODS

Patients

A total of two hundred and nine patients with chronic gastritis, who were diagnosed through gastroscopy and mucosal biopsy, were included in the present study. All patients, who resided in Shandong province, were investigated by the Institute of Basic Theory, Chinese Academy of Traditional Chinese Medicine from 1999 to 2001. Among them 103 were males and 106 were females, aged from 45 to 72 with a mean age of 55 years old. Gastric biopsies were histologically evaluated for activity and chronicity of gastritis, and the presence of AT and/or IM according to the criterion of the visual analogue scale in Sydney classification and grading of gastritis[8]. The patients consisted of 76 with mild chronic atrophic gastritis (CAG), 22 with severe (CAG), 22 with mild IM, 58 with severe IM and 31 with DYS accompanied with mild IM. All patients had not received any anti- *H. pylori* treatment.

Diagnosis of H. pylori infection

Two hundred and nine specimens of gastric mucosa were obtained from each patient via endoscopy. Gastric mucosa was sampled from the area of greater curvature at gastric antrum, and *H. pylori* was determined by pathological staining with hematoxylin and eosin (HE) followed by Giemsa staining. Under microscope, *Helicobacter-like organisms* can be identified as a typical curve like S or C. They look like a short bacilli or globular body with a slight curve.

Detection of anti-H. pylori IgG and IgA antibodies

Blood was sampled twice from patients. Enzyme-linked immunoadsorbent assays (ELISA) were used to detect the levels of serum anti-*H. pylori* IgG and IgA antibodies. The test kits for the detection of anti-*H. pylori* -IgG and anti-*H. pylori* -IgA were purchased from Bioseed Co., USA. The value of the optical density (OD) was read by a microtiter plate reader at 450 nm.

Clinical presentations observation

35 clinical presentations were observed as follows: (1) Symptoms of the digestive system including appetite, distending fullness in the stomach, stomachache, distending fullness in the abdomen, pain in the hypochondrium, pain in the abdomen, singultus, nausea, vomit, acid regurgitation and epigastric upset, and heartburn; (2) General status including ear, eye, physique, complexion, stool, urine, oropharynx, taste, swollen, head, limbs, chest, hand and foot; (3) Spirit and psychological status including spirit, sleep, and emotion; (4) Glossoscopy including quality of tongue, body of tongue, and fur of tongue and (5) Pathogenic factors including smoking, alcohol, dietary bias, and dietary regularity. Each investigated symptom consisted of two to four subordinate items.

Statistical analysis

A SPSS 10.0 statistical package program was used for data analysis. The variables were processed by chi-square test, student' s *t* test, ANVOA analysis, and bivariate correlate analysis, where appropriate.

k-means cluster analysis

The *k*-means cluster analysis method has been applied in many areas including data mining, statistics, biology, and machine learning, and so on[9]. In this study, the relationship between the *H. pylori* infection and the 35 clinical presentations of patients was analyzed by this method. The diagnostic accuracy was obtained by the *k*-means algorithms. The distance between clusters was further verified by an ANOVA test.

RESULTS

As shown in Table 1, the detected positive rates of *H. pylori* varied were 72.7 % (16/22) in mild IM, 84.5 % (49/58) in severe IM, 67.7 % (21/31) in DYS, 51.3 % (39/76) in mild CAG, and 68.2 % (15/22) in severe CAG, respectively. Analyses of chi-square test showed that the detected positive rates of *H. pylori* were similar in mild IM, mild CAG, DYS, and severe CAG groups. The *H. pylori* positive rate in severe IM group was statistically higher than those in other groups (all $P<0.01$).

Table 2 shows the detective positive rates of *H. pylori* for the CG patients in relation to gender and age. There was no significant difference between the male (62.1 %, 64/103) and the female patients (71.7 %, 76/106) ($P>0.05$). The *H. pylori* infection rate was highest in the ages from 42 to 49 (59/80, 73.8 %). However, the ANVOA analysis showed that there was no significant difference among four groups with different ages ($P>0.05$). Bivariate correlation analysis also indicated that the detected positive rate of *H. pylori* was not remarkably associated with the age of patients ($r=0.0814$, $P=0.241$).

Table 3 lists the levels of serum anti- *H. pylori* IgG and IgA at different statge of CG. Both serum anti- *H. pylori* IgG and IgA levels were remarkably higher in *H. pylori* positive patients than those negative for *H. pylori* ($P<0.001$-0.01). In *H. pylori* positive patients the IgG level was significantly greater in severe CAG than in mild CAG ($P<0.01$). In *H. pylori* negative patients both the serum IgG and IgA levels increased significantly in severe IM, compared to those in mild IM ($P<0.01$-0.05). There was no significant difference in IgG and IgA levels between mild and severe IM in the presence of *H. pylori* infection ($P>0.05$).

Table 1 The detected positive rates of *H. pylori* at different stages of CG

H. pylori	Mild CAG	Severe CAG	Mild IM	Severe IM	DYS	Total
Number	76	22	22	58	31	209
Positive %	39 (51.3%)	15 (68.2%) [a]	16 (72.7%)	49 (84.5%)[b]	21 (67.7%)	140
Negative %	37 (48.7%)	7 (31.8%)	6 (27.3%)	9 (15.5%)	10 (32.3%)	69

CAG, chronic atrophic gastritis; IM, intestinal metaplasia; DYS, dysplasia. [a]$P<0.05$, [b]$P<0.01$, mild IM *vs* severe IM; mild CAG *vs.* severe CAG.

Table 2 The detected positive rates of *H. pylori* for CG patients in relation to gender and age

H. pylori	Males	Females	70-77 years old	60-69 years old	50-59 years old	42-49 years old
Number	103	106	16	47	66	80
Positive (%)	64 (62.1%)	76 (71.7%)	10 (62.5%)	32 (68.1%)	39 (59.1%)	59 (73.8%)
Negative (%)	39 (37.9%)	30 (28.3%)	6 (37.5%)	15 (31.9%)	27 (40.9%)	21 (26.2%)

Table 3 Comparison of serum anti-*H. pylori* IgG and IgA levels (the optical density value) at different stages of CG

	Mild CAG		Severe CAG		Mild IM		Severe IM		DYS	
	H. pylori (+)	*H. pylori* (-)	*H. pylori* (+)	*H. pylori* (-)	*H. pylori* (+)	*H. pylori* (-)	*H. pylori* (+)	*H. pylori* (-)	*H. pylori* (+)	*H. pylori* (-)
IgG(1)	2.86±1.8[b]	0.38±0.27	4.48±2.14[bc]	0.53±0.27	3.86±1.87[b]	0.14±0.07	3.1±2.34[a]	0.55±0.29[d]	2.74±1.67[b]	0.23±0.17
IgG(2)	3.26±2.16[b]	0.46±0.24	4.52±3.27[a]	0.54±0.29	4.44±2.56[b]	0.3±0.18	3.5±1.98[b]	0.54±0.29	3.33±1.87[b]	0.72±0.97
IgA(1)	0.85±0.7[b]	0.24±0.22	0.99±0.49[b]	0.21±0.16	0.83±0.39[b]	0.1±0.06	0.93±0.79	0.33±0.16[d]	0.94±0.89[b]	0.13±0.13
IgA(2)	0.96±0.83[b]	0.25±0.21	1.08±0.59[a]	0.27±0.16	0.99±0.72[a]	0.12±0.07	0.89±0.63[a]	0.32±0.19[d]	0.78±0.6[b]	0.15±0.13

CAG, chronic atrophic gastritis; IM, intestinal metaplasia; DYS, dysplasia. (1) The first detection. (2) The second detection. [a]$P<0.01$, [b]$P<0.001$, *H. pylori* (+) *vs. H. pylori* (-). [c]$P<0.05$, *H. pylori* (+) mild CAG *vs. H. pylori* (+) severe CAG; [d]$P<0.05$, *H. pylori* (-) mild IM *vs. H. pylori* (-) severe IM.

Table 4 Diagnostic accuracy of *H. pylori* infection determined by different assemblages of symptoms

Attributes	Assemblages of symptoms	Accuracy (%)	
		H. pylori (+)	*H. pylori* (-)
Pathogenic factors and general status	Smoking, alcohol, limbs, hand and foot (all[a])	70.7%	42.3%
Pathogenic factors, general status and tongue	Smoking, alcohol, dietary regularity, limbs, and tongue quality (all[a])	74.3%	39.1%
Pathogenic factors and digestive symptoms	Smoking, alcohol, limbs, hand and foot, distending fullness in the stomach, stomachache, distending fullness in the abdomen, and nausea (all[a])	51.4%	52.2%
Digestive symptoms	Appetite, distending fullness in the stomach, stomachache, distending fullness in the abdomen, pain in the hypochondrium, pain in the abdomen, singultus, nausea, vomit, acid regurgitation and epigastric upset, heartburn, and stool (all[a])	71.4%	26.1%
Digestive symptoms and tongue	Distending fullness in the stomach, stomachache, pain in the abdomen, nausea, and fur of tongue (all[a])	72.1%	26.1%
General status	Taste, swollen, head, limbs, chest, hand and foot, spirit and sleep, emotion, complexion (all[a])	50.7%	40.6%
Total symptoms	35 items[b]	65.7 %	40.6 %

[a]P<0.05-0.001, the difference between two classes tested by the ANOVA analysis. [b]P<0.05-0.001, except dietary bias, dietary regularity, urine, oropharynx, eye, ear, physique, tongue quality, and tongue body.

Table 4 shows the diagnostic accuracy of *H. pylori* infection determined by different assemblages of clinical presentations. The overall diagnostic accuracy based on 35 presentations was 65.7 %. It could be improved by 5.7 % when the only digestive symptoms were engaged, or by 8.6 % when further information were referred such as the assemblage of pathogenic factors (smoking, alcohol), general status (tired limbs), and tongue observation according to the traditional Chinese medicine (TCM) method. However, the diagnostic accuracy could be decreased by the improper assemblages such as the general symptoms only, the pathogenic factors accompanied with some common digestive symptoms (distending fullness in the stomach, stomachache, distending fullness in the abdomen, and nausea) which had no special significance for the positive or negative *H. pylori*.

DISCUSSION

An increasing number of studies support a close relationship between *H. pylori* infection and CG, as previous described. However, the correlation between *H. pylori* infection, serum antibody and clinical symptoms at different stages of CG has not been well investigated so far. The chi-square test results in Table 1 show that the detected positive rates of *H. pylori* increase significantly in patients with mild CAG (51.3 %, 39/76), DYS and mild IM (67.7 %, 21/31), severe CAG (68.2 %, 15/22), and mild IM (72.7 %, 16/22). They reach the highest value in patients with severe IM (84.5 %, 49/58) (P<0.01). However, *H. pylori* infection exhibited no remarkable association with patient' s gender (62.1 % in males; 71.7 % in females) and age (r=0.08, P=0.241).

It has been reported that the adherence of *H. pylori* may play an important role in the pathogenesis of severe histological changes in CAG[10], IM[11] and DYS[12]. Our investigation further explored the statistic probability of *H. pylori* infection at different stages of CG. Based on these, we suggest that *H. pylori* infection may be the key factor in accelerating the occurrence and development of CG, since *H. pylori* is a pathogenic bacterium that can adhere to gastric mucosa until the atrophy and intestinal metaplasia occurring in the course of CG.

A mostly pathological mechanism of *H. pylori* infection is the immunopathological response of host. When CG occurs, a detectable specific humoral immunological response will be established. The appearance of serum antibodies such as IgG and IgA may indicate an extensive immunoreaction causing by *H. pylori* infection. The serum anti-*H. pylori* -IgG antibody, therefore, acts as a highly accurate, simple and noninvasive method in monitoring the status of *H. pylori* infection[5, 13]. In our study, both serum anti-*H. pylori* IgG and IgA are remarkably higher in *H. pylori* positive patients than those negative for *H. pylori* (P<0.001-0.01). On the one hand, in the presence of *H. pylori* infection the IgG level in severe CAG increased significantly, compared to those in mild CAG (P<0.01). These imply that the serum anti-*H. pylori* IgG and IgA are appropriate indicators to evaluate the status of *H. pylori* infection in the process of CG. On the other hand, in absence of *H. pylori* infection both serum IgG and IgA are significantly greater in severe IM than those in mild IM (P<0.01-0.05), whereas no significant difference (P>0.05) was observed between mild and severe IM in the presence of *H. pylori* infection. The increase of antibody may be due to the reminiscence of *H. pylori* infection, resulting in a certain arrearage between serum antibody and *H. pylori*. It is reported that the IgA response of gastric mucoa in CG patients can be detected even in the quiescent period of negative *H. pylori* infection due to the recent exposure to the bacterial antigens[6].

The clinical situations of CG patients are intricate. They are divergent by the pathological changes of gastric mucosa, and are affected by environmental factors[14, 15]. By means of the cluster analysis method, we found that the proper assemblages such as digestive symptoms, pathogenic factors (smoking, alcohol), general status (tired limbs), and the tongue could improve the diagnostic accuracy of *H. pylori* infection. However, the improper assemblages, such as the general symptoms only, or the pathogenic factors accompanied with some common digestive symptoms decreased the diagnostic accuracy. A preferable symptomatic assemblage has been proposed in the present study. Based on this, the diagnostic accuracies of up to 74.3 % and 40.5 %, respectively, for positivity and negativity of *H. pylori* infection have been obtained. It has been demonstrated clinically that smoking, alcohol[16] and the tongue change[17] are pathogenic factors for the *H. pylori* infection. Our study indicates that the symptomatic assemblages rather than an individual factor are closely related to the clinic significance of *H. pylori* infection. Furthermore, it has been known that the validity of CG treatment in traditional Chinese medicine (TCM) is based on the differentiation of symptom-complexes[18, 19]. Our investigation suggests that *H. pylori*-related symptomatic assemblages can be taken into consideration in practicality and methodology during the diagnoses and treatment of CG. More effective symptomatic assemblages and their effects

on *H. pylori* infection are still required.

In conclusion, the early genesis and further progression of CG are associated with *H. pylori* infection, which can be characterized by the increase of serum anti-*H. pylori* IgG and IgA with a certain arrearage. Due to the intricate clinical situation of CG, effective symptomatic assemblages are required in diagnosing *H. pylori* infection.

REFERENCES

1 **Aguilar GR**, Ayala G, Fierros-Zarate G. *Helicobacter pylori*: Recent advances in the study of its pathogenicity and prevention. *Salud Publica Mex* 2001; **43**: 237-247

2 **Gao HJ**, Yu LZ, Bai JF, Peng YS, Sun G, Zhao HL, Miu K, Lu XZ, Zhang XY, Zhao ZQ. Multiple genetic alterations and behavior of cellular biology in gastric cancer and other gastric mucosal lesions: *H. pylori* infection, histological types and staging. *World J Gastroenterol* 2000; **6**: 848-854

3 **Zhuang XQ**, Lin SR. Research of *Helicobacter pylori* infection in precancerous gastric lesions. *World J Gastroentero* 2000; **6**: 428-429

4 **Prinz C**, Schoniger M, Rad R, Becker I, Keiditsch E, Wagenpfeil S, Classen M, Rosch T, Schepp W, Gerhard M. Key importance of the *Helicobacter pylori* adherence factor blood group antigen binding adhesin during chronic gastric inflammation. *Cancer Res* 2001; **61**: 1903-1909

5 **Zhu Y**, Lin J, Li D, Du Q, Qian K, Wu Q, Zheng S. *Helicobacter pylori* antigen and its IgG, IgA-type specific immunocomplexes in sera from patients with *Helicobacter pylori* infection. *Chin Med J (Engl)* 2002; **115**: 381-383

6 **Futagami S**, Takahashi H, Norose Y, Kobayashi M. Systemic and local immune responses against *Helicobacter pylori* urease in patients with chronic gastritis: distinct IgA and IgG productive sites. *Gut* 1998; **43**: 168-175

7 **Stankiewicz JA**, Chow JM. A diagnostic dilemma for chronic rhinosinusitis: definition accuracy and validity. *Am J Rhinol* 2002; **16**: 199-202

8 **Dixon MF**, Genta RM, Yardley JH, Correa P. Classification and grading of gastritis: the updated sydney system. International workshop on the histopathology of gastritis houston 1994. *Am J Surg Pathol* 1996; **20**: 1161-1181

9 **Han JW**, Kamber M. Data mining: concepts and techniques. *Morgan Kaufmann Publishers, USA* 2001: 16

10 **Domellof L**. Reversal of gastric atrophy after *Helicobacter pylori* eradication: is it possible or not? *Am J Gastroenterol* 1998, **93**: 1407-1408

11 **Meining A**, Stolte M. Close correlation of intestinal metaplasia and corpus gastritis in patients infected with *Helicobacter pylori*. *Z Gastroenterol* 2002; **40**: 557-560

12 **Gao H**, Wang JY, Shen XZ, Liu JJ. Effect of *Helicobacter pylori* infection on gastric epithelial cell proliferation. *World J Gastroenterol* 2000; **6**: 442-444

13 **Figueroa G**, Faundez G, Troncoso M, Navarrete P, Toledo MS. Immunoglobulin G antibody response to infection with coccoid forms of *Helicobacter pylori*. *Clin Diagn Lab Immunol* 2002; **9**: 1067-1071

14 **Kipen HM**, Fiedler N. The role of environmental factors in medically unexplained symptoms and related syndromes: conference summary and recommendations. *Environ Health Perspect* 2002; **110**(Suppl 4): 591-595

15 **Brown LM**, Thomas TL, Ma JL, Chang YS, You WC, Liu WD, Zhang L, Pee D, Gail MH. *Helicobacter pylori* infection in rural China: demographic, lifestyle and environmental factors. *Int J Epidemiol* 2002; **31**: 638-645

16 **Kamada T**, Haruma K, Komoto K, Mihara M, Chen X, Yoshihara M, Sumii K, Kajiyama G, Tahara K, Kawamura Y. Effect of smoking and histological gastritis severity on the rate of *H. pylori* eradication with omeprazole, amoxicillin, and clarithromycin. *Helicobacter* 1999; **4**: 204-210

17 **Ozdemir A**, Mas MR, Sahin S, Saglamkaya U, Ateskan U. Detection of *Helicobacter pylori* colonization in dental plaques and tongue scrapings of patients with chronic gastritis. *Quintessence Int* 2001; **32**: 131-134

18 **Chen ZQ**, Chen GL, Li XW, Zhao YQ, Shi LJ. Plasma L-ENK, AVP, ANP and serum gastrin in patients with syndrome of Liver-Qi-stagnation. *World J Gastroenterol* 1999; **5**: 61-63

19 **Zhang XC**, Gao RF, Li BQ, Ma LS, Mei LX, Wu YZ, Liu FQ, Liao ZL. Clinical and experimental study of therapeutic effect of Weixibaonizhuan pills on gastric precancerous lesions. *World J Gastroenterol* 1998; **4**: 24-27

Edited by Xia HHX

P.O.Box 2345, Beijing 100023, China
Fax: +86-10-85381893
E-mail: wjg@wjgnet.com www.wjgnet.com

World J Gastroenterol 2003;9(4):759-764
World Journal of Gastroenterology
 ISSN 1007-9327

• BASIC RESEARCH •

Immunotolerance of liver allotransplantation induced by intrathymic inoculation of donor soluble liver specific antigen

Chang-Ku Jia, Shu-Sen Zheng, Qi-Yong Li, Ai-Bin Zhang

Chang-Ku Jia, Shu-Sen Zheng, Qi-Yong Li, Ai-Bin Zhang, Department of Hepatobiliary Pancreatic Surgery, Key Lab of combined Multi-Organ Transplantation, Ministry of Public Health, The First Affiliated Hospital of College of Medicine, Zhejiang University, Hangzhou 310003, China
Supported by Science and Technology Department of Zhejiang Province Foundation, No.011106206
Correspondence to: Dr. Chang-Ku Jia, Department of Hepatobiliary Pancreatic Surgery, The First Affiliated Hospital of College of Medicine, Zhejiang University, Hangzhou 310003, China. jiachk @sohu.com
Telephone: +86-571-87236570 **Fax:** +86-571-87236570
Received: 2002-10-08 **Accepted:** 2002-11-14

Abstract

AIM: To study the effects of liver specific antigen (LSA) on the immunoreaction of liver allotransplantation and its significance.

METHODS: Orthotopic liver transplantation was used in this study. Group I: syngeneic control (Wistar-to-Wistar); Group II: acute rejection (SD-to-Wistar). Group III: acute rejection treated by intramuscular injection of cyclosporine A (CsA) (SD-to-Wistar+CsA). Group IV: Intrathymic inoculation of SD rat LSA one week before transplantation (LSA+SD-to-Wistar). The common situation and survival time, rejection grades, NF-κB activity of splenocytes and intragraft cytokine gene expression were observed to analyze the acute rejection severity and immune state of animals.

RESULTS: The common situation of Wistar-to-Wistar group was very good after the transplantation and no signs of rejection were found. Recipients of SD-to-Wistar group lost body weight progressively. All died within 9 to 13 days after transplantation with the median survival time of 10.7±0.51 days. It was an optimal control for acute rejection. The common situation of SD-to-Wistar+CsA group was bad during CsA medication but only with mild rejection. As for LSA+SD-to-Wistar group, 5 of 6 recipients survived for a long time and common situation was remarkably better than that of SD-to-Wistar group and SD-to-Wistar+CsA group. Its rejection grades were significantly lower than that of SD-to-Wistar group (P=0.026). Furthermore, no significant discrepancies of rejection were found between SD-to-Wistar group and LSA+SD-to-Wistar group at day7 and day12 (P=0.067). NF-κB activity, IFN-γ and IL-2mRNA expression were significantly inhibited in LSA+SD-to-Wistar group compared with that of SD-to-Wistar group (P<0.05).

CONCLUSION: LSA is an important transplantation antigen which involves in the immunorejection of liver transplantation directly. We reported for the first time that intrathymic inoculation of LSA can induce immnotolerance of liver allotransplantation and grafts can survive for a long time thereby, thus leading to a novel way to liver transplantation immunotolerance.

Jia CK, Zheng SS, Li QY, Zhang AB. Immunotolerance of liver allotransplantation induced by intrathymic inoculation of donor soluble liver specific antigen. *World J Gastroenterol* 2003; 9 (4): 759-764
http://www.wjgnet.com/1007-9327/9/759.htm

INTRODUCTION

Although MHC-antigens have been extensively studied, the problem of rejection in liver transplantation was not resolved completely. Liver transplantation are not strict for HLA matching and both grafts and recipients can survive for a long time after immunotherapy[1]. On the other hand, given HLA multiple loci matching in some cases, the likelihood of grafts dysfunction and rejection increased, which suggested that matching for HLA type may exert a dualistic effect on liver transplantation[1,2]. No satisfactory explanations have been made about it up to date; and most studies were limited to HLA antigens themselves with the results still remaining controversial.

The specific antigens expressed only in liver cell membrane or liver cytoplasma and encoded by loci not linked to the MHC gene were called liver specific antigen (LSA). It was reported that this antigen could be detected in sera of almost all liver allotransplantation recipients but its effects remained unknown yet[3]. Thus in this experiment, we aimed to find whether LSA was an transplantation antigen and its possible mechanism of inducing the tolerance of liver allotransplantation using intrathymic LSA inoculation pathway. And the roles of LSA in thymus tolerance were discussed in this research too.

MATERIALS AND METHODS

Materials

Inbred male Wistar and male SD rats weighing 200 to 250 g were purchased from Shanghai Experimental Animal Center; there were also materials used in this study as following: [γ-^{32}P]ATP (Furui bioengineering Corp, Beijing); EMSA assay kit (Promega); NF-κB double stranded oligonucleotide, 5'-AGTTGAGGGGACTTTCCCAGGC-3', 3'-TCAACTCCCCTGAAAGGGTCCG-5' (Santa Cruz), NF-κB double stranded mutant oligonucleotide, 5'-AGTTGAGG-CGACTTTCCCAGGC-3', 3'-TCAACTCCGCTGAAAG GGTCC G-5' (Santa Cruz); TRIzol Reagent (Gibco, BRL); MuLV (MBI, Fermentas); Ultracentrifugator (Beckman); CHRIST lyophilizer (B.Braun Biotech).

Methods

Isolation of LSA Preparation of liver specific protein S100 was carried out by the method previously described[4]. The protein contents was measured according to the method of Bradford. Then the protein was lyophilized by CHRIST lyophilizer and stored at -80 ℃.

Surgical procedure, experimental groups and sample harvesting Rats were anesthetized with ether inhalation. Orthotopic rat liver transplantation was performed by Kamada's two-cuff technique[5]. The animals surviving less

then 3 days after the transplantation were attributed to technical errors and were excluded from this study. Wistar rats serving as recipients were randomly divided into four groups, Group I: syngeneic control (Wistar-to-Wistar); Group II: acute rejection (SD-to-Wistar); Group III: acute rejection treated with intramuscular injection of CsA 3.0 mg/kg/d (SD-to-Wistar+CsA); Group IV: Intrathymic inoculation of 10 mg SD rat LSA one week before transplantation (LSA+SD-to-Wistar). All groups were subdivided into day 1, 3, 5, 7, 12 subgroup (n=3 each) after the transplantation respectively for sample harvesting and another subgroups (n=6) for observation of common situation and survival time. For observation of common situation and survival time in Group III, after the therapy of CsA for 12 days, animals received no additional immunosuppression. Graft specimens were harvested to determine morphological changes and cytokine gene expression. Recipient splenocytes were isolated and the NF-κB activity were determined.

Histopathological examination Grafted liver samples were fixed in 10 % buffered formalin and embed in paraffin. Five micrometers think sections were affixed to slides, deparaffinized, and stained with hematoxylin and eosin to assess morphologic changes and severity of acute rejection by the Kemnitz' s standard[6].

Cytokine reverse transcription-polymerase chain reaction Primer sequences and reaction conditions: Primers sequences used were as follow: IL-2 sense primer, 5'-GACGCTTGTCCTCCTTGT CA-3', IL-2 antisense primer, 5'-ACCACAGTTGCTGGCTCATC-3' (size3 72bp); IFN-γ sense primer, 5'-ACTGCCAAGGCACACTCATT-3', IFN-γ antisense primer, 5'-AGGTGCGAT TCGATGACACT-3' (size 235bp); β-actin sense primer, 5'-TCGTACCA CTGGCATTGTGA-3', β-actin antisense primer, 5'-TCCTGCTTGCTGATCCACAT-3' (size 645bp). Amplifications were performed under the following conditions: 95 ℃ for 2 minutes, 94 ℃ for 45 seconds, 56 ℃ for 45 seconds, 72 ℃for 45 seconds, totally 32 cycles. The final extension step was performed by one cycle at 72 ℃ for 10 minutes. Reaction buffer: 10×Buffer 2.5 μl, 10 mM dNTP 1 μl, MgCl 2 μl, cDNA 2 μl and 1 μl of each primer, ddH_2O was added to get the final volume of 25 μl. RT-PCR: Total RNA was prepared from grafted liver with TRIzol Reagent according to the manufacturer' s recommendations. For cDNA synthesis, 4 ug total RNA was reverse transcribed with MuLV reverse transcriptase according to the manufacturer' s recommendations. Two microliters from the resulting cDNA solution were then amplified using specific oligonucleotides under the reaction conditions using β-actin as a "housekeeping gene" in a volume of 25 ul PCR buffer. Reaction products were run by electrophoresis on a 1.5 % agarose gel for 30-40 min at 100 V in 0.5×Tris/borate/EDTA buffer, and visualized with ethidium bromide under UV light. Relative expression of cytokines were defined as optical density ratio (cytokine/β-actin) analyzed by Kodak digital science scanning system.

NF-kB activity of splenocytes and EMSA competitive inhibition NF-κB activity was detected by gel electrophoretic mobility shift assay (EMSA): Splenocytes of recipients were isolated and nuclear extracts were prepared according to the method described by Kravchenko[7]. The contents of protein were determined by the method of Bradford. NF-κB oligonucleotide was end-labeled with [γ-^{32}P]ATP according to the manufacturer' s recommendations. For EMSA, 10 ug of each nuclear extract was mixed with 5×binding buffer at room temperature for 10 min. Then 1 ul [γ-^{32}P] ATP -labeled double strand NF-κB oligonucleotide probe was added in and incubated at room temperature for 20 min. The DNA/protein complex was electrophoresed on 4 % nondenaturing polyacrylamide gels in 0.5×Tris/borate/EDTA buffer to separate probe binding to NF-κB and free probe. Radioactive bands were detected by autoradiography at -70 ℃ followed by radiography to detect the level of retardation. The results were expressed as relative optical density (ROD)[8]. To study whether the method of EMSA was specific, standard nuclear extract of Hela cells was used to bind with NF-κB protein. The specificity of binding was confirmed by 100 fold excess unlabeled NF-κB oligonucleotide as a specific competitor, 100 fold excess unlabeled non-related oligonucleotide as a nonspecific competitor and 100 fold excess unlabeled mutant NF-κB oligonucleotide as a mutant competitor. All unlabeled oligonucleotides were preincubated with Hela nuclear extract at room temperature for 10 min then labeled NF-κB oligonucleotide was added. The left steps were the same as mentioned above.

Statistics analysis

All data were expressed as mean ±SD and analyzed by one-way repeated measures analysis of variance (ANOVA) using SPSS software (version 11.0 for windows). Pearson correlation analysis was used between parameters. P<0.05 was considered as statistically significant.

RESULTS

Postoperative common situation and survival time

The common situation of rats in the Wistar-to-Wistar group was very good after the transplantation. Recipients drank normally after 3rd day of posttransplantation. Normal coat recovered at day 7 with increase of body weight and all recipients survived for a long time. Recipients of rats in the SD-to-Wistar group ate badly with tarnished coat and progressive loss of body weight; all died within 9 to 13 days after the transplantation; median survival time was 10.7±0.51 days. Although 5 of 6 recipients of rats in the SD-to-Wistar+CsA group survived for a long time (one dead from abdominal inflammation and liver abscess day on 14 after the transplantation), they also drank badly with tarnished coat and ceased increase of body weight during CsA medication, which recovered after the cease of drug treatment. As for the LSA+SD-to-Wistar group, 5 of 6 recipients survived for a long time (one dead of bile duct obstruction on day 15 after the transplantation) and their common situation were remarkably better than that of rats in the SD-to-Wistar group and SD-to-Wistar+CsA group.

Histopathologic examination

No signs of rejection were found at any time point in the Wistar-to-Wistar group with minimal portal inflammatory infiltrates. In the SD-to-Wistar group, a few portal lymphocyte infiltrations combined with minimal vein endothelialitis on day 1 was found but there was no evidence of rejection. Significant portal lymphocyte infiltration with degeneration of hepatic parenchyma in some cases can be found on day 3 and day 5 with average rejection grade of 1.83 and 2.67, respectively. Severe inflammatory cells infiltration, severe vein subendothelialitis with bridging hepatocellular necrosis could be found on both day 7 and day 12 with rejection grade of 2.87 and 3, respectively. Owing to the immunosuppressive effect of CsA, rejection was greatly inhibited in the SD-to-Wistar+CsA group. No evidence of rejection was found at the first three time points. But mixed inflammatory infiltration and endothelialitis could be found on day 7 and day 12, in which grade 1 rejection was diagnosed. As for the LSA+ SD-to-Wistar group, rejection grades was 0 and 1 on day 1 and 3, respectively. Mixed but mainly lymphocytic infiltration was found in both portal tract and parenchyma without focal necrosis of the hepatic parenchyma on day 5, 7 and 12. Thus their rejection grades were all defined as 1.25 which were significantly lower

than that in the SD-to-Wistar group (P=0.026). Furthermore, no significant discrepancies of rejection grades on day7 and day 12 were found between the the SD-to-Wistar+CsA group and LSA+SD-to-Wistar group (P=0.067) (Figure 1).

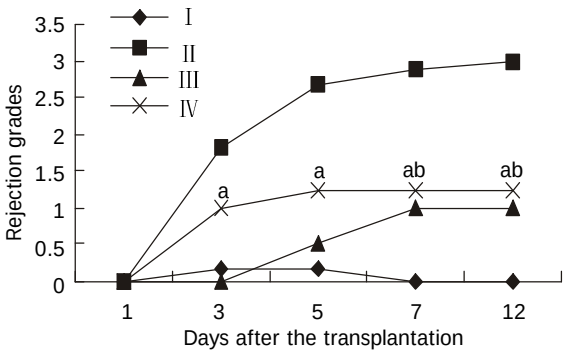

Figure 1 Rejection grades of grafted liver in different groups. Data were expressed as mean±SD. I, Wistar-Wistar group; II, SD-Wistar group; III, SD-Wistar+CsA group; IV, LSA+SD-Wistar group; Rejection grades of group IV were significantly lower than that in groupII at all but day 1 time point. No significant discrepancies were found between groupIV and groupIII on day 7 and day 12 time points. [a]P<0.05 *vs* groupII, [b]P>0.05 *vs* group III.

Expression of cytokine gene

The kinetic changes of intragraft IL-2 mRNA expression in different groups were shown in Figure 2: no expression was detected at any time point in the Wistar-to-Wistar and the SD-to-Wistar+CsA group, whereas high level expression was detected at all time points in the SD-to-Wistar group and reached to the peak on day 7 and 12 after the transplantation (P<0.001, *vs* the Wistar -to-Wistar group). Low level expression was only detected on day 5 in the LSA+SD-to-Wistar group which was significantly lower than that in the SD-to-Wistar group (P<0.001). Intragraft IFN-γ mRNA expression in different groups was shown in Figure 3. Very weak IFN-γ mRNA expression was detected at any time point in the Wistar-to-Wistar group after the liver transplantation, whereas there was very strong expression in the SD-to-Wistar group at all time points (P=0.006, *vs* the Wistar -to-Wistar group). The expression of IFN-γ mRNA was significantly inhibited in the SD-to-Wistar+CsA group which was significantly lower than that in the SD-to-Wistar group (P<0.001). As for group IV, its kinetic change was similar to that in the SD-to-Wistar group but was significantly lower than that in the SD-to-Wistar group at any time points (P=0.046). Expression of IL-2 and IFN-γ mRNA was correlated to the histopathological damage.

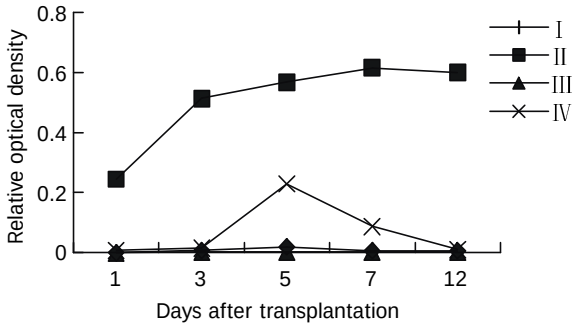

Figure 2 The kinetic change of intragraft IL-2mRNA expression in different groups. I, Wistar-Wistar group; II, SD-Wistar group; III, SD-Wistar+CsA group; IV, LSA+SD-Wistar group; IL-2mRNA expression of group IV were significantly lower than that in group II at all time point (P<0.05).

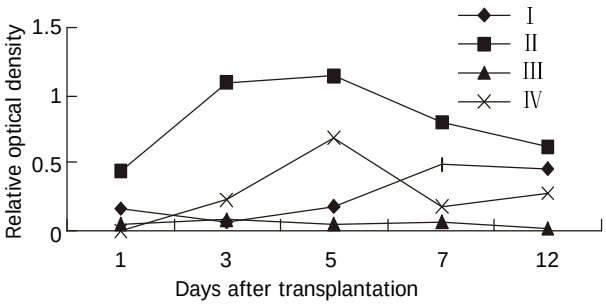

Figure 3 The kinetic change of Intragraft IFN-γ mRNA expression in different groups. I, Wistar-Wistar group; II, SD-Wistar group; III, SD-Wistar+CsA group; IV, LSA+SD-Wistar group; IL-2mRNA expression of group IV were significantly lower than that in group II at all time point (P<0.05).

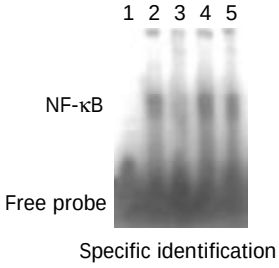

Figure 4 EMSA specific competitive inhibition. Lane 1, negative control; Lane 2, positive control; Lane 3, specific competition; Lane 4, non-specific competition; Lane 5, mutant competition.

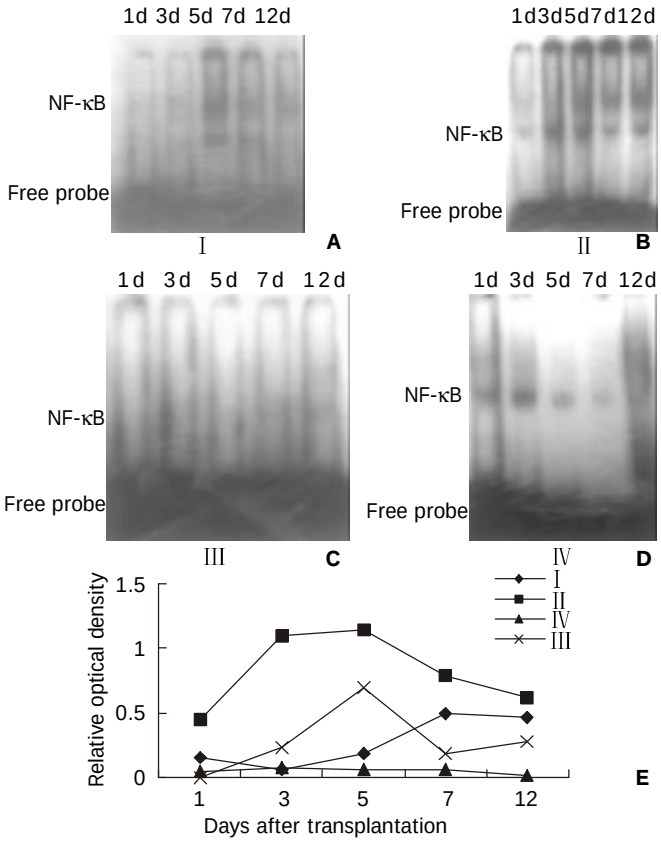

Figure 5 NF-κB activity of splenocytes at different time points after the transplantation. A, Wistar-Wistar group; B, SD-Wistar group; C, SD-Wistar+CsA group; D, LSA+SD-Wistar group; E, the kinetic change of NF-κB activity. NF-κB activity of group IV were significantly lower than that in group II at all time point (P<0. 05).

EMSA specific competitive inhibition and NF-kB activity of splenocytes

The results of EMSA competitive inhibition showed that no NF-κB activity was found after the specific competition, whereas NF-κB activity was the same as the positive control after the nonspecific competition and mutant competition (Figure 4). This results showed that this method was specific. NF-κB activity of splenocytes in Figure 5 showed the autoradiographic results of splenocyte NF-κB DNA binding activity in different groups (A, B, C, D). Low NF-κB activity was only detected on day 5 and day 7 in the Wistar-to-Wistar syngeneic group after the transplantation. In contrast, NF-κB activity increased from day 3 after the transplantation in the SD-to-Wistar group and was significantly higher than that in the syngeneic group at all time points (P=0.001). Only very weak DNA binding activity was found on day 12 in the SD-to-Wistar+CsA group and NF-κB activity was also inhibited in the LSA+SD-to-Wistar group which was significantly lower than that in the SD-to-Wistar group (P=0.003). NF-κB activity was significantly inhibited in the SD-to-Wistar+CsA and LSA+SD-to-Wistar group (Figure 5E).

Correlation analysis

A good correlation was found between the activity of NF-κB and intragraft IL-2 as well as IFN-γ mRNA expression in this study (pearson correlation analysis, r=0.737 and r=0.742 respectively, P<0.01,n=20). While intragraft IL-2 and IFN-γ mRNA expression were correlated to histopathological damage (pearson correlation analysis, r=0.856 and r=0.680 respectively, P<0.01,n=20).

DISCUSSION

Allotransplantation tolerance can be induced by intrathymic inoculation of donor cellular antigen[9-12], and also by intrathymic inoculation of donor soluble MHC antigen[13-15]. However, intrathymic inoculation of donor soluble non-MHC antigen have not been reported heretofore. In this study, we inoculated donor LSA into recipient thymus before the liver transplantation so that rejection was greatly inhibited. Only mild rejection was found in grafts and was significantly lower than that in the non-LSA inoculated group and similar to that in the CsA treated group. Recipients survived for a long time due to the induction of immunotolerance.

Although the rejection grades in the LSA+SD-to-Wistar group was increased obviously from day 3 and peaked at day 5 after transplantation, there was no significant difference between time points except for day 1 (P>0.05). This rejection kinetic change in the LSA+SD-to-Wistar group was similar to that in the Wistar -Wistar group and was significantly lower than that in the SD-to-Wistar group (P=0.026). Furthermore, the rejection grades in the LSA+SD-to-Wistar group did not significantly differ from that in the SD-to-Wistar+CsA group on day 7 and day 12 time point after the transplantation (P=0.067), which showed that intrathymic inoculation of LSA could greatly alleviate rejection. However, rejection in the SD-to-Wistar group was increased continuously and the rejection grade on day 3 after the transplantation was significantly different from its peak one (P<0.05). It was an optimal acute rejection control. As for the SD-to-Wistar+CsA group, rejection was greatly suppressed due to the effect of CsA and recipients survived for a long time, which was consistent with previous reports[16]. The rejection grades in all but SD-to-Wistar+CsA group was increased rapidly within groups when compared with that on day 1 after the transplantation (Figure 1) showed that the high immunoresponses starting from day 3 to day 5 after the transplantation was the "rejection crisis" phase[17]. Rejection crisis phase in the SD-to-Wistar+CsA group was postponed to start from day 5 to day 7 after the transplantation due to the strong immunosuppressive effect of CsA. Meanwhile, that rejection grades was not increase on day 7 after the transplantation both in the SD-to-Wistar+CsA group and LSA+SD-to-Wistar group and recipients survived for a long time suggested that the pathological damage in these two groups may be "self-limited". Given longer harvesting time point, more could probably be found.

For the expression of IL-2mRNA, the most related cytokine to rejection, detected using RT-PCR in grafts, low level expression was only detected on day 5 in the LSA+SD-to-Wistar group and it was significantly lower than that in the SD-to-Wistar group (P<0.001) (Figure 2). Although the expression of IFN-γ mRNA, another important cytokine to rejection, was slightly higher than that in the Wistar-to-Wistar group (P=0.427), it was also significantly inhibited in the LSA+SD-to-Wistar group (P<0.046,*vs* SD-to-Wistar group) (Figure3). IL-2 and IFN-γ are the representative cytokines secreted by Th1 cells which play important roles in transplant rejection[18-20]. Both intragraft IFN-γ mRNA and protein were increased when grafts were rejected[21,22]. IFN-γ not only increases expression of MHC class I and class II antigens of intragraft, but stimulates cells without expression of MHC class II antigens at quiescent state to express MHC class II antigens[23]. Thus inhibiting the synthesis and secretion of IL-2 and IFN-γ is one of the mainly target for preventing transplantation rejection all the while.

As an important nuclear transcription factor, NF-κB is a specific sequence binding protein which can bind to promoters or enhancers of multiple genes including closely related cytokines and adhesion molecules to organ transplantation rejection[24], thus extensively regulating the expression of these genes. Apart from that the change of NF-κB activity exerts crucial effects on the proliferation and activation of immune cells, NF-κB is also an important antiapoptotic nuclear factor[25,26]. So the change of NF-κB activity may play a crucial role in the immunoresponses and directly influence the immunoreaction after the transplantation. In its quiescent state, NF-κB is localized in cytoplasm in a complex with its inhibitory proteins (IκBs)[27,28], which mask its nuclear localization signal and prevent its from translocation to the nucleus. NF-κB is activated through phosphorylation and IκBs is subsequently degraded and then translocated into nucleus to bind with specific DNA sequences to regulate the expression of related genes[26]. NF-κB regulates the transcription of IL-2 mRNA through binding to its binding sites in down-stream of IL-2 gene promoter. It has been demonstrated *in vitro* that activated NF-κB can directly result in high level expression of IL-2 mRNA and promote the proliferation and activation of T lymphocyte[29]. IFN-γ gene belongs to lymphokine gene family and is related to transplantation rejection. Its transcription parallels that of other lymphokine genes such as IL-2 whose promoter activity can be enhanced by NF-κB protein[30,31]. In this regard, the ubiquitous factor NF-κB controlling a number of cytokines may have roles in the transcription of IFN-γ gene. It has also been demonstrated that NF-κB interacts with NF-AT to coregulate the gene expression of IFN-γ *in vitro*[32] but not *in vivo* especially in the organ transplantation rejection. We used rat orthotopic liver transplantation model to study the relationship between the activity of NF-κB and the expression of IL-2 and IFN-γ mRNA and its mechanisms with or without CsA and LAS treatment. A good correlation was found between the activity of NF-κB and the expression of intragraft IL-2 as well as IFN-γ mRNA in this study (pearson correlation analysis, r=0.737 and r=0.742 respectively, P<0.01, n=20). While the expression of intragraft IL-2 and IFN-γ mRNA were correlated

to the histopathological damage (pearson correlation analysis, r=0.856 and r=0.680 respectively, P<0.01, n=20). Thus it is believable that allotransplantation rejection is partly due to the activation of NF-κB at least. Both CsA and intrathymic inoculation of donor LSA can inhibit the activity of NF-κB and further inhibit the expression of IL-2 and IFN-γ mRNA and rejection after the transplantation.

We preliminarily discuss the specific tolerance mechanisms induced by LSA: T lymphocytes recognition process of tissue specific antigens is MHC-restricted which includes direct and indirect recognition and the latter is the main one. In this experiment, before the transplantation, protein antigen was used to inoculate recipient thymus. No APC and MHC molecules of donor existed, so the recognition of LSA should be indirect. Modern immunology believes that TCR recognizes neither MHC molecules nor antigen peptides alone. What it recognizes is surface information of MHC-antigen peptides complex. So it is believed that although LSA is organ specific, space conformation, electric charge qualities and distributions of MHC-antigen peptides complex are not the same due to its polymorphism, thus activating allolymphocytes[33]. But large numbers of activated lymphocytes may be clonally deleted due to high dose antigen immunization, which coincides with the "high-dose/activation- associated tolerance" mechanism[34]; In addition, thymus reeducation may also be one of the mechanisms of this tolerance.T lymphocytes of recipient recognize donor LSA as self by reeducation mechanism.

Therefore it was postulated that given multiple MHC loci matching, the processing ability of tissue specific antigens by recipient MHC molecules will be enhanced or be equal to that of by donor' s, thus bring about indirect recognition of T lymphocytes changing into direct recognition and increasing the occurrence of hepatopathy and rejection after the transplantation. This may be one of the reasons why mutiple MHC loci matching, especially DR matching, can increase the rates of grafted liver dysfunction and rejection[1,2]. This may be just as what Desquenne postulated that it should make it easier to induce tolerance of skin antigen as well as other tissue specific antigen when MHC incompatibilities prevail[35]. Besides, special attention must be paid to the LSA+SD-to-Wistar group. The common situation of recipients without any transient immunosuppression were much better than that in the non-LSA or CsA-treated group and no such complications as inflammations happened. It showed that the tolerance did not result from down-regulation of body' s immunofunction, in contrast recipients' immunuofunction was normal. This is perhaps the optimal condition to induce donor specific tolerance and do not affect body' s immunofunction. Reasonable explanation is that strong immunoreaction towards to liver parenchymal cells happened when transplanted liver was rejected. Thus the tolerance induced by LSA is towards to hepatocytes and is in real sense a donor and organ specific one.

The results of this experiment not only demonstrated that thymus had unusual effects on the tolerance induction, but also that allotolerance to non-MHC antigen can be induced after contacting of thymus microenvironment to non-MHC antigen. It may suggest that if immunodominant character or immunodominant non-MHC antigens were identified, differences of other MHC and non-MHC antigen may be neglected, thus leading to long-term allografts survival across complete MHC barrier. It also suggested that MHC antigens may be not the only obstacles to successful transplantation. It is reported here for the first time that intrathymic inoculation of LSA can induce permanent and specific immunotolerance of liver allotransplantation, which show that hepatocytes are directly involved in the immunoreaction of liver transplantation. It' s an important supplement to the traditional theory of liver transplantation rejection which considers that rejection is mainly involved in liver vascular bed, bile ducts and nonparenchymal cells, thus leading to a novel way to liver transplantation immunotolerance.

REFERENCES

1 **Donaldson P**, Underhill J, Doherty D, Hayllar K, Calne R, Tan KC, O'Grady J, Wight D, Portmann B, Williams R. Influence of human leukocyte antigen matching on liver allograft survival and rejection: "the dualistic effect". *Hepatology* 1993; **17**: 1008-1015

2 **Doran TJ**, Derley L, Chapman J, McCaughan G, Painter D, Dorney S, Sheil AG. Severity of liver transplantation rejection is associated with recipient HLA type.*Transplant Proc* 1992; **24**: 192-193

3 **Yan YH**, Liu GZ. Transplantation antigens. In: YiZhi MianYi Xue. *Wuhan: Hubei Science and Technology Press* 1998: 45-47

4 **Lohse AW**, Dienes HP, Meyer zum Buschenfelde KH. Suppression of murine experimental autoimmune hepatitis by T-cell vaccination or immunosuppression. *Hepatology* 1998; **27**: 1536-1543

5 **Kamada N**, Calne RY. A surgical experience with five hundred thirty liver transplants in the rat. *Surgery* 1983; **93**: 64-69

6 **Kemnitz J**, Ringe B, Cohnert TR, Gubernatis G, Choritz H, Georgii A. Bile duct injury as a part of diagnostic criteria for liver allograft rejection. *Hum Pathol* 1989; **20**: 132-143

7 **Kravchenko VV,** Pan Z, Han J, Herbert JM, Ulevitch RJ, Ye RD. Platelet-activating factor induces NF-kappa B activation through a G protein-coupled pathway. *J Biol Chem* 1995; **270**: 14928-14934

8 **Gong JP**, Liu CA, Wu CX, Li SW, Shi YJ, Li XH. Nuclear factor kB activity in patients with acute severe cholangitis. *World J Gastroenterol* 2002; **8**: 346-349

9 **Fujii Y,** Sugawara E, Hayashi K, Sano S. Neonatal intrathymic splenocyte injection yields prolonged cardiac xenograft survival. *Acta Med Okayama* 1998; **52**: 83-88

10 **Oluwole OO**, Depaz HA, Gopinathan R, Ali A, Garrovillo M, Jin MX, Hardy MA, Oluwole SF. Indirect allorecognition in acquired thymic tolerance: induction of donor-specific permanent acceptance of rat islets by adoptive transfer of allopeptide-pulsed host myeloid and thymic dendritic cells. *Diabetes* 2001; **50**: 1546-1552

11 **Torchia MG**, Aitken RM, Thliveris A. The effect of thymic inoculation to induce tolerance of allogeneic thyroid grafts in the outbred rabbit. *Histol Histopathol* 1998; **13**: 1061-1068

12 **Blom D**, Morrissey N, Mesonero C, Zuo XJ, Jordan S, Fisher T, Bronsther O, Orloff MS. Tolerance induction by intrathymic inoculation prevents chronic renal allograft rejection. *Transplantation* 1998; **65**: 272-275

13 **Chowdhury NC**, Saborio DV, Garrovillo M, Chandraker A, Magee CC, Waaga AM, Sayegh MH, Jin MX, Oluwole SF. Comparative studies of specific acquired systemic tolerance induced by intrathymic inoculation of a single synthetic Wistar-Furth (RT1U) allo-MHC class I (RT1.AU) peptide or WAG (RT1U)-derived class I peptide. *Transplantation* 1998; **66**: 1059-1066

14 **Fandrich F**, Zhu X, Schroder J, Dresske B, Henne-Bruns D, Oswald H, Zavazava N. Different in vivo tolerogenicity of MHC class I peptides. *J Leukoc Biol* 1999; **65**: 16-27

15 **Stadlbauer TH**, Schaub M, Magee CC, Kupiec Weglinski JW, Sayegh MH. Intrathymic immunomodulation in sensitized rat recipients of cardiac allografts: requirements for allorecognition pathways. *J Heart Lung Transplant* 2000; **19**: 566-575

16 **Gassel HJ**, Otto C, Gassel AM, Meyer D, Steger U, Timmermann W, Ulrichs K, Thiede A. Tolerance of rat liver allografts induced by short-term selective immunosuppression combining monoclonal antibodies directed against CD25 and CD54 with subtherapeutic cyclosporine. *Transplantation* 2000; **69**: 1058-1067

17 **Sharland A**, Shastry S, Wang C, Rokahr K, Sun J, Sheil AG, McCaughan GW, Bishop GA. Kinetics of intragraft cytokine expression, cellular infiltration, and cell death in rejection of renal allografts compared with acceptance of liver allografts in a rat model: early activation and apoptosis is associated with liver graft acceptance.*Transplantation* 1998; **65**: 1370-1377

18 **Coito AJ**, Shaw GD, Li J, Ke B, Ma J, Busuttil RW, Kupiec-Weglinski JW. Selectin-mediated interactions regulate cytokine networks and macrophage heme oxygenase-1 induction in cardiac allograft recipients.*Lab Invest* 2002; **82**: 61-70

19 **Ring GH**, Saleem S, Dai Z, Hassan AT, Konieczny BT, Baddoura FK, Lakkis FG. Interferon-gamma is necessary for initiating the acute rejection of major histocompatibility complex class II-disparate skin allografts. *Transplantation* 1999; **67**: 1362-1365
20 **Boehler A**, Bai XH, Liu M, Cassivi S, Chamberlain D, Slutsky AS, Keshavjee S. Upregulation of T-helper 1 cytokines and chemokine expression in post-transplant airway obliteration. *Am J Respir Crit Care Med* 1999; **159**: 1910-1917
21 **Moudgil A**, Bagga A, Toyoda M, Nicolaidou E, Jordan SC, Ross D. Expression of gamma-IFN mRNA in bronchoalveolar lavage fluid correlates with early acute allograft rejection in lung transplant recipients. *Clin Transplant* 1999; **13**: 201-207
22 **Affleck DG**, Bull DA, Albanil A, Shao Y, Brady J, Karwande SV, Eichwald EJ, Shelby J. Interleukin-18 production following murine cardiac transplantation: correlation with histologic rejection and the induction of INF-gamma.*J Interferon Cytokine Res* 2001; **21**: 1-9
23 **Gill RG**, Coulombe M, Lafferty KJ. Pancreatic islet allograft immunity and tolerance: the two-signal hypothesis revisited. *Immunol Rev* 1996; **149**: 75-96
24 **Baeuerle PA, Baltimore D**. NF-κB: ten years after. *Cell* 1996; **87**: 13-20
25 **Fonteh AN**, Marion CR, Barham BJ, Edens MB, Atsumi G, Samet JM, High KP, Chilton FH. Enhancement of mast cell survival: a novel function of some secretory phospholipase A(2) isotypes. *J Immunol* 2001; **167**: 4161-4171
26 **Akari H**, Bour S, Kao S, Adachi A, Strebel K. The human immunodeficiency virus type 1 accessory protein Vpu induces apoptosis by suppressing the nuclear factor kappaB-dependent expression of antiapoptotic factors. *J Exp Med* 2001; **194**: 1299-1311
27 **Granville DJ**, Carthy CM, Jiang H, Levy JG, McManus BM, Matroule JY, Piette J, Hunt DW. Nuclear factor-kappaB activation by the photochemotherapeutic agent verteporfin. *Blood* 2000; **95**: 256-262
28 **Tenjinbaru K**, Furuno T, Hirashima N, Nakanishi M. Nuclear translocation of green fluorescent protein-nuclear factor kappaB with a distinct lag time in living cells. *FEBS Lett* 1999; **444**: 1-4
29 **Kalli K**, Huntoon C, Bell M, McKean DJ. Mechanism responsible for T-cell antigen receptor-and CD28-or interleukin 1 (IL-1) receptor-initiated regulation of IL-2 gene expression by NF-kappaB. *Mol Cell Biol* 1998; **18**: 3140-3148
30 **Herndon TM**, Juang YT, Solomou EE, Rothwell SW, Gourley MF, Tsokos GC. Direct transfer of p65 into T lymphocytes from systemic lupus erythematosus patients leads to increased levels of interleukin-2 promoter activity. *Clin Immunol* 2002; **103**: 145-153
31 **Zhou XY**, Yashiro-Ohtani Y, Nakahira M, Park WR, Abe R, Hamaoka T, Naramura M, Gu H, Fujiwara H. Molecular mechanisms underlying differential contribution of CD28 versus non-CD28 costimulatory molecules to IL-2 promoter activation. *J Immunol* 2002; **168**: 3847-3854
32 **Sica A**, Dorman L, Viggiano V, Cippitelli M, Ghosh P, Rice N, Young HA. Interaction of NF-kappaB and NFAT with the interferon-gamma promoter. *J Biol Chem* 1997; **272**: 30412-30420
33 **Liblau RS**, Tisch R, Shokat K, Yang X, Dumont N, Goodnow CC, McDevitt HO. Intravenous injection of soluble antigen induces thymic and peripheral T-cells apoptosis. *Proc Natl Acad Sci USA* 1996; **93**: 3031-3036
34 **Bishop GA**, Sun J, Sheil AG, McCaughan GW. High-dose/activation-associated tolerance: a mechanism for allograft tolerance. *Transplantation* 1997; **64**: 1377-1382
35 **Desquenne-Clark L**, Kimura H, Naji L, Silvers WK. Comparison of the abilities of MHC-compatible bone marrow cells and lymph node cells to induce tolerance of skin allografts in rats. *Transplantation* 1993; **56**: 1230-1233

Edited by Xu XQ

P.O.Box 2345, Beijing 100023, China
Fax: +86-10-85381893
E-mail: wjg@wjgnet.com www.wjgnet.com

World J Gastroenterol 2003;9(4):765-770
World Journal of Gastroenterology
 ISSN 1007-9327

• BASIC RESEARCH •

Expression of growth hormone receptor and its mRNA in hepatic cirrhosis

Hong-Tao Wang, Shuang Chen, Jie Wang, Qing-Jia Ou, Chao Liu, Shu-Sen Zheng, Mei-Hai Deng, Xiao-Ping Liu

Hong-Tao Wang, Jie Wang, Qing-Jia Ou, Chao Liu, Department of Hepato-biliary Surgery, Sun Yat-Sen Memorial Hospital, the Second Affiliated Hospital, Sun Yat-Sen University, Guangzhou 510120, Guangdong Province, China
Shuang Chen, Department of Gastroenteral Surgery, Sun Yat-Sen Memorial Hospital, the Second Affiliated Hospital, Sun Yat-Sen University, Guangzhou 510120, Guangdong Province, China
Shu-Sen Zheng, Molecular Medical Laboratory Center, Sun Yat-Sen Medical College, Sun Yat-Sen University, Guangzhou 510089, Guangdong Province, China
Mei-Hai Deng, Department of General Surgery, the Third Affiliated Hospital, Sun Yat-Sen University, Guangzhou 510630, Guangdong Province, China
Xiao-Ping Liu, Department of General Surgery, Shenzhen Central Hospital, Peking University, Shenzhen 518036, China
Supported by the Natural Science Foundation of Guangdong Province, No.984213 and Academic Foundation of Sun Yat-Sen University of Medical Sciences and Ministry of Health for Project 211, No.F000099075
Correspondence to: Dr. Hong-Tao Wang, M.D., Ph.D., Department of Hepato-biliary Surgery, Sun Yat-Sen Memorial Hospital, the Second Affiliated Hospital, Sun Yat-Sen University, Guangzhou 510120, Guangdong Province, China. sumswht@hotmail.com
Telephone: +86-20-81332020 **Fax:** +86-20-81332853
Received: 2002-10-05 **Accepted:** 2002-11-06

Abstract

AIM: To investigate the expression of growth hormone receptor (GHR) and mRNA of GHR in cirrhotic livers of rats with the intension to find the basis for application of recombinant human growth hormone (rhGH) to patients with liver cirrhosis.

METHODS: Hepatic cirrhosis was induced in Sprague-Dawley rats by administration of thioacetamide intraperitoneally for 9-12 weeks. Collagenase IV was perfused in situ for isolation of hepatocytes. The expression of GHR and its mRNA in cirrhotic livers was studied with radio-ligand binding assay, RT-PCR and digital image analysis.

RESULTS: One class of specific growth hormone-binding site, GHR, was detected in hepatocytes and hepatic tissue of cirrhotic livers. The binding capacity of GHR (R_T, fmol/mg protein) in rat cirrhotic liver tissue (30.8±1.9) was significantly lower than that in normal control (74.9±3.9) at the time point of the ninth week after initiation of induction of cirrhosis (n=10, P<0.05), and it decreased gradually along with the accumulation of collagen in the process of formation and development of liver cirrhosis (P<0.05). The number of binding sites (×10^4/cell) of GHR on rat cirrhotic hepatocytes (0.86±0.16) was significantly lower than that (1.28±0.24) in control (n=10, P<0.05). The binding affinity of GHR among liver tissue, hepatocytes of various groups had no significant difference (P>0.05). The expression of GHR mRNA (riOD, pixel) in rat cirrhotic hepatic tissues (23.3±3.1) was also significantly lower than that (29.3±3.4) in normal control (n=10, P<0.05).

CONCLUSION: The growth hormone receptor was expressed in a reduced level in liver tissue of cirrhotic rats, and lesser expression of growth hormone receptors was found in a later stage of cirrhosis. The reduced expression of growth hormone receptor was partly due to its decreased expression on cirrhotic hepatocytes and the reduced expression of its mRNA in cirrhotic liver tissue.

Wang HT, Chen S, Wang J, Ou QJ, Liu C, Zheng SS, Deng MH, Liu XP. Expression of growth hormone receptor and its mRNA in hepatic cirrhosis. *World J Gastroenterol* 2003; 9 (4): 765-770
http://www.wjgnet.com/1007-9327/9/765.htm

INTRODUCTION

Liver cirrhosis is a common pathway of a variety of chronic liver diseases[1] and is associated with high protein catabolism, low anabolism and negative nitrogen balance[2] resulting in hypoproteinemia which contributes to ascites, dysfunction of coagulation and suppressed immune reponses[3] as pathophysiological outcomes. In fact, progressive nutrition deficiencies and muscle wasting are universal problems and critical predictors of morbidity, mortality and survival[4, 5] after surgical intervention. Early reports showed that cirrhotic patients requiring emergency abdominal surgery exhibited a higher mortality[6]. In retrospective studies of liver transplant recipients, protein-calorie malnutrition had been associated with adverse outcomes in patients with end-stage liver diseases[7, 8]. A prospective study showed that cirrhotic patients with hypermetabolism and body mass loss had a much higher mortality rate after liver transplantation than those with normometabolism[9]. Nutritional support is critical for patients with hepatic cirrhosis. Yet, studies have shown that aggressive nutritional support is essential but not effective enough to prevent protein loss and optimize the care of these patients in severe catabolic illness, including cirrhosis[10, 11].

Recent research has investigated the role of exogenous growth factor therapy in catabolic illness. Recombinant human growth hormone (rhGH) has been used in catabolic states such as after abdominal operation[12], organ transplantation[13], major trauma[14] and severe burns[15] to enable them to survive an aggressive surgery and gain access to a new life[16]. After treatment of rhGH, donor site healing rate in children with severe burns enhanced and thus decreased a 14-day hospitalization time[17-19], Mortality rates in severely burned adults dropped 26 %[20]. Cell-mediated immunity significantly enhanced, wound infection rates and length of hospitalization in a large group of post surgical patients decreased[21]. Some clinical trial reported that growth hormone enhanced nitrogen retention in patients with chronic obstructive lung diseases[22], severe sepsis[23, 24] and wasting status of AIDS[25, 26] and in fasted adult volunteers. Although there are many controversies[27-31], it has been confirmed that rhGH is an effective drug to accelerate protein anabolism[32] and plays a central role in metabolic intervention with a significant cost-effect benefit[33].

The action of growth hormone depends on its binding with growth hormone receptor on cell membrane[34]. Whether the cirrhotic hepatocytes express growth hormone receptors (GHR), and the relationship between the GHR expression and the staging of liver cirrhosis are not clear. So, we adopted multiple techniques such as radioligand binding assay and RT-PCR to measure the changes of GHR and its mRNA in an experimental liver cirrhosis model at cellular and histological levels for understanding of biological feature of expression of GHR in cirrhotic hepatocytes.

MATERIALS AND METHODS

Induction of liver cirrhosis

Liver cirrhosis in rats was induced by daily intraperitoneal injection of 3 % thioacetamide (TAA, Shanghai, China) 50 mg/kg for 9 to 12 weeks[35, 36]. Two hundreds male Sprague-Dawley rats (200-300 g, Medical Animal Center, Sun Yat-Sen University) were randomized and allotted to two groups, normal group (n=82) received saline intraperitoneally everyday; and cirrhotic group (n=118) received drugs for induction of hepatic cirrhosis. From each group, 80 rats were available for analysis. Rats were fed with regular chow and water *ad libitum* in cages placed in a room with 12-hour light-dark cycle and constant humidity and temperature (25 ℃).

At the 3rd, 6th, 9th, 12th week and the 15th week (3 weeks after withdrawal of TAA) after induction of liver cirrhosis 10 rats from each group were fasted overnight and sacrificed. Liver tissue samples were obtained after hepatic sinusoids were flushed by perfusion of liver with normal saline through the portal vein. Tissue samples from the right major liver lobe were obtained and frozen in liquid nitrogen immediately and then stored at -80 ℃ until use, or fixed in 10 % neutral buffered formaldehyde solution and dehydrated and embedded in paraffin for regular pathological examination.

Digital image analysis

Liver collagen content was calculated by histomorphometric measurement in 4-μm sections with Masson' s trichrome stain. Under photographic analytic microscope (Carl Zeiss Axiotron, OPTON, Germeny), three random areas in each section of liver slide were chosen and captured in RGB format with 24-bit true colors at a resolution of 768×512 in real time by the JVC ky-F30B 3-CCD color video camera with digital conversion connected with a computer system of Kontron IBAS2.5 (OPTON, Germeny) for digital image analysis. The total area and the area of fibrosis with positive staining were automatically selected, outlined and evaluated by planimetry. The relative content of collagen (RCC %) was expressed as a percentage of positive staining area in the total area[37, 38].

Hepatocyte isolation

At 9-12 weeks of the study, livers in 10 rats from each group were perfused *in situ* through portal vein with collagenase (type IV, 90 or 120 U/ml)[39, 40]. Hepatocytes were isolated at 4 ℃ by centrifugation (50×g, 5 min or 1×g, 10 min). Cells were re-suspended for radio-ligand binding assay in RPMI 1640 medium without serum to a final concentration of 1.0×10^6 cell/ml with a purity of more than 98 % and a viability of more than 90 % determined by trypan-blue exclusion.

Total RNA isolation

Total RNA of liver tissue was prepared from 10 rats in each group at the 9th week during the induction of cirrhosis by a single-step method[41]. Integrity and quality of RNA were tested by electrophoresis in 1 % agarose-formaldehyde gels stained with ethidium bromide. The RNA concentration was evaluated at spectrophotometric absorbance at 260 nm.

Primers for RT-PCR

Primers for the PCR amplification of GHR transcripts were purchased from Sangon Co. (Shanghai, China). The primers used for detection of GHR mRNA by RT-PCR were specific for the intracellular domain of the rat GHR, thus excluding detection of the smaller transcripts encoding GH-binding protein (GHBP)[42]. The forward primer (GHR4548) was 5' -*ATGTGAGATCCAGACAACG-3' with the first base *A at the 5' end as an unmatched base of the original G and spanned from 876 to 894 located in exon 7 and the reverse one 5' -ATGTCAGGGTCATAACAGC-3' spanned from 1 356 to 1 374 located in exon 10. The PCR product was supposed to be 499 bp in length.

RT-PCR

RT-PCR was performed using the MasterAmp™ RT-PCR kit (Epicentre, Madison, USA) for detection of GHR mRNA[43]. The procedure of RT-PCR was similar to that of literature[44]. Negative controls in RT-PCR included reactions in the absence of RNA sample or primers or RT reaction to detect possible contamination of genomic DNA in RNA samples. The experiment was considered ineffective if there was any incidental band in lane of negative control. 10 μl of each PCR products was subjected to electrophoresis for about 1 hour on 1 % agarose gel using electrophoresis apparatus (Bio-Rad, UK) and visualized by staining with ethidium bromide. The bands were observed using a ultraviolet gel device (UVI, UK) and captured into its computer system for digital image analysis. The level of GHR mRNA in each sample was expressed as: iOD (pixel)=the average optical density of each band×its area (pixel).

Membrane microsome preparation

The microsomal liver membrane fraction was prepared by differential centrifugation of liver homogenate according to Papotti[45]. About 1 g tissue from rat livers was chopped and homogenized with an electric homogenizer (Vorsicht, Malaysia) in ice-cold (4 ℃) phosphate buffer (PBS) containing 0.25 M sucrose. The mixture was centrifuged at 1 500×g for 15 minutes. The supernatant was collected and centrifuged at 30 000×g for 30 minutes. The pellet was re-suspended in 3M $MgCl_2$ for 5 minutes to remove endogenous GH binding[46] and centrifuged, the pellet was suspended in PBS. Protein concentration of the solution was determined by Lowry method.

GH binding assay

In radioreceptor assay, 100 μl (approximately 20 000 cpm) of ^{125}I-hGH (NEN Inc, Boston, USA) with a specific activity of about 108 μCi/μg, 100 μl of unlabeled hGH in PBS and 100 μl of liver membrane microsomes or liver cells were mixed and incubated at 4 ℃ over night. Parallel incubations were performed with various amounts of hGH (0-3nM divided into 7-9 concentration gradients) in duplicate. An excess of hGH was used to determine nonspecific binding. At the end of the incubation, bound and free hormones were separated by filtration (0.18 μm mesh filters, Shanghai, China)[47]. The pellets on membrane were subjected to a gamma counter (SNγ682, Rihuan, Shanghai, China). GH binding affinity constant (Kd, nM) and binding capacity (R_T, fmol/mg protein) or numbers of ^{125}I-GH binding sites of hepatocytes ($\times10^4$/cell) were calculated by Scatchard analysis using the LIGAND program[48, 49].

Statistical analysis

Results were expressed as the mean ± SEM ($\bar{x}\pm s$) and analyzed by ANOVA and least significant difference (LSD) method with an acceptance of significance as $P<0.05$.

RESULTS

Changes of lobular structure and RCC in the development of liver cirrhosis

In control group, no evident pathological change of lobular structure was found in liver tissue over 15 weeks. In cirrhotic model group, 4 stages of pathological changes were manifested during the development of liver cirrhosis: (1) scattered necrosis and cellular degeneration at the 3rd week; (2) fibrous proliferation at the 6th week; (3) pseudo-lobule formation at the 9th week; (4) massive nodule formation at the 12th week and (5) partial reversion of cirrhosis at the 15th week.

In control group, there was no significant change of RCC (P>0.05) among the different time points during the period of 15 weeks (Table 1). While compared with that of the control group at the same time point, RCC kept no significant change at the 3rd week (P>0.05) and increased significantly at the 6th, 9th, 12th and 15th week respectively (P<0.05) in the cirrhotic model group. When compared among the different time points in the cirrhotic model group, RCC increased gradually at the 3rd, 6th, 9th week and reached to its turning point at the 12th week (P<0.05), then went down, but still above normal level at the 15th week.

Table 1 Dynamic alteration of RCC, R_T and Kd in cirrhotic liver tissues

Time	RCC (%)		RT (fmol / mg protein)		Kd (nM)	
	Control Group	Model Group	Control Group	Model Group	Control Group	Model Group
3rd week	1.29±0.23	1.56±0.35	75.8±5.1	55.2±4.5[b]	0.62±0.03	0.61±0.07
6th week	1.19±0.21	10.8±2.5[ab]	77.3±4.3	42.6±2.1[ab]	0.64±0.05	0.58±0.06
9th week	1.16±0.18	20.2±3.6[ab]	74.9±3.9	30.8±1.9[ab]	0.61±0.09	0.60±0.04
12th week	1.27±0.25	28.0±4.3[ab]	73.2±5.4	17.5±2.5[ab]	0.60±0.08	0.59±0.07
15th week	1.13±0.24	15.2±2.6[ab]	71.5±4.9	20.8±1.6[b]	0.58±0.06	0.61±0.09

[a]P<0.05 *vs* a previous time point, [b]P<0.05 *vs* control group. RCC: relative content of collagen (%) indicating severity of liver fibrosis; R_T: total binding capacity of receptors (fmol / mg protein) corresponding to the quantity of receptors; K_d: dissociation constant in equilibrium (nM) which is equal to the affinity of receptors.

GH binding in the development of liver cirrhosis

GH binding assay was carried out using liver membrane microsomes from rats at different time points in various groups and specific binding for ^{125}I-hGH was detected in all samples. The Scatchard analysis of GH binding capacity (R_T) and affinity (Kd) on each sample was performed and a single class of specific GH-binding sites on liver cell membranes, that is GHR, was revealed in both normal and cirrhotic liver tissue samples by linear Scatchard plots (Figure 1).

No significant change of R_T and Kd was found in liver tissue samples during the period of 15 weeks in control group (P>0.05) (Table 1 and Figure 1). While compared with that of the control group at the same time point, R_T decreased significantly (P<0.05) at the 3rd, 6th, 9th, 12th and 15th week although no change of Kd was observed in cirrhotic model group. When compared among the different time points in the cirrhotic model group, R_T decreased gradually at the 3rd, 6th, 9th week and reached to its lowest point (P<0.05) at the 12th week, then increased but still under normal level at the 15th week.

The correlation analysis manifested a significant negative linear correlation between R_T and RCC in rat liver cirrhotic tissue (r=-0.82, n=50, P<0.05) (Figure 2).

Quantitative analysis of GH binding sites on rats hepatocytes

There were linear Scatchard plots of normal and cirrhotic hepatocytes, which indicated the presence of a single class of specific GH-binding sites, GHR, on hepatocyte membranes. The quantity of GH-binding sites (×10^4/cell) on hepatocytes of cirrhotic model group (0.86±0.16) was significantly less than that (1.28±0.24) in normal control group (n=10, P<0.05) while the affinity (Kd, nM) of hepatocytes from model group (0.56±0.08) and control group (0.61±0.11) was similar (n=10, P>0.05).

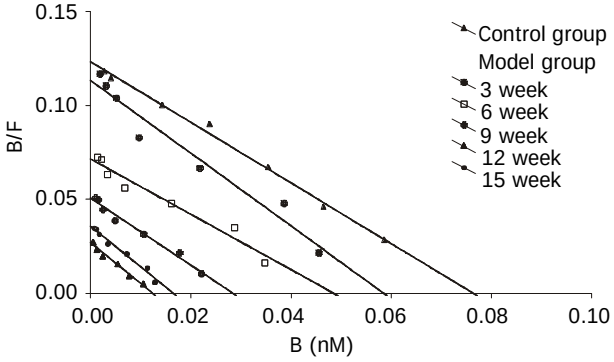

Figure 1 Scatchard analysis of GH-binding in rat liver tissue. Microsomes of liver tissues were incubated with ^{125}I-labeled hGH and increased concentrations of unlabeled hGH. The bound / free radioactivity ratio (Y axis) was plotted as a rectilineal function of bound hormone (X axis). GH binding capacities (Bmax=intercept on X axis, R_T=Bmax / protein concentration) and affinities (Kd=negative reciprocal of slope) were calculated from the competition assays by Scatchard analysis.

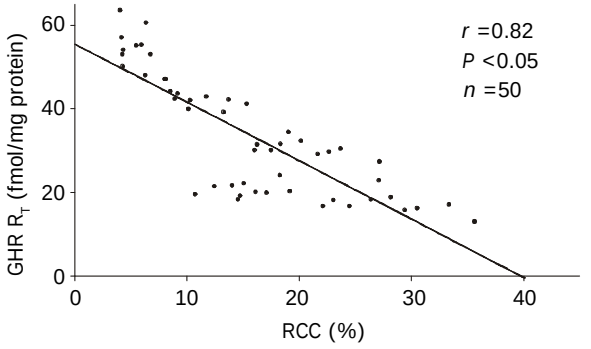

Figure 2 Correlation between R_T (quantity of GHR) and RCC (degree of cirrhosis) in rat cirrhotic liver samples.

GHR mRNA detected by RT-PCR

A specific band of RT-PCR products (499 bp in length) was detected in liver tissue samples from both control group and cirrhotic model group, indicating that GHR mRNA was expressed in both groups. The level of GHR mRNA (iOD, pixel) in cirrhotic liver (23.3±3.1) was lower than that (29.3±3.4) in normal liver (n=10, P<0.05) (Figure 3).

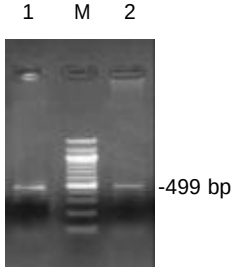

Figure 3 Comparison of GHR mRNA expression in liver tissue in normal control group and cirrhotic model group (the result of RT-PCR). Lane M: 100 bp DNA ladder; Lane 1: Normal control group; Lane 2: Cirrhotic model group.

DISCUSSION

Much has been done regarding the expression of GHR and signal transduction[34, 47, 50, 51], but the expression of GHR in some pathological states such as cirrhotic hepatocytes, malignant cells is not clear. Chang[52] reported that ^{125}I-rhGH binding activity in 6 cases of hepatocellular carcinoma and adjacent cirrhotic liver tissue could not be detected and believed that the GHR in cirrhotic hepatic tissue disappeared although the study only examined one aspect of the GHR, GH binding. Another study[53] showed that specific binding of ^{125}I-hGH in liver tissue from liver transplant of 17 cases with end-stage liver diseases was lower than that in normal control, but only in 3 cirrhotic livers Scatchard analysis was performed for calculation of GH binding capacity and affinity. In this setting of tissue-based GH binding assay, it was not convincing enough to clear up the controversy about the expression of GHR on cirrhotic liver cells. So, GH binding assay at cellular level was used to analyze the expression of GHR on hepatocytes or in liver tissue of rats with cirrhosis. We have demonstrated that the growth hormone receptor was expressed on cirrhotic hepatocytes and lesser expression of GHR was found in a later stage of cirrhosis.

In present study, ^{125}I-hGH binding activity of cirrhotic hepatic tissue was studied with radioligand binding assay, and a single class of growth hormone specific binding sites with normal affinity was detected in the cirrhotic hepatic tissue, which indicated the expression of GHR in cirrhotic hepatic tissue. These results were compatible with those of clinical specimens from liver transplants[53].

The relationship between the GHR expression in cirrhotic tissue and the stage of liver cirrhosis has not been reported. In our study, ^{125}I-hGH binding capacity (*i.e.* the quantity of GHR) decreased significantly even in the early stage of cirrhosis, and gradually decreased during the development of liver fibrosis and dropped to the lowest level in late stage of cirrhosis on week 12 after induction of hepatic cirrhosis, then increased but still below the normal level after withdrawal of TAA. This implicated that the quantity of GHR in liver tissue altered dynamically without any significant change of GH binding affinity over the development or recovery of liver cirrhosis. In other words, GHR expression was suppressed in the process of formation of liver cirrhosis. The more severe the cirrhosis was, the more significant the down regulation of GHR expression would be.

GH binding varied among liver samples[47,53]. Our results indicated that GH binding capacity in rat cirrhotic liver tissue differed in various stages of liver cirrhosis, and only slight variation (data not listed) of such binding was found in liver tissue with the same time point during the development of cirrhosis. Therefore, histological staging of liver cirrhosis was one of the important factors predisposing the down-regulation of GHR expression[54].

Fibrotic tissue accumulated in the portal area during the reconstruction of lobule of cirrhotic liver while hepatocytes regenerated continuously after repeated necrosis in the development of liver cirrhosis. The fibrous structure, hepatocytes and interstitial cells with heterogeneous distribution and various combination in cirrhotic tissue should be considered respectively as we analyzed the expression of growth hormone receptor. In the present study, the result of GH-binding capacity (R_T) in cirrhotic liver tissue indicated the GHR expression on membrane microsomes in hepatocytes and interstitial cells and could be affected by non-parenchymal cells rather than fibrotic tissue[53]. The quantitative measurement of GH binding sites on parenchymal cells from cirrhotic livers had not been reported previously. Therefore Scatchard analysis was resorted to again and a single class of growth hormone specific binding sites with normal affinity was detected in isolated cirrhotic hepatocytes, suggesting the expression of GHR on cirrhotic hepatocytes disassociated *in vitro*. It was found that the binding sites on cirrhotic hepatocytes was significantly decreased as compared with that on normal hepatocytes, which implied that cirrhotic hepatocytes expressed GHR in a reduced level without any significant difference of binding affinity. So, the decreased expression of GHR in cirrhotic liver tissue should be attributed not only to accumulation of interstitial cells but to the reduced expression of GHR on cirrhotic hepatocytes themselves also.

It is possible that the reduced level of GH binding is partly owing to the reduced population of hepatocytes and increased numbers of interstitial cells in cirrhotic livers. But the mechanisms of the reduced GHR expression on cirrhotic hepatocytes has not been defined yet. The reduced GH binding level was unlikely due to changes in the receptor itself. Occupancy of the receptors by endogenous GH and ligand-induced internalization of GHR may affect the measurement of the binding, since dissociation of GH from its receptor and recycling of GHR is incomplete in several hours[55]. Therefore, GH binding was determined on microsomes that had been desaturated by exposure to 3M $MgCl_2$ for 5 minutes[46]. It was reported that the specific binding of ^{125}I-labelled bovine GH to a GHR-enriched low density membrane fraction from regenerating rat liver was reduced to 10-35 % between 12 and 24 h and remained low until 48 h after partial hepatectomy[46], which indicated the amount of functional GHR on hepatocytes was decreased with repeated degeneration, necrosis and regeneration in the microenvironment of cirrhosis. In this situation several cytokines such as IL-1β, TNF-α and glucocorticoids seemed to be involved in the likely mechanism of the reduced GHR expression[40, 56, 57].

It is necessary to investigate the changes of GHR and its mRNA simultaneously in order to understand the biological events at different levels. Shen[53] reported that the reduced expression of GHR mRNA identified by ribonuclease protection assay in human cirrhotic livers was in the similar order of magnitude as reduction in GH binding. Relative quantity of GHR mRNA in liver tissue of cirrhotic rats was tested with RT-PCR assay and a similar result of our study indicated that the expression of GHR mRNA in cirrhotic liver tissue was lower than that in normal controls. Accordingly, it was suggested that the reduced GH binding may be secondary to reduced GHR gene expression and decreased GHR synthesis.

In summary, GH binding assay with staging analysis of liver cirrhosis was applied and our study showed that the growth hormone receptor was expressed with normal binding affinity on cirrhotic hepatocytes and expression of growth hormone receptors in a later stage of cirrhosis reduced significantly. These results implicated that there was a physiological basis of GHR for GH action in cirrhotic livers, but the sensitivity of cirrhotic hepatocytes to growth hormone might be decreased. Further investigations should be concentrated on the signal transduction of GHR in cirrhotic hepatocytes[58].

REFERENCES

1 **Strong RW**. Liver transplantation: current status and future prospects. *J R Coll Surg Edinb* 2001; **46**: 1-8

2 **Dichi JB**, Dichi I, Maio R, Correa CR, Angeleli AY, Bicudo MH, Rezende TA, Burini RC. Whole-body protein turnover in malnourished patients with child class B and C cirrhosis on diets low to high in protein energy. *Nutrition* 2001; **17**: 239-242

3 **Sobhonslidsuk A**, Roongpisuthipong C, Nantiruj K, Kulapongse S, Songchitsomboon S, Sumalnop K, Bussagorn N. Impact of liver cirrhosis on nutritional and immunological status. *J Med Assoc Thai* 2001; **84**: 982-988

4 **Alberino F**, Gatta A, Amodio P, Merkel C, Di Pascoli L, Boffo G,

Caregaro L. Nutrition and survival in patients with liver cirrhosis. *Nutrition* 2001; **17**: 445-450
5 **Mendenhall CL**, Tosch T, Weesner RE, Garcia-Pont P, Goldberg SJ, Kiernan T, Seeff LB, Sorell M, Tamburro C, Zetterman R. VA cooperative study on alcoholic hepatitis. II. Prognostic significance of protein-calorie malnutrition. *Am J Clin Nutr* 1986; **43**: 213-218
6 **Maull KI**, Turnage B. Trauma in the cirrhotic patient. *South Med J* 2001; **94**: 205-207
7 **Moukarzel AA**, Najm I, Vargas J, McDiarmid SV, Busuttil RW, Ament ME. Effect of nutritional status on outcome of orthotopic liver transplantation in paediatric patients. *Transplant Proc* 1990; **22**: 1560-1563
8 **Harrison J**, McKiernan J, Neuberger JM. A prospective study on the effect of recipient nutritional status on outcome in liver transplantation. *Transpl Int* 1997; **10**: 369-374
9 **Muller MJ**, Lautz HU, Plogmann B, Burger M, Korber J, Schmidt FW. Energy expenditure and substrate oxidation in patients with cirrhosis: the impact of cause, clinical staging and nutritional state. *Hepatology* 1992; **15**: 782-794
10 **Streat S**, Beddoe A, Hill GL. Aggressive nutritional support does not prevent protein loss despite fat gain in septic intensive care patients. *J Trauma* 1987; **27**: 262-266
11 **Le Cornu KA**, McKiernan FJ, Kapadia SA, Neuberger JM. A prospective randomized study of preoperative nutritional supplementation in patients awaiting elective orthotopic liver transplantation. *Transplantation* 2000; **69**: 1364-1369
12 **Wong WK**, Soo KC, Nambiar R, Tan YS, Yo SL. The effect of recombinant growth hormone on nitrogen balance in malnourished patients after major abdominal surgery. *Aust N Z J Surg* 1995; **65**: 109-113
13 **Rodeck B**, Kardorff R, Melter M, Ehrich JH. Improvement of growth after growth hormone treatment in children who undergo liver transplantation. *J Pediatr Gastroenterol Nutr* 2000; **31**: 286-290
14 **Petersen SR**, Holaday NJ, Jeevanandam M. Enhancement of protein synthesis efficiency in parenterally fed trauma victims by adjuvant recombinant human growth hormone. *J Trauma* 1994; **36**: 726-733
15 **Singh KP**, Prasad R, Chari PS, Dash RJ. Effect of growth hormone therapy in burn patients on conservative treatment. *Burns* 1998; **24**: 733-738
16 **Iglesias P**, Diez JJ. Clinical applications of recombinant human growth hormone in adults. *Expert Opin Pharmacother* 1999; **1**: 97-107
17 **Herndon DN**, Hawkins HK, Nguyen TT, Pierre E, Cox R, Barrow RE. Characterization of growth hormone enhanced donor site healing in patients with large cutaneous burns. *Ann Surg* 1995; **221**: 649-656
18 **Aili Low JF**, Barrow RE, Mittendorfer B, Jeschke MG, Chinkes DL, Herndon DN. The effect of short-term growth hormone treatment on growth and energy expenditure in burned children. *Burns* 2001; **27**: 447-452
19 **Hart DW**, Herndon DN, Klein G, Lee SB, Celis M, Mohan S, Chinkes DL, Wolf SE. Attenuation of posttraumatic muscle catabolism and osteopenia by long-term growth hormone therapy. *Ann Surg* 2001; **233**: 827-834
20 **Knox J**, Demling R, Wilmore D, Sarraf P, Santos A. Increased survival after major thermal injury: the effect of growth hormone therapy in adults. *J Trauma* 1995; **39**: 526-530
21 **Vara-Thorbeck R**, Guerrero JA, Rosell J, Ruiz-Requena E, Capitan JM. Exogenous growth hormone: effects on the catabolic response to surgically produced acute stress and on postoperative immune function. *World J Surg* 1993; **17**: 530-537
22 **Pape GS**, Friedman M, Underwood LE, Clemmons DR. The effect of growth hormone on weight gain and pulmonary function in patients with chronic obstructive lung disease. *Chest* 1991; **99**: 1495-1500
23 **Koea JB**, Breier BH, Douglas RG, Gluckman PD, Shaw JH. Anabolic and cardiovascular effects of rhGH in surgical patients with sepsis. *Br J Surg* 1996; **83**: 196-202
24 **Li W**, Li J, Xu B, Yin L, Wang L, Gu J, Ren JA, Quan ZF. Effect of recombinant human growth hormone with total parenteral nutrition on albumin synthesis in patients with peritoneal sepsis. *Zhonghua Waike Zazhi* 1998; **36**: 643-645
25 **Schambelan M**, Mulligan K, Grunfeld C, Daar ES, LaMarca A, Kotler DP, Wang J, Bozzette SA, Breitmeyer JB. Recombinant human growth hormone in patients with HIV-associated wasting. A randomized, placebo-controlled trial. Serostim Study Group. *Ann Intern Med* 1996; **125**: 873-882
26 **Waters D**, Danska J, Hardy K, Koster F, Qualls C, Nickell D, Nightingale S, Gesundheit N, Watson D, Schade D. Recombinant human growth hormone, insulin-like growth factor 1, and combination therapy in AIDS-associated wasting. A randomized, double-blind, placebo-controlled trial. *Ann Intern Med* 1996; **125**: 865-872
27 **O'Leary MJ**, Ferguson CN, Rennie M, Hinds CJ, Coakley JH, Preedy VR. Effect of growth hormone on muscle and liver protein synthesis in septic rats receiving glutamine-enriched parenteral nutrition. *Crit Care Med* 2002; **30**: 1099-1105
28 **Losada F**, Garcia-Luna PP, Gomez-Cia T, Garrido R N M, Pereira JL, Marin F, Astorga R. Effects of Human Recombinant Growth hormone on Donor-site Healing in Burned Adults. *World J Surg* 2002; **26**: 2-8
29 **Carroll PV**, Van den Berghe G. Safety aspects of pharmacological GH therapy in adults. *Growth Horm IGF Res* 2001; **11**: 166-172
30 **Takala J**, Ruokonen E, Webster NR, Nielsen MS, Zandstra DF, Vundelinckx G, Hinds CJ. Increased mortality associated with growth hormone treatment in critically ill adults. *N Engl J Med* 1999; **341**: 785-792
31 **Jeschke MG**, Barrow RE, Herndon DN. Recombinant human growth hormone treatment in pediatric burn patients and its role during the hepatic acute phase response. *Crit Care Med* 2000; **28**: 1578-1584
32 **Raguso CA**, Genton L, Kyle U, Pichard C. Management of catabolism in metabolically stressed patients: a literature survey about growth hormone application. *Curr Opin Clin Nutr Metab Care* 2001; **4**: 313-320
33 **Wilmore DW**. Postoperative protein sparing. *World J Surg* 1999; **23**: 545-552
34 **Carter-Su C**, Schwartz J, Smit LS. Molecular mechanism of growth hormone action. *Annu Rev Physiol* 1996; **58**: 187-207
35 **Dashti H**, Jeppsson B, Hagerstrand I, Hultberg B, Srinivas U, Abdulla M, Bengmark S. Thioacetamide and carbon tetrachloride-induced liver cirrhosis. *Eur Surg Res* 1989; **21**: 83-91
36 **Jeong DH**, Jang JJ, Lee SJ, Lee JH, Lim IK, Lee MJ, Lee YS. Expression patterns of cell cycle-related proteins in a rat cirrhotic model induced by CCl4 or thioacetamide. *J Gastroenterol* 2001; **36**: 24-32
37 **Huang J**, Cai MY, Wei DP. HLA class I expression in primary hepatocellular carcinoma. *World J Gastroenterol* 2002; **8**: 654-657
38 **Noutsias M**, Pauschinger M, Ostermann K, Escher F, Blohm JH, Schultheiss H, Kuhl U. Digital image analysis system for the quantification of infiltrates and cell adhesion molecules in inflammatory cardiomyopathy. *Med Sci Monit* 2002; **8**: MT59-71
39 **Imanishi H**, Kothary PC, Bhora FY, Eckhauser FE, Raper SE. Impaired phorbol ester-induced hepatocyte proliferation in cirrhosis. *J Surg Res* 1995; **58**: 435-440
40 **Thissen JP**, Verniers J. Inhibition by interleukin-1 beta and tumor necrosis factor-alpha of the insulin-like growth factor I messenger ribonucleic acid response to growth hormone in rat hepatocyte primary culture. *Endocrinology* 1997; **138**: 1078-1084
41 **Chomczynski P**, Sacchi N. Single-step method of RNA isolation by acid guanidinium thiocyanate- phenol- chloroform extraction. *Anal Biochem* 1987; **162**: 156-159
42 **Wolf M**, Bohm S, Brand M, Kreymann G. Proinflammatory cytokines interleukin 1 beta and tumor necrosis factor alpha inhibit growth hormone stimulation of insulin-like growth factor I synthesis and growth hormone receptor mRNA levels in cultured rat liver cells. *Eur J Endocrinol* 1996; **135**: 729-737
43 **Rzucidlo SJ**, Bounous DI, Jones DP, Brackett BG. Acute acetaminophen toxicity in transgenic mice with elevated hepatic glutathione. *Vet Hum Toxicol* 2000; **42**: 146-150
44 **Zhao J**, van Tol HT, Taverne MA, van der Weijden GC, Bevers MM, van den Hurk R. The effect of growth hormone on rat preantral follicles *in vitro*. *Zygote* 2000; **8**: 275-283
45 **Papotti M**, Ghe C, Cassoni P, Catapano F, Deghenghi R, Ghigo E, Muccioli G. Growth hormone secretagogue binding sites in peripheral human tissues. *J Clin Endocrinol Metab* 2000; **85**: 3803-3807

46 **Husman B**, Andersson G. Regulation of the growth hormone receptor during liver regeneration in the rat. *J Mol Endocrinol* 1993; **10**: 289-296

47 **Hocquette JF**, Postel-Vinay MC, Kayser C, de Hemptinne B, Amar-Costesec A. The human liver growth hormone receptor. *Edocrinology* 1989; **125**: 2167-2174

48 **Golda V**, Fickova M, Pinterova L, Jurcovicova J, Macho L, Zorad S. Terguride attenuates prolactin levels and ameliorates insulin sensitivity and insulin binding in obese spontaneously hypertensive rats. *Physiol Res* 2001; **50**: 175-182

49 **Reynaud D**, Demin P, Pace-Asciak CR. Hepoxilin A3-specific binding in human neutrophils. *Biochem J* 1996; **313**: 537-541

50 **Husman B**, Andersson G, Norstedt G, Gustafsson JA. Characterization and subcellular distribution of somatogenic receptor in rat liver. *Endocrinology* 1985; **116**: 2605-2611

51 **van Neste L**, Husman B, Moller C, Andersson G, Norstedt G. Cellular distribution of somatogenic receptors and insulin-like growth factor-I mRNA in the rat liver. *J Endocrinol* 1988; **119**: 69-74

52 **Chang TC**, Lin JJ, Yu SC, Chang TJ. Absence of growth-hormone receptor in hepatocellular carcinoma and cirrhotic liver. *Hepatology* 1990; **11**: 123-126

53 **Shen XY**, Holt RI, Miell JP, Justice S, Portmann B, Postel-Vinay MC, Ross RJ. Cirrhotic liver expresses low levels of the full-length and truncated growth hormone receptors. *J Clin Endocrinol Metab* 1998; **83**: 2532-2538

54 **Wang H**, Chen S, Ou Q, Deng M, Liu X. Expression of growth hormone receptor and its mRNA in cirrhotic livers. *Zhonghua Yixue Zazhi* 2002; **82**: 168-171

55 **Allevato G**, Billestrup N, Goujon L, Galsgaard ED, Norstedt G, Postel-Vinay MC, Kelly PA, Nielsen JH. Identification of phenylalanine 346 in the rat growth hormone receptor as being critical for ligand-mediated internalization and down-regulation. *J Biol Chem* 1995; **270**: 17210-17214

56 **Tonshoff B**, Mehls O. Interactions between glucocorticoids and the growth hormone-insulin-like growth factor axis. *Pediatr Transplant* 1997; **1**: 183-189

57 **Wang P**, Li N, Li JS, Li WQ. The role of endotoxin, TNF-α, and IL-6 in inducing the state of growth hormone insensitivity. *World J Gastroenterol* 2002; **8**: 531-536

58 **Wang H**, Deng M, Ou Q, Wei J, Liu X, Chen S. Effects of rhGH on the expression of growth hormone receptor of liver cells in a murine experimental cirrhosis model. *Zhonghua Putong Waike Zazhi* 2002; **17**: 93-95

Edited by Ren SY

P.O.Box 2345, Beijing 100023, China
Fax: +86-10-85381893
E-mail: wjg@wjgnet.com www.wjgnet.com

World J Gastroenterol 2003;9(4):771-774
World Journal of Gastroenterology
 ISSN 1007-9327

• BASIC RESEARCH •

Influence of methionine/valine-depleted enteral nutrition on nucleic acid and protein metabolism in tumor-bearing rats

Yin-Cheng He, Jun Cao, Ji-Wei Chen, Ding-Yu Pan, Ya-Kui Zhou

Yin-Cheng He, Jun Cao, Ji-Wei Chen, Ding-Yu Pan, Ya-Kui Zhou, Department of general surgery, Zhongnan Hospital, Wuhan University, Wuhan 430071, China
Supported by Hubei Provincial Health Department, No.W98016 and The Education Department of Hubei Province, China, No. 2001A14005
Correspondence to: Dr. Yin-Cheng He, Department of general surgery, Zhongnan Hospital, Wuhan University, Wuhan 430071, China. w030508h@public.wh.hb.cn
Telephone: +86-27-67812963
Received: 2002-10-17 **Accepted:** 2002-11-16

Abstract

AIM: To investigate the effects of methionine/valine-depleted enteral nutrition (EN) on RNA, DNA and protein metabolism in tumor-bearing (TB) rats.

METHODS: Sprague-Dawlley (SD) rats underwent jejunostomy for nutritional support. A suspension of Walker-256 carcinosarcoma cells was subcutaneously inoculated. 48 TB rats were randomly divided in 4 groups: A, B, C and D. The TB rats had respectively received jejunal feedings supplemented with balanced amino acids, methionine-depleted, balanced amino acids and valine-depleted for 6 days before injection of 740 KBq ^{3}H- methionine/valine via jejunum. The ^{3}H incorporation rate of the radioactivity into RNA, DNA and proteins in tumor tissues at 0.5, 1, 2, 4 h postinjection of tracers was assessed with liquid scintillation counter.

RESULTS: Incorporation of ^{3}H into proteins in groups B and D was (0.500±0.020) % to (3.670±0.110) % and (0.708±0.019) % to (3.813±0.076) % respectively, lower than in groups A [(0.659±0.055) % to (4.492±0.108) %] and C [(0.805±0.098) % to (4.180±0.018) %]. Incorporation of ^{3}H into RNA, DNA in group B was (0.237±0.075) % and (0.231±0.052) % respectively, lower than in group A (P<0.01). There was no significant difference in uptake of ^{3}H by RNA and DNA between group C and D (P>0.05).

CONCLUSION: Protein synthesis was inhibited by methionine/valine starvation in TB rats and nucleic acid synthesis was reduced after methionine depletion, thus resulting in suppression of tumor growth.

He YC, Cao J, Chen JW, Pan DY, Zhou YK. Influence of methionine/valine-depleted enteral nutrition on nucleic acid and protein metabolism in tumor-bearing rats. *World J Gastroenterol* 2003; 9(4): 771-774
http://www.wjgnet.com/1007-9327/9/771.htm

INTRODUCTION

Parenteral nutrition (PN) is now a supportive therapy commonly used for cancer patients. However, some studies have suggested that PN with amino acid balanced solutions may prompt tumor growth[1-3]. Previous studies have shown that tumor growth was inhibited by a diet or PN lacking in methionine/valine. However, the mechanism is not yet known[4-15]. In this study, we prepared methionine/valine-free amino acid imbalance solutions to investigate the effects of methionine/valine depleted EN on RNA, DNA and protein metabolism in TB rats.

MATERIALS AND METHODS

Radiopharmaceuticals

^{3}H-methionine (^{3}H-Met, specfic activity of 148 MBq· mg^{-1}) and ^{3}H-valine (^{3}H-Val, specfic activity of 240 MBq· mg^{-1}) was purchased from Chinese institute of atomic energy. The radiochemical purity was over 95 %.

Catheterization of jejunostomy

SD rats weighing (160±20) g were purchased from the animal center of Wuhan University, China. They were allowed to acclimate for one week. After fasting for 12 hours, rats were anesthetized with i.p. sodium pentobarbital (40 mg· kg^{-1}). The animals were undergone catheterization of jejunostomy (day 0). A silicone rubber catheter (2 mm ID, 3 mm OD) was inserted into the proximal jejunum. The catheter passed through a subcutaneous tunnel and emerged between the scapulae. The catheter was sutured to the animal' s back to protect the lines and was connected to a swivel so that animals can move without any restrictions in individual metabolic cages. The cannulation system consists of an microinfusion pump, a swivel, rat-harness and a silicone-tube-jejunostomy. Coprophagy was prevented by an own model of faecal collection cup. Animals were fasted for 48 hours after operation but they were provided with water ad libitum, and then given normal rat diets.

Preparation of TB rats

Walker-256 carcinosarcoma cells were obtained from Chinese Center of Culture Preservation. On day 0, the rats were inoculated subcutaneously in the right flank with 10^7 tumor cells of approximately 0.1 ml of cell suspension. Tumors were palpable in 7 days after transplantation.

Jejunal feeding

Enteral feedings were found to be a safe and cost-effective method for providing nutrition to cancer-bearing patients. On day 8, 48 TB rats were randomly divided into four groups (12 rats per group) and received enteral nutrition (jejunal feeding): Group A: TB rats were fed enteral nutrition solutions composed of balanced amino acids for 6 days before injection of 740 KBq ^{3}H-MET.

Group B: TB rats were fed methionine-depleted enteral nutrition solutions for 6 days before injection of 740 KBq ^{3}H-Met.

Group C: TB rats were fed enteral nutrition solutions composed of balanced amino acids for 6 days before injection of 740 KBq ^{3}H-Val.

Group D: TB rats were fed valine-depleted enteral nutrition solutions for 6 days before injection of 740 KBq ^{3}H-Val.

TB rats received continuous jejunal tube infusion with pump

for nutritional support at a daily dose of 330 ml· kg^{-1}, non-protein calorie was approximately 1160K J· kg^{-1}. A microinfusion pump was used for constant administration of EN solutions. TB rats were not fed during the entire infusion experiment, however they had free access to water.

Composition of amino acid solutions

Table 1 lists the components of amino acid solutions.

Table 1 Composition of amino acid solutions ($g \cdot L^{-1}$)

Amino acids	Balanced amino acids (Group A, C)	Methionine-depleted (Group B)	Valine-depleted (Group D)
Isoleucine	5.5	5.5	5.5
Leucine	7.5	7.5	7.5
Lysine	7.0	7.0	7.0
Methionine	6.0	-	6.0
Phenylalanine	4.0	4.0	4.0
Threonine	5.0	5.0	5.0
Tryptophan	1.5	1.5	1.5
Valine	6.0	6.0	-
Arginine	6.0	6.0	6.0
Histidine	3.0	3.0	3.0
Proline	4.0	4.0	4.0
Tyrosine	1.0	1.0	1.0
Alanine	20.0	20.0	20.0
Glycine	7.5	7.5	7.5
Aspartic acid	4.0	4.0	4.0
Total amino acid	88.0	82.0	82.0
Total N	14.1	13.1	13.1

Composition of EN solutions

Table 2 summarizes the daily EN compositions infused into various groups.

Table 2 Compositions of EN solutions ($ml \cdot L^{-1}$)

Amino acids	Balanced amino acids (group A, C)	Methionine-depleted (group B)	Valine-depleted (group D)
Amino acid solutions	350	350	350
50 % Glucose	300	300	300
20 % Intralipid	100	100	100
Electrolytes, vitamine	250	250	250
Total calorie ($KJ \cdot L^{-1}$)	3 513.3	3 507.9	3 507.9
Total N ($g \cdot L^{-1}$)	4.9	4.6	4.6
Non-protein calorie / N	122	131	131

Specimen sampling

After the infusions were completed, three rats per group were respectively killed by cervical dislocation at 0.5, 1, 2 and 4 hours postinjection of tracers. The whole tumor was dissected and used for the tissue uptake of radioactivity.

Nucleic acid and protein analysis

To assess the incorporation of the radioactivity into macromolecular materials, portions of the tumor tissues (70-120 mg) were divided into the acid-soluble fraction (ASF) and the acid-precipitate fraction (APF). Radiolabeled APF was divided into four fractions: lipids, RNA, DNA and proteins. To analyze ^{3}H-Met and ^{3}H-Val metabolites, the tumor tissues were homogenated in 1 ml of ice-cold 0.4 M $HClO_4$. The homogenate was centrifuged at 3 000 rpm for 5 min. The precipitate was resuspended in 1 ml of 0.4 M $HClO_4$. This wash was repeated twice. The precipitate was resuspended in 5 ml of $CHCl_3$: CH_3OH (2:1,V/V). After centrifugation at 3 000 rpm for 10 min, the $CHCl_3$: CH_3OH phase was separated. This extraction was repeated twice. The combined $CHCl_3$: CH_3OH fraction contains radiolabeled lipids. The precipitate was dissolved in 1 ml of 0.3 M KOH. After incubation of the solution at 37 ℃ for 1 hour to hydrolyze RNA, 0.32 ml of 3 N $HClO_4$ was added. The mixture was kept on ice for 5 min. The precipitate was then separated and washed with 1 ml 0.5 M $HClO_4$ as described above. The combined supernatant was designated as the alkaline-labile fraction containing the RNA hydrolysate. The precipitate was resuspended in 1 ml of 0.5 M $HClO_4$ and heated at 90 ℃ for 15 min to hydrolyze DNA. The solution was kept on ice for 5 min, and precipitate was separated and washed with 0.4 M $HClO_4$ twice. The combined supernatant and the final precipitate were assessed as the acid-labile fraction containing hydrolysates of DNA and protein fraction, respectively.

The radioactivities of fractions were counted by liquid scintillation counter. The tissue radioactivity was expressed as differential uptake ratio (DUR).

$$DUR = \frac{\text{Counts of tumor tissue (cpm)/sample weight (g)}}{\text{Injection dose counts (cpm)/body weight (g)}}$$

Statistical analysis

Student *t* test was used to examine the data. The difference was considered significant when *P* value was less than 0.05.

RESULTS

Three TB rats died of intestinal fistula, diarrhea, infection of abdominal cavity. Table 3 represented incorporation of ^{3}H into nucleic acids and proteins in TB rats after treatment.

Table 3 Incorporation (DUR,%) of ^{3}H into nucleic acids and proteins in TB rats after treatment

Group		0.5 h	1 h	2 h	4 h
RNA	A	0.208±0.002	0.300±0.002	0.349±0.007	0.405±0.007[c]
	B	0.149±0.012	0.249±0.009	0.260±0.010	0.389±0.010
	C	0.200±0.007	0.250±0.036[b]	0.283±0.029[ac]	0.326±0.014[c]
	D	0.180±0.013	0.210±0.024	0.300±0.034	0.320±0.030[b]
DNA	A	0.210±0.013	0.300±0.020	0.339±0.039	0.400±0.002[c]
	B	0.179±0.010[a]	0.204±0.039[a]	0.240±0.028[a]	0.300±0.015[b]
	C	0.200±0.011	0.250±0.040	0.283±0.031[c]	0.340±0.057[c]
	D	0.180±0.015	0.220±0.024	0.308±0.007	0.320±0.035
Proteins	A	0.659±0.055	2.410±0.149	3.450±0.125	4.492±0.108[c]
	B	0.500±0.020[b]	2.000±0.203[b]	2.890±0.090[bc]	3.670±0.110[b]
	C	0.805±0.098	2.510±0.010	3.540±0.101[c]	4.180±0.018[c]
	D	0.708±0.019	1.887±0.020[b]	2.916±0.085[b]	3.813±0.076[b]

[a]$P<0.05$, [b]$P<0.01$, *vs* group A or C. [c]Number of rats=2.

DISCUSSION

Influence of Methionine/Valine-depleted enteral nutrition on protein metabolism in TB rats

Patients with malignant tumors often show severe protein-amino acid metabolism disorder and uncorrectable negative nitrogen balance. Researchers have begun to reconsider the prescription of amino acid imbalance solution for cancer patients. Total parenteral nutrition deprived of methionine or valine cause tumor growth inhibition, but also have no significantly negative influences on the host animals[16-18].

Table 3 shows the ^{3}H incorporation rate in tumor tissues at

various times after ^{3}H-Met/Val injections. Regardless of Methionine/Valine-depleted enteral nutrition, the radioactivity into nucleic acids and proteins increased with time. In proteins we found an accumulation of the label which was up to 3-10-fold higher than in DNA and RNA. It represents the principle pathway for methionine and valine anabolism. Accumulation of ^{3}H-Met/Val into malignant tissue is thought to be due to amino acid metabolism of cancer cells such as increased active transport and incorporation of amino acid into protein fractions. In the complete absence of Methionine or Valine, the ^{3}H incorporation rate of the radioactivity into proteins in tumor tissues was from 75.8 % to 87.9 % of the control value. That is to say, in agreement with Xiao' s study[5], protein synthesis was inhibited by methionine/valine depletion, in this case suppressing tumor growth[19-26].

Although essential amino acids are indispensable for physical well-being, the body lacks the ability to synthesize these compounds. Amino acids are an important materials of protein synthesis, amino acid imbalance are considered to principally involving alterations in intracellular protein synthesis, the deprivation of essential amino acids (Met, Val) leads to inhibit activity of tumor growth[27,28].

Influence of Methionine/Valine-depleted enteral nutrition on RNA and DNA in TB rats

Methionine adenosyltransferase is the enzyme which is responsible for the synthesis of S-adnosyl-L-methionine (SAM) using methionine and adnosine triphosphate (ATP). Most of SAM are used in transmethylation reaction in which methyl groups are added to compounds and SAM is converted to S-adenosylhomocysteine. SAM is the principal biological methyl donor. SAM can easily transfer its methyl group to a large variety of acceptor substrates including rRNA, tRNA, mRNA, DNA, proteins, phospholipides, biological amines, and a long list of small molecules[29-33]. So ^{3}H-Met is also incorporated into nucleic acids by transmethylation via S-adenosyl-L-methionine. Methionine depleted enteral nutrition can decrease methylation of tumor tissues and lead to further reduction in nucleic acid synthesis and inhibition of cancer growth at molecular levels.

Table 3 showed that the RNA and DNA incorporation rate in group B was lower than in control group (group A). Based on these findings, cancer cells were known to have lower levels of DNA and RNA synthesis on methionine-depleted enteral nutrition.

Theoretically, it is considered that ^{3}H-Val is incorporated into proteins but not into other high-molecular materials such as nucleic acids. The incorporation of ^{3}H-Val was detected in nucleic acids at negligible amounts, which possibly reflects contamination by labeled proteins during the experimental processes. However, because no metabolic pathway for the DNA incorporation of ^{3}H-Val is considered, the radioactivity in the acid-labile fraction is probably derived from basic proteins such as chromosomal histones.

REFERENCES

1 **Bozzetti F,** Gavazzi C, Cozzaglio L, Costa A, Spinelli P, Viola G. Total parenteral nutrition and tumor growth in malnourished patients with gastric cancer. *Tumori* 1999; **85**: 163-166

2 **Sasamura T,** Matsuda A, Kokuba Y. Tumor growth inhibition and nutritional effect of d-amino acid solution in AH109A hepatoma-bearing rats. *J Nutr Sci Vitaminol* 1998; **44:** 79-87

3 **Forchielli ML,** Paolucci G, Lo CW. Total parenteral nutrition and home parenteral nutrition: an effective combination to sustain malnourished children with cancer. *Nutr Rev* 1999; **57:** 15-20

4 **Sasamura T,** Matsuda A, Kokuba Y. Nutritional effects of a D-methionine-containing solution on AH109A hepatoma-bearing rats. *Biosci Biotechnol Biochem* 1998; **62:** 2418-2420

5 **Xiao HB,** Cao WX, Yin HR, Lin YZ, Ye SH. Influence of L-methionine-deprived total parenteral nutrition with 5-fluorouracil on gastric cancer and host metabolism. *World J Gastroenterol* 2001; **7:** 698-701

6 **Nagahama T,** Goseki N, Endo M. Doxorubicin and vincristine with methionine depletion contributed to survival in the Yoshida sarcoma bearing rats. *Anticancer Res* 1998; **18:** 25-31

7 **Cao WX,** Cheng QM, Fei XF, Li SF, Yin HR, Lin YZ. A study of preoperative methionine-depleting parenteral nutrition plus chemotherapy in gastric cancer patients. *World J Gastroenterol* 2000; **6:** 255-258

8 **Tang B,** Li YN, Kruger WD. Defects in methylthioadenosine phosphorylase are associated with but not responsible for methionine-dependent tumor cell growth. *Cancer Res* 2000; **60:** 5543 –5547

9 **Komatsu H,** Nishihira T, Chin M, Doi H, Shineha R, Mori S, Satomi S. Effects of caloric intake on anticancer therapy in rats with valine-depleted amino acid imbalance. *Nutr Cancer* 1997; **28:** 107-112

10 **Yoshida S,** Ohta J, Shirouzu Y, Ishibashi N, Harada Y, Yamana H, Shirouzu K. Effect of methionine-free total parenteral nutrition and insulin-like growth factor I on tumor growth in rats. *Am J Physiol* 1997; **273:** E10-16

11 **Komatsu H,** Nishihira T, Chin M, Doi H, Shineha R, Mori S, Satomi S. Effect of valine depleted total parenteral nutrition on fatty liver development in tumor-bearing rats. *Nutrition* 1998; **14:** 276-281

12 **Tan Y,** Xu M, Guo H, Sun X, Kubota T, Hoffman RM. Anticancer efficacy of methioninase *in vivo*. *Anticancer Res* 1996; **16:** 3931-3936

13 **Guo H,** Tan Y, Kubota T, Moossa AR, Hoffman RM. Methionine depletion modulates the antitumor and antimetastatic efficacy of ethionine. *Anticancer Res* 1996; **16**: 2719-2723

14 **Sasamura T,** Matsuda A, Kokuba Y. Effects of D-methionine-containing solution on tumor cell growth *in vitro*. *Arzneimittelforschung* 1999; **49:** 541-543

15 **Bozzetti F, Gavazzi C,** Miceli R, Rossi N, Mariani L, Cozzaglio L, Bonfanti G, Piacenza S. Perioperative total parenteral nutrition in malnourished, gastrointestinal cancer patients: a randomized, clinical trial. *JPEN* 2000; **24:** 7-14

16 **Yoshioka T,** Wada T, Uchida N, Maki H, Yoshida H, Ide N, Kasai H, Hojo K, Shono K, Maekawa R, Yagi S, Hoffman RM, Sugita K. Anticancer efficacy *in vivo* and *in vitro*, synergy with 5-fluorouracil, and safety of recombinant methioninase. *Cancer Res* 1998; **58:** 2583-2587

17 **Jin D,** Phillips M, Byles JE. Effects of parenteral nutrition support and chemotherapy on the phasic composition of tumor cells in gastrointestinal cancer. *JPEN* 1999; **23**: 237-241

18 **Machover D,** Zittoun J, Broet P, Metzger G, Orrico M, Goldschmidt E, Schilf A, Tonetti C, Tan Y, Delmas-Marsalet B, Luccioni C, Falissard B, Hoffman RM. Cytotoxic synergism of methioninase in combination with 5-fluorouracil and folinic acid. *Biochem Pharmacol* 2001; **61**: 867-876

19 **Nishihira T,** Takagi T, Mori S. Leucine and manifestation of antitumor activity by valine-depleted amino acid imbalance. *Nutrition* 1993; **9:** 146-152

20 **Nishihira T,** Takagi T, Kawarabayashi Y, Izumi U, Ohkuma S, Koike N, Toyoda T, Mori S. Anti-cancer therapy with valine-depleted amino acid imbalance solution. *Tohoku J Exp Med* 1988; **156:** 259-270

21 **Nishihira T,** Komatsu H, Sagawa J, Shineha R, Mori S. Prevention of fatty liver and maintenance of systemic valine depletion using a newly developed dual infusion system. *JPEN* 1995; **19:** 199-203

22 **Machover D,** Zittoun J, Saffroy R, Broet P, Giraudier S, Magnaldo T, Goldschmidt E, Debuire B, Orrico M, Tan Y, Mishal Z, Chevallier O, Tonetti C, Jouault H, Ulusakarya A, Tanguy ML, Metzger G, Hoffman RM. Treatment of cancer cells with methioninase produces DNA hypomethylation and increases DNA synthesis. *Cancer Res* 2002; **62:** 4685-4689

23 **Hoshiya Y,** Kubota T, Inada T, Kitajima M, Hoffman RM. Methionine-depletion modulates the efficacy of 5-fluorouracil in human gastric cancer in nude mice. *Anticancer Res* 1997; **17:** 4371-4375

24 **Poirson-Bichat F,** Goncalves RA, Miccoli L, Dutrillaux B, Poupon

MF. Methionine depletion enhances the antitumoral efficacy of cytotoxic agents in drug-resistant human tumor xenografts. *Clin Cancer Res* 2000; **6**: 643-653

25 **Poirson-Bichat F,** Lopez R, Bras Goncalves RA, Miccoli L, Bourgeois Y, Demerseman P, Poisson M, Dutrillaux B, Poupon MF. Methionine deprivation and methionine analogs inhibit cell proliferation and growth of human xenografted gliomas. *Life Sci* 1997; **60:** 919-931

26 **Hoshiya Y,** Kubota T, Matsuzaki SW, Kitajima M, Hoffman RM. Methionine starvation modulates the efficacy of cisplatin on human breast cancer in nude mice. *Anticancer Res* 1996; **16:** 3515-3517

27 **Samuels SE,** Knowles AL, Tilignac T, Debiton E, Madelmont JC, Attaix D. Protein metabolism in the small intestine during cancer cachexia and chemotherapy in mice. *Cancer Res* 2000; **60:** 4968-4974

28 **Poirson-Bichat F,** Gonfalone G, Bras-Goncalves RA, Dutrillaux B, Poupon MF. Growth of methionine-dependent human prostate cancer (PC-3) is inhibited by ethionine combined with methionine starvation. *Br J Cancer* 1997; **75:** 1605-1612

29 **Lu SC**. Methionine adenosyltransferase and liver disease: it's all about SMA. *Gastroenterology* 1998; **114:** 403-407

30 **Zhu SS,** Xiao SD, Chen ZP, Shi Y, Fang JY, Li RR, Mason JB. DNA methylation and folate metabolism in gastric cancer. *World J Gastroenterol*, 2000; **6**(Suppl 3): 18

31 **Avila MA,** Carretero MV, Rodriguez EN, Mato JM. Regulation by hypoxia of methionine adenosyltransferase activity and gene expression in rat hepatocytes. *Gastroenterology* 1998; **114:** 364-371

32 **Cao WX,** Ou JM, Fei XF, Zhu ZG, Yin HR, Yan M, Lin YZ. Methionine-dependence and combination chemotherapy on human gastric cancer cells *in vitro. World J Gastroenterol* 2002; **8:** 230-232

33 **Cui J,** Yang DH, Bi XJ, Fan ZR. Methylation status of *c-fms* oncogenein HCC and its relationship with clinical pathology. *World J Gastroenterol* 2001; **7:** 136-139

Edited by Xu JY

P.O.Box 2345, Beijing 100023, China
Fax: +86-10-85381893
E-mail: wjg@wjgnet.com www.wjgnet.com

World J Gastroenterol 2003;9(4):775-778
World Journal of Gastroenterology
 ISSN 1007-9327

• BASIC RESEARCH •

Action of progesterone on contractile activity of isolated gastric strips in rats

Fang Wang, Tian-Zhen Zheng, Wei Li, Song-Yi Qu, Di-Ying He

Fang Wang, Insititute of Infectious Diseases, the Third Military Medical University Afflicated Southwest Hospital, Chongqing 400038, China
Tian-Zhen Zheng, Wei Li, Song-Yi Qu, Department of Physiology, Lanzhou Medical College, Lanzhou 730000, China
Di-Ying He, Department of Physical Culture, Gansu College of Education, Lanzhou 730000, China
Supported by Natural Science Foundation of Province of Gansu Province, No: ZR-96-085
Correspondence to: Fang Wang, Insititute of Infectious Diseases, the Third Military Medical University Afflicated Southwest Hospital, Chongqing 400038, China. kaixin919@163.com
Telephone: +86-23-68754475-8020 **Fax:** +86-23-65334998
Received: 2002-07-23 **Accepted:** 2002-08-23

Abstract

AIM: To study the effect of progesterone on contractile activity of isolated gastric strips in rats.

METHODS: Wistar rats were sacrificed to remove whole stomach. Then, the stomach was opened and the mucosal layer was removed. Parellel to either the circular or the longitudial fibers, muscle strips were cut from fundus, body, antrum and pylorus. Each muscle strip was suspended in a tissue chamber containing 5 mL Krebs solution. Then the motility of gastric strips in tissue chambers was simultaneously recorded. The preparations were subjected to 1 g load tension and washed with 5 ml Krebs solution every 20 min. After 1 h equilibration, progesterone or antagonists were added in the tissue chamber separately. The antagonists were added 3 min before using progesterone (50 μmol·L^{-1}).

RESULTS: Progesterone decreased the resting tension of fundus and body longitudinal muscle (LM) (P<0.05). It inhibited the mean contractile amplitude of body and antrum LM and circular muscle (CM), and the motility index of pyloric CM (P<0.05). The inhibition of progesterone on the mean contractile amplitude could be partially blocked by phentolamine in LM of the stomach body (the mean contractile amplitude of body LM decreased from -7.5±5.5 to -5.2±4.5 P<0.01), and by phentolamine or indomethacin in CM of body (The inhibition of progesterone on the mean contractile amplitude of body CM decreased from -5.6±3.0 to -3.6±2.7 by phentolamine and from -5.6±3.0 to -3.5±2.5 by indomethacin, P<0.01). Hexamethonium, propranolol and L-NNA (inhibitor of NO synthetase) didn't affect the action of progesterone (P>0.05).

CONCLUSION: The study suggested that progesterone can inhibit the contractile activity of isolated gastric strips in rats and the mechanism seems to be a direct one except that the action on gastric body is mediated through prostaglandin and adrenergic α receptor partly.

Wang F, Zheng TZ, Li W, Qu SY, He DY. Action of progesterone on contractile activity of isolated gastric strips in rats. *World J Gastroenterol* 2003; 9(4): 775-778
http://www.wjgnet.com/1007-9327/9/775.htm

INTRODUCTION

Nausea and vomiting are extremely common complaints of pregnancy and may precede even the patients are aware that she is pregnant[1-4]. However, it's mechanism is poorly understood. The questions of whether gastric emptying of solids and liquids differs in men and women and whether emptying is influenced by the action of sex hormones on gastric smooth muscle remain unresolved[5-8]. Whether gastric emptying of solids and liquids differs in women during the menstrual cycle is controversial[9-12]. The results of several clinical and physiological studies have suggested that the aforementioned complaints of pregnancy may be related, at least in part, to decrease of resting tension within the lower esophageal sphincter and changes in gastric motility[3,13-15]. The fact that a high serum sex hormone concentration is the characteristic of pregnancy tempts researchers to investigate the hormonal factor associated with gastrointestinal dysmotility. However, so far, the effect of pregnancy and sex hormone on gastric motility remains controversial. We studied the action of progesterone on the gastric strips in rats and explored the possible mechanism concerned.

MATERIALS AND METHODS

Materials

Progesterone, purchased from sigma, was dissolved and diluted in 1, 2-propanecol; hexamethonium and N*w*-Nitro-L-Arginine (L-NNA), Sigma; indomethacin, Jiangsu Taicang Pharmaceutical Factory; propranolol, Beijing Second Pharmaceutical Factory; Phentolamine, Beijing Thirteen Pharmaceutical Factory; 1, 2-propanecol, Tianjing Chemical Factory; Krebs buffer solution [(mmol·L^{-1}: NaCl 120. 6, KCl 5.9, NaH_2PO_4 1.2, $MgCl_2$ 1.2, $NaHCO_3$ 15.4, $CaCl_2$ 2.5, $C_6H_{12}O_6$ 11.5, pH=7.4)].

JZ-BK external isometric force transducer, BK company; LMS-ZB two channel recorder, Chengdu Equipment Factory.

Wistar rats, 200-250 g, were provided by the Animal Center of Lanzhou Medical College.

Methods

Wistar rats were fasted with free access to water for 24 h, and sacrificed to remove whole stomach. Then, the stomach was opened along the great curvature, and rinsed with Krebs solution. The stomach was pinned on a wax block with mucosa side up, and the mucosal layer was gently rubbed with a tweezers. Parellel to either the circular or the longitudial fibers, muscle strips (8×2 mm) were cut and named logitudinal muscle (LM) of fundus, circular muscle (CM) and LM of body and antrum and CM of pylorus[16,17].

Each muscle strip with the mucosa removed was suspended in a tissue chamber containing 5 mL Krebs solution, constantly warmed by circulating water jacket at 37 ℃ and supplied with 95 % O_2 and 5 % CO_2. One end of the strip was fixed to a hook on the bottom of the chamber while the other end was connected by a thread to an external isometric force transducer at the top. Motility of gastric strips in tissue chambers were simultaneously recorded on recorders. Preparations were subjected to 1 g load tension and washed with 5 ml Krebs

solution every 20 min. After 1 h equilibration, progesterone (5, 10, 50 μmol· L^{-1}) or antagonist was added in the tissue chamber (all were the final concentration) separately 3 min before using progesterone (50 μmol· L^{-1})[16-20].

Analysis of data

We measured the resting tension of all strips, the mean contractile amplitude of body and antrum strips, and the motility index (MI= Σ [amplitude×duration]) of pyloric strip. Frequencies of contraction were determined by counting the contraction waves. Values of the results was presented as $\bar{x}\pm s$. Statistical significances were measured by *t* test[16,17].

RESULTS

Effect of progesterone on spontaneous contraction of gastric strips

Progesterone significantly decreased the resting tension of fundus and body LM (Table 1). It decreased the mean contractile amplitude of body and antrum, and the motility index of pylorus (Table 2). However it didn' t influence the gastric contractile frequency (P>0.05).

Effect of antagonists added progesterone on spontaneous contraction of gastric strips

Hexamethonium (10 μmol· L^{-1}), L-NNA (100 μmol· L^{-1}) or propranolol (1 μmol· L^{-1}) added 3 min before admistrated progesterone didn' t influence the decreasing effect of progesterone on the gastric strips in rats (P>0.05), but phentolamine (1 μmol· L^{-1}) partly blocked its effect on the mean contractile amplitude of body LM and CM, and indomethacin (10 μmol· L^{-1}) also decreased the effect on the mean contractile amplitude of body CM (Table 3).

DISCUSSION

It has been shown from humans and animals that pregnancy is associated with alternations in the motor activity of the gastrointestinal tract, such as decreased gallbladder contractivity and lower esophageal sphincter pressure, reduced gastric emptying, small intestine and colonic transit[13-15,21-29]. Although the factors responsible for the impaired gastric motility are obscure, there is evidence to suggest that pregnancy is associated with disturbances in the myoelectric and mechanical properties of gastrointestinal smooth muscle.

Table 1 Effect of progesterone on the resting tension of gastric smooth muscle in rats

Progesterone μmol· L^{-1}	Resting tension / g					
	Fundus	Body		Antrum		Pylorus
	LM	LM	CM	LM	CM	CM
5	-0.08±0.12[a]	-0.008±0.08	0	0.01±0.05	0	0
10	-0.08±0.08[b]	-0.05±0.11	-0.03±0.06	0.04±0.09	0	0
50	-0.09±0.06[d]	-0.12±2.0[a]	0.01±0.15	0.02±0.04	0	-0.03±0.10

The values were expressed as differences in resting tension between 3 min before and after the addition of progesterone (5, 10 and 50 μmol· L^{-1}) (The same in Tab 2). The resting tension of each strip in control (progesterone 0 μmol· L^{-1}) was 1. LM: longitudinal muscle; CM: circular muscle. $\bar{x}\pm s$, n=12, [a]P<0.05, [b]P<0.01, [d]P<0.001, *vs* control by paired t test.

Table 2 Effect of progesterone on the mean contractile amplitude of body and antrum, and the motility index of pylorus in rats

Progesterone μmol· L^{-1}		Contractile amplitude / mm				Motility index / $cm.s^{-1}$
		Body		Antrum		Pylorus
		LM	CM	LM	CM	CM
5	B	13.4±17.0	12.0±13.2	13.6±8.6	14.1±15.0	92.4±16.2
	C	0.2±0.4	-0.9±3.0	-0.5±0.8[a]	-0.8±1.7	1.7±4.8
10	B	12.8±17.6	11.2±14.0	14.0±7.1	13.6±12.9	98.5±20.0
	C	-2.1±3.8[a]	-1.5±1.6[b]	-1.8±2.0[b]	-3.1±1.8[d]	-22.5±16.6[d]
50	B	12.0±16.9	11.8±12.9	12.6±8.0	12.6±14.8	110.2±22.8
	C	-7.5±5.5[a]	-5.6±3.0[d]	-5.4±3.8[d]	-5.8±3.8[d]	-47.4±31.2[d]

B: basic values in 3 min before addition of progesterone; C: changes in 3 min after addition of progesterone (The same in Tab 3). $x\pm s$, n=12. [a]P<0.05, [b]P<0.01, [d]P<0.001, *vs* corresponding B by paired *t* test.

Table 3 Effect of progesterone on the mean contractile amplitude of body after indomethacin or phentolamine pretreatment in rats

Gastric body muscle	Contractile amplitude / mm									
	Pr		I + Pr				Ph + Pr			
	B	C	B	C	B	C	B	C	B	C
LM	12.0±16.9	-7.5±5.5[b]	12.9±17.1	-0.1±6.0	12.5±18.4	-8.2±6.9[b]	12.1±19.2	1.4±3.8	15.4±16.5	-5.2±4.5[d]
CM	11.8±12.9	-5.6±3.0[b]	12.2±14.0	1.2±5.2	12.6±13.2	-3.5±2.5[d]	11.7±12.6	0.2±0.5	11.4±13.0	-3.6±2.7[d]

Phentolamine (1 μmol· L^{-1}) or indomethacin (10 μmol· L^{-1}) was added 3 min before the addition of progesterone (50 μmol· L^{-1}). $\bar{x}\pm s$, n=12. Pr: progesterone, I: indomethacin, Ph: phentolamine. [b]P<0.001 *vs* corresponding B by paired *t* test; [d]P<0.01 *vs* Pr alone by two samples mean *t* test.

In our study, progesterone decreased the resting tension of fundus, which might be a cause of changed gastric motility during pregnancy. It had been agreed that decreased fundic resting tension mainly influenced the gastric emptying of liquids. Ryan also reported[30] that pregnancy was associated with decreased gastric emptying of liquids in the guinea pig. The observation in our study that hexamethonium, L-NNA and propranolol didn' t influence the effect of progesterone suggesting that the action of progesterone was not mediated via NO, β or N_1 receptors. Since phentolamine blocked partly the effect of body LM and CM, and indomethacin decreased that of body CM showed that the effect of the hormone on body LM partly via a receptor, and on body CM via prostaglandin and a receptor. In addition, the effect of progesterone might act on gastric smooth muscle cells directly. Progesterone receptor had been found in normal human gastric tissues. Another evidence was addition of progesterone to isolated denervated gallbladder muscle strips inhibited contraction in response to both acetylcholine or cholecystokinin[31].

Parkman reported[14] that spontaneous and bethanechol induced phasic antrum contraction of pregnant guinea pigs were significantly reduced in force compared with control virgin animals, and intracellular electrical recordings were obstained from antral smooth muscle cells to investigate the mechanism of the decreased contractivity of antral smooth muscle during pregnancy. The results showed that there were similar resting membrance potentials, slow wave frequency and slow wave duration *vs* those of the control, but the upstroke amplitude, plateau amplitude and number of spike per slow wave decreased significantly. Further study suggested that the decreased force of spontaneous antral contractions was associated with a reduction in the underlying electrical slow wave depolarization. Electrogastrogram recordings also suggested that gastric dysrhythmias were objective pathophysiologic event associated with symptoms of nausea and vomiting during pregnancy[14,32,33].

Exogeneous progesterone also inhibited the myoelectric and mechanical activity of gastrointestinal smooth muscle. Electrical spike potentials recorded from chronically implanted electrodes in the antrum and jejunum of ovariectomized dogs by Milenory decreased after 4 d of progesterone addition (2 $mg \cdot kg^{-1} \cdot d^{-1}$) and the propagation velocity of the basic electrical rhythm from the antral region of the progesterone-treated animals also decreased[34]. In another example, progesterone had been shown to reduce the propagation velocity of gestrointestinal slow waves possibly by decreasing the degree of electrical coupling between smooth muscle cells[35]. Dysrhythmias were also induced in healthy, nonpregnant women by administration of progesterone in the dose that reproduces plasma level seen in pregnancy. The above results suggested that the inhibitory effect of progesterone on the gastric smooth muscle may contribute to the gastric dysmotility during pregnancy.

REFERENCES

1 **Chandra K**, Magee L, Koren G. Discordance between physical symptoms versus perception of severity by women with nausea and vomiting in pregnancy (NVP). *BMC Pregnancy Childbirth* 2002; **2**: 5-8

2 **Chandra K**, Einarson A, Koren G. Taking ginger for nausea and vomiting during pregnancy. *Can Fam Physician* 2002; **48**: 1441-1442

3 **Singer AJ**, Brandt LJ. Pathophysiology of the gastrointestinal tract during pregnancy. *Am J Gastrointestinal* 1991; **86**: 1695-1712

4 **DiIorio C**, van Lier D, Manteuffel B. Patterns of nausea during first trimester of pregnancy. *Clin Nurs Res* 1992; **1**: 127-140

5 **Hutson WR**, Roehrkasse RL, Wald A. Influence of gender and menopause on gastric emptying and motility. *Gastroenterology* 1989; **96**: 11-17

6 **Degen LP**, Phillips SF. Variability of gastrointestinal transit in healthy women and men. *Gut* 1996; **39**: 299-305

7 **Bennink R**, Peeters M, Van den Maegdenbergh V, Geypens B, Rutgeerts P, DeRoo M, Mortelmans L. Comparison of total and compartmental gastric emptying and antral motility between healthy men and women. *Eur J Nucl Med* 1998; **25**: 1293-1299

8 **Datz FL**, Christian PE, Moore J. Gender-related differences in gastric emptying. *J Nucl Med* 1987; **28**: 1204-1207

9 **Horowitz M**, Maddern GJ, Chatterton BE, Collins PJ, Petrucco OM, Seamark R, Shearman DJ. The normal menstrual cycle has no effect on gastric emptying. *Br J Obstet Gynaecol* 1985; **92**: 743-746

10 **Gill RC**, Murphy PD, Hooper HR, Bowes KL, Kingma YJ. Effect of the menstrual cycle on gastric emptying. *Digestion* 1987; **36**: 168-174

11 **Caballero-Plasencia AM**, Valenzuela-Barranco M, Martin-Ruiz JL, Herrerias-Gutierrez JM, Esteban-Carretero JM. Are there changes in gastric emptying during the menstrual cycle? *Scand J Gastroenterol* 1999; **34**: 772-776

12 **Bovo P**, Paola Brunori M, di Francesco V, Frulloni L, Montesi G, Cavallini G. The menstrual cycle has no effect on gastrointestinal transit time. Evaluation by means of the lactulose H2 breath test. *Ital J Gastroenterol* 1992; **24**: 449-451

13 **Koch KL**. Gastrointestinal factors in nausea and vomiting of pregnancy. *Am J Obstet Gynecol* 2002; **185**: S198-203

14 **Parkman HP,** Wang MB, Ryan JP. Decreased electromechanical activity of guinea pig circular muscle during pregnancy. *Gastroenterology* 1993; **105**: 1306-1312

15 **Jones MJ,** Mitchell RW, Hindocha N, James RH. The lower oesophageal sphincter in the first trimester of pregnancy: comparison of supine with lithotomy positions. *Br J Anaesth* 1988; **61**: 475-476

16 **Qu SY**, Zheng TZ, Li W. Comparative study of ranitidine and cimetidine on contractile activity of isolated gastric muscle strips in rats. *Xin Xiaohuabingxue Zazhi* 1997; **5**: 75-76

17 **Wang F**, Luo JQ, Zhen TZ, Qu SY, Li W, He DY. Effect of oxytocin on the contractile activity of gastric strips of rats *in vitro*. *Zhongguo Yaolixueyudulixue Zazhi* 1999; **13**: 285-287

18 **Qu SY**, Zhen TZ, Li W. Effect of cholecystokinin and secretin on contractile activity of isolated gastric muscle strips in guinea pigs. *Shenlixuebao* 1995; **47**: 305-309

19 **Xie DP**, Li W, Qu SY, Zhen TZ, Yang YL, Ding YH, Wei YL, Chen LB. Effect of areca on contraction of colonic muscle strips in rats . *World J Gastroenterol* 2002; **8**: 350-352

20 **Li W**, He DY, Zhen TZ, Wang F, Qu SY. Effect of estradiol on the contractile activity of bladder strips of rats *in vitro*. *Jichuyixue Yu Lingchuang* 2001; **21**: 186-187

21 **Ryan JP**. Effect of pregnancy on intestinal transit: comparison of results using radioactive and non-radioactive test meals. *Life Sci* 1982; **31**: 2635-2640

22 **Scott LD**, Lester R, Van Thiel DH, Wald A. Pregnancy-related changes in small intestinal myoelectric activity in the rat. *Gastroenterology* 1983; **84**: 301-305

23 **Baron TH,** Ramirez B, Richter JE. Gastrointestinal motility disorders during pregnancy. *Ann Intern Med* 1993; **118**: 366-375

24 **Shah S**, Hobbs A, Singh R, Cuevas J, Ignarro LJ, Chaudhuri G. Gastrointestinal motility during pregnancy: role of nitrergic component of NANC nerves. *Am J Physiol Regul Integr Comp Physiol* 2000; **279**: R1478-R1485

25 **Bainbridge ET**, Nicholas SD, Newton JR, Temple JG. Gastro-oesophageal reflux in pregnancy. Altered function of the barrier to reflux in asymptomatic women during early pregnancy. *Scand J Gastroenterol* 1984; **19**: 85-89

26 **Ryan JP**, Bhojwani A. Colonic transit in rats: effect of ovariectomy, sex steroid hormones, and pregnancy. *Am J Physiol* 1986; **251** (1Pt1): G46-50

27 **Brock-Utne JG**, Dow TG, Dimopoulos GE, Welman S, Downing JW, Moshal MG. Gastric and lower oesophageal sphincter (LOS) pressures in early pregnancy. *Br J Anaesth* 1981; **53**: 381-384

28 **Everson GT,** McKinley C, Lawson M, Johnson M, Kern F Jr. Gallbladder function in the human female: effect of the ovulatory cycle,pregnancy, and contraceptive steroids. *Gastroenterology* 1982; **82**: 711-719

29 **Braverman DZ**, Johnson ML, Kern F Jr. Effects of pregnancy and contraceptive steroids on gallbladder function. *N Engl J Med* 1980; **302**: 362-364
30 **Ryan JP**, Bhojwani A, Wang MB. Effect of pregnancy on gastric motilily *in vivo* and *in vitro* in the guinea pig. *Gastroenterology* 1987; **93**: 29-34
31 **Everson GT**. Gastrointestinal motility in pregnancy. *Gastroenterol Clin North Am* 1992; **21**: 751-776
32 **Chen JD**, Mittal RK. Nausea and vomiting in pregnancy and cutaneous electrogastrogram. *Gastroenterology* 1993; **104**: 1569-1571
33 **Abell TL**. Nausea and vomiting of pregnancy and the electrogastrogram: old disease, newtechnology. *Am J Gastroenterol* 1992; **87**: 689-691
34 **Milenory K**. Effect of estradiol, progesterone and oxytocin on smooth muscle activity. In: *Physiology of Smooth Muscle*, edited by Bulbring E, Shuba MF. *New York: Raven* 1976: 395-402
35 **Bortoff A**. Progesterone reduces slow wave propagation velocity and decrease electrical coupling between intestinal muscle cells. In: Weinbeek M. *Motility of Digestive Tract. New York: Raven* 1982: 445-450

Edited by Wu XN

P.O.Box 2345, Beijing 100023, China
Fax: +86-10-85381893
E-mail: wjg@wjgnet.com www.wjgnet.com

World J Gastroenterol 2003;9(4):779-783
World Journal of Gastroenterology
 ISSN 1007-9327

• BASIC RESEARCH •

Relative efficacy of some prokinetic drugs in morphine-induced gastrointestinal transit delay in mice

AD Suchitra, SA Dkhar, DG Shewade, CH Shashindran

AD Suchitra, SA Dkhar, DG Shewade, CH Shashindran, Department of Pharmacology, JIPMER, Pondicherry 605006, INDIA
Correspondence to: DG Shewade, Department of Pharmacology, JIPMER, Pondicherry 605006, INDIA. shewade@eth.net
Telephone: +91-413-2278693 **Fax:** +91-413-2272067
Received: 2002-10-05 **Accepted:** 2002-11-04

Abstract

AIM: To study the relative efficacy of cisapride, metoclopramide, domperidone, erythromycin and mosapride on gastric emptying (GE) and small intestinal transit (SIT) in morphine treated mice.

METHODS: Phenol red marker meal was employed to estimate GE and SIT in Swiss albino mice of either sex. The groups included were control, morphine 1 mg/kg (s.c. 15 min before test meal) alone or with (45 min before test meal p.o.) cisapride 10 mg/kg, metoclopramide 20 mg/kg, domperidone 20 mg/kg, erythromycin 6 mg/kg and mosapride 20 mg/kg.

RESULTS: Cisapride, metoclopramide and mosapride were effective in enhancing gastric emptying significantly ($P<0.001$) whereas other prokinetic agents failed to do so in normal mice. Metoclopramide completely reversed morphine induced delay in gastric emptying followed by mosapride. Metoclopramide alone was effective when given to normal mice in increasing the SIT. Cisapride, though it did not show any significant effect on SIT in normal mice, was able to reverse morphine induced delay in SIT significantly ($P<0.001$) followed by metoclopramide and mosapride.

CONCLUSION: Metoclopramide and cisapride are most effective in reversing morphine-induced delay in gastric emptying and small intestinal transit in mice respectively.

Suchitra AD, Dkhar SA, Shewade DG, Shashindran CH. Relative efficacy of some prokinetic drugs in morphine-induced gastrointestinal transit delay in mice. *World J Gastroenterol* 2003; 9(4): 779-783
http://www.wjgnet.com/1007-9327/9/779.htm

INTRODUCTION

Opioids are effective analgesics for moderate to severe pain[1]. Morphine is the most commonly prescribed opioid agonist for the treatment of chronic pain[2, 3]. However, when opioids are given to alleviate pain they cause undesirable gastrointestinal (GI) side effects namely nausea, vomiting and reduced gastrointestinal transit[4]. Reduced GI transit can cause gastroesophageal reflux disease, bloating and idiopathic constipation[5].

The pathophysiology of GI delay due to opioids has been well described. Possible etiologies include increased stationary segmentation, reduced peristalsis and depression of secretory activity[6]. Due to the paucity of the data to guide practitioners in the management of GI side effects of opioids much of the information is extrapolated from different patient populations experiencing the same symptoms due to different etiologies.

Use of opioid antagonists such as naloxone, nalmefene, for opioid-induced GI delay[7-10], is limited by their cost and tendency to cause withdrawal symptoms in the doses used[10,11]. Peripherally acting methyl naltrexone and ADL-2698 (Alvimopan) are in the stage of investigational[11].

Mosapride, cisapride, metoclopramide, erythromycin and domperidone are commonly used prokinetic agents. At present, the data supporting their relative efficacy in opioid induced GI delay are lacking. Further their distinct mechanism of action leaves a scope for variation in their efficacy. The present work attempts to study the relative efficacy of various prokinetic drugs such as cisapride, metoclopramide, domperidone, erythromycin and mosapride on small intestinal transit (SIT) and gastric emptying (GE) in morphine treated mice.

MATERIALS AND METHODS

Animals

Randomly bred healthy adult Swiss albino mice of either sex weighing between 20-25 g were obtained from JIPMER animal house, Pondicherry. One week prior to the experimentation, six mice were housed in separate cages and had free access to food and water. The experiments were conducted between 09:00 AM and 1:00 PM. The animals were fed with the pellets obtained from Prestige Agro-industries, Aurangabad. The study was approved by the institutional animal ethics committee.

Drugs and chemicals

Morphine sulphate (Govt. opium and alkaloid works, Ghazipur), cisapride (Torrent Pharmaceuticals, Ahmedabad), metoclopramide hydrochloride (Ipca laboratories Ltd., Mumbai), domperidone (Torrent Pharmaceuticals, Ahmedabad), erythromycin ethylsuccinate (Emil pharmaceutical industries Pvt Ltd, Thane), mosapride citrate (Alembic chemical works Co. Ltd. Vadodara) and Thiopentone sodium (Abbot laboratories, Mumbai) were used. Other chemicals used were of analytical grade. Carboxymethyl cellulose (1 %, 0.2 ml) was used as vehicle to administer prokinetic drugs.

Phenol red meal

Phenol red indicator weighing 25 mg was dissolved in 50 ml of distilled water and filtered. The filtrate was heated to 70 ℃ and methylcellulose (0.75 g) was added to it with continuous stirring. The mixture was then cooled to 37 ℃.

Gastric emptying (GE) and small intestinal transit (SIT)

The standard method of phenol red marker meal as performed by earlier workers was employed[12,13]. Mice were deprived of food for 24 h prior to experimentation but had free access to water, and 0.5 ml of phenol red meal was administered with the aid of the oral feeding syringe. Animals were killed by cervical dislocation under i.v. thiopentone sodium anesthesia 15 min after the administration of the meal. Abdomen was

opened and stomach was dissected out after careful ligation at the cardiac and pyloric ends, and was washed with normal saline. The stomach was cut into pieces and homogenized with 25 ml of 0.1 N NaOH. To this 5 ml homogenate 0.5 ml of trichloroacetic acid (20 %w/v) was added and centrifuged at 3 000 rpm for 20 minutes. To one ml of supernatant 4 ml of 0.5 N NaOH was added. The absorbance of this pink colored liquid was measured using spectrophotometer at 560nm (Model: HITACHI 150-20). This correlates with the concentration of phenol red in the stomach, which in turn depends upon the gastric emptying. The percentage gastric emptying is derived as (1-X/Y) 100 where, X is absorbance of phenol red recovered from the stomach of animals sacrificed 15 minutes after test meal. Y is mean (n=5) absorbance of phenol red recovered from the stomachs of control animals (killed at 0 min following test meal).

The small intestine was dissected out from the pylorus and ileocaecal junction and the point to which meal had traversed was secured with thread to avoid change in the length of the transit due to handling. The total length of the small intestine and distance traveled by phenol red meal was measured. The small intestinal transit (SIT) was calculated considering the distance traveled by phenol red meal divided by total length of the small intestine multiplied by 100. Small intestinal transit was expressed as mean ±sem. The observer was blinded for the drugs administered to the mice.

Drug treatment

Control groups received the equal volumes of vehicle through corresponding routes. The groups included were control, morphine 1 mg/kg (s.c.), cisapride 10 mg/kg (p.o.), metoclopramide 20 mg/kg (p.o.), domperidone 20 mg/kg (p.o.), erythromycin 6 mg/kg (p.o.) and mosapride 20 mg/kg (p.o.). The doses were selected based on the earlier reports[14,17], recommended clinical doses[18,20] and prior pilot experiments. Cisapride, metoclopramide, domperidone, erythromycin and mosapride in the dose mentioned above were given alone 45 minutes before the administration of phenol red meal. Morphine (s.c.) was injected 15 minutes before the administration of the meal.

Statistical analysis

Statistical analysis was carried out using Graph pad (Prism) soft ware. One way analysis of variance (ANOVA) for small intestinal transit and gastric emptying was applied separately followed by bonferroni post-test for multiple comparisons. Values were expressed as mean ± sem. P<0.05 was considered significant.

RESULTS

Since significant difference was not noticed among inter-day and animals receiving saline or 1 % carboxymethyl cellulose, data from these groups were pooled to serve as control group. Similar results obtained from morphine (1 mg/kg s.c.) treated groups were pooled. Morphine in the dose of 1 mg/kg (s.c.) caused significant decrease (61 %) in SIT (P<0.001) and (43 %) in gastric emptying (P<0.05).

Gastric emptying

Cisapride, metoclopramide and mosapride in the doses employed increased gastric emptying significantly (P<0.001) by 126 %, 102 %, 89 % respectively compared with control animals, while domperidone and erythromycin failed to show any significant effect (Table 1, Figure 1). When combined with morphine (1 mg/kg s.c.) only metoclopramide and mosapride reversed morphine induced delay significantly (P <0.05) (Table 2, Figure 2).

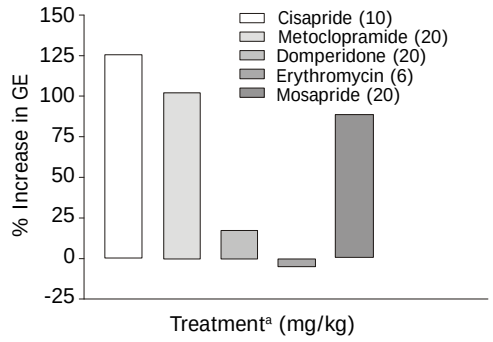

Figure 1 Percentage increase in gastric emptying by various prokinetic agents in mice. ([a]Prokinetic agents were administered 45 minutes orally prior to the test meal).

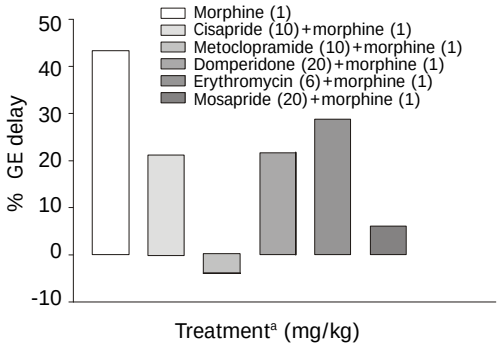

Figure 2 Effect of prokinetic agents on morphine induced delay of gastric emptying in mice. ([a]Prokinetic agents were administered 45 minutes orally and morphine (s.c.) 15 minutes prior to test meal).

Table 1 Effect of prokinetic agents on gastric emptying and small intestinal transit in mice

Treatment* (mg / kg)	GE (%)	SIT(%)
Control	41.15±3.76	51.11±1.59
Cisapride (10) p.o.	92.98±1.76[a]	61.46±3.01
Metoclopramide (20) p.o.	83.14±5.59[a]	76.63±2.13[a]
Domperidone (20) p.o.	48.15±2.31	58.94±1.25
Erythromycin (6) p.o.	39.08±5.10	52.91±1.50
Mosapride (20) p.o.	77.88±0.54[a]	57.53±1.19

Each value represents mean±sem, n=10 in control group and n=5 in prokinetic drug treated group. *prokinetic agents were given 45 minutes prior to test meal. [a]P<0.001 *vs* the control group.

Table 2 Effect of prokinetic agents on morphine induced delay in gastric emptying and small intestinal transit in mice

Treatment* (mg / kg)	GE (%)	SIT(%)
Control	41.15±3.76	51.11±1.59
Morphine(1) s.c.	23.30±2.83[a]	19.73±1.25[b]
Morphine (1) s.c. + Cisapride (10) p.o.	32.34±2.52	46.28±2.00[d]
Metoclopramide (20) p.o	42.77±2.04[c]	34.01±1.75[d]
Domperidone (20) p.o	32.16±3.48	28.63±2.47
Erythromycin (6) p.o	29.39±2.53	31.19±1.08
Mosapride (20) p.o	38.59±1.98[c]	38.01±1.61[d]

Each value represents mean ±sem, n=5 in treatment group and n=10 in control and morphine treated group. *prokinetic agents were given 45 minutes and morphine 15 minutes prior to the test meal. [a]P<0.05 and [b]P<0.001 *vs* control group. [c]P<0.05 and [d]P<0.001 *vs* morphine treated group.

Small intestinal transit

Only metoclopramide *per se*, significantly (P<0.001) increased SIT by 50 % (Figure 3). However, when combined with morphine (1 mg/kg, s.c.) cisapride showed maximum efficacy followed by mosapride and metoclopramide (Figure 4). Domperidone and erythromycin did not exhibit any significant effect (Table 2).

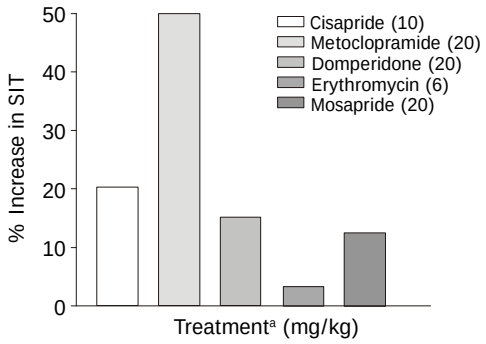

Figure 3 Effect of various prokinetic agents on small intestinal transit in mice. ([a]Prokinetic agents were administered orally 45 minutes prior to test meal).

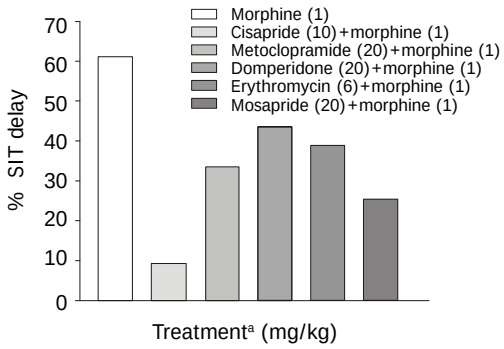

Figure 4 Effect of Prokinetic agents on morphine induced delay of small intestinal transit in mice. ([a]Prokinetic agents were administered orally 45 minutes and morphine s.c.15 minutes prior to test meal).

DISCUSSION

Opioids cause decrease in gastric emptying and intestinal motility, which leads to nausea, abdominal bloating and constipation[21]. Both exogenous and endogenous opioids inhibit propulsive movements of the intestine by interfering with the enteric regulation of propulsive motility[22]. They interact with μ and δ opioid receptors and cause decrease in cyclic AMP. Opioids increase the calcium dependent potassium conductance and thus, hyperpolarize myentric neurons, which reduce the entry of calcium during the action potential leading to decrease in intracellular calcium and thereby decreasing peristalsis[23].

In mice μ agonists administered subcutaneously produced dose-related inhibitions of gastrointestinal transit[24]. In our study there was significant decrease (61 %) in SIT with morphine (1 mg/kg s.c.) compared with control animals (P<0.001). Decrease in SIT seen with 1 mg/kg (s.c) of morphine is in agreement with earlier reports[14,16,17].

Prokinetic agents used to reverse morphine induced delay in GI transit showed variation in their efficacy. Cisapride (10 mg/kg, p.o.) though, did not show significant increase in SIT compared with control, it was most effective in reversing morphine induced delay in SIT (Figure 4). This finding is consistent with a clinical study where the effect of cisapride was significantly greater than that of metoclopramide[16]. Cisapride in the dose of 10 mg/kg (p.o.) showed significant increase in gastric emptying when compared with control animals but in morphine induced delay in gastric emptying it fails to show significant effect in overcoming the inhibition (Table 2).

Rectal administration of cisapride 30 mg 8th hourly had modest benefit in reversing small intestinal transit following intravenous meperidine in patients undergoing major abdominal surgery[25]. This may reflect an inability of cisapride to attain effective plasma concentrations when given rectally and this is supported by an another report where rectal cisapride was not able to overcome gastric stasis produced by morphine[26]. Above observations indicate that in morphine treated mice, cisapride is more effective in reversing morphine induced delay in SIT rather than delay in gastric emptying.

Similar differential effect of metoclopramide and cisapride on the abdominal surgery induced decrease in transit was seen in which metoclopramide further inhibited whereas cisapride ameliorated the inhibition of transit[27].

In our study metoclopramide (20 mg/kg p.o.) was found to be the most effective prokinetic agent when compared to control animals (Figure 3). Metoclopramide is a 5-HT_4 agonist, 5-HT_3 antagonist and antagonises the inhibitory effect of dopamine in the gastrointestinal tract. Despite above actions, it was only marginally effective in reversing morphine induced delay in SIT (Figure 2).

Metoclopramide in the dose of 20 mg/kg p.o. significantly increased gastric emptying when compared with controls (Table 1). In morphine induced gastric emptying delay, it reversed the morphine effect completely (Figure 2). In a clinical study conducted by McNeill *et al*, it was shown that i.v. metoclopramide antagonised the opioid premedication induced delay in gastric emptying but not i.m. metoclopramide[28]. There is also evidence that the effectiveness of metoclopramide may depend on the route of administration[29,30].

Domperidone is a peripherally acting dopamine antagonist. Domperidone (20 mg/kg, p.o.) alone did not show any significant prokinetic effect as against control animals (Table 2). In our study, it was seen that in reversing morphine induced delay, though it could not significantly increase SIT, its efficacy was similar to that of metoclopramide (Figure 4). Since there is a risk of extrapyramidal effects with metoclopramide, domperidone may be useful in opioid induced delay in gastrointestinal transit where metoclopramide is contraindicated. Domperidone in the dose of 20 mg/kg p.o. did not show any significant increase in gastric emptying in normal and morphine treated animals (Table1 and Table 2).

Erythromycin, a motilinomimetic in the dose of 6 mg/kg (p.o.) did not show any significant prokinetic effect (Table 1) and had the least efficacy in reversing morphine induced delay in gastrointestinal transit (Table 2). Erythromycin in the dose of 1 mg/kg did not show any effect in postoperative ileus[27]. Erythromycin even at 40 mg/kg did not show any prokinetic effect in rats though motilin immunoreactivity has been demonstrated in the rat intestine[31]. The motilin receptor status of mouse upper GI tract is not documented. De Winter *et al* suggested by their experiments that rat might not be the ideal species to test erythromycin[27]. The fact that erythromycin was not effective in our study indicates that mice too may not be the ideal species for these type of studies.

Mosapride, a derivative of cisapride so far was not tested in morphine-induced delay in small intestinal transit. In our study though it did not show significant prokinetic effect in the dose (20 mg/kg p.o.) used, however it was less effective than 10 mg cisapride in reversing morphine induced delay in SIT. Efficacy of mosapride and metoclopramide in reversing morphine effect on GE cannot be differentiated from the available data.

A look at the SIT values (Table 1) indicates that metoclopramide has maximum efficacy in normal mice while cisapride is most efficacious in reversing morphine induced delay in SIT followed by metoclopramide and mosapride (Table 2). The above differences may be due to interactions taking place at various levels viz. the central and the peripheral nervous system. It is known that morphine suppresses the cholinergic outflow[32], while metoclopramide enhance cholinergic outflow[20] via 5-HT_4 and D_2 receptor interaction. It is also known that cisapride is non-selective 5-HT_4 receptor agonist with affinity for D_2, 5-HT_2, α_1 adrenergic and muscarinic receptors[33]. Further, mosapride a 5-HT_4 agonist shows efficacy less than cisapride in reversing morphine effects on SIT and less than metoclopramide in GE. The intrinsic activity of mosapride was less than that observed for cisapride which indicates that it may act as a partial agonist[34]. Role of heterogenicity in 5-HT_4 receptors in the differential effect of 5-HT_4 agonists cannot be ruled out[35].

Mechanism underlying the stimulation of gastric and small intestinal motility by prokinetic agents is 5-HT_4 receptor activation that involve cholinergic nerves. However the mechanism underlying the different profile of the effect of 5-HT_4 agonists on gastric emptying and small intestinal transit remains unexplained.

Gastric emptying in normal mice was enhanced by cisapride, metoclopramide and mosapride (Figure 1) but in morphine treated mice metoclopramide was most effective followed by mosapride (Figure 2). This suggests that in morphine treated mice, 5-HT_4 pathways may not play a major role. Effect of cisapride and metoclopramide on other receptors contributes predominantly in reversing the effect of morphine on SIT and gastric emptying respectively.

Results of this study and earlier reports indicate that efficacy of prokinetic agents is dependent on factors such as pathophysiology, species, site of gastrointestinal tract and pharmacological profile of the drug.

CONCLUSIONS

Morphine in the dose of 1 mg/kg (s.c.) inhibited the small intestinal transit by 61 % and to a lesser extent, gastric emptying (43 %) under the experimental conditions. Metoclopramide has significant prokinetic effect when compared with cisapride, domperidone, mosapride and erythromycin in normal mice. Metoclopramide, cisapride and mosapride enhance gastric emptying significantly compared to domperidone and erythromycin in normal mice. All the prokinetic agents used in our study differ in their prokinetic effects in counteracting the effect of morphine induced GI inertia. Cisapride is most effective in reversing morphine induced SIT delay followed by metoclopramide and mosapride. In morphine-induced GE delay metoclopramide is most effective followed by mosapride.

REFERENCES

1 **Barnett M**. Alternative opioids to morphine in palliative care: a review of current practice and evidence. *Postgrad Med J* 2001; **77**: 371-378

2 **Moulin DE**, Iezzi A, Amireh R, Sharpe WK, Boyd D, Merskey H. Randomised trial of oral morphine for chronic non-cancer pain. *Lancet* 1996; **347**: 143-147

3 **McQuay H**. Opioids in pain management. *Lancet* 1999; **353**: 2229-2232

4 **Murphy DB**, Sutton JA, Prescott LF, Murphy MB. Opioid-induced delay in gastric emptying: a peripheral mechanism in humans. *Anesthesiology* 1997; **87**: 765-770

5 **McCallum RW**. Review of the current status of prokinetic agents in gastroenterology. *Am J Gastroenterol* 1985; **80**: 1008-1016

6 **De Luca A**, Coupar IM. Insights into opioid action in the intestinal tract. *Pharmacol Ther* 1996; **69**: 103-115

7 **Meissner W,** Schmidt U, Hartmann M, Kath R, Reinhart K. Oral naloxone reverses opioid-associated constipation. *Pain* 2000; **84**: 105-109

8 **Cheskin LJ**, Chami TN, Johnson RE, Jaffe JH. Assessment of nalmefene glucuronide as a selective gut opioid antagonist. *Drug Alcohol Depend* 1995; **39**: 151-154

9 **Culpepper-Morgan JA**, Inturrisi CE, Portenoy RK, Foley K, Houde RW, Marsh F, Kreek MJ. Treatment of opioid-induced constipation with oral naloxone: a pilot study. *Clin Pharmacol Ther* 1992; **52**: 90-95

10 **Yuan CS**, Foss JF, O'Connor M, Toledano A, Roizen MF, Moss J. Methylnaltrexone prevents morphine-induced delay in oral-cecal transit time without affecting analgesia: a double-blind randomized placebo-controlled trial. *Clin Pharmacol Ther* 1996; **59**: 469-475

11 **Schmidt WK**. Alvimopan* (ADL 8-2698) is a novel peripheral opioid antagonist. *Am J Surg* 2001; **182**(5A Suppl): 27S-38S

12 **Barquist E**, Bonaz B, Martinez V, Rivier J, Zinner MJ, Tache Y. Neuronal pathways involved in abdominal surgery-induced gastric ileus in rats. *Am J Physiol* 1996; **270**(4 Pt 2): R888-R894

13 **Matsuda H**, Li Y, Yamahara J, Yoshikawa M. Inhibition of gastric emptying by triterpene saponin, momordin, in mice: roles of blood glucose, capsaicin-sensitive sensory nerves, and central nervous system. *J Pharmacol Exp Ther* 1999; **289**: 729-734

14 **Fickel J**, Bagnol D, Watson SJ, Akil H. Opioid receptor expression in the rat gastrointestinal tract: a quantitative study with comparison to the brain. *Brain Res Mol Brain Res* 1997; **46**: 1-8

15 **Rowbotham DJ**, Nimmo WS. Effect of cisapride on morphine-induced delay in gastric emptying. *Br J Anaesth* 1987; **59**: 536-539

16 **Bianchi G**, Ferretti P, Recchia M, Rocchetti M, Tavani A, Manara L. Morphine tissue levels and reduction of gastrointestinal transit in rats. Correlation supports primary action site in the gut. *Gastroenterology* 1983; **85**: 852-858

17 **Patil CK**, Kulkarni SK. Effect of physostigmine and cisapride on morphine-induced delayed gastric transit in mice. *Ind J Pharmacol* 2000; **32**: 321-323

18 **Brogden RN**, Carmine AA, Heel RC, Speight TM, Avery GS. Domperidone. A review of its pharmacological activity, pharmacokinetics and therapeutic efficacy in the symptomatic treatment of chronic dyspepsia and as an antiemetic. *Drugs* 1982; **24**: 360-400

19 **Pandolfino JE**, Howden CW, Kahrilas PJ. Motility-modifying agents and management of disorders of gastrointestinal motility. *Gastroenterology* 2000; **118**: S32-S47

20 **Harrington RA**, Hamilton CW, Brogden RN, Linkewich JA, Romankiewicz JA, Heel RC. Metoclopramide. An updated review of its pharmacological properties and clinical use. *Drugs* 1983; **25**: 451-494

21 **Murphy DB**, Sutton JA, Prescott LF, Murphy MB. Opioid-induced delay in gastric emptying: a peripheral mechanism in humans. *Anesthesiology* 1997; **87**: 765-770

22 **Wong CL**. Central and peripheral inhibitory effects of morphine on intestinal transit in mice. *Exp Clin Pharmacol* 1986; **8**: 479-483

23 **Pasricha PJ**. Prokinetic agents, antiemetics and agents used in irritable bowel syndrome. In Hardman JG, Limbard LE, eds The pharmacological basis of therapeutics. McGraw-Hill, New York, 2001: 1021-1036

24 **Pol O**, Ferrer I, Puig MM. Diarrhea associated with intestinal inflammation increases the potency of mu and delta opioids on the inhibition of gastrointestinal transit in mice. *J Pharmacol Exp Ther* 1994; **270**: 386-391

25 **Benson MJ**, Roberts JP, Wingate DL, Rogers J, Deeks JJ, Castillo FD, Williams NS. Small bowel motility following major intra-abdominal surgery: the effects of opiates and rectal cisapride. *Gastroenterology* 1994; **106**: 924-936

26 **Kluger MT**, Plummer JL, Owen H. The influence of rectal cisapride on morphine-induced gastric stasis. *Anaesth Intensive Care* 1991; **19**: 346-350

27 **De Winter BY**, Boeckxstaens GE, De Man JG, Moreels TG, Schuurkes JA, Peeters TL, Herman AG, Pelckmans PA. Effect of different prokinetic agents and a novel enterokinetic agent on postoperative ileus in rats. *Gut* 1999; **45**: 713-718

28 **McNeill MJ**, Ho ET, Kenny GN. Effect of i.v. metoclopramide on gastric emptying after opioid premedication. *Br J Anaesth* 1990; **64**: 450-452
29 **Bateman DN**, Kahn C, Davies DS. Concentration effect studies with oral metoclopramide. *Br J Clin Pharmacol* 1979; **8**: 179-182
30 **Bateman DN**, Kahn C, Mashiter K, Davies DS. Pharmacokinetic and concentration-effect studies with intravenous metoclopramide. *Br J Clin Pharmacol* 1978; **6**: 401-407
31 **Trudel L**, Tomasetto C, Rio MC, Bouin M, Plourde V, Eberling P, Poitras P. Ghrelin / motilin-related peptide is a potent prokinetic to reverse gastric postoperative ileus in rat. *Am J Physiol Gastrointest Liver Physiol* 2002; **282**: G948-G952
32 **Cherubini E**, Morita K, North RA. Opioid inhibition of synaptic transmission in the guinea-pig myenteric plexus. *Br J Pharmacol* 1985; **85**: 805-817
33 **Briejer MR**, Akkermans LM, Schuurkes JA. Gastrointestinal prokinetic benzamides: the pharmacology underlying stimulation of motility. *Pharmacol Rev* 1995; **47**: 631-651
34 **Yoshida N**. Pharmacological effects of the gastroprokinetic agent mosapride citrate. *Nippon Yakurigaku Zasshi* 1999; **113**: 299-307
35 **Mine Y**, Yoshikawa T, Oku S, Nagai R, Yoshida N, Hosoki K. Comparison of effect of mosapride citrate and existing 5-HT4 receptor agonists on gastrointestinal motility *in vivo* and *in vitro*. *J Pharmacol Exp Ther* 1997; **283**: 1000-1008

Edited by Ma JY and Xu XQ

P.O.Box 2345, Beijing 100023, China
Fax: +86-10-85381893
E-mail: wjg@wjgnet.com www.wjgnet.com

World J Gastroenterol 2003;9(4):784-787
World Journal of Gastroenterology
 ISSN 1007-9327

• BASIC RESEARCH •

Effect of transforming growth factor beta and bone morphogenetic proteins on rat hepatic stellate cell proliferation and trans-differentiation

Hong Shen, Guo-Jiang Huang, Yue-Wen Gong

Hong Shen, Guo-Jiang Huang, Yue-Wen Gong, Departments of Internal Medicine, Biochemistry and Medical Genetics, Faculty of Medicine, University of Manitoba, Winnipeg, Manitoba, Canada
Correspondence to: Dr. Yue-Wen Gong, John Buhler Research Centre, 803G - 715 McDermot Avenue, Winnipeg, Manitoba, Canada, R3E 3P4. ygong@ms.umanitoba.ca
Telephone: +1-204-7893567 **Fax:** +1-204-7893987
Received: 2002-10-04 **Accepted:** 2002-11-04

Abstract

AIM: To explore different roles of transforming growth factor beta (TGF-β) and bone morphogenetic proteins (BMPs) in hepatic stellate cell proliferation and trans-differentiation.

METHODS: Hepatic stellate cells were isolated from male Sprague-Dawley rats. Sub-cultured hepatic stellate cells were employed for cell proliferation assay with WST-1 reagent and Western blot analysis with antibody against smooth muscle alpha actin (SMA).

RESULTS: The results indicated that TGF-β1 significantly inhibited cell proliferation at concentration as low as 0.1 ng/ml, but both BMP-2 and BMP-4 did not affect cell proliferation at concentration as high as 10 ng/ml. The effect on hepatic stellate cell trans-differentiation was similar between TGF-β1 and BMPs. However, BMPs was more potent at trans-differentiation of hepatic stellate cells than TGF-β1. In addition, we observed that TGF-β1 transient reduced the abundance of SMA in hepatic stellate cells.

CONCLUSION: TGF-β may be more important in regulation of hepatic stellate cell proliferation while BMPs may be the major cytokines regulating hepatic stellate cell trans-differentiation.

Shen H, Huang GJ, Gong YW. Effect of transforming growth factor beta and bone morphogenetic proteins on rat hepatic stellate cell proliferation and trans-differentiation. *World J Gastroenterol* 2003; 9(4): 784-787
http://www.wjgnet.com/1007-9327/9/784.htm

INTRODUCTION

Transforming growth factor beta (TGF-β) and bone morphogenetic proteins (BMPs) are the members of TGF-β superfamily[7, 23]. Their biological effects are mediated through the receptors that have serine-threonine kinase activity[1, 24]. However, they bind to their respective receptors. Moreover, the molecules involved in their signal transduction are different. It is generally considered that signal transduction pathway of BMPs is mediated by Smads 1, 5, and 8, while the signaling molecules of TGF-β are Smads 2 and Smads 3[17, 29, 33]. The role of TGF-β in hepatic fibrogenesis has been investigated because of the effect of TGF-β on extracellular matrix (ECM) production and degradation[3, 27, 32]. But the effects of BMP on hepatic fibrogenesis have not been studied extensively. With recent understanding of hepatic fibrogenesis, hepatic stellate cells play an important role in the development of hepatic fibrosis[8, 14]. It is documented that hepatic stellate cells are the main cell type that synthesize and secret ECM in the liver. In addition, hepatic stellate cells migrate, proliferate and contract in response to liver injury, which contribute to the development of scar formation and portal hypertension. The effects of TGF-β1 on hepatic stellate cell proliferation and activation have been documented with some studies showed the inhibitory effect of TGF-β1[2, 6, 25, 26] while others exhibited no effect on hepatic stellate cell proliferation[20, 28]. However, there are no reports about the effects of BMPs on hepatic stellate cell proliferation and trans-differentiation. Therefore, the objective of this study is to examine the effects of TGF-β1 and BMPs on rat hepatic stellate cell proliferation and expression of smooth muscle alpha actin (SMA) - a marker of hepatic stellate cell trans-differentiation.

MATERIALS AND METHODS

Materials

Collagenase D, pronase, DNase 1, cell proliferation reagent WST-1, and monoclonal antibody against smooth muscle alpha actin were purchased from Roche Diagnostics (Laval Quebec). Rabbit antibody against mouse IgG conjugated to horseradish peroxidase, and Enhanced Chemiluminescence Detection Kit were from Amersham Pharmacia Biotech, Inc. (Baie d' Urfe, Quebec). Dulbecco' s Modified Eagle Medium (DMEM), fetal bovine serum (FBS) and Nycodenz were obtained from GIBCO/BRL (Burlington, Ontario). TGF-β1, BMP-2 and BMP-4 were purchased from R&D systems (Minneapolis, MN).

Isolation of rat hepatic stellate cells

Male Sprague-Dawley rats (450-550 gram body weight) were purchased from Central Animal Care of the University of Manitoba and maintained under 12-hour light/dark cycles with food and water ad libitum. In conducting the research described in this report, all animals received humane care in compliance with the Institution' s guidelines (Animal Protocol No. 98-053), which is in accordance with the Canadian Council on Animal Care' s criteria. Hepatic stellate cells were isolated from rat liver by two steps of collagenase and pronase methods as previously described[10]. The liver was perfused via the portal vein first with Ca^{2+} free Hanks' balanced salt solution (HBSS), pH7.4, for 10 minutes at 37 ℃ and then with Ca^{2+} HBSS containing 0.125 mg/ml collagenase D, 0.5 mg/ml pronase and 15 μg/ml DNase 1 for 20 minutes. After being dispersed gently, the cells were incubated with 0.125 mg/ml collagenase D, 0.5 mg/ml pronase and 15 μg/ml DNase 1 for another 12 minutes with constant low speed stirring at 37 ℃. Cell suspension was filtered through a 100 μm mesh. After removing hepatocytes

by centrifugation at 500 rpm on a bench-top centrifuge, Hepatic stellate cells were separated from other non-parenchymal cells by density gradient centrifugation on 11.3 % Nycodenz with sodium chloride at 1 400 g for 17 minutes at 8 ℃. Hepatic stellate cells were harvested from the interface between suspension buffer on the top and 11.3 % Nycodenz solution, washed and plated on uncoated plastic tissue culture dishes (Costar) at a density of 25 000 cells/cm^2. Hepatic stellate cells were identified by the typical star-like configuration under light microscopic appearance. The purity was always higher than 95 %. Hepatic stellate cells were incubated in DMEM supplemented with 10 % FBS, antibiotics (100 IU/ml penicillin and 100 mg/ml streptomycin) and 2 mM L-glutamine at 37 ℃ in a humidified atmosphere of 5 % CO_2. The first change of culture medium was made 24 hours after seeding and then change the medium every 48 hours. Sub-cultured Hepatic stellate cells were obtained from 9-day-old primary culture hepatic stellate cells by detaching from the dishes with trypsin-EDTA.

Cell proliferation assay

Cell proliferation was measured by cell proliferation reagents WST-1[12]. Sub-cultured hepatic stellate cells (2×10^3) in 200 μl culture medium were seeded into 96 well plates. After incubation for 24 hours, the medium was changed with 100 μl of fresh culture medium containing different concentrations of recombinant TGF-β1, BMP-2 and BMP-4. The media and reagents were changed every other day. Cell proliferation was documented after 3, 6, 9 days of treatment. At the end of treatment, 10 μl of WST-1 reagent were added into wells and incubated for 2 hours. The absorbence of the treated samples against a blank control was measured using a THERMOmax microplate reader (ELISA) (molecular Devices Co., Menlo Park, CA) with 420nm as detection wavelength and 650nm as reference wavelength for WST-1 assay.

Western blot analyses of SMA

Sub-cultured hepatic stellate cells were lysed in 100 μl protein extract solution (1 mM Tris-HCl pH7.5, 1 mM EDTA pH 8.0, 10 mM NaCl, 1 % sodium dodecyl sulfate (SDS), 1 mM PMSF and 0.25 M sucrose)[11]. Cell membrane was broken by sonicating the cells for 1 minutes with Sonicator (Vibra Cell, Sonics and Material Inc. Danbury, CT) and cell debris was pelleted by centrifugation at 14 000 rpm at 4 ℃ for 5 minutes. Protein concentration was determined by Lowry method[9]. 20 g of protein from each sample was mixed with gel loading buffer (2×: 125 mM Tris-HCl, pH6.8, 4 % SDS, 20 % glycerol, 0.1 % bromophenol blue and 2.5 % β-mercaptoethanol), boiled for 5 minutes, separated on 12 % SDS-polyacrylamide gel under reducing conditions, and transferred to Nitroplus-2000 membrane (Micron Separations Inc. Westborough, MA). Nonspecific antibody binding was blocked by pre-incubation of the membranes in 1×Tris-buffered-saline (TBS) containing 5 % skim milk for 1 hour at room temperature. Membranes were then incubated overnight at 4 ℃ with primary antibody against SMA at dilution of 1:1 000 in 1×TBS containing 2 % skim milk. After washing, they were incubated for 1 hour at room temperature with sheep anti-mouse IgG at 1:1 000 dilutions. Bands were visualized by employing the enhanced chemiluminescence kit per the manufacturer' s instruction.

Statistical analyses

Statistical significance of differences was performed by employing the ANOVA and Fisher' s PLSD test as Post hoc test with StatView software (version 5.0, SAS Institute Inc. Cary, NC). Differences were considered to be significant when *P* was less than 0.05.

RESULTS

Effect of TGF-b1, BMP2 and BMP4 on rat hepatic stellate cell proliferation

Effect of TGF-β1, BMP2 and BMP4 on rat hepatic stellate cell proliferation was shown in Figure 1. TGF-β1 significantly inhibited hepatic stellate cell proliferation after 6 days of incubation at the concentrations of 0.1, 0.5 and 1 ng/ml, respectively, $P<0.05$ (Figure 1A). The inhibition was more dramatic at 9-days treatment of TGF-β1, $P<0.01$. However, both BMP2 and BMP4 did not affect hepatic stellate cell proliferation at the concentration as high as 10 ng/ml (Figure 1B and 1C).

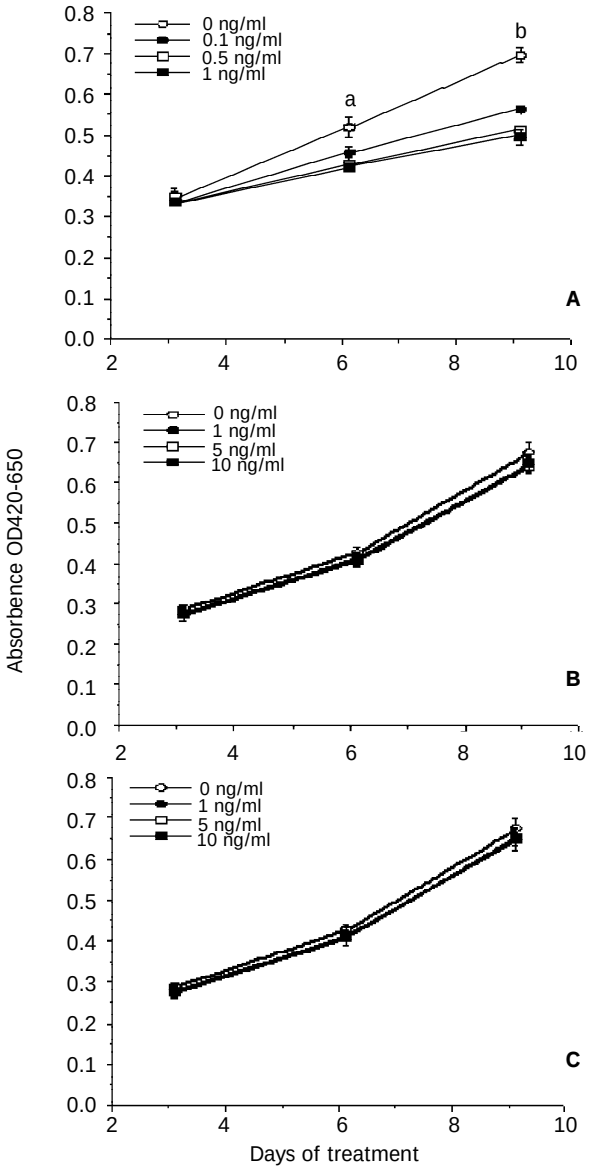

Figure 1 Regulating effect of TGF-β1, BMP-2 and BMP-4 on the proliferation of rat hepatic stellate cells. Hepatic stellate cells were incubated with TGF-β1 (A), BMP-2 (B) and BMP-4 (C) as described in Materials and methods. The data represent mean ± SE from ten wells. The experiments were repeated two times. Denotes: a represents $^aP<0.05$ *vs* the concentrations of 0.1, 0.5 and 1 ng/ml, b means $^bP<0.01$*vs* the concentrations of 0.1, 0.5 and 1 ng/ml.

Effect of TGF-b1, BMP-2 and BMP-4 on SMA expression

TGF-β1, BMP-2 and BMP-4 increased the expression of SMA, which is well recognized by the antibody as a 42-kDa protein. BMP-2 and BMP-4 seemed to have more potent effect on the expression of SMA than TGF-β1. After incubation with TGF-

β1 (concentrations from 0.1 to 1 ng/ml) for 3 days, SMA level was only elevated about 50 % as compared with control group (Figure 2). While after BMP-2 or BMP-4 treatment, SMA level was two to four times higher than that of the untreated group (Figure 3). Moreover, we observed that the abundance of SMA in hepatic stellate cells was reduced after 3 hours of TGF-β1 treatment. The abundance of SMA was reduced to about 20 % of original level and the level of SMA was elevated (about 60 % higher than original level) after 18 hours' treatment (Figure 4).

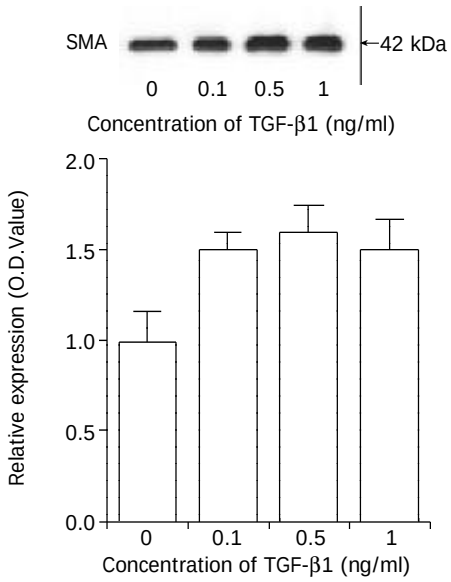

Figure 2 Regulating effect of TGF-β1 on rat hepatic stellate cell trans-differentiation. Hepatic stellate cells were incubated with different concentrations of TGF-β1 for three days. The media and TGF-β1 were changed every other day. Western blot was performed as described in Materials and methods. The top panel represents typical Western blot of SMA. The lower panel represents histogram of densitometric data from four-separated Western blot (mean ± SE).

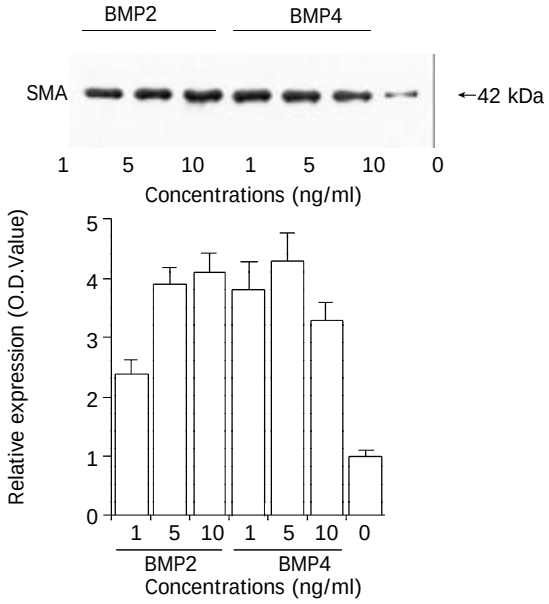

Figure 3 Regulating effect of BMP-2 and BMP-4 on hepatic stellate cell trans-differentiation. Hepatic stellate cells were incubated with different concentrations of BMP-2 or BMP-4 for three days. The media and BMPs were changed every other day. Western blot was performed as described in Materials and methods. The top panel represents typical Western blot of SMA. The lower panel represents histogram of densitometric data from four-separated Western blot (mean ± SE).

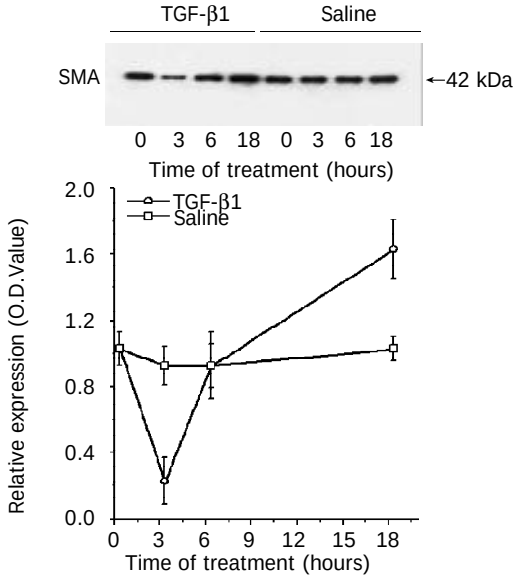

Figure 4 Regulating effect of TGF-β1 on SMA protein expression. Hepatic stellate cells were cultured for three days and the media were removed. Media with 1 ng/ml TGF-β1 or saline were added into culture dishes and cells were collected at different times as indicated. The data represent mean ± SE from four experiments.

DISCUSSION

Hepatic stellate cells are non-parenchymal liver cells located at the perisinusoidal space. Recent studies have demonstrated that these cells proliferate and activate in response to liver injury. It is now established that hepatic stellate cells are the cell type involved in hepatic fibrogenesis[4, 5]. It is known that the proliferation of these cells is one response during hepatic fibrogenetic process. The other feature of these cells is their trans-differentiation, which is indicated by increased expression of SMA[19]. During the trans-differentiation process of hepatic stellate cells, these cells are trans-differentiated into myofibroblast-like phenotype. To understand hepatic fibrogenesis, it is important to know the mechanism of proliferation and trans-differentiation of hepatic stellate cells. In this report, we employed TGF-β1 and BMPs to examine their effects on hepatic stellate cell proliferation and trans-differentiation. Our study indicated that both TGF-β1 and BMPs were important in the trans-differentiation of hepatic stellate cells. However, BMP-2 and BMP-4 had more potent effect on trans-differentiation of these cells than TGF-β1 did. The difference can be due to the different signaling proteins involved in TGF-β1 and BMPs signal transduction. It is known that Smads are the intracellular molecules for both TGF-β and BMP signal transduction pathways[17, 29, 33]. However, Smad-2 and Smad-3 are believed to mediate TGF-β signal transduction while Smad-1, Smad-5 and Smad-8 mediate BMP signaling[13, 16, 18, 21]. It has been demonstrated that Smad-3 is not necessary to the trans-differentiation of hepatic stellate cells but is required for TGF-β1 mediated cell proliferation[31]. Although TGF-β1 had some effect on the trans-differentiation of hepatic stellate cells in this study, it might not be related to Smad-2 and Smad-3. It has been documented that TGF-β1 can phosphorylate Smad-1 in human breast cancer cells[22]. However, it still remained be tested what is the mechanism mediating the transient reduction of SMA by TGF-β1 in hepatic stellate cells. The direct TGF-β1 regulation of SMA gene expression could not be excluded.

The inhibitory effect of TGF-β1 on hepatic stellate cell proliferation was consistent with effect of TGF-β1 on most mammalian cells. It inhibited the proliferation of hepatic stellate

cells. Studies relating the effect of TGF-β1 on hepatic stellate cell proliferation from other groups have revealed some conflicting results. Most of the studies indicated that TGF-β1 inhibited the proliferation of hepatic stellate cells[2, 6, 25, 26, 28] while few studies had found no significant effect on these cell proliferation[14, 20]. The difference of TGF-β1 regulation of hepatic stellate cells may be related to stage of cell differentiation or the period of TGF-β1 treatment. One of the interesting findings in this study is that both BMP-2 and BMP-4 did not affect the proliferation of hepatic stellate cells. It is well known that the main role of BMPs is bone morphogenesis, which is a sequential cascade with three key phases: chemotaxis and mitosis of mesenchymal cells, differentiation of the mesenchymal cells initially into cartilage, and replacement of the cartilage by bone. Its function is more related to differentiation then proliferation[15, 30]. Therefore, no effect of BMPs on hepatic stellate cell proliferation is well consistent with their functions.

CONCLUSION

Our study documented that both TGF-β and BMPs play important roles in hepatic stellate cell proliferation and trans-differentiation. TGF-β is more important in the regulation of hepatic stellate cell proliferation while BMPs is more potent in the regulation of trans-differentiation of hepatic stellate cells. However, the *in vitro* observations of TGF-β and/or BMPs on hepatic stellate cell proliferation and trans-differentiation may represent one aspect of the complex interaction among varieties of factors in human body.

ACKNOWLEDGEMENTS

This work was supported by grants from Canadian Institute of Health Research and Manitoba Medical Service Foundation.

REFERENCES

1 **Atfi A**, Lepage K, Allard P, Chapdelaine A, Chevalier S. Activation of a serine/threonine kinase signaling pathway by transforming growth factor type beta. *Proc Natl Acad Sci USA* 1995; **92**: 12110-12114
2 **Bachem MG**, Riess U, Gressner AM. Liver fat storing cell proliferation is stimulated by epidermal growth factor/transforming growth factor alpha and inhibited by transforming growth factor beta. *Biochem Biophys Res Commun* 1989; **162**: 708-714
3 **Baricos WH**, Cortez SL, Deboisblanc M, Xin S. Transforming growth factor-beta is a potent inhibitor of extracellular matrix degradation by cultured human mesangial cells. *J Am Soc Nephrol* 1999; **10**: 790-795
4 **Brenner DA**, Waterboer T, Choi SK, Lindquist JN, Stefanovic B, Burchardt E, Yamauchi M, Gillan A, Rippe RA. New aspects of hepatic fibrosis. *J Hepatol* 2000; **32**: 32-38
5 **Davis BH**, Kresina TF. Hepatic fibrogenesis. *Clin Lab Med* 1996; **16**: 361-375
6 **Davis BH**, Rapp UR, Davidson NO. Retinoic acid and transforming growth factor beta differentially inhibits platelet-derived-growth-factor-induced Ito-cell activation. *Biochem J* 1991; **278**: 43-47
7 **Derynck R**, Chen RH, Ebner R, Filvaroff EH, Lawler S. An emerging complexity of receptors for transforming growth factor-beta. *Princess Takamatsu Symp* 1994; **24**: 264-275
8 **Friedman SL**. Hepatic stellate cells. *Prog Liver Dis* 1996; **14**: 101-130
9 **Fryer HJ**, Davis GE, Manthorpe M, Varon S. Lowry protein assay using an automatic microtiter plate spectrophotometer. *Anal Biochem* 1986; **153**: 262-266
10 **Gong W**, Roth S, Michel K, Gressner AM. Isoforms and splice variant of transforming growth factor beta-binding protein in rat hepatic stellate cells. *Gastroenterology* 1998; **114**: 352-363
11 **Gong Y**, Blok LJ, Perry JE, Lindzey JK, Tindall DJ. Calcium regulation of androgen receptor expression in the human prostate cancer cell line LNCaP. *Endocrinology* 1995; **136**: 2172-2178
12 **Gong Y**, Zhang M, Minuk GY. Regulation of transforming growth factor-beta1 gene expression and cell proliferation in human hepatocellular carcinoma cells (PLC/PRF/5) by tamoxifen. *J Lab Clin Med* 1999; **134**: 90-95
13 **Goumans MJ,** Mummery C. Functional analysis of the TGFbeta receptor/Smad pathway through gene ablation in mice. *Int J Dev Biol* 2000; **44**: 253-265
14 **Gressner AM**. Transdifferentiation of hepatic stellate cells (Ito cells) to myofibroblasts: a key event in hepatic fibrogenesis. *Kidney Int Suppl* 1996; **54**: S39-S45
15 **Hogan BL**. Bone morphogenetic proteins in development. *Curr Opin Genet Dev* 1996; **6**: 432-438
16 **Hullinger TG**, Pan Q, Viswanathan HL, Somerman MJ. TGFbeta and BMP-2 activation of the OPN promoter: roles of smad- and hox-binding elements. *Exp Cell Res* 2001; **262**: 69-74
17 **Itoh S**, Itoh F, Goumans MJ, Ten Dijke P. Signaling of transforming growth factor-beta family members through Smad proteins. *Eur J Biochem* 2000; **267**: 6954-6967
18 **Kawabata M**, Imamura T, Miyazono K. Signal transduction by bone morphogenetic proteins. *Cytokine Growth Factor Rev* 1998; **9**: 49-61
19 **Khan MA**, Poulos JE, Brunt EM, Li L, Solomon H, Britton RS, Bacon BR, Di Bisceglie AM. Hepatic alpha-smooth muscle actin expression in hepatitis C patients before and after interferon therapy. *Hepatogastroenterology* 2001; **48**: 212-215
20 **Knittel T**, Janneck T, Muller L, Fellmer P, Ramadori G. Transforming growth factor beta 1-regulated gene expression of Ito cells. *Hepatology* 1996; **24**: 352-360
21 **Lagna G,** Hemmati-Brivanlou A. A molecular basis for Smad specificity. *Dev Dyn* 1999; **214**: 269-277
22 **Liu X**, Yue J, Frey RS, Zhu Q, Mulder KM. Transforming growth factor beta signaling through Smad1 in human breast cancer cells. *Cancer Res* 1998; **58**: 4752-4757
23 **Massague J**. The transforming growth factor-beta family. *Annu Rev Cell Biol* 1990; **6**: 597-641
24 **Massague J**, Weis-Garcia F. Serine/threonine kinase receptors: mediators of transforming growth factor beta family signals. *Cancer Surv* 1996; **27**: 41-64
25 **Matsuoka M**, Pham NT, Tsukamoto H. Differential effects of interleukin-1 alpha, tumor necrosis factor alpha, and transforming growth factor beta 1 on cell proliferation and collagen formation by cultured fat-storing cells. *Liver* 1989; **9**: 71-78
26 **Meyer DH**, Bachem MG, Gressner AM. Modulation of hepatic lipocyte proteoglycan synthesis and proliferation by Kupffer cell-derived transforming growth factors type beta 1 and type alpha. *Biochem Biophys Res Commun* 1990; **171**: 1122-1129
27 **Paulus W**, Baur I, Huettner C, Schmausser B, Roggendorf W, Schlingensiepen KH, Brysch W. Effects of transforming growth factor-beta 1 on collagen synthesis, integrin expression, adhesion and invasion of glioma cells. *J Neuropathol Exp Neurol* 1995; **54**: 236-244
28 **Pinzani M**, Gesualdo L, Sabbah GM, Abboud HE. Effects of platelet-derived growth factor and other polypeptide mitogens on DNA synthesis and growth of cultured rat liver fat-storing cells. *J Clin Invest* 1989; **84**: 1786-1793
29 **Schiffer M**, von Gersdorff G, Bitzer M, Susztak K, Bottinger EP. Smad proteins and transforming growth factor-beta signaling. *Kidney Int Suppl* 2000; **77**: S45-S52
30 **Schmitt JM**, Hwang K, Winn SR, Hollinger JO. Bone morphogenetic proteins: an update on basic biology and clinical relevance. *J Orthop Res* 1999; **17**: 269-278
31 **Schnabl B**, Kweon YO, Frederick JP, Wang XF, Rippe RA, Brenner DA. The role of Smad3 in mediating mouse hepatic stellate cell activation. *Hepatology* 2001; **34**: 89-100
32 **Tipton DA**, Dabbous MK. Autocrine transforming growth factor beta stimulation of extracellular matrix production by fibroblasts from fibrotic human gingiva. *J Periodontol* 1998; **69**: 609-619
33 **Visser JA**, Themmen AP. Downstream factors in transforming growth factor-beta family signaling. *Mol Cell Endocrinol* 1998; **146**: 7-17

Edited by Xu XQ

P.O.Box 2345, Beijing 100023, China
Fax: +86-10-85381893
E-mail: wjg@wjgnet.com www.wjgnet.com

World J Gastroenterol 2003;9(4):788-790
World Journal of Gastroenterology
 ISSN 1007-9327

• BASIC RESEARCH •

IL-11 up-regulates Tie-2 expression during the healing of gastric ulcers in rats

Chun-Yang Wen, Masahiro Ito, Hui Wang, Long-Dian Chen, Zhao-Min Xu, Mutsumi Matsuu, Kazuko Shichijo, Toshiyuki Nakayama, Masahiro Nakashima, Ichiro Sekine

Chun-Yang Wen, Mutsumi Matsuu, Kazuko Shichijo, Toshiyuki Nakayama, Ichiro Sekine, Department of Molecular Pathology, Atomic Bomb Disease Institute, Nagasaki University School of Medicine, Japan
Chun Yang Wen, Long-Dian Chen, Zhao-Min Xu, Department of Digestive Disease, Nanjing Gu-Lou Hospital, Medical School of Nanjing University, Nanjing 210008, Jiangsu Province, China
Masahiro Ito, Department of Pathology, National Nagasaki Medical Center, Japan
Hui Wang, Department of Infectious Disease, Rui Jin Hospital, Shanghai Second Medical University, Shanghai 200025, China
Masahiro Nakashima, Tissue and Histopathology Section Division of Scientific Data Registry, Atomic Bomb Disease Institute, Nagasaki University School of Medicine, Japan
Correspondence to: Chun-Yang Wen, M.D., Ph.D., Department of Molecular Pathology, Atomic Bomb Disease Institute, Nagasaki University School of Medicine, 1-12-4 Sakamoto, Nagasaki 852-8523, Japan. cywen518@net.nagasaki-u.ac.jp
Telephone: +81-95-849-7107 **Fax:** +81-95-849-7108
Received: 2002-11-29 **Accepted:** 2003-01-13

Abstract

AIM: To investigate Tie-2 expression during the repair of acetic acid-induced gastric ulcers in rats treated with recombinant human IL-11 (rhIL-11) and in untreated control animals.

METHODS: Gastric ulcers were induced in male Wistar rats by applying acetic acid to the fundus of the stomach. RhIL-11 (100 μg/kg twice daily, subcutaneously) was administered from two days before ulcer induction and continued for five days after the induction. Control rats received bovine serum albumin. Gastric specimens were collected at 3 and 5 days after the induction of ulcer for immunohistochemical observation, Western blotting, and reverse transcription polymerase chain reaction (RT-PCR).

RESULTS: Immunohistochemical and Western blot analysis demonstrated that Tie-2 expression was enhanced in the rhIL-11-treated rats compared with the control animals at both intervals.

CONCLUSION: These findings suggested that IL-11 could accelerate ulcer healing, in part, by up-regulating Tie-2 expression and promoting angiogenesis.

Wen CY, Ito M, Wang H, Chen LD, Xu ZM, Matsuu M, Shichijo K, Nakayama T, Nakashima M, Sekine I. IL-11 up-regulates Tie-2 expression during the healing of gastric ulcers in rats. *World J Gastroenterol* 2003; 9(4): 788-790
http://www.wjgnet.com/1007-9327/9/788.htm

INTRODUCTION

IL-11 is a kind of pleiotropic cytokine that stimulates stem cell proliferation and affects multiple types of cells[1]. RhIL-11 may be useful in accelerating the recovery of both hematopoietic cells and gastrointestinal mucosal cells after cytoablative therapies[2]. RhIL-11 is in Phase II clinical trials for the treatment of thrombocytopenia that occurs secondary to chemotherapy[3]. Gross and microscopic evidence suggested that rhIL-11 treatment could improve acute colitis caused by both chemically-induced damage and chronic inflammatory bowel disease[4]. Bruce *et al*[5] recently reported that short-term treatment with rhIL-11 was well tolerated in patients with active Crohn's disease. Our previous study demonstrated that rhIL-11 facilitates gastric ulcer healing in rats[6].

Angiogenesis is critical to ulcer healing since it regulates nutrient and oxygen delivery to the injured site and, thus, controls the healing rate. Tie-2 (tek) is a member of the endothelial cell-specific receptor tyrosine kinase family[7, 8], and is essential for the formation of the embryonic vasculature[9]. Our recent study suggests that Tie-2 plays an important role in the angiogenesis associated with the healing of gastric ulcers[10]. The present study examined the effect of IL-11 on Tie-2 expression in acetic acid-induced gastric ulcers by comparing with in the rhIL-11-treated and control rats.

MATERIALS AND METHODS

Materials

This study was approved by the Animal Care Committee of Nagasaki University. Male Wistar rats, purchased from Charles River Japan (Atsugi, Japan) at 7 weeks of age, were housed 3 or 4 per cage in an air-conditioned room(24 ℃, 12 hr light cycle) at the Laboratory Animal Center of Nagasaki University. The animals were fed with laboratory chow (F2, Japan CLEA, Tokyo, Japan) and tap water ad libitum.

Induction of gastric ulcer

Gastric ulcers were induced by luminal application of a 40 % acetic acid solution as reported previously[11]. Under ether anesthesia, the stomach was exposed via a midline incision and the anterior and posterior walls of the gastric fundus were clamped together with ring forceps (ID, 6 mm). The acetic acid solution was injected into the clamped portion through the forestomach using 21 gauge needles. After forty-five seconds, the acid solution was removed, the abdomen closed and the animals fed and housed as above.

Treatment

RhIL-11 (Genetics Institute, Andover, MA, USA), courtesy of Yamanouchi Pharmaceutical Co., Ltd. (Tokyo, Japan), was diluted in 0.1 % bovine serum albumin (BSA) and administered subcutaneously (100 μg/kg/twice daily) for seven consecutive days beginning two days before ulcer induction as described previously (n=16)[12]. Control animals (n=16) received the same volume of 0.1 % BSA twice daily. Eight rhIL-11-treated and eight untreated rats were sacrificed 3 and 5 days after the induction of gastric ulcers. Gastric tissues were collected for Western blot analysis, and reverse transcription polymerase chain reaction (RT-PCR). Tissues were fixed in 4 % paraformaldehyde solution for immunohistochemical examination of Tie-2 expression.

Immunohistochemistry analysis

Paraformaldehyde-fixed and paraffin-embedded tissues were cut into 4 μm sections, deparaffinized in xylene and rehydrated in phosphate-buffered saline. The tissues were subsequently preincubated in 3 % H_2O_2 for 30 minutes, followed by incubation in bovine serum to prevent nonspecific binding, and then incubated overnight at 4 ℃ (2 μg/ml) with rabbit anti-mouse Tie-2 (C-20, Santa Cruz Biotechnology, Inc., Santa Cruz, CA). The slides were subsequently incubated in biotinylated anti-rabbit immunoglobulin G followed by avidin-horseradish peroxidase and the reaction product was resolved using DAB (Vectastain ABC kit; Vector Laboratories, Burlingame, CA).

Western blot analysis

Fresh gastric tissues obtained from ulcerated areas were immediately frozen, suspended in RIPA buffer (50 mM Tris, 150 mM NaCl, 1 % NP-40, 1 % sodium deoxycholate and 0.05 % SDS, pH 7.4), broken into pieces on ice and subjected to three freeze-thaw cycles. Insoluble cell debris was removed by centrifugation at 14 000×g at 0 ℃ for 10 minutes. The protein concentrations in the resultant supernates were quantified using a protein assay reagent (Bio-Rad Laboratories, Hercules, CA). Data from four rats were recorded at each time point and the assays were performed in duplicate. The proteins (30 μg) were separated by polyacrylamide gel electrophoresis (PAGE) under denaturing and reducing conditions, and transferred to a Hybond ECL Nitrocellulose Membrane (Amersham Life Science, Buckinghamshire, U.K.). The membranes were rinsed in TBS, blocked with 5 % low-fat dried milk in TBS containing 0.1 % Tween 20 (TTBS), and incubated for 2 hours at room temperature in a 1:500 dilution of mouse anti-rat Tie-2 antibodies. After extensive washing with TTBS, the membranes were incubated for 1 hour in TTBS with 1:2 000 dilution of horseradish-peroxidase-conjugated goat anti-mouse immunoglobulin G containing 3 % low-fat dried milk. The membranes were washed, developed with a horseradish peroxidase chemiluminescence detection reagent (ECL Plus System, Amersham, N.D.), and exposed to Hyperfilm ECL (Amersham).

RT-PCR analysis

Total RNA was prepared from gastric tissue using the acid guanidine phenol method. RNA (1 μg) was incubated at 37 ℃ for 1 hour in 50 μl reverse transcriptase buffer containing 20 units RNAsin (Promega Corp., Madison, WI), 100 pmol of random hexamer primers (Boehringer Mannheim, Germany), and 400 units Moloney murine leukemic virus reverse transcriptase (GIBCO/BRL). Reverse transcription was terminated by heating to 95 ℃ for 10 minutes, and 20 % of the resulting cDNA was used for PCR. PCR samples were incubated with 50 pmol of each primer and 2.5 units of Taq DNA polymerase. The rat Tie-2 PCR primers were as followings: 5'-TGTTCCTGTGCCACAGGCTG-3' (sense) and 5'-CACTGTCCCATCCGGCTTCA-3' (antisense). The human β-actin PCR primers were as followings: 5'-TCCTCCCTGGAGAAGAGCTA-3' (sense) and 5'-AGTACTTGCGCTCAGGAGGA-3' (antisense). The Tie-2 and β-actin primers were predicted to amplify 317 and 313 bp DNA products, respectively. Primer pairs were chosen to span introns of their respective rat genes. Samples were subjected to 40 cycles of PCR amplification, each cycle consisting of denaturation at 95 ℃ for 3 minutes, annealing at 50 ℃ for 1 minute, and primer extension at 72 ℃ for 1 minute. An aliquot of each amplification mixture was subjected to electrophoresis on 2 % agarose gel, and DNA was visualized by ethidium bromide staining.

RESULTS

Immunohistochemistry results

Immunohistochemical staining of Tie-2 was weakly positive in the endothelial cells of pre-existing vessels in the gastric wall. Tie-2 expression in the endothelial cells of new capillaries was enhanced in the rhIL-11-treated rats (Figure1A) compared with the control rats (Figure1B) after 3 and 5 days of the induction of ulcers.

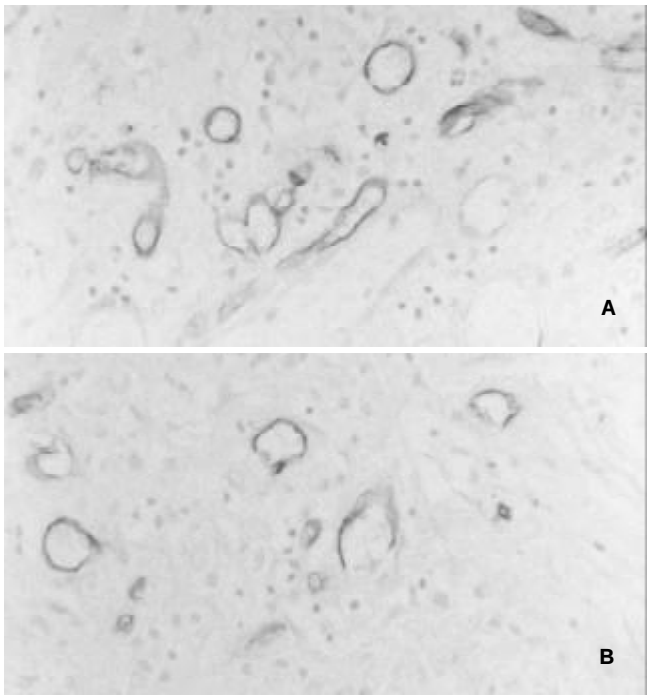

Figure 1 Three days after the induction of gastric ulcers, Tie-2 expression in the endothelial cells of new capillaries was enhanced in the rhIL-11-treated rats (A) in comparison to the untreated control animals (B).

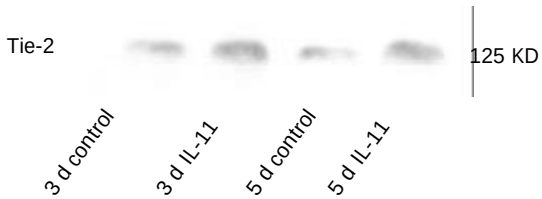

Figure 2 Western blots demonstrating Tie-2 expression. RhIL-11 treatment increased Tie-2 expression significantly 3 and 5 days after the induction of gastric ulcers compared with untreated control rats.

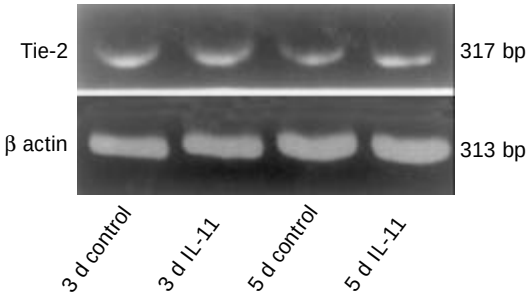

Figure 3 RT-PCR analysis of Tie-2 mRNA expression in ulcerative gastric tissues, using the specific primer pairs predicted to amplify Tie-2(317 bp) and β-actin (313 bp). Lanes 1-4: rhIL-11-treated rats on days 3(lane 2) and 5(lane 4) and the untreated control rats on day 3(lane 1) and 5(lane 3).

Western blotting results

A major band of 125 KD representing Tie-2 protein was detected in the Western blots. Tie-2 expression was increased significantly after the appearance of ulcers in the rhIL-11-treated rats compared with the untreated control animals on day 3 and day5 (Figure2).

RT-PCR results

Tie-2 mRNA was detected between rhIL-11-treated rats and the control animals after3 and 5 days of the induction of gastric ulceration. β-actin mRNA, a constitutively expressed transcript, was detected in all of the samples from both the rhIL-11 and untreated rats (Figure3).

DISCUSSION

Angiogenesis occurs in many physiological and pathological processes, including embryonic development, wound healing, and tumor growth[13, 14]. Ulcer healing consists of two processes, epithelial regeneration and mesenchymal reconstruction. The process of mesenchymal reconstruction consists of angiogenesis, fibrosis and smooth muscle regeneration. Therefore, angiogenesis is central to the formation of granulation tissue since newly formed vessels are required to supply oxygen and nutrients to the regenerating tissue. Tie-2 is a receptor tyrosine kinase expressed by endothelial cells[15,16] and it has been reported to play an important role in embryonic angiogenesis[17]. Furthermore, our own recent study revealed that Tie-2 was important in the angiogenesis that occurs during the healing of gastric ulcers[10].

Our previous study was the first to demonstrate that IL-11 could promote gastric ulcer healing in rat model[6]. This effect of IL-11 on the repair of mucosal injury most likely reflects its trophic action on mucosal epithelial and smooth muscle cells. RhIL-11 also exhibits an anti-apoptotic effect on the gastric mucosa. RhIL-11 most likely acts on epithelial cells via the regeneration of epithelial cell facilitated by IL-11 receptor. Concomitant smooth muscle hyperplasia may induce tissue contraction, thus promoting healing. The importance of smooth muscle contraction at the base of the ulcer has been previously demonstrated[18]. Interestingly, IL-11 inhibits the production of nitric oxide, an agent that can relaxs smooth muscle cells[19].

Our immunohistochemical and Western blot data showing that rhIL-11 enhanced Tie-2 expression suggest that Il-11 accelerates healing by promoting angiogenesis. The results of this study demonstrate that rhIL-11 up-regulates Tie-2 expression during the healing of gastric ulcer in rats and suggest that rhIL-11 may have clinical benefits in the treatment of gastric ulcers.

REFERENCES

1 **Du XX**, Williams DA. Interleukin-11: a multifunction growth factor derived from the hematopoietic microenvironment. *Blood* 1994; **83**: 2023-2030

2 **Gordon MS**, McCaskill-Stevens WJ, Battiato LA, Loewy J, Loesch D, Breeden E, Hoffman R, Beach KJ, Kuca B, Kaye J, Sledge GW Jr. A phase I trial of recombinant human interleukin-11 (neumega rhIL-11 growth factor) in women with breast cancer receiving chemotherapy. *Blood* 1996; **87**: 3615-3624

3 **Gordon MS**. Thrombopoietic activity of recombinant human interleukin-11 in cancer patients receiving chemotherapy. *Cancer Chemother Pharmacol* 1996; **38**: S96-S98

4 **Keith JC Jr**, Albert L, Sonis ST, Pfeiffer CJ, Schaub RG. IL-11, a pleiotropic cytokine: Exciting new effects of IL-11 on gastrointestinal mucosal biology. *Stem Cells* 1994; **12**: 79-90

5 **Bruce ES**, Simmy B, Charles AS, Malcolm R, Seymour K, John WS, Philip BM Jr, Michael AS, Susan G, Stephen BH, Gary WV, Alan LB, Vance DR, Bruce S, Bin C, John L, Michael FD, Holly R, Mark S, Ullrich SS. Preliminary evaluation of safety and activity of recombinant human interleukin 11 in patients with active Crohn's disease. *Gastroenterology* 1999; **177**: 58-64

6 **Wen CY**, Ito M, Matsuu M, Fukuda E, Shichijo K, Nakashima M, Nakayama T, Sekine I. Mechanism of the antiulcerogenic effect of IL-11 on acetic acid-induced gastric ulcer in rats. *Life Sci* 2002; **70**: 2997-3005

7 **Schnurch H**, Risau W. Expression of tie-2, a member of a novel family of receptor tyrosine kinases, in the endothelial lineage. *Development* 1993; **199**: 957-968

8 **Maisonpierre PC**, Goldforb M, Yancopoulos GD, Gao G. Distinct rat genes with related profiles of expression define a TIE receptor tyrosine kinase family. *Oncogene* 1993; **8**: 1631-1637

9 **Sato TN**, Tozawa Y, Deutsch U, Wolburg-Buchholz K, Fujiwara Y, Gendron-Maguire M. Distinct roles of the receptor tyrosine kinases Tie-1 and Tie-2 in blood vessel formation. *Nature* 1995; **376**: 70-74

10 **Wen CY**, Ito M, Chen LD, Matsuu M, Shichijo K, Nakayama T, Nakashima M, Xu ZM, Ohtsuru A, Hsu CT, Sekine I. Expression of Tie-2 and Angiopoietin-1 and -2 in early phase of ulcer healing. *J Gastroenterol* 2003 (in press)

11 **Tsukimi Y**, Okabe S. Changes in gastric function and healing of chronic gastric ulcers in aged rats. *Jpn J Pharmacol* 1995; **68**: 103-110

12 **Potten CS**. Interleukin-11 protects the clonogenic stem cells in murine small-intestinal crypts from impairment of their reproductive capacity by radiation. *Int J Cancer* 1995; **62**: 356-361

13 **Millauer B**, Longhi MP, Plate KH, Shawver LK, Risau W, Ullrich A. Dominant-negative inhibition of Flk-1 suppresses the growth of many tumor types *in vivo*. *Cancer Res* 1996; **56**: 1615-1620

14 **Nakayama T**, Ito M, Ohtsuru A, Naito S, Nakashima M, Fagin JA, Yamashita S, Sekine I. Expression of the Ets-1 proto-oncogene in human gastric carcinoma. *Am J Pathol* 1996; **149**: 1931-1939

15 **Sato TN**, Qin Y, Kozak CA, Audus KL. Tie-1 and Tie-2 define another class of putative receptor tyrosine kinase genes expressed in early embryonic vascular system. *Proc Natl Acad Sci USA* 1993; **90**: 9355-9358

16 **Maisonpierre PC**, Goldfarb M, Yancopoulos GD, Gao G. Distinct rat genes with related profiles of expression define a TIE receptor tyrosine kinase family. *Oncogene* 1993; **8**: 1631-1637

17 **Korhonen J**, Polvi A, Partanen J, Alitalo K. The mouse tie receptor tyrosine kinase gene: expression during embryonic angiogenesis. *Oncogene* 1994; **12**: 395-403

18 **Tsukimi Y**, Okabe S. Acceleration of healing of gastric ulcers induced in rats by liquid diet: importance of tissue contraction. *Jpn J Pharmacol* 1994; **66**: 405-412

19 **Trepicchio WL**, Bozza M, Pedneault, Dorner AJ. Recombinant human IL-11 attenuates the inflammatory response through down-regulation of proinflammatory cytokine release and nitric oxide production. *J Immunol* 1996; **157**: 3627-3634

Edited by Xu XQ

P.O.Box 2345, Beijing 100023, China
Fax: +86-10-85381893
E-mail: wjg@wjgnet.com www.wjgnet.com

World J Gastroenterol 2003;9(4):795-799
World Journal of Gastroenterology
 ISSN 1007-9327

• BASIC RESEARCH •

Changes of microvascular architecture, ultrastructure and permeability of rat jejunal villi at different ages

Yan-Min Chen, Jin-Sheng Zhang, Xiang-Lin Duan

Yan-Min Chen, Xiang-Lin Duan, Life Science College, Hebei Normal University, Shijiazhuang 050016, Hebei Province, China
Jin-Sheng Zhang, Department of Otolaryngology, Wayne State University School of Medicine, Detroit, Michigan 48201, USA
Supported by Natural Science Foudation of Hebei Province Educational Committee, No.2002136 and Natural Science Foudation of Hebei Province, No.303158
Correspondence to: Xiang-Lin Duan, Life Science College, Hebei Normal University, Shijiazhaung 050016, Hebei Province China. chyanmin@163.com
Telephone: +86-311-6049941 Ext 86480 **Fax:** +86-311-5828784
Received: 2002-11-26 **Accepted:** 2002-12-20

Abstract

AIM: To investigate the changes of microvascular architecture, ultrastructure and permeability of rat jejunal villi at different ages.

METHODS: Microvascular corrosion casting, scanning electron microscopy, transmission electron microscopy and Evans blue infiltration technique were used in this study.

RESULTS: The intestinal villous plexus of adult rats consisted of arterioles, capillary network and venules. The marginal capillary extended to the base part of the villi and connected to the capillary networks of adjacent villi. In newborn rats, the villous plexus was rather simple, and capillary network was not formed. The villous plexus became cone-shaped and was closely arrayed in ablactation rats. In adult rats, the villous plexus became tongue-shaped and was enlarged both in height and width. In aged rats, the villous plexus shrank in volume and became shorter and narrower. The diametral ratio of villous arteriole to villous venule increased as animals became older. The number of endothelial holes, the thickness of basal membrane and the permeability of microvasculature were increased over the entire course of development from newborn period to aged period.

CONCLUSION: The digestive and absorptive functions of the rat jejunum at different ages are highly dependent upon the state of villous microvascular architecture and permeability, and blood circulation is enhanced by collateral branches such as marginal capillary, through which blood is drained to the capillary networks of adjacent villi.

Chen YM, Zhang JS, Duan XL. Changes of microvascular architecture, ultrastructure and permeability of rat jejunal villi at different ages. *World J Gastroenterol* 2003; 9(4): 795-799
http://www.wjgnet.com/1007-9327/9/795.htm

INTRODUCTION

The microvasculature of intestinal villi play an important role in the process of digestion, absorption and mucosal barrier protection[1,2]. Intestinal diseases, such as diarrhea and enteritis, are reported to be related to the change of microvasculature[3,4]. More recent studies on the intestinal microvasculature demonstrated that the damage to surface microvasculature is an early event inducing mucosal injury in the intestine[5-7]. However, these studies were only limited in collecting pathological or clinical data, and tissue materials were obtained from adult subjects[8-10]. In addition, little information is available regarding the changes of microvasculature throughout different age periods. Therefore, the current work was meant to elucidate the morphological and permeability changes of jejunal microvasculature at different ages. Microvascular corrosion casting technique, scanning electron microscopy (SEM), transmission electron microscopy (TEM), Evans blue infiltration methods were used and morphometry was conducted in this study.

MATERIALS AND METHODS

Animals

Fifty-four male Sprague-Dawley rats were used. They were divided into 4 groups according to their ages after birth: (1) newborn rats (1 day, *n*=9); (2) ablactation rats (3 weeks, *n*=15); (3) adult rats (3 months, *n*=15) and (4) aged rats (24 months, *n*=15). For the groups with 15 animals, six were used for corrosion casting, three were observed under TEM, the other six were used to determine the permeability with Evans blue infiltration technique. The newborn rats were too small to be used in determining the permeability. All rats were fasting for 12 hours prior to each experiment.

Microvascular corrosion casting and SEM

Methyl-methacrylate and methacrylate were mixed at a ratio of 9:1. Polymerization was allowed by adding benzoyl-methacrylate at 80 ℃. The viscosity of this solution was maintained to a level corresponding to that of 30 % glycerine. The solution was cooled for later use. The microvascular architecture was then performed in the following procedure. Animals were deeply anesthetized with ether and a catheter was inserted into the thoracic aorta. One percent of saline solution (500 ml/kg i.m.) was perfused to flush the blood out of cardiovascular system, and this step was immediately followed by a perfusion of 5 ml methyl-methacrylate. Meanwhile, the same volume of the pre-prepared solution mixed with N, N-dimethylaniline (1 % of the total volume) was added, serving as a polymerization accelerator. twelve hours later when polymerization was completed, the small intestine was sampled and stored in a 10 % NaOH solution for 1-2 weeks. The tissue was rinsed with tap water until the corroded tissue was washed out, and then trimmed under the dissection microscope and dried at 40 ℃ for 48 hours. The dried tissue was then coated using an IB-3 ionic splashing and shooting device. Photomicrographs were taken under a Hitachi S-570 scanning electron microscope.

TEM

Small pieces of the jejunum were immersed in phosphate-buffered 3 % glutaraldehyde for 2 hours, and then postfixed in phosphate-buffered 1 % OsO_4 for 2 hours. After postfixation, the tissue was dehydrated with ethanol and embedded in Epon

812. Ultra-thin sections stained with uranyl acetate and lead citrate were observed and photomicrographs were taken under a Hitachi TEM S-600.

Quantification of microvascular permeabilityof the jejunal tissue

Evans blue was used to measure the permeability of microvasculature. Rats were anesthetized with ether, and Evans blue (75 mg/kg i.m.) in 0.9 % saline solution was injected into a femoral vein. Two hours later, rats were perfused transcardially with 0.9 % saline solution (500 ml/kg i.m.). Evans blue was extracted from the jejunum by incubation in 5 ml of formamide at 54 ℃ for 24 hours. Evans blue was then quantified by measuring its absorption at wavelength of 620 nm using spectrometer. Results were expressed as μg Evans blue/gram fresh tissue.

Data processing

According to the methods of stereology[11], the measurement and calculation of the thickness of basal membrane (nm), the number of endothelial hole (per mm capillary perimeter) and plasmalemmal vesicles (per mm^2 endothelium) were conducted on the photographs of TEM. Results were expressed as mean ± SEM, and statistics was performed using Student' s *t* test.

RESULTS

Microvascular architecture of adult rats villi

The villous plexi stood on the surface of the ileum. Between the adjacent villous plexi there were numerous different cryptal plexi. The villous plexus consisted of villous arteriole, villous capillary network and the villous venule. The villous capillaries connected to each other in a form of "net-basket" (Figure 1). The villous arteriole coming from the arterial plexus in the submucosa reached the base of the villi through the cryptal plexus gap, extending to the tip along the axis of the villi. The villous arterioles did not bifurcate within the villi, but formed the villous capillary network at the tips of the villi in the pattern of a "netted bag". This villous capillary wrapped the villous arteriole. The villous venules were formed in the middle and upper part of the villi, through which the blood from capillary venules converged into the venous plexus in the submucosa (Figure 1).

In addition, there was a straight capillary along the margin of the villous capillary network, and it is called marginal capillary. Its diameter was twice that of its adjacent capillaries (Figures 1 and 2). This capillary ran along the villous margin and did not merge into the villous venules of itself. It reached the base of the villi and connected to the basal part of its adjacent villous capillary networks (Figure 2).

Changes of microvascular architecture of jejunal villi at different ages

In newborn rats, the villous plexus was rather simple and was composed of only one or two loops of capillary vessels. A capillary network was not formed at this age and villous arteriole and venule could not be differentiated (Figure 3). For the ablactation rats, the villous plexus became cone-shaped and was closely arrayed. The marginal capillary was as wide as villous arteriole. Each villous plexus had only one villous venule and was formed in the basal part of the villi. However, the diametral ratio of villous arteriole to it was very small (Figure 4). In adult rats, the villous plexus became tongue-shaped and was enlarged both in height and width. Each villous plexus usually had one villous venule which was formed in the middle and upper part of the villi, but the wide villi had two venules that were zygomorphous (Figure 1). In the aged rats, the villous plexus shrank in volume and became shorter and narrower. The capillaries were irregularly arrayed (Figure 5). The villous arteriole became wider and lower than villous venule (Figure 6). The diametral ratio of villous arteriole to venule was increased as animals became older (Table 1).

Changes of endothelial ultrastructure of villous capillary at different ages

Under TEM, the endothelium of capillary in the vicinity of epithelium of villi was so polarized that the nucleus was far away from epithelium and the side near the epithelium was thin. In the endothelium of newborn rats, bigger nucleus, more cytoplast as well as several plasmalemmal vesicles were seen, but no endothelial hole and basal membrane were observed. However, endothelial hole and basal membrane were found in ablactation animals (Figure 7). For the adult rats, a plenty of plasmalemmal vesicles were noticed in the endothelium (Figure 8). The endothelium in the aged rats, however, became thinner whereas its basal membrane became thicker. Endothelial holes were found to be increased whereas plasmalemmal vesicles were decreased (Figure 9). The number of endothlial holes, the thickness of basal membrane and the permeability of microvasculature were increased over the entire course of development from newborn period to aged period (Table 2).

Changes of microvascular permeability of villi at different ages

The microvascular permeability at different ages was determined with Evans Blue infiltration technique. The amount of Evans blue that penetrated into intestinal tissue was 28.1 μg/g tissue in ablactation rats and 64.4 μg/g tissue in adult rats. The microvascular permeability of the aged rats was twice as high as that of the adult rats (Table 2).

Table 1 Comparison of the microvascular architecture of villi at different ages (mean±SEM)

	Ablactation rats	Adult rats	Aged rats
Diameter of arteriole (μm)	6.17±1.51	10.47±2.25[a]	16.73±3.28[c]
Diameter of venule (μm)	20.43±3.17	25.45±3.07[b]	25.50±3.34
Ratio: arteriole/venule	0.30±0.04	0.41±0.04[a]	0.65±0.06[c]

[a]$P<0.01$, [b]$P<0.05$ *vs* ablactation rats; [c]$P<0.01$ *vs* adult rats.

Table 2 Comparison of the endothelial ultrastructure of villi at different ages (mean±SEM)

	Newborn	Ablactation	Adult	Aged rats
Endothelial holes (number/μm)		3.01±0.38	3.51±0.35[b]	5.19±0.48[d]
Plasmalemmal vesicles (number/0.1 μm^2)	17.7±4.25	39.1±10.36[a]	75.3±12.13[c]	38.0±11.14[d]
Basal membrane (nm)		25.2±5.26	43.5±5.86[c]	60.5±6.89[d]
Vascular permeability (μg/g)		28.1±4.64	64.4±9.34[c]	116.4±15.63[d]

[a]$P<0.01$ *vs* newborn rats; [b]$P<0.05$, [c]$P<0.01$ *vs* ablactation rats; [d]$P<0.01$ *vs* adult rats.

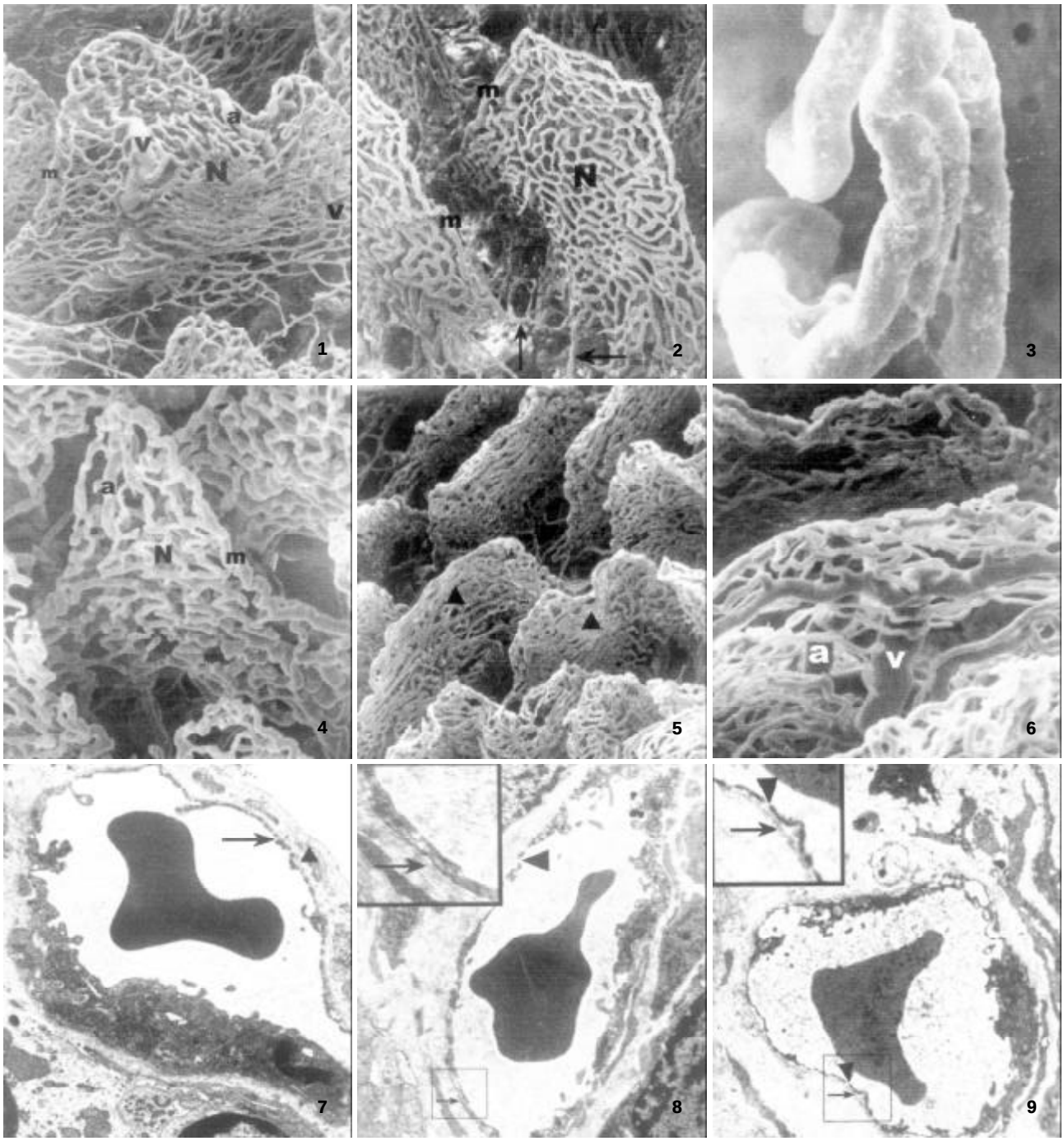

Figure 1 The microvascular architecture of adult rat jejunal villi, showing the villous arteriole (a), the villous capillary network (N), the villous venule(v), the marginal capillary(m) ×150.
Figure 2 The microvascular architecture of adult rat jejunal villi,showing the marginal capillary(m) connecting to the basal part of its adjacent villous plexus (↑) ×130.
Figure 3 The microvascular architecture of newborn rat jejunal villi, ×400.
Figure 4 The microvascular architecture of ablactation rat jejunal villi, showing the villous arteriole (a), The villous capillary network(N),the marginal capillary(m) ×300.
Figure 5 The microvascular architecture of aged rat jejunal villi ×100.
Figure 6 The microvascular architecture of aged rat jejunal villi, showing the villous arteriole(a), the villous venule(v) ×250.
Figure 7 The capillary endothelium of ablactation rats, showing the endothelial hole (↑) and the basal membrane (▲) ×8 000.
Figure 8 The capillary endothelium of adult rats, showing the basal membrane (↑) and the endothelial hole (▲) ×8 000.
Figure 9 The capillary endothelium of aged rats, showing the basal membrane (↑) and the endothelial hole (▲) ×8 000.

DISCUSSION

Injection of certain materials into blood vessels enables three dimensional visualization of vascular architecture and has provided abundant information which is not available by reconstruction of serial sections[12-14]. A line of evidence demonstrated in rats, horses and human embryos, that the "fountain type" microvascular architecture of mammalian small intestine is common[15-17]. Among these studies, Ohashi *et al*[16] found that two or more villous venules originating in the base of villi. The results of our study appear to suggest that the villous venules of the rat small intestine are formed in the middle and upper part of the villi, not in the base and at the tip. The villous venules are shorter than villous arterioles, and do not form arterio-venous anastamoses. There is big difference

in diameter between villous venules and villous arteries. The former is about one third of that of the latter. All of these properties are important in creating a low blood pressure and speedy circulatory system in the villous capillary network, which is important to the process of nutritional absorption and transportation[18].

We found that branching did not take place when the villous arterioles climbed towards the tip of the villous and the capillary networks were not formed until the villous arteria reached the tip of the villous. After entering the villi, blood was supplied to the tip portion of villi and partially to its surrounding area. The cryptal plexus mainly supplied the blood to the basal part of the villi, which lacked artery terminals and branches. Therefore, this collateral circulation can provide blood supplies to the villi. Although there was supplementary blood supply in the base of the villi, blood supply was inefficient due to a long distance of transportation from the branching point at the tips of villi which were full of arterial blood[19]. Therefore, the villi at the tip received much more arterial blood supply than in the base. From the base to the tip of the villi, the absorption rate of epithelium increased proportionately with the volume of its blood supply. However, there were still aging cells at the tip of villous that were less dynamic physiologically than the younger cells at the basal part. The cells of villi at the tip might not be able to adapt themselves very well to any abnormal blood circulation, and therefore would easily lose their normal physiology under certain harsh conditions[20]. Injuries due to hypoxia usually emerged later in both intestinal crypts and basal part of villi than in the apical area of villi[21]. This may indicate that the crypts, as compared with villi, are relatively more resistant to hypoxic injuries. Such resistance is important in maintaining the optimal endocrine function and the regenerative capability of mucosa even after shock resulting from excessive blood loss.

Our results also showed that there were marginal capillaries on both sides of the small intestinal villi. These capillaries descended from the apical part of the villi to the basal part along its margin. It crossed the cryptal plexus and connected to the capillary network. So far, there have been no report regarding this connection. Before this study, it had been considered that there was only one venous return path from the small intestinal capillary. In other words, blood from capillary venules converged into the venous plexus in the submucosa[16,17,22]. Studies on marginal capillary have been developed since Mohiuddin[19] described the marginal capillary. It was reported recently that marginal capillary was more manifest in jejunum than in ileum[23,24], but its relationship with its adjacent villous plexus was not found in both jejunum and ileum. It is thus considered that the marginal capillary transports blood to the villous margin. Therefore, the findings from the this study regarding the marginal capillary and its relation with its adjacent villi suggest that the collateral circulation may exist before the venous return from the villi. That is, the marginal capillary delivers blood partially into the adjacent villous capillary networks. This architecture of the villous plexus may have been adapted to the movement of intestines as well as to the digestive and absorptive activities. After eating, the small intestine speeds up its motility. Villi not only have tight contacts with the chyme but also are subjected to mechanical pressure from the passing chyme. If the villous venules are depressed, blood return to the villi will be blocked. Therefore, blood can be collected into the adjacent villous plexi through the marginal capillary. This helps maintain a normal blood circulation in the villi, and their digestive and absorptive functions are carried out normally.

In the newborn rat villi, capillary network was not formed although only simple microvascualr architecture was formed. The later developed capillary network is probably due to the formation of slender transcapillary tissue pillars, which give rise to new vascular meshes[25,26]. During villous formation, the developing vascular nets played an important role and the apical capillary loop in a villous was anchored to epithelial basal membrane or to the adjoining matrixes[27]. After 3 weeks, the villous microvascular architecture tended to grow in full scale. During ablactation period, the villous capillary network was formed, and the diametral ratio of villous arteriole to villous venule was one-third, which consolidated the normal digestion and absorption. The villous plexus in adult rats became higher and wider, providing more nutrition for the body. In aged rats, the tip of the villous plexus caved in, the position of villous venule was relatively high. The increases in diametral ratio of villous arteriole to villous venule caused high blood pressure, which degraded the transportation and absorption of nutrition. All of these demonstrate the important role of the vascular architecture in maintaining an efficient absorption of nutrition for the malfunctional intestines in the aged animals.

The primary penetrating vessels in the submucosa formed an extensive submucosal plexus that supplied the tunica serosa, tunica muscularis, and tunica mucosa[28]. Fewer branches of this plexus supply the muscle layers, and most of branches run towards the mucosa and to supply blood to the villous and the cryptal plexus[29]. Therefore the vascular permeability mainly depends on the villous plexus, namely vascular architecture and endothelial structure. Under normal physiological condition, small molecules can easily enter or come out of blood vessels, but the large size substances must be transported through endothelial hole or plasmalemmal vesicle[30]. Since there were no endothelial holes and very few plasmalemmal vesicles in newborn rats, these large size substances must be selected to pass through the endothelium, which may be a protection for the immature immune system. The emergence of a few of endothelial holes and plasmalemmal vesicles during ablactation period indicate that the big molecular substances can be transported. The endothelium of adult rats have a plenty of plasmalemmal vesicles, and microvascular permeability was twice as high as that of the ablactation rats. In the aged rats, the endothelium became thinner, and the number of plasmalemmal vesicles became smaller while the number of endothelial holes became bigger. The diametral ratio of villous arteriole to villous venule increased as animals become older. The blood pressure was higher in old rat villi. The larger number of endothelial holes and higher blood pressure resulted in double increase in the microvascular permeability of the aged rats as compared with the adult rats. The thickened basal membrane may be due to a compensatory response, which may prevent any injurants from entering the blood vessels in the aged rats. Based upon the above information, one can say that aging or degradation of blood vessels may underlie the mechanisms of systematic aging.

In summary, the microvascular architectures of rat intestinal villi are complex. Each villi has its own blood supply and venous return paths. Furthermore, one villi can supply blood to its adjacent villi through the marginal capillary. These complex connections in the villi help avoid a shortage of blood supply or blockade of venous blood return. Normal digestive and absorptive functions are thus protected. With regard to the small intestine of other species, whether there is a marginal capillary and venous return collateral circulation is a matter of future study.

REFERENCES

1 **Matheson PJ**, Wilson MA, Garrison RN. Regulation of intestinal blood flow. *J Surg Res* 2000; **93**: 182-196

2 **Mailman D**. Blood flow an intestinal absorption. *Fed Proc* 1982; **41**: 2096-2100

3 **Lun H**. Investigative survey of the intestinal blood vessels. *Jiepouxue Zazhi* 1997; **20**: 197-199

4 **Laroux FS**, Grisham MB. Immunological basis of inflammatory bowel disease: role of the microcirculation. *Microcirculation* 2001; **8**: 283-301

5 **Abbas B**, Boyle FC, Wilson DJ, Nelson AC, Carr KE. Radiation induced changes in the blood capillaries of rat duodenal villi:a corrosion cast,light and transmission electron microscopical study. *J Submicrosc Cytol Pathol* 1990; **22**: 63-70

6 **Kelly DA**, Piasecki C, Anthony A, Dhillon AP, Pounder RE, Wakefield AJ. Focal reduction of villous blood flow in early indomethacin enteropathy: a dynamic vascular study in the rat. *Gut* 1998; **42**: 366-373

7 **Ruh J**, Vogel F, Schmidt E, Werner M, Klar E, Secchi A, Gebhard MM, Glaser F, Herfarth C. Effects of hydrogen peroxide scavenger Catalase on villous microcirculation in the rat small intestine in a model of inflammatory bowel disease. *Microvasc Res* 2000; **59**: 329-337

8 **Hu S,** Sheng ZY. The effects of anisodamine and dobutamine on gut mucosal blood flow during gut ischemia / reperfusion. *World J Gastroenterol* 2002; **8**: 555-557

9 **Nakajima Y,** Baudry N, Duranteau J, Vicaut E. Microcirculation in intestinal villi: a comparison between hemorrhagic and endotoxin shock. *Am J Respir Crit Care Med* 2001; **164**: 1526-1530

10 **Dabareiner RM,** Snyder JR, Sullins KE, White NA 2nd, Gardner IA. Evaluation of the microcirculation of the equine jejunum and ascending colon after ischemia and reperfusion. *Am J Vet Res* 1993; **54**: 1683-1692

11 **Zheng FS**. Steric metrology of cell morphology. *Beijing: The Former Beijing Medical University and PUMC Press* 1990

12 **Kondo S**. Microinjection methods for visualization of the vascular architecture of the mouse embryo for light and scanning electron microscopy. *J Electron Microsc* 1998; **47**: 101-113

13 **Poonkhum R,** Pongmayteegul S, Meeratana W, Pradidarcheep W, Thongpila S, Mingsakul T, Somana R. Cerebral microvascular architecture in the common tree shrew (Tupaia glis) revealed by plastic corrosion casts. *Microsc Res Tech* 2000; **50**: 411-418

14 **Zahner M,** Wille KH. Vascular system in the large intestine of the dog. *Anat Histol Embryol* 1996; **25**: 101-108

15 **Bellamy JE**, Latshaw WK, Nielsen NO. The vascular architecture of the porcine small intestine. *Can J Comp Med* 1973; **37**: 56-62

16 **Ohashi Y**, Kita S, Murakami T. Microcirculation of the rat small intestine as studied the injection replica scanning electron microscope method. *Arch Histol Jpn* 1976; **39**: 271-282

17 **Dart AJ**, Snyder JR, Julian D, Hinds DM. Microvascular circulation of the small intestine in horse. *Am J Vet Res* 1992; **53**: 995-1000

18 **Hummel R,** Schnorr B. The system of blood vessels of the small intestine of ruminants. *Anat Anz* 1982; **151**: 260-280

19 **Mohiuddin A**. Blood and lymph vessels in the jejunal villi of the white rat. *Anat Rec* 1966; **156**: 83-89

20 **Jiang L,** Zhao XM, Tian N, Liu YY, Li XH, Jiang CG. Simulation study of hemodynamic of small intestinal villosity microvessels in vitro. *Zhongguo Bingli Shengli Zazhi* 1999; **15**: 60-62

21 **Morini S**, Yacoub W, Rastellini C, Gaudio E, Watkins SC, Cicalese L. Intestinal microvascular patterns during hemorrhagic shock. *Dig Dis Sci* 2000; **45**: 710-722

22 **Metry JM**, Neff M, Knoblauch M. The microcirculatory system of the intestinal mucosa of the rat. An injection cast and scanning electron microscopy study. *Scand J Gastroenterol Suppl* 1982; **71**: 159-162

23 **Tahara T,** Yamamoto T. Morphological changes of the villous microvascular architecture and intestinal growth in rats with streptozotocin-induced diabetes. *Virchows Arch A Pathol Anat Histopathol* 1988; **413**: 151-158

24 **Kamyshova VV,** Karelina NR, Mironov AA, Mironov VA. Morphofunctional features of different divisions of the microcirculatory bed of jejunal villi in the white rat. *Arkh Anat Gistol Embriol* 1985; **88**: 44-50

25 **Patan S**, Alvarez MJ, Schittny JC, Burri PH. Intussusceptive microvascular growth:a common alternative to capillary sprouting. *Arch Histol Cytol* 1992; **55**(Suppl): 65-75

26 **Karelina NR**. Circulatory bed of the small intestinal villi of newborn infants. *Arkh Anat Gistol Embriol* 1978; **75**: 64-71

27 **Hashimoto H**, Ishikawa H, Kusakabe M. Divelopment of vascular networks during the morphogenesis of intestinal villi in the fetal mouse. *Kaibogaku Zasshi* 1999; **74**: 567-576

28 **Yarbrough TB**, Snyder JR, Harmon FA. Jejunal microvasculature of the llama and alpaca. *Am J Vet Res* 1995; **56**: 1133-1137

29 **Chen YM**, Li J, Zhang J, Duan XL. The intestinal microvascular architecture of rat. *Shijie Huaren Xiaohua Zazhi* 2000; **8**: 1291-1293

30 **Komuro T,** Hashimoto Y. Three-dimensional structure of the rat intestinal wall (mucosa and submucosa). *Arch Histol Cytol* 1990; **53**: 1-21

Edited by Ma JY

P.O.Box 2345, Beijing 100023, China
Fax: +86-10-85381893
E-mail: wjg@wjgnet.com www.wjgnet.com

World J Gastroenterol 2003;9(4):800-803
World Journal of Gastroenterology
 ISSN 1007-9327

• BASIC RESEARCH •

Pleckstrin homology domain of G protein-coupled receptor kinase-2 binds to PKC and affects the activity of PKC kinase

Xing-Long Yang, Ya-Li Zhang, Zhuo-Sheng Lai, Fei-Yue Xing, Yu-Hu Liu

Xing-Long Yang, Ya-Li Zhang, Zhuo-Sheng Lai, Yu-Hu Liu, Institute of Gastroenterology, NanFang Hospital, First Military Medical University 510515, Guangzhou, Guangdong Province, China
Fei-Yue Xing, Key lab. for shock and microcirculation of PLA, Department of Preclinical Medicine, First Military Medical University 510515, Guangzhou, Guangdong Province, China
Correspondence to: Xing-Long Yang, Institute of Gastroenterology, NanFang Hospital, First Military Medical University 510515, Guangzhou, Guangdong Province, China. foru3000@hotmail.com
Telephone: +86-20-61364633 **Fax:** +86-20-61641544
Received: 2002-10-04 **Accepted:** 2002-11-28

Abstract

AIM: To study the detail mechanism of interaction between PKC and GRK_2 and the effect of GRK_2 on activity of PKC.

METHODS: The cDNA of pleckstrin homology (PH) domain located in GRK_2 residue 548 to 660 was amplified by PCR with the mRNA of human GRK_2 (β1-adrenergic receptor kinase) as template isolated from human fresh placenta, the expression vector pGEX-PH inserted with the aboved cDNA sequence for GRK_2 PH domain protein and the expression vectors for GST (glutathion-s-transferase) -GRK_2 PH domain fusion protein, BTK (Bruton's tyrosine kinase) PH domain and GST protein were constructed. The expression of GRK_2 in culture mammalian cells (6 cell lines: PC-3,MDCK, SGC7901, Jurkat cell etc.) was determined by SDS-PAGE and Co-immunoprecipitation. The binding of GRK_2 PH domain, GST-GRK_2 PH domain fusion protein and BTK PH domain to PKC *in Vitro* were detected by SDS-PAGE and Western blot, upon prolonged stimulation of epinephrine, the binding of GRK_2 to PKC was also detected by western blot and Co-immunoprecipitation.

RESULTS: The binding of GRK_2 PH domain to PKC *in Vitro* was confirmed by western blot, as were the binding upon prolonged stimulation of epinephrine and the binding of BTK PH domain to PKC. In the present study, GRK_2 PH domain was associated with PKC and down-regulated PKC activity, but Btk PH domain up-regulated PKC activity as compared with GRK_2 PH domain.

CONCLUSION: GRK_2 can bind with PKC and down-regulated PKC activity.

Yang XL, Zhang YL, Lai ZS, Xing FY, Liu YH. Pleckstrin homology domain of G protein-coupled receptor kinase-2 binds to PKC and affects the activity of PKC kinase. *World J Gastroenterol* 2003; 9(4): 800-803

http://www.wjgnet.com/1007-9327/9/800.htm

INTRODUCTION

G protein-coupled receptor kinase-2 (GRK), also known as β1-adrenergic receptor kinase (β-ARK1), plays an important role in agonist-induced desensitization of the β-adrenergic receptors. Activation of protein kinase C (PKC) is able to stimulate phosphorylation and activation of GRKs and induce desensitization of G protein-coupled receptor. However, the detail mechanism of interaction between PKC and GRK_2 and the effect of GRK_2 on activity of PKC remain unknown. Pleckstrin homology (PH) domain is a kind of functional domain containing 120 amino acids, which exist on many protein molecules that involved in cellular signal transduction. A PH domain located in GRK_2 residue 548 to 660 may play a significant role in mediating interaction between PKC and GRK_2. In the present study, we showed that PKC could associate with PH domain of GRK_2 in pull-down assay *in vitro*. Co-immunoprecipitation displayed binding of PKC to GRK_2 in intact Jurkat cells after prolonged stimulation of epinephrine. Assay of PKCβ1 kinase activity indicated that the binding of the PH domain of GRK_2 to PKCβ1 could down-regulate the activity of PKCβ1 kinase. Thus, GRK_2 may play a negative feedback regulatory role on PKCβ1 activity in interaction between GRK_2 and PKCβ1.

G protein-coupled receptor kinase-2 is a member of the GRK family existing of at least 6 GRKs[1]. GRKs are implicated in agonist-induced phosphorylation and homologous desensitization of G protein-coupled receptor (GPR). Phosphorylation sites of the GPR by GRK are located in the carboxyl tail of the receptor and involved amino acid residues at positions serine 404 408, and 410[2]. These phosphorylation sites are thought to initiate desensitization of GPR.

It has been recently reported that protein kinase C (PKC) could phosphorylate and activate GRK which sequentially mediated desensitization of GPR[3]. In addition, PKC could directly phosphorylate GPR and initiate desensitization of the receptors[4]. Thus, PKC likely participates in phosphorylation and homologous desensitization of adrenergic receptor at multiple levels. Furthermore, both activated GRK and PKC are recruited to the specific membrane and GRK may localize on the membrance via its PH domain binding to phosphatidylinositol phosphates. Both recruitment to membrane will facilitate the association of PKC with GRK. Deletion or mutation of the PH domain will abolish GRK faculty of phosphorylating and activating GPR[5]. PH domain of GRK plays a pivotal role in mediating the phosphorylation and desensitization of the receptors. However, as to detail mechanism of PKC, how to interact with and activate GRK remains unclear.

PH domain has been distinguished from more than 100 molecules that are implicated in signaling and other biological function. The main function of PH domains is to mediate protein-phospholipid and protein-protein interaction. Up to now, several molecules such as phosphatidylinositol phosphates, Gβγ, RACK1, PKC, Gα subunit-12 and F-actin have been identified as ligands of PH domains. It was reported by Yao *et al*(1994)[6] that the PH domain of Btk and Itk interacted with protein kinase C. Afterwards, the interactions between PKC and other PH domains of the molecules were also confirmed by different groups. Those PH domains that bind to PKC share a high homology in 1^{st}-4^{th} β strands[7] which formats a relatively reserved face binding to PKC. But other PH domains that can interact with PKC remain to be identified.

PKC is a family of serine/threonine protein kinase, which plays significant roles in numerous cellular responses (including cell proliferation, differentiation, growth control, tumor progression, apoptosis etc.)[8]. Besides the event of PKC phosphorylating GRK_2 discussed above, PKC can phosphorylate GRK_5 and modulate the activity of GRK_5[9]; PKC can also lead to olfactory signal termination and desensitization[17] via other GRK_2; Agonist stimulation results in oxytocin receptor interaction with GRK and PKC[10]. Moreover, PKC presents a manner of phosphorylating directly to muscarinic receptor and leading to the desensitization receptor[11].

Like most interaction between signaling molecules, PKC is likely associated with GRK_2 before phosphorylating and activating GRK_2. To elucidate detail mechanism of interaction between GRK_2 and PKC, we reported the study on interaction between PKC and GRK_2. It is expected that present study will provide new insights into understanding of the modulation mechanism of PKC in GRK_2 mediating signaling pathway. It is also expected that the present investigation can illustrate the importance of the GRK_2 PH domain in interaction with PKC.

MATERIALS AND METHODS

Materials

Anti-GRK_2, anti-PKCb1 and secondary antibodies conjugated with horseradish peroxidase were purchased from Santa Cruz Biotechnology. **PKC assay kit (Sigma TECT™ PKC assay system) and reverse transcription kit** were from Promega. **Glutathione-agarose beads** was from Sigma. **Expression vector pGEX-4T-1 and ECL detection kit** (for western blotting) were from Amersham Pharmacia Biotech. **PVDF membrane** was from Millipore. **Rabbit IgG** was from Sino-American company (China). **Protein A-agarose** was from Pierce Inc.

Methods

Construction of expression vector pGEX-PH The mRNA of human GRK_2 (β1-adrenergic receptor kinase) was isolated from fresh human placenta[12], and reverse transcription was performed according to the kit protocol. cDNA of PH domain (residue 548 to 660)[13] was amplified by PCR with oligonucleotides containing BamHI sites (forward, CGGGATCCGGCCACGAGGAAGACTAC) and EcoRI sites (reverse, GGAATTCTCACCGCTGCACCAGCTGCTG). The products were purified from agarose gel and the resulting fragments were digested with Bam HI and EcoRI, respectively. The resulting fragments were ligated in frame between Bam HI and EcoRI sites of plasmid pUC-19. The resulting plasmid (termed pUC-PH) was resolved by sequencing. The fragments were excised from pUC-PH and ligated in frame into expression vector pGEX-4T-1, named pGEX-PH.

Expression and purification of GST fusion protein GST-GRK_2 PH domain, Btk PH domian and GST were expressed in *Escherichia coli* strain DH5α. Here was Btk PH domian positive control[6]. The expression was induced with 0.2 mM of IPTG at 26 ℃ for 1 hour in LB medium containing 1 % glucose. Briefly, the bacteria were resuspended in ice-cold STE buffer (10 mM Tris-HCl, 150 mM NaCl,1.0 mM EDTA,1.0 mM phenylmethylsulfonyl fluoride and 0.1 mg/ml lysozyme, pH 8.0) on ice for 20 min. The treated bacteria were added dithiothreitol to 5.0 mM and sarkosyl to 1.5 % on ice until the solution became viscous, and then lysed by sonicate (30-40 output,1 min×2, at 4 ℃). Cell lysate was centrifuged at 10 000×g for 20 min at 4 ℃. Component of both supernatant and the pellet was separated by SDS-PAGE to determine the distribution of the fusion protein. The supernatant was added Triton X-100 to 2 %, and then filtered with 0.45 mm membrane. The solution was saved as the fraction containing interested proteins, and then the treated glutathione-agarose beads were added to solution at 4 ℃ for 2 hours with occasional gentle mixing. The beads were washed with PBS and centrifuged at 800×g, 4 ℃ for 3 min×5 times. The pellet was subjected to SDS-PAGE in 12 % gels. In order to utilize 1 equivalent amount of GST and fusion proteins for the following assay, the protein concentration was modulated according to band sizes in SDS-GAGE gel.

Determination of GRK2 expression in mammalian cell lines MDCK, SGC7901, DU145, PC-3, U937 and Jurkat cells were maintained in Dulbecco' s modified eagle' s medium or 1640 medium with 10 % (v/v) new born bovine serum and a 5 % CO_2 humidified atmosphere at 37 ℃. In brief, the 10^7 cells were harvested by centrifuging or scraping off, respectively, washed by PBS at 4 ℃ and then incubated with 1 ml of lysis buffer (20 mM Tris-HCl, pH 7.5, 10 mM KCl, 1 mM EDTA, 0.5 mM phenylmethylsulfonyl fluoride, 10 μg/ml leupeptin and 1 μg/ml aprotinin) on ice for 20 min with casually and vigorously vortexing. The mixtures were centrifuged at 12 000×g for 10 min at 4 ℃. The supernatants were saved as GRK_2-contained or PKB-contained preparations for western blot.

Cell culture and lysis Jurkat T lymphocytes were maintained as above with RPMI 1640 medium. The 2×10^7 cells were divided into 2 parts and were serum-freed for 8 h. followed by 0.5 h treatment without (Control) or with epinephrine. The stimulation was stopped by removal of the medium and adding 3 ml of ice-cold phosphate-buffered saline, which was also used for two similar washing steps with centrifugation at 500×g for 5 min.

Protein-protein interaction assay Approximately 20 μg of the GST and GST fusion proteins immobilized on glutathione-agarose beads was incubated with the 0.3 ml of Jurkat T lymphocyte supernatant at room temperature for 2 hours with gentle mixing. The beads were then washed five times with 1 ml of ice-cold PBST (PBS with 0.05 % tween-20). The eventual bead pellet was resolved by SDS-PAGE. Equivalent amount of the fusion protein or GST alone was used for the following assay.

Western blot-the resolved proteins were electrotransferred onto PVDF membrane. The membrane was blocked by incubating with 5 % gelatin in PBST at 37 ℃ for 1 h with gentle vibration, and then incubated with 1 μg of anti-PKCβ1 antibody at 4 ℃ overnight. The membrane was then washed 5 times with PBST and incubated with horseradish peroxidase-conjugated anti-rabbit secondary antibody at room temperature for 1 h with gentle vibration. The membrane was finally washed 6 times with PBST to remove unbound secondary antibody and visualized by using ECL (Amersham Pharmacia Biotech).

Co-immunoprecipitation assays 10^7 Jurkat cells were lysed in 1 ml of lysis buffer (20 mM sodium phosphate, pH 7.5, 500 mM NaCl, 0.1 % SDS, 1 % NP-40, 0.5 % sodium deoxycholate, 0.02 % sodium azide, 0.5 mM phenylmethylsulfonyl fluoride, 2 μg/ml leupeptin and 2 μg/ml aprotinin). Briefly, 10 μg of anti-PKCβ1, or anti-GRK_2 antibodies and rabbit IgG were added to 200 μl of the lysate, respectively, then the samples were incubated overnight at 4 ℃. The products were added 40 ml of immobilized protein A (Pierce Inc) and incubated at room temperature for 2 h with gentle mixing. The products were added 0.5 ml lysis buffer (without protease inhibitor) and centrifuged at at 500×g, 4 ℃ for 3 min. The supernatant was discarded and this procedure was repeated for 6 times. In brief, the pellets were subjected to SDS-PAGE. The proteins were electrotransferred onto PVDF membranes. The membranes were blocked with gelatin and incubated with anti-PKCβ1 or anti-GRK_2 antibodies, respectively. The membranes were probed and visualized as described above.

PKC kinase assay The fusion proteins and GST were purified as described above, and washed extensively with PBST. After washing, the GST-fusion proteins and GST were eluted with

20 mM of reduced glutathione in 50 mM Tris· HCl (pH 8.0). The eluted proteins were concentrated using a Centricon (Millipore). Protein concentrations were determined with Bradford reagent (Bio-Rad). Equivalent amounts of the protein were added to the 100 μl lysate of Jurkat cells. According to manufacturer' s instruction (Sigma TECT™ PKC assay system), the activity of PKC in the lysate was determined by subtracting the radioactivity of the reaction with control buffer and 100 μM PKC peptide inhibitor from that of the reaction without activated buffer nor the PKC inhibitor. The experiment was performed in triplicate samples for each groups. The data were presented as percentage of PKC activity and the control was used as 100 %.

RESULTS

Binding of GRK_2 PH domain to PKC in vitro

To search for potential binding between the expressed proteins (GST-GRK_2 PH domain, GST-Btk PH domain and GST) and PKCβ1, the proteins immobilized on glutathione-agarose beads were added to lysate of Jurkat cells, and then the products were subjected to SDS-PAGE and Western blot. The potential PKCβ1 was probed with anti- PKCβ1 antibody. As shown in Figure 1, the GST fusion proteins encompassing GRK_2 PH domain and GST-Btk PH domain associated specifically with PKCβ1 because the GST did not pull out PKCβ1 under the same experimental conditions. Binding of Btk PH domain to PKCβ1 was formerly approved. We confirmed the binding of GRK_2 PH domain to PKCβ1 which was specific *in vitro*.

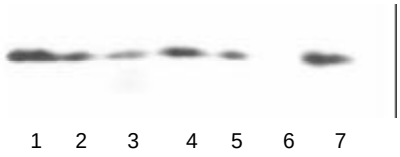

Figure 1 The binding of PH domain to PKC by Western blot with the antibody to PKC. Lane 1, 2, 3, 4 and 5 were the GST-PH domains of IRS-1, GRF/c, β-ARK1, PLCγ/n and Btk, respectively; lane 6 was the GST; lane 7 was lysate of Jurkat cells.

Determination of expression of GRK_2 in cultured mammalian cells

In order to detect the association of GRK_2 with PKC *in vivo*, GRK_2 expression of 6 cell lines were confirmed by western blot in advance. The same amount of the protein was utilized in SDS-PAGE. The results indicated GRK_2 were expressed in PC-3, MDCK,7901 and Jurkat cell lines. The GRK_2-antibody could react with GRK_1 in MDCK and 7901 cell lines,and the antibody could specifically recognize GRK_2 in Jurkat cells. Thus, the following Co-immunoprecipitation assays was performed in Jurkat cells.

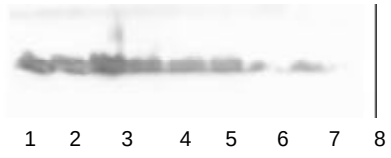

Figure 2 The expressing of GRK_2 by Western blot with the antibody to GRK2. Lane 1, 2, 3, 4 were the results of Western blot in PC-3, MDCK, 7901 and Jurkat cell line respectively. Lane 5,6 was GST.

Binding of GRK_2 to PKC upon prolonged stimulation of epinephrine

Phosphorylation and activation of GRK by PKC enhance desensitization of G protein-coupled receptor. In the pull-down assay, our result indicated that the PH domain of GRK_2 was associated specifically with PKC *in vitro*. To determine the association of PKC with GRK_2 *in vivo* after stimulation of the agonist of β-ARK, 100 μm epinephrine was added to the cells in 1640 medium for 30 min. Co-immunoprecipitation was performed with specific anti-GRK_2 and anti-PKC antibodies in co-precipitation and detection of PKC and GRK. After stimulation of 100 μm epinephrine for 30 min, PKC was detected out in the precipitate of GRK antibody and GRK was detected out in precipitate of PKC antibody, respectively. In contrast, the PKC did not bind to GRK_2 in the intact cells without stimulation of epinephrine. Thus, the results indicated that the association of PKC with GRK_2 was involved in GRK_2 activation and desensitization of G protein-coupled receptor.

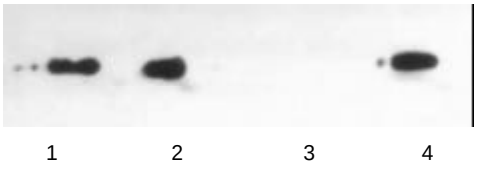

Figure 3 After stimulation of epinephrine, Co-immunoprecipitation was performed with anti-GRK_2 and anti-PKC in co-precipitation and detection of PKC and GRK_2. Lane 1 was PKC detected in precipitate of GRK antibody, lane 2 was GRK_2 detected in precipitate of PKC antibody.Lane 3 indicated the PKC did not bind to GRK_2 in the intact cells without stimulation of epinephrine ,lane 4 was the lysate of Jurkat cell.

Effects of GRK_2 and Btk PH domains on PKC activity

Effects of proteins on PKC activity were determined as described under the experimental Procedures. After purification as described above, the expressed proteins were eluted and dialysed in PBS. Equivalent amounts (20 μg) of GST-GRK_2 PH domain, GST-Btk PH domain and GST were added to the lysate of Jurkat cell lysate (100 μl) in determining PKC activity. When Btk associated with PKC, Btk activity was down-regulated by PKC and PKC activity was up-regulated by Btk PH domain. In the present study, GRK_2 PH domain was associated with PKC and down-regulated PKC activity but Btk PH domain up-regulated PKC activity as compared with GST and untreated cells.

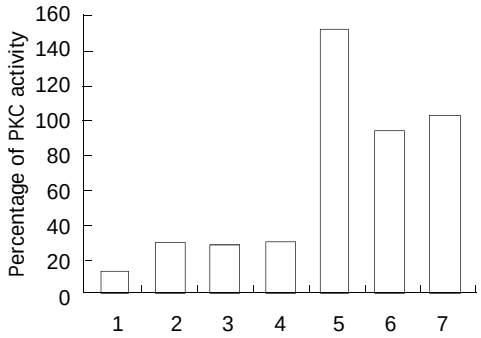

Figure 4 Effects of the PH domain on PKC activity measured by protein kinase C Assay System. The volume was percentage of PKC activity. The data were representation of two experiments. Lanes 1, 2, 3, 4 and 5 were GST-PH domain of IRS-1, GRF/c, β-ARK1, PLC γ/n and Btk, respectively; lane 6 wasthe GST; lane 7 was lysate of Jurkat cells.

DISCUSSION

The GRK family is composed of six members, namly GRK 1-6. Of these, GRK_2 phosphorylates G protein-coupled receptors (GPCRs) and plays an important role in mediating homologous desensitization of GPCRs. Chuang' s work showned the activity of GRK_2 was increased[14] in a protein kinase C (PKC)-dependent manner. Further study demonstrated that PKC could directly phosphorylate GRK. This study suggested that GRK could be

activated via phosphorylation of PKC. Recent work had led to the identification of phosphorylation site at GRK_2, the study of Krasel and co-worker showed that PKC phosphorylated GRK_2 at serine 29[15], but the detail mechanism of PKCβ1 recognizing and binding to GRK_2 remains unknown. In present study, we reported that GRK_2 could bind to PKC via its carboxyl-terminal PH domain *in vitro*, which was a fundamental event in mediating interaction between PKC and GRK_2. The present result suggested the GRK ph domain had an analogous fashion to PH domain of Btk and Itk, which could interact with protein kinase C[6] in our previous study. The PH domain of GRK_2 is probably involved in directly binding of GRK_2 to PKC and facilitates phosphorylation and activation of GRK_2 by PKC.

Stimulation of agonist (epinephrine) on adrenergic receptor results in association of PKCβ1 with GRK_2 in Jurkat cells. GRK_2 could through its PH domain can directly bind to PKC and then be phosphorylated by PKC. But in intact cells (without stimulation of epinephrine), PKC and GRK_2 are in dissociated state. The epinephrine stimulation on adrenergic receptor may activate phospholipase C (PLC), and initiates a cascade of events. The stimulation causes PLC-mediated hydrolysis of inositol phospholipids, and results in calcium mobilization and production of second messenger diacylglycerol (DAG). The DAG and Ca^{++} are activators of PKC, and cause activation of PKC[16]. In the present study, activated PKC is likely to bind to and phosphorylate GRK_2 directly, which phosphorylates G-protein coupled receptor and results in receptor desensitization. In this signaling pathway, activation of PKC appears to be prior to receptor desensitization and is of fundamental importance in regulating the receptor desensitization.

Those PH domains from Btk, β-spectrin, dynamin and amino-terminal of AFAP-110 known directly binding to PKC share a high homology at first three β-sheets[7]. These β-sheets form conserved structure elements and may specifically bind to PKC. Table 1 showed the residue comparison of PH domains from GRK_2 and GRK_3 with these PH domains. The PH domain of GRK_2 and GRK_3 matches that consensus well. This may form a structured base of PH domains binding to PKC.

Table 1 First three β sheets of PH domains of GRK_2 and GRK_3 are compared with other PH domain known or predicted to bind to PKC

PH domain (source)	β1	β2	β3
Btk	ESIFLKT--SQQKKKTSPLS--NFKKRLFLLT-VH-KLSYYEYDF		
β-spectrin	MEGFLNRKH-EWEAHNKKASSR-SWHNVYCVIN-NQ--EMGFYKDAK		
Dynamin	RKGWLTI---NNIGIMKGGS----KEYWFVLT--AE--NLSWYKDDE		
AFAP, Nt PH domain	ICAFLLRKK-RFGQ----------WTKLLCVIK-EN--KLLCYKSSK		
Consensus	1* +*	++*****	+L 1p
GRK_2	MHGYMSKM--GNPFLTQ-----WQRRYFYLF---PN--RLEWRGEGEA		
GRK_3	MHGYMLKL--GNPFLTQ-----WQRRYFYLF---PN--RLEWRGEGES		

Consensus sequence is shown and symbols used are as in the paper of Baisden *et al*. 1 indicates aromatic residues, + indicates positively charged residues, *indicates hydrophobic residues, indicates polar residues. The sequences of GRK_2 and GRK_3 from Zheng *et al*[18].

The previous study revealed PKC inhibited the activity of Btk kinase via binding to Btk PH domain[6], but the binding effect on PKC activity remains unclear. In the present study, the effects on PKC activity of Btk and GRK_2 PH domains were determined with GST. Compared with GST or control, Btk PH domain could increase PKC kinase activity, but GRK_2 PH domain inhibited PKC kinase activity. The mechanism of activation or inhibition of PKC activity might lie in the PH domains binding to PKC regulatory domain and regulating activity of PKC kinase. Biological function of Btk PH domain inhibiting PKC activity will be laid in future investigation. The present study indicated that PKC through its binding to the PH domain of GRK and facilitates phosphorylation and activation of GRK by PKC when stimulated by epinephrine. On the other hand, GRK_2 PH domain appeared to play a negative feedback regulatory role on PKC activity. GRK_2 immediately turns off PKC kinase activity on GRK after PKC completed phosphorylation and activation of GRK.

REFERENCES

1 **Sallese M,** Iacovelli L, Cumashi A, Capobianco L, Cuomo L, De Blasi A. Regulation of G protein-coupled receptor kinase subtypes by calcium sensor proteins. *Biochim Biophys Acta* 2000; **1498**:112-121

2 **Diviani D,** Lattion AL, Cotecchia S. Characterization of the phosphorylation sites involved in G protein-coupled receptor kinase- and protein kinase C-mediated desensitization of the alpha1B-adrenergic receptor. *J Biol Chem* 1997; **272**: 28712-28719

3 **Winstel R,** Freund S, Krasel C, Hoppe E, Lohse MJ. Protein kinase cross-talk: Membrane targeting of the beta-adrenergic receptor kinase by protein kinase C. *Proc Natl Acad Sci USA* 1996; **93**: 2105-2109

4 **Garcia-Sainz JA,** Vazquez-Prado J, Del Carmen Medina L. Alpha 1-adrenoceptors: function and phosphorylation. *Eur J Pharmacol* 2000; **389**: 1-12

5 **Touhara K**. Effects of mutations in pleckstrin homology domain on beta-adrenergic receptor kinase activity in intact cells. *Biochem-Biophys Res Commun* 1998; **252**: 669-674

6 **Yao L,** Kawakami Y, Kawakami T. The pleckstrin homology domain of Bruton tyrosine kinase interacts with protein kinase C. *Proc Natl Acad Sci USA* 1994; **91**: 9175-9179

7 **Baisden JM,** Qian Y, Zot HM, Flynn DC. The actin filment-associated protein AFAP-110 is an adaptor protein that modulates changed in actin filament integrity. *Oncogene* 2001; **20**: 6435-6447

8 **Nishizuka Y.** The protein kinase C family and lipid mediators for transmembrane signaling and cell regulation. *Alcohol Clin Exp Res* 2001; **25**: 3S-7S

9 **Pronin AN,** Benovic JL. Regulation of the G protein-coupled receptor kinase GRK5 by protein kinase C. *J Biol Chem* 1997; **272**: 3806-3812

10 **Berrada K,** Plesnicher CL, Luo X, Thibonnier M. Dynamic interaction of human vasopressin / oxytocin receptor subtypes with G protein-coupled receptor kinases and protein kinase C after agonist stimulation. *J Biol Chem* 2000; **275**: 27229-27237

11 **Hosey MM,** Benovic JL, DebBurman SK, Richardson RM. Multiple mechanisms involving protein phosphorylation are linked to desensitization of muscarinic receptors. *Life Sci* 1995; **56**: 951-955

12 **Chomczynski P,** Sacchi N. Single-step method of RNA isolation by acid guanidinium thiocyanate-phenol-chloroform extraction. *Anal Biochem*. 1987; **162**: 156-159

13 **Chuang TT,** LeVine H 3rd, De Blasi A. Phosphorylation and activation of beta-adrenergic receptor kinase by protein kinase C. *J Biol Chem* 1995; **270**: 18660-18665

14 **Chuang TT**, Sallese M, Ambrosini G, Parruti G, De Blasi A. High expression of beta-adrenergic receptor kinase in human peripheral blood leukocytes. Isoproterenol and platelet activating factor can induce kinase translocation. *J Biol Chem* 1992; **267**: 6886-6892

15 **Krasel C,** Dammeier S, Winstel R, Brockmann J, Mischak H, Lohse MJ. Phosphorylation of GRK_2 by protein kinase C abolishes its inhibition by calmodulin. *J Biol Chem* 2001; **276**: 1911-1915

16 **Rasmussen H,** Isales CM, Calle R, Throckmorton D, Anderson M, Gasalla-Herraiz J, McCarthy R. Diacylglycerol production, Ca2+ influx, and protein kinase C activation in sustained cellular responses. *Endocr Rev* 1995; **16**: 649-681

17 **Bruch RC,** Kang J, Moore ML Jr, Medler KF. Protein kinase C and receptor kinase gene expression in olfactory receptor neurons. *J Neurobiol* 1997; **33**: 387-394

18 **Zheng J,** Cahill SM, Lemmon MA, Fushman D, Schlessinger J, Cowburn D. Identification of the binding site for acidic phospholipids on the PH domain of dynamin: implications for stimulation of GTPase activity. *J Mol Biol* 1996; **255**: 14-21

Edited by Wu XN

P.O.Box 2345, Beijing 100023, China
Fax: +86-10-85381893
E-mail: wjg@wjgnet.com www.wjgnet.com

World J Gastroenterol 2003;9(4):804-807
World Journal of Gastroenterology
 ISSN 1007-9327

• BASIC RESEARCH •

Collagen fiber angle in the submucosa of small intestine and its application in gastroenterology

Yan-Jun Zeng, Ai-Ke Qiao, Ji-Dong Yu, Jing-Bo Zhao, Dong-Hua Liao, Xiao-Hu Xu, Gregersen Hans

Yan-Jun Zeng, Ai-Ke Qiao, Shantou University, Guangdong, 515031, China; Beijing University of Technology, Beijing, 100022, China
Ji-Dong Yu, Beijing Polytechnic University, Beijing, 100022, China
Jing-Bo Zhao, Department Gastrointestinal Surgery, Aalborg University, Denmark; China-Japan Friendship Hospital, Beijing, 100029, China
Dong-Hua Liao, Beijing University of Technology, Beijing, 100022, China; Department Gastrointestinal Surgery, Aalborg University, Denmar
Xiao-Hu Xu, Shantou University, Guangdong, 515031, China
Gregersen Hans, Department Gastrointestinal Surgery, Aalborg University, Denmar
Correspondence to: Yan-Jun Zeng, Professor and Director of Biomechanics & Medical Information Institute, Beijing University of Technology, No.100 Pingleyuan, Chaoyang District, Beijing 100022, China. yjzeng@bjpu.edu.cn
Telephone: +86-10-67392172 **Fax**: +86-10-67392297
Received: 2002-07-10 **Accepted:** 2002-07-25

Abstract

AIM: To propose a simple and effective method suitable for analyzing the angle and distribution of 2-dimensional collagen fiber in larger sample of small intestine and to investigate the relationship between the angles of collagen fiber and the pressure it undergoes.

METHODS: A kind of 2-dimensional visible quantitative analyzing technique was described. Digital image-processing method was utilized to determine the angle of collagen fiber in parenchyma according to the changes of area analyzed and further to investigate quantitatively the distribution of collagen fiber. A series of intestinal slice's images preprocessed by polarized light were obtained with electron microscope, and they were processed to unify each pixel. The approximate angles between collagen fibers were obtained via analyzing the images and their corresponding polarized light. The relationship between the angles of collagen fiber and the pressure it undergoes were statistically summarized.

RESULTS: The angle of collagen fiber in intestinal tissue was obtained with the quantitative analyzing method of calculating the ratio of different pixels. For the same slice, with polarized light angle's variation, the corresponding ratio of different pixels was also changed; for slices under different pressures, the biggest ratio of collagen fiber area was changed either.

CONCLUSION: This study suggests that the application of stress on the intestinal tissue will change the angle and content of collagen fiber. The method of calculating ratios of different pixel values to estimate collagen fiber angle was practical and reliable. The quantitative analysis used in the present study allows a larger area of soft tissue to be analyzed with relatively low cost and simple equipment.

Zeng YJ, Qiao AK, Yu JD, Zhao JB, Liao DH, Xu XH, Hans G. Collagen fiber angle in the submucosa of small intestine and its application in gastroenterology. *World J Gastroenterol* 2003; 9(4): 804-807
http://www.wjgnet.com/1007-9327/9/804.htm

INTRODUCTION

Several G.I. diseases can change the collagen fiber structure in the G.I. tract[1-4]. The collagen fiber content and its distribution outside the cell are closely related to some diseases. For example, systemic sclerosis (scleroderma) will replace smooth muscle and deposit large amounts of collagen instead. Gastrointestinal sclerdema is a common clinical disorder; however, due to its complicated etiology, most of them are not easily diagnosed and all the patients with such disease manifested distinct collagen fiber transformations. Early collagen fiber transformations are swelling and homogenization and then become thickened, sclerosed and arranged in a close order[5-9]. Collagen synthesis is increased especially the ratio of fine collagen fibers; at the same time, the smooth muscle fiber bundles become homogeneous, sclerosed and atrophic. There are changes occurred in the orientation of collagen fibers[10-13]. Obstructive diseases could also change the collagen structure and content[14-16]. In normal tissue the submucosal layer consist almost entirely of collagen, which is called the skeleton of the small intestine, and it is well known that the fibers run in a cross-cross pattern with 30 degrees angle in longitudinal direction[17-20]. The directional distribution of collagen fibers has a very important role in studying the function and self-repair of soft tissue[21].

The application of digital image-processing technology in medicine field has offered an accurate, simple, convenient and rapid method for the measurement and analysis of large amounts of medical images, especially for the quantitative analysis of smaller pictures, such as microscopic images. At the present time, the techniques for the quantitatively analyzing the distribution of collagen fibers consist mainly of several kinds as follows: that is, the method of quantitatively polarized light microscopy, small angle beam dispersion, image analysis and X-ray diffraction. These methods will sometimes be constrained by the image size, time cost or image connecting, and 90° orientation of template etc[23].

The purpose of this paper is to propose a method suitable for analyzing the angle and distribution of 2-dimensional collagen fiber in larger sample and to investigate the relationship between the angles of collagen fiber and the pressure it undergoes. At the same time, this paper also offers an effective method for research of the large area collagen fiber distribution.

MATERIALS AND METHODS

Isolation of small intestine

Seven Sprague-Dawley (250-300 g body wt) rats were used in this sdudy. They were fasted but free access to water for 24 hours before experiment. Approval of the protocol was obtained from the Danish Animal Experiment Committee. After animal was euthanized by cervical dislocation, its abdomen was opened and the small intestine was separated from the adjacent organs. An 18-cm-long segment from the middle part of small intestine was cut and excised within 2 min, then transferred to an organ bath containing oxygenated Krebs-Ringer-bicarbonate solution at pH 7.4 with 6 % Dextran and 2 mL EGTA.

Procedures

The specimen was further cut into six 3-cm-long segments. One of the six segments served as control and was fixed in 4 % formalin in no-load condition. The 5 segments left had one end ligated while the other end was connected via a tube to a fluid container for application of different pressures, which were 2, 5, 10, 15 and 20 cm H_2O respectively. Before we pressurized the intestinal segments, we placed some microbeads on surface of the middle part of the segments. Then the outlet was clamped to maintain the volume. After applying pressure for 3 minutes, a record of the whole intestine segment and the part with dots was obtained using video-camera (SONY CCD/RGB, JAPAN) to monitor the whole process (refer to Figure 1) performed under room temperature.

After the specimen was fixed in 4 % formalin for 24 hours, 1.0 cm long and 0.5 cm long transverse sections were taken from the middle part of specimen and dehydrated in a series of graded ethanol (70 %, 90 %, 95 % and 100 %) and embedded in paraffin respectively. 5 μm serial slices were cut and stained with picrosirius red for collagen analysis and HE (hemotoxylin and eosin) for general histological observation[22-26].

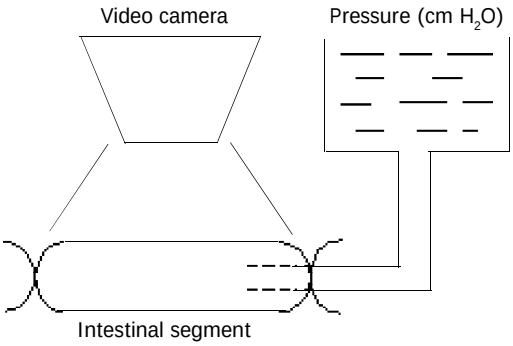

Figure 1 Slice record.

Image acquire

A series of polarized images of intestine slice was acquired by the recorder through microscope at every δ degree angle, and then stored in computer through image collecting card with TIFF format (RGB system type). The TIFF format, a very popular in use currently to reflect the details of the slice images distinctly, and the pixel values in the polarized images are suitable for the principles presented previously very well[27-29]. Therefore we took the TIFF form to verify the method' s feasibility and practicality.

In polarized light microscope, polarized light is delivered onto the sample to be analyzed and handled after being passed through two filter glasses. When the angle between optical axis of the two polarizing lens is 0 degree (that is, both of the two optical axis are parallel to the muscle direction), the blackest image area will be the part where the collagen fiber angle is 90 or 0 degree to the optical axis. Such an image area is also the part where the pixel values are minimum. Therefore, through image analysis we can find out all the area where the collagen fibers are parallel to muscle direction and thereby figure out the area ratio between the study area and the entire analysis Area (abcd). In the slice image analysis, the collagen fiber manifested as some pink striation (f) and the muscle fiber (e) some buff [4] (refer to Figure 2).

Rotating the polarizing eyepiece while maintaining the objective lens and the experiment sample stable can make muscle fiber direction coincide with the optical axis of polarizing objective. When the polarizing eyepiece is rotated δ degree, all the areas where the collagen fiber are δ degree or 90 + δ degree with the muscle fiber will present in the blackest part[21], in this way, their ratio to the entire analyzing area can be figured out as well.

Accordingly, we can obtain the relationship between the angle and its area ratio to the entire area. Since the collagen fiber distribution is uniform, that is, reticular in shape, its longitude and latitude lines are +30 degree and -30 degree to the muscle fiber direction. The area ratio for which is therefore the biggest, we can utilize the area ratio to reckon the collagen fiber angle.

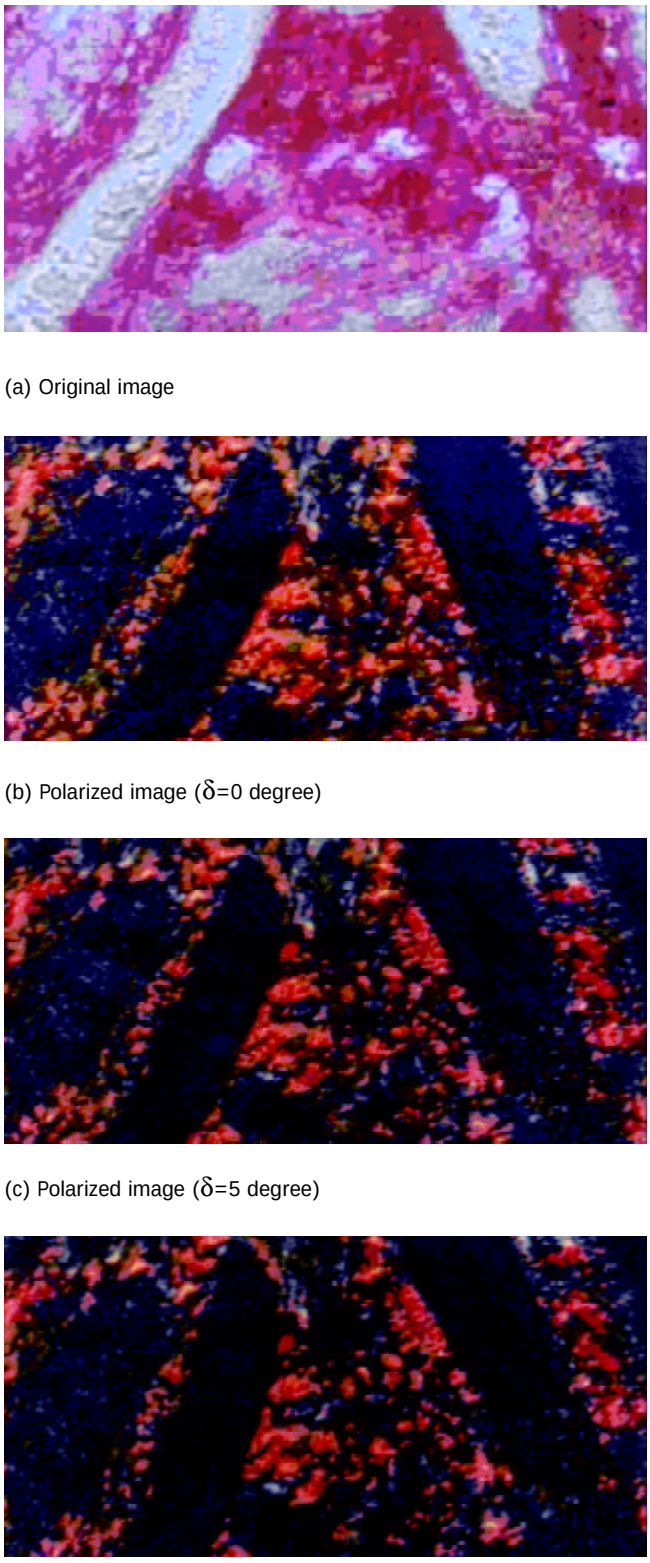

(a) Original image

(b) Polarized image (δ=0 degree)

(c) Polarized image (δ=5 degree)

(d) Polarized image (δ=10 degree)

Figure 2 Image processing.

Image processing

The image processing is the key part of the research, which is eventually based on the analysis of every image' s pixels, namely, first to normalize the pixel value and then to use proper algorithms to obtain results. When all the data are summed up, the distribution relationship of collagen fibers can be obtained reversely through the regression curve.

Since the scope of the images recorded is so large that there can include a great deal of muscle tissue and other unrelated background (Figure 2), which should be removed by the image filter before the analysis. The area selected for analysis should be done on the original image before it was polarized.

In this study, the background noises were excluded directly with a frequency domain strengthening method because both of the edge and noise in the image correspond to the high frequency section of the image' s Fourier transformation, we could weaken this part of the frequency to lessen its influence in the frequency domain[30-33].

Data processing

For the purpose of saving much more information of each pixel, the matrix was unified. Take matrix F (m,n) as the basis for further processing, the data less than the chosen threshold value were considered as the collagen fiber area in the polarized image. Figure out the pixel' s number that was less than the chosen threshold value s (j)[34,35]. And made:

$$b(j)=\frac{s(j)}{m\times n};$$

b(j) was equal to the area ratio of collagen fiber and the chosen observed area in polarized image j. From this we got series of the ratio sequence, which were stored into array Y(j).

RESULTS

According to the steps mentioned above, the calculation results were shown in Table 1, where the first column listed the pressures the tissue were received and the first row was the polarized light angles being rotated. We found that for the same slice, with polarized light angle' s variation, its corresponding area ratio is not identical; for each tissue under different pressures, its biggest area ratio is not identical either. To obtain the smooth curve showing the relationship between the angle and the corresponding ratio, we made a nonlinear normality on the sample data[36], the abscissa of the curve was δ' s integer multiple and the ordinate the series value in array Y(i) (Figure 3).

The relationship between pressures tissue received and their corresponding fiber angle was shown in Figure 4.

The relationship between pressures tissue received and their corresponding biggest ratio was shown in Figure 5.

We tested other intestinal slice' s images (of the same animal) and found that their properties above were similar by and large.

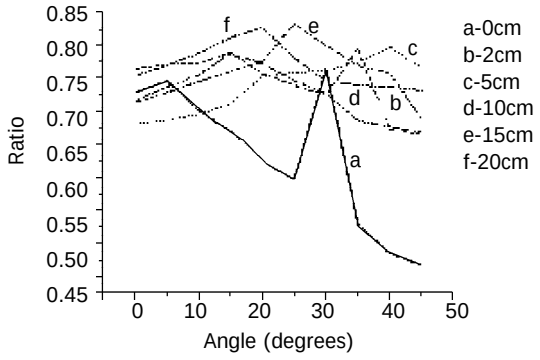

Figure 3 Relationship between angles of polarized light and their corresponding pixel ratio in series of slice images.

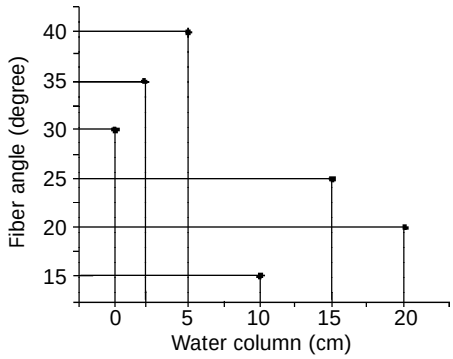

Figure 4 Relationship between pressures tissue received and their corresponding fiber angle.

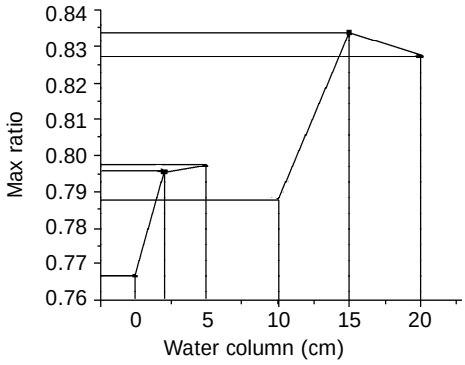

Figure 5 Relationship between pressures tissue received and their corresponding biggest ratio.

DISCUSSION

From the data in Table 1, we found that in the same tissue sample there exist obvious alterations in the collagen area ratio

Table 1 Area ratio of slice image at different angles within various distension pressures (δ=5°, *is the biggest area ratio of this slice image)

δ	0°	5°	10°	15°	20°	25°	30°	35°	40°	45°
H_2O										
0 cm	.7288	.7465	.7016	.6694	.6238	.5978	.7666*	.5290	.4852	.4669
2 cm	.7649	.7713	.7732	.7890	.7576	.7399	.7245	.7956*	.6730	.6654
5 cm	.6817	.6874	.6959	.7118	.7535	.7591	.7632	.7744	.7976*	.7664
10 cm	.7162	.7375	.7563	.7877*	.7730	.7469	.7272	.6866	.6764	.6684
15 cm	.7139	.7285	.7455	.7611	.7760	.8337*	.8000	.7693	.7580	.6873
20 cm	.7548	.7700	.7885	.8125	.8270*	.7807	.7457	.7400	.7372	.7320

as the angles of polarized light changed; In different slice' s images with different pressures, its biggest ratio was also not identical (Figure 4), and the biggest value was fairly obvious. However, it can not be determined whether the magnitude of collagen fiber angle and the fiber content are all in direct proportion with the pressure that the intestines received (Figure 4, Figure 5), because this depends some degree on the way how it receives the pressure. Using other methods to change its stress still needs to be tested in future experiments. The method of calculating ratios of different pixel values to estimate collagen fiber angle has its feasibility and reliability, which allows a larger area of soft tissue being analyzed with relatively low cost and simple equipment. The disadvantage of this method is the difficulty in determining an appropriate threshold value as well as a definite scope suitable for analyzing which have very important influence on the study results. At the same time, the less δ is to be selected, the more accurate the angle will be.

This paper has tried to acquire the collagen fiber angle of soft tissue in intestine slice through introducing a quantitative analysis method for calculating different pixel values whose validity is verified with computer program, and suggested a practical and effective method for basic research on G.I. disease.

REFERENCES

1 **Sacks MS**, Gloeckner DC. Quantification of the fiber architecture and biaxial mechanical behaviour of porcine intestinal submucosa. *J Biomed Mater Res* 1999; **46**: 1-10

2 **Clarke KM,** Lantz GC, Salisbury SK, Badylak SF, Hiles MC, Voytik SL. Intestine submucosa and polypropylene mesh for abdominal wall repair in dogs. *J Surg Res* 1996; **60**: 107-114

3 **Badylak SF,** Lantz GC, Coffoy A, Geddes LA. Small intestinal submucosa as a large diameter vascular graft in the dog. *J Surg Res* 1989; **47**: 74-80

4 **Fackler K**, Klein L, Hiltner A, Microsc J. Polarizing light microscopy of intestine and its relationship to mechanical behaviour. *J Microsc* 1981; **124**: 305-311

5 **Klein L**, Eichelberger H, Mirian M, Hiltner A. Ultrastructural properties of collagen fiberils In rat intestine. *Connective Tissue Res* 1983; **12**: 71-78

6 **Gabella G**. The cross-ply arrangement of collagen fibers in the submucosa of the mammalian small Intestine. *Cell Tissue Res* 1987; **248**: 491-497

7 **Doering CW**, Jalil JE, Janicki JS, Pick R, Aghili S, Abrahams C, Weber KT. Collagen network remodeling and diastolic stiffness of the rat left ventricle with pressure overload hypertrophy. *Cardiovasc Res* 1988; **22**: 686-695

8 **Whittaker P**, Boughner DR, Kloner RA. Role of collagen in acute myocardial infarct expansion. *Circulation* 1991; **84**: 2123-2134

9 **Yao YL**, Xu B, Zhang WD, Song YG. Gastrin, somatostatin, and experimental disturbance of the gastrointestinal tract in rats. *World J Gastroenterol* 2001; **7**: 399-402

10 **Jalil JE**, Janicki JS, Pick R, Abrahams C, Weber KT. Fibrosis-induced reduction of endomyocardium in the rat after isoproterenol treatment. *Circ Res* 1989; **65**: 258-264

11 **Jorgensen CS,** Assentoft JE, Knauss D, Gregersen H, Briggs GA, Jorgensen Claus S. Small intestine wall distribution of elastic stiffness measured with 500 MHz scanning acoustic microscopy. *Ann Biomed Eng* 2001; **29**: 1059-1063

12 **Eghbali M**, Robinson TF, Seifter S, Blumenfeld OO. Collagen accumulation in heart ventricles as a functiion of growth and aging. *Cardiovasc Res* 1989; **23**: 723-729

13 **Zou XP**, Liu F, Lei YX, Li ZS. Change and role of β-endorphine in plasma and gastric mucosa during the development of rat gastric stress ulceration. *Shanghai Shengwu Yixue Gongcheng* 2001; **22**: 3-5

14 **Jiang ZL**, Li HH, Liu B, Teng ZZ, Qing KR. Biomechanical properties of arteries in experimental hypotensive rats. *Shengwu Yixue Gongchengxue Zazhi* 2001; **18**: 381-384

15 **Wang ZS**, Chen JDZ. Blind separation of slow waves and spikes from gastrointestinal myoelectrical recordings. *IEEE Transactions on Information Technology in Biomedicine* 2001; **5**: 133-137

16 **Cui JH**, Krueger U, Henne-Bruns D, Kremer B, Kalthoff H. Orthotopic transplantation model of human gastrointestinal cancer and detection of micrometastases. *World J Gastroenterol* 2001; **7**: 381-386

17 **James X**, Horace HS, Nabil S, Helena TF, Gateno J, Wang DF, Tideman H. Three-dimensional virtual-reality surgical planning and soft-tissue prediction for orthognathic sugery. *IEEE Transaction on Information Technology in Biomedicine* 2001; **5**: 97-107

18 **Zhao J**, Sha H, Zhou S, Tong X, Zhuang FY, Gregersen H. Remodelling of zero-stress state of small intestine in streptozotocin-induced diabetic rats. Effect of gliclazide. *Dig Liver Dis* 2002; **34**: 707-716

19 **Orberg JM**, Klein L, Hiltner A. Scanning electron microscopy of collagen fibers in intestine. *Connective Tissue Research* 1982; **9**: 187-193

20 **Orberg J**, Baer E, Hiltner A. Organization of collagen fibers in the intestine. *Connective Tissue Research* 1983; **11**: 285-297

21 **Komuro T**. The lattice arrangement of the collagen fibers in the submucosa of the rat small intestine: scanning electron microscopy. *Cell Tissue Res* 1988; **251**: 117-121

22 **Gabella G**. The collagen fibrils in the collapsed and the chronically stretched intestinal wall. *J Ultrastruct Res* 1983; **85**: 127-138

23 **Dickey JP**, Hewlett BR, Dumas GA, Bednar DA. Measuring collagen fiber orientation: A two-dimensional quantitative macroscopic technique. *J Biomech Eng August* 1998; **120**: 537-540

24 **Pu YP,** Li YH, Han YS, Yuan CW, Wu L. Rat keratinocyte primary cultures based on conductive polypyrrole primary cell culture technique. *J Biomed Eng* 2001; **18**: 416-418

25 **Liu XP**, Li YM, Qiu XC, Li J, Yang YL. Effect and mechanism of melatonin on hemorheology in morphine withdrawal rats. *Beijing Shengwu Yixue Gongcheng* 2001; **20**: 143-145

26 **Jiang ZL**, Yang XQ, Ji KH, Chen EY. Effect of endothelin on zero-stress state of arties in spontaneously hypertensive rats (SHR). *Zhongguo Shengwu Yixue Gongcheng Xuebao* 2001; **20**: 289-292

27 **Whittaker P**, Kloner RA, Boughner DR, Pickering JG. Quantitative assessment of myocardial collagen with picrosirius red staining and circularly polarized light. *Basic Res Cardiol* 1994; **89**: 397-410

28 **Slayter EM**. Optical methods in biology. *New York Wiley* 1970: 268-338

29 **Chandraratna PA**, Whittaker P, Chandraratna PM, Gallet J, Kloner RA, Hla A. Characterization of collagen by high-frequency ultrasound: evidence for different acoustic properties based on collagen fiber morphologic characteristics. *Am Heart J* 1997; **133**: 364-368

30 **Pickering JG**, Boughner DR. Quantitative assessment of the age of fibrotic lesions using polarized light microscopy ang digital image analysis. *Am J Pathol* 1991; **138**: 1225-1231

31 **Zhang YJ**. Objective image quality measures and their applications in segmentation evaluation. *Journal of Electronics* 1997; **14**: 97-103

32 **Liu ZW**, Zhang YJ. Image retrieval using both color and texture features. *Tongxun Xuebao* 1999; **20**: 36-40

33 **Dong YN**. A New method for efficiently implementing parallel image ratations. *Dianzi Xuebao* 2001; **29**: 1671-1675

34 **Xue JH**, Zhang YJ, Lin XG. MAP pixel clustering method based on SEM estimation of scatter-plot for low quality image. *Dianzi Xuebao* 1999; **27**: 95-98

35 **Zhang YJ,** Xu Y, Liu ZW, Yao YR, Li Q. A test-bed for retrieving images with extracted features, *Zhongguo Tuxiang Tuxing Xuebao* 2001; **6**: 439-443

36 **Crowe JA,** Gibson NM, Woolfson MS, Somekh MG. Wavelet transform as a potential tool for ECG analysis and compression. *J Biomed Eng* 1992; **14**: 268-272

Edited by Zhu L

P.O.Box 2345, Beijing 100023, China
Fax: +86-10-85381893
E-mail: wjg@wjgnet.com www.wjgnet.com

World J Gastroenterol 2003;9(4):808-812
World Journal of Gastroenterology
 ISSN 1007-9327

• BASIC RESEARCH •

Hormonal regulation of dipeptide transporter (PepT1) in Caco-2 cells with normal and anoxia/reoxygenation management

Bing-Wei Sun, Xiao-Chen Zhao, Guang-Ji Wang, Ning Li, Jie-Shou Li

Bing-Wei Sun, Ning Li, Jie-Shou Li, Department of General Surgery, School of Medicine, Nanjing University, Nanjing 210093, Jiangsu Province, China
Research Institute of General Hospital, Chinese PLA General Hospital of Nanjing Military Area, Nanjing 210002, Jiangsu Province, China
Xiao-Chen Zhao, Guang-Ji Wang, Center of Drug Metabolism and Pharmacokinetics, China Pharmaceutical University, Nanjing 210009, Jiangsu Province, China
Supported by National Natural Science Foundation of China, No. 39970862
Correspondence to: Dr. Bing-Wei Sun, Research Institute of General Surgery, Chinese PLA General Hospital of Nanjing Military Area, 305 East Zhongshan Road, Nanjing 210002, Jiangsu Province, China. sunbinwe@hotmail.com
Telephone: +86-25-3387871 Ext 58088 **Fax:** +86-25-4803956
Received: 2002-10-04 **Accepted:** 2002-11-12

Abstract

AIM: To determine the regulation effects of recombinant human growth hormone (rhGH) on dipeptide transporter (PepT1) in Caco-2 cells with normal culture and anoxia/reoxygenation injury.

METHODS: A human intestinal cell monolayer (Caco-2) was used as the in vitro model of human small intestine and cephalexin as the model substrate for dipeptide transporter (PepT1). Caco-2 cells grown on Transwell membrane filters were preincubated in the presence of rhGH in the culture medium for 4 d, serum was withdrawn from monolayers for 24 h before each experiment. The transport experiments of cephalexin across apical membromes were then conducted; Caco-2 cells grown on multiple well dishes (24 pore) with normal culture or anoxia/reoxygenation injury were preincubated with rhGH as above and uptake of cephalexin was then measured.

RESULTS: The transport and uptake of cephelaxin across apical membranes of Caco-2 cells after preincubation with rhGH were significantly increased compared with controls (P=0.045, 0.0223). Also, addition of rhGH at physiological concentration (34 nM) to incubation medium greatly stimulates cephalexin uptake by anoxia/reoxygenation injuried Caco-2 cells (P=0.0116), while the biological functions of PepT1 in injured Caco-2 cells without rhGH were markedly downregulated. Northern blot analysis showed that the level of PepT1 mRNA of rhGH-treated injured Caco-2 cells was greatly increased compared to controls.

CONCLUSION: The present results of rhGH stimulating the uptake and transport of cephalexin indicated that rhGH greatly upregulates the physiological effects of dipeptide transporters of Caco-2 cells. The alteration in the gene expression may be a mechanism of regulation of PepT1. In addition, Caco-2 cells take up cephalexin by the Proton-dependent dipeptide transporters that closely resembles the transporters present in the intestine. Caco-2 cells represent an ideal cellular model for future studies of the dipeptide transporter.

Sun BW, Zhao XC, Wang GJ, Li N, Li JS. Hormonal regulation of dipeptide transporter (PepT1) in Caco-2 cells with normal and anoxia/reoxygenation management. *World J Gastroenterol* 2003; 9(4): 808-812
http://www.wjgnet.com/1007-9327/9/808.htm

INTRODUCTION

Transport of protein in the form of small peptides (di/tripeptides) across the small intestinal wall is a major route of dietary protein absorption. The H^+-coupled dipeptide transporter, PepT1, is known to be located in the intestine and the kidney, and plays an important role in the absorption of di/tripeptide; in addition, it mediates the intestinal absorption of β-lactam antibiotics, angiotensin-converting enzymeinhibitors, and other peptide-like drugs[1].

To investigate the properties of the human dipeptide transporter, the human intestinal cell line Caco-2 as an in vitro model was employed. The dipeptide transporters normally found in the small intestine are present in Caco-2 cells[2-4]. Also, Caco-2 cells spontaneously differentiate in culture to polar cells possessing microvilli and enterocytic properties[5]. Confluent monolayers form tight junctions between cells[5], and exhibit dome formation[6] and electrical properties of an epithelium[7]. These cells have been evaluated in detail as a model to study both transcellular and paracellular transport of nutrients and drugs in the gut[8-12].

Previous studies have shown that some hormones metabolically regulate the expression of the intestinal dipeptide transporter[13,14]. For example, as the key hormone, insulin increases the membrane population of PepT1 by increasing its translocation from a preformed cytoplasmic pool[14]. However, little is known whether another important hormone, growth hormone (GH), also metabolically regulate the functions of PepT1. The present study was undertaken to evaluate the potential effects of recombinant human growth hormone (rhGH) for the study of the properties of the human PepT1. Especially, we observed the regulation effects of rhGH to PepT1 in Caco-2 cells which were normally cultured or anoxia/reoxygenation injuried. Because dipeptide and some β-lactam antibiotics (cephalexin, cefaclor etc.) share certain structural features such as a peptide bond with an α-amino group and a terminal carboxylic acid group (as illustrated in Figure 1 for cephalexin), it is not surprising that these compounds share a common transport mechanism. Unlike dipeptides, these orally absorbed antibiotics are not hydrolyzed by intestinal peptidases. Consequently, these kinds of drugs are ideal substrates to characterize the PepT1[15-17]. In this study, the uptake and transport of cephalexin were examined.

MATERIALS AND METHODS

Materials

Cephalexin (Figure 1) was obtained from Nanjing No.2 Pharma.Co. Ltd. rhGH was purchased from Laboratoires Serono S.A. (Switzerland). All other chemicals were purchased from Sigma (St. Louis, MO), unless specified. Cell culture

reagents were obtained from Gibco (Grand Island, NY) and culture supplies from Corning (Corning, NY) and Falcon (Lincoln Park, NJ).

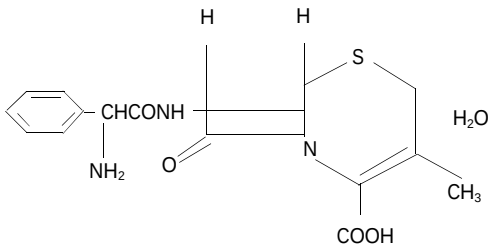

Figure 1 Structure of cephalexin used in this study.

Cell culture

The human adenocarcinoma cell line Caco-2 was obtained from American Tissue Culture Collection (ATCC, Rockville. MD, U.S.A). The cells were passaged as previously described[18]. Caco-2 cells were grown in Dulbecco' s Modified Egle' s Medium supplemented with 1 % nonessential amino acids, 10 % fetal calf serum (FCS), 1 000 UL^{-1} penicillin, and 1 $mg \cdot L^{-1}$ streptomycin (Complete DMEM). For transport Studies, Caco-2 cells were seeded on the polycarbonate filter (0.4-μm pores, 4.71-cm^2 growth area) in the Transwell Cell Culture Chamber System (Costar, Cambridge, MA) at a density of 600 000 cells/filter. The cell monolayers were cultured with 1.5 and 2.6 ml of complete DMEM at the apical and the basolateral chamber, respectively. To assess the integrity of the monolayer, transepithelial electrical resistance (TEER) was monitored by measuring the transmembrane resistance. After subtracting intrinsic resistance (filter alone without cell monolayers) from the total resistance, TEER was corrected for surface area and expressed as Ω cm^2. Transport studies were carried out with cell monolayers that were 21-25 days old. For uptake studies, cells were seeded in the collagen-coated multiwell dishes (24 pore) with the same cell density. All the medium were replaced every day when each experiment began. Monolayers were kept at 37 ℃, 5 % CO_2, and 90 % related humidity.

Transport studies

Before the transport experiments, the culture medium was replaced every day from both sides of the monolayers, 1.5 ml pH 7.0 culture medium with 34nM rhGH were added to apical chamber of Transwell, while 2.6 ml pH 7.0 culture medium without rhGH were added to basolateral chamber. Then Caco-2 cells were cultured for 4 days. The controls were incubated with PH 7.0 culture medium both in apical side and basolateral side. All the monolayers were washed during each experiment. The apical chamber were then filled with 1.5 ml solution containing 1 mM cephalexin. Transport was examined within the time range of 0, 5, 10, 30, 60, 90, and 120 min. At the end of the incubation period, the inserts of Transwell were removed and the transport samples were obtained from the basolateral chambers. The concentrations of cephalexin of the transport samples were determined by High Performance Liquid Chromatography (HPLC, LC-10AT SHIMADIU, Japan) using an isocratic solvent system described previously[19] and the OD value was monitored at 254 nm.

Uptake studies

Using the same way as the transport experiments, the Caco-2 cells cultured in the multiwell dishes (24 pore) were cultured for 4 d with 34 nM rhGH. After washing the monolayers, the transport medium with 1 mM cephalexin was added to the pores and uptake was measured at 0, 5, 10, 30, 60, 90, and 120 min. At the end of the incubation period, cell monolayers were washed with pH 7.4 PBS to remove any extracellular cephalexin. Accumulated concentrations of cephalexin were determined by HPLC after the cells were lysed.

Anoxia-reoxygenation cells model

After Caco-2 cells were plated, media within the wells was reduced to a uniformly thin layer to reduce the diffusion distances for atmospheric gases, while maintaining cell ability. During culture, the monolayers were normally exposed to an atmosphere consisting of 95 % air and 5 % CO_2. Anoxia was produced with an atmosphere of 95 % N_2 and 5 % CO_2 for 90 min, reoxygenation was produced by restoration of the 95 % air, 5 % CO_2 for 30 min. After the period of reoxygenation, the volume of media was restored to the initial volume of 1.0 ml[20] (Figure 2).

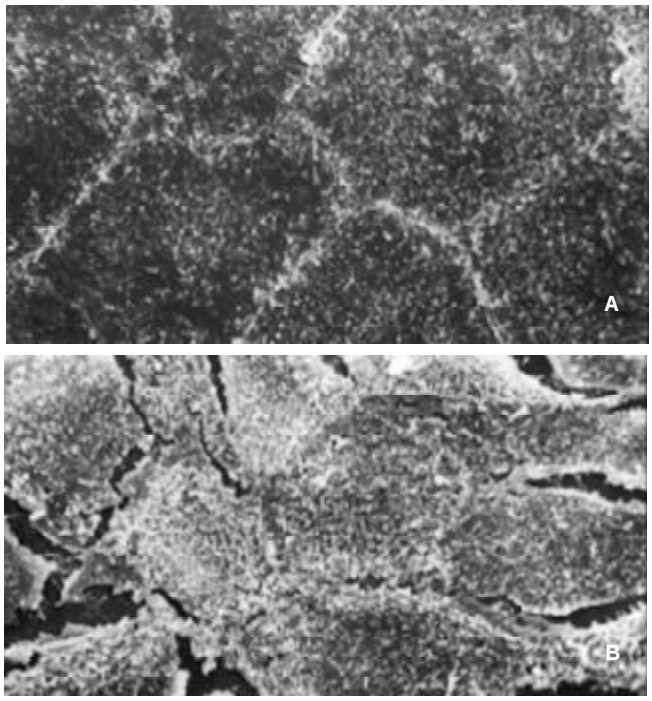

Figure 2 Appearance of scan electronic microscopy of Caco-2 cells. (A) Tight junction formation of normal Caco-2 cells. ×1 000; (B) Tight junction of A/R Caco-2 cells was destroyed partially. ×1 000.

Protein determination

Cells were lysed for 20 min or ice in 2 % Nonidet P-40, 0.2 % SDS, 1 mM dithiothreitol (DTT) in PBS, and total cellular protein was determined using Dc Protein Assay Reagent (BioRad).

Concentration dependence of cephalexin transport

To examine the kinetics of cephalexin transport by rhGH-treated Caco-2 cells, the different concentrations of cephalexin range of 20 to 80 $\mu g \cdot ml^{-1}$ were used.

Northern blotting

Total RNAs were isolated from the Caco-2 cell fractions by extraction with acid guanidine thiocyanate-phenol-chloroform. Total RNAs were denatured by heating at 70 ℃ in 10 $mmol \cdot L^{-1}$ 3-(N-morpholino) propanesulfonic acid (pH 7.0) containing 5 $mmol \cdot L^{-1}$ sodium acetate, 1 $mmol \cdot L^{-1}$ ethylenediaminetetraacetic acid (EDTA), 2.2 $mol \cdot L^{-1}$ formaldehyde, and 50 % (vol/vol) formamide for 5 minutes and subjected to electrophoresis in 1.2 % agarose gel containing 2.2 $mol \cdot L^{-1}$ formaldehyde. Resolved RNA was transferred to hybridization

and was performed in a solution that contains 50 % formamide, 5x sodium chloride-sodium phosphate-EDTA, 2x Denhardt' s solution, and 1 % sodium dodecyl sulfate (SDS). The membranes were exposed and analyzed by Fuji BAS-2000 system. The cDNA probe was prepared from human cDNA libraries.

Sense 5' TTTGGATCCCGGAGTAAGGCATTTCCCAAG 3',
Antisense 5' CCGAAGCTTTCAGGAAGGAGCCTGAGAATATGAG 3'.

Statistical analysis

Data were expressed as mean ±SE. Differences between experimental groups were assessed by analysis of Variance. *P* values of <0.05 were considered statistically significant.

RESULTS

Transepithelial cephalexin transport in Caco-2 cell with normal culture

Caco-2 cells were seeded at a high density of 600 000 cells/ filter, the transport of 1 mM cephalexin across rhGH-treated Caco-2 monolayers, apical-to-basolateral, was examined at PH 6.0 in the donor and pH 7.4 in the receiver compartment. Integrity of the monolayers was monitored by TEER. The apical-to-basolateral transport of cephalexin was significantly increased compared with the controls (P=0.0045) (Figure 3).

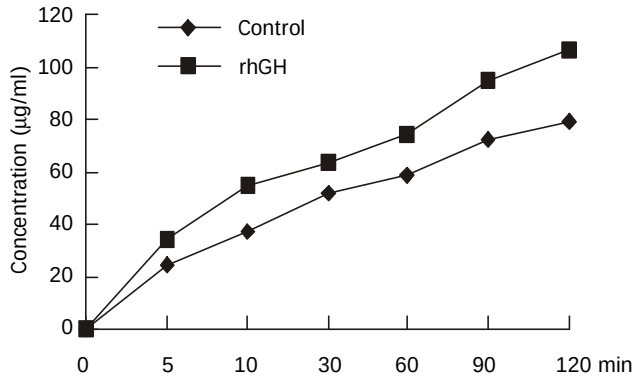

Figure 3 Transport of 1 mM cephalexin in Caco-2 cells. Caco-2 cells were cultured with rhGH in apical side for 4 days. The controls were incubated with PH 7.0 culture medium without rhGH both in apical side and basolateral side. All the monolayers were washed in each experiment. The apical chambers were then filled with 1.5 ml solution containing 1 mM cephalexin. Transport was examined within the time range of 0, 5, 10, 30, 60, 90, and 120 min. At the end of the incubation period, the inserts of Transwell were removed and the transport samples were obtained from the basolateral chambers. The concentrations of cephalexin of the transport samples were determined by HPLC. The apical-to-basolateral transport of cephalexin was significantly increased compared with the controls (P=0.0045).

Uptake of cephalexin in Caco-2 cells with normal culture

Uptake experiments with cephalexin were performed 6-8 days affter seeding and 18 h after media replacement. Cephalexin uptake was measured in the presence and absence of 34nM of rhGH. The differences were significant (P=0.0223), and the results were summarized in Figure 4.

Uptake of cephalexin in anoxia/reoxygenation Caco-2 cells model

Caco-2 monolayers were initially subjected to a 90-minute period of anoxia followed by a 30-minute period of reoxygenation. This was selected as optimal for the main body of the experiment on the basis of the results of our initial experiments. Consequently, the effect of the presence of rhGH on cephalexin uptake via the PepT1 of anoxia/reoxygenation Caco-2 cells were examined (Figure 5). The present studies indicated that uptake and transport of cephalexin by the normal and anoxia/reoxygenation Caco-2 cells were significantly increased under the influence of rhGH.

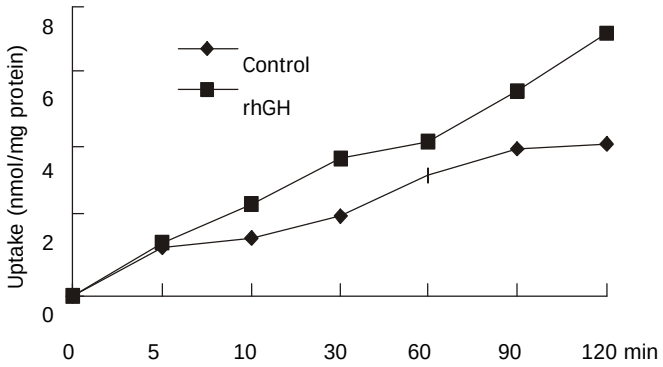

Figure 4 Uptake of 1 mM cephalexin in Caco-2 cells. Caco-2 cells cultured in the multiwell dishes (24 pore) were cultured for 4 d with 34 nM rhGH. After washing the monolayers, the transport medium with 1 mM cephalexin was added to the pores and uptake was measured at 0, 5, 10, 30, 60, 90, and 120 min. At the end of the incubation period, cell monolayers were washed with PH 7.4 PBS to remove any extracellular cephalexin. Accumulated concentrations of cephalexin were determined by HPLC after the cells were lysed. The differences were significant (P=0.0223).

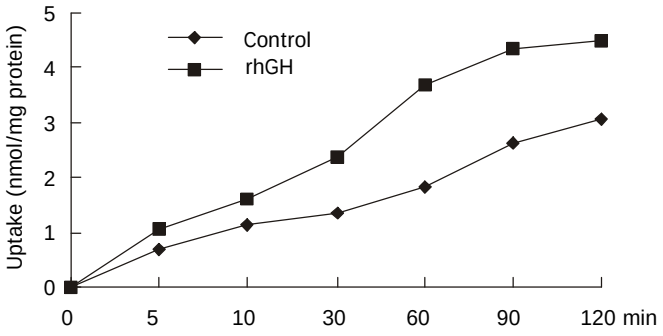

Figure 5 Uptake of 1 mM cephalexin in Caco-2 cells with anoxia / reoxygenation injury. Caco-2 monolayers were initially subjected to a 90-minute period of anoxia followed by a 30-minute period of reoxygenation. The effect of the presence of rhGH on cephalexin uptake via the PepT1 of anoxia / reoxygenation Caco-2 cells was examined. The differences were significant (P=0.0116).

Northern blot analysis

Northern blots of Poly $(A)^+$ RNA, prepared from anoxia/ reoxygenation Caco-2 cells grown either under control conditions or in medium supplemented with 34nM rhGH, were probed separately with ^{32}P-labelled hPepT1 and β-actin cDNAs. The studies showed that the level of mRNA in rhGH-treated Caco-2 Cells was increased 1.3-fold compared with the controls.

Concentration dependence of cephalexin transport

Transport experiments were performed across the rhGH-treated Caco-2 cells using the different concentrations of cephalexin range of 20 to 80 μg· ml^{-1}. The results (Figure 6) indicated that the transport of cephalexin was increased both in rhGH-treated Caco-2 cells and Controls. However, the extent of upregulation of rhGH on the transport was greater than the controls followed the increase of the concentration of cephalexin.

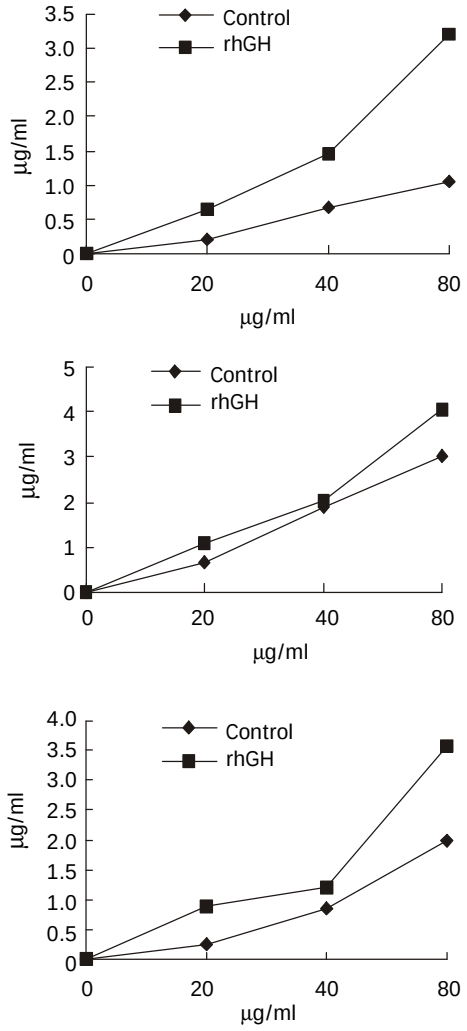

Figure 6 Concentration-dependent transport of cephalexin. The kinetics of cephalexin transport by rhGH-treated Caco-2 cells showed that the transport level of Caco-2 cells was in accordance with the concentration of cephalexin. The concentrations of cephalexin range of 20 to 80 μg· ml^{-1} were used. Transport was determined at the different time-point (a, 15 min; b, 30 min; c, 45 min). The extent of upregulation of rhGH on the transport was greater than the controls followed the increase of the concentration of cephalexin.

DISCUSSION

The nutritional importance of amino acid uptake in the form of short-chain peptides (di/tripeptides) is well known[21]. The intraluminal products of protein digestion are predominantly small peptides[22]. A significant fraction of the dietary amino nitrogen is absorbed as intact dipeptide rather than free amino acids. Absorption of these small peptieds from the gastrointestinal (GI) tract of mammals occurs via the dipeptide transporter (PepT1). Previous studies have shown that the functions of intestine (including PepT1) were changed under the influence of many factors[23,24]. PepT1 seems to play important roles in nutritional and pharmacological therapies; for example, it has allowed the use of small peptide as a source of nitrogen for enteral feeding and the use of oral route for delivery of peptididomimetic drugs such as β-lactam antibiotics. PepT1 was located at the brush-border membranes of the absorptive epithelial cells along the small intestine but absent in crypt and goblet cells[25,26].

To examine the functions of PepT1, we used Caco-2 cells (the human adenocarcinoma cell line) as a unique in vitro intestinal model[27]. One clear advantage of the Caco-2 cells is that the cells stay viable throughout the transport studies. Also, a monolayer of cells may be grown on a porous support to represent an intact epithelium. Some β-lactam anibiotics (cephalexin) and dipeptied share certain structural features, and they are generally in the D-form, which allows them to escape hydrolysis by cytoplasmic peptidases. So these compounds share a common transport mechanism[28]. In this study, we employed cephalexin as an ideal substrate.

The previous studies have shown that the insulin stimulates dipeptide transport by increasing membrane insertion of PepT1 from a preformed cytoplasmic Pool[14], and choleratoxin decreases dipeptide transport by inhibiting the activity of PepT1 through an increase in the intracellular concentration of adenosine 3' , 5;-cyclic monophosphate[21]. It remains unclear, however, whether another key hormone, human growth hormone (hGH), also shows some significant importance. Strong evidence has demonstrated that growth hormone (GH) is an important growth factor for intestine[28]. Complete GH depletion due to hypophysectomy caused pronounced hypoplasia of small intestinal mucosa with decreased villus height and reduced crypt cell proliferation[29]. Simple replacement of GH can restore mucosal proliferative activity[30]. rhGH promotes normal growth and development in the body by changing chemical activity in cells. It activates protein production in muscle cells and the release of energy from fats. rhGH significantly improves the anabolism in parenterally fed[31]. It is typically used to stimulate growth in children with hormone deficiency, or to treat people with severe illness, burns or sepsis where destruction of human tissue and muscle occurs[32-34]. Many of the effects of human growth hormone are brought about by the insulin-like growth factor 1 (IGF-1), which the growth hormone stimulates. IGF-1 plays an important part in growth-promoting effects of rhGH[32]. The present studies showed that the uptake and transport of cephalexin in Caco-2 cells were greatly increased by using of rhGH. In addition, a specific injured cell model, anoxia/reoxygenation Caco-2 cells model, was established in our present experiment. The uptake of cephalexin in the injured Caco-2 cells was markedly decreased while the cephalexin uptake was significantly increased in the injured Caco-2 cells with treatment of rhGH. These results indicate that the functions of PepT1 in Caco-2 cells were upregulated by rhGH. The investigation of concentration-dependent transport of cephalexin in Caco-2 cells showed that the transport was increased both in rhGH-treated Caco-2 cells and controls. However, the upregulating extent of rhGH on the transport of cephalexin was greater than controls following the increase of the concentration of cephalexin. Northern blot analysis showed that the level of PepT1 mRNA of injured Caco-2 cells with rhGH treatment were increased. This result also provides novel information about the mechanism of regulation action of rhGH. It has suggested that the alteration in the gene expression may be a mechanism of regulation of PepT1.

Use of this experimental design leads to the following three questions. What is the detail mechanism of upregulating the functions of PepT1 by rhGH? How does the rhGH receptor distribute in Caco-2 cells? How does the rhGH receptor change in anoxia/reoxygenation Caco-2 cells? Clearly, the present study needs to be followed by further studies on physiology and biology of hormonal regulation of PepT1.

REFERENCES

1 **Hsu CP**, Walter E, Merkle HP, Rothen-Rutishauser B, Wunderli-Allenspach H, Hilfinger JM, Amidon GL. Function and immunolocalization of over expressed human intestinal H^+/peptide cotransporter in adenovirus-transduced Caco-2 cells. *AAPS PharmSci* 1999; **1**: E12

2 **Vincent ML**, Russell RM, Sasak V. Folic acid uptake characteristics of a human colon carcinoma cell line, Caco-2. A newly-described cellular model for small intestinal epithelium. *Hum Nutr Clin Nutr* 1985; **39**: 355-360

3 **Mohrmann I**, Mohrmann M, Biber J, Murer H. Sodium-dependent transport of Pi by an established intestinal epithelial cell line(Caco-2). *Am J Physiol* 1986; **250**(3 Pt 1): G323-330

4 **Blais A**, Bissonnette P, Berteloot A. Common characteristics for Na+-dependent sugar transport in Caco-2 cells and human fetal colon. *J Member Biol* 1987; **99**: 113-125

5 **Rousset M**, Laburthe M, Pinto M, Chevalier G, Rouyer-Fessard C, Dussaulx E, Trugnan G, Boige N, Brun JL, Zweibaum A. Enterocytic differentiation and glucose utilization in the human colon tumar cell line Caco-2: modulation by forskolin. *J Cell Physiol* 1985; **123**: 377-385

6 **Romond MJ**, Martinot-Peignoux M, Erlinger S. Dome formation in the human colon carcinoma cell line Caco-2 in culture. Influence of ouabain and permeable supports. *Biol Cell* 1985; **54**: 89-92

7 **Grasset E**, Pinto M, Dussaulx E, Zweibaum A, Desjeux JF. Epithelial properties of human colonic carcinoma cell line Caco-2: electrical parameters. *Am J Physiol* 1984; **247**(3 Pt 1): C260-267

8 **Milovic V**, Turchanowa L, Stein J, Caspary WF. Transepithelial transport of putrescine across monolayers of the human intestinal epithelial cell line, Caco-2. *World J Gastroenterol* 2001; **7**: 193-197

9 **Hidalgo IJ,** Raub TJ, Borchardt RT. Characterization of the human colon carcinoma cell line (Caco-2) as a model system for intestinal epithelial permeability. *Gastroenterology* 1989; **96**: 736-749

10 **Artursson P**. Epithelial transport of drugs in cell culture. I: A moded for studying the passive diffusion of drugs over intestinal absorptive (Caco-2) cells. *J Pharm Sci* 1990; **79**: 476-482

11 **Artursson P**, Karlsson J. Correlation between oral drug absorption in humans and apparent drug permeability coefficients in human intestinal epithelial (Caco-2) cells. *Biochem Biophys Res Commun* 1991; **175**: 880-885

12 **Artursson P**. Cell cultures as models for drugs absorption across the intestinal mucosa. *Crit Rev Ther Drug Carrier Syst* 1991; **8**: 305-330

13 **Thamotharan M**, Bawani SZ, Zhou X, Adibi SA. Hormonal regulation of oligopeptide transporter PepT1 in a human intestinal cell line. *Am J Physiol* 1999; **276**(4 Pt 1): C821-826

14 **Nielsen CU**, Amstrup J, Steffansen B, Frokjaer S, Brodin B. Epidermal growth factor inhibits glycylsarcosine transport and hPepT1 expression in a human intestinal cell line. *Am J Physiol Gastrointest Liver Physiol* 2001; **281**: G191-199

15 **Ganapathy V**, Mendicino JF, Leibach FH. Transport of glycyl-L-proline into intestinal and renal brush border vesicles from rabbit. *J Biol Chem* 1981; **256**: 118-124

16 **Rajendran VM**, Ansari SA, Harig JM, Adams MB, Khan AH, Ramaswamy K. Transport of glycyl-L-proline by human intestinal brush border membrane vesicles. *Gastroenterology* 1985; **89**: 1298-1304

17 **Berteloot A.** Membrane potential dependence of glutamic acid transport in rabbit jejunal brush-border membrane vesicles: K+ and H+ effects. *Biochim Biophysi Acta* 1986; **861**: 447-456

18 **Dantzig AH**, Bergin L. Uptake of the cephalosporin, cephalexin, by a dipeptide transport carrier in the human intestinal cell line, Caco-2. *Biochim Biophys Acta* 1990; **1027**: 211-217

19 **Dantzig AH**, Bergin L. Carrier-mediated uptake of cephalexin in human intestinal cells. *Biochim Biophys Res Commun* 1988; **155**: 1082-1087

20 **Ratych RE**, Chuknyiska RS, Bulkley GB. The primary localization of free radical generation after anoxia / reoxygenation in isolated endothelial cells. *Surgery* 1987; **102**: 122-131

21 **Ferraris RP**, Diamond J, Kwan WW. Dietary regulation of intestional transport of the dipeptide carnosine. *Am J Physiol* 1988; **255**(2 Pt 1): G143-150

22 **Ganapath V**, Brandsch M, Leibanch FH. Intestinal transport of amino acids and peptides. In: Johnson LR, ed. Physiology of the gastrointestinal tract. Volum 2. 3rd ed. *New York: Raven* 1994: 1773-1794

23 **Li YS**, Li JS, Li N, Jiang ZW, Zhao YZ, Li NY, Liu FN. Evaluation of various solutions for small bowel graft preservation. *World J Gastroenterol* 1998; **4**: 140-143

24 **Liang LJ**, Yin XY, Luo SM, Zheng JF, Lu MD, Huang JF. A study of the ameliorating effects of carnitine on hepatic steatosis induced by total parenteral nutrition in rats. *World J Gastroenterol* 1999; **5**: 312-315

25 **Ogihara H**, Saito H, Shin BC, Terada T, Takenoshita S, Nagamachi Y, Inui K, Takata K. Immuno-localization of H^+/peptide cotransporter in rat digestive tract. *Biochem Biophys Res Commun* 1996; **220**: 848-852

26 **Adibi SA**. The oligopeptide transporter (PepT1) in human intestine: Biology and Function. *Gastroenterology* 1997; **113**: 332-340

27 **Dantzig AH**, Bergin L. Uptake of the cephalosporin, cephalexin, by a dipeptide transport carrier in the human intestinal cell line, Caco-2. *Biochim Biophys Acta* 1990; **1027**: 211-217

28 **Zhou X**, Li YX, Li N, Li JS. Effect of bowel rehabilitative therapy on structural adaptation of remnant small intestine: animal experiment. *World J Gastroenterol* 2001; **7**: 66-73

29 **Bastie MJ**, Balas D, Laval J, Senegas-Balas F, Bertrand C, Frexinos J, Ribet A. Histological variations of jejunal and ileal mucosa on days 8 and 15 after hypophysectomy in rat: morphometrical analysis on light and electron microscopy. *Acta Anat (Basel)* 1982; **112**: 321-337

30 **Scow RO**, Hagan SN. Effect of testosterone Propionate and growth hormone on growth and chemical composition of muscle and other tissues in hypophy sectomized male rats. *Endocrinology* 1965; **77**: 852-858

31 **Gu Y**, Wu ZH. The anabolic effects of recombinant human growth hormone and glutamine on parenterally fed, short bowel rats. *World J Gastroenterol* 2002; **8**: 752-757

32 **Jeschke MG,** Herndon DN, Wolf SE, Debroy MA, Rai J, Lichtenbelt BJ, Barrow RE. Recombinant human growth hormone alters acute phase reactant proteins, cytokine expression, and liver morphology in burned rats. *J Surg Res* 1999; **83**: 122-129

33 **Roth E,** Valentini L, Semsroth M, Holzenbein T, Winkler S, Blum WF, Ranke MB, Schemper M, Hammerle A, Karner J. Resistance of nitrogen metabolism to growth hormone treatment in the early phase after injury of patient with multiple injuries. *J Trauma* 1995; **38**: 136-141

34 **Postel-Vinay MC,** Finidori J, Sotiropoulos A, Dinerstein H, Martini JF, Kelly PA. Growth hormone receptor: structure and signal transduction. *Ann Endocrinol* 1995; **56**: 209-212

Edited by Xu JY

P.O.Box 2345, Beijing 100023, China
Fax: +86-10-85381893
E-mail: wjg@wjgnet.com www.wjgnet.com

World J Gastroenterol 2003;9(4):813-817
World Journal of Gastroenterology
 ISSN 1007-9327

• BASIC RESEARCH •

Experimental study on the feasibility and safety of radiofrequency ablation for secondary splenomagely and hypersplenism

Quan-Da Liu, Kuan-Sheng Ma, Zhen-Ping He, Jun Ding, Xue-Quan Huang, Jia-Hong Dong

Quan-Da Liu, Kuan-Sheng Ma, Zhen-Ping He, Jun Ding, Jia-Hong Dong, Institute of Hepatobiliary Surgery, Southwest Hepatobiliary Surgery Hospital, Southwest Hospital, Third Military Medical University, Chongqing, 400038, China
Xue-Quan Huang, Department of Radiology, Southwest Hospital, Third Military Medical University, Chongqing, 400038, China
Supported by the "Tenth-Five" Fundamental Medical Scientific Research Projects of PLA, China, No. 02Z005
Correspondence to: Dr. Quan-Da Liu, Institute of Hepatobiliary Surgery, Southwest Hepatobiliary Surgery Hospital, Southwest Hospital, Third Military Medical University, Chongqing, 400038, China. liuquanda@sina.com
Telephone: +86-23-65398541
Received: 2002-10-08 **Accepted:** 2002-11-09

Abstract

AIM: To assess the feasibility and safety of radiofrequency ablation (RFA) in treatment of secondary splenomagely and hypersplenism.

METHODS: Sixteen healthy mongrel dogs were randomly divided into two groups, group I (n=4) and group II (n=12). Congestive splenomegaly was induced by ligation of splenic vein and its collateral branches in both groups. At the end of 3rd week postoperation, RFA in spleen was performed in group II *via* laparotomy, complications of RFA were observed, CT scan was performed and the spleens were obtained. The radiofrequency (RF) thermal lesions and histopathology of spleen were examined regularly.

RESULTS: No complication or death was observed in both groups; CT revealed that the splenomegaly lasted over 2 months after ligation of splenic vein; the segmental RF lesions included hyperintense zone of coagulative necrosis and more extensive peripheral hypointense infarcted zone, the latter was called "bystander effect". The infarcted zone would be absorbed and subsequently disappeared in 4-6 weeks after RFA accompanied with shrinkage of the remnant spleen. The fundamental histopathological changes of splenic lesions caused by RF thermal energy included local coagulative necrosis, peripheral thrombotic infarction zone, subsequent tissue absorption and fibrosis in the zone of thrombotic infarction, the occlusion of vessels in remnant viable spleen, deposition of extensive fibrous protein, and disappearance of congestive splenic sinusoid - "splenic carnification". Those pathologic changes were underline of shrinkage of spleen.

CONCLUSION: It is feasible and safe to perform RFA in spleen to treat experimental splenomegaly and hypersplenism. The RFA could be safely performed clinically via laparotomy or laparoscopic procedure while spleen was strictly separated from surrounding organs.

Liu QD, Ma KS, He ZP, Ding J, Huang XQ, Dong JH. Experimental study on the feasibility and safety of radiofrequency ablation for secondary splenomagely and hypersplenism. *World J Gastroenterol* 2003; 9(4): 813-817
http://www.wjgnet.com/1007-9327/9/813.htm

INTRODUCTION

Radiofrequency ablation (RFA) was developed in 1990s and thereafter evolved rapidly as a minimally invasive technique for the treatment of primary and secondary malignant tumors in solid organs[1-25]. The fundamental principle is that alternating electric current operated in the range of radiofrequency (460-500 kHz) can produce a focal thermal injury in living tissue, the tip of the electrode conducts the current, causing local ionic agitation and subsequent frictional heat (90-110 ℃). Temperatures over 60 ℃ produce uniform tissue coagulative necrosis, a 2-5 cm spherical thermal injury can be produced with each ablation. The potential benefits of these techniques over conventional surgical options include tumor ablation in nonsurgical candidates with low morbidity, and being used on an outpatient basis[1-15].

One of the most manifestations of liver cirrhosis with portal hypertension was hypersplenism secondary to splenic congestion with intrasplenic sequestration and destruction of erythrocytes, leucocytes and platelets resulting in anemia, leucopenia and thrombocytopenia[26]. Splenectomy is a routine therapy for hypersplenism and can correct the abnormal hematologic parameters[26,27]. However, with the awareness of the role and importance of the spleen in the immune system, splenic conservative methods have gained prominence in the treatment of benign conditions of the spleen[27-29]. Several minimally invasive treatment modalities such as transcatheter selective splenic arterial embolization[30], absolute alcohol or ethanolamine oleate intrasplenic injection[31,32] have been investigated clinically, but the clinical applications were restricted due to associated complications.

In order to establish an effective therapy for hypersplenism with splenomegaly, animal model with splenomegaly was induced by ligation of splenic vein (LSV), the computerized tomographic (CT) and pathologic changes of the thermal lesions in spleen after RFA were observed, and the feasibility and safety of RFA for secondary splenomagely and hypersplenism and its potential clinical prospective were investigated.

MATERIALS AND METHODS

Animals and experimental design

Sixteen healthy adult mongrel dogs (12 to 17 kg) were randomly divided into two groups. LSV *plus* Laparotomy were performed in Group I (n=4), and LSV *plus* RFA were done in Group II (n=12).

After fasting overnight, the animals were anesthetized generally with sodium pentobarbital (25 mg/kg) and maintained with supplemental doses of sodium pentobarbital. The great saphenous vein was cannulated for transfusion with 500 ml of acetate Ringer' s solution. Midline incision was used to access the spleen, splenic veins in both groups were ligated at the confluent to portal vein, and then the main branches of splenic vein were further ligated separately at the splenic hilus in order to minimize collateral formation. The animals were cared in cages at 24±2 ℃ and fed with standard diet and water ad libitum after operation. At the end of the third week, under general anesthesia again, the animals in group I were performed laparotomy only; and both laparotomy and RFA of spleen were done in group II.

Ablation procedures

RFA was performed with the RF 2000 generator system (Radio Therapeutics Corp., CA, USA), which consists of a generator generating [pup to 90 W in power, a leVeen monopolor array needle electrode (3.5 cm maximum array diameter), and tow electrode pads (grounding pads) placed on the animal' s shaved thighs. The leVeen needle electrode is a 15-gauge, 15-20 cm in length insulated cannula containing 10 individual hook-shaped retractable electrode arms that deployed in situ after placement of the needle electrode in splenic parenchyma. The probe was inserted perpendicularly into the splenic parenchyma in lateral region of superior or inferior pole of spleen, and the spleen was elevated to avoid to contact with adjacent organs and skin. A 90 W monopolar radiofrequency generator (RF 2000, Radiotherapeutics) was used as the energy source. Power output was initially set at 30 W and manually titrated 10 W per 60 sec until the maximum power. Thereafter, impedance could rise with automatic power adjustment until power output was terminated. The electrode 0.5 cm retrograded in situ and above session repeated. The needle track was cauterized on needle removal.

During RFA procedure, the temperatures on the sites of thermal lesions, hilum of spleen and the tail of pancreas were measured frequently by thermosensors, and cold saline was used to lower the temperature on the hilum of spleen, and tail of pancreas. Five-hundred ml of acetate Ringer' s solution and 0.8M IU of penicillin were given intravenously.

Observation of animals

The complications during RFA, such as hemorrhage, thermal injury of other organs, the appetites, eating and activities of animals, morbidity and mortality after RFA were carefully documented.

CT imaging and histopathology on splenic lesions

Splenic sizes in group I after LSV were documented with CT scans (Siemens Medical System, Germany) at 3, 6, 9 weeks after laparotomy. CT imaging (plain scan plus enhancement) performed for the dogs in group II after RFA on day 1, and at 1, 2, 4, 6 and 9 weeks after RFA to study the thermal injured lesions in spleens. Two dogs in group II were killed immediately after CT scan, and all dogs were sacrificed at the end of the 9th week. Before sacrificing the dogs, spleens were removed, specimen of liver and pancreas were harvested and fixed in 10 % formaldehyde, and routine histopathological studies were processed and examined under light microscopy.

RESULTS

Animals

The RFA procedure took 30 to 58 minutes, the temperatures on 0.5 cm in depth of thermal lesion in spleens were over 100 ℃ as reaching to the maximum impedance. The temperatures on the hilum of spleen were 45-50 ℃, the temperatures was kept below 42 ℃ with iced cold saline. There was a temperature gradient rising from lateral to center of splenic hilum due to blood inflow. Thus, choosing puncture site on lateral region of superior or inferior pole of spleen could enlarge the size of thermal lesions, and approximately 40-50 % of spleen could be damaged on each episode of RFA. Minor or mild bleeding from the puncture site of spleen immediately after inserting the electrode may occur and would be stopped automatically in 5 minutes due to thermal coagulation if the electrode was kept still. The animals could well tolerate the RFA, distressing in 5 dogs due to high tension of spleen capsule caused by thermal injury was resolved after administration of tranquilizer. The dogs fasted on the day of RFA were lethargic or anorexic. All dogs were fed normally after RFA. Restlessness, vomiting and anorexia, significant body weights change and complications of surgery such as gastrointestinal perforation, peritonitis, intra-abdominal hemorrhage, rupture of spleen or hydrothorax and death were not observed at all.

CT imaging of spleens

Splenomegaly in group I could persisted over 2 months. The enhanced CT revealed that each RF thermal lesion could destroy one lobe or multiple splenic segments, and the splenic capsule was intact except small part of hilum. The ablated lesion included two zones: (a) hyperintense zone of coagulative necrosis; (b) more extensive peripheral hypointense infarcted zone - the latter was called "bystander effect". No perisplenic or splenic abcess was formed (Figure 1). The infarcted zone would be absorbed in 4 to 6 weeks after RFA, and subsequently disappeared in two months, and the size of remnant spleen shrunk significantly (Figure 2, 3).

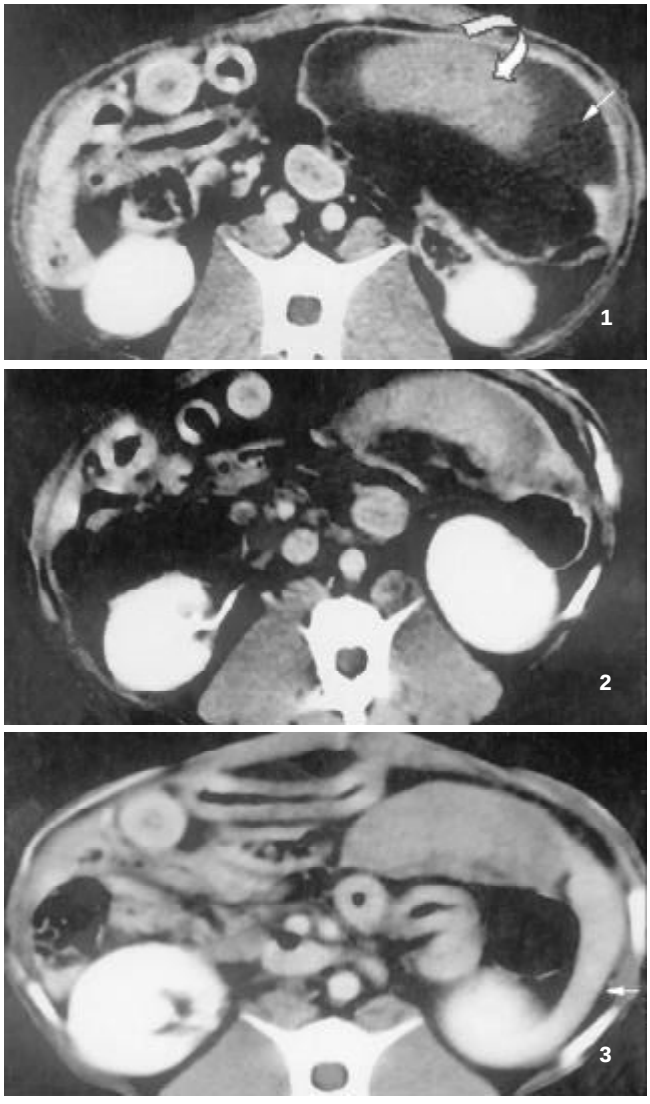

Figure 1 Enhanced CT demonstrated multiple segmental ablated lesion at the end of 2nd week after RFA, the splenic capsule was continuous, the thermal lesion included 2 zones, namely hyperintense zone of coagulative necrosis and peripheral hypointense infarcted zone; no perisplenic or splenic abcess was seen.

Figure 2 The lesion of infarcted zone was mostly absorbed at the end of 6th week after RFA.

Figure 3 The lesion of infarcted zone was absorbed absolutely at the end of 9th week after RFA, however, the lesion of coagulative necrosis hardly altered, the remnant spleen shrinked significantly (arrow).

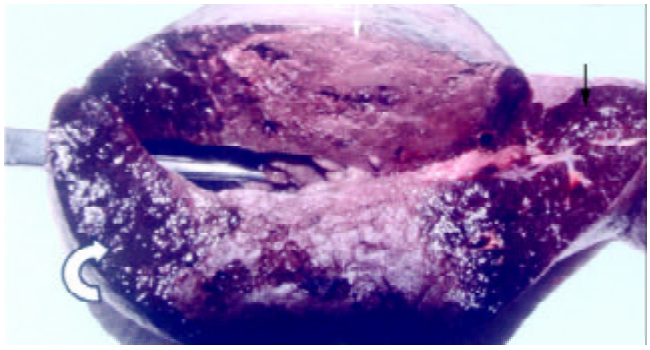

Figure 4 The appearance of the spleen the day after RFA, showed the lesion included the zone of soid-yellow dry necrosis (white arrow) and dark-red zone of thrombotic infarction (curve arrow), and the bright red normal spleen (black arrow); each ablation created a lesion with maximum diameter of 9 cm.

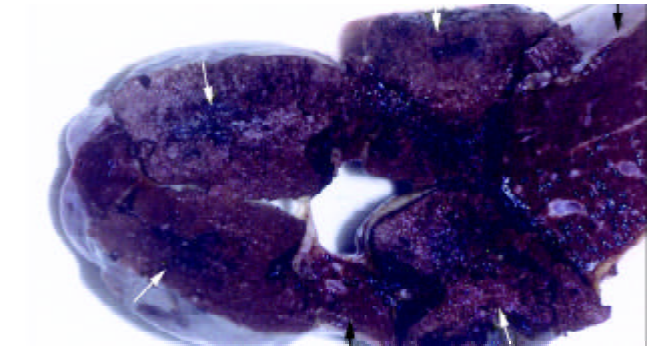

Figure 5 The lesion of infarcted zone was absorbed absolutely at the end of 9th week after RFA, however, the lesion of coagulative necrosis hardly altered (arrow).

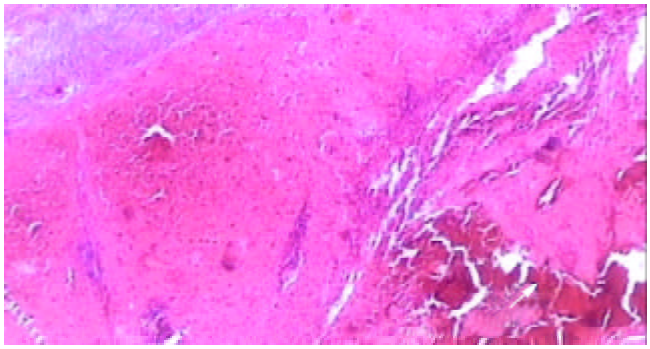

Figure 6 Light microscopic appearance of the coagulative necrosis at the end of 2nd week after RFA, the intrasplenic hemorrhage at the probe insertion site could see (arrow), the splenic capsule thickened (HE. ×40).

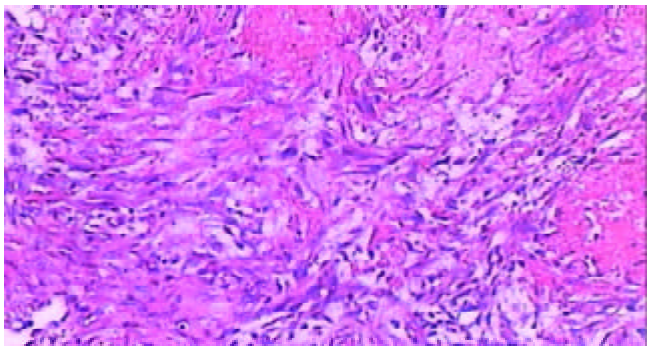

Figure 7 Microscopic examination at the junction of the necrotic region and infarcted region at the end of 2nd week after RFA, massive fibroblasts and inflammatory cells aggregated, the microthrombus dissolved (HE. ×200).

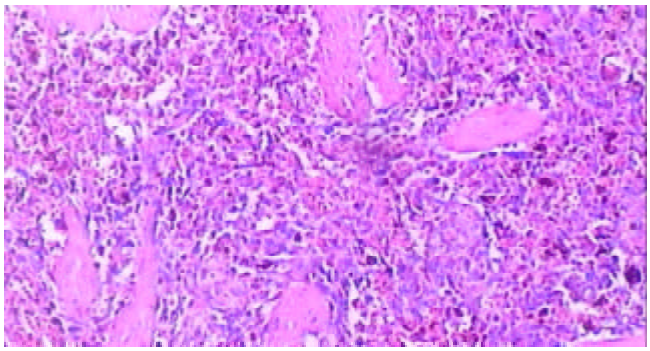

Figure 8 Microscopic examination of the thrombotic infarction at the end of 4th week after RFA, the microthrombus dissolved, and extensive macrophages with hemosiderin deposition presented (HE. ×100).

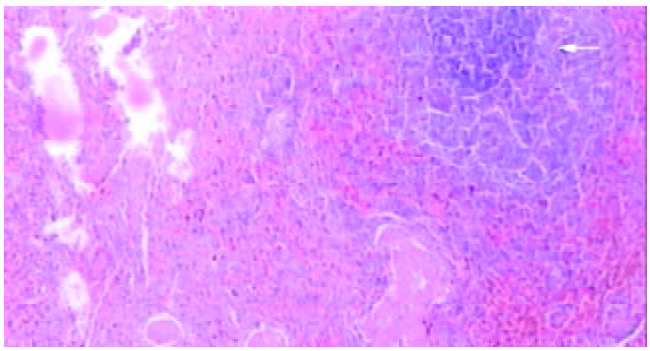

Figure 9 Microscopic appearance of "plenic carnification"of the normal viable splenic tissue distant form ablative lesion at the end of 9th week after RFA, the tissue structure consolidated, larger vessels occluded, extensive fibrous protein deposited, and the congestive splenic sinusoid disappeared; however, the structure of splenic lymphoid nodule was intact (arrow) (HE. ×40).

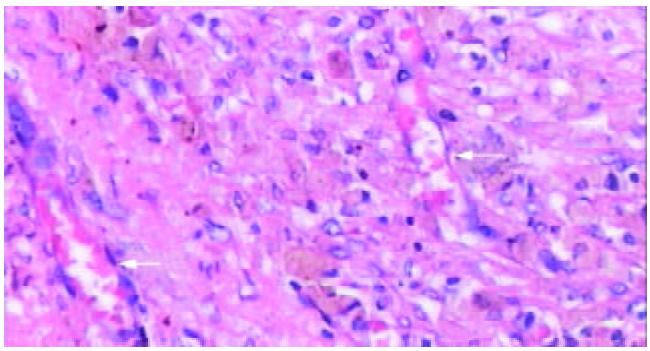

Figure 10 The typical appearance of poorly vascularized splenic tissue due to "plenic carnification" after RFA. The splenic sinusoid disappeared, tissue structure consolidated, granular hemosiderin deposition and sparsely neovascularized vessels (arrow) presented clearly (HE. ×200).

Histopathology

Splenomegaly in gross appearance was existed in 2 months after ligation of splenic veins. The areas of ablated lesions had dot swollen dark red appearance, the spleens shrunk significantly and approached to the normal size at the end of ninth week after RFA. The macroscopic and microscopic of liver and pancreas were normal. The omentum was adherent to the ablated surface of the spleen in most cases. The appearances of cut surface of the ablated lesions matched

with the CT imaging, including the zone of soil-yellow dry necrosis and zone of thrombotic infarction (Figure 4), and the lesions became dry necrosis after the thrombotic infarction was absorbed (Figure 5). No obvious intrasplenic hemorrhage except the puncture tract was seen with microscopic examination (Figure 6). The RF energy caused focal tissue coagulative necrosis, massive vessels in the spleen were damaged thermally and occluded, consequently broad microthrombus leaded to the peripheral thrombotic infarction, which is called as bystander effect corresponding to the CT finding. Thrombotic infarction zone had absorbed by macrophages gradually in 4-6 weeks, where fibroblasts proliferation and local fibrosis were demonstrated. Even though some part of spleen appeared normal and viable, there had obvious thickened intima, occluded vessels, extensive fibrous protein deposition, and the absence of congestive splenic sinusoid, which we called as splenic carnification, the most important pathological basis of the shrunken spleen (Figure 7-10).

DISCUSSION

Hypersplenism is one of the common manifestations, 70-80 % patients with cirrhotic hypertension present with various degrees of splenomegaly and hypersplenism. The immune function in patients with hypersplenism would be reduced due to leucopenia, thrombocytopenia and erythropenia. Splenectomy is the traditional treatment for hypersplenism. However, patients with cirrhotic splenomegaly and hypersplenism often have many complications, which are the contraindication of splenectomy. Furthermore, endoscopic ligation or sclerosing of varices for esophageal varices bleeding due to cirrhotic portal hypertension was advocated as first line treatment in western countries, splenectomy plus devascularization are commonly abandoned[33-38]. With the awareness of the role and importance of the spleen in the immune system, it is recommended to reserve the splenic tissue and function as much as in the treatment of benign conditions of the spleen. Thereby, new safe, effective and minimal invasive modalities should be established.

Radiofrequency ablation (RFA) technique is a safe and effective minimally invasive modality and has been clinically used in treatment of many malignant tumors and some benign tumors in solid organs[1-25]. Until now, only two cases in treatment of colorectal and renal splenic metastasis using RFA were reported[39, 40], no data of experimental or clinical study regarding the safety and efficacy of RFA for hypersplenism is available. The safety and effectiveness may be the cardinal considerations that impede the attempts. The limited necrotic volume identical to the lesion in liver for hepatocellular carcinoma with 3-5 cm maximal diameter could scarcely reduce the size of splenomegaly, consequently could be futile to ameliorate cytopenia for hypersplenism. However, theoretically, RFA could be used for hypersplenism due to portal hypertension: (a) spleen is a solid organ, thermal energy can cause focal tissue coagulative necrosis, and the RF heat energy has the role of electric coagulation[39,40]; (b) certain time of RF thermal energy can lead to endothelial cells degeneration of vessels and sinus, thrombosis, and occlusion of vessels and splenic sinusoid, therefore produces effect of ablating larger lesion[17]; (c) puncture of spleen with needle is relative safe, the morbidity rate of biopsy reported using 18-22 gauge needles for splenic lesions including splenomegaly is 0-5.2 %, without mortality[41-43]; (d) the inflammatory reaction and neovascularization at the site of RFA lesion could create extensive collateral circulation between portal-cava vein systems, and reduce blood inflow to portal vein due to smaller spleen, sequentially depress the portal hypertension[28]. Clinically, we performed RFA for splenomegaly intraoperatively before splenectomy, only minor or mild bleeding occurred but stopped within few minutes (data not shown), and we found this procedure was practicable.

For these reasons, we carried out the study on RFA for splenomegaly and hypersplenism in canine models (the blood counts of peripheral samples in splenomegaly models also showed thrombocytopenia, erythropenia without leucopenia, which is similar to the result of Sahin *et al*[44], and the hematologic abnormalities could be corrected by RFA; data not shown), results of preliminary study confirmed part of above presumptions.

First, RFA procedure for spleen is relative safe. Although bleeding occurred immediately following inserting of electrodes into the spleen, it ceased soon due to thermal coagulation. In order to avoid the potential risks, several important steps should be followed, the puncture site must be kept away from large vessels at hilum of spleen, the electrode should be fixed to reduce bleeding; the spleen should be elevated to avoid to contact with adjacent organs and skin; cool saline should be used on the surface of the hilum of spleen, tail of pancreas to reduce energy deposition and avoid thermal damage of pancreas. In our preliminary experiment, dog' s thighs were burned due to insufficient shave of thigh and thus incomplete attachment of electrode pads; and another dog died from severe burning of internal organs, because spleen was not isolated from skin and intra-abdominal viscera. However, no morbidity and mortality occurred after procedures above in experiment were followed strictly. In addition, puncture of needle at lower pole of spleen is preferable to reduce the pulmonary complications and referred pain. If this procedure were used clinically, exposure and protection of spleen would be helpful in avoiding complications.

Second, the area of RF thermal ablated lesion is so large that compasses one lobe or multiple segments of spleen. The area of coagulative necrosis zone in spleen is similar to that of RF lesion in liver[12,25], but the RFA in spleen also has "bystander effect" - the RF energy causes multiple segmental thrombotic infarction, enables for the management of hypersplenism effectively. The RF energy triggers occlusion of broad intrasplenic microthrombi and vessels, and absorption of area with thrombotic infarction. Even in the remaining normal splenic tissue, obvious occluded vessels, extensive fibrous protein deposition with no congestion of splenic sinusoid are still existed. The changes of "splenic carnification" are responsible for the shrinking of the remnant spleen, which could explain precisely why splenic RFA ameliorated the cytopenia.

In summary, it is feasible and safe to perform RFA in spleen to treat secondary splenomegaly and hypersplenism in a canine model, and yet its clinical application is worthy of further study. The peculiar radiological and pathological splenic changes after RFA could be used as clinical indicators for therapeutic effect and the follow-up in the therapy of hypersplenism. With the development of technique, such as RFA with the minimally invasive procedures, it would provide promising effect on selected patients with hypersplenism[17].

REFERENCES

1 **Ma K**, Min C, Ian HX, Jiahong D. Prevention and cure of complications from multiple-electrode radiofrequency treatment of liver tumors. *Dig Dis* 2001; **19**: 364-366
2 **Liu LX**, Jiang HC, Piao DX. Radiofrequence ablation of liver cancers. *World J Gastroenterol* 2002; **8**: 393-399
3 **Tang ZY**. Hepatocellular carcinoma-Cause, treatment and metastasis. *World J Gastroenterol* 2001; **7**: 445-454
4 **Qin LX**, Tang ZY. The prognostic significance of clinical and pathological l features in hepatocellular carcinoma. *World J Gastroenterol* 2002; **8**: 193-199

5 **Wu MC**, Shen F. Progress in research of liver surgery in China. *World J Gastroenterol* 2000; **6**: 773-776
6 **Makin GB**, Breen DJ, Monson JR. The impact of new technology on surgery for colorectal cancer. *World J Gastroenterol* 2001; **7**: 612-621
7 **Wood BJ**, Ramkaransingh JR, Fojo T, Walther MM, Libutti SK. Percutaneous tumor ablation with radiofrequency. *Cancer* 2002; **94**: 443-451
8 **Primrose JN**. Treatment of colorectal metastases: surgery, cryotherapy, or radiofrequency ablation. *Gut* 2002; **50**: 1-5
9 **Seidenfeld J**, Korn A, Aronson N. Radiofrequency ablation of unrespectable primary liver cancer. *J Am Coll Surg* 2002; **194**: 813-828
10 **Goldberg SN**, Kamel IR, Kruskal JB, Reynolds K, Monsky WL, Stuart KE, Ahmed M, Raptopoulos V. Radiofrequency ablation of hepatic tumors: increased tumor destruction with adjuvant liposomal doxorubicin therapy. *AJR Am J Roentgenol* 2002; **179**: 93-101
11 **Hall-Craggs MA**, Vaidya JS. Minimally invasive therapy for the treatment of breast tumors. *Eur J Radiol* 2002; **42**: 52-57
12 **Morimoto M**, Sugimori K, Shirato K, Kokawa A, Tomita N, Saito T, Tanaka N, Nozawa A, Hara M, Sekihara H, Shimada H, Imada T, Tanaka K. Treatment of hepatocellular carcinoma with radiofrequency ablation: radiologic-histologic correlation during follow-up periods. *Hepatology* 2002; **35**: 1467-1475
13 **Elias D**, De Baere T, Smayra T, Ouellet JF, Roche A, Lasser P. Percutaneous radiofrequency thermoablation as an alternative to surgery for treatment of liver tumour recurrence after hepatectomy. *Br J Surg* 2002; **89**: 752-756
14 **Machi J**, Uchida S, Sumida K, Limm WM, Hundahl SA, Oishi AJ, Furumoto NL, Oishi RH. Ultrasound-guided radiofrequency thermal ablation of liver tumors: percutaneous, laparoscopic, and open surgical approaches. *J Gastrointest Surg* 2001; **5**: 477-489
15 **Parikh AA**, Curley SA, Fornage BD, Ellis LM. Radiofrequency ablation of hepatic metastases. *Semin Oncol* 2002; **29**: 168-182
16 **Kosari K**, Gomes M, Hunter D, Hess DJ, Greeno E, Sielaff TD. Local, intrahepatic, and systemic recurrence patterns after radiofrequency ablation of hepatic malignancies. *J Gastrointest Surg* 2002; **6**: 255-263
17 **Dick EA**, Taylor-Robinson SD, Thomas HC, Gedroyc WM. Ablative therapy for liver tumours. *Gut* 2002; **50**: 733-739
18 **Zagoria RJ**, Chen MY, Shen P, Levine EA. Complications from radiofrequency ablation of liver metastases. *Am Surg* 2002; **68**: 204-209
19 **Yamagami T**, Nakamura T, Kato T, Matsushima S, Iida S, Nishimura T. Skin injury after radiofrequency ablation for hepatic cancer. *AJR Am J Roentgenol* 2002; **178**: 905-907
20 **Poon RT**, Fan ST, Tsang FH, Wong J. Locoregional therapies for hepatocellular carcinoma: a critical review from the surgeon's perspective. *Ann Surg* 2002; **235**: 466-486
21 **Kim RY**, Weintraub JL, Susman J, Haskal ZJ. Radiofrequency ablation for hemobilia secondary to hepatocellular carcinoma. *J Vasc Interv Radiol* 2002; **13**: 3117-3120
22 **de Baere T**, Bessoud B, Dromain C, Ducreux M, Boige V, Lassau N, Smayra T, Girish BV, Roche A, Elias D. Percutaneous radiofrequency ablation of hepatic tumors during temporary venous occlusion. *AJR Am J Roentgenol* 2002; **178**: 53-59
23 **Yohannes P**, Pinto P, Rotariu P, Smith AD, Lee BR. Retroperitoneoscopic radiofrequency ablation of a solid renal mass. *J Endourol* 2001; **15**: 845-849
24 **Izzo F**, Thomas R, Delrio P, Rinaldo M, Vallone P, DeChiara A, Botti G, D'Aiuto G, Cortino P, Curley SA. Radiofrequency ablation in patients with primary breast carcinoma: a pilot study in 26 patients. *Cancer* 2001; **92**: 2036-2044
25 **Lee JD**, Lee JM, Kim SW, Kim CS, Mun WS. MR imaging-histopathologic correlation of radiofrequency thermal ablation lesion in a rabbit liver model: observation during acute and chronic stages. *Korean J Radiol* 2001; **2**: 151-158
26 **Bolognesi M**, Merkel C, Sacerdoti D, Nava V, Gatta A. Role of spleen enlargement in cirrhosis with portal hypertension. *Dig Liver Dis* 2002; **34**: 144-150
27 **Trobs RB**, Bennek J. Partial splenectomy, transposition of the spleen to the abdominal wall or splenohepatoplasty in portal hypertensive rats. Effects on portal venous pressure and homeostasis- microscopical appearance of the transposed spleen. *Eur J Pediatr Surg* 1998; **8**: 155-162
28 **Jiang HC**, Sun B, Qiao HQ, Xu J, Piao DX, Yin H. Clinical application of serial operations with preserving spleen. *World J Gastroenterol* 2001; **7**: 876-879
29 **Zhang H**, Chen J, Kaiser GM, Mapudengo O, Zhang J, Exton MS, Song E. The value of partial splenic autotransplantation in patients with portal hypertension: a prospective randomized study. *Arch Surg* 2002; **137**: 89-93
30 **Obatake M**, Muraji T, Kanegawa K, Satoh S, Nishijima E, Tsugawa C. A new volumetric evaluation of partial splenic embolization for hypersplenism in biliary astresia. *J Pediatr Surg* 2001; **36**: 1615-1616
31 **Liu FQ**, Chu GW, Tong JM, Zhang XJ, Qin DJ, Liu YL, Chen GH. Studies of treatment of hypersplenism with injection of absolute alcohol into spleens. *Shijie Huaren Xiaohua Zazhi* 2000; **8**: 1381-1384
32 **Shina S**, Aoyama H, Shiratori Y, Mutoh H, Kurita M, Ota S, Terano A, Sugimoto T. Ultrasound-guided percutaneous injection of ethanolamine oleate for hypersplenism. *Invest Radiol* 1990; **23**: 651-657
33 **Idezuki Y**. Progress and changes in surgery: portal hypertension. *World J Surg* 1998; **22**: 759-766
34 **Sharara AI**, Rockey DC. Gastroesophageal variceal hemorrhage. *N Engl J Med* 2001; **345**: 669-681
35 **Krige JE**, Bornman PC. Endoscopic treatment of oesophageal varices. *S Afr J Surg* 2000; **38**: 82-88
36 **Rossle M**. Prevention of rebleeding from oesophageal-gastric varices. *Eur J Gastroenterol Hepatol* 2001; **13**: 343-348
37 **Russo MW**, Brown RS Jr. Endoscopic treatment of patients with portal hypertension. *Gastrointest Endosc Clin N Am* 2001; **11**: 1-14
38 **Gow PJ**, Chapman RW. Modern management of oesophageal varices. *Postgrad Med J* 2001; **77**: 75-81
39 **Marangio A**, Prati U, Luinetti O, Brunetti E, Filice C. Radiofrequency ablation of colorectal splenic metastasis. *AJR Am J Roentgenol* 2002; **178**: 1481-1482
40 **Wood BJ**, Bates S. Radiofrequency thermal ablation of a splenic metastasis. *J Vasc Interv Radiol* 2001; **12**: 261-263
41 **Keogan MT**, Freed KS, Paulson EK, Nelson RC, Dodd LG. Imaging-guided percutaneous biopsy of focal splenic lesions: update on safety and effectiveness. *AJR Am J Roentgenol* 1999; **172**: 933-937
42 **Muraca S**, Chait PG, Connolly BL, Baskin KM, Temple MJ. US-guided core biopsy of the spleen in children. *Radiology* 2001; **218**: 200-206
43 **Civardi G**, Vallisa D, Berte R, Giorgio A, Filice C, Caremani M, Caturelli E, Pompili M, De Sio I, Buscarini E, Cavanna L. Ultrasound-guided fine needle biopsy of the spleen: high clinical efficacy and low risk in a multicenter Italian study. *Am J Hematol* 2001; **67**: 93-99
44 **Sahin M**, Tekin S, Aksoy F, Vatansev H, Seker M, Avunduk MC, Kartal A. The effects of splenic artery ligation in an experimental model of secondary hypersplenism. *J R Coll Surg Edinb* 2000; **45**: 148-152

Edited by Ren SY

P.O.Box 2345, Beijing 100023, China
Fax: +86-10-85381893
E-mail: wjg@wjgnet.com www.wjgnet.com

World J Gastroenterol 2003;9(4):818-823
World Journal of Gastroenterology
 ISSN 1007-9327

• BASIC RESEARCH •

Analysis of gene expression profile of pancreatic carcinoma using cDNA microarray

Zhi-Jun Tan, Xian-Gui Hu, Gui-Song Cao, Yan Tang

Zhi-Jun Tan, Xian-Gui Hu, Gui-Song Cao, Yan Tang, Department of General Surgery, Changhai Hospital, Second Military Medical University, Shanghai 200433, China
Correspondence to: Xian-Gui Hu, Department of General Surgery, Changhai Hospital, Second Military Medical University, Shanghai 200433, China. hxgchw@sh163.net
Telephone: +86-21-25070571 **Fax:** +86-21-25070571
Received: 2002-11-06 **Accepted:** 2002-12-07

Abstract

AIM: To identify new diagnostic markers and drug targets, the gene expression profiles of pancreatic cancer were compared with that of adjacent normal tissues utilizing cDNA microarray analysis.

METHODS: cDNA probes were prepared by labeling mRNA from samples of six pancreatic carcinoma tissues with Cy5-dUTP and mRNA from adjacent normal tissues with Cy3-dUTP respectively through reverse transcription. The mixed probes of each sample were then hybridized with 12 800 cDNA arrays (12 648 unique human cDNA sequences), and the fluorescent signals were scanned by ScanArray 3 000 scanner (General Scanning, Inc.). The values of Cy5-dUTP and Cy3-dUTP on each spot were analyzed and calculated by ImaGene 3.0 software (BioDiscovery, Inc.). Differentially expressed genes were screened according to the criterion that the absolute value of natural logarithm of the ratio of Cy5-dUTP to Cy3-dUTP was greater-than 0.69.

RESULTS: Among 6 samples investigated, 301 genes, which accounted for 2.38 % of genes on the microarry slides, exhibited differentially expression at least in 5. There were 166 over-expressed genes including 136 having been registered in Genebank, and 135 under-expressed genes including 79 in Genebank in cancerous tissues.

CONCLUSION: Microarray analysis may provide invaluable information on disease pathology, progression, resistance to treatment, and response to cellular microenvironments of pancreatic carcinoma and ultimately may lead to improving early diagnosis and discovering innovative therapeutic approaches for cancer.

Tan ZJ, Hu XG, Cao GS, Tang Y. Analysis of gene expression profile of pancreatic carcinoma using cDNA microarray. *World J Gastroenterol* 2003; 9(4): 818-823
http://www.wjgnet.com/1007-9327/9/818.htm

INTRODUCTION

The morbidity of pancreatic carcinoma has taken an upward trend all over the world. In occidental countries, the morbidity of pancreatic carcinoma has increased by 3 to 7 times in nearly thirty years, and pancreatic carcinoma has become one of the ten commonest malignant tumors. In China, the morbidity was 1.16/100 000 in Shanghai in 1963, and reached on 3.80/100 000 in 1974. Then, it took the 14th place of the morbidity of the malignant tumors, and jumped to fifth in 1984. The statistical results showed that it was 5.1/100 000, which was four times higher than that of twenty years before. In some medical centers, curative resections were given to minority of patients in early stage who were highly selected, and their five-year survival of these patients might even rise to 15 to 25 percent. But generally speaking, treatment of pancreatic cancer is still a serious challenge to us. The key problem to improve the current situation of treatment is to seek novel diagnostic markers, effective adjunctive therapy and mechanism of genesis and evolution of pancreatic cancer. Hence, more and more attention has been paid to the research on molecular pathology and related genes of pancreatic cancer.

Over the past decade, many studies involving pancreatic cancer have searched for cancer-causing gene. As a result, several cancer-related genes have been identified. DPC4, p53, and p16 are the three most frequently inactivated tumor suppressor genes. Other tumor suppressor genes that are altered in pancreatic cancer include BRCA2, ALK-5, MKK4, and STK11. Mutations of K-ras oncogene are commonly seen in pancreatic cancer, with it' s incidence as high as 90 %. Some other cancer-related genes, such as Her-2/neu, COX-2, VEGF have also been reported to be overexpressed in pancreatic cancer. Development and progression of pancreatic cancer is a very complicated process, so it is reasonable to predict that many other genes, as yet undiscovered, might be potential tumor markers or drug targets.

Microarray is the technique that a large number of cDNAs are arranged orderly on the carrier, such as glass chip or else in high density. Data are obtained by examining the signals of fluorescence, analyzed and compared by computer software. A large number of genes can be examined simutaneously, accurately, and effectively in one experiment. In this study, we have used a high-density cDNA microarray technique to assess the gene expression profile of pancreatic carcinoma versus adjacent normal tissue. Several genes, we identified, may be involved in pancreatic tumorigenesis as well as it' s potential clinical biomarkers that may be used to improve early diagnosis, and to constitute potential novel therapeutic targets.

MATERIALS AND METHODS

Materials

cDNA microarray slides used in this study were fabricated in United Gene Technique, Ltd. Briefly, each slide has 12 800 spots, containing 112 genes as negative control, such as ripe U2 RNA gene (8 spots), HCV coat protein gene (8 spots), spotting solution (96 spots); and 40 housekeeping genes as positive control. Each slide has 12 648 unique human cDNA sequences. Six samples of pancreatic carcinoma were obtained from patients undergoing pancreaticoduodenectomy in department of general surgery, Changhai Hospital, the Second Military Medical University. All cases were proved pathologically as carcinoma of pancreatic head. Normal tissues as control were taken from tissue adjacent to the cutting margin of the carcinoma and proved pathologically to be free from tumor invasion. Samples were snap-frozen in liquid nitrogen within 15 to 20 minutes after resection and then stored at -80 ℃.

Cy3-dUTP and Cy5-dUTP were purchased from Amersham Phamacia Biotech, Inc. and Oligotex mRNA Midi Kit from Quagen, Inc. ScanArray 3 000 scanner was manufactured by General Scanning, Inc. ImaGene3.0 software came from BioDiscovery, Inc.

Methods

Probe preparation Total RNA isolated from pancreas tissues and normal adjacent tissues by using modified single step extraction. Briefly, frozen tissues were crushed down and homogenized in solution D and 1 % mercaptoethanol. The supernatant was then extracted by phenol: chloroform (1:1) two times, and phenol: chloroform (5:1) and NaAc (PH=4.5) once. Afterward, the supernatant was precipitated in equal volume of isopropanol at -20 ℃ for 1.5 hours and was precipitated in LiCl for purification. Both kinds of mRNAs were purified using Oligotex mRNA Midi Kit. The fluorescent cDNA probes were prepared by reverse transcription and then purified, according to the protocol of Schena (Schena *et al*., 1995). The mRNA from normal tissue was labeled with Cy3- dUTP, and that from cancerous tissue with Cy5- dUTP. Then the two probes were mixed with equivalence, precipitated by ethanol, and resolved in 20 μl hybridization buffer (5×SSC + 0.4 % SDS, 50 % Formamide, 5×denhardt' s solution).

Hybridization Microarray slides were pre-hybridized in hybridization buffer, which contained 0.5 mg/ml denatured clupeine DNA, at 42 ℃ for 6 hours. After denatured at 95 ℃ for 5 minutes, the probes mixture were added on the pre-hybridized slides and sealed with cover glass. After hybridizing in HybChamber at 60 ℃ for 15 to 17 hours, the slides were subsequently washed in solutions of 2×SSC + 0.2 % SDS, 0.1×SSC+0.2 % SDS and 0.1×SSC respectively for 10 minutes, then dried at room temperature.

Scanning and analysis The slides were scanned by ScanArray 3 000 laser scanner at two wavelengths to obtain fluorescence intensities for both dyes (Cy3 and Cy5). The original value of each spot was normalized by the values of 40 housekeeping genes selected on the slides. The fluorescence intensities of Cy3 and Cy5 were analyzed and the ratios of Cy5 to Cy3 were calculated by ImaGene 3.0 software. The intensities of two fluorescent signals represented the quantities of two tagged probes. The ration of Cy5 to Cy3 of certain spot on the slides demonstrated that mRNA abundance of this gene expressed in cancerous tissues versus normal.

RESULTS

Verification of micrearray technique system

There were 12 800 spots on each slide, including 6 170 known genes and 6 478 unknown ones. In order to monitor entire process of microarray technique system, negative and positive control genes were set on the slides. They were ripe U2 RNA gene (8 spots), HCV coat protein gene (8 spots), spotting solution (96 spots), which served as negative control; and 40 housekeeping genes as positive control. In present study, the individual result of six hybridization showed that all of positive control signals are distinct, and all of negative control signals were very low. These prove the reliability of the data.

Table 1 Over-expressed genes in pancreatic carcinoma

Accession number	Gene name	Gene function	Ratio value
U06863	Alpha 1 (III) collagen	Extracellular metrix	33.89
X91148	Microsomal triglyceride transfer protein	Microsomal triglyceride transfer	21.89
AF017986	Secreted apoptosis related protein 1 (SARP1)	Repress apoptosis	20.32
Y00755	Extracellular matrix protein BM-40	Extracellular metrix	20.23
Z74616	Alpha2 (I) collagen	Extracellular metrix	12.52
D32039	Proteoglycan PG-M(V3)	Extracellular metrix	11.90
J03607	40-kDa keratin intermediate filament precursor	Extracellular metrix	11.62
AF144103	Novel chemokine family member with altered expression in human head and neck squamous cell carcinoma	Cytokine	9.93
AF141201	Ubiquitin fusion-degradation 1 protein (UFD1)	Protease	8.29
X02761	Fibronectin (FN)	Extracellular metrix	8.01
U06863	Follistatin-related protein precursor	Nucleoprotein	6.92
M14219	Chondroitin / dermatan sulfate proteoglycan (PG40) core protein	Extracellular metrix	6.65
M17783	Glia-derived nexin (GDN)	Protease inhibitor	6.49
U59877	Low-Mr GTP-binding protein (RAB31)	Signal transduction	5.97
AF000989	Thymosin beta 4 Y isoform (TB4Y)	Thymosin isoform	5.71
L20688	GDP-dissociation inhibitor protein (Ly-GDI)	Signal transduction	5.62
X57351	1-8D gene from interferon-inducible gene	Signal transduction	5.51
U18728	Lumican	Extracellular metrix	5.15
L02326	Lambda-like gene	Immunity correlation	4.77
M14144	Vimentin	Extracellular metrix	4.64
J05633	Integrin beta-5 subunit	Cell adhesion molecule	4.42
AF070523	JWA protein	-	4.32
M27749	Immunoglobulin-related 14.1 protein	Immunity correlation	4.28
S83308	Sry-related HMG box gene (SOX5)	Transcription factor	4.16
U05875	Interferon gamma receptor accessory factor-1 (AF-1)	Immunity correlation	3.92
M17733	Thymosin beta-4	Thymosin isoform	3.89
M20259	Thymosin beta-10	Thymosin isoform	3.75
M36501	Alpha-2-macroglobulin	Protease inhibitor	3.72
AF026977	Microsomal glutathione S-transferase 3 (MGST3)	Oxidation-reduction	3.62
M14630	Prothymosin-α	Nucleoprotein	3.45

Table 2 Under-expressed genes in pancreatic carcinoma

Accession number	Gene name	Gene function	Ratio value
U96628	Nuclear antigen H731-like protein	Tumor suppressor	0.16
U72649	B-cell translocation gene 2 (BTG2)	Tumor suppressor	0.18
Y15409	Putative glucose 6-phosphate translocase	Gluconeogenesis	0.18
Z21507	Elongation factor-1-delta	Translation factor	0.20
L13463	Helix-loop-helix basic phosphoprotein (G0S8)	Cell cycle correlation	0.21
S68805	L-arginine:glycine amidinotransferase	Amino transferase	0.22
AF041474	BAF53a (BAF53a)	Chromatin reformation	0.22
X05130	Prolyl 4-hydoxylase beta subunit	Hydroxylase	0.22
AF067855	Geminin	Cell cycle correlation	0.25
D87810	Phosphomannomutase	Glycometabolism	0.25
D28540	CDC10 homologue	Cell cycle correlation	0.27
L37368	RNA-binding protein	RNA metabolism	0.27
Y00711	Lactate dehydrogenase B (LDH-B)	Dehydrogenase	0.27
M24103	Trans-golgi network glycoprotein 51 (TGN)	-	0.29
M64930	Protein phosphatase 2A beta subunit	Signal transduction	0.29
X81197	Archain	Membranin	0.31
U75686	Polyadenylate binding protein	Signal transduction	0.32
AF133659	ATP-binding cassette 7 iron transporter (ABC7)	Iron transfer	0.32
M61832	S-adenosylhomocysteine hydrolase (AHCY)	Hydrolase	0.33
Z23064	HnRNP G protein	RNA-binding protein	0.34
X85960	TRK-T3 oncogene	Oncogene	0.35
L18887	Calnexin	Calcium binding protein	0.35
J02966	Mitochondrial ADP / ADT translocator	ATP / ADP transport	0.35
X78678	Ketohexokinase	Glycometabolism	0.35
M58460	75-kD autoantigen (PM-Sc1)	Autoantigen	0.35
L12711	Transketolase (tk)	Ribose metabolism	0.35
S75311	Glycosyl phosphatidylinositol (GPI)-linked glycoprotein CD24	Signal transduction	0.35
U46838	MCM105 protein	Cell cycle correlation	0.36
Y11312	Phosphoinositide 3-kinase	Signal transduction	0.36
U83908	PDCD4 (programmed cell death 4)	Tumor suppressor	0.36

Judgement of differentially expressed genes

Hybridization of each couple of probes repeated two times. The standard of determination for differentially expressed genes was that, the absolute value of natural logarithm of the ratio of Cy5 to Cy3 was greater than 0.69, that was to say change of gene expression was above 2 times, and the signal value of either Cy3 or Cy5 needed to be greater than 600.

Genes expressed differentially

Among 6 samples investigated, 301 genes, which accounted for 2.38 % of genes on the microarry slides, exhibited differentially expression at least in 5. There were 166 over-expressed genes including 136 having been registered in Genebank, and 135 under-expressed genes including 79 in Genebank. Some of these genes, which took superior places of differentially expression, were listed in Table 1 and Table 2.

DISCUSSION

There are altogether 215 previously reported genes differently expressed in cancer tissues in our research, including urokinase plasminogen activator surface receptor (uPAR)[1], glyceraldehyde-3-phosphate dehydrogenase (GAPDH), lumican[2], phospholipase A2[3], vascular cell adhesion molecule 1[4], which have been reported to play certain role in evolution of pancreatic carcinoma. However, the relationship between the majority of these genes and development of pancreatic carcinoma has not been covered in any study up to the present. These genes are involved in various cytobiological functions, such as signal transduction, transcription and translation, cytoskeleton, cell adhesion, extracellular matrix and matrix degradation, cell cycle and apoptosis, chromosome instability, tumor suppressor genes, enzyme, and "others". Moreover, some genes exhibit differently expression in pancreatic cancer in our study, as well as in other cancers. They are fibronectin[5], caltractin[6], glyceraldehyde-3-phosphate dehydrogenase (GAPDH)[7], lipocortin II, uPAR[8] in hepatic cancer; FN[9], glutathione peroxidase[10], phospholipase A2[11], thymosin beta-10[12], uPAR[13], uracil DNA glycosylase[14] in colorectal cancer; N-cadherin[15], uPAR[16], alpha-2-macroglobulin[17], caltractin[6], syntenin[18] in gastric cancer; phospholipase A2[19] in cholangiocarcinoma; fibronectin[20], glutathione peroxidase[21,22], prothymosin alpha[23,24], thymosin beta-10[25], uPAR[26], caltractin[6], GAPDH[27], proteoglycan PG-M(V3), syntenin[18], lumican[28] in mammary cancer and glutathione peroxidase[29], SPARC/osteonectin[29], thymosin beta-10[30], uPAR[31] in thyroid carcinoma. These data indicated that we have obtained the same results by using cDNA microarray as by other methods. Meanwhile, these confirmed the feasibility, accuracy and effectiveness of microarray as a method to investigate the expression profiles of pancreatic cancer. On the other hand, we might get the conclusion that genesis and progression of various neoplasms have some common mechanisms. Further study on these common mechanisms might lead us go into depth the knowledge of molecular biology of cancer, and find the key to the improvement of diagnosis and treatment of cancer.

Pancreatic carcinoma is one of the most malignant tumors, and is characterized by aggressive growth behavior and high incidence rate of recurrence. During proliferation of a primary tumor or the establishment of metastatic foci, there is

continuous remodeling of the extracellular matrix including various degrees of biosynthesis, reformation and degradation. Among over-expressed genes, several genes, such as alpha1 (III) collagen, extracellular matrix protein BM-40, alpha2 (I) collagen, proteoglycan PG-M (V3), fibronectin, chondroitin/ dermatan sulfate proteoglycan (PG40) core protein, lumican, vimentin, chondroitin sulfate proteoglycan versican V0 splice-variant, and versican V2 splice-variant core protein, component analysis related to extracellular metrix (ECM), take the superior places. Versican belongs to the family of large aggregating proteoglycans (PGs). In mammals, versican appears as four possible spliced variants, V_0, V_1, V_2, and V_3. It has been described that the versican-rich extracellular matrices exert an anti-adhesive effect on the cells, thus facilitating tumor cell migration and invasion. Besides decreasing cell adhesion, versican is also able to increase the cell proliferation. The study on melanoma has shown that this PG could serve as a good marker for primary malignant as well as metastatic lesion[32]. Lumincan is the member of the small leucine-rich proteoglycan (SLRP) family, whose members are known as keratocan, mimecan, decorin, biglycan, fibromodulin, epiphycan, osteoadherin, and lumican. SLRP proteins can modulate cellular behaviour, including cell migration and proliferation during embryonic development, tissue repair, and tumor growth. In breast cancer tissues, lumican mRNA is reported to be overexpressed. Furthermore, its high expression level was associated with high tumor grade, low estrogen receptor levels, and young age of patients[28]. It is also found that lumican is not synthesized by the exocrine components of the normal pancreas, but that these cells ectopically synthesize and secrete the lumican in cancer tissues, which may play a role in pancreatic cancer cell growth[2]. Extracellular matrix protein BM-40, an anti-adhesive protein, is proposed to modulate cell migration and vascular morphogenesis either by directly interacting with ECM proteins or by initiating a receptor-mediated signaling event. It may directly affect cell motility by inducing intracellular changes of cytoplasmic components; or indirectly promote cell migration by modulating the expression of proteolytic enzymes that degrade the ECM, such as collagenase, stromelysin and MMP-9. It may promote infiltration of tumor cells, serve as a cellular marker of invasion, and correlate to angiogenesis[33]. Fibronectin connects with the cancer cell via its receptors, including intergrins $\alpha_5\beta_1$ and $\alpha v\beta_3$. The abilities in adhesion to fibronectin and migration increased markedly, after hepatocellular carcinoma cells were transfected with H-ras oncogene[34]. In addition, fibronectin is the primary protein involved in the displacement of MMP-2 produced by adjacent normal cells to cancer tissues[35]. MMP-2 can associate with the cell surface through its COOH-terminal and hemopexin-like domain via a number of mechanisms, including binding to cell-associated collagen I and IV. In our present study, we also find that collagen I and IV overexpress in cancerous tissues. This may enhance the fibronectin-induced displacement of MMP-2, and facilitates invasion of cancerous cells. Vimentin is also a component of ECM. Enhanced expression of the vimentin is associated with high degree of motility, poor differentiation and metastasis of prostate carcinoma[36]. It has been shown that vimentin was immunohistochemically positive in basaloid squamous carcinoma of esophagus[37]. Moreover, uPAR and cathepsin O2 are also found to be over-expressed in our study. All of these changes endow pancreatic cancer with the trait of aggressive growth, and may be potential markers of invasion.

On the other hand, recurrence to chemotherapy after resection remains a major obstacle to the cure of pancreatic cancer. It is well known that cancerous cells are surrounded by an extensive stroma of ECM at both primary and metastatic sites, which contains, among other proteins, fibronectin, laminin and collgen IV. Adhesion of pancreatic cancer cells to these proteins confers resistance to apoptosis induced by standard chemotherapeutic agents. The study on small-cell lung cancer showed that β1-integrin-mediated cell adhesion to ECM proteins results in tyrosine phosphorylation, which, weaken persistent chemotherapy-induced DNA damage, prevents caspase activation and apoptosis[38]. Alpha-tubulin[39], lipocortin II and uracil DNA glycosylase[14] were also found to be contributed to resistance to chemotherapy. These genes over-express in pancreatic cancer in our study, and may play the same role. It is indicated that the regulation routes of these genes may be potential targets for treatment of pancreatic carcinoma.

There are still some genes that should be mentioned. Prothymosin alpha (PTA) is a nuclear protein that is present throughout the cell cycle. It has been shown that it binds histones in vitro and has been proposed to affect the chromatin state. PTA is expressed in various human tumor tissues of different origins, supporting the idea that PTA expression is required for tumor growth. Recent study has shown that in breast cancer, whose tumor with low or moderate PTA level demonstrated a statistically significant decreased rate of tumor recurrence and a statistically significant increased overall survival in comparison with those whose tumor had high PTA levels. It is proposed that PTA could be used as a predictor of the potential malignancy of breast tumors that might help to identify patients at high risk of fatality[23,24]. Fas-binding protein and secreted apoptosis related protein-1 (SARP-1) are proposed to repress apoptosis. SARP-1 may inhibit phosphorylation of liberated β-catenin and degradation by ubiquitin-protease system via Wnt signaling way. Subsequently, β-catenin accumulates in cytoplasm, and cell apoptosis is suppressed. SARP-1 thus promotes excessive proliferation and transformation. Fas-binding protein can arrest Fas-induced apoptosis. Thymosin beta-4 and Thymosin beta-10 are also up-regulated. These genes may serve as markers for measuring proliferation of pancreatic cancer cells.

There are two tumor suppressors, B-cell translocation gene 2 (BTG2) and programmed cell death 4 (PCDC4), which are down-regulated in cancer tissues. PDCD4 gene is homologous to the mouse gene (MA-3/Pdcd4/A7-1), which is associated with apoptosis and is shown to suppress tumor promoter-induced neoplastic transformation. The ORF of human PDCD4 encodes a protein of 458 aa with a predicted molecular size of 50.6 kDa. It has been demonstrated that PDCD4 protein inhibits neoplastic transformation and must be down-regulated for progression to occur[40]. BTG2, which is induced by p53, displays an antiproliferative activity in different cell types, such as fibroblasts and PC12 cells. It is well known that the control of the cell cycle plays an essential role in cell growth and in the activation of important cellular processes, such as differentiation and apoptosis. pRb and p53 are two molecules identified as key regulators of the cell cycle. Some suggestions came from a recent report, which showed that BTG2 interacted with a protein-arginine N-methyltransferase (Prmt1) by positively modulating its activity. Prmt1, in turn, has been found to bind the interferon receptors and to be required for interferon-mediated growth inhibition. A further investigation on BTG2 demonstrated that this gene inhibited G_1/S progression in an Rb-dependent manner and that this effect was correlated with its ability to inhibit cyclin D_1 expression. Furthermore, the impairment in the ability of BTG2 to lower cyclin D_1 levels, seen in consequence of mutations of the BTG2 molecule, correlated with the extent of impairment in growth arrest[41].

DNA replication is initiated at discrete sites on chromosomes through the coordinate action of a number of replication initiation factors. It is believed that a complex of proteins called

the origin recognition complex (ORC) associates with specific DNA sequences near origins of replication to recruit other replication initiation factors during the G_1 phase of the cell cycle. The other replication initiation factors, Cdc6p, Cdt1p, and the Mcm2-7p complex, associate with the origin sequence in an ORC-dependent reaction to form a pre-replicative complex (pre-RC). At the G_1-S transition, the activation of cyclin-dependent kinases leads to the recruitment of elongation factors, CDC45, DNA polymerases, and RPA to the pre-RCs at origins. The action of these replication elongation proteins leads to the initiation of DNA synthesis, the hallmark of S phase. Geminin interacts with Cdt1p and prevents the recruitment of the Mcm2-7p complex to origins during S, G_2, and early M phases of the cell cycle and thereby inhibits replication initiation, leading to the expectation that the protein acts as an inhibitor of cell proliferation[42]. The research on these under-expressed genes may render invaluable information to find novel targets for the treatment of pancreatic cancer.

In summary, though some genes have been missed in present study, the genes we have identified may be important to the tumorigenesis of pancreatic cancer, and potential to serve as tumor markers or drug targets.

REFERENCES

1 **Han H**, Bearss DJ, Browne LW, Calaluce R, Nagle RB, Von Hoff DD. Identification of differentially expressed genes in pancreatic cancer cells using cDNA microarray. *Cancer Res* 2002; **62**: 2890-2896

2 **Ping Lu Y**, Ishiwata T, Asano G. Lumican expression in alpha cells of islets in pancreas and pancreatic cancer cells. *J Pathol* 2002; **196**: 324-330

3 **Kashiwagi M**, Friess H, Uhl W, Berberat P, Abou-Shady M, Martignoni M, Anghelacopoulos SE, Zimmermann A, Buchler MW. Group II and IV phospholipase A(2) are produced in human pancreatic cancer cells and influence prognosis. *Gut* 1999; **45**: 605-612

4 **Tempia-Caliera AA**, Horvath LZ, Zimmermann A, Tihanyi TT, Korc M, Friess H, Buchler MW. Adhesion molecules in human pancreatic cancer. *J Surg Oncol* 2002; **79**: 93-100

5 **Nejjari M**, Hafdi Z, Gouysse G, Fiorentino M, Beatrix O, Dumortier J, PourreyronC, Barozzi C, D'errico A, Grigioni WF, Scoazec JY. Expression, regulation, and function of alpha V integrins in hepatocellular carcinoma: an *in vivo* and *in vitro* study. *Hepatology* 2002; **36**: 418-426

6 **Tian DY**, Hayashi M, Yoshida T, Sakakura T, Kawarada Y, Tanaka T. Overexpression of caltractin gene in tumor-infiltrating lymphocytes. *Int J Oncol* 1998; **13**: 1135-1140

7 **Yamagata M**, Mori M, Begum NA, Shibuta K, Shimoda K, Barnard GF. Glyceraldehyde-3-phosphate dehydrogenase mRNA expression in hepatocellular carcinoma. *Int J Oncol* 1998; **12**: 677-683

8 **Zhou L**, Hayashi Y, Itoh T, Wang W, Rui J, Itoh H. Expression of urokinase-type plasminogen activator, urokinase-type plasminogen activator receptor, and plasminogen activator inhibitor-1 and -2 inhepatocellular carcinoma. *Pathol Int* 2000; **50**: 392-397

9 **Lopez-Conejo MT**, Olmo N, Turnay J, Lopez De Silanes I, Lizarbe MA. Interaction of fibronectin with human colon adenocarcinoma cells: effect on the *in vivo* tumorigenic capacity. *Oncology* 2002; **62**: 371-380

10 **Skrzydlewska E**, Stankiewicz A, Sulkowska M, Sulkowski S, Kasacka I. Antioxidant status and lipid peroxidation in colorectal cancer. *J Toxicol Environ Health A* 2001; **64**: 213-222

11 **Osterstrom A**, Dimberg J, Fransen K, Soderkvist P. Expression of cytosolic and group X secretory phospholipase A (2) genes in human colorectal adenocarcinomas. *Cancer Lett* 2002; **182**: 175-182

12 **Nimmrich I**, Erdmann S, Melchers U, Finke U, Hentsch S, Moyer MP, Hoffmann I, Muller O. Seven genes that are differentially transcribed in colorectal tumor cell lines. *Cancer Lett* 2000; **160**: 37-43

13 **Baker EA**, Bergin FG, Leaper DJ. Plasminogen activator system, vascular endothelial growth factor, and colorectalcancer progression. *Mol Pathol* 2000; **53**: 307-312

14 **Dusseau C**, Murray GI, Keenan RA, O'Kelly T, Krokan HE, McLeod HL. Analysis of uracil DNA glycosylase in human colorectal cancer. *Int J Oncol* 2001; **18**: 393-399

15 **Yanagimoto K**, Sato Y, Shimoyama Y, Tsuchiya B, Kuwao S, Kameya T. Co-expression of N-cadherin and alpha-fetoprotein in stomach cancer. *Pathol Int* 2001; **51**: 612-618

16 **Choi YK**, Yoon BI, Kook YH, Won YS, Kim JH, Lee CH, Hyun BH, Oh GT, Sipley J, KimDY. Overexpression of urokinase-type plasminogen activator in human gastric cancercell line (AGS) induces tumorigenicity in severe combined immunodeficient mice. *Jpn J Cancer Res* 2002; **93**: 151-156

17 **Allgayer H**, Babic R, Grutzner KU, Beyer BC, Tarabichi A, Schildberg FW, HeissMM. Tumor-associated proteases and inhibitors in gastric cancer: analysis of prognostic impact and individual risk protease patterns. *Clin Exp Metastasis* 1998; **16**: 62-73

18 **Koo TH**, Lee JJ, Kim EM, Kim KW, Kim HD, Lee JH. Syntenin is overexpressed and promotes cell migration in metastatic human breastand gastric cancer cell lines. *Oncogene* 2002; **21**: 4080-4088

19 **Wu T**, Han C, Lunz JG 3rd, Michalopoulos G, Shelhamer JH, Demetris AJ. Involvement of 85-kd cytosolic phospholipase A (2) and cyclooxygenase-2 in theproliferation of human cholangiocarcinoma cells. *Hepatology* 2002; **36**: 363-373

20 **Jiang Y**, Harlocker SL, Molesh DA, Dillon DC, Stolk JA, Houghton RL, Repasky EA, Badaro R, Reed SG, Xu J. Discovery of differentially expressed genes in human breast cancer using subtracted cDNA libraries and cDNA microarrays. *Oncogene* 2002; **21**: 2270-2282

21 **Perquin M**, Oster T, Maul A, Froment N, Untereiner M, Bagrel D. The glutathione-related detoxification system is increased in human breastcancer in correlation with clinical and histopathological features. *J Cancer Res Clin Oncol* 2001; **127**: 368-374

22 **Gorodzanskaya EG**, Larionova VB, Zubrikhina GN, Kormosh NG, Davydova TV, Laktionov KP. Role of glutathione-dependent peroxidase in regulation of lipoperoxide utilization in malignant tumors. *Biochemistry* 2001; **66**: 221-224

23 **Bianco NR**, Montano MM. Regulation of prothymosin alpha by estrogen receptor alpha: molecular mechanismsand relevance in estrogen-mediated breast cell growth. *Oncogene* 2002; **21**: 5233-5244

24 **Magdalena C**, Dominguez F, Loidi L, Puente JL. Tumour prothymosin alpha content, a potential prognostic marker for primarybreast cancer. *Br J Cancer* 2000; **82**: 584-590

25 **Santelli G**, Califano D, Chiappetta G, Maria Teresa Vento, Bartoli PC, Zullo F, Trapasso F, Viglietto G, Fusco A. Thymosin beta-10 gene overexpression is a general event in human carcinogenesis. *Am J Pathol* 1999; **155**: 799-804

26 **Gong SJ**, Rha SY, Chung HC, Yoo NC, Roh JK, Yang WI, Lee KS, Min JS, Kim BS, Chung HC. Tissue urokinase-type plasminogen activator receptor levels in breast cancer. *Int J Mol Med* 2000; **6**: 301-305

27 **Revillion F**, Pawlowski V, Hornez L, Peyrat JP. Glyceraldehyde-3-phosphate dehydrogenase gene expression in human breast cancer. *Eur J Cancer* 2000; **36**: 1038-1042

28 **Leygue E**, Snell L, Dotzlaw H, Troup S, Hiller-Hitchcock T, Murphy LC, Roughley PJ, Watson PH. Lumican and decorin are differentially expressed in human breast carcinoma. *J Pathol* 2000; **192**: 313-320

29 **Takano T**, Hasegawa Y, Matsuzuka F, Miyauchi A, Yoshida H, Higashiyama T, Kuma K, Amino N. Gene expression profiles in thyroid carcinomas. *Br J Cancer* 2000; **83**: 1495-1502

30 **Takano T**, Hasegawa Y, Miyauchi A, Matsuzuka F, Yoshida H, Kuma K, Amino N. Quantitative analysis of thymosin Beta-10 messenger RNA in thyroid carcinomas. *Jpn J Clin Oncol* 2002; **32**: 229-232

31 **Kim SJ**, Shiba E, Taguchi T, Tsukamoto F, Miyoshi Y, Tanji Y, Takai S, Noguchi S. uPA receptor expression in benign and malignant thyroid tumors. *Anticancer Res* 2002; **22**: 387-393

32 **Touab M**, Villena J, Barranco C, Arumi-Uria M, Bassols A. Versican is differentially expressed in human melanoma and may play a role intumor development. *Am J Pathol* 2002; **160**: 549-557

33 **Vajkoczy P**, Menger MD, Goldbrunner R, Ge S, Fong TAT, Vollmar B, Schilling L, Ullrich A, Hirth KP, Tonn JC, Schmiedek P, Rempel SA. Targeting angiogenesis inhibits tumor infiltration

and expression of the pro-invasive protein SPARC. *Int J Cancer* 2000; **87**: 261-268

34 **Wang Q**, Lin ZY, Feng XL. Alterations in metastatic properties of hepatocellular carcinoma cell following H-ras oncogene transfection. *World J Gastroenterol* 2001; **7**: 335-339

35 **Saad S**, Gottlieb DJ, Bradstock KF, Overall CM, Bendall LJ. Cancer cell-associated fibronectin induces release of matrix metalloproteinase-2from normal fibroblasts. *Cancer Res* 2002; **62**: 283-289

36 **Lang SH**, Hyde C, Reid IN, Hitchcock IS, Hart CA, Bryden AA, Villette JM, Stower MJ, Maitland NJ. Enhanced expression of vimentin in motile prostate cell lines and in poorly differentiated and metastatic prostate carcinoma. *Prostate* 2002; **52**: 253-263

37 **Zhang XH**, Sun GQ, Zhou XJ, Guo HF, Zhang TH. Basaloid squamous carcinoma of esophagus: a clinicopathological, immunohistochemical and electron microscopic study of sixteen cases. *World J Gastroenterol* 1998; **4**: 397-403

38 **Rintoul RC**, Sethi T. Extracellular matrix regulation of drug resistance in small-cell lung cancer. *Clin Sci* 2002; **102**: 417-424

39 **Kyu-Ho Han E**, Gehrke L, Tahir SK, Credo RB, Cherian SP, Sham H, Rosenberg SH, Ng S. Modulation of drug resistance by alpha-tubulin in paclitaxel-resistant humanlung cancer cell lines. *Eur J Cancer* 2000; **36**: 1565-1571

40 **Cmarik JL**, Min H, Hegamyer G, Zhan S, Kulesz-Martin M, Yoshinaga H, Matsuhashi S, Colburn NH. Differentially expressed protein Pdcd4 inhibits tumor promoter-induced neoplastic transformation. *Proc Natl Acad Sci U S A* 1999; **96**: 14037-14042

41 **Guardavaccaro D**, Corrente G, Covone F, Micheli L, Dagnano I, Starace G, Caruso M, Tirone F. Arrest of G_1 S progression by the p53-inducible gene PC3 is Rb dependent andrelies on the inhibition of cyclin D1 transcription. *Mol Cell Biol* 2000; **20**: 1797-1815

42 **Wohlschlegel JA**, Dwyer BT, Dhar SK, Cvetic C, Walter JC, Dutta A. Inhibition of eukaryotic DNA replication by geminin binding to Cdt1. *Science* 2000; **290**: 2309-2312

Edited by Xu JY

P.O.Box 2345, Beijing 100023, China
Fax: +86-10-85381893
E-mail: wjg@wjgnet.com www.wjgnet.com

World J Gastroenterol 2003;9(4):824-828
World Journal of Gastroenterology
 ISSN 1007-9327

• BASIC RESEARCH •

Association of two polymorphisms of tumor necrosis factor gene with acute biliary pancreatitis

Dian-Liang Zhang, Jie-Shou Li, Zhi-Wei Jiang, Bao-Jun Yu, Xing-Ming Tang, Hong-Mei Zheng

Dian-Liang Zhang, Jie-Shou Li, Zhi-Wei Jiang, Bao-Jun Yu, Xing-Ming Tang, Research Institute of General Surgery, Jinling Hospital, School of Medicine, Nanjing University, Nanjing 210093, Jiangsu Province, China
Hong-Mei Zheng, Department of Nephrology, the Hospital affiliated with Binzhou Medical College, Binzhou 256603, Shandong Province, China
Supported by the 10th five-year plan for medicine and health, PLA, No.013012 and is also supported by the General Hospital of Nanjing Command, No.2002059
Correspondence to: Dian-Liang Zhang and Jie-Shou Li, Research Institute of General Surgery, Jinling Hospital, Nanjing 210093, China. phdzdl@yahoo.com
Telephone: +86-25-4825061 **Fax:** +86-25-4803956
Received: 2002-10-08 **Accepted:** 2003-01-02

Abstract

AIM: To investigate TNF-α-308 and TNFB polymorphisms in acute biliary pancreatitis (ABP) and to related them to the plasma TNF-α levels.

METHODS: Genomic DNA was prepared from peripheral blood leukocytes. Genotypes and allele frequencies were determined in patients (n=127) and healthy controls (n=102) using restriction fragment length polymorphism analysis of polymerase chain reaction (PCR) products. Reading the size of digested bands from polyacrylamide gel demonstrated the two alleles TNF1 and TNF2, or the two alleles TNFB1 and TNFB2.

RESULTS: The frequencies of TNF2 polymorphism and TNFB2 polymorphism were both similar in patients with mild or severe pancreatitis, so were in pancreatitis patients and in controls. Patients with septic shock showed a significantly higher prevalence of the TNF2 than those without. No significant differences were found in the genotype distribution of TNF-α-308 and TNFB among different groups. Plasma TNF-α levels did not differ significantly in ASBP patients displaying different alleles of the TNF gene studied.

CONCLUSION: Results indicate that TNF gene polymorphisms studied play no part in determination of disease severity or susceptibility to acute biliary pancreatitis; however, TNF2 polymorphism is associated with septic shock from ASBP. Genetic factors are not important in determining plasma TNF-α levels in ASBP.

Zhang DL, Li JS, Jiang ZW, Yu BJ, Tang XM, Zheng HM. Association of two polymorphisms of tumor necrosis factor gene with acute biliary pancreatitis. *World J Gastroenterol* 2003; 9(4): 824-828
http://www.wjgnet.com/1007-9327/9/824.htm

INTRODUCTION

In China and most other countries, gallstones are the most common cause of acute pancreatitis. There are reports that gallstones account for between one third and two thirds of cases, with an average of 40 to 50 %[1]. Acute severe pancreatitis (ASP) is a serious disease, with highly persistent morbidity and mortality. Generally speaking, the natural course of severe acute pancreatitis progresses in two phases. The first 14 days are characterized by the systemic inflammatory response syndrome resulting from the release of inflammatory mediators. The second stage, beginning approximately 2 weeks after the onset of the disease, is dominated by septic-related complications resulting from infection of pancreatic necrosis or bacteria translocation. Today, with improvements in the care of the critically ill, many patients with ASP survive over early systemic inflammatory response and enter a second phase of illness dominated by sepsis and the consequences of organ failure. More than two thirds of deaths in ASP are due to late septic organ complications[2]. However, the susceptibility and mechanism of septic shock related to ASP are still unclear.

Tumor necrosis factor-α (TNF-α), the early cytokine to be released, is a principal mediator of immune responses to endotoxin. It can be produced in large amounts in several organs during ASP and is also believed to mediate pathophysiological changes[3,4]. Systemic release of TNF-α is associated with septic shock and fatal outcome. TNF-α levels are increased in patients with ASP and septic shock and appear to correlate with clinical outcome.

Because of its short half-life, the value of TNF-α as a marker of susceptibility or severity for ASP is limited. The production and response of TNF-α are partly regulated at the transcription level, the role of polymorphisms of TNF promoter in determination inflammatory disease susceptibility or as a marker of severity has been the subject of intense research[5]. There are many single nuclear polymorphisms within the TNF-α gene promoter. The TNF-α gene shows a polymorphism at position -308 in the promoter region. This polymorphism results in two allele forms, 1 in which a guanine defines the common allele TNF1 and 1 in which an adenosine defines the uncommon allele TNF2[6]. The TNF2 allele has been associated with a variety of inflammatory disorders, including systemic lupus erythematosus, dermatitis herpetiformis, and celiac disease[7]. Furthermore, TNF2 allele has been found to be a stronger transcription activator than the TNF1 allele[8-12], resulting in higher TNF-α levels. Moreover, TNF2 polymorphism has been associated with morbidity and mortality of severe forms of cerebral malaria[13], mucocutaneous leishmaniasis[14], meningococcal disease[15] and septic shock[16].

A polymorphism is also found at position +252 located in the first intron of the TNFβ gene, with a G in the TNFB1 allele and an A in the TNFB2 allele[17]. In contrast to TNF-α, which is expressed mainly by macrophages, TNFβ is expressed and released by lymphocytes. Genes encoding either cytokine are positioned next to each other within the cluster of human leukocyte antigen class III genes on chromosome 6. With respect to high homology and location in the genome, evolutionary studies suggest a common ancestor for both genes that duplicated during evolution. The TNFB1 allele has been associated with a higher TNFβ response at both the mRNA and the protein levels[17]. Furthermore, some studies have found

that the TNFB2 allele results in a higher TNF-α secretory capacity than the TNFB1 allele[8], and higher plasma TNF-α levels[18], whereas others could not confirm this observation.

The present study was focused on ABP. The aim was to investigate TNF-α-308 and TNFB polymorphisms in ABP patients, and to related the polymorphisms studied to plasma TNF-α levels.

MATERIALS AND METHODS

Subjects

127 consecutive patients with a first attack of unequivocal acute biliary pancreatitis (ABP) were prospectively considered from January 2001 to August 2002. The diagnosis of acute pancreatitis was based on clinical criteria, an increased -amylase activity (enzymatic colorimetric test) in serum and CT verification of pancreatitis. Etiology of acute pancreatitis was gallstones, in the presence of appropriate radiological of endoscopic retrograde cholangiopancreatography (ERCP) findings. Pancreatitis is classified as severe when APACHE II score is ⩾8[19] and CT severity index ⩾4[20]. Septic shock was defined according to ACCP/SCCM consensus conference criteria[21]. The control Group came from 102 healthy volunteers. In order to be eligible for the enrollment, all of the subjects from the two groups had to be yellow Chinese Han. The exclusion criteria were defined as follows: (1) age > 75 years; (2) cardiac failure(class>III); (3) liver insufficiency (Child C); (4) White blood cell counts $<0.4\times10^9$/L; (5) immunosuppression; (6) there was a delay of more than 36 hours from onset of abdominal pain and hospitalization; (7) patients who had clinical, radiological, or ERCP evidence suggestive of a diagnosis of chronic pancreatitis. The study was approved by the local Ethics Committee and informed consent had been obtained from the patient or a close relative.

Measurement of plasma TNF-α concentrations

Peripheral venous plasma samples were collected (EDTA anticoagulation) from only ASBP patients at admission, centrifuged and stored at -70 ℃ before analysis. Plasma TNF-alpha concentrations were measured by enzyme immunoassay kit (Quantikine HS Human TNF-alpha immunoassay. kit, R & D Systems, Inc, Minneapolis, MN). The limit of sensitivity was 2.5 pg/mL.

TNF-α-308 G to A substitution

Each patient's DNA was extracted from whole blood using Wizard Genomic DNA Purification kit (Promega) according to the manufacture's instruction. PCR was used to amplify a 107 basepairs fragment of the TNF-α genomic sequence using primers. Upstream: 5' -AGGCAATAGGTTTTGAGGGCCAT3', downstream: 5' -TCCTCCCTGCTCCGATTCCG 3' (Nanjing Bio Eng Co.Ltd.). The following PCR protocol was used: 94 ℃ for 3 minutes; 35 cycles of 94 ℃ for 45 seconds, 60 ℃ for 45 seconds, 72 ℃ for 45 seconds; 72 ℃ for 5 minutes using reagents purchased from Promega on a Gene Cycler™ (BIO-RAD, Japan). The PCR product was digested directly with 2 U NcoI restriction enzyme (Promega) at 37 ℃ for 6 hours. Digested DNA was analyzed on 5 % polyacrylamide gels. Ethidium bromide staining of the gel demonstrated the original 107 basepairs fragment (homozygous patients for allele TNF2, lacking NcoI site), three fragments of 102, 87 and 20 basepairs (heterozygous patients), or two fragments of 87 and 20 basepairs of size (homozygous patients for the allele TNF1), (Figure 1).

TNF-β NcoI polymorphism

A 782 basepairs fragment of the TNF-β genomic sequence, including the polymorphic NcoI site, was amplified using PCR. The following nucleotide sequences were used for PCR amplification[18]: 5' -CCGTGCTTCGTGCTTTGGACTA 3' and 5' -AGAGGGGTGGATGCTTGGGTTC3' (Nanjing Bio Eng Co.). The following PCR protocol was used: 95 ℃ for 3 minutes; 37 cycles of 95 ℃ for 1 minute, 50 ℃ for 1 minute, 72 ℃ for1 minute; 72 ℃ for 5 minutes using reagents purchased from Promega on a Gene Cycler™ (BIO-RAD, Japan). The PCR product was digested directly with 2 U NcoI restriction enzyme (Promega) at 37 ℃ for 6 hours. Digested DNA was analyzed on 5 % polyacrylamide gels. Ethidium bromide staining of the gel demonstrated the original 782 basepairs fragment (homozygous patients for allele TNFB2), three fragments of 782, 586 and 196 basepairs (heterozygous patients), or two fragments of 586 and 196 basepairs of size (homozygous patients for the allele TNFB1), (Figure 2).

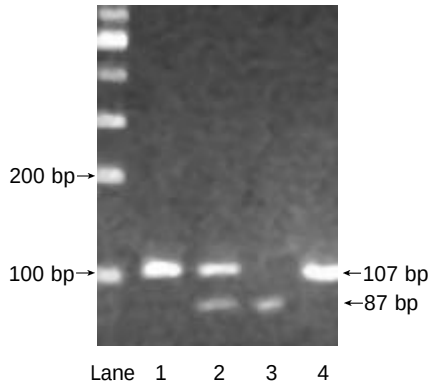

Figure 1 Lane1 and 4, TNF2 homozygote; Lane 2, TNF1/TNF2 heterozygote; Lane 3, TNF1 homozygote.

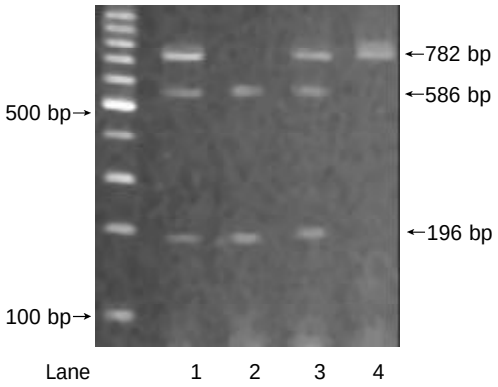

Figure 2 Lane 1 and 3, TNFB1/TNFB2 heterozygote; Lane 2, TNFB1 homozygote; Lane 4, TNFB2 homozygote.

Statistical analysis

Comparison of allelic and genotype frequencies was examined for statistical significance with chi-square test. Descriptive data of continuous variables were tested by Student's *t*-test. Plasma TNF-α levels were reported as median ± SD. Analysis was completed by SPSS 10.0, and a 2-tailed $P<0.05$ was considered statistically significant.

RESULTS

Characteristics of the patients

According to the selected criteria, 61 patients (36 females, males 25) with acute severe pancreatitis were studied. The mean age (± SD) was 54.6±19 years. APACHE II, 11.5±1; CT, 6±1. Of these, 18 had developed septic shock. The APACHE II score and CT score at the time of admission was similar in both septic shock and no septic shock patients. This study was

undertaken in selected patients with acute mild biliary pancreatitis (AMBP, *n*=66) as defined by APOCHE II score[19] and CT severity index[20], and matched with ASBP for age, sex, and cause of pancreatitis. Patients with AMBP had an uneventful recovery. The control group included 102 healthy volunteers, the mean age (± SD) was 44.5±10 years. The distribution of gender was 59 females and 43 males.

Two polymorphisms of tumor necrosis factor gene

The frequency distribution of genotypes for TNF polymorphisms studied is shown in Table 1. There was no significant difference in the TNF-308 or TNFB genotype frequency distributions between patients with mild or severe disease. For the TNF-308 polymorphism, TNF2 was found in 18 (29.5 %) of patients with ASBP compared with 17 (25.8 %) of patients with AMBP (χ^2=0.223, *P*=0.636). Likewise TNFB2 occurred in 42 (68.9 %) of patients with ASBP compared with 44 (66.7 %) of patients with AMBP (χ^2=0.147, *P*=0.702).

Further there were no significant differences in the TNF-308 or TNFB genotype frequency distributions between patients with ABP and controls (Table 1). As to TNF2 frequency, it was found in 35 (27.6 %) of patients with ABP compared with 26 (25.5 %) of controls (χ^2=0.124, *P*=0.725). Likewise TNFB2 occurred in 86 (67.7 %) of patients with ABP compared with 63 (61.8 %) of controls (χ^2=0.882, *P*=0.348 respectively).

TNF2 was found in 9 (50 %) of ASBP patients who developed septic shock compared with 9 (20.1 %) of ASBP patients with no septic shock (χ^2=5.155, *P*=0.023). However, TNFB2 occurred in 13 (72.2 %) of ASBP patients with septic shock compared with 29 (67.4 %) of ASBP patients with no septic shock (χ^2=0.135, *P*=0.713), (Table 2).

Table 1 Comparison of TNF Genotype among different groups

	TNF-308			TNFB		
	G/G	G/A	A/A	1/1	1/2	2/2
ASBP	43 (70.5)	15 (24.6)	3 (4.9)	19 (31.1)	25 (41.0)	17 (27.9)
AMBP	49 (74.2)	14 (21.2)	3 (4.5)	22 (33.3)	26 (39.4)	18 (27.3)
	χ^2=0.040, *P*=0.980			χ^2=0.197, *P*=0.906		
ABP	92 (72.4)	29 (22.8)	6 (4.7)	41 (32.3)	51 (40.1)	35 (27.6)
Control	76 (74.5)	21 (20.6)	5 (4.9)	39 (38.2)	35 (34.3)	28 (27.5)
	χ^2=2.545, *P*=0.280			χ^2=3.594, *P*=0.166		

Note. Comparison by chi-square test. No significant differences were found in the distribution of each genotype frequency [no. (%)] between any of the two groups.

Table 2 Comparison of TNF2 frequency and TNFB2 frequency between septic shock group and no septic shock group

	Septic shock (*n*=18)	No septic shock (*n*=43)	*P*
TNF2	9 (44.4%)	9 (20.9%)	0.023
TNFB2	13 (72.2%)	29 (67.4%)	0.713

Patients with septic shock showed a significantly higher prevalence of the TNF2 than those without. No such association was seen in TNFB2.

Baseline concentrations of TNF-α at inclusion in ASBP

Plasma TNF-α levels at inclusion were detectable in all of the patients with ASBP and shown in Figure 3. At inclusion, among the 61 patients who were admitted for ASBP, 31 (50.8 %) had an increased concentration of TNF-α (normal value <20 pg/mL). There was no significant difference in baseline concentrations of TNF-α, between ASBP patients who developed septic shock and ASBP patients who didn't.

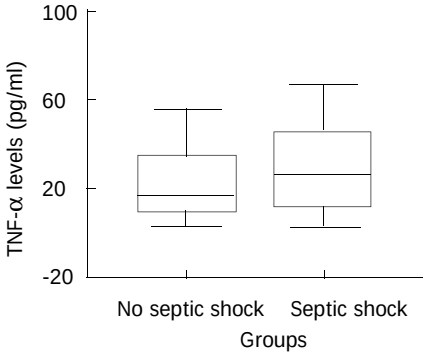

Figure 3 Baseline concentrations of TNF-α at inclusion in ASBP complicated by septic shock or not. *P*=0.643. No significant differences were found in baseline TNF-α levels between septic shock group and no septic shock group.

Association of two polymorphisms of TNF gene with TNF-α levels

In ASBP patients, no association was found in baseline TNF-α levels between TNF2 carrier and TNF1 carrier (30.73±23.05 *vs* 25.65±22.63, *P*=0.430), neither was found between TNFB2 carrier and TNFB1 carrier (25.53±23.71 *vs* 30.73±20.38, *P*=0.412), (Figure 4 and Figure 5).

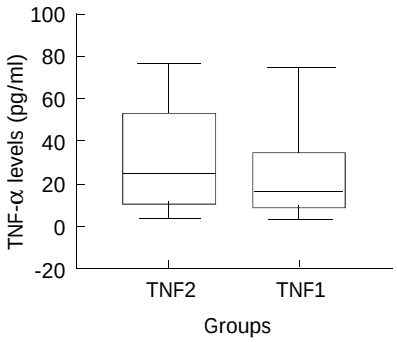

Figure 4 Comparison of TNF-α levels (pg/mL) in ASBP patients based on TNF2 allele. No significant difference was found in TNF-α levels between TNF2 carrier and TNF1 carrier.

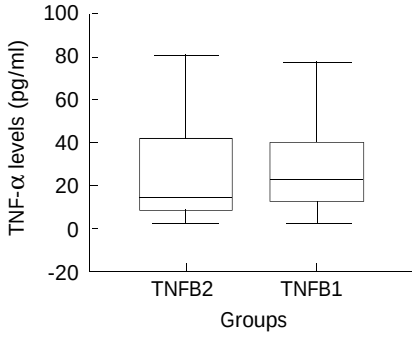

Figure 5 Comparison of TNF-α levels (pg/mL) in ASBP patients based on TNFB2 allele. No significant difference was found in TNF-α levels between TNFB2 carrier and TNFB1 carrier.

DISCUSSION

In the study we have found no association between either TNF-α-308 or TNFB biallelic polymorphism and ASBP or ABP, and thus no evidence that these loci contribute to ASBP susceptibility

or severity. This was in line with previous study[22, 23]. However, the distribution of TNF-α-308 polymorphisms within the ASBP patients varied, and TNF2 allele was found significantly more frequently in the septic sock patients than in no septic shock ones ($P<0.05$). The association between the septic shock patients and TNF polymorphism was restricted to the TNF-α-308 polymorphism (TNF2 allele), no such association being seen with TNFB2. The finding of an apparent association between the TNF-α-308 polymorphism and the septic shock raises the possibility that genetic factors may play a role in controlling the onset of septic shock related to ASBP.

In our study an increased TNF-α value was documented in 50.8 % of ASBP patients at inclusion. This finding confirms two previous clinical studies in which TNF-α was documented in 29 % to 78 % of patients studied[24, 25]. However, there was no significant difference in baseline TNF-α levels between patients who developed septic shock and patients who didn' t. The result suggested that plasma baseline TNF-α level was of little value predicting whether septic shock would occur in ASP.

In sepsis and other diseases TNF polymorphisms have been associated with morbidity and mortality of severe forms[13-16,26]. The present study did not found an association in the distribution of either TNF2 allele frequency or TNFB2 allele frequency between ASBP patients and AMBP patients ($\chi^2=0.223$, $P=0.636$ and $\chi^2=0.147$, $P=0.702$ respectively). The results showed no correlation between the gene polymorphisms studied and disease severity. Comparison of TNF2 allele frequency or TNFB2 allele frequency in patients with ABP and in healthy controls suggested that these polymorphisms studied did not influence disease susceptibility ($\chi^2=0.124$, $P=0.725$ and $\chi^2=0.882$, $P=0.348$ respectively). However, significant difference was found in TNF2 allele frequencies between septic shock patients and non-septic shock patients ($\chi^2=5.155$, $P=0.023$). Indeed, only in severe forms of cerebral malaria[13], mucocutaneous leishmaniasis[14], meningococcal disease[15] and septic shock[16], were morbidity and mortality linked with TNF2 allele or TNFB2 allele. In mild conditions, no such relationship was found between sepsis and the TNF2 allele[27]. As to TNF-α-308 and TNFB genotype, there were no significant difference in the distribution of either type between ASBP patients and AMBP patients, neither was found between ABP patients and controls. It suggested that TNF-α-308 genotype and TNFB genotype were both not related to the susceptibility or severity of ABP.

Although polymorphisms may only be markers of other functionally significant gene polymorphism, at least one of the TNF gene polymorphisms studied is known to have functional significance. It seems that environmental factors trigger cytokine secretion, genetic factors may be important in determining levels of secretion[28]. In vitro studies have identified that individuals may demonstrate consistent differences in leukocyte cytokine secretion[29] and that these difference are probably genetically predetermined[28]. In our study, plasma TNF-α concentrations of ASBP patients with TNF2 allele or TNFB2 allele were not significantly higher than that of patients without TNF2 allele or TNFB2 allele respectively. It suggested that there was no significant correlation between TNF-α concentration and TNF2 or TNFB2 allele carriage. However, many factors could influence plasma TNF-α concentrations. Of these, an important one is its relatively short half-life[30], so we were at great risk of missing the intravascular secretion of this cytokine. Another reason for low plasma TNF-α concentrations may be the breakdown of TNF-α by enzyme released from pancreas into circulation[31, 32]. Furthermore, this detectable level does not take into account the membrane-bound form of TNF-α. In addition, in complex biologic systems, the effect of a single gene polymorphism in determining cytokine production may be minimized through the interaction of other factors[33]. Maybe circulating TNF-α levels do not correspond with the TNF2 and TNFB2 polymorphisms, however, circulating TNF-α levels might be under a multifactoral regulatory process. Local TNF-α levels might be of greater importance and under more control by specific polymorphisms.

To the best of our knowledge, there have two different studies on the association of two polymorphisms of tumor necrosis factor gene with acute severe pancreatitis[23, 35], and our results are in line with theirs. However, they both failed to study the association of two polymorphisms with septic shock due to ASBP. The finding of our study for the first time, to our knowledge, raise the possibility that TNF2 allele may play some role in the susceptibility of septic shock related to ASBP. However, the role, if any, of genetic factors in influencing the occurrence of septic shock awaits confirmation in further prospective studies. If the association between TNF2 allele and septic shock is confirmed, it would have implications not only for understanding of mechanisms of septic shock from ASBP, but also in the clinical management of patients, with the possibility that TNF2 carriers at high risk of septic shock may be identifiable early in the disease course, allowing early and aggressive therapy to be instituted. In addition, the study offers new opportunities for studying intervention with anti-TNF therapies. Determining a patient' s TNF2 genotype before starting the treatment may permit the selection of a TNF2 group of high-risk patients who could benefit from treatment with anti-TNF. Such a possibility deserves further study, since an effective therapy for ASBP patients with septic shock would have important clinical and economic consequences.

In conclusion, our study demonstrated that there was no association between acute biliary pancreatitis and the two polymorphisms of tumor necrosis factor gene studued; however, TNF2 allele were associated with the susceptibility to septic shock related to acute sever biliary pancreatitis. Genetic factors are not important in determining plasma TNF-α levels in ASBP.

REFERENCES

1 **Forsmark CE.** The clinical problem of biliary acute necrotizing pancreatitis: epidemioloty, pathophysiology, and diagnosis of biliary necrotizing pancreatitis. *J Gastrointest Surg* 2001; **5:** 235

2 **Schmid SW,** Buchler MW. The role of infection in acute pancreatitis. *Gut* 1999; **45:** 311-316

3 **Xia Q,** Jiang JM, Gong X, Chen GY, Li L, Huang ZW. Experimental study of Tong Xia purgative method in ameliorating lung injury in acute necrotizing pancreatitis. *World J Gastroenterol* 2000; **6**: 115-118

4 **Grewal HP,** Kotb M, el Din AM, Ohman M, Salem A, Gaber L, Gaber AO. Induction of tumor necrosis factor in severe acute pancreatitis and its subsequent reduction after hepatic passage. *Surgery* 1994; **115:** 213-221

5 **Chiche JD,** Siami S, Dhainaut JF, Mira JP. Cytokine polymorphisms and susceptibility to severe infectious disease. *Sepsis* 2001; **4:** 209-215

6 **Wilson AG,** de Vries N, Pociot F, di Giovine FS, van der Putte LB, Duff GW. An allelic polymorphism within the human tumor necrosis factor α promoter region is strongly associated with HLA A1, B8, and DR3 alleles. *J Exp Med* 1993; **177:** 557-560

7 **McManus R,** Wilson AG, Mansfield J, Weir DG, Duff GW, Kelleher D. TNF2, a polymorphism of the tumor necrosis-α gene promoter, is a component of the celiac disease major histocompatibility complex haplotype. *Eur J Immunol* 1996; **26:** 2113-2118

8 **Pociot F,** Briant L, Jongeneel CV, Molvig J, Worsaae H, Abbal M, Thomsen M, Nerup J, Cambon-Thomsen A. Association of tumor necrosis factor (TNF) and class II major histocompatibility complex alleles with the secretion of TNF-α and TNF-β by human mononuclear cells: a possible link to insulin-dependent diabetes mellitus. *Eur J Immunol* 1993; **23:** 224-231

9 **Kroeger KM,** Carville KS, Abraham LJ. The -308 tumor necrosis factor α promotor polymorphism effects transcription. *Mol Immunol* 1997; **34:** 391-399

10 **Wilson AG,** Symons JA, McDowell TL, McDevitt HO, Duff GW. Effects of a polymorphism in the human tumor necrosis factor α promoter on transcriptional activation. *Proc Natl Acad Sci USA* 1997; **94:** 3195-3199

11 **Braun N,** Michel U, Ernst BP, Metzner R, Bitsch A, Weber F, Rieckmann P. Gene polymorphism at position –308 of the tumor-necrosis-factor-alpha (TNF-alpha) in multiple sclerosis and it's influence on the regulation of TNF-alpha production. *Neruosci Lett* 1996; **215:** 75-78

12 **Brinkman BM,** Zuijdeest D, Kaijzel EL, Breedveld FC, Verweij CL. Relevance of the tumor necrosis factor alpha (TNF-α)-308 promoter polymorphism in TNF alpha gene regulation. *J Inflamm* 1996; **46:** 32-41

13 **McGuire W,** Hill AV, Allsopp CE, Greenwood BM, Kwiatkowski D. Variation in the TNF-alpha promoter region associated with susceptibility to cerebral malaria. *Nature* 1994; **371:** 508-510

14 **Cabrera M,** Shaw MA, Sharples C, Williams H, Castes M, Convit J, Blackwell JM. Polymorphism in tumor necrosis factor genes associated with mucocutaneous leishmaniasis. *J Exp Med* 1995; **182:** 1259-1264

15 **Nadel S,** Newport MJ, Booy R, Levin M. Variation in the tumor necrosis factor-alpha gene promoter region may be associated with death from meningococcal disease. *J Infect Dis* 1996; **174:** 878-880

16 **Mira JP,** Cariou A, Grall F, Delclaux C, Losser MR, Heshmati F, Cheval C, Monchi M, Teboul JL, Riche F, Leleu G, Arbibe L, Mignon A, Delpech M, Dhainaut JF. Association of TNF2, a TNF-alpha promoter polymorphism, with septic shock susceptibility and mortality: a multicenter study. *JAMA* 1999; **282:** 561-568

17 **Messer G,** Spengler U, Jung MC, Honold G, Blomer K, Pape GR, Riethmuller G, Weiss EH. Polymorphic structure of the tumor necrosis factor (TNF) locus: an Ncol polymorphism in the first intron of the human TNF-β gene correlates with a variant amino acid in position 26 and a reduced level of TNF-β production. *J Exp Med* 1991; **173:** 209-219

18 **Stuber F,** Petersen M, Bokelmann F, Schade U. A genomic polymorphism within the tumor necrosis factor locus influences plasma tumor necrosis factor-α concentrations and outcome of patients with severe sepsis. *Crit Care Med* 1996; **24:** 381-384

19 **Dominguez-Munoz JE**, Carballo F, Garcia MJ, de Diego JM, Campos R, Yanguela J, de la Morena J. Evaluation of the clinical usefulness of APACHEII and SAPS systems in the initial prognostic classification of acute pancreatitis: a multicenter study. *Pancreas* 1993; **8:** 682-686

20 **Balthazar EJ,** Robinson DL, Megibow AJ, Ranson JH. Acute pancreatitis: value of CT in establishing prognosis. *Radiology* 1990; **174:** 331-336

21 **Muckart DJ,** Bhagwanjee S. American college of chest physicians / society of critical care medicine consensus conference definitions of the systemic inflammatory response syndrome and allied disorders in relation to critically injured patients. *Crit Care Med* 1997; **25:** 1789-1795

22 **Zhang D**, Li J, Jiang Z, Yu B, Tang X. Significance of tumor necrosis factor-alpha gene polymorphism in patients with acute severe pancreatitis. *Zhonghua Yixue Zazhi* 2002; **82**: 1529-1531

23 **Sargen K,** Demaine AG, Kingsnorth AN. Cytokine gene polymorphisms in acute pancreatitis. *JOP* 2000; **1:** 24-35

24 **de Beaux AC,** Goldie AS, Ross JA, Carter DC, Fearon KC. Serum concentrations of inflammatory mediators related to organ failure in patients with acute pancreatitis. *Br J Surg* 1996; **83:** 349-353

25 **Brivet FG,** Emilie D, Galanaud P. Pro- and anti-inflammatory cytokines during acute severe pancreatitis: an early and sustained response, although unpredictable of death. Parisian Study Group on Acute Pancreatitis. *Crit Care Med* 1999; **27:** 749-755

26 **Majetschak M,** Flohe S, Obertacke U, Schroder J, Staubach K, Nast-Kolb D, Schade FU, Stuber F. Relation of a TNF Gene Polymorphism to Severe Sepsis in Trauma Patients. *Ann Surg* 1999; **230:** 207-214

27 **Stüber F,** Udalova IA, Book M, Drutskaya LN, Kuprash DV, Turetskaya RL, Schade FU, Nedospasov SA. –308 tumor necrosis factor (TNF) polymorphism is not associated with survival in severe sepsis and is unrelated to lipopolysaccharide inducibility of the human TNF promotor. *J Inflam* 1996; **46:** 42-50

28 **Westendorp RG,** Langermans JA, Huizinga TW, Elouali AH, Verweij CL, Boomsma DI, Vandenbroucke JP, Vandenbrouke JP. Genetic influence on cytokine production and fatal meningococcal disease. *Lancet* 1997; **349**: 170-173

29 **van der Linden MW,** Huizinga TW, Stoeken DJ, Sturk A, Westendorp RG. Determination of tumor necrosis factor-alpha and interleukin-10 production in a whole blood stimulation system: assessment of laboratory error and individual variation. *J Immunol Methods* 1998; **218**: 63-71

30 **Kaufmann P,** Tilz GP, Lueger A, Demel U. Elevated plasma levels of soluble tumor necrosis factor receptor (sTNFp60) reflect severity of acute pancreatitis. *Intensive Care Med* 1997; **23**: 841-848

31 **Steer ML.** How and where does acute pancreatitis begin? *Arch Surg* 1992; **127**: 1350-1353

32 **Dominguez-Munoz JE,** Carballo F, Garcia MJ, de Diego JM, Rabago L, Simon MA, de la Morena J. Clinical usefulness of polymorphonuclear elastase in predicting the severity of acute pancreatitis: results of a multicentre study. *Br J Surg* 1991; **78**: 1230-1234

33 **Powell JJ,** Fearon KC, Siriwardena AK, Ross JA. Evidence against a role for polymorphisms at tumor necrosis factor interleukin-1 and interleukin-1 receptor antagonist gene loci in the regulation of disease severity in acute pancreatitis. *Surgery* 2001; **129:** 633-640

Edited by Ren SY

P.O.Box 2345, Beijing 100023, China
Fax: +86-10-85381893
E-mail: wjg@wjgnet.com www.wjgnet.com

World J Gastroenterol 2003;9(4):829-832
World Journal of Gastroenterology
 ISSN 1007-9327

• CLINICAL RESEARCH •

The development of a new bioartificial liver and its application in 12 acute liver failure patients

Yi-Tao Ding, Yu-Dong Qiu, Zhong Chen, Qing-Xiang Xu, He-Yuan Zhang, Qing Tang, De-Cai Yu

Yi-Tao Ding, Yu-Dong Qiu, Zhong Chen, Qing-Xiang Xu, Qing Tang, De-Cai Yu, Hepatobiliary Surgery Department, affiliated Drum Tower Hospital of Medical College of Nanjing University, Hepatobiliary Institute of Nanjing University; Hepatobiliary Surgery Institute of Nanjing, Jiangsu Province, 210008, China
He-Yuan Zhang, Biochemistry Department in Nanjing University, Jiangsu Province, China
Supported by the Public Health Bureau of Jiangsu Province, China, BQ200020 and Social Development Plan of Scientific and Technological Council of Nanjing Municipal, China. SS200002
Correspondence to: Dr. Yi-Tao Ding, Hepatobiliary Surgical Department, Affiliated Drum Tower Hospital of Medical College in Nanjing University, Zhongshan road, 321, Nanjing, 210008, Jiangsu Province, China. xqx008@hotmail.com
Telephone: +86-25-3304616-11601 **Fax:** +86-25-3317016
Received: 2002-07-31 **Accepted:** 2002-09-12

Abstract

AIM: Bioartificial liver is a hope of supporting liver functions in acute liver failure patients. Using polysulfon fibers, a new bioartificial liver was developed. The aim of this study was to show whether this bioartificial liver could support liver functions or not.

METHODS: Hepatocytes were procured from swine using Seglen's methods. The bioartificial liver was constructed by polysulfon bioreactor and more than 10^{10} hepatocytes. It was applied 14 times in 12 patients, who were divided into 7 cases of simultaneous HBAL and 5 cases of non-simultaneous HBAL. Each BAL treatment lasted 6 hours. The general condition of the patients and the biochemical indexes were studied.

RESULTS: After treatment with bioartificial liver, blood ammonia, prothrombin time and total bilirubin showed significant decrease. 2 days later, blood ammonia still showed improvment. within one month period, 1 case (1/7) in simultaneous group died while in non-simultaneous group 2 cases (2/5) died. The difference was significant. Mortality rate was 25 %.

CONCLUSION: The constructed bioartificial liver can support liver functions in acute liver failure. The simultaneous HBAL is better than non-simultaneous HBAL.

Ding YT, Qiu YD, Chen Z, Xu QX, Zhang HY, Tang Q, Yu DC. The development of a new bioartificial liver and its application in 12 acute liver failure patients. *World J Gastroenterol* 2003; 9 (4): 829-832

http://www.wjgnet.com/1007-9327/9/829.htm

INTRODUCTION

Acute liver failure (ALF) is commonly seen in the mainland of China. The patients are always characterized by infection of hepatitis B. Liver cell damage is the main reason of ALF. When the amount of normal cells decrease below its limit, liver function will deteriorate and a vicious cycle will be formed.

Liver transplantation (LT) has already been a wise choice for these patients[1-3]. The 1 year survival rate could be improved to more than 70 % when LT is applied[4,5]. But the donor is scarce, so it limits the wide practice of LT. Many patients exacerbated and died during the period of waiting donor liver.

Bioartificial liver (BAL) is designed to take the responsibility of supporting liver functions temporarily in acute liver failure[6-9]. It consists of a semi-permeable membrane and living allogeneic or syngeneic liver cells. The flow of blood or plasma from the patient can exchange the substances with those cells through this membrane. The ammonia and other toxins in blood then are detoxified, as well as some useful factors are secreted into blood. Many scholars reported that BAL was effective and could be used as a bridge to LT[8-10]. Also this technique gave the chance of spontaneous recovery of the native function because of liver cell regeneration in some cases[8,11].

It is estimated that 1×10^9 hepatocytes are the lowest limit that are needed in BAL[10]. Such large number of hepatocytes are very difficult to be cultured in a small bioreactor. Enlarging the volume of the bioreactor and adding a hepatocytes cell pool are both good methods to solve such problems.

Using a bioreactor made of polysulfon, we developed a bioartificial liver recently and applied it in 12 patients. The results were exciting.

MATERIALS AND METHODS

Animals

Healthy Chinese experimental miniature swine were purchased from the Animal Center of Beijing Agriculture University. On receipt, swine were kept in a temperature and humidity controlled environment (20-25 ℃, humidity 50-70 %) in a 12/12 hour light/dark cycle and fed with a cereal based diet with free access to water. More than a week later, they were used to get the hepatocytes. 12 hours before procedure only free water *ad libitum* was allowed. The animals were treated in accordance with the guidelines established by Affiliated Drum Tower Hospital of Medical College of Nanjing University.

Hepatocytes preparation

Hepatocytes were isolated from the swine by in situ liver perfusion and enzymatic collagenase digestion according to the process described by Seglen[12]. Briefly, under katamine (50 mg/kg) anesthesia, a median laparotomy and cannulation of the portal vein were performed. The inferior vena cava was ligated just above the renal vein and then was cannulated close to the heart. The liver was perfused at 4 ℃ and pH 7.6 with 3 000 ml Hanks solution through the portal vein. Then the liver was circularly perfused with 500 ml 0.5 ‰ collagenase IV solution (Gibco, New York, USA) at a constant flow of 20 ml/minute. The softened liver was then excised and hepatocytes were separated from the connective liver tissue by gentle

agitation. The resulting cell suspension was filtered though 50 μm sterile metal mesh. The cells were washed three times, suspended in non serum RPMI 1640 culture medium (Sigma, Louis, USA) with 200 μg/L hydrocortisone, 1 mg/L HGF, 10 μg/L EGF, 20 μg/L NGF, 100 μg/Linsulin, 4 μg/L glucagon, 6.25 mg/L transferrin, 10 mg/L linoleic acid, 2 mmol glutamine, 0.5 g/L bovine serum albumin, 3nmol sodium selenate, 0.1 μg/L $CuSO_4 \cdot 5H_2O$, 50pM $ZnSO_4 \cdot 7H_2O$, 15 mmol HEPES, 200 μg/L cefaperazone, 1×10^5U/Lpenicillin and 100 mg/L streptomycin. Cell viability was determined by the trypanum exclusion test. Only suspentions with cell viability of ⩾95 % were used. Cells suspension was then stirring incubated overnight in that non serum RPMI 1640 culture medium at 37 ℃.

Configuration of bioartificial liver

Polysulfon bioreactor was purchased from TECA Corp. (Hongkong, China). The molecular cutoff of the membrane was 100 kD. Total fiber internal surface area was 1 620 cm^2, external surface area was 2 060 cm^2. Before use, the bioreactor was sterilized and rinsed by 3 000 ml normal saline. A hepatocytes reservoir, a rolling pump and a circulation cycle were designed to connect to the extra-fiber compartment of bioreactor. The aim was to ensure more than 10^{10} hepatocytes being used and enough nutrition could be provided. Then the cultured suspended cells were filled into the extra-fiber compartment of bioreactor. The rolling rate of the pump was 80 ml/minute.

Blood was removed from the patient through a double lumen catheter in superficial femoral vein at a rate of 100 ml/minute and run through a plasma separator. The separated plasma passed through a charcoal column or bilirubin absorption column and then run into the intra-fiber compartment of bioreactor in simultaneous HBAL, while in non- simultaneous HBAL the plasma run directly into the intra-fiber compartment of bioreactor. The reacted plasma were then reconstituted with red blood cells and returned to the patient via the venous cannula. (Figure 1).

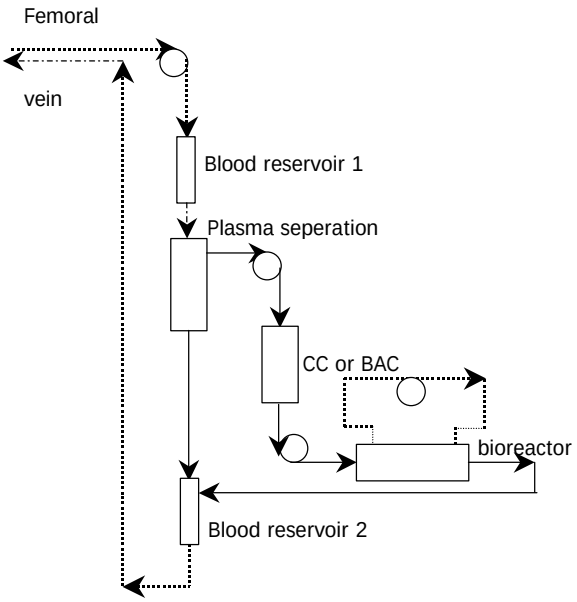

Figure 1 The constructed bioartificial liver. CC: charcoal column. BAC: bilirubin absorption column.

Clinical use

12 patients, which include 9 male and 3 female, suffering from acute liver failure were adopted to this study. The age ranged from 13 to 56. All the patients were found having hepatitis B infection (Table 1). Before the BAL supporting treatment, an evaluation of the patient's psychic state was conducted by a psychologist, and an agreement of BAL application was signed by the patient and/or his direct relatives.

The treatment regimen included simultaneous HBAL and non-simultaneous HBAL. The only difference was bilirubin absorption treatment or plasma exchange treatment being used 1day before the bioreactor was applied in non-simultaneous HBAL while in simultaneous HBAL they were applied simultaneously. Other traditional treatments were all the same. Some liver function indexes and the one month mortality rate were used to evaluate the function of BAL.

Table 1 Clinical data of the patients

Patient No.	Sex	Age	Hepatitis B infection	Regimen of treatment	Number of treatment	Result
1	M	13	+	HBAL(CC)	1	Improved
2	M	38	+	1. HBAL(BAC)	1	Improved
				2. BAL	1	
3	F	34	+	HBAL(BAC)	1	Improved
4	M	55	+	HBAL(BAC)	1	Death
5	M	52	+	HBAL(BAC)	1	Improved
6	M	46	+	HBAL(BAC)	1	Improved
7	M	58	+	HBAL(BAC)	1	Improved
8	M	33	+	PE and BAL	1	Improved
9	F	50	+	PE and BAL	2	Death
10	F	52	+	HF and BAL	1	Death
11	M	40	+	HF and BAL	1	Improved
12	M	30	+	BAC and BAL	1	Improved

M: male, F: female, +: positive, HBAL: hybrid bioartificial liver, BAL: bioartificial liver, (CC): with charcoal column, (BAC): with bilirubin absorption column, PE and BAL: plasma exchange and 24 hours later BAL only, HF and BAL: hemofiltration and 24 hours later BAL only, BAC and BAL: bilirubin absorption and 24 hours later BAL only.

Statistical analysis

Mortality rate was expressed as percentage. Others were expressed as mean ± SD. Paired T test was used (SPSS software, SPSS Inc. USA). Probability of less than 0.05 was accepted as significant.

RESULTS

In 12 patients, 14 times BAL treatments were conducted. The period of one BAL treatment lasted 6 hours. All patients experienced the procedure successfully.

3 patients died soon after the procedure and 9 were improved. The mortality rate was 25 %. The criteria of improvement included improvement of general condition of the patient, persistent hepatic function improvement, improved psychic state, and recovery.

In biochemical test, ALT showed slight decrease in post-treatment period and restored to pre-treatment level 2 days later. No change in blood albumin. Blood ammonia, prothrombin time and total bilirubin indexes showed significant decrease after treatment. 2 days later, only blood ammonia still maintained significant low level (Figure 2).

In non-simultaneous HBAL, the mortality rate was 40 %. While in simultaneous HBAL, the mortality rate was 14.3 %. Significant difference was found comparing them (Figure 3).

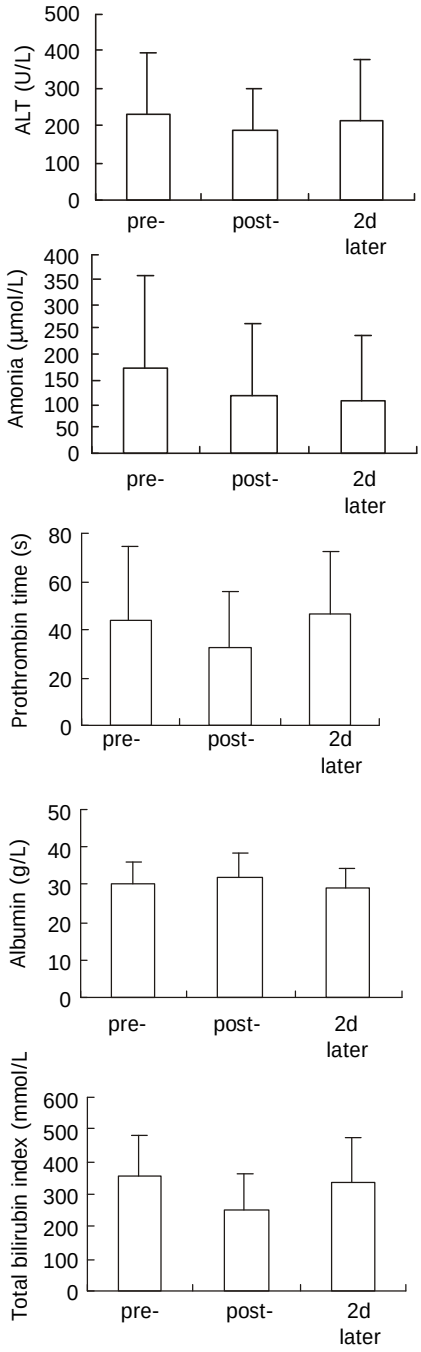

Figure 2 Change of ALT, ammonia, prothrombin time, albumin and total bilirubin index in 12 patients. Compared with pre-, ammonia, prothrombin time and total bilirubin index showed significant decreace in post-. 2 days later, only ammonia showed significant lowing. pre-: pre-treatment, post-: post-treatment, 2d later: 2 days after the treatment. Paired T test was used to test the difference.

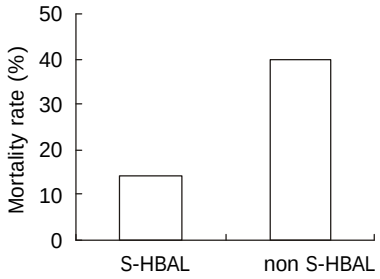

Figure 3 The mortality rate of simultaneous HBAL and non-simultaneous HBAL. Significant difference was found between this two groups (P<0.05).

Typical case report: A male, aged 38 years old, was admitted for "fatigue and yellow urine for a week". Physical examination showed yellowish face, moderate jaundice in skin and sclera, palpable liver that was 2 cm below the costal arch in right mid-clavicular line, and tenderness in right upper abdomen. Laboratory examination showed positive HBs antibody, Hbe antibody and HBc antibody, abnormal liver function. B type ultrasound examination showed image of liver injury. The diagnosis was severe acute hepatitis with hepatitis B virus infection. After admission, the patient was given conventional treatment without any improvement and ran downhill. One week later, He received a simultaneous HBAL (bilirubin absorption) treatment. Total bilirubin and prothrombin time decreased immediately. 6 days later he received another HBAL treatment because of worsening some biochemical indexes. 2 weeks after that the patient was recovered and was waiting for liver transplantation. (Table 2).

Table 2 Change of some biochemical index after the HBAL treatment

	Time	ALT (U/L)	GOT (U/L)	TBI (μmol/L)	DBI (μmol/L)	TP (g/L)	ALB (g/L)	PT (s)
	Admission	77.5	58.8	341.8	265.4	60.1	32.8	68.8
	2 hours later	58.7	52.5	343.0	255.2	52.4	31.9	32.2
HBAL	4 hours later	66.3	69.5	345.7	280.4	52.9	31.4	40.9
(BA)	6 hours later	68.7	79.9	260.8	291.6	54.5	31.4	26.7
	2 days later	80.6	68.0	423.2	336.0	70.4	37.1	20.2
	Before HBAL	421.2	371.9	375.4	109.0	44.6	27.4	21.9
	2 hours later	427.9	412.0	389.0	102.1	42.7	26.5	28.5
HBAL	4 hours later	431.8	411.4	373.9	99.5	43.0	26.7	28.7
	6 hours later	371.0	218.0	339.8	122.1	45.6	28.8	17.4
	2 days later	301.2	159.6	444.6	125.7	43.6	26.5	28.7

HBAL: hybrid bioartificial liver; BA: bilirubin absorption.

DISCUSSION

ALF is a severe disease in clinical practice with a mortality rate of 30-80 %[1-5]. OLT is thought to be the most effective method to improve the prognosis. But it is greatly limited due to shortage of donor liver[3,4]. HBAL is designed to take responsibility of improving the poor physical state of the patients and supporting liver function for a short time which may serve as a bridge to OLT[6-11].

The ideal HBAL should support the patients to pass through the worst period of the course by its metabolic, synthetic, toxin and drug degradational functions. When it works, immune reactions to the living cells may be avoided[13,14], while toxins and some useful factors might be capable to pass the membrane freely.

Construction of HBAL

The external BAL is being studied in many medical centers. Living hepatocytes are first needed in this apparatus. Human hepatocytes are the ideal choice. But the only available human livers are all used for liver transplantation. Human cell strains from some liver neoplasmas were also reported. But the danger of this application is unknown. Porcine hepatocytes are the commonest choice of many centers, because pigs are cheap and easy to get, without any ethical contradictions of killing them.

When the liver cells are procured, the membranes might be damaged by the enzymes or the mechanical factors[15]. The damaged membrane needs 1 to 3 days for recovery[16]. Our experience shows 1 day stirring culture of the procured hepatocytes is enough.

Enough viable hepatocytes are also important in BAL. It was estimated that 1×10^9 hepatocytes are the lowest limit[10]. Such a large number of hepatocytes are very difficult to live and maintain its function in a small bioreactor, through which hepatocytes may exchange substance with blood. If the volume of bioreactor is enlarged greatly, hemodynamics of the patient may be disturbed. We designed a two cycles bioreactor. The first cycle was to supply the nutrition and the other one was to connect to a cell reservoir which ensured 10^{10} cells were used in this system.

The toxins in blood are sometimes harmful to living hepatocytes. To decrease this effect, mechanical filtration or absorption is used in this system. Due to long period of time to construct the system and urgent situation of the patient requiring this treatment, we designed a non-simultaneous HBAL, that used mechanical filtration or carbon absorption or bilirubin absorption or plasma exchange first, then BAL was applied the next day. The results were not satisfactory. The mortality rate was higher than the simultaneous HBAL.

Effects of HBAL

The material of the bioreactor and the characters of it are most important. Polysulfon was chosen because of its good histocompatibility with body and little toxicity. In dialysis medicine the polysulfon is already widely used as dialyzer. The molecular cut-off is another important index for the bioartificial liver. If it is large enough, cells in it may not be protected completely. Otherwise the toxins cannot be detoxified and useful factors secreted by hepatocytes cannot enter the body. The molecular cut-off we choosed was 100 kD because IgG is about 150 kD and albumin or hepatic growth factor is about 70-80 kD.

Our experiments showed that BAL could function well when applied to the patients. The ammonia, prothrombin time and total bilirubin showed significant decrease in post-treatment examination. ALT also showed a slight decrease in post-treatment study, although no significant difference was found.

Also HBAL showed a delayed reaction, 2 days after application as ammonia still showed significant decrease. We considered that this function might be due to the synthetic function of HBAL.

REFERENCES

1 **Emond JC,** Whitington PF, Thistlethwaite JR, Cherqui D, Alonso EA, Woodle IS, Vogelbach P, Busse-Henry SM, Zucker AR, Broelsch CE. Transplantation of two patients with one liver. *Ann Surg* 1990; **212:** 14-22

2 **Shaw BW**. More questions than answers. *Liver Transplant Surg* 1995; **1:** 404-407

3 **Everhart JE**, Lombardero M, Detre KM, Zetterman RK, Wiesner RH, Lake JR, Hoofnagle JH. Increased waiting time for liver transplantation results in higher mortality. *Transplantation* 1997; **64**: 1300-1306

4 **Bilsuttil W,** Klintmalm B. Transplantation of the liver Philadelphia. W. B. *Saunders Company* 1996: 861

5 **Emond JC,** Whitington PF, Thistlethwaite JR, Alonso EM, Broelsch CE. Reduced-size orthotopic liver transplantation: use in the management of children with chronic liver disease. *Hepatology* 1989; **10**: 867-872

6 **Friedman AL**. Why bioartificial liver support remains the holy grail. *ASAIO* 1998; **44:** 241-243

7 **Kamihira M**, Yamada K, Hamamoto R, Iijima S. Speroid formation of hepatocytes using synthetic polymer. *Ann NY Acad Sci* 1997; **831**: 398-407

8 **Sussman NL,** Gislason GT, Conlin CA, Kelly JH. The Hepatix extracorporeal liver assist device: Initial clinical experience. *Artif Organs* 1994; **18:** 390-396

9 **Dixit V**. Development of a bioartificial liver using isolated hepatocytes. *Artif Organs* 1994; **18**: 371-384

10 **Hui T**, Rozga J, Demetriou AA. Bioartificial liver support. *J Hepatobiliary Surg* 2001; **8**: 1-15

11 **Suh KS**, Lilja H, Kamohara Y, Eguchi S, Arkadopoulos N, Neuman T, Demetriou AA, Rozga J. Bioartificial liver treatment in rats with fulminant hepatic failure: effect on DNA-binding activity of liver-enriched and grouth-associated transcription factors. *J Surg Res* 1999; **85**: 243-250

12 **Seglen PO**. Preparation of isolated rat liver cells. *Methods Cell Biol* 1976; **13**: 23-28

13 **Rozga J**, Williams F, Ro MS, Neuzil DF, Giorgio TD, Backfisch G, Moscioni AD, Hakim R, Demetriou AA. Development of a bioartificial liver: properties and function of a hollow fiber module inoculated with liver cells. *Hepatology* 1993; **17**: 258-265

14 **Cuervas-Mons V,** Colas A, Rivera JA, Prados E. *In vivo* efficacy of a bioartificial liver in improving spontaneous recovery from fulminant hepatic failure: a controlled study in pigs. *Transplantation* 2000; **69**: 337-344

15 **Flendrig LM,** La-Soe JW, Jorning GGA, Steenbeek A, Karlsen OT, Bovee WMM, Ladiges NC, te Velde AA, Chamuleau RA. In vitro evaluation of a novel bioreactor based on an integral oxygenator and spirally wound nonwoven polyester matrix for hepatocyte culture as small aggregates. *J Hepatol* 1997; **26:** 1379-1392

16 **Chen Z**, Ding Y, Zhang H. Cryopreservation of suckling pig hepatocytes. *Ann Clin Lab Sci* 2001; **31**: 391-398

Edited by Xu JY

P.O.Box 2345, Beijing 100023, China
Fax: +86-10-85381893
E-mail: wjg@wjgnet.com www.wjgnet.com

World J Gastroenterol 2003;9(4):833-835
World Journal of Gastroenterology
 ISSN 1007-9327

• CLINICAL RESEARCH •

Serum positive cagA in patients with non-ulcer dyspepsia and peptic ulcer disease from two centers in different regions of Turkey

Ender Serin, Uður Yilmaz, Ganiye Künefeci, Birol Özer, Yüksel Gümürdülü, Mustafa Güçlü, Fazilet Kayaselçuk, Sedat Boyacioðlu

Ender Serin, Ganiye Künefeci, Birol Özer, Yüksel Gümürdülü, Mustafa Güçlü, Ba kent University Faculty of Medicine, Department of Gastroenterology, Adana Teaching and Medical Research Center, Dadaloðlu Mahallesi, 39 Sokak, No: 6, 01250 Adana, Turkey
Uður Yilmaz, Sedat Boyacioðlu, Ba°kent University Faculty of Medicine, Department of Gastroenterology, Ankara Hospital, Dadaloðlu Mahallesi, 39 Sokak, No: 6, 01250 Adana, Turkey
Fazilet Kayaselçuk, Ba°kent University Faculty of Medicine, Department of Pathology, Adana Teaching and Medical Research Center Dadaloðlu Mahallesi, 39 Sokak, No: 6, 01250 Adana, Turkey
Correspondence to: Ender Serin, Baþkent Üniversitesi Týp Fakültesi, Adana Uygulama ve Araþtýrma Merkezi, Dadaloðlu Mahallesi, 39 Sokak, No: 6, 01250 Adana, Turkey. eserin@baskent-adn.edu.tr
Telephone: +90-322-3272727 **Fax:** +90-322-3271273
Received: 2002-12-07 **Accepted:** 2003-01-03

Abstract

AIM: To investigate and compare frequencies of serum positive cagA in patients from two separate regions of Turkey who were grouped according to the presence of peptic ulcer disease or non-ulcer dyspepsia.

METHODS: One hundred and eighty *Helicobacter pylori*-positive patients with peptic ulcer disease or non-ulcer dyspepsia were included in the study. One hundred and fourteen patients had non-ulcer dyspepsia and 66 had peptic ulcer disease (32 with gastric ulcers and/or erosions and 34 with duodenal ulcers). Each patient was tested for serum antibody to *H. pylori* cagA protein by enzyme immunoassay.

RESULTS: The total frequency of serum positive cagA in the study group was 97.2 %. The rates in the patients with peptic ulcers and in those with non-ulcer dyspepsia were 100 % and 95.6 %, respectively. These results were similar to those reported in Asian studies, but higher than those that have been noted in other studies from Turkey and Western countries.

CONCLUSION: The high rates of serum positive cagA in these patients with peptic ulcer disease and non-ulcer dyspepsia were similar to results reported in Asia. The fact that there was high seroum prevalence regardless of ulcer status suggests that factors other than cagA might be responsible for ulceration or other types of severe pathology in *H. pylori*-positive individuals.

Serin E, Yilmaz U, Künefeci G, Özer B, Gümürdülü Y, Güçlü M, Kayaselçuk F, Boyacioðlu S. Serum positive cagA in patients with non-ulcer dyspepsia and peptic ulcer disease from two centers in different regions of Turkey. *World J Gastroenterol* 2003; 9(4): 833-835
http://www.wjgnet.com/1007-9327/9/833.htm

INTRODUCTION

Helicobacter pylori (*H. pylori*) infection is very common, especially in developing countries; however, patients with this infection rarely develop clinically significant conditions, such as peptic ulcer disease. This situation has prompted researchers to investigate the possible roles of host and environmental factors, and factors related to the bacterium itself in cases that show severe pathologies[1-3]. Earlier works identified associations between *H. pylori* strains that harbor cytotoxin-associated gene A (cagA) and significant gastroduodenal pathology; however, the results of more recent studies are conflicting. In Europe, investigators have reported a significantly higher seroprevalence of cagA antigen in gastroduodenal ulcer cases than that in non-ulcer dyspepsia cases[4,5]. In contrast, most studies from Asian countries have noted that there was no significant difference between these patient groups with respect to anti-cagA antibody positivity[5-7]. Interpretation of these findings has been further complicated by reports from Japan and China. Some of these results differ from those of other Asian studies, and are in line with findings in Western countries[8,9].

Turkey is geographically situated between two continents that are reported to have different cagA seroprevalence rates. Our aim in this study was to compare the frequencies of serum positive cagA in Turkish patients with peptic ulcer disease and those with non-ulcer dyspepsia.

MATERIALS AND METHODS

General data of patients

The study included 180 patients (79 males and 101 females; mean age 43.4±11.2 years old) with dyspepsia who were confirmed *H. pylori*-positive by rapid urease testing. The patients came from two Baskent University medical centers in two different Turkish cities. Ninety-nine were from the southern city of Adana, and 81 were from Ankara in central Turkey. Individuals who met at least one of the following criterias were excluded from the study: history of *H. pylori* eradication treatment; anti-secretory and/or non-steroidal anti-inflammatory drug therapy in the 4 weeks prior to the study; chronic organ failure (chronic renal, pulmonary, or liver disease); chronic alcohol intake and cigarette smoking.

Methods

Gastric specimens from the antrum and corpus of each patient from the Adana Hospital were examined with hematoxylin/eosin and Giemsa stains. For each specimen, chronic inflammation, neutrophil activity, and *H. pylori* density were scored separately, according to the updated Sydney system: 0=normal, 1=mild, 2=moderate, and 3=severe[10]. We modified the four-point scale for histological scoring slightly in order to facilitate statistical analysis. Scores of 0-1 were categorized together as "low score" and scores of 2-3 were categorized together as "high score." The same pathologist examined all the histological sections.

Three groups were divided according to the patients' endoscopic findings: a non-ulcer dyspepsia (NUD) group (n=114); a duodenal ulcer (DU) group (n=34); and a gastric ulcer and/or erosion (GU/E) group (n=32).

Enzyme immunoassay (Equipar Diagnostici, Rome, Italy) was used to test for the presence of serum IgG and IgA

antibodies to *H. pylori* cagA protein. Since there is no international standard for IgG levels, this was quantitated by means of a standard curve calibrated in arbitrary units per milliliter (Uarb/mL). Serum levels above 5 Uarb/mL were considered to indicate positivity.

Statistical analysis

The unpaired Student's *T*-test and the χ^2 test were used to analyze the data, as appropriate. It was considered to be statistical significant when $P<0.05$.

RESULTS

Of the 180 patients, 175 (97.2 %) were cagA (+). The rate serum positive cagA in the NUD group was 95.6 %, and they were 100 % in both DU and GU/E groups. The overall rate in each hospital and the group rates in each center were shown in Table 1. The NUD, DU, and GU/E groups had similar mean serum levels of IgG-type cagA antibodies (45.2±40.3 Uarb/mL, 54.3±42.4 Uarb/mL, and 51.2±41.3 Uarb/mL, respectively; $P>0.05$).

Table 1 The rates of serum positive cagA overall and according to endoscopic diagnosis in the patients from the two different centers

	cagA+		
	Adana hospital *n* (%)	Ankara hospital *n* (%)	*P*
Total patients	98/99 (98.9)	77/81 (95.1)	NS
NUD patients	73/74 (98.6)	36/40 (90.0)	NS
GU/E patients	12/12 (100)	20/20 (100)	NS
DU patients	13/13 (100)	21/21 (100)	NS

Denotes: NUD: Non-ulcer dyspepsia; DU: Duodenal ulcer; GU/erosion: Gastric ulcer and/or erosions.

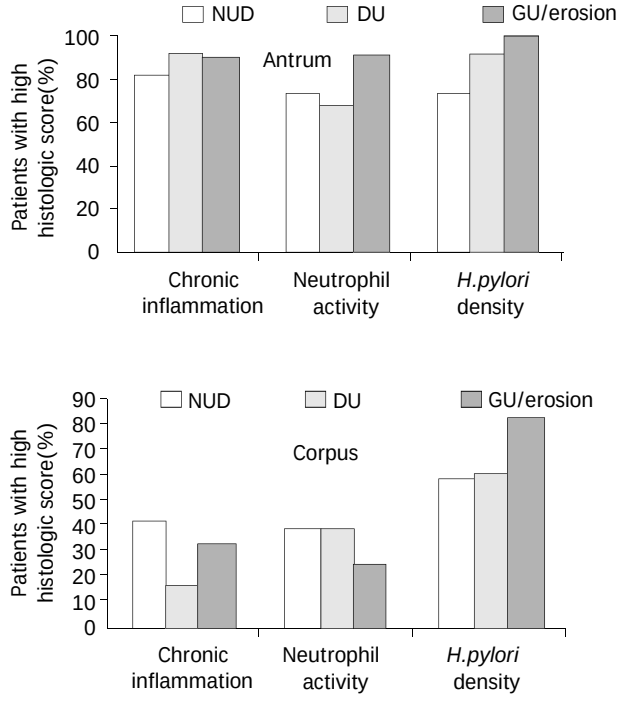

Figure 1 The percentages of patients with high scores (moderate or severe findings) for inflammation, neutrophil activity, and *H. pylori* density in the antrum and corpus. (NUD: Non-ulcer dyspepsia; DU: Duodenal ulcer; GU/erosion: Gastric ulcer and/or erosions).

In each group, the percentages of patients with high scores for each histologic parameter were calculated. Separate calculations were made for the antrum and the corpus specimens. The results were then compared to demonstrate whether there was any difference among gastroduodenal pathologies (NUD, DU, and GU/E) with respect to severity of gastritis and *H. pylori* density in each stomach region (Figure 1). In the antrum, there were no significant differences in the group rates for chronic inflammation, neutrophil activity, and *H. pylori* density ($P>0.05$), and all three groups had very high frequencies of high scores for chronic inflammation and *H. pylori* density. Analysis of the corpus findings showed that the DU group had a lower percentage of patients with high inflammation scores than those in the other two groups ($P<0.05$). Also, the GU/E group had a higher percentage of patients with high *H. pylori* density scores than those in the other two groups ($P<0.05$).

DISCUSSION

Many studies have suggested that cagA+ strains of *H. pylori* are associated with severe gastrointestinal lesions, such as severe gastritis, peptic ulcer disease, and gastric cancer[11-13]. In infected patients, the cagA protein is translocated into epithelial cells and induces structural changes in these cells[14,15]. A number of investigations have shown that infection with these strains leads to increased secretion of interleukin-8, which plays a pivotal role in the inflammatory response[16,17]. Despite these findings and observations, recent studies of the frequency of cagA+ *H. pylori* strains in patients with NUD have suggested that factors other than cagA may contribute to severe gastrointestinal pathologies[5-7].

Studies of patients with and without peptic ulcer disease in different countries, and in different regions within countries, have revealed wide variations in cagA serum prevalence in these two groups. This variation is evident if we compared the data from our study group overall (180 *H. pylori*-positive patients from health centers in central and southern Turkey) and a previously published study of patients from western Turkey[18]. The latter report showed that the rate of serum positive cagA was significantly higher in peptic ulcer patients than that in NUD patients, whereas our results showed higher but similar rates when our patients were categorized in these two groups. When we analyzed our data of patients categorized according to hospital/city origin (Table 1), the overall rates of serum positive cagA were similar, and the corresponding rates were similar when the patients were divided into NUD, GU/E, and DU groups. These observations supported the suggestion that cagA should not be considered a universal marker for the prediction of severe gastrointestinal pathology. The reasons for, and the clinical aspects associated with this variation in serum positive cagA are not clear. Two possible reasons for the discrepancy among studies even from same country are the possible differences between commercial kits in the detection of cagA antibody in the sera of patients and variation in the prevalence of serum positive cagA strains even in areas showing geographical proximity.

In our study, we were unable to compare the severity of gastritis and *H. pylori* density in patients with cagA(+) and cagA(-) strains because almost all of the 180 patients tested positive for cagA antibodies, regardless of the endoscopic diagnosis. We performed an indirect analysis in attempt to determine whether cagA+ *H. pylori* strains were associated with severe gastritis. For this, we focused only on individuals with high histological scores, and determined the percentage of patients in each group that had high scores for chronic inflammation, neutrophil activity, and *H. pylori* density, respectively. The NUD, GU/E, and DU groups all had very high frequencies of high inflammation scores in the antrum.

However, in the corpus, the DU group had a significantly lower frequency of high inflammation scores than the other two groups. These findings suggested that cagA may have some impact on the severity of gastritis, but not on duodenal ulcer development. Previous work has shown a negative correlation between severe corpus gastritis and the presence of DU, most likely due to changes in the pattern of gastric acid secretion[19,20]. Our findings were in line with this reported relationship.

Figura *et al* reported that most patients with NUD have both cagA(+) and cagA(-) strains of *H. pylori* simultaneously, and suggested that a particular pathological finding may be determined by the dominant strain that colonizes a particular gastric area[21]. This may explain the conflicting results of different studies concerning the serum prevalence of cagA in NUD patients. According to this concept, a patient with anti-cagA antibody in his or her serum may clinically show NUD if the majority of the *H. pylori* organisms in the gastric mucosa are cagA(-).

There is also another possible explanation for why some patients with cagA(+) strains develop milder upper gastrointestinal pathology than those who show more severe pathology but have the same bacterial strain. The reason may be variations in genetic make-up, as a number of different cagPaI genes are required for the cagA protein to be able to enter epithelial cells. Investigation has shown that inactivation of some of these genes abolishes cagA delivery and phosphorylation[14,22].

In conclusion, our findings reveal that the rates of cagA serum prevalence are high and similar in *H. pylori*-positive patients from two Turkish cities that are approximately half thousand of kilometers apart. These rates indicate that cagA serum prevalence in the Turkish population is close to the rates reported in Asian countries. The fact that we observed similar frequencies of cagA(+) *H. pylori* strains in all our dyspeptic patients, regardless of ulcer status, suggests that factors other than cagA may contribute to severe gastrointestinal pathology in patients with *H. pylori*.

REFERENCES

1 **Go MF**. What are the host factors that place an individual at risk for *Helicobacter pylori*-associated disease? *Gastroenterology* 1997; **113**(Suppl 6): S15-S20

2 **Kurata JH**, Nogawa AN. Meta-analysis of risk factors for peptic ulcer. Nonsteroidal anti-inflammatory drugs, *Helicobacter pylori* and smoking. *J Clin Gastroenterol* 1997; **24**: 2-17

3 **Atherton JC**. The clinical relevance of strain types of *Helicobacter pylori*. *Gut* 1997; **40**: 701-703

4 **Warburton VJ**, Everett S, Mapstone NP, Axon AT, Hawkey P, Dixon MF. Clinical and histological associations of cagA and vacA genotypes in *Helicobacter pylori* gastritis. *J Clin Pathol* 1998; **51**: 55-61

5 **Jenks PJ**, Megraud F, Labigne A. Clinical outcome after infection with *Helicobacter pylori* does not appear to be reliably predicted by the presence of any of the genes of the cag pathogenicity island. *Gut* 1998; **43**: 752-758

6 **Hua J**, Zheng PY, Yeoh KG, Ho B. The status of the cagA gene does not predict *Helicobacter pylori*-associated peptic ulcer disease in Singapore. *Microbios* 2000; **102**: 113-120

7 **Yang JC**, Wang TH, Wang HJ, Kuo CH, Wang JT, Wang WC. Genetic analysis of the cytotoxin-associated gene and the vacuolating toxin gene in *Helicobacter pylori* strains isolated from Taiwanese patients. *Am J Gastroenterol* 1997; **92**: 1316-1321

8 **Takata T**, Fujimoto S, Anzai K, Shirotani T, Okada M, Sawae Y, Ono J. Analysis of the expression of CagA and VacA and the vacuolating activity in 167 isolates from patients with either peptic ulcers or non-ulcer dyspepsia. *Am J Gastroenterol* 1998; **93**: 30-34

9 **Ching CK**, Wong BC, Kwok E, Ong L, Covacci A, Lam SK. Prevalence of CagA-bearing *Helicobacter pylori* strains detected by the anti-CagA assay in patients with peptic ulcer disease and in controls. *Am J Gastroenterol* 1996; **91**: 949-953

10 **Dixon MF**, Genta RM, Yardley JH, Correa P. Classification and grading of gastritis The updated Sydney System. International Workshop on the Histopathology of Gastritis, Houston 1994. *Am J Surg Pathol* 1996; **20**: 1161-1181

11 **Crabtree JE**, Taylor JD, Wyatt JI, Heatley RV, Shallcross TM, Tompkins DS, Rathbone BJ. Mucosal IgA recognition of *Helicobacter pylori* 120 kDa protein, peptic ulceration, and gastric pathology. *Lancet* 1991; **338**: 332-335

12 **Kuipers EJ**, Perez-Perez GI, Meuwissen SG, Blaser MJ. *Helicobacter pylori* and atrophic gastritis: importance of the cagA status. *J Natl Cancer Inst* 1995; **33**: 28-32

13 **Rudi J**, Kolb C, Maiwald M, Zuna I, von Herbay A, Galle PR, Stremmel W. Serum antibodies against *Helicobacter pylori* proteins VacA and CagA are associated with increased risk for gastric adenocarcinoma. *Dig Dis Sci* 1997; **42**: 1652-1659

14 **Asahi M**, Azuma T, Ito S, Ito Y, Suto H, Nagai Y, Tsubokawa M, Tohyama Y, Maeda S, Omata M, Suzuki T, Sasakawa C. *Helicobacter pylori* cagA protein can be tyrosine phosphorylated in gastric epithelial cells. *J Exp Med* 2000; **191**: 593-602

15 **Segal ED**, Cha J, Lo J, Falkow S, Tompkins LS. Altered states: involvement of phosphorylated CagA in the induction of host cellular growth changes by *Helicobacter pylori*. *Proc Natl Acad Sci USA* 1999; **96**: 14559-14564

16 **Crabtree JE**, Covacci A, Farmery SM, Xiang Z, Tompkins DS, Perry S, Lindley IJ, Rappuoli R. *H. pylori*-induced interleukin-8 expression in gastric epithelial cells associated with cagA-positive phenotype. *J Clin Pathol* 1995; **48**: 41-45

17 **Sharma SA**, Tummuru M, Miller G, Blaser MJ. Interleukin-8 response of gastric epithelial cell lines to Helicobacter pylori stimulation *in vitro*. *Infect Immun* 1995; **63**: 1681-1687

18 **Demirturk L**, Ozel AM, Yazgan Y, Solmazgul E, Yildirim S, Gultepe M, Gurbuz AK. CagA status in dyspeptic patients with and without peptic ulcer disease in Turkey: association with histopathological findings. *Helicobacter* 2001; **6**: 163-168

19 **Kim HY**, Kim YB, Park CK, Yoo JY, Graham DY. Co-existing gastric cancer and duodenal ulcer disease: Role of *Helicobacter pylori* infection. *Helicobacter* 1997; **2**: 205-209

20 **El-Zimaity HMT**, Gutierrez O, Kim JG, Akamatsu T, Gurer IE, Simjee AE, Graham DY. Geographic differences in the distribution of intestinal metaplasia in duodenal ulcer patients. *Am J Gastroenterol* 2001; **96**: 666-672

21 **Figura N**, Vindigni C, Covacci A, Presenti L, Burroni D, Vernillo R, Banducci T, Roviello F, Marrelli D, Biscontri M, Kristodhullu S, Gennari C, Vaira D. CagA-positive and -negative *H. pylori* strains are simultaneously present in the stomach of most patients with non-ulcer dyspepsia: relevance to histological damage. *Gut* 1998; **42**: 772-778

22 **Odenbreit S**, Puls J, Sedlmaier B, Gerland E, Fischer W, Haas R. Translocation of *Helicobacter pylori* CagA into gastric epithelial cells by type IV secretion. *Science* 2000; **287**: 1497-1500

Edited by Xu XQ

P.O.Box 2345, Beijing 100023, China
Fax: +86-10-85381893
E-mail: wjg@wjgnet.com www.wjgnet.com

World J Gastroenterol 2003;9(4):836-842
World Journal of Gastroenterology
 ISSN 1007-9327

• CLINICAL RESEARCH •

Study on the classification of chronic gastritis at molecular biological level

Goang-Yao Yin, Wu-Ning Zhang, Xue-Fen He, Yi Chen, Xiao-Jing Shen

Goang-Yao Yin, Xue-Fen He, Xiao-Jing Shen, Wuxi No.3 Peoples Hospital, Wuxi 214041, Jiangsu Province, China
Wu-Ning Zhang, Yi Chen, Department of National Microanalysis Center, Fudan University, Shanghai 200433, Shanghai, China
Correspondence to: Dr. Goang-Yao Yin, Wuxi No.3 Peoples Hospital, 230 Eastern Tonghhui Road Wuxi 214041, Jiangsu Province,China. yinyao@pub.wx.jsinfo.net
Received: 2002-10-04 **Accepted:** 2002-12-03

Abstract

AIM: To explore the pathophysiologibasis for the fact that patients with digestive tract symptoms do not necessarily have gastric mucosal pathology and those without clinical symptoms do not necessarily have no gastric mucosal pathology.

METHODS: The ultrastructure, trace elements, cAMP, DNA, SOD and LPO in the gastric mucosa and its epithelial cells of 188 patients without organic lesions of heart, lung, liver, gallbladder, pancreas, kidney or intestine and basically histopathological normal persons (F) were detected synchronously by SEM, TEM, EDAX, Image analysis system RIA and ^{3}H-TdR Lymphocyte Transfer Test.

RESULTS: The content of Zn, Cu, cAMP and ^{3}H-TdR LCT in gastric mucosa and the content of Zn, Cu, DNA and LPO in gastric mucosa epithelial nuclei of each group were shown as belows: Normal control (4.1±1.0, 5.2±0.8, 15.9±1.5, 1079.7±227.4, 7.6±0.4, 58.4±0.3, 12.6±2.7, 2.6±0.6); CSG without symptoms group (3.7±1.2, 5.1±1.8, 15.6±0.9, 924.5±234.9, 7.8±0.3, 58.6±0.4, 13.0±3.1, 2.9±0.4); CAG without symptoms group (3.3±1.0, 4.8±0.9, 14.9±0.7, 887.7±243.6, 7.8±0.3, 58.7±0.3, 14.3±2.8, 3.1±0.4); F type with symptoms group (3.5±1.4, 4.5±1.0, 15.7±1.4, 932.1±2449.3, 7.9±0.4, 58.7±0.5, 13.5±4.6, 2.9±0.7); CSG with symptoms group (2.8±1.9, 4.0±1.5, 14.2±1.8, 867.3±240.5, 8.1±0.5, 58.9±0.5, 15.2±3.2, 4.2±0.7); CAG with symptoms group (2.0±1.8, 3.4±1.5, 13.4±1.8, 800.9±221.8, 8.6±0.4, 59.3±0.5, 16.5±3.1, 4.5±0.6). The contents of Zn, Cu in mitochonondria and SOD in gastric mucosa of each group were shown as belows: Normal control group (9.2±0.5, 58.3±0.3, 170.5±6.1), CSG without symptoms group (8.9±0.5, 58.2±0.3, 167.2±5.3), CAG without symptoms group (8.8±0.4, 57.5±0.2, 166.1±4.2); F type with symptoms group (8.9±0.5, 58.0±0.3, 167.9±5.7), CSG with symptoms group (8.6±0.5, 57.8±0.3, 163.3±5.6); CAG with symptoms group (8.3±0.4, 57.5±0.3, 161.2±4.3). There were significant differences in these cases, P<0.05-0.001. There were synchronous changes of gastric mucosa epithelial cellular ultrastructure. The "background lesions" (focal atrophic gastritis, focal intestinal metaplasia, micro-ulcer) in nonfocal gastric mucosa of all groups had significant differences (P<0.05-0.001).

CONCLUSION: Disease with symptoms, disease without symptoms, nondisease with symptoms occur on the basis of the quantitative changes of gastric mucosa epithelial cellular ultrastructure and related bioactive substances.

Yin GY, Zhang WN, He XF, Chen Y, Shen XJ. Study on the classification of chronic gastritis at molecular biological level. *World J Gastroenterol* 2003; 9(4): 836-842
http://www.wjgnet.com/1007-9327/9/836.htm

INTRODUCTION

After undergoing gastroscopy with mucosal biopsy, patients with digestive traet symptoms and volunteer blood donors without any clinical symptoms were found to be of two types: those with gastric mucosa pathological changes, and others without evident pathology. In order to explore the pathophysiological basis, we detected synchronously the epithelial cell ultrastracture, trace element, cAMP, DNA, gastric mucosa SOD, serum LPO and ^{3}H-TdRLCT by means of histopathology, SEM, TEM with EDAX, image analysis technique, RIA and chemiluminescence method. The results were reported as follows.

MATERIALS AND METHODS

Materials

188 patients with digestive tract symptoms, had been ruled out from organic lesions of heart, lung, liver, gallbladder, pancreas, kidney or intestine by physical examination, fluoroscopy of chest, GI x-ray examination, type ultrasonography, blood biochemistry, gastroscopy with histopathological examination. According to diagnostic criteria of "the standards for the classification of chronic gastritis, gastroscopy antrophic gastritis", 68 cases were diagnosed as CSG (43 males, 25 females, average age 43, average course of disease 4a); 64 cases as CAG (37 males, 27 females, average age 47, average course of disease 6a.); 56 cases as having basically normal gastric mucosa (F group) (22 males, 34 females, average age 39, average course of disease 2a). Among 42 volunteer blood donors without any clinical symptoms, through gastroscopy and histopathological biopsy, 18 cases were diagnosed as CSG (13 males, 5 females, average age 39), 9 cases as CAG (7 males, 2 females, average age 41); 15 cases as having basically normal gastric mucosa (6 males, 9 females, average age 37) thus also referred to as normal control group (NC group).

Methods

Daring gastroscopy, three pieces of gastric mucosa were taken from the focal, nonfocal areas of antral region of stomach and body of stomach for histopathological examination, SEM, TEM, the determination of cAMP and SOD. Blood specimens were taken to determine LPO and ^{3}H-TdRLCT. For the study of gastric mucosa ultrastructure and determination of its trace elements, 501B SEM with 9100/60 EDAX were used ttaking three pieces of specimens from each patient and determine the weight percentage (WT%)[1-4] of each element between the elements of gastric mucosa. Radioimmuno-assay was adopted

to detect gastric mucosa cAMP content (pmol/g)[5], blood ^{3}H-TdRLCT (Bq/L)[5]. For the observation of gastric mucosa epithelial cellular ultrastructure and the determination of its trace elements, EM 430 TEM with 9100/60 EDAX[1-4] were used. The three pieces of mucosa specimens of every patient were magnified in unison by five magnifying powers (3 600, 7 200, 14 000, 19 000, 29 000) to randomly take pictures of the panoramagram, local area and organelle and to determine the atomic number percentage (AT %) of each nuclear and mitochondrial element between the trace elements. 50 nuclei and 50 mitochondria of each patient were determined, with average WT% of each element taken as its actual WT%. For the determination of DNA in gastric mucosa epithelial nuclei, IBAS 2000 image analysis technique was used to determine IOD with gastric mucosa cell smear after. Feulgen staining, taken as the relative content of nuclear DNA[4]. Chemiluminescence method was adopted to determine the activity of SOD (u/g) in gastric mucosa[5]. Thiobarbituric acid development process was adopted to determine serum LPO (umol/L)[5].

Statistical method

χ^2 and *t* test.

RESULTS

Histopathological changes of gastric mucosa

In NC group and F group, there were extremely small number of mononuclear cells and lymphocytes in lamina propria of gastric mucosa, there was no abnormality in gastric gland. Therefore their gastric mucosa were defined as relatively normal. In CG gastric mucosa, in there were various degrees of infiltration of lymphocyte, plasmocyte, eosinophil and neutropil in lamina propria, there were various degrees of degeneration necrosis, erosion and atrophy in mucosa epithelial cells. Glands decreased due to destruction and some glands had cystic dilatation. As for the inflammatory cell infiltration degree in gastric mucosa and the decrease degree of original glands (<1/3 low-grade, >1/3 <2/3 middle-degree, >2/3 heavy-grade). There was greater significant difference in CSG without symptom (CSG-woS) group, CAG without symptom (CAG-woS) group, CSG with symptom (CSG-wS) group. CAG with smptom (CAG-wS) group than in HC group and F group (P<0.05-0.001). There was significant difference between the first four groups (P<0.05-0.001, Table 1).

Ultrastructure of gastric mucosa

The relatively normal gastric mucosa had clear surface, which was divided by crisscross small groves into many lesser gastric areas, assuming convolution shape, in which there were many gastric pits (the mouths of gastric glands). The gastric pits were shaped like craters and their concaver walls had round or oval epithelial cells of almost the same size (Figure 1). When magnified, the surfaces of cells were found to be rough and uneven, with short and thin microvilli as well as many semiciroular cumuli, several micro processus and small fossae. The fossae were marks left by cumuli after rupture and excretion of mucus. The crater periphery projections were shaped like dykes. The gastric antrum mucosa were rough, apparently folded, the small craters were mostly groves of different lengths with deep bottoms. In low power observation, as far as gastric mucosa of chronic gastritis was concerned, the crisscross groves of the focal mucosa are shallow, the convolution structures were smooth and even, craters were deformed and of different sizes at different heights and ill-distributed; the dykes form projections that are undulating, of different width (Figure 2). In high power observation, the focal gastric mucosa had scattering denatured, diabrotic and necrotic exfoliated epithelial cells, on it' s surfaces S-shape helicobacter pylori were found (Figure 3). Massive epithelial cells were diabrotic, anabrotic and exfoliated forming micro ulcers. The ulcers spread from their centers, with adjacent cells crushed and destructed, in irregular shapes and arrangement. The epithelial cells of the crater walls were atrophic and denatured of different sizes and derangement (Figure 5), and the cells became diabrotic and necrotic and had inflammatory cell infiltration (Figure 6). The glands propria of the serious cases were shaped like grid framework structure (Figure 7). The surfaces of the epithelial cells of IM gastric mucosa were covered with a thick coating, villi were invisible, and the intercellular boundaries were not clear (Figure 8). The hollowed crateriform cells were round or polygon cavities, with ejected mucus at mouths scattering like tiny white dots. In nonfocal gastric mucosa, focal atrophic inflammatory changes, IM cell population, micro ulcers and helicobacter pylori (can be found also), they were generally referred to as "background lesion".

Comparing CSG-woS group, CAG-woS group, CSG-wS group and CAG-wS group, there were significant differences in background lesion of nonfocal gastric antrum mucosa (P<0.05-0.001). The incidence rate of background lesion of nonfocal gastric mucosa is especially high in CAG-wS group (Table 2).

The ultrastructure of gastric mucosa epithelial cells

The mucous cells on epithelial cell surface of relatively normal gastric mucosa were columanar epithelial cells covering endogastric surfaces and inside wall of gastric pits. Their free surfaces had short microvilli and muclei were relatively big, at the bottoms of the cells. In cytoplasm were mucous granules of various sizes, a great deal of RERs and scattered mitochondria. The mucous neck cells were distributed over the necks of gastric glands, round or crescent shape. In the upper part of cytoplasmic nuclei, there were a great deal of secretory granules, developed Golgi' s bodies, a few RERs and scattered mitochondria. On the tops of cells were a few short thick micro villi. Chief cells were distributed over the bodies and bottoms of gastric glands and their nuclei were round. In cytoplasms there are many parallel RERs, a great deal of secretory granules, well-developed Golgi' s bodies and scattered mitochondria (Figure 9). The parietal cells were big and conic in shape and their conical tops turned towards gland cavities. The nuclei were in the centers of the cells. The cytosols are filled with vesicular smooth RERs (secreting hydrochloric acid), intracellular canaliculi (conveying hydrochloric acid) and many mitochondria. The endocrine cells lay between chief cells and parietal cells. They were small and their nuclei are round, at the bottoms of cellular matrixes. In cytoplasms, there are great deal of spherical endocrine granules, RERs, and a few mitochoncdria, Golgi' s bodies lie nearby nuclei (Figure 10). The normal gastric mucosa epithelial cell nuclei were round or oval; the nuclei envelopes are slightly bending; lobulated nuclei were few; the nucleocyotoplasmic ratio was less than 1; the nuclei chromatins were scattered, associated with nucleoli or distributed around the nuclei. The light bright zones between heterochromatins in the nucleoli were euchromatins; the nucleoli had high electron density without capsules (Figure 11). The normal epithelial cell mitochondria of gastric mucosa were round or oval, scattered around nuclei. The mitochondria consist of outer membrane, inner membrane, outer ventricle, inner ventricle and cristae. Crista, the inward folded inner membrane, was a hollow canal leading to outer ventricle. Some mitochondrial cristae lead directly to

cytoplasms. Cristas were generally in tabular arrangement, parall to each other and vertical to mitochondrial long axes (Figure 12). The free surfaces of epithelial cells of CG gastric mucosa have dropped off micro villi. The intercellular space expands and cell conjuctions decrease; mitochondria decrease, become swollen or cristae breake and had vacuolar degeneration (Figure 13). RERs dilate and were in circular arrangement. The Golgi' s bodies became atrophic and had lost their typical structures; the cytoplasmic secretory granules decreased; nuclei expand or shrink; parietal cell intracytoplasmic canaliculi dilate and micro villi become short and thin or even disappear. The karyoplasmic ratio of the cells with undifferenciated nuclei and IM cells of CG gastric mucosa epithelial cells were greater than 1 and there is increase in nuclear lobulation (Figure 14), interchromatic granules, peri-chromatic granular density and euchromatins. The nucleoli were hypertrophic and lie close to nuclear margins (referred to as nucleolar margination). The obsolescent epithelial nuclei shrink and the nucleocyto-plasmic ratio was still less. The hetero chromatins lie densely around nuclei; the electron density was low in the center of nuclei and nuclei were loop in shape (referred to as chromatic margination) (Figure 15). The shrinked nuclei were denticular, in which the electron density was moderately homogeneous and chromatins were not found (referred to as chromatic homogenization). As for the above changes, there was significant difference between NC group, CSG-woS group, CAG-woS group, F-wS group, CSG-wS group and CAG-wS group (P<0.05-0.001, Table 3). There were mitochondrial swelling, hypertrophy, pyknosis, hyaline degeneration as well as vacuolar degeneration in epithelial cells of CG gastric mucosa. Deformed mitochondria were in C-shape or U-shape. There were zigzag, longitudinal, sparse, pyknosis and deranged cristae (Figure 16). There was an decrease in the number of mitochondria and their cristae. In the above changes, there Is significant difference between NC group. CSG-woS group. CAG-woS group. F-wS group CSG-wS group and CAG-wS group (P<0.05-0.001, Table 4).

Gastric mucosa trace elements, cAMP, SOD and blood ^{3}H-TdRLCT

Under the direct vision of SEM with EDAX probe that automatically detected the samples within 0.1-0.01 mm^2 range all the elements under 12 in atomic number and automatically calculates the weight percentage (WT%) of each element in the element series. 15 points were fixed in the three pieces of mucosa from every patient to carry out 15 detections and in every detection, 21 elements were detected to get their respective average WT% as its actual WT%. Zn and Cu were taken as index. The gastric mucosa Zn, Cu, cAMP, SOD and ^{3}H-TdRLCT decrease progressively in the sequence of NC group CSG-woS group, CAG-woS group, F-wS group. CSG-wS group and CAG-wS group (P<0.05-0.001, Table 5).

Biochemical changes in gastric mucosa and blood serum

The quantity of nuclei DNA, Zn, Cu and serum LPO increased progressively in the sequence of NC group, CSG-woS group, CAG-woS group, F-wS group, CSG-wS group, CAG-wS group. While mitochondrial Zn, Cu, decreased progressively in the same sequence and there were significant differences between these groups (P<0.05-0.001, Table 6).

Table 1 Degree of inflammatory cell infiltration compared with the degree of decrease of original glands in gastric mucosa *n*(%)

Group	*n*	Degree of inflammatory cell infiltration			Degree decrease of glands propria		
		<1/3	>1/3<2/3	>2/3	<1/3	1/3<2/3	>2/3
NC	15						
CSG-woS	18	11(61.1)	6(33.3)	1(5.6)	1(5.6)		
CAG-woS	9	5(55.6)	3(33.3)	1(11.1)	5(55.6)^{d}	3(33.3)	
F-TwS	56						
CSG-wS	68	26(38.2)^{c}	32(47.1)	10(14.7)			
CAG-Ws	64	19(29.7)^{df}	21(32.8)	24(37.5)^{df}	23(35.9)^{d}	23(35.9)	18(28.1)

Compared with NC group. ^{a}P<0.05, ^{b}P<0.01; compared with CSG-woS group. ^{c}P<0.05, ^{d}P<0.01; compared with CAG-woS group. ^{e}P<0.05, ^{f}P<0.01, Compared with F-wS group, ^{g}P<0.05, ^{h}P<0.01, Compared with CSG-wS group, ^{i}P<0.05, ^{j}P<0.01, In table 2-6, the marks are the same as here.

Table 2 Focal background lesions in non-focal site of gastric mucosa *n* (%)

Focal lesions	CSG-woS (*n*=18)		CAG-woS (*n*=9)		CSG-wS (*n*=68)		CAG-Ws (*n*=64)	
	Gastric antrum	Gastric body	Gastric antrum	Gastric body	Gastric antrum	Gastric body	Gastric antrum	Gastric body
Atrophic inflammatory lesion	1 (5.6)	0 (0.0)	1 (11.1)^{a}	0 (0.0)	21 (30.9)^{bd}	11 (16.2)	47 (73.4)^{bdj}	27 (42.2)^{j}
IM	4 (22.2)	1 (5.6)	5 (55.6)^{b}	2 (22.2)^{b}	27 (39.7)^{bc}	5 (7.4)^{d}	59 (92.2)^{bdj}	13 (20.3)^{b}
Micro ulcer	1 (5.6)	1 (5.6)	3 (33.3)^{b}	1 (11.1)^{a}	11 (16.2)	2 (2.9)^{c}	28 (43.8)^{bdj}	9 (14.1)^{aj}

Table 3 Ultrastructures of gastric mucosa epithelial cell nuclei *n* (%)

Group	*n*	Appearance		Chromatin		Nucleoli	
		nucleoplasmic ratio >1	nuclear lobulation	margination or homogeneity	perinuclear concentration	hypertrophy or margination	looping
NC	15			1 (6.7)	1 (6.7)		
CSG-woS	18	1(5.6)		4 (22.2)^{b}	1 (5.6)	1 (5.6)	1 (5.6)
CAG-woS	9	2(22.2)^{d}	2(22.2)	7 (77.8)^{bd}	3 (33.3)^{bd}	2 (22.2)^{d}	4 (44.4)^{d}
F-TwS	56			3 (5.4)^{df}	3 (5.4)^{f}	1 (1.8)^{f}	
CSG-wS	68	5(5.7)^{f}	2(2.9)^{f}	7 (10.3)^{cf}	5 (7.4)^{f}	2 (2.9)^{f}	2 (2.9)^{f}
CAG-Ws	64	20(31.3)^{dj}	9(29.7)^{j}	33 (51.6)^{bdhj}	29 (45.3)^{dfhj}	27 (42.2)^{dfhj}	14 (21.9)^{dgi}

Table 4 Mitochondria ultrastructures of gastric mucosa epithelial cells. ($\bar{x}\pm s$)

Group	*n*	Number	Swelling & overgrowth (%)	Matrix-discoloration (%)	Vacuolar degencration (%)	Pyknosis (%)	Crista number	Crista fragmentation & derangement (%)
NC	15	86.5±27.3	3.4±1.6	3.0±1.1	2.9±1.9	1.1±0.8	12.8±3.2	2.2±1.1
CSG-woS	18	85.3±22.2	3.9±1.1	3.9±2.2	3.2±1.2	1.4±0.9	11.4±2.4	3.1±1.3
CAG-woS	9	83.8±17.3	4.4±2.4	4.3±2.9	3.3±1.1	1.7±0.8	11.4±2.1	3.2±1.2
F-TwS	56	83.1±22.8	5.4±2.9^{bd}	4.4±2.4	2.9±1.8	1.2±0.7	11.2±2.3	3.9±1.2^{bc}
CSG-wS	68	65.4±21.1^{bdfh}	7.2±3.8^{bdfg}	7.9±5.0^{bdfh}	6.4±4.5^{bdfh}	1.9±0.9^{bch}	8.2±3.2^{bdfh}	5.8±3.1^{bdfh}
CAG-wS	64	52.2±20.8^{bdfhj}	10.9±4.5^{bdfhj}	11.7±8.6^{bdfhj}	11.6±7.7^{bdfhj}	3.7±1.1^{bdfhj}	6.9±3.5^{bdfhji}	8.9±3.7^{bdfhj}

Table 5 Gastric mucosa trace elements, cAMP and ^{3}H-TdRLCT ($\bar{x}\pm s$)

Group	*n*	Gastric mucosa				Blood
		Zn (WT%)	Cu (WT%)	cAMP (Pmol/g)	SOD (u/g)	^{3}H-TdRLCT (Bq/L)
NC	15	4.1±1.0	5.2±0.8	15.9±1.5	170.5±6.1	1079.7±227.4
CSG-woS	18	3.7±1.2	5.1±1.8	15.6±0.9	167.2±5.3	924.5±234.9
CAG-woS	9	3.3±1.0	4.8±0.9	14.9±0.7^{a}	166.1±4.2^{a}	887.7±243.6
F-TwS	56	3.5±1.4^{a}	4.5±1.0^{a}	15.7±1.4^{e}	167.9±5.7	932.1±2449.3^{a}
CSG-wS	68	2.8±1.9^{bcg}	4.0±1.5^{aceg}	14.2±1.8^{bdeh}	163.3±5.6^{bdh}	867.3±240.5^{bc}
CAG-wS	64	2.0±1.8^{bdfhi}	3.4±1.5^{bdfhj}	13.4±1.8^{bdfhi}	161.2±4.3^{bdfhi}	800.9±221.8^{bdi}

Table 6 Epithelial nuclei and mitochondria Zn, Cu in gastric mucosa ($\bar{x}\pm s$)

Group	*n*	Nuclei			Mitochondria		Serum
		Zn (AT%)	Cu(AT%)	DNA(IOD)	Zn (AT%)	Cu(AT%)	LPO(umol/L)
NC	15	7.6±0.4	58.4±0.3	12.6±2.7	9.2±0.5	58.3±0.3	2.6±0.6
CSG-woS	18	7.8±0.3	58.6±0.4	13.0±3.1	8.9±0.5	58.2±0.3	2.9±0.4
CAG-woS	9	7.8±0.3^{a}	58.7±0.3^{a}	14.3±2.8	8.8±0.4^{a}	57.5±0.2^{bd}	3.1±0.4
F-TwS	56	7.9±0.4^{a}	58.7±0.5^{a}	13.5±4.6	8.9±0.5^{a}	58.0±0.3^{af}	2.9±0.7
CSG-wS	68	8.1±0.5^{bdfh}	58.9±0.5^{bdh}	15.2±3.2^{bcg}	8.6±0.5^{bh}	57.8±0.3^{bdfh}	4.2±0.7^{bdfh}
CAG-Ws	64	8.6±0.4^{bdfhj}	59.3±0.5^{bdfhj}	16.5±3.1^{bdehi}	8.3±0.4^{bdfhj}	57.5±0.3^{bdhj}	4.5±0.6^{bdfhi}

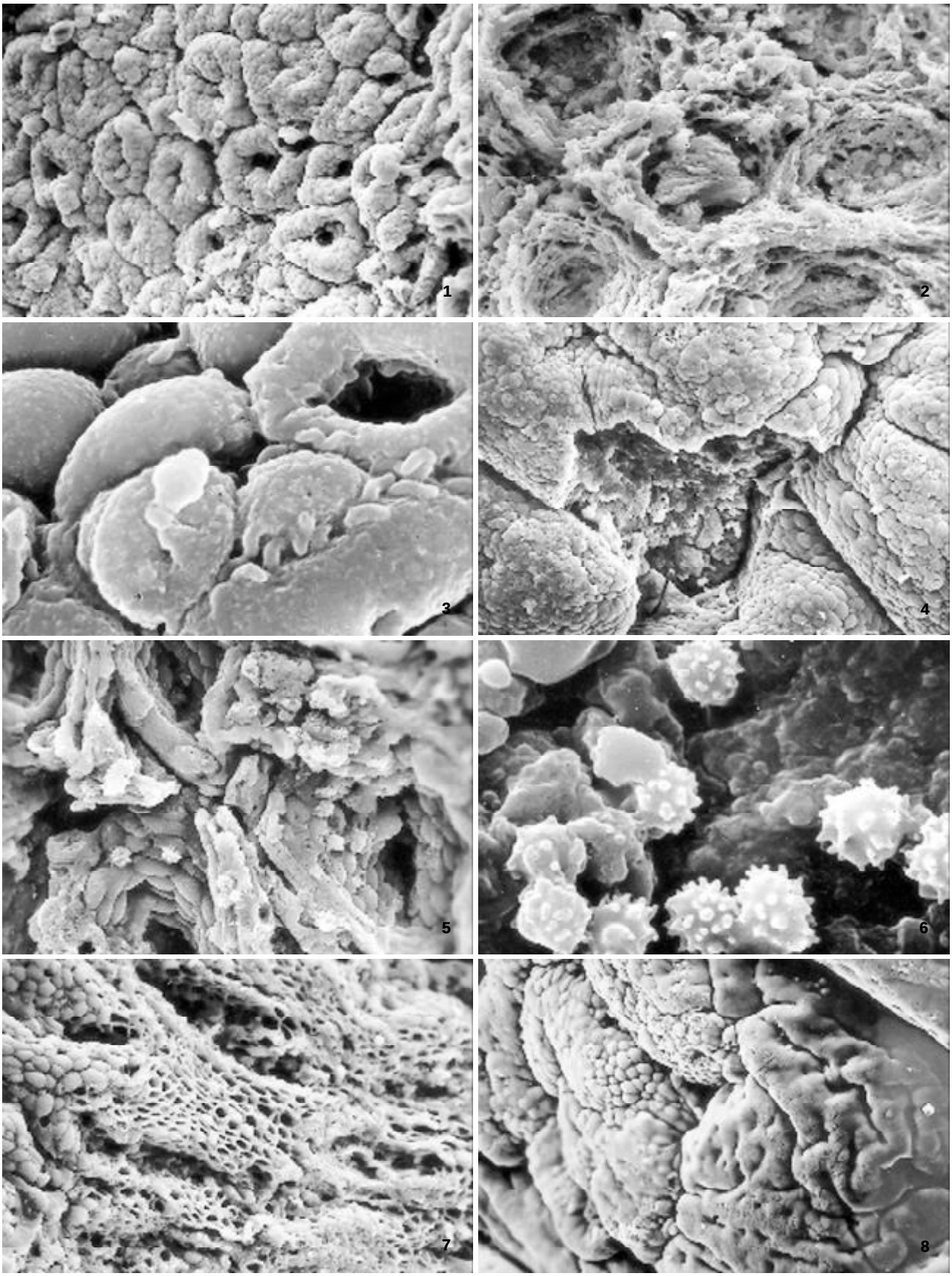

Figure 1 Mouth of gastric glands, like craters, The concaver walls have round or oval epithelial cells, of almost same size. ×160.
Figure 2 Craters are deformed, the crater periphery projections are of different heights and width. ×320.
Figure 3 On cell surfaces, S-shape *Helicobacter pylori* are found. ×2 500.
Figure 4 Micro ulcers. ×320.
Figure 5 Epithelial cells of crater concave walls are atrophic, denatured, of different sizes and deranged. ×640.
Figure 6 Inflammatory cell infiltration . ×2 500.
Figure 7 Glands propria of grid framework structure. ×320.
Figure 8 Surface of IM gastric mucosa epithelial is thickly coated, villi are invisible, intercellular boundaries are not clear. ×320.

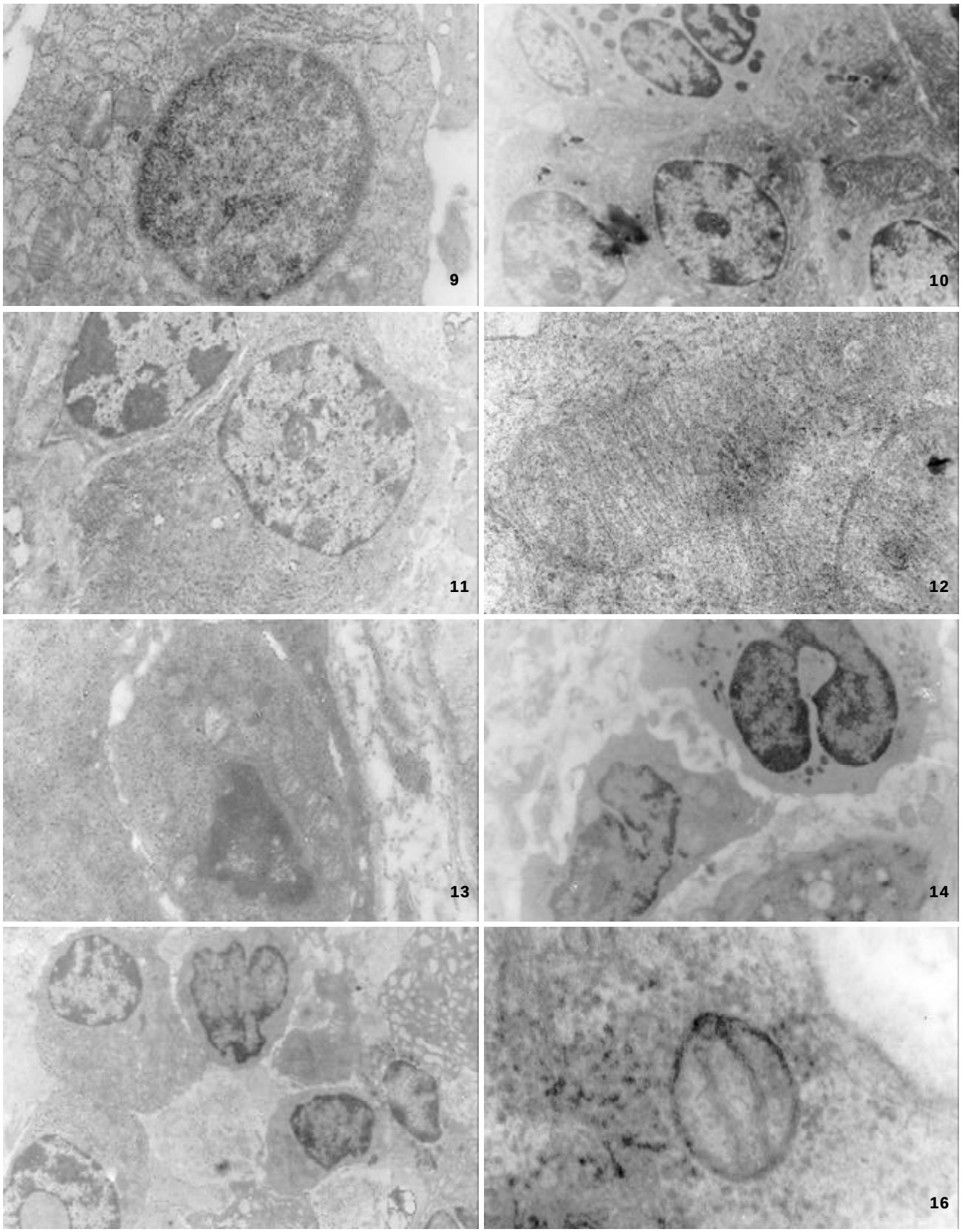

Figure 9 Normal epithelial nuclei are round, there are RERS, secretory granules, Golgi's bodies and mitochondrias in cytoplasms. ×7 200.
Figure 10 The normal epithelial secretory cells are relatively small, nuclei are round, a great deal of spherical incretory granules in cytoplasms. ×14 000.
Figure 11 Normal gastric mucosa epithelial nuclei are round. or oval, nucleocyotoplasmic ratio <1; the nucleoli have no capsules. ×14 000.
Figure 12 Normal cristas are hollow canals leading to outer ventricles. cristas are vertical to mitochondrial long axles. ×14 000.
Figure 13 Intercellular space expands, decrease of cellular conjuctions; mitochondria decrease, swollen or cristae break, have vacuolar degeneration. ×29 000.
Figure 14 Nucleocytoplasmic ratio >1, lobulated nuclei. ×7 200.
Figure 15 Heterochromatins lie densely around nuclei, the electron density is low in the centers of nuclei. the nuclei are loop in shape (referred to as chromatic homogenization). ×14 000.
Figure 16 Longitudinal cristas, sparse cristae, deranged cristae. ×14 000.

DISCUSSION

Compared with NC group, 188 patients with digestive tract symptoms without other orangic disease and 27 patients without any clinical symptoms have a tendency of decreasing of quality in the submicrostructure of gastric mucosa epithelial cells -mitochonclria. The incidence rate of karyoplasmic ratio > 1, mucleari lobulation, chromatin peripheral granule densification, hypertrophy of nucleoli, mitochondrial degeneration, and quantitive changes of nucleolar DNA, Zn, Cu and LPO incread progressively in the sequence of NC group. CSG-woS group, CAG-woS group, F-wS group, CSG-wS group and CAG- wS group. While gastric mucosa Zn, Cu, cAMP, SOD and mitochondrial Zn, Cu and the number of mitochondria and crista decread progressively in the same sequence.

When gastric mucosa is damaged by noxious substances or ischemia, the metabolism of Zn, Cu becomes disordered with the body and thus enzyme system is disturbed. In human body, Zn is the important component and activator of over a hundred varieties of enzymes such as carbonic anhydrase, DNA polymerase, peptase, phosphatase, peroxide dismutase etc. By regulating the activity of these enzymes, it participates and regulates the metabolism of sugars, lipids, proteins, nuclei acid and vitamins, contends for mercaptan to inhibit free radical reaction. Cu participates the composition of over 30 kinds of proteins and enzymes in the body, regulates the protein metabolism and influences cellular respiration and division. When the level of Zn and Cu in the body declines, the synthesis and activity of SOD will be inhibited. Because of NADPH oxidation reduction circulation and the catalytic function of xanthine oxidase, a great deal of oxygen free radicals will be produced, far beyond the clearing ability of SOD. The excessive accumulated oxygen free radicals react in peroxidation with unsaturated fatty acid of inner and outer mitochondrial membranes and produce LPO, therefore serum LPO level will rise. The inner and outer mitochondrial membranes will accordingly be damaged, resulting in the decrease and derangement of mitochondrial cristae, the change of the ratio of mitochondrial ventricle diameter to cavity diameter and eventfully the retrograde affection, the decrease of ATP production, inadequate energy supply, which in turn cause debility, structural atrophy, decrease of gastric acid secretion and even cytonecrosis. The participation of Zn and Cu dependence enzymes is essential in nuclear protein synthetic metabolism (including DNA duplication) and mitochondrial energy metabolism. When nuclear took in more Zn and Cu, the protein synthsis was brisk, nuclei division and hyperplasia were accelerated, which increased the chance of gene mutation. As the second messenger substance, cAMP regulate some vital activities in the body. Once the quantity of cyclic nucleoside phosphate in nuclei changes abnormally, pathological state will occur. The quantitive changes of cAMP result in the changes of cellular metabolism, immunity and vegetative functions. The decrease of cyclic nucleoside phosphate, especially cAMP in the body results in the inhibition of sympathetic nerve (including purinergic nerve) function, and relative hyperfunction of parasympathetic nerve function. As a result, digestive tract symptoms occur such as abdominal distention, loose stool, involuntary drooling, poor appetite, pale enlarged tongue with tooth marks. Through influencing lymphocyte metabolism, the quantitive changes of Zn and cAMP in turn influence cell respiration, differentiation and inhibit lymphocyte transformation[4,6-13] and cause decline of ^{3}H-TdRLCT level. As a result: (1) When gastric mucosa Zn, Cu and blood ^{3}H-TdRLCT are nearly equal to that of NC group and gastric mucosa cAMP was markedly lower than that of HC group, clinical phenomena as CSG-woS and CAG-woS will occur; (2) When gastric mucosa Zn, Cu and ^{3}H-TdRLCT were markedly lower than that of NC group and gastric mucosa cAMP is nearly equal to that of NC group, the phenomenon of F type with symptoms (non -disease with symptoms) will occur; (3) When the levels of gastric mucosa Zn, Cu, cAMP and ^{3}H-TdRLCT were all markedly lower than those of NC group, the clinical phenomena such as CSG-wS and CAG-wS will occur. The occurrences of these clinical phenomena were consistent with the change of gastric mucosa ultrastructure and histopathology, forming the pathophysiological basis in the classification of chronic gastritis. Thus it can be seen that changes of gastric mucosa epithelial cell ultrastructures and the quantitive changes of their bioactive substances are the pathophysiological bases that determines the classification of chronic gastritis with different classification has respective clinical symptoms.

REFERENCES

1 **Yin GY**, Zhang WN, He XF, Chen Y, Shen XJ. Detection of ultrastructural changes and contents DNA, Zn, Cu and LPO in subgroups of chronic gastritis. *Shijie Huaren Xiaohua Zazhi* 2002; **10**: 663-667

2 **Yin GY**, Zhang WN, Shen XJ, Chen Y, He XF. Ultrastructural and molecular diological changes of chronic gastritis and gastric cancer: a comparative study. *Shijie Huaren Xiaohua Zazhi* 2002; **10**: 668-672

3 **Yin GY**, Zhang WN, He XF, Chen Y, Shen XJ. Alterations of ultrastructures, trace elements, cAMP and cytoimmunity in subgroups of chronic gastritis. *Shijie Huaren Xiaohua Zazhi* 2002; **10**: 673-676

4 **Yin GY,** Zhang WN, He XF, Chen Y, Yin YF, Shen XJ. Histocytepathological study on gastric mucosa of spleen deficiency syndromes. *Zhongguo Zhongxiyi Jiehe Zazhi* 1999; **19**: 660-663

5 **Yin GY**, Xu FC, Zhang WN, Li GC, He XF, Chen Y, Shen XJ. The effect of weikangfu on cytopathology of gastric mucosa tissue when treating gastric precancerosis lesion of patients with spleen deficiency syndromes. *Zhongguo Zhongxiyi Jiehe Zazhi* 2000; **6**: 241-243

6 **Yin GY**, Zhang WN, Xu FC, He XF, Chen Y, Shen XJ. Effect of Weikangfu chongji on ultrastructure of precancerosis gastric mucosa of patients with spleen deficiency Syndromes. *Zhongguo Zhongxiyi Jiehe Zazhi* 2000; **20**: 667-670

7 **Yin GY**, Zhang WN, Xu FC, Chen Y, He XF, Li GC, Shen XJ. Study on the modern pathophysiologic basis of the syndrome classification of spleen deficiency with chronic gastritis and of (treatment) verification of clinical syndromes and prescriptions. *Jiangsu Yiyao Zazhi* 2001; **27**: 46-47

8 **Yin GY,** He XF, Yin YF, Du YQ, Jiao JH. Study on mitochondrial ultrastructure, trace elements and correlative factors of gastric mucosa in patients with spleen deficiency syndrome. *Zhongguo Zhongxiyi Jiehe Zazhi* 1996; **15**: 719-723

9 **Yin GY**, Zhang WN, Xu FC, He XF, Chen Y, Shen XJ. Effect of weikangfu chongji on epithelial cellular ultrastructure of precancerotic gastric mucosa of patients with spleen deficiency syndrome. *Jiangsu Yiyao Zazhi* 2000; **26**: 514-517

10 **Yin GY,** Zhang WN, Xu FC, He XF, Chen Y, Li GC, Shen XJ. Effect of weikangfu on Zn, Cu and DNA in precancerosis gastric mucosa epithelial nuclei and mitochondria of patients with spleen deficiency syndromes. *Zhongguo Zhongxiyi Jiehe Zazhi* 2000; **8**: 221-224

11 **Yin GY**, Zhang WN, Shen XJ, Chen Y, He XF. A comparative study on ultrastructure of chronic gastritis grastric mucosa IM, ATP and their molecular biology. *Jiangsu Yiyao Zazhi* 2002; **28**: 4-7

12 **Yin GY**, He XF, Zhang WN, Chen Y. Relationship between the classification of spleen deficiency and the quantitative changes of bio-active substances in mitochondria of gastric mucosa epithelical cell nuclei. *Zhongguo Zhongxiyi Jiehe Zazhi* 1999; **7**: 145-148

13 **Yin GY**, Zhang WN, Li GC, Huang JR, Chen Y, He XF, Shen XJ. Therapeutic effect of weikangfu on gastric precancerosis disordddeer with spleen deficiency syndrome and its effect of gastric mucosal zinc, copper, cyclic adenosine monophosphate, superoxide dismutase,lipid peroxide and ^{3}H-TdR lymphocyte conversion test. *Zhongguo Zhongxiyi Jiehe Zazhi* 2000; **20**: 176-179

Edited by Xu JY

P.O.Box 2345, Beijing 100023, China
Fax: +86-10-85381893
E-mail: wjg@wjgnet.com www.wjgnet.com

World J Gastroenterol 2003;9(4):843-846
World Journal of Gastroenterology
 ISSN 1007-9327

• CLINICAL RESEARCH •

The influence of Enteral Nutrition in postoperative patients with poor liver function

Qing-Gang Hu, Qi-Chang Zheng

Qing-Gang Hu, Qi-Chang Zheng, Department of Surgery, Xiehe hospital, Tongji Medical College, Huazhong University of Science and Technology, Wuhan 430022, Hubei Province, China
Supported by the Scientific Foundation of Wuhan city, No.92251106
Correspondence to: Dr. Qing-Gang Hu, Department of Surgery, Xiehe hospital, Tongji Medical College, Huazhong University of Science and Technology, Wuhan 430022, Hubei Province China. mailbox_1@163.net
Telephone: +86-27-85726201 **Fax**: +86-10-85726942
Received: 2002-08-09 **Accepted:** 2002-09-03

Abstract

AIM: To investigate the safety, rationality and the practicality of enteral nutritional (EN) support in the postoperative patients with damaged liver function and the protective effect of EN on the gut barrier.

METHODS: 135 patients with liver function of Child B or C grade were randomly allocated to enteral nutrition group (EN, 65 cases), total parenteral nutrition group (TPN, 40 cases) and control group (CON, 30 cases). Nutritional parameters, hepatic and kidney function indexes were measured at the day before operation, 5th and 10th day after the operation respectively. Comparison was made to evaluate the efficacy of different nutritional support. Urinary concentrations of lactulose(L) and mannitol(M) were measured by pulsed electrochemical detection(HPLC-PED) and the L/M ratio calculated to evaluate their effectiveness on protection of gut barrier.

RESULTS: No significant damages in hepatic and kidney function were observed in both EN and TPN groups between pre- and postoperatively. EN group was the earliest one reaching the positive nitrogen balance after operation and with the lowest loss of body weight and there was no change in L/M ratio after the operation (0.026±0.004) at the day 1 before operation, 0.030±0.004 at the day 5 postoperative and 0.027±0.005 at the day 10 postoperative), but the change in TPN group was significant at the day 5 postoperative (0.027±0.003 *vs* 0.038±0.009,$P<0.01$).

CONCLUSION: EN is a rational and effective method in patients with hepatic dysfunction after operation and has significant protection effect on the gut barrier.

Hu QG, Zheng QC. The influence of Enteral Nutrition in postoperative patients with poor liver function. *World J Gastroenterol* 2003; 9(4): 843-846
http://www.wjgnet.com/1007-9327/9/843.htm

INTRODUCTION

Liver is the central organ for production and utilization of nutrients and plays a key role in metabolism. In chronic liver disease severe protein-calorie malnutrition can seriously damaging the capacity of liver regeneration, however nutritional support can improve the postoperative outcome[1]. Parenteral nutrition (PN) has been used clinically[2], but its limitations of the incomplete nutritional constituent[3], catheter-related or endogenous complication[4], metabolic complications and liver dysfunction restrict its use in hepatic damaged patients[5]. In the mid 1980s, along with the recognition of the relevance of the gut barrier and endogenous infection[6,7], enteral nutrition (EN) has been widely used[8], but how does it effect on poor liver function remaining unclarified.

It is the aim of this study: (1) To investigate the safety, rationality and feasibility in performing EN in postoperative patients with poor liver function. (2) To study the influence of EN on gut barrier.

MATERIALS AND METHODS

Patients and groups

According to the later Enrolled criterion, 135 patients were enrolled and randomly divided into 3 groups: EN (n=65), TPN (n=40) and CON (n=30) (Table 1).

Enrolled criterion is: (1) Hospitalized adult patients from July 1998 to October 2001 with chronic liver damage requiring operative treatment; (2) The hepatic function was graded as Child B or C; (3) A patience of at least 7 days' nutritional support after the operation; (4) Except the primary disease, no other factors affecting the metabolism (5) With the agreement of the patients to join the program.

Table 1 Grouping of patients

	CON (n=30)			TPN(n=40)			EN(n=65)		
	Cases	Grade		Cases	Grade		Cases	Grade	
		B	C		B	C		B	C
PVH	13	10	3	14	8	6	21	10	11
HCC	4	2	2	11	7	4	10	5	5
CLA	1	-	1	3	1	2	8	-	8
ROBD	7	3	4	7	3	4	15	5	10
CLT	3	1	2	3	2	1	10	3	7
Others	2	1	1	2	-	2	1	-	1

PVH: Portal venous hypertension; HCC: hepatocellular carcinomar; CLA: Cholangiocarcinoma; ROBD: Reoperation of bile duct; CLT: cholelithiasis.

Reagents used

(1) 20 % and 30 % Intralipid (Beijing, Fresenius); (2) 8.5 % Novamin (Sino-swed Pharmaceutical Corp. LTD); (3) Nutrison Fibre (Nutrisia); (4) manitol (Sigma); (5) lactulose (Sigma).

Procedures

Deferent Nutrition supports were used: In TPN group, 30 cal· kg^{-1}· d^{-1} energy and 0.16 g· kg^{-1}· d^{-1} nitrogen were given. 1/4-1/3 nonprotein calories were provided by fat and carbohydrate. The ratio of N: nonprotein calorie=1:168. The source of nitrogen was Novamin (8.5 %) and the source of fat was from Intralipid (20 % or 30 %). Essential trace elements

and vitamins were given and the solution was given via peripheral infusion from the day 1 after the operation and lasted at least 7 days. In EN group, Nutrison Fibre was given. After 2 days of TPN, EN begun on the day 3 after the operation via the jejunostomy tube placed during the operation. On the first day, 500 ml Nutrison Fibre was given, which was increased progressively each day till 1 500 ml/d while TPN was deceased progressively till totally substituted. This was used given at least for 7 days. The temperature of Nutrison Fibre were kept at 25-30 ℃ and infused in 12-24 h. The rate was adjusted according to the need. In CON group, nutritional support was not performed or performed not regularly.

The sample preparation including: (1) urine sample: The patient drank the test solution, containing 2 g lactulose, 1 g mannitol in fasted condition or injected on 1 day before operation, 5th and 10th day after the operation respectively. Urine was collected for a total of 6 h and being added 0.1 ml of 10 g/L thimerosal as preservative. The total volume was recorded and 20 ml sample was stored at -20 ℃ until analysis by the HPLC-PED; (2) blood sample: Venous blood samples were achieved during fasting on 1 day before operation, 5th and 10th day after operation respectively for analysis.

Such Monitoring markers were measured: (1) Nutritional status marker: Transferrin (TRF), Prealbumin (PAB), Total protein (TP), Albumin (ALB), the alteration of weight (w) and circumference of upper arm (COUA) postoperatively, and accumulative nitrogen balances in the first 7 days after operation (ANE); (2) Liver and kidney function, electrolytes: Total bilirubin (TB), Direct bilirubin (DB), Albumin (ALB), Total protein (TP), Alanine aminotransferase (ALT), Aspartate aminotransferase (AST), Creatinine (Cr), Blood urea nitrogen(BUN), Potassium (k+), Sodium (Na+), Calcium (Ca2+); (3) Gut barrier marker: Urinary ratio of lactulose and Mannitol (L/M)[9,10].

Statistical analysis

The data was expressed as mean ± standard error. Experimental results were analyzed by analysis of variance and *t* tests for multiple comparisons. $P<0.05$ was considered statistically significant.

RESULTS

All 135 patients, except one cirrhotic patient (CON) with portal hypertension died due to MSOF at the 26th day after operation, all completed the treatment and were discharged. In EN group, there were 32 patients complained for abdominal distention and diarrhea but disappeared by adjusting the temperature and infusion rate, given domperidone or antidiarrheal agent.

Nutritional status marker (Table 2)

In all three groups, on the 5th day postoperatively, the level of TRF, TP, and ALB declined significantly ($P<0.05$), but in EN and TPN groups, they recovered on the 10th day. Comparing with TPN, the level of TP in EN group on the 10th day was higher with significant difference ($P<0.05$). In CON group, on the 10th day PO, the level of TRF, PAB, TP and ALB were all significantly lower than these in EN and TPN groups ($P<0.05$). The W and COUA loss in CON group were significantly more than those in EN and TPN groups ($P<0.05$), and in EN group were lower than that in TPN group. Among these, EN group reached positive nitrogen balance the earliest ($P<0.05$).

Table 2 Changes of nutritional status

Parameters	Control(n=30)			TPN(n=40)			EN(n=65)		
	1st BO*	5th PO**	10th PO	1st BO	5th PO	10th PO	1st BO	5th PO	10th PO
TRF(g/L)	1.1±0.6	0.9±0.3	0.8±0.6	1.2±0.4	1.0±0.6	1.2±0.3	1.3±0.6	1.2±0.5	1.2±0.6
PAB(mg/L)	657±232	591±220	595±213	690±214	669±228	667±239	681±228	719±177	690±221
TP(g/L)	63.6±12.9	46.3±9.7	48.1±9.7	66.6±12.2	48.3±10.1	50.4±9.6	70.1±7.9	55.7±7.8	63.5±8.9
ALB(g/L)	30.8±4.9	29.2±5.9	29.1±4.8	31.4±4.9	30.8±7.1	31.8±5.0	36.5±6.1	30.7±4.0	32.9±3.9
ANE	32.4±10.8 mg· kg^{-1}· 7 d^{-1}			105.3±9.4 mg· kg^{-1}· 7 d^{-1}			185.3±8.4 mg· kg^{-1}· 7 d^{-1}		
W(kg)	-3.3±1.7			-2.4±1.1			-2.1±0.9		
COUA	23.5±1.2	-	22.2±1.3	23.6±1.1	-	23.2±1.3	24.4±2.6	-	23.7±2.2

BO: Before operation; PO: After operation;ANE: accumulated nitrogen banlance; W: weight change; COUA: circumference of upper arm.

Table 3 Changes of liver and kidney function, electrolytes

Parameters	Control(n=20)			TPN(n=26)			EN(n=30)		
	1st BO	5th PO	10th PO	1st BO	5th PO	10th PO	1st BO	5th PO	10th PO
TB (μmol/L)*	92.3±37.8	71.7±34.5	41.8±35.8	86.3±46.8	68.7±33.8	45.7±33.2	119.8±73.0	96.3±54.4	64.3±47.3
DB(μmol/L)*	53.3±28.6	39.2±23.3	16.5±11.7	50.4±33.7	38.4±22.6	17.7±12.3	60.8±50.2	42.8±32.7	31.9±29.2
TP(g/L)*	63.6±12.9	46.3±9.7	48.1±9.7	66.6±12.2	48.3±10.1	50.4±9.6	70.1±7.9	55.7±7.8	63.5±8.9
ALB(g/L)	30.8±4.9	29.2±5.9	29.1±4.8	31.4±4.9	30.8±7.1	31.8±5.0	36.5±6.1	30.7±4.0	32.9±3.9
AST(U/L)#	71.7±28.9	91.3±33.5	78.7±28.1	73.4±30.6	89.9±35.7	67.7±39.1	94.8±47.8	104.4±80.7	69.6±23.8
ALT(U/L)#	54.7±31.1	101.4±44.9	85.3±33.7	58.7±32.3	99.3±56.2	78.7±35.5	109.1±82.7	148.4±180	67.1±50.1
Cr(μmol/L)	72.9±28.8	82.1±23.3	69.5±37.9	73.9±35.3	80.1±22.9	67.5±33.7	77.4±16.5	80.6±24.7	77.1±19.6
BUN(mmol/L)	6.9±3.3	8.4±3.5	5.9±3.4	7.1±4.1	8.2±3.7	5.6±3.2	5.5±1.8	6.9±4.9	6.0±3.2
K(mmol/L)	3.9±0.5	5.3±1.1	3.8±0.7	3.8±0.6	4.4±0.9	4.3±1.1	4.1±0.5	4.3±0.8	4.4±0.2
Na(mmol/L)	136.5±14.7	139.3±18.3	145.8±15.4	132.7±15.9	140.3±13.7	138.8±7.3	138.3±7.1	135.3±5.7	137.0±7.4
Ca(mmol/L)	2.35±0.39	1.99±0.18	2.17±0.31	2.32±0.43	2.67±0.27	2.27±0.34	2.21±0.22	2.07±0.14	2.24±0.17

*among all 3 groups, between day 1 preopratively and day 10 postoperatively, $P<0.01$; # at day 10 postoperatively, the levels were lower in EN and TPN group than in CON group, $P<0.05$.

Liver and kidney function, electrolytes (Table 3)

After operation, the levels of TB, DB declined significantly in all three groups ($P<0.01$). Same increase could be found in patients with hepatic lobectomy, radical operation of Cholangiocarcinoma, severe portal hypertension and emergency operation, but with no statistical significance. On the 10th PO, the levels of AST and ALT were lower in EN and TPN group than those in CON group ($P<0.05$), but no difference was seen between EN and TPN group. The levels of Cr and BUN increased in EN and TPN group on the 5th day, but recovered on the 10th day. No electrolyte imbalance occurred in EN and TPN group.

Gut barrier marker (Table 4)

In EN group, the L/M ratio did not chang after operation. In TPN and CON groups, they increased on the 5th day ($P<0.01$) and declined at 10th day. In both TPN and CON groups, the difference of L/M ratio between preoperation and postoperation was significant.

Table 4 Changes of L / M ratio

	1st BO	5th PO	10th PO
CON(n=30)	0.028±0.004	0.037±0.017	0.031±0.010
TPN(n=40)	0.027±0.003	0.038±0.009	0.030±0.006
EN(n=65)	0.026±0.004	0.030±0.004	0.027±0.005

DISCUSSION

Present status of clinical nutritional support in patients with poor hepatic function

The liver plays a central role in nutritional homeostasis and any liver disease can lead to abnormal nutrient metabolism with the subsequent malnutrition. Severe protein-calorie malnutrition in patients with advanced liver disease can seriously undermine the capacity for liver regeneration and functional restoration. Appropriate nutritional support is helpful to these patients.

PN and EN are two major nutritional supports clinically. What has been proved is that long-term TPN may aggravate the liver damage[11]. In recent years, there have been some advance in studies on various formulas including the branched chain amino acid (BCAA)[13] and MCT/LCT[14] in patients with poor hepatic function[12], but there are still some problems: (1) How does lipid affect the nutrient metabolism; (2) What is the rational and safe dose and the suitable percentage of lipid supplied as the energy source[15,16]; (3) The expensive cost. These problems impede the extensive use of PN which on long-term use may cause atrophy of intestinal mucosa and lead to the gut barrier dysfunction[17]. The consequent enteric bacterial translocation would also cause endogenous infection even multiple organ failure (MOF) and death. EN is a more physiological, cheaper and has protection function on gut barrier. But when using EN[18,19], the later three facts are inevitable: (1)The gastrointestinal tract should be intact; (2) Patient should be able to tolerate the indwelling nasogastric tube;(3) In case of hypertonic, patient may have abdominal distention, diarrhea, and sometimes nausea and vomiting and enhancement of the liver burden. There had been reported on using EN in patients with alcoholic cirrhosis and obstructive jaundice[20,21], but in patients with worse liver function or sustain the hepatic lobectomy, radical operation of cholangiocarcinoma, severe portal hypertension with upper gastrointestinal hemorrhage, the selection of nutritional support is troublesome.

Evaluation of EN and its influence on liver function

En has been proven to be an efficient nutritional support[22,23], which is prefer to TPN. In this study, in both EN and PN groups, the patients' nutritional status was much better than CON group. Compare with PN groups, in weight loss and circumference of upper arm, EN group were much less and the positive nitrogen balance was reached much earlier.

Liver is the key organ in maintaining the carbohydrate, lipid and protein metabolism and the stabilization of internal environment. Also it is the site of biochemical pathways responsible for production and utilization of nutrients and other chemicals. It plays a central role in carbohydrate, lipid and nitrogen metabolism. Therefore it is not surprising that chronic liver disease has great metabolic impact. On the base of this, the impact and irritated responsiveness of the operation may aggravate the burden of liver and ultimately affect the outcome of the patients[24-26]. On the other hand, we can suspect that if the nutrients were absorbed via liver, the liver could utilize the nutriment as the substrate to repair and rebuilt hepatic cell so as to promote its recover[27]. Whether it is beneficial or harmful, our study have performed some useful study in finding this method for support sufficient nutriment at the same time to avoid further liver damage in such patients.

In 42/65 patients of Child C grade EN group, after EN, had their levels of ALT, AST, TB and DB declined, and their Cr and BUN did not increased. There were no signs of aggravating damage of liver and kidney. The successful use of Nutrison Fibre indicates that whether the BCAA is absolutely necessary in EN needs further study.

EN can protect the gut barrier

In patients with poor liver function, infection is a familiar complication and threat[28]. Except for the depression of cellular immunity[29], the bacteria translocation is the most probable reason of infection after the operation[30]. Because of the translocation of the germ and endotoxin, the consequent systemic inflammatory reaction and sepsis and the dysfunction of renal, lung and cardiac system would even threaten the patient' s life. The gut barrier plays a the major role in preventing bacteria translocation and block the subsequent malign reaction, which is the "trigger" of MSOF[31,32]. Keeping the integrity of gut barrier is important to decrease the morbidity and mortality after operation.

In our study, the L/M probe was selected to monitor the status of gut barrier. The result showed: the L/M ratio of EN group was 0.026±0.004 in day 1 before the operation, 0.030±0.004 in day 5 postoperatively and 0.027±0.005 in day 10 postoperatively, the change was not significant, but it was markedly elevated in TPN and CON group after operation as follow. It indicated: EN could protect the gut barrier remarkably, the rational mechanisms were (1) The stimulation on the bowl wall may increase the blood perfusion[33,34]; (2) The stimulation on the bowl wall may accelerate the secretion of pancreas and biliary duct to prevent shrinking of gut mucosa; (3) EN supplies the substrate of intestinal mucosal cell metabolism directly; (4) The fiber[35-38] ingredient of Nutrison may also protect the gut barrier.

Clinical observation

In our study, we found through the upper jejunostomy tube placed during the operation, good nutrition support and good tolerance and good controllability are approached. The tube can be hold for at least 4 weeks. With good nursery, it can be kept fairly long, the longest one in our study is 94 days and no complications occurred.

In our study, the rate of ascites was 83.6 %, 93.3 % and 90.0 % in EN group, PN group and CON group, respectively, till discharge, the subsidence of them were 86.6 %, 61.3 % and 75 %. In EN group the ascites subsided earliest and liver function recovered faster.

The lowest rate of fever and the shortest fever time indicated that the risk of infection is low in EN. It is owed to the protection of the gut barrier.

REFERENCES

1 **Zhang LH**, Li JS. Perioperative nutrition in hepatic surgery. *Gandan Waike Zazhi* 1994; **2**: 121-123
2 **Yeatman TJ**. Nutritional support for the surgical oncology Patient. *JMCC* 2000; **7**: 563-565
3 **Jeejeebhoy KN**. Enteral and parenteral nutrition: evidence-based approach. *Proc Nutr Soc* 2001; **60**: 399-402
4 **Waitzberg DL**, Plopper C, Terra RM. Access routes for nutritional therapy. *World J Surg* 2000; **24**: 1468-1476
5 **Nompleggi DJ**, Bonkovsky HL. Nutritional supplement in chronic liver disease: an analytical review. *Hepatology* 1994; **19**: 518-533
6 **Wu CT**, Huang QC, Li ZL. The increase of intestinal mucosal premeability and bacterial translocation. *Shijie Huaren Xiaohua Zazhi* 1999; **7**: 605-606
7 **Wilmore DW**, Smith RJ, O'D-wyer ST, Jacobs DO, Ziegler TR, Wang XD. The gut: a central organ after surgical stress. *Surgery* 1988; **104**: 917-923
8 **Zhu WM**, Li L. Enteral nutritional support. *Zhongguo Shiyong Waike Zazhi* 2001; **21**: 506-510
9 **Sun M**, Liu YW, Liu W, Deng GY, Tang WS, Jiang ZM. Lactulose mannitol ratio in patients after operation. *Zhonghua Waike Zazhi* 1999; **37**: 298-300
10 **Hu QG**, Zheng QC. The effect of enteral nutrition on gut barrier in patients with hepatic dysfunction. *Parenteral&Enteral Nutrition* 2002; **9**: 1-3
11 **Bavdekar A**, Bhave S, Pandit A. Nutrition management in chronic liver disease. *Indian J Pediatr* 2002; **69**: 427-431
12 **Fang CH**, Yang JZ. Arginine regulation of cellular immunity in patients with obstructive jaundice. *Huaren Xiaohua Zazhi* 1998; **6**: 902-904
13 **Abou-Assi S**, Vlahcevic ZR. Hepatic encephalopathy. Metabolic consequence of cirrhosis often is reversible. *Postgrad Med* 2001; **109**: 52-54, 57-60, 63-65 passim
14 **Qin HL**, Wu ZH. Influence of lipofundin vs intralipid on surgical patients with liver diseases. *Zhongguo Linchuang Yingyang Zazhi* 1999; **7**: 129-132
15 **Ling PR**, Ollero M, Khaodhiar L, McCowen K, Keane-Ellison M, Thibault A, Tawa N, Bistrian BR. Disturbances in essential fatty acid metabolism in patients receiving long-term home parenteral nutrition. *Dig Dis Sci* 2002; **47**: 1679-1685
16 **Jia QB**, Wu YT, Mao HX, Wang BY, Tang Y. The influence of fat emulsion on liver function and fatty metabolism in patients after surgery of obstructive jaundice. *Zhongguo Linchuang Yingyang Zazhi* 1999; **7**: 112-114
17 **Takagi K**, Yamamori H, Toyoda Y, Nakajima N, Tashiro T. Modulating effects of the feeding route on stress response and endotoxin translocation in severely stressed patients receiving thoracic esophagectomy. *Nutrition* 2000; **16**: 355-360
18 **Zhou X**, Chen QP. Prevention and cure of complications of enteral nutrition. *Shijie Huaren Xiaohua Zazhi* 2000; **8**: 1393-1394
19 **Zhi XT**, Shou NH. Accommodation and contraindication of enteral nutrition. *Shijie Huaren Xiaohua Zazhi* 2000; **8**: 1389-1390
20 **Teran JC**. Nutrition and liver diseases. *Curr Gastroenterol Rep* 1999; **1**: 335-340
21 **Wu XT**, Yan LN. Enteral nutrition in liver disease and pancreatic disease. *Shijie Huaren Xiaohua Zazhi* 2000; **8**: 1397-1398
22 **Li JS**. The experience of nutritional surpport in gastric surgery. *Zhonghua Putong Waike Zazhi* 2000; **15**: 172-173
23 **Zhu L**, Yang ZC, Li A, Cheng DC. Protective effect of early enteral feeding on postburn impairment of liver function and its mechanism in rats. *World J Gastroenterol* 2000; **6**: 79-83
24 **Li N**, Li JS. Improve and prospect of surgical nutrition in current 20 years. *Zhongguo Shiyong Waike Zazhi* 2002; **22**: 6-8
25 **Wu GH**, Wu ZH. Selection of perioperative nutrition. *Zhonghua Putong Waike Zazhi* 2000; **15**: 766-767
26 **Heubi JE**, Wiechmann DA, Creutzinger V, Setchell KD, Squires R Jr, Couser R, Rhodes P. Tauroursodeoxycholic acid (TUDCA) in the prevention of total parenteral nutrition-associated liver disease. *J Pediatr* 2002; **141**: 237-242
27 **Mochizuki H**, Togo S, Tanaka K, Endo I, Shimada H. Early enteral nutrition after hepatectomy to prevent postoperative infection. *Hepatogastroenterology* 2000; **47**: 1407-1410
28 **Xu BH**, Wang X, Wang XX, Wang BT, Li JG. 52 cases of discompensated in liver cirrhosis with multiple organ falliure. *Huaren Xiaohua Zazhi* 1998; **6**: 918
29 **Zhang J**, Liu YH, Jiang XH, Xu KS. Relationship between endotoxemia and cellular immunity in obstructive jaundice. *Huaren Xiaohua Zazhi* 1998; **6**: 305-306
30 **Xu DZ**, Lu Q, Deitch EA. Elemental diet-induced bacterial translocation associated with systemic and intestinal immune suppression. *Journal of Parenteral and Enteral Nutrition* 1998; **22**: 37-41
31 **Yue MX**. Research method in therapy of multiple organ failure. *Huaren Xiaohua Zazhi* 1998; **6**: 729-730
32 **Sugiura T**, Tashiro T, Yamamori H, Takagi K, Hayashi N, Itabashi T, Toyoda Y, Sano W, Nitta H, Hirano J, Nakajima N. Effects of total parenteral nutrition on endotoxin translocation and extent of the stress response in burned rats. *Nutrition* 1999; **15**: 570-575
33 **Fu TL**, Chen QP. The protection of enteral nutrition on gut barrier. *Shijie Huaren Xiaohua Zazhi* 2000; **8**: 1395-1396
34 **Zhu WM**, Li L. Enteral nutritional support in gastric surgery. *Shijie Huaren Xiaohua Zazhi* 2000; **8**: 1396-1397
35 **Zheng QC**, Wang JJ, Li JS, Zhang SX. Elemental diet supplemented with intestinal nutrient ingredients protects stressed rat's gut barrier. *Zhonghua Linchuang Yingyang Zazhi* 1997; **5**: 145-148
36 **Gong SJ**, Luo MD, Chen DW, Quan SW, Shen J, Chu BF, Zhang YC, Cai W, Tang QY, Xia ZM, Feng Y. Elementary diet supplemented with fiber in alimentary tract operative patients. *Shijie Huaren Xiaohua Zazhi* 2001; **9**: 483-484
37 **Yu Y**, Tian HM, Shi ZG, Yao YM, Wang YP, Lu LR, Yu Y, Chang GY, Ma NS, Sheng ZY. Relationship between endotoxemia and dysfunction of intestinal immuno-barrier after scald in rats. *Huaren Xiaohua Zazhi* 1998; **6**: 703-704
38 **Wu WX**, Xu Q, Hua YB, Shen LZ. Early enteral nutrition after colorectal resections: a prospective clinical trial. *Shijie Huaren Xiaohua Zazhi* 1999; **7**: 1024-1029

Edited by Wu XN

P.O.Box 2345, Beijing 100023, China
Fax: +86-10-85381893
E-mail: wjg@wjgnet.com www.wjgnet.com

World J Gastroenterol 2003;9(4):847-850
World Journal of Gastroenterology
 ISSN 1007-9327

• CLINICAL RESEARCH •

Operative stress response and energy metabolism after laparoscopic cholecystectomy compared to open surgery

Kai Luo, Jie-Shou Li, Ling-Tang Li, Kei-Hui Wang, Jing-Mei Shun

Kai Luo, Jie-Shou Li, Ling-Tang Li, Kei-Hui Wang, Jing-Mei Shun, Research Institute of General Surgery, Nanjing General hospital, Nanjing Command of People' s Liberation Army, and Clinical School of Medical College, Nanjing University, Nanjing Jiangsu Province 210002, China
Supported by grants from the Health Department of General Logistics Department of People' s Liberation Army, China, No 01Z011
Correspondence to: Dr. Kai Luo, Research Institute of General Surgery, Nanjing General Hospital, Nanjing Command of People' s Liberation Army, and Clinical School of Medical College, Nanjing University, Nanjing 210002, Jiangsu Province, China. lokai@jlonline.com
Telephone: +86-25-4491878
Received: 2002-03-14 **Accepted:** 2002-08-13

Abstract

AIM: To determine the least invasive surgical procedure by comparing the levels of operative stress hormones, response-reactive protein (CRP) and rest energy expenditure (REE) after laparoscopic (LC) and open cholecystectomy (OC).

METHODS: Twenty-six consecutive patients with noncomplicated gallstones were randomized for LC (14) and OC (12). Plasma concentrations of somatotropin, insulin, cortisol and CRP were measured. The levels of REE were determined.

RESULTS: In the third postoperative day, the insulin levels were lower compared to that before operation ($P<0.05$). In the first postoperative day, the levels of somatotropin and cortisol were higher in OC than those in LC. After operation the parameters of somatotropin, CRP and cortisol increased, compared to those in the preoperative period in the all patients ($P<0.05$). In the all-postoperative days, the CRP level was higher in OC than that in LC (7.46±0.02; 7.38±0.01, $P<0.05$). After operation the REE level all increased in OC and LC ($P<0.05$). In the all-postoperative days, the REE level was higher in OC than that in LC (1438.5±418.5; 1222.3±180.8, $P<0.05$).

CONCLUSION: LC results in less prominent stress response and smaller metabolic interference compared to open surgery. These advantages are beneficial to the restoration of stress hormones, the nitrogen balance, and the energy metabolism. However, LC can also induce acidemia and pulmonary hypoperfusion because of the penumoperitonium it uses during surgery.

Luo K, Li JS, Li LT, Wang KH, Shun JM. Operative stress response and energy metabolism after laparoscopic cholecystectomy compared to open surgery. *World J Gastroenterol* 2003; 9(4): 847-850

http://www.wjgnet.com/1007-9327/9/847.htm

INTRODUCTION

The superiority of laparoscopic cholecystectomy (LC) has justified its universal usage in recent years. It induces less surgical response compared to open cholecystectomy (OC). A great many literatures had proved such an advantage[1-4]. However, there were few studies concerning the difference between LC and OC in operative stress response and energy metabolism. In this prospective, randomized study, we compared the effects of LC and OC on body oxygen supply, metabolic hormones and response-reactive protein (CRP) levels, body energy metabolism, and acid-base balance.

MATERIALS AND METHODS

Clinical data

Twenty-six patients with uncomplicated gallstones were recruited for the study from April 2001 to Oct. 2001. They were randomized to undergo LC (n=14) or OC (n=12). The two groups of patients had comparable demographic data (Table 1). All enrolled patients were asymptotic for at least 6 weeks prior to admission without any history of abdominal surgery. Ultrasonography was routinely performed to exclude the common bile duct stone. The patients with jaundice, severe infection, or metabolic abnormities were also excluded in this study. Anesthesia was induced and maintained using a standard intravenous protocol in both groups. LC was undertaken by a standard 4-trochar approach with electrocautery dissection; pneumoperitoneum was established with carbon dioxide (CO_2) insufflation, and OC was performed via a sub-costal incision.

Table 1 Comparison of general conditions between the two groups

Group	Number	M/F	Median age (yrs)	Height (cm)	BW (Kg)
OC	12	3/9	45.5±12.6	161.3±7.1	61.0±3.6
LC	14	6/8	46.6±15.8	163.9±6.1	65.8±9.4

Blood samples and evaluation method

Fast venous blood was taken at 6 AM on the day prior to surgery, and days 1 and 3 postoperatively. Samples should be analyzed within 2 hours after stored *in vitro*. All hormones were quantitatively assayed. In CRP assay, rate immunonephetometry with specific protein analyzer (BN 100 Analyzer) was adopted. Growth hormones (GH) levels were determined by double-antibody RIA with reagents from Jiuding Bio-medical Co. Ltd, Tianjing. Serum cortisol and insulin analysis were both carried out by competitive RIA, using reagents from 3V Diagnostic Technique Co. Ltd. and Chinese Institute of Atomic Energy, respectively.

Energy metabolism was assessed by indirect calorimeter on the day prior to operation, and days 1 and 3 postoperatively. During analysis, patients should be reposed, with ambient temperature 18-26 ℃ and humidity 50-60 %. Oxygen consumption (VO2) and CO2 production (VCO2) per unit time were determined at first. Then, based on the indirect calorimetery theory, REE and RQ were figured out according to the value of VO2 and VCO2. All energy consumption measurements were carried out using Medical Graphics Critical Care Monitor Desktop Analysis System (Medical Graphics Co.,

Minneapolis, MN). Artery and acid-base balance were assayed by automatic gas analyzer.

Statistical analysis

Data were given as means and standard error of the mean. The intergroup comparison was made using the Student' s *t* test. All the statistical procedures were accomplished with SPSS 8.0. A two-tailed $P<0.05$ was taken as significant.

RESULTS

Median surgical duration was not different between the LC (50.9±8.9 min) and OC (58.5±6.3 min) group ($P>0.05$), while the length of hospital stay and the time to first passage of flatus were significantly shorter in LC than those in OC group (Table 2).

Table 2 Postoperative intestinal transit recovery

	OC (*n*=12)	LC (*n*=14)
Time to first passage of flatus (days)	2.8±0.4	1.5±0.3[a]
Postoperative length of stay (days)	6.7±0.2	3.2±0.3[a]

[a]$P<0.05$ *vs* OC.

Insulin levels rose significantly on the 3rd postoperative day above baseline measurements in OC group, with no intergroup difference throughout the postoperative period. GH levels elevated in both groups at all phases postoperatively. However, there was a more prominent response in patients undergoing OC. A significant intergroup difference was detected on day 1 following operation with higher values for OC than that for LC. Cortisol levels increased from baseline on both of the postoperative days in the two groups, but more remarkably in OC group. Intergroup comparison indicated that concentrations were significantly higher in patients undergoing OC on day 1, postoperatively. But on the 3rd postoperative day, cortisol concentrations were comparable in the two groups (Table 3).

Table 3 GH, Insulin, and cortisol levels before and after surgery

	Prior to surgery	1st postoperative day	3rd postoperative day
Insulin			
LC (*n*=14)	14.4±2.1	16.1±2.8	14.6±2.5
OC (*n*=12)	17.9±2.1	17.2±3.4	12.3±0.9[b]
GH			
LC	1.0±0.2	2.7±1.0[ab]	1.5±0.5[b]
OC	1.8±0.4	5.4±2.5[b]	2.2±0.9
Cortisol			
LC	0.46±0.01	0.56±0.11[ab]	0.74±0.05[b]
OC	0.71±0.15	1.12±0.25[b]	0.89±0.02[b]

[a]$P<0.05$, *vs* OC [b]$P<0.05$, *vs* the preoperative period.

In OC groups, REE levels raised 165.3Kcal from baseline on day 1 postoperatively. The difference was significant. But on the 3rd postoperative day, it was 57.3Kcal higher than baseline only (not significant). A similar pattern was seen in the patients undergoing LC, and there was a marked increase (60.1Kcal) on day 1 but not on day 3. On both of the postoperative days, REE levels were significantly higher in OC than those in LC group. RQ fell significantly from baseline on the 1st postoperative day in both groups. There was a significant elevation of CRP concentrations from baseline levels in both groups. However, in patients undergoing OC, the increase was more remarkable. CRP levels were significantly higher in OC than those in LC group on both of the postoperative days (Table 4).

Table 4 REE, RQ, and CRP levels before and after surgery

	Prior to surgery	1st postoperative day	3rd postoperative day
REE			
LC (*n*=14)	1162.2±159.6	1222.3±180.8[ab]	1152.8±150.2[a]
OC (*n*=12)	1273.2±304.8	1438.5±418.5[b]	1330.5±353.8
RQ			
LC	0.87±0.10	0.78±0.06[b]	0.85±0.09
OC	0.88±0.12	0.78±0.04[b]	0.84±0.08
CRP			
LC	8.00±0.01	15.10±2.47[ab]	34.44±7.88[ab]
OC	12.37±3.55	64.50±15.20[b]	94.25±13.43[b]

[a]$P<0.05$, *vs* OC [b]$P<0.05$, *vs* the preoperative period.

Artery oxygen pressure did not change remarkably after surgery in OC group, while it declined significantly on the 1st postoperative day in the LC group and returned to preoperative levels on the 3rd day. Oxygen saturation (SO2) in blood fell significantly on the 1st postoperative day in both groups. On the 3rd day, it was much higher in LC than that in OC group. There was no significant change of PCO2 in both groups after surgery. (Table 5) On the 3rd postoperative day, HCO3- level and BE rose significantly in LC group, and BE was significantly higher in LC than that in OC group. PH was significantly lower in LC than that in OC group on the 1st postoperative day (Table 6).

Table 5 Artery PO2, PCO2 and SO2 before and after surgery

	Prior to surgery	1st postoperative day	3rd postoperative day
PO2			
LC (*n*=14)	87.7±4.0	75.9±3.2[b]	80.94±4.3
OC (*n*=12)	80.2±2.2	86.5±9.2	79.81±0.6
PCO2			
LC	36.79±1.19	37.09±1.64	34.48±1.75
OC	35.01±1.76	31.83±2.63	37.96±1.88
SO2			
LC	96.4±0.40	94.6±0.86[b]	95.4±0.40[a]
OC	95.4±0.40	92.73±1.70[b]	94.0±0.67

[a]$P<0.05$, *vs* OC [b]$P<0.05$, *vs* the preoperative period.

Table 6 REE, RQ, and CRP levels before and after surgery

	Prior to surgery	1st postoperative day	3rd postoperative day
REE			
LC (*n*=14)	22.5±0.61	21.7±0.61	22.15±0.83
OC (*n*=12)	21.02±0.58	20.32±2.1	24.8±0.72[b]
RQ			
LC	-1.77±0.48	-2.85±0.46	-1.77±0.78[a]
OC	-1.66±0.54	-2.17±1.38	1.23±0.65[b]
CRP			
LC	7.40±0.006	7.387±0.008[a]	7.43±0.008[b]
OC	7.42±0.013	7.46±0.022	7.44±0.018

[a]$P<0.05$, *vs* OC [b]$P<0.05$, *vs* the preoperative period.

DISCUSSION

Laparoscopic cholecystectomy is becoming the choice of surgery for uncomplicated cholelithiasis because it had induced less tissue trauma response throughout the course of wound healing compared to open cholecystectomy. Surgery stimulates a series of hormonal and metabolic changes that constitute the stress response. Surgery also induces neurohormonal events that include activation of sympathetic nervous system and stimulation of hypothalamic-pituitary -adrenal axis initially. Then the adrenal cortex is activated, promoting the release of neurohormonal transmitters that would influence the intensity of postoperative pain and duration of postoperative ileus[5-7]. ACTH, catecholamine, cortisol, and glucagon all played crucial roles in the mediation of stress response. In response to sepsis and trauma, massive catecholamine, cortisol, and glucagons are released, while serum insulin concentrations decrease relatively, and decrease of insulin levels is in correlation with the severity of the sepsis and trauma[8-12]. In the present study, we found a marked decrease of insulin levels from baseline in OC group on the 3rd postoperative day, while the intergroup different was not significant on either 1st or 3rd postoperative day. GH and cortisol levels increased from baseline in both groups on the 1st and 3rd postoperative day, and there was a more marked increase in OC group. On the 1st postoperative day GH and cortisol concentrations were both higher in OC than those in LC group.

The cytokines and CRP were objective markers of operative stress response as well as the mediators of host immunologic reaction. Derived from immune system or other tissues, TNF, IL-1 and IL-6 were the major mediators of the acute-phase response[13-15]. In a recent study, Bruce and coworkers[16] examined the changes of CRP, IL-1 Ra, IL-6, and TNF-a in LC and OC patients after surgery. A marked and persistent raise of IL-6 levels was detected from 8 hours to 7 days postoperatively in OC group, while the concentrations of CRP and albumin were comparable in the two groups. IL-1ra levels were significantly raised as early as 4 hours following incision in OC group, compared to LC group. IL-6 levels rose significantly and early (1 hour) in both groups, but there was a more prominent and prolonged response in patients undergoing OC. Significant intergroup difference of IL-6 levels was present as early as 8 hours following incision[17-21]. In our study, we found that CRP levels rose significantly from baseline on both day 1 and day 3 after surgery in the two groups, but more prominently in OC group.

In response to the surgical trauma, the body usually presents with a hyper-metabolic state. Such a state is directly linked to the activation of sympathetic nervous system, the increase of oxygen and energy consumption, the negative nitrogen balance, and the synthesis of CRP. All surgical traumas will induce neuroendocrine activation and protein catabolism, and the nitrogen excretion is therefore increased (mainly as BUN, sometimes as SCr)[22,23]. The amount of the increased nitrogen excretion was determined by the extent of stress, which is proportional to the intensity of injury response. Thus, the degree of metabolic restoration could be acquired using systemic nitrogen balance measurements[8]. To our knowledge, this study is the first to assess the effect of mini-invasive surgery on body REE consumption. In the study, we observed the perioperative changes of REE levels of LC and OC groups using indirect calorimeter. As the result, REE increased significantly (165.3 Kcal) from baseline in the 1st postoperative day in OC group, while on the 3rd day the elevation was not significant (57.3 Kcal). The LC group also revealed marked increase (60.1 Kcal) in the 1st postoperative day, but not in the 3rd day. The intergroup difference of REE levels was significant (with higher levels in OC group) at all phases postoperatively. RQ decreased significantly on the 1st postoperative day in both groups. Thus, our study revealed that LC was less invasive and induced less host stress response and metabolic disturbance compared with traditional OC and it therefore might be more beneficial to the restoration of nitrogen balance and metabolism.

During LC, pneumoperitoneum is induced by insufflation of carbon dioxide, which may be accompanied with disturbance of acid-base balance and pulmonary perfusion[24-27]. Open surgery, on the other hand, usually results in pulmonary dysfunction. Previous studies have shown that on the 1st postoperative day, FVC and FEV1 decreased 40-70 % in patients undergoing OC, compared to 20-40 % in patients undergoing LC. There are possibly two explanations for this. One is that postoperative wound pain often causes shallow respiration, which may lead to small bronchiole closure, the pulmonary blood shunt, and hence the hyponoxia. Increased oxygen consumption after surgery may be another explanation[28-31]. In this study, we observed that artery oxygen consumption fell significantly from baseline on day 1 and restored to preoperative levels on the day 3 postoperatively in LC patients, with no significant reduction in OC patients. SO2 decreased significantly on the 1st postoperative day on both groups, and on the 3rd postoperative day it was higher in LC group than in OC group. Penumoperitonium could explain the reduced oxygen supply at early postoperative phases in LC patients. However, the influence of wound pain on respiration is more pronounced and permanent OC than in LC patients, this may be the reason why the intergroup difference is significant on the 3rd postoperative day. HCO3 and BE raised significantly from baseline in OC group on the 3rd postoperative day, and BE was significantly higher in LC group than that in OC group on the day. PH levels were much lower in LC group than those in OC group on the 1st postoperative day. This is possibly because of the postoperative acidemia elicited by the retention of CO2 during pneumoperitonium. Much attention should be paid to this change during LC.

In conclusion, LC results in less prominent stress response and metabolic interference compared to open surgery. These advantages are beneficial to the restoration of stress hormones, the nitrogen balance, and the energy metabolism. However, LC can also induce acidemia and pulmonary hypoperfusion because of the penumoperitonium it uses during surgery.

REFERENCES

1 **Chen L,** Dai N, Shi X, Tao S, Zhang W. Life quality of patients after cholecystectomy. *Zhonghua Waike Zazhi* 2002; **40**: 762-765

2 **Champault A**, Vons C, Dagher I, Amerlinck S, Franco D. Low-cost laparoscopic cholecystectomy. *Br J Surg* 2002; **89**: 1602-1607

3 **Bosch F,** Wehrman U, Saeger HD, Kirch W. Laparoscopic or open conventional cholecystectomy: clinical and economic considerations. *Eur J Surg* 2002; **168**: 270-277

4 **Topcu O**, Ka rakayali F, Kuzu MA, Ozdemir S, Erverdi N, Elhan A, Aras N. Comparison of long-term quality of life after laparoscopic and open cholecystectomy. *Surg Endosc* 2003; **17**: 291-295

5 **Dubois M,** Pickar D, Cohen MR, Roth YF, Macnamara T, Bunney WE Jr. Surgical stress in humans is accompanied by an increase in plasma beta-endorphin immunoreactivity. *Life Sci* 1981; **29**: 1249-1254

6 **Hearing SD**, Thomas LA, Heaton KW, Hunt L. Effect of cholecystectomy on bowel function: a prospective, controlled study. *Gut* 1999; **45**: 889-894

7 **Fox JE,** Daniel EE. Exogenous opiates: their local mechanisms of action in the canine small intestine and stomach. *Am J Physiol* 1987; **253**(2 Pt 1): G179-188

8 **Byrne J,** Hallett JW Jr, Ilstrup DM. Physiologic responses to laparoscopic aortofemoral bypass grafting in an animal model. *Ann Surg* 2000; **231**: 512-518

9 **Blanc-louvry IL,** Coquerel A, Koning E. Operative stress response

is reduced after laparoscopic compared to pen cholecystectomy. *Dig Dis Sic* 2000; **45**: 1703-1713

10 **Emirer S**, Karadayi K, Simsek S, Erverdi N, Bumin C. Comparison of postoperative acute-phase reactants in patients who underwent laparoscopic v open cholecystectomy: a randomized study. *J Laparoendosc Adv Surg Tech A* 2000; **10**: 249-252

11 **Schauer PR**, Sirinek KR. The laparoscopic approach reduces the endocrine response to elective cholecystectomy. *Am Surg* 1995; **61**: 106-111

12 **Yoshida S,** Ohta J, Yamasaki K, Kamei H, Harada Y, Yahara T, Kaibara A, Ozaki K, Tajiri T, Shirouzu K. Effect of surgical stress on endogenous morphine and cytokine levels in the plasma after laparoscopoic or open cholecystectomy. *Surg-Endosc* 2000; **14**: 137-140

13 **Mendoza-Sagaon M**, Hanly EJ, Talamini MA, Kutka MF, Gitzelmann CA, Herreman-Suquet K, Poulose BF, Paidas CN, De Maio A. Comparison of the stress response after laparoscopic and open cholecystectomy. *Surg Endosc* 2000; **14**: 1136-1141

14 **Leung KL**, Lai PB, Ho RL, Meng WC, Yiu RY, Lee JF, Lau WY. Systemic cytokine response after laparoscopic-assisted resection of rectosigmoid carcinoma: A prospective randomized trial. *Ann Surg* 2000; **231**: 506-511

15 **Sendt W,** Amberg R, Schoffel U, Hassan A, von-Specht BU, Farthmann EH. Local inflammatory peritoneal response to operative trauma: studies on cell activity, cytokine expression, and adhesion molecules. *Eur J Surg* 1999; **165**: 1024-1030

16 **Bruce DM**. FRCS And simith M. Minimal Access Surgery for cholelithiasis induces an attenuated acute phase response. *Am J Surg* 1999; **178**: 232-234

17 **Jess P**, Schultz K, Bendtzen K, Nielsen OH. Systemic inflammatory responses during laparoscopic and open inguinal hernia repair: a randomised prospective study. *Eur J Surg* 2000; **166**: 540-544

18 **Chaudhary D,** Verma GR, Gupta R, Bose SM, Ganguly NK. Comparative evaluation of the inflammatory mediators in patients undergoing laparoscopic versus conventional cholecystectomy. *Aust N Z J Surg* 1999; **69**: 369-372

19 **Mansour MA**, Stiegmann GV, Yamamoto M, Berguer R. Neuroendocrine stress response after minimally invasive surgery in pigs. *Surg Endosc* 1992; **6**: 294-297

20 **Kristiansson M,** Saraste L, Soop M, Sundqvist KG, Thorne A. Diminished interleukin-6 and C-reactive protein responses to laparoscopic versus open cholecystectomy. *Acta Anaesthesiol Scand* 1999; **43**: 146-152

21 **Janicki K**, Bicki J, Radzikowska E, Pietura R, Madej B, Burdan F. C-reactive protein (CRP) as a response to postoperative stress in laparoscopic cholecystectomy using the abdominal wall lift, with performed pneumoperitoneum (CO2), and in open cholecystectomy. *Ann Univ Mariae Curie Sklodowska* 2001; **56**: 397-402

22 **Bistrian BR.** A simple technique to estimate severity of stress. *Surg Gynecol Obstet* 1979; **148**: 675-678

23 **Cerra FB**, Siegal JH, Border JR. Correlations between metabolic and cardiopulmonary measurement in patients after trauma, general surgery and sepsis. *J trauma* 1979; **19**: 621-629

24 **Coskun I,** Hatipoglu AR, Topaloglu A, Yoruk Y, Yalcinkaya S, Caglar T. Laparoscopic versus open cholecystectomy: effect on pulmonary function tests. *Hepatogastroenterology* 2000; **47**: 341-342

25 **Mimica Z**, Biocic M, Bacic A, Banovic I, Tocilj J, Radonic V, Ilic N, Petricevic A. Laparoscopic and laparotomic cholecystectomy: a randomized trial comparing postoperative respiratory function. *Respiration* 2000; **67**: 153-158

26 **Singh-Ranger D**. Pulmonary function after laparoscopic and open cholecystectomy. *Surg Endosc* 2002; **16**: 1496-1497

27 **Koivusalo AM**, Kellokumpu I, Scheinin M, Tikkanen I, Makisalo H. A comparison of gasless mechanical and conventional carbon dioxide pneumoperitoneum methods for laparoscopic cholecystectomy. *Anesth Analg* 1998; **86**: 153-158

28 **Ali J,** Gana TJ. Lung volumes 24 h after laparoscopic cholecystectomy - justification for early discharge. *Can Respir J* 1998; **5**: 109-113

29 **Chumillas MS**, Ponce JL, Delgado F, Viciano V. Pulmonary function and complications after laparoscopic cholecystectomy. *Eur J Surg* 1998; **164**: 433-437

30 **Larsen JF**, Ejstrud P, Svendsen F, Pedersen V, Redke F. Systemic response in patients undergoing laparoscopic cholecystectomy using gasless or carbon dioxide pneumoperitoneum: a randomized study. *J Gastrointest Surg* 2002; **6**: 582-586

31 **Hendolin HI,** Paakonen ME, Alhava EM, Tarvainen R, Kemppinen T, Lahtinen P. Laparoscopic or open cholecystectomy: a prospective randomised trial to compare postoperative pain, pulmonary function, and stress response. *Eur J Surg* 2000; **166**: 394-399

Edited by Zhang JZ

P.O.Box 2345, Beijing 100023, China
Fax: +86-10-85381893
E-mail: wjg@wjgnet.com www.wjgnet.com

World J Gastroenterol 2003;9(4):851-857
World Journal of Gastroenterology
 ISSN 1007-9327

• CLINICAL RESEARCH •

Ultrastructure and molecular biological changes of chronic gastritis, gastric cancer and gastric precancerous lesions: a comparative study

Goang-Yao Yin, Wu-Ning Zhang, Xiao-Jing Shen, Yi Chen, Xue-Fen He

Goang-Yao Yin, Xiao-Jing Shen, Xue-Fen He, Wuxi No.3 Peoples Hospital, Wuxi 214041, Jiangsu Province, China
Wu-Ning Zhang, Yi Chen, Department of National Microanalysis Center, Fudan University, Shanghai 200433, Shanghai, China
Correspondence to: Dr. Goang-Yao Yin, Wuxi No.3 Peoples Hospital, 230 Eastern Tonghhui Road Wuxi 214041, Jiangsu Province,China. yinyao@pub.wx.jsinfo.net
Received: 2002-10-04 **Accepted:** 2002-12-03

Abstract

AIM: To carry out a comparative study on ultrastructure and molecular biological changes of chronic gastritis (CG), gastric cancer (GC) aand gastric precancerous lesions.

METHODS: By the use of histochemical staining, SEM with EDAX, TEM with EDAX, image analysis technique, RIA and chemiluminescence method, gastric mucosa of 168 patients were synchronously analyzed in morphology, trace elements, DNA, cAMP, SOD, ^{3}H-TdR LCT and serum LPO were also done.

RESULTS: The incidence of epithelial nucleoplasmic ratio >1, lobulated nuclei, inter-chromatin aggregation of granules, nucleolar hypertrophy, and the content of DNA, Zn, Cu in nuclei and serum LPO of each group were showed as belows: normal control group (0.0, 0.0, 6.7, 0.0, 12.6±2.7, 7.6±0.4, 58.4±0.3, 2.6±0.6), CSG group (5.7, 2.9, 7.4, 2.9, 15.2±3.1, 8.1±0.5, 58.9±0.5, 4.2±0.7), CAG group (31.3, 29.7, 45.3, 42.2, 16.5±3.1, 8.6±0.4, 59.3±0.5, 4.5±0.6), CA group (100.0, 100.0, 72.2, 50.0, 30.7±8.2, 8.8±0.3, 59.5±0.4, 6.8±1.6), ATP^{++}group (61.5, 38.5, 23.1, 38.5, 23.5±8.9, 8.3±0.4, 59.1±0.4, 5.1±1.2), IM^{++}+ ATP^{++}group (77.8, 55.5, 33.3, 44.4, 25.1±7.2, 8.4±0.5, 59.5±0.4, 6.5±1.1), IM^{+++}+ATP^{++} group (100.0, 100.0, 75.0, 62.5, 28.5±9.1, 8.9±0.5, 59.7±0.4, 7.6±0.7), $IMII_b$ group (100.0, 62.5, 75.0, 50.0, 27.3±10.3, 8.6±0.3, 59.5±0.4, 6.1±0.9); whereas the content of Zn, Cu in mitochondria and cAMP, SOD in gastric mucosa, and ^{3}H-TdR LCT of each group were showen as belows: normal control group (9.2±0.5, 58.3±0.3, 15.9±1.5, 170.5±6.1, 1079.7±227.4), CSG group (8.6±0.5, 57.8±0.3, 14.6±1.8, 163.3±5.6, 867.3±240.5), CAG group (8.3±0.4, 57.5±0.3, 13.4±1.8, 161.2±4.3, 800.9±221.8), CA group (8.9±0.4, 57.1±0.3, 10.2±3.9, 152.2±3.8, 325.7±186.8), ATP^{++} group (9.1±0.4, 57.0±0.3, 12.4±1.8, 161.5±3.8, 642.9±174.3), IM^{++}+ ATP^{++} group (8.6±0.4, 56.9±0.3, 12.0±2.3, 152.2±2.5, 326.3±160.3), IM^{+++}+ATP^{++} group (8.5±0.3, 56.8±0.2, 10.4±0.9, 147.4±2.6, 316.1±170.7), $IMII_b$ group (8.6±0.3, 56.9±0.3, 11.9±1.9, 150.0±2.8, 318.9±145.8), there were significant differences between groups (P<0.05-0.01).

CONCLUSION: There was a significant difference between CG and GC in their ultrastructure and molecular biology. Only on the condition of changes of internal environment in combination with the harmful effect of external environment, chronic atrophic gastritis can then develop into gastric cancer. Hence it might have similar epithelial cell ultrastructure and molecular biological changes in ATP^{++}, $IMII_b$ and cancer, hence there were similar patterns of occurrence, development and transformation. Recognition of this trend might help to explore problems of prevention and cure.

Yin GY, Zhang WN, Shen XJ, Chen Y, He XF. Ultrastructure and molecular biological changes of chronic gastritis, gastric cancer and gastric precancerous lesions: a comparative study. *World J Gastroenterol* 2003; 9(4): 851-857
http://www.wjgnet.com/1007-9327/9/851.htm

INTRODUCTION

We conducted histochemical staining, detection of cAMP, SOD and DNA of gastric mucosa of 168 patients with chronic gastritis (CG) or gastric cancer (GC); SEM and TEM with EDAX were used to synchronously determine ultrastructures and trace elements and image analysis technique was used to determine nuclear DNA. ^{3}H-TdR LCT and serum LPO were also cared out. Following was the comparative study.

MATERIALS AND METHODS

Materials

168 patients definitely diagnosed as suffering from CSG, CAG and GC were our subjects of study. According to "The standards for the classification of chronic gastritis, for gastrofiberscopic diagnosis and for histopathological diagnosis of atrophic gastritis", gastric mucosa tissue slices underwent HE staining and $AB_{PH2.5}$/PAS, Hid/$AB_{PH2.5}$ and HiD/$AB_{PH2.5}$ histochemical staining. ATP was classified into low-grade, middle-grade and heavy-grade and IM into IM I_a, IM I_b, IM II_a, IM II_b. 68 cases were definitely diagnosed as CSG, including 43 males, 25 females, average age 43 years, average course of disease 4a, 26 cases without IM or ATP; 31 cases with concomitant or solitary IM-19 cases low-grade, 10 cases middle-grade and 2 cases heavy-grade; 9 cases with solitary ATP-8 cases low-grade, 1 case middle-grade; 2 cases with IM and concomitant ATP, IM and ATP were both middle-grade. 64 cases were definitely diagnosed as CAG, including 37 males, 27 females, average age 47 years average course of disease 6a, 3 cases without IM or ATP; 39 cases with concomitant solitary IM (17 cases low-grade, 4 cases middle-grade and 18 cases heavy-grade); 8 cases with solitary ATP (2 cases low-grade, 6 cases middle-grade.) 14 cases with IM concomitant ATP (12 cases middle-grade IM, 2 cases heavy-grade IM, 8 cases low-grade ATP, 6 cases middle-grade ATP). 36 cases were definitely diagnosed as GC, including 22 males, 14 females, average age 52 years, average course of disease, 2a, all with IM or ATP. 12 cases with solitary IM (6 cases low-grade, 3 cases middle-grade, 3 cases heavy-grade); 7 cases with solitary ATP (1 case low-grade, 6 cases middle-grade);

17 cases with IM concomitant ATP (5 cases middle-grade IM, 12 cases heavy-grade IM; 7 cases low-grade ATP, 9 cases middle-grade ATP, 1 case heavy-grade ATP). Of the 45 healthy volunteers who underwent gastroscopy and biopsy, 15 cases had basically normal gastric mucosa tissues, including 6 males 9 females, average age 37, and they were referred to as normal control (NC) group.

Methods

Under gastroscopy, three pieces of gastric mucosa were taken from the focal and nonfocal areas in antral region and body of stomach as specimens for section preparation, SEM, TEM, detection of DNA, cAMP and SOD. Blood was taken for ^{3}H-TdRLCT and LPO. For the observation of gastric mucosa ultrastracture and determination of its trace elements[1-4], 501B SEM with 9100/60 EDAX was used to observe the three pieces of specimens of each patient, under the direct vision of SEM, the EDAX probe automatically detected the samples within 0.1-0.01 mm^2 range all the elements under 12 in atomic number and automatically calculated the weight percentage (WT%) of each element in element series. 15 points were fixed in the three pieces of mucosa of every patient to carry out 15 detections, and the average WT% of each element was taken as its actual WT%. In every detection, 21 elements such as Na, Mg, Al, Si, P, S, K, Ca, Fe, Cu, Zn, Ti, Cr etc were detected, and weight percentage (WT%) of each element between elements of gastric mucosa was calculated.

By using EM430 TEM with 9100/60 EDAX, three pieces of mucosa specimens of every patient were magnified in unison by five magnifying powers (3 600, 7 200, 14 000, 19 000, 29 000) to randomly take the pictures of the panoramagram, local area and organelle and to detect the atomic number percentage (AT%) of each nuclear and mitochondrial element between trace elements[5-10]. After gastric mucosa cell smear was stained by Feulgen staining, IBAS 2000 image analysis technique was adopted to detect IOD, which is taken as the relative content of nuclear DNA[7,8]. RIA was adopted to detect the content of gastric mucosa cAMP (Pmol/g); chemiluminescence method was adopted to detect the activity of SOD (u/g)[4]. ^{3}H-TdRLCT. (Bq/L whole blood) was carried out; thiobarbituric acid development process was adopted to detect serum LPO (u mol/L)[4].

Statistical method

χ^2 and t test.

RESULTS

Histopathology of gastric mucosa

Between NC group. CSG group. CAG group and CA group, there were significant differences in the incidence rate and degree of different types of IM and ATP in glands propria of gastric mucosa (P<0.05-0.001, Table 1). The surface of normal gastric mucosa was isolated by crisscross small groves into many lesser gastric areas, assuming convolution shape (Figure 1). In these areas, there were many gastric pits (the mouths of gastric glands), which were shaped like craters. The concave walls had round or oval epithelial cells of almost the same size. In CSG gastric mucosa there were scattered denatured, diabrotic and necrotic exfoliated epithelical cells, on whose surface S-shape *Helicobacter pylori* (HP) were found (Figure 2). Massive epithelial cells became diabrotic, anabrotic and exfoliated forming micro ulcers. The ulcers spred out from their centers, with adjacent cells crushed, destructed in irregular shapes and arrangement. In CSG gastric mucosa, cyst was found accidentally (Figure 3), the epithelial cells of crater walls were atrophic and denatured, of different sizes and deranged; the cells became diabrotic and necrotic and had inflammatory cell infiltration and the glands propria of the serious cases were shaped like grid framework structure (Figure 4). The surfaces of the epithelial calls of IM gastric mucosa were thickly coated, villi were invisible and the intercellular boundaries were not clear (Figure 5). SEM was not able to definitely indentify gastric mucosa ATP, but only able to distinguish whether cells were hyperplastic or not. Degeneration, hyperplasia or cellular regeneration occured in gastric mucosa. The hyperplastic cells are of different sizes and states and the active memberanes were shaped like lesser tubercles (Figure 6, 7). The cells of gastric cancer were different sizes and shapes, deranged, characterized by obvious heteromorphic nature, conglobated and shaped like grapes or cauliflower. There were nearby or basal infiltration, destruction and ulceration of cancer cells, which have developed into ulcers.

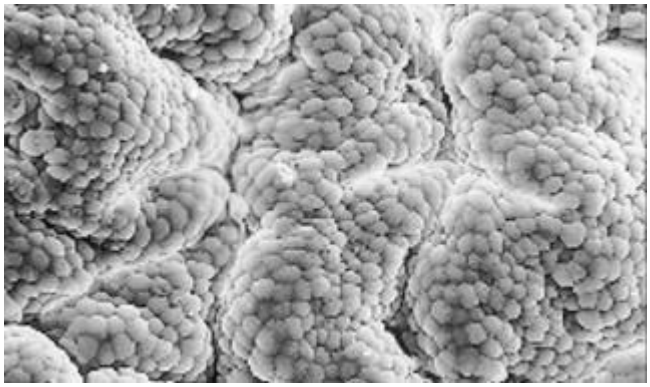

Figure 1 Convolution shape of mucosa surface. ×320.

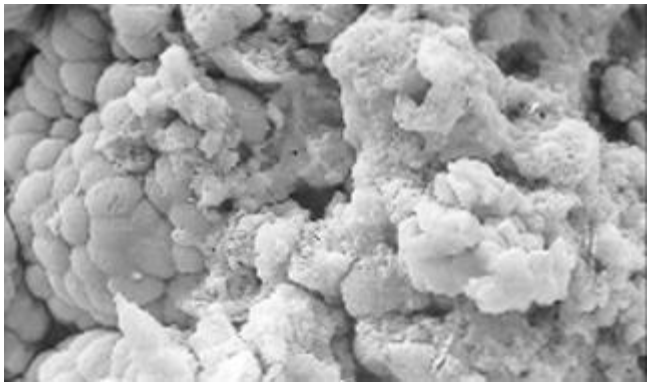

Figure 2 Degeneration, diabrosis, necrosis and exfoliation of gastric mucosa epithelial cells. ×640.

Figure 3 Cysts of gastric mucosa. ×64.

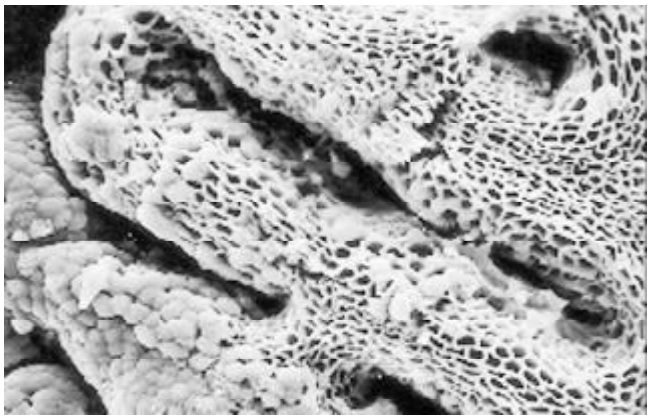

Figure 4 Atrophic and denatured glands propria in grid framework structure. ×320.

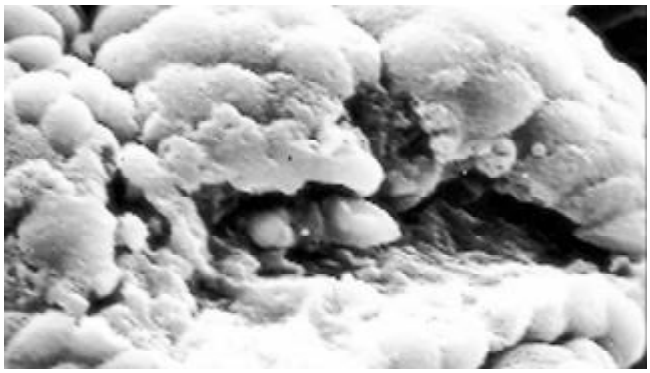

Figure 5 The surface of IM cells is thickly coated, intercellular boundaries are not clear. ×1 250.

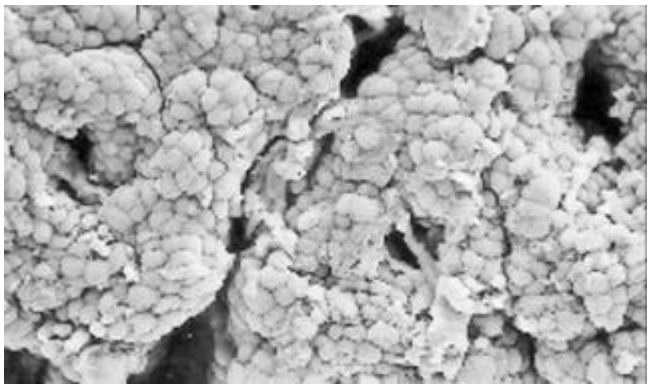

Figure 6 The hyperplastic cells are of different sizes and states, the active membranes are shaped like lesser tubercles. ×320.

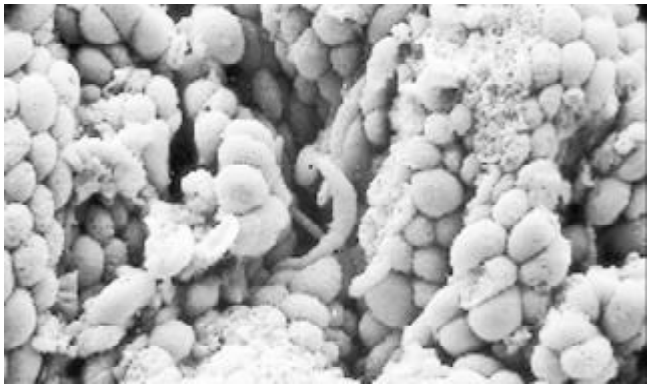

Figure 7 The hyperplastic cells are of different sizes and states, the active membranes are shaped like lesser tubercles. ×640.

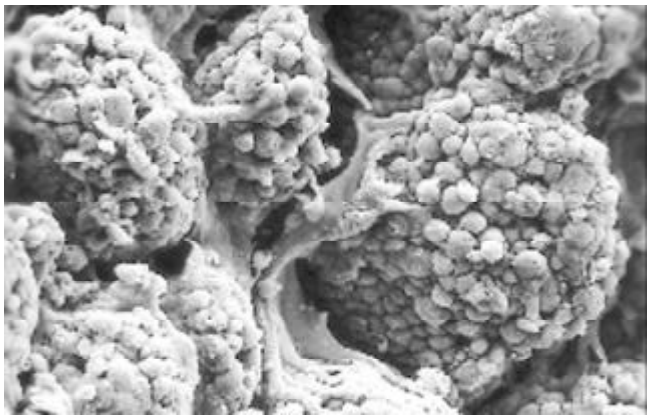

Figure 8 The cells of gastric cancer are conglobated and shaped like grapes. ×320.

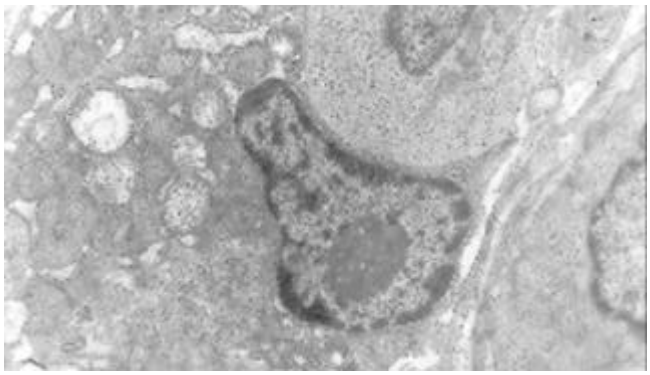

Figure 9 There is an increase in inter chromatinic grandules densification, nucleolar grandules become thick nucleoli expand with irregular margins. ×14 000.

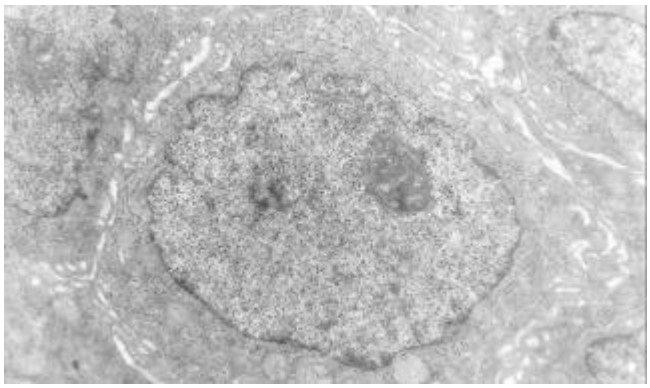

Figure 10 Nucleolar margination. ×7 200.

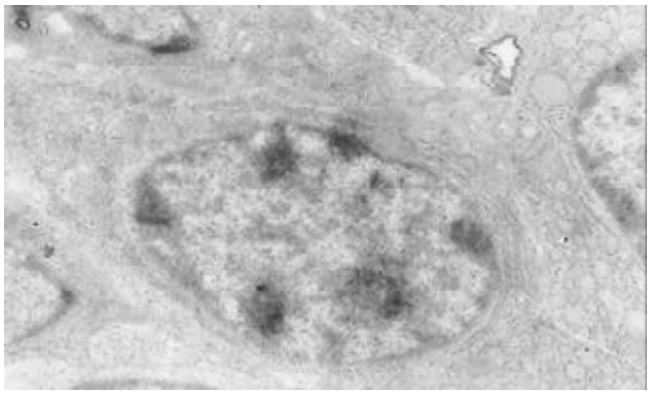

Figure 11 Multi nucleoli. ×14 000.

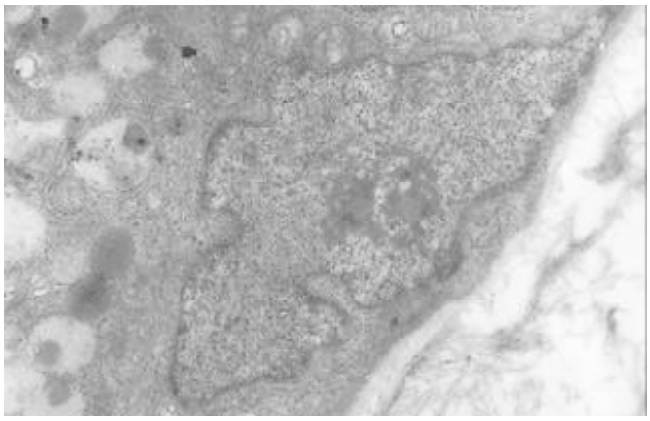

Figure 12 Nucleolar division. ×14 000.

Figure 13 Intranuclear inclusion. ×14 000.

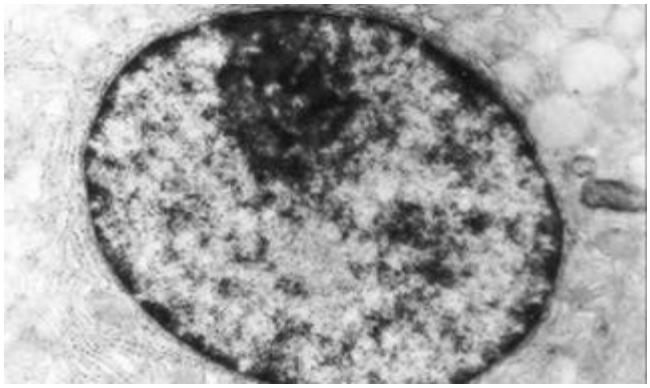

Figure 14 The densification of inter chromatinic grandules. ×14 000.

The ultrastructure of gastric mucosa epithelial cells

The mucous cells on epithelial cell surface of relatively normal gastric mucosa were columna epithelial cells covering endogastric surfaces and inside wall of gastric pit. Their free surfaces had short micro villi; the mucous neck cells were distributed over the necks of gastric glands, and on the tops of these cells were a few short thick micro villi. Chief cells were distributed over the bodies and bottoms of gastric glands; parietal cells were big and conic and their conical tops turned towards gland cavities; the endocrine cells lied between chief cells and parietal cells and they were small, and their nuclei are round or oval, the nuclei envelopes are slightly bent, lobulated nuclei were few, the nucleocyotoplasmic ratio was less than 1.

The nuclear chromatins were scattered, or associated with nucleoli or along nuclear perimeters. The light bright zones between heterochromatins in the nucleoli are euchromatins; the nucleoli had high electron density without capsule. Mitochondria were round or oval, scattering around nuclei. The mitochondria consisted of outer membrane, inner membrane, outer ventricle, inner ventricle and cristae. Crista, the inward folded inner membrane, was a hollow canal leading to outer ventricle. Some mitochondrial cristae directly led to cytoplasms. Cristae were generally in tabular arrangement, parallel to each other and vertical to mitochondrial long axes. In cytoplasms were many parallel rough surfaced endoplasmic reticuluas (RERs), secretory granules, well-developed Golgi' s bodies and scattered mitochondria. The free surfaces of epithelial cells of CG gastric mucosa had dropped micro villi; the intercellular space expanded and cell conjuctions decreased; the karyoplasmic ratio of both ill-differentiated epithelial cells and IM cells was greater than 1, and lobulated nuclei increased; nucleolar granules became thick and nucleoli expanded with irregular margins (Figure 9).

There occured nucleolar margination (Figure 10), multinucleoli (Figure 11) and nucleolar division (Figure 12). The obsolescent epithelial nuclei shrank and the karyoplasmic ratio was still less; the heterochromatins lied densely around nuclei; the electron density was low in the center of nuclei and nuclei were loop in shape. (referred to as chromatin margination); the shrunk nuclei were denticular, in which the electron density was moderately homogeneous and chromatins were not found (referred to as chromatin homogenization). There were mitochondrial swelling, hypertrophy, pyknosis, hyaline degeneration as well as vacuolar degeneration. The deformed mitochrondrias were in C-shape or U-shape. There were zigzag, longitudinal, sparse and pyknosis cristae, and deranged cristas. There was an decrease in the number of mitochondrias and their cristae. There were mitochondrial decreases in number, mitochondrial swelling, or crista fragmentation, vacuolar degeneration, and RERs in circular arrangement; the Golgi' s bodies become atrophic and had lost their typical structures; the cytoplasmic incretory granules decreased. There were still greater epithelial cell changes in cancer cells of gastric cancer than in cells of gastric mucosa of chronic gastritis, intranuclear inclusion appeared (Figure 13). There was an increase in peri-chromatinic and interchromatinic granular densification (Figure 14). In euchromatins; there was a significant difference between CSG group and CAG group in nucleolar margination and nucleolar looping (P<0.05-0.001, Table 2, 3); between IM II_b group, ATP^{++} group, IM^{++}+ATP^{++} group and IM^{+++}+ATP^{++} group, compared with NC group, CSG group and CAG group, the difference was also significant (P<0.05-0.001, Table 2, 3). There is no significant difference between IM^{+++}+ATP^{++} group, IM II_b group and CA group (P>0.05, Table 2, 3).

The biochemical assay in gastric mucosa and serum

The content of nuclear Zn and Cu increased progressively in the sequence of NC group, CSG group, CAG group and CA group; the content of mitochondrial Zn and Cu decreased progressively in the same sequence. There was significant differences between these groups (P<0.05-0.001, Table 4). The content of Zn, Cu, cAMP and SOD in gastric mucosa decreased progressively in the same sequence; the content of DNA increased progressively in the above sequence. There were significant differences between these groups (P<0.05-0.001, Table 5). The content of ^{3}H-TdRLCT decreased in the sequence of NC group, CSG group, CAG group and CA group; content of serum LPO increased in the same sequence; there was significant difference between these groups (P<0.05-0.001, Table 6). Between IMIII_b group, ATP^{++} group, IM^{++}+ATP^{++} group and IM^{+++}+ATP^{++} group, NC group, CSG group and CAG group, there was also significant difference (P<0.05-0.001, Table 4, 5, 6). Between IM^{+++}+ATP^{++} group, IM II_b group and CA group, There was no significant difference (P>0.05, Table 4, 5, 6).

Table 1 Comparison between classification of IM and grading of ATP in CG and GC gastric mucosa *n* (%)

Groups	*n*	IM classification				Grading of ATP						
		I_a	I_b	II_a	II_b	ATP^+	ATP^{++}	$IM^{++}+ATP^+$	$IM^{++}+ATP^{++}$	$IM^{+++}+ATP^+$	$IM^{+++}+ATP^{++}$	$IM^{+++}+ATP^{+++}$
NC	15	2(13.3)	1(6.7)									
CSG	68	16(23.5)	8(11.8)	6(8.8)	3(4.4)	8(11.8)	1(1.5)		2(2.9)			
CAG	64	16(25.0)^b	11(17.2)^b	13(20.3)^d	13(20.3)^d	2(3.1)^d	6(9.4)^d	7(10.9)	5(7.8)^c	1(1.5)	1(1.6)	
CA	36		4(11.1)	9(25.0)^c	16(44.4)^{df}	1(2.8)^d	6(16.7)^d	3(8.3)	2(5.6)^c	4(11.1)^f	7(19.4)^f	1(2.8)

Either Solitary IM or IM with concomitant ATP in CSG, CAG or CA is included in IM classification statistically, compared with NC group. $^aP<0.05$, $^bP<0.01$; compared with CSG group. $^cP<0.05$, $^dP<0.01$; compared with CAG group. $^eP<0.05$, $^fP<0.01$. In table 2-6, the marks are the same as here.

Table 2 The ultrastructures of epithelial nuclei of gastric mucosa in CG and GC *n* (%)

Group	*n*	Appearce		Chromatin		Nucleons	
		Nucleoplasmic ratio >1	Nucleus lobulated	Margination or homogeneity	Perinuclcar concentrated	Hypertrophy or margination	looping
NC	15			1(6.7)	1(6.7)		
CSG	68	5(5.7)	2(2.9)	7(10.3)	5(7.4)	2(2.9)	2(2.9)
CAG	64	20(1.3)^d	19(9.7)^d	33(51.6)^{bd}	29(45.3)^{bd}	27(42.2)^d	14(21.9)
CA	36	36(00.0)^{bf}	36(00.0)^{bf}	17(47.2)^d	26(72.2)^{bdf}	18(50.0)^d	17(47.2)^{df}
$IMII_b$	8	8(100.0)^b	5(62.5)^h	5(62.5)^b	6(75.0)^b	4(50.0)	3(37.5)
ATP^{++}	13	8(61.5)^{hi}	5(38.5)^{hj}	4(30.8)^{bgj}	3(23.1)^{bhj}	5(38.5)	1(7.7)^{hj}
$IM^{++}+ATP^{++}$	9	7(77.8)^{hhik}	5(55.5)^{hk}	3(33.3)^{bgj}	3(33.3)^{bhj}	4(44.4)	3(33.3)^l
$IM^{+++}+ATP^{++}$	8	8(100.0)^{ln}	8(100.0)^{jkm}	5(62.5)^{bkm}	6(75.0)^{blm}	5(62.5)^{lm}	3(37.5)^l

Compared with CA group, $^gP<0.05$, $^hP<0.01$, Compared with $IMII_b$ group, $^iP<0.05$, $^jP<0.01$, Compared with ATP^{++} group, $^kP<0.05$, $^lP<0.01$. Compared with $IM^{++}+ATP^{++}$ group, $^mP<0.05$, $^nP<0.01$. In table 3-6, the marks are the same as here.

Table 3 Mitochondria utrastructures of gastric mucosa epithelial cells in CG and GC ($\bar{x}\pm s$)

Group	*n*	Number	Swelling or Ovegrowth (%)	Matrix fading (%)	Vacuolar degeneration (%)	Pyknosis (%)	Crista number	Fragmentation and derangement of cristas(%)
NC	15	86.5±27.3	3.4±1.6	3.0±1.1	2.9±1.9	1.1±0.8	12.8±3.2	2.2±1.1
CSG	68	65.4±21.1^b	7.2±3.8^b	7.8±5.0^b	6.4±4.5^b	1.9±0.9^b	8.2±3.2^b	5.8±3.1^b
CAG	64	52.2±20.8^{bd}	10.9±4.5^{bd}	11.7±8.6^{bd}	11.6±7.7^{bd}	3.7±1.1^{bd}	6.9±3.5^{bc}	8.9±3.7^{bd}
CA	36	38.8±31.5^{bde}	12.9±4.2^{bde}	15.6±5.4^{bdf}	14.6±5.8^{bde}	3.9±0.6^{bd}	8.1±1.9^{bde}	10.5±2.7^{bde}
$IMII_b$	8	36.8±30.8^b	13.8±3.2^b	14.1±4.3^b	12.5±3.9^b	3.3±0.8^{bg}	9.3±2.1^b	7.6±1.1^{bh}
ATP^{++}	13	49.1±27.9^b	11.3±2.9^b	8.3±3.5^{bh}	9.3±4.7^b	1.9±0.5^{bhj}	11.3±1.8^{hi}	5.2±1.2^{bhj}
$IM^{++}+ATP^{++}$	9	41.3±30.8^b	12.8±2.1^b	12.1±2.8^{bg}	11.2±3.7^b	2.3±0.3^{bhjk}	11.0±1.5^{ahi}	6.2±1.3^{bhi}
$IM^{+++}+ATP^{++}$	8	35.4±31.5^b	13.3±4.3^b	15.2±5.3^{bl}	12.8±4.3^b	3.9±0.5^{bbln}	8.4±2.1^{bln}	8.6±1.0^{bhln}

Table 5 Gastric mucosa Zn, Cu, DNA, cAMP and SOD in CG and GC ($\bar{x}\pm s$)

Group	*n*	Zn (WT%)	Cu(WT%)	DNA(IOD)	cAMP(pmol/g)	SOD(u/g)
NC	15	4.1±1.0	5.2±0.8	12.6±2.7	15.9±1.5	170.5±6.1
CSG	68	2.8±1.9^b	4.0±1.5^a	15.2±3.1^b	14.6±1.8^b	163.3±5.6^b
CAG	64	2.0±1.8^{bc}	3.4±1.5^{bd}	16.5±3.1^{bc}	13.4±1.8^{bc}	161.2±4.3^{bc}
CA	36	1.5±1.2^{bde}	2.8±0.9^{bde}	30.7±8.2^{bdf}	10.2±3.9^{bdf}	152.2±3.8^{bdf}
$IMII_b$	8	1.7±0.9^b	3.5±0.9^b	27.3±10.3^b	11.9±1.9^b	150.0±2.8^b
TP^{++}	13	2.7±1.3^{bhi}	4.4±0.9^{ahi}	23.5±8.9^{bg}	12.4±1.8^{bg}	161.5±3.8^{aj}
$IM^{++}+ATP^{++}$	9	2.3±1.5^b	4.1±0.9^{bh}	25.1±7.2^b	12.0±2.3^b	152.2±2.5^{bl}
$IM^{+++}+ATP^{++}$	8	1.5±0.8^{bkm}	2.9±0.8^{bhin}	28.5±9.1^b	10.4±0.8^{bil}	147.4±2.6^{bhln}

Table 4 Nuclear and mitochondriaL Zn, Cu of gastric mucosa in CG and GC ($\bar{x}\pm s$)

Group	*n*	Nuclear		Mitochondria	
		Zn (AT%)	Cu(AT%)	Zn (AT%)	Cu(AT%)
NC	15	7.6±0.4	58.4±0.3	9.2±0.5	58.3±0.3
CSG	68	8.1±0.5^{b}	58.9±0.5^{b}	8.6±0.5^{b}	57.8±0.3^{b}
CAG	64	8.6±0.4^{bd}	59.3±0.5^{bd}	8.3±0.4^{bd}	57.5±0.3^{bd}
CA	36	8.8±0.3^{bde}	59.5±0.4^{bde}	8.9±0.4^{bde}	57.1±0.3^{bde}
IMII$_{b}$	8	8.6±0.3^{b}	59.5±0.4^{b}	8.6±0.3^{b}	56.9±0.3^{b}
ATP^{++}	13	8.3±0.4^{bhi}	59.1±0.4^{bhi}	9.1±0.4^{i}	57.0±0.3^{b}
IM^{++}+ ATP^{++}	9	8.4±0.5^{bg}	59.5±0.4^{bk}	8.6±0.4^{bl}	56.9±0.3^{b}
IM^{+++}+ATP^{++}	8	8.9±0.5^{bl}	59.7±0.4^{b}	8.5±0.3^{bgl}	56.8±0.2^{bh}

Table 6 LPO and ^{3}H-TdRLCT of CG and GC ($\bar{x}\pm s$)

Group	*n*	LPO(umol/L)	^{3}H-TdRLCT(Bq/L)
NC	15	2.6±0.6	1079.7±227.4
CSG	68	4.2±0.7^{b}	867.3±240.5^{b}
CAG	64	4.5±0.6^{bc}	800.9±221.8^{bc}
CA	36	6.8±1.6^{bdf}	325.7±186.8^{bdf}
IMII$_{b}$	8	6.1±0.9^{b}	318.9±145.8^{b}
ATP^{++}	13	5.1±1.2^{bhi}	642.9±174.3^{bhj}
IM^{++}+ ATP^{++}	9	6.5±1.1^{b}	326.3±160.6^{bk}
IM^{+++}+ATP^{++}	8	7.6±0.7^{bgjlm}	316.1±170.7^{bl}

DISCUSSION

Chronic gastritis, CAG in particular, is generally acknowledged as precancer ous state. However, not all CAGs are likely to develop into gastric cancer because there is significant difference between chronic gastritis and gastric cancer in the ultrastructure and molecular biology of gastric mucosa. In the grading and classification of IM, grading of ATP of gastric mucosa, incidence rate of epithelial karyoplasmic ratio >1, incidence rate of perichromatinic granular densification and of nucleolar hypertrophy, the number of mitochondria and cristae as well as the incidence rate of mitochondrial deqeneration; as well as in the quantitative changes of nuclear DNA, Zn, Cu, cAMP, SOD and serum LPO and ^{3}H-TdRLCT, there were significant differences between NC group, CSG group, CAG group, CA group, IM II$_{b}$ group, ATP^{++} group, IM^{++}+ATP^{++} group and IM^{+++}+ATP^{++} group (P<0.05-0.0001); There was no significant difference between IM^{+++}+ATP^{++} group, IM II$_{b}$ group and CA group (P>0.05). There are similar epithelial ultrastructures and molecular biochemical changes in ATP^{++}, IM II$_{b}$ and CA. Consequently they should have similar law of occurrence, development and transformation, which might contribute to the exploration of prevention and treatment of the disease.

Clinically, only a few chronic gastritis patients' gastric mucosa epithelial cells are likely to develop into cancer cells, but it is essential that there should be a process which causes genetic variation of cells, the key of which is the quantitative changes of epithelial nuclear DNA. The DNA molecular is coded with nucleotide sequence fragments of special genetic codes, every fragment is a functional group, referred to as gene. The gene order has great stability. Only when intracellular cAMP declines, cytodifferentiation is disturbed.The metabolism of Zn, Cu in the body is disturbed, which in turn disturbs the enzyme system and inhibits the synthesis and activity of SOD; because of the NADPH oxidation reduction circulation and the catalytic function of xanthine oxidase, a great deal of oxygen free radicals are produced far beyond the cleaning ability of SOD. The excessive accumulated oxygen free radicals react in lipid peroxidation with unsaturated fatty acid of inner and outer membranes of mitochondria, producing LPO. Thus level of serum LPO rises. The inner and outer membranes of mitochondria are destructed, causing decrease and derangement of mitochondrial cristae, mitochondrial degeneration decrease of adenosine triphosphate production, and inadequate energy supply of gastric mucosa epithelial cells. When nuclei take up more Zn and Cu, the protein synthesis is enhaneed nuclear division and hyperplasia are accelerated; through influencing lymphocyte metabolism, the quantitative changes of Zn and cAMP in turn inhibit lymphocyte transformation and result in the decline of ^{3}H-TdRLCT level and immunity of the organism. The above changes of intraorganism environment, only if stimulated by certain external causes such as ionizaing radiation, chemical injuries, infection S-shape HP and virus, are likely to cause the change of sequences in gene group, which is referred to as gene mutation; and genetic codes change accordingly, the changed codes are transferred to heterogenous cell descendants, causing cellular differentiation disturbance and even cancerous change. Human body is an integrity organism, in which the components of tissue and cell, and the bioactive substances including trace elements, enzymes, hormones, immunity and messenger substances exist with a definite content and a definite quantitative ratio. It' s important to measure the "absolute" content of each bioactive substance, but it' s more important to measure quantitative ratio of each bioactive substance because it can explain the trends and laws of variation of the whole body and inner circumstance[9,10]. These ratios in normal body keep in a state of dynamic balance within a definite range. If this balance is broken, pathological phenomena and functional disturbance will arise. The ratio fluctuation of bioactive substances higher or lower than normal value, can lead to a series of ratio variation, and then cause both a definite disease diagnosed by modern medicine and clinical expression of Chinese medical syndrome (a synthesis of symptoms without peculiarity). The composite nature of Chinese medicine treats disease through adjusting the above mentioned pathological ratio is one of it' s therapeutic mechanisms. This is why Chinese medicines have multilevel, multitarget, two-way adjusting effects on human body, and how the medicines regulate pathological ratio. It' s a slow process for Chinese medicines to regulate pathological ratio, so It' s therapeutic effect is slow too. Measuring the "quantitative ratio" of a series of bioactive substances not only will be the research direction of medical science and biological science, but also the research kernel of the basic theory of traditional Chinese medicine[11-13].

REFERENCES

1 **Yin GY**, Zhang WN, He XF, Chen Y, Shen XJ. Detection of ultrastructural changes and contents DNA, Zn, Cu and LPO in subgroups of chronic gastritis. *Shijie Huaren Xiaohua Zazhi* 2002; **10**: 663-667

2 **Yin GY**, Zhang WN, Shen XJ, Chen Y, He XF. Ultrastructural and molecular diological changes of chronic gastritis and gastric cancer: a comparative study. *Shijie Huaren Xiaohua Zazhi* 2002; **10**: 668-672

3 **Yin GY**, Zhang WN, He XF, Chen Y, Shen XJ. Alterations of ultrastructures, trace elements, cAMP and cytoimmunity in subgroups of chronic gastritis. *Shijie Huaren Xiaohua Zazhi* 2002; **10**: 673-676

4 **Yin GY,** Zhang WN, He XF, Chen Y, Yin YF, Shen XJ. Histocytepathological study on gastric mucosa of spleen deficiency syndromes. *Zhongguo Zhongxiyi Jiehe Zazhi* 1999; **19**: 660-663

5 **Yin GY**, Xu FC, Zhang WN, Li GC, He XF, Chen Y, Shen XJ. The effect of weikangfu on cytopathology of gastric mucosa tissue

when treating gastric precancerosis lesion of patients with spleen deficiency syndromes. *Zhongguo Zhongxiyi Jiehe Zazhi* 2000; **6**: 241-243

6 **Yin GY**, Zhang WN, Xu FC, He XF, Chen Y, Shen XJ. Effect of Weikangfu chongji on ultrastructure of precancerosis gastric mucosa of patients with spleen deficiency Syndromes. *Zhongguo Zhongxiyi Jiehe Zazhi* 2000; **20**: 667-670

7 **Yin GY**, Zhang WN, Xu FC, Chen Y, He XF, Li GC, Shen XJ. Study on the modern pathophysiologic basis of the syndrome classification of spleen deficiency with chronic gastritis and of (treatment) verification of clinical syndromes and prescriptions. *Jiangsu Yiyao Zazhi* 2001; **27**: 46-47

8 **Yin GY,** He XF, Yin YF, Du YQ, Jiao JH. Study on mitochondrial ultrastructure, trace elements and correlative factors of gastric mucosa in patients with spleen deficiency syndrome. *Zhongguo Zhongxiyi Jiehe Zazhi* 1996; **15**: 719-723

9 **Yin GY**, Zhang WN, Xu FC, He XF, Chen Y, Shen XJ. Effect of weikangfu chongji on epithelial cellular ultrastructure of precancerotic gastric mucosa of patients with spleen deficiency syndrome. *Jiangsu Yiyao Zazhi* 2000; **26**: 514-517

10 **Yin GY,** Zhang WN, Xu FC, He XF, Chen Y, Li GC, Shen XJ. Effect of weikangfu on Zn, Cu and DNA in precancerosis gastric mucosa epithelial nuclei and mitochondria of patients with spleen deficiency syndromes. *Zhongguo Zhongxiyi Jiehe Zazhi* 2000; **8**: 221-224

11 **Yin GY**, Zhang WN, Shen XJ, Chen Y, He XF. A comparative study on ultrastructure of chronic gastritis grastric mucosa IM, ATP and their molecular biology. *Jiangsu Yiyao Zazhi* 2002; **28**: 4-7

12 **Yin GY**, He XF, Zhang WN, Chen Y. Relationship between the classification of spleen deficiency and the quantitative changes of bio-active substances in mitochondria of gastric mucosa epithelical cell nuclei. *Zhongguo Zhongxiyi Jiehe Zazhi* 1999; **7**: 145-148

13 **Yin GY**, Zhang WN, Li GC, Huang JR, Chen Y, He XF, Shen XJ. Therapeutic effect of weikangfu on gastric precancerosis disordddeer with spleen deficiency syndrome and its effect of gastric mucosal zinc, copper, cyclic adenosine monophosphate, superoxide dismutase,lipid peroxide and ^{3}H-TdR lymphocyte conversion test. *Zhongguo Zhongxiyi Jiehe Zazhi* 2000; **20**: 176-179

Edited by Xu JY

P.O.Box 2345, Beijing 100023,China
Fax: +86-10-85381893
E-mail: wjg@wjgnet.com www.wjgnet.com

World J Gastroenterol 2003;9(4):858-861
World Journal of Gastroenterology
 ISSN 1007-9327

• CLINICAL RESEARCH •

Neuroendocrine markers in adenocarcinomas: an investigation of 356 cases

Gen-You Yao, Ji-Lin Zhou, Mao-De Lai, Xiao-Qing Chen, Pei-Hui Chen

Gen-You Yao, Ji-Lin Zhou, Mao-De Lai, Xiao-Qing Chen, Pei-Hui Chen, Department of Pathology, Zhejiang University Medical School, Hangzhou 310031, China
Supported by Fundation of Health Bureau of Zhejiang Province
Correspondence to: Gen-You Yao, Research fellow of Pathology, Department of Pathology, Zhejiang University Medical School, Hangzhou, 310031 China. yaogy@zjuem.zju.edu.cn
Telephone: +86-0571-87217167
Received: 2002-10-25 **Accepted:** 2002-11-18

Abstract

AIM: To investigate the incidence of neuroendocrine (NE) cells and their hormone products in adenocarcinomas and evaluate their significance in clinical pathology and prognosis.

METHODS: By using tissue sectioning and immunocytochemistry, 356 cases of adenocarcinomas were studied to examine the presence of chromorgranin and polypeptide hormones in adenocarcinoma samples from our hospital.

RESULTS: The positive rate of NE cells and hormone products was 41.5 % (54/130) and 59.3 % (32/54), respectively in large intestinal adenocarcinoma cases; 39.6 % (38/96) and 36.8 % (14/38), respectively in gastric cancer cases; 38.1 % (8/21) and 50.0 % (4/8), respectively in prostatic cancer cases; 21.0 % (17/81) and 17.6 % (3/17), respectively in breasr cancer cases; 17.9 % (5/28) and 60.0 % (3/5), respectively in pancreatic cancer cases. Among carcinomas of large intestine, pancreas and breast, the highly differentiated NE cell numbers were higher than the poorly differentiated NE cell numbers; while the gastric carcinoma cases had more poorly differentiated NE cells than highly differentiated NE cells. The higher detection rate of NE cells and their hormone products, the higher 5-year survival rate among the large intestine cancer cases.

CONCLUSION: Close correlation was observed between NE cells and their hormone products with the cancer differentiations. For colorectal carcinomas, there is a close correlation of the presence of NE cells and their hormone products with the tumor staging and prognosis.

Yao GY, Zhou JL, Lai MD, Chen XQ, Chen PH. Neuroendocrine markers in adenocarcinomas: an investigation of 356 cases. *World J Gastroenterol* 2003; 9(4): 858-861
http://www.wjgnet.com/1007-9327/9/858.htm

INTRODUCTION

Compared with neuroendocrine cancers, little investigation is carried out on the relationship of neuroendocrine cells and their hormone products in non- neuroendocrine cancers, especially in the common adenocarcinoma cases. By using nine different antibodies and immunocytochemistry, NE cells and their hormone products in 356 adenocarcinamas was observed with the aim of revealing the incidence and distribution of NE cells and the correlation between the cancer differentiation with the biological behaviors was evaluated.

MATERIALS AND METHODS

Materials

All the 365 adenocarcima samples were got from the first affiliated hospital of Zhejiang University Medical College from 1975 to 1994. There were 96 cases of gastric cancer samples (31 samples were got from the clinical biopsy; 65 samples were got from radical operation and 22 samples had lymph nodes metastasis); there were 130 case of large intestine cancer samples got from radical operations (110 cases had the follow-up data); there were 81 and 28 case of breast and panereatic cancer, respectively. The remaining 21 samples were got from prostatic cancer biopsy.

Methods

All the samples were fixed with 10 % formaldehyde with paraffin embedding and continuous sectioning at 4 μM in thickness. Gross pathological observation was made on the HE stain slides followed by immunocytochemistry. All the samples were treated with anti-chromogranin serum fot the primary screening positive cases. Further immunocytochemistry was carried out for those positive NE samples by using peptide hormone antibodies such as ST (diluted at 1:10 000, provided by the 4th Military Medical Academy) and other Dako's antibodies (somatostatin diluted at 1:300; glucagon diluted at 1:800; pancreatic polypeptide diluted at 1:800; gastrin diluted at 1:350; insulin diluted at 1:150; ACTH diluted at 1:800 and calcitonin diluted at 1:150). The immunostains were done by ABC method and coloured with AEC. The antiserum of serotonin and gastrin was used in the gastric mucosa; the pancreas tissue was used to detect the chromogranin, somatostatin, glucagon, insulin and pancreatic polypeptide; calcitonin antiserum was used in the medullary carcinoma of the thyroid gland while ACTH in the pituitary was used as the positive control. The negative control was carried out by using normal sheep serum to replace the 1st antibody. Based on the chromoganin positive NE cell numbers, all the samples were divided into three grades as the following. Negative: there was no NE cells; Positive(+): the number of NE cells was fewer than 5/mm^2; Super positive (++): the number of NE cells was over 5/mm^2.

Statistical analysis

The date were analysed by χ^2 test.

RESULTS

Morphology of NE cells and their incidence

Among the five common adenocarcinomas from different tissue sources, the incidence rate was 41.5 % (54/130) for the large intestinal carcinomas; 39.6 % (38/96) for the gastric carcinoma; 38.1 % (8/21) for the prostatic carcinoma; 21.0 % (17/81) for the breast cancer and 17.9 % (5/28) for the pancreatic cancers, respectively. The highest incidence was

seen in large intestinal carcinomas while the lowest in the pancreatic carcinomas. When observing the chromoganin stained slides, clear edges of NE cells and brownish granules could be seen in the cytoplasm under the microscopy. In the low differentiated carcinomas, the NE cells presented as an oval, round or irregular shape without polarizations. Abnormal structural characteristics were observed among these low differentiated NE cells, which was similar to the adjacent tumor cells; while for those highly differentiated carcinomas, the NE cells were pyramid or bar shaped with the apex pointing to the cavity of the gland. A few NE cell processes could be observed reaching the gland cavity surfaces. The distribution of NE cells were scattered or localized infiltrating all the layers with the cancer cells. NE cells could be seen in both of the primary carcinoma and the metastasis sites.

Relationship between NE cells and carcinoma differentiation

No exact correlation between NE cells and carcinoma differentiation was observed among different carcinomas. The highly differentiated NE cell incidences were 41.7 % (5/12) for the large intestinal carcinomas, 42.9 % (3/7) for the pancreas carcinomas and 32.5 % (14/43) for the breast cancers, which was much higher than that of the low differentiated carcinomas. Prostatic carcinomas had the same tendency but there was no statistical significance due to fewer case numbers. In the low differentiated gastric carcinomas, 50 % (27/54) had the positive NE cells, which was significantly higher than that of the highly differentiated carcinomas.

Distribution of hormone products of NE cells in tumors

From Table 1, the number of hormone products types was more in large intestinal and gastric carcinomas (5 types of hormone products); hormone products detected in breast cancers were the fewest (only three in 17 cases). Most of them were the tumor origin tissue hormones, but few of them were ecotopic hormones.

Relationship between positive cell of hormone products and tumor differentiation

In the large intestinal carcinomas, 9 cases were low differentiated carcinomas whose positive cell percentage of hormone products against the total NE cells was 27.0 %, which was obviously lower than that in high differentiated carcinomas (15 cases with the percentage of 43.9 %) (χ^2=115.9, P<0.01); It was also the same in the highly differentiated large intestinal carcinomas whose percentage was lower than that in the normal mucus membrane (10 cases with the percentage of 83.1 %) (χ^2=212.3, P<0.01) and the mucus membranes adjacent to the tumors (25 cases with the percentage of 88.7 %) (χ^2=168.8, P<0.01). The gastric carcinoma had the similar results: the positive cell percentage of hormone products against the total NE cells was 17.5 %. But in the positive cells of hormone products from 5 gastric sinus mucus membranes, the positive cell percentage of hormone products against the total NE cells was 78.6 % (χ^2=1611.8, P<0.01); the samples adjacent to the gastric sinus areas had the obviously higher percentage (46.6 %, χ^2=266.4, P<0.01). Significant difference was also observed between the percentage of the adjacent mucus membrane tissues of the tumors and the normal mucus membranes (χ^2=242.0, P<0.01).

Ecotopic hormones and tumor differentiation

Except for the pancreatic carcinomas, ecotopic hormones were revealed in other four types of the adenocarcinomas. One of the large intestinal carcinomas cases showed gastrin positive; Six gastric carcinoma cases showed ACTH positive; Two prostatic cancer cases were glucagons positive; One breast cancer case was somatostain positive while another breast cancer case was calcitonin positive. Except for the large intestinal and gastric carcinomas, all the other nine cases were low differentiated carcinomas among the ecotopic hormone carcinomas.

NE cells and tumor differentiation

Observed in large intestinal carcinomas, Dukes A stage accounted for 41.7 % of the NE cell (++) cases (12 cases), which was much higher than that in NE(-) group (19.7 %,76 cases). (χ^2=4.668, P<0.05). Among the 110 cases with following-up, the 5-year survival rate was 81.8 % in NE cell (++) group, which was obviously higher than that in the NE (+) group (45.7 %, 35 cases) (χ^2=4.000, P<0.05) and in NE cell (-) group (42.2 %, 64 cases) (χ^2=4.397, P<0.05).

Among the 32 hormone products positive cases with polypeptide hormones (PH), Dukes A stage cases accounted for 44.1 %, which was higher than that of NE cell positive cases with hormone products negative (36.1 %), yet no statistical difference was found between the two groups (χ^2=0.351, P>0.05). In hormone products (+) group (17 cases), the 5-year survival rate was 70.6 %, which was higher than that of hormone products (-) group (37.9 %, 29 cases) (χ^2=4.148, P<0.05).

DISCUSSION

The commonly used staining methods for revealing NE cells include silver staining, neuron-specific enolase (NSE), synaptophysin (SY) and chromorgranin (CG) immunocytochemistry. Silver staining is the traditional staining method with less specificity and sensitivity. Although NSE, CG and SY are all the common markers, NSE has poor specificity with distributions in different tissues but is localized in the cytoplasm. CG is distributed in neuroendocrine granules. Both CG and SY are good markers and corresponding to

Table 1 Distribution of hormone productions of NE cells in tumors

Type	NE Positive Case	Serotonin Case (%)	Somatostatin Case (%)	Glucagon Case (%)	P P Case (%)	Gastrin Case (%)	Calcitonin Case (%)	ACTH Case (%)
Colorectal carcinomas	54	30(55.6)	14(25.9)	11(20.4)	5(9.3)	1(1.9)	0	0
Gastric carcinomas	38	5(13.2)	5(13.2)	5(13.2)	0	3(7.9)	0	6(15.8)
Pancreatic Carcinomas	5	1(20.0)	0	1(20.0)	2(40.0)	0	0	0
Breast Carcinomas	17	1(5.9)	1(5.9)	0	0	0	1(5.9)	0
Prostatic Carcinomas	8	4(50.0)	0	2(25.0)	0	0	0	0

respective subcellular structures. CG is a specific matrix component of endocrine granules[1-3]. While SY is localized within small capsule membranes related to the secretion granules, whose specificity and sensitivity are less than those of CG. That' s why CG is considered as a realistic marker for NE cells[4-8]. Studies have confirmed that CG could be served as a new way of revealing NE cells and for the diagnosis of NE tumors[9].

Our study demonstrated that NE cell numbers were closely correlated to the tumor differentiation in large intestinal, pancreatic, breast and prostatic carcinomas[10]. The higher differentiated tumors had the higher incidence of the NE cells[8]. That was contradicted to our gastric carcinoma observations, but corresponding to the publication reports[11]. Further studies are needed to be conducted to reveal these differences to see if they are related to the embryology, etiology and tissue development of the tumors.

No serial report were seen about the hormone products of NE cells from the common adenocarcinomas. We observed 5 types of adenocarcinomas and found out that large intestinal and gastric carcinomas had the higher hormone products in their NE cells; but in the gastric and highly differentiated carcinomas, they had lower hormone products in NE cell than those of poor differentiated carcinomas. The hormone products were more in the large intestinal and gastric carcinomas than those in normal mucus membranes and tissues adjacent to the carcinomas. Neoplastic NE cells had lower hormone products and they were decreased with anaplasia which may be due to the fact that these cells were in immature state with lower hormone synthesis. Thus, the amount of hormone products in NE cells of the carcinomas can serve as an index for the determination of tumor differentiation and the diagnosis of benign and malignant tumors[12-15].

Based on the study of the large intestinal carcinomas, we found that hormone products and distribution of NE cells were closely correlated to the tumor grade, clinical pathological stage of the tumor and prognosis of the patients[16-23]. Carcinomas with NE (++) releasing PH were the early stage carcinomas. The higher 5-year survival rate may be due to the somatostatin' s inhibition of the tumors[24-29]. Zollinger-Ellison syndrome was reported in some gastric carcinoid cases[30-32], but our study only revealed there were only different hormone products but without sign and symptoms of Zollinger-Ellison syndrome as well as other hormone signs and symptoms, which may be the fact that the hormone products produced by NE cells were not enough in the inactivated form or inactivated by the liver enzymes. Further study is required to examine whether these hormone products participate in the immune regulations of the tumor or the hormone products exert the direct effects on the tumor development and growth.

REFERENCES

1 **Papotti M**, Macri L, Finzi G, Capella C, Eusebi V, Bussolati G. Neuroendocrine differentiation in carcinomas of the breast:a study of 51 cases. *Semin Diagn Pathol* 1989; **6**: 174-188

2 **Van Laarhoven HA**, Gratama S, Wereldsma JC. Neuroendocrine carcinoid tumours of the breast: a variant of carcinoma with neuroendocrine differentiation. *J Surg Oncol* 1991; **46**: 125-132

3 **Giovanella L**, Marelli M, Ceriani L, Giardina G, Garancini S, Colombo L. Evaluation of chromogranin A expression in serum and tissues of breast cancer patients. *Int J Biol Markers* 2001; **16**: 268-272

4 **Kimura N**, Sasano N, Yamada R, Satoh J. Immunohistochemical study of chromogranin in 100 cases of pheochromocytoma, carotid body tumour, medullary thyroid carcinoma and carcinoid tumour. *Virchows Arch A Pathol Anat Histopathol* 1988; **413**: 33-38

5 **Kimura N**, Hoshi S, Takahashi M, Takeha S, Shizawa S, Nagura H. Plasma chromogranin A in prostatic carcinoma and neuroendocrine tumors. *J Urol* 1997; **157**: 565-568

6 **Portel-Gomes GM**, Grimelius L, Johansson H, Wilander E, Stridsberg M. Chromogranin A in human neuroendocrine tumors: an immunohistochemical study with region-specific antibodies. *Am J Surg Pathol* 2001; **25**: 1261-1267

7 **Bernini GP**, Moretti A, Ferdeghini M, Ricci S, Letizia C, D'Erasmo E, Argenio GF, Salvetti A. A new human chromogranin 'A' immunoradiometric assay for the diagnosis of neuroendocrine tumours. *Br J Cancer* 2001; **84**: 636-642

8 **Yao GY,** Chen PH, Lai MD, Hong LY. Study of 9 neuroendocrine markers in pancreatic tumors. *Zhenjiang Yike Daxue Xuebao* 1995; **24**: 56-58

9 **Chen FX,** Corti A, Siccardi AG. DIBIT; San Raffaele H. Characterizzation of antigenic sites of Human Chromogranin A. *Shanghai Mian Yixue Zazhi* 1998; **18**: 215-219

10 **di Sant'Agnese PA.** Neuroendocrine differentiation in prostatic carcinoma: an update. *Prostate Suppl* 1998; **8**: 74-79

11 **Chen BF**, Yin H. Neuro-endocrine type of gastric carcinoma. Immunohistochemical and electron microscopic studies of 100 cases. *Chin Med J* 1990; **103**: 561-564

12 **Yu JY**, Wang LP, Meng YH, Hu M, Wang JL, Bordi C. Classification of gastric neuroendocrine tumors and its clinicopahologic significance. *World J Gastroenterol* 1998; **4**: 158-161

13 **Chabot V,** de Keyzer Y, Gebhard S, Uske A, Bischof-Delaloye A, Rey F, Dusmet M, Gomez F. Ectopic ACTH Cushing's syndrome: V3 vasopressin receptor but not CRH receptor gene Expression in a pulmonary carcinoid tumor. *Horm Res* 1998; **50**: 226-231

14 **Mao C,** el Attar A, Domenico DR, Kim K, Howard JM. Carcinoid tumors of the pancreas. Status report based on two cases and review of the world's literature. *Int J Pancreatol* 1998; **23**: 153-164

15 **Duchesne G,** Cassoni A, Pera M. Radiosensitivity related to neuroendocrine and endodermmal differentiation in lung carcinoma lines. *Radiother Oncol* 1988; **13**: 153-161

16 **Tezel E**, Nagasaka T, Nomoto S, Sugimoto H, Nakao A. Neuroendocrine-like differentiation in patients with pancreatic carcinoma. *Cancer* 2000; **89**: 2230-2236

17 **Yao G**, Zhou J, Zhao Z. Studies on the DNA content of breast carcinoma cells with neuroendocrine differentiation. *Chin Med J* 2002; **115**: 296-298

18 **Maluf HM**, Zukerberg LR, Dickersin GR, Koerner FC. Spindle-cell argyrophilic mucin-producing carcinoma of the breast. Histological, ultrastructural, and immunohistochemical studies of two cases. *Am J Surg Pathol* 1991; **15**: 677-686

19 **Scopsi L,** Andreola S, Pilotti S, Testori A, Baldini MT, Leoni F, Lombardi L, Hutton JC, Shimizu F, Rosa P. Argyrophilia and granin (chromogranin / secretogranin) expression in Female breast carcinomas. Their relationship to survival and other disease parameters. *Am J Surg Pathol* 1992; **16**: 561-576

20 **Grabowski P**, Schindler I, Anagnostopoulos I, Foss HD, Riecken EO, Mansmann U, Stein H, Berger G, Buhr HJ, Scherubl H. Neuroendocrine differentiation is a relevant progostic factor in stage III-IV colorectal cancer. *Eur J Gastroenterol Hepatol* 2001; **13**: 405-411

21 **Sapino A,** Papotti M, Righi L, Cassoni P, Chiusa L, Bussolati G. Clinical significance of neuroendocrine carcinoma of the breast. *Ann Oncol* 2001; **12**(Suppl 2): S115-117

22 **Matsui T,** Kataoka M, Sugita Y, Itoh T, Ichihara T, Horisawa M, Koide A, Ichihara S, Nakao A. A case of small cell carcinoma of the stomach. *Hepatogastroenterology* 1997; **44**: 156-160

23 **Yang GC,** Rotterdam H. Mixed (composite) glandular-endocrine cell carcinoma of the stomach. Report of a case and review of liteerature. *Am J Surg Pathol* 1991; **15**: 592-598

24 **Upp JR Jr**, Olson D, Poston GJ, Alexander RW, Townsend CM Jr, Thompson JC. Inhibition of growth of two human pancreatic adenocarcinomas in vivo by somatostatin analog SMS 201-995. *Am J Surg* 1988; **155**: 29-35

25 **Anderson JV**, Bloom SR. Neuroendocrine tumours of the gut: long-term therapy with the somatostatin analogue SMS 201-995. *Scand J Gastroenterol Suppl* 1986; **119**: 115-128

26 **Oda Y,** Tanaka Y, Naruse T, Sasanabe R, Tsubamoto M, Funahashi H. Expression of somatostatin receptor and effects of somatostatin analog on pancreatic endocrine tumors. *Surg Today* 2002; **32**: 690-694

27 **O'Byrne KJ,** Carney DN. Somatostatin and the lung. *Lung Can-*

cer 1993; **10**: 151-172

28 **Taylor JE,** Moreau JP, Baptiste L, Moody TW. Octapeptide analogues of somatostatin inhibit the clonal growth and vasoactive intestinal peptide-stimulated cyclic AMP formation in human small cell lung cancer cells. *Peptides* 1991; **12**: 839-843

29 **Taylor JE,** Bogden AE, Moreau JP, Coy DH. *In vitro* and *in vivo* inhibition of human small cell lung carcinoma (NCI-H69) growth by a somatostatin analogue. *Biochem Biophys Res Commun* 1988; **153**: 81-86

30 **Diaz-Sanchez CL**, Molano Romero RA, Martinez Gonzalez M, Marquez Rivera ML, Halabe-Cherem J. Gastric neuroendocrine tumor. *Rev Gastroenterol Mex* 1998; **63**: 97-100

31 **Tomassetti P**, Migliori M, Lalli S, Campana D, Tomassetti V, Corinaldesi R. Epidemiology, clinical features and diagnosis of gastroenteropancreatic endocrine tumours. *Ann Oncol* 2001; **12** (Suppl 2): S95-99

32 **Eriksson B**, Oberg K, Stridsberg M. Tumor markers in neurodocrine tumors. *Digestion* 2000; **621**: 33-38

Edited by Xu XQ

P.O.Box 2345, Beijing 100023,China
Fax: +86-10-85381893
E-mail: wjg@wjgnet.com www.wjgnet.com

World J Gastroenterol 2003;9(4):862-864
World Journal of Gastroenterology
 ISSN 1007-9327

• CLINICAL RESEARCH •

Primary jejunoileal neoplasmas: a review of 60 cases

Yun-Sheng Yang, Qi-Yang Huang, Wei-Feng Wang, Gang Sun, Li-Hua Peng

Yun-Sheng Yang, Qi-Yang Huang, Wei-Feng Wang, Gang Sun, Li-Hua Peng, Department of Gastroenterology, China PLA General Hospital, Beijing 100853, China
Correspondence to: Yun-Sheng Yang M.D.&Ph.D, Department of Gastroenterology, China PLA General Hospital, Beijing 100853, China. yangys@163bj.com
Telephone: +86-10-66939747 **Fax:** +86-10-68154357
Received: 2002-07-12 **Accepted:** 2002-08-13

Abstract

AIM: Primary neoplasmas of the jejunum and ileum are infrequent and lack specific manifestations and inaccessibility of conventional endoscopy, so the diagnosis of these tumors are usually delayed. So far the data of primary jejunoileal neoplasmas is still scarce, especially in Chinese medical literature in English. There may be some differences among the Chinese and the westerners in jejunoileal neoplasmas.

METHODS: A retrospective analysis was made on clinical findings and pathological types.

RESULTS: Of the 60 patients with jejunal or ileal neoplasmas, the most frequent symptom was abdominal pain (57 %), followed by tarry stool (43 %) and hematochezia (10 %). Abdominal mass (40 %) was the most common finding on physical examination, followed by anemia and weight loss (35 %). 67 % of the jejunoileal neoplasms were located in the jejunum. Among the malignant neoplasmas (68 %), malignant stroma (47 %) was most common, while the benign stromoma (20 %) was the most common benign neoplasmas. Preoperatively, 40 patients (67 %) were diagnosed as small bowel neoplasmas, of which 34 were found by enteroclysis. Abdominal mass was shown by CT in 18 cases and by ultrasonography in 13. The mean duration of symptoms before diagnosis was 7 months. In 41 patients with malignant tumors, the duration of symptoms before diagnosis exceeded 12 months in 21 cases, lymphatic or distant metastases were found in 26 (63 %)cases during operation. An emergency laparotomy was performed in 4 patients (7 %) owing to intestinal obstruction or perforation.

CONCLUSION: Primary jejunoileal neoplasmas in Chinese present some difference from Westerners on clinical features and histopathologic types. Enteroclysis remains the major relevant diagnostic procedure in this study, the misdiagnotic rate is high preoperatively due to failure of detection by conventional imaging procedures such as CT and inaccessibility of routine endoscopy. For the suspected patients, combined application of aforementioned procedures may facilitate early diagnosis. The wireless capsule endoscopy may improve the diagnostic rate of jejunoileal neoplasmas in the future.

Yang YS, Huang QY, Wang WF, Sun G, Peng LH. Primary jejunoileal neoplasmas: a review of 60 cases. *World J Gastroenterol* 2003; 9(4): 862-864
http://www.wjgnet.com/1007-9327/9/862.htm

INTRODUCTION

Primary neoplasmas of jejunum and ileum, benign or malignant, are infrequent. Clinical manifestations of jejunoileal neoplasmas are nonspecific and the neoplasma-related symptoms occur late, moreover, such neoplasms are beyond the scope of conventional gastroscopy or colonoscopy. The rarity, nonspecific and inaccessibility make them liable to be overlooked, with delayed or erroneous diagnosis[1], and are responsible for high mortality rates. So far the data on small bowel cancers are scarce[2]. To our knowledge, there may be some differences between the Chinese and the Westerner in jejunoileal neoplasmas. Herein we reported a series of consecutive cases of primary jejunal and ileal neoplasmas in our hospital over the past 8 years, and analyzed their clinical manifestations, pathologic types and diagnostic process.

MATERIALS AND METHODS

Cases of primary jejunal and ileal neoplasmas from January 1993 to August 2001 were retrieved through the inpatient computer registry system of PLA General Hospital, Beijing. The medical records were reviewed by the authors. Cases of duodenal and metastatic small bowel tumors were excluded. A total of 60 cases of primary jejunal and ileal neoplasmas were collected. All cases underwent surgery and were confirmed by histopathology.

RESULTS

Demographic features

There were 42 males (70 %) and 18 females (30 %) with an average age of 48 years (16-77 years). The majority (51 %) of patients were over 50 years of age.

Clinical manifestations

Symptoms, signs and complications were listed in the following Table 1. Abdominal pain and tarry stool were the most common symptoms in both benign and malignant jejunoileal tumors. Abdominal mass and anemia were common findings on physical examination in both benign and malignant neoplasmas, while the weight loss was frequent in malignant ones. Complications at presentation such as intestinal obstruction and perforation were more common in malignant tumors.

Table 1 Clinical manifestations of 60 cases of jejunoileal tumors

	Benign (*n*)	Malignant (*n*)	Total
Symptoms			
Abdominal pain	8	26	34 (57%)
Tarry stool	9	17	26 (43%)
Hematochezia	2	4	6 (10%)
Signs			
Abdominal mass	9	15	24 (40%)
Anemia	6	15	21 (35%)
Weight loss	1	20	21 (35%)
Complications			
Intestinal obstruction	2	5	7 (12%)
Intestinal perforation	0	1	1

Histopathology and sites of distribution

Histopathology and sites of distribution of jejunoileal neoplasmas were summarized in Table 2. Of the 60 cases, 40 (67 %) were located in the jejunum, and 20 (33 %) in the ileum. Malignant tumors (*n*=41, 68 %) was nearly twice that of the benign ones (*n*=19, 32 %). Benign and malignant stromoma were predominant histological entities.

Table 2 Histopathology and distribution sites of 60 cases of jejunal and ileal tumors

Tumor types	Jejunum	Ileum	Total
Benign	14 (23.3%)	5 (8.3%)	19 (≈32%)
Stromoma	8	4	12 (20%)
Adenoma	2	0	2 (3.3%)
Angioleiomyoma	2	0	2 (3.3%)
Lipoma	0	1	1 (1.7%)
Lymphangioma	1	0	1 (1.7%)
Neurofibroma	1	0	1 (1.7%)
Malignant	26 (43%)	15 (25%)	41 (≈68%)
Malignant stromoma	17	11	28 (46.7%)
Adenocarcinoma	7	1	8 (13.3%)
Non-Hodgkin's lymphoma	0	2	2 (3.3%)
Carcinoid	0	1	1 (1.7%)
Neuroendocrine carcinoma	1		1 (1.7%)
Malignant histiocytosis	1	0	1 (1.7%)
Total	40(67%)	20(33%)	60 (100%)

Diagnostic procedures

Before operation, small intestinal diseases were suspected in 73 % (44/60) on admission. There were 40/60 patients (67 %) correctly diagnosed preoperatively. Among the 40 patients, 34 jejunoileal neoplasmas were correctly diagnosed by enteroclysis. Other preoperative diagnoses were made by angiography, colonoscopy, CT and Ultrasonography. Angiography was performed in 5 cases, of which 4 (80 %) of them were discovered preoperatively. One case of lymphoma of terminal ileum was detected by colonoscopy, and one jejunal tumor was diagnosed by CT scan only.

Of the 60 patients, 56 underwent CT scan, abdominal masses or intestinal wall thickening were visualized in 18 (32 %) cases, but two of them were misinterpreted as ovarian cancer, one as renal lipoma and one as intestinal tuberculosis. Ultrasonography was carried out in all 60 patients, and solid abdominal masses were demonstrated in 13 (22 %).

20 patients remained obscure diagnosis preoperatively, final diagnoses were disclosed during laparotomy. The mean duration of symptoms before diagnosis was 7 months. In 41 patients with malignant neoplasms, the duration of symptoms exceeded 12 months in 21 (52 %) cases.

Surgical findings

Of the 60 patients, three cases of intestinal obstruction and one case of intestinal perforation underwent emergency laparotomy (7 %). The rest underwent selective laparotomy (93%).

Of the 41 of malignant tumors, the masses within the intestinal walls were found in 15 without metastases; local lymph node metastasis in 12, distant and mesenteric lymph node metastasis in 9, liver metastases in 4 and urinary bladder metastasis in 1, the total rate of metastases was 63 % among the malignant tumors. lymph node metastasis was commonest in 51 % of malignant tumors.

DISCUSSION

Primary neoplasmas of jejunum and ileum are only <2 % of the gastrointestinal malignant tumors, the incidence was 1.4 per 100 000 compared to 35.7/100 000 for colorectal and 92.9/100 000 for breast cancer[2,3]. The jejunoileal neoplasmas are preponderant in male with a ratio of 2:1 between male and female[3,4]. Our result showed 70 % in male and 30 % in female, similar to that reported in the literature. The patients with jejunoileal tumors were usually eld people with an average age of over 50 years[1-5], in this article, 51 % were over 50 years.

The small bowel neoplasmas located in the jejunum usually more frequent than that in ileal. In our results, the jejunal neoplasmas were twice as many as the ileal ones, higher than that reported in the literature[4]; but the ratio of malignant and benign in small bowel tumors was concordant with those in the literature[7]. As to the histopathologic types, the commonest pathologies of jejunoileal tumors were lymphoma, adenocarcinoma and carcinoids, followed by leiomyosarcomas, neuroendocrine tumors and other entities in Western countries[1-7], which were significantly different from those in our study, in which the benign and malignant stromoma was predominant. In addition, some very rare tumors were seen in our investigation including angioleiomyoma, lymphangioma and malignant histiocytosis etc. The above results indicated that there were some differences between the Chinese and the Westerners in the pathologic types of jejunoileal tumors.

The clinical manifestations of jejunoileal neoplasmas were nonspecific and symptoms usually occurred late. The abdominal pain, gastrointestinal bleeding and weight loss were most frequent complaints in our patients and as well as in the other reports[4-6], followed by nausea and/or vomiting[4,6]. Abdominal mass and anemia were the most common physical findings in our study and related literatures[4,6], followed by abdominal distension, muscle guarding and rigidity[4]. The diagnosis of small bowel neoplasmas was often made when symptoms presented several months late, the median duration of symptoms before diagnosis was 7 months in our study, 3.6 and 6 months in others[4,6]. The metastasises of jejunoileal neoplasms were common as they were usually identified late, the metastatic rate of leiomyosarcoma ranged from 24 % to 50 %, with the liver being most frequently involved[5], distant metastasis occurred in 27 %[2]. In our study, metastasis was found in 63 % of the malignant tumors, lymph node metastasis was the commonest (51 %) similar to that reported in the literature[4], followed by liver metastases in 10 % of cases.

The preoperative diagnosis of primary jejunoileal neoplasmas remains difficult for clinicians owing to the nonspecific symptomatic presentation. The enteroclysis, enteroscopy and imaging methods have been used generally for small bowel diseases. Radiographic study of small bowel malignant tumors showed abnormality in 87 %[4]. In our study, 34 cases of jejunoileal neoplasmas were diagnosed by enteroclysis. Both ultrasonography (US) and CT are also useful for detection of small bowel tumours. CT was found to detect leiomyoma and leiomyosarcoma most successfully and had the additional advantage of locating metastatic lesions[5]. Moreover, CT offered the possibility of a preoperative staging by evaluating tumour extension through the bowel wall, involvement of lymph node and possible metastases[8]. Other preoperative diagnoses were made through angiography, colonoscopy, CT and Ultrasonography. Angiography was performed in 5 cases, of which 4 (80 %) of small intestinal neoplasmas were discovered preoperatively. A case of lymphoma of terminal ileum was detected by colonoscopy, and one case of jejunum tumor was diagnosed by CT scan only.

Of the 60 patients, 56 underwent CT scan, abdominal masses or intestinal wall thickening were visualized in 18 (32 %), but two cases were misinterpreted as ovarian cancer, one as renal lipoma and one as intestinal tuberculosis. Ultrasonography was

carried out in all 60 patients, and the solid abdominal masses were demonstrated in 13 cases (22 %).

Final diagnoses were disclosed during laparotomy for those 20 patients whose diagnoses remained obscure preoperatively. The mean duration of symptoms before diagnosis was 7 months. In 41 patients with malignant neoplasms, the duration of symptoms exceeded 12 months in 21 cases (52 %).

Jejunum and ileum are difficult to visualize directly. Colonoscopy with retrograde ileoscopy is useful in the diagnosis of neoplasm of the terminal ileum[4]. Enteroscopy is capable of observing most of the small intestine[5], but it is hard for the patients to endure. Small bowel enteroclysis is still a good choice for the detection of jejunoileal neoplasms[6], albeit a third of cases of this series may be missed in the examination. Angiography is carried out in only a small proportion of patients, though it is relatively sensitive, especially for those lesions with abundant vascularity, the expense and invasive property limit its application[7]. Spiral CT is thought to be comparatively accurate in detecting small bowel tumors[8], however its diagnostic accuracy is poor in this series with possible misinterpretations, probably due to lack of experience of some radiologists in this field. Despite the interference by intestinal gas, ultrasonography proves to be helpful in a fifth of cases to demonstrate thickened intestinal wall or unsuspected mass. Wireless capsule endoscopy is optimal for those patients without intestinal obstruction when it is available. Laparotomy is justified in those suspected cases as a last resort.

Thanks to a variety of investigations, the correct diagnosis is reached in the majority of patients before operation, though the delay between the onset of symptoms and the final diagnosis is often significant. As a result, more than 60 % of patients with malignant tumors has advanced beyond the early stage of neoplasm. Recognition of this entity, with high index of suspicion, rational application of aforementioned investigation procedures, the advent of capsule endoscopy and justified early laparotomy, may facilitate the diagnosis and improve the outcome.

REFERENCES

1 **Baillie CT**, Williams A. Small bowel tumors: a diagnostic challenge. *J R Coll Surg Edinb* 1994; **39**: 8-12

2 **DiSario JA**, Burt RW, Vargas H, McWhorter WP. Small bowel cancer: epidemiological and clinical characteristics from a population-based registry. *Am J Gastroenterol* 1994; **89**: 699-701

3 **North JH**, Pack MS. Malignant tumors of the small intestine: a review of 144 cases. *Am Surg* 2000; **66**: 46-51

4 **Garcia Marcilla JA**, Sanchez Bueno F, Aguilar J, Parrilla Paricio P. Primary small bowel malignant tumors. *Eur J Surg Oncol* 1994; **20**: 630-634

5 **Blanchard DK**, Budde JM, Hatch GF 3rd, Wertheimer-Hatch L, Hatch KF, Davis GB, Foster RS Jr, Skandalakis JE. Tumors of the small intestine. *World J Surg* 2000; **24**: 421-429

6 **O'Boyle CJ**, Kerin MJ, Feeley K, Given HF. Primary small intestinal tumours: increased incidence of lymphoma and improved survival. *Ann R Coll Surg Engl* 1998; **80**: 332-334

7 **Brucher BL**, Roder JD, Fink U, Stein HJ, Busch R, Siewert JR. Prognostic factors in resected primary small bowel tumors. *Dig Surg* 1998; **15**: 42-51

8 **Maccioni F**, Rossi P, Gourtsoyiannis N, Bezzi M, Di Nardo R, Broglia L. US and CT findings of small bowel neoplasms. *Eur Radiol* 1997; **7**: 1398-1409

Edited by Wu XN

P.O.Box 2345, Beijing 100023,China
Fax: +86-10-85381893
E-mail: wjg@wjgnet.com www.wjgnet.com

World J Gastroenterol 2003;9(4):865-867
World Journal of Gastroenterology
 ISSN 1007-9327

• CLINICAL RESEARCH •

Prospective study of scoring system in selective intraoperative cholangiography during laparoscopic cholecystectomy

Xiao-Dong Sun, Xiao-Yan Cai, Jun-Da Li, Xiu-Jun Cai, Yi-Ping Mu, Jin-Min Wu

Xiao-Dong Sun, Xiao-Yan Cai, Jun-Da Li, Xiu-Jun Cai, Yi-Ping Mu, Jin-Min Wu, Department of General Surgery, The Affiliated Sir Run Run Shaw Hospital, Zhejiang University Medical College, Hangzhou 310016, Zhejiang Province, China
Correspondence to: Dr Xiao-Dong Sun, Department of General Surgery, The Affiliated Sir Run Run Shaw Hospital, Zhejiang University Medical College, Hangzhou 310016, Zhejiang Province, China. s.xiaodong@sohu.com
Telephone: +86-571-86090073 **Fax:** +86-571-86044817
Received: 2002-07-26 **Accepted:** 2002-08-23

Abstract

AIM: To evaluate of scoring system in predicting choledocholithiasis in selective intraoperative cholangiography (IOC) during laparoscopic cholecystectomy (LC).

METHODS: The scoring system of predicting choledocholithiasis was developed during the retrospective study in 264 cases, and was tested in 184 to evaluate its predictive value in choledocholithiasis.

RESULTS: The scoring system was developed in a retrospective study of 264 cases, the statistical analyses showed the predictive factors included sex, transaminase levels, alkaline phosphatase level, bilirubin level, and common bile duct diameter on ultrasonography. The scoring system was used in 184 cases prospectively, of which, 3 of 162 (1.9 %) cases scoring <3 had choledocholithiasis, 17 of 22 (77.3 %) cases scores≥3 had choledocholithiasis. A case of scores≥3 or more prospectively should be considered highly intraoperative cholangiography during laparoscopic cholecystectomy.

CONCLUSION: The scoring system can predict choledocholithiasis and is helpful in selection patietns for intraoperative cholangiography.

Sun XD, Cai XY, Li JD, Cai XJ, Mu YP, Wu JM. Prospective study of scoring system in selective intraoperative cholangiography during laparoscopic cholecystectomy. *World J Gastroenterol* 2003; 9(4): 865-867
http://www.wjgnet.com/1007-9327/9/865.htm

INTRODUCTION

Laparoscopic cholecystectomy (LC) has been extensively accepted since Mouret first successfully finished the procedure in 1987[1]. Whether intraoperative cholangiogram (IOC) during LC should be applied routinely is still controversial. Thus, we develop a scoring system to predict choledocholithiasis and recommend selection of IOC during LC.

MATERIALS AND METHODS

Retrospective study

Two hundred sixty-four cases of LC from January 1996 to June 1999 were analyzed. Before operation, choledocholithiasis in cases with cholecystolithiasis was not discovered by ultrasonography (US). During operation, 54 cases of cholecystolithiasis with choledocholithiasis and 210 cases of cholecystolithiasis without choledocholithiasis were confirmed by IOC. Sex, age, history of pancreatitis, jaundice, transaminase levels, alkaline phosphatase level, bilirubin level and diameter of common bile duct (CBD) on ultrasonography were evaluated as predictors of choledocholithiasis, and scoring system of selective IOC was designed.

Prospective study

From January 2000 to June 2001, the scoring system was carried out prospectively in 184 patients undergoing LC. Following evaluation, LC and IOC were performed, then the correlation of scoring results with choledocholithiasis was studied.

RESULTS

No choledocholithiasis in 264 patients undergoing LC was discovered by ultrasonography prior to operation. During LC, IOC found choledocholithiasis in 54 patients (Table 1).

Table 1 Factors predicting choledocholithiasis in 264 patients

Factor	No of cases with choledocholithiasis (54 cases)	No of cases without choledocholithiasis (210 cases)	Percentage (%)	*P*
Sex				
Male	27	40	40	<0.05
Female	27	170	14	
Age				
<55ys	34	112	23	
⩾55ys	20	98	17	<0.05
Pancreatitis				
Present	15	30	33	>0.05
Absent	39	180	18	
Jaundice				
Present	10	22	31	>0.05
Absent	44	188	19	
Transaminase				
Normal	31	201	13	
Elevated	23	9	72	<0.05
Alkaline phosphatase				
Normal	36	189	16	
Elevated	18	21	46	<0.05
Bilirubin				
Normal	31	205	13	
Elevated	23	5	82	<0.05
CBD diameter on US				
⩽8 mm	33	204	14	
>8 mm	21	6	78	<0.05

Multivariate analysis found that independent predictors of choledocholithiasis included sex, serum level of transaminase, alkaline phosphatase, and bilirubin, and CBD diameter on US. Therefore, the scoring system in regression analysis was established (Table 2).

Table 2 Scoring system of predicting choledocholithiasis

Factor	Criteria	Score
Sex	Female	0
	Male	1
Transaminase	Normal	0
	Elevated	2
Alkaline phosphatase	Normal	0
	Elevated	2
Bilirubin	Normal	0
	Elevated	3
CBD diameter on US	≤8 mm	0
	>8 mm	3
Total		11

The scoring system was used in 184 patients undergoing LC before operation. During LC, all of the patients were performed IOC(Table 3).

Table 3 Results of scores in 184 patients before LC

	Score											
	0	1	2	3	4	5	6	7	8	9	10	11
No of patients	107	49	6	3	1	2	1	3	2	2	2	6

During LC, choledocholithiasis was found in 20 patients by IOC, the relationship between scores and choledocholithiasis was showed in Table 4.

Table 4 Relationship between scoring results and choledocholithiasis in 184 patients undergoing LC

Score	No of patients with choledocholithiasis	No of patients without choledocholithiasis	Percentage
<3	3	159	1.9
≥3[a]	17	5	77.3

[a]$P<0.05$ *vs* score of less than 3.

A significant difference in predicting value scoring 3 or more and that of less than 3 was found according to the χ^2 test. Thus, evaluation of LC patient with scoring system preoperatively would be helpful in predicting choledocholithiasis. If patient were scored more than 3, IOC should be performed during LC.

DISCUSSION

With the popularization of laparoscope, the age of microtraumatic surgery has come and great changes have occurred in surgical operation and surgical ideology[2]. Gallstone is one of the common primary diseases of biliary tract. LC has become a conventional method to treat patient with symptomatic gallstones. IOC is one of the accurate and safe procedure used in LC, is helpful in finding abnormality of pancreaticobiliary tract[3], avoiding common bile duct injury[4-8], and detecting choledocholithiasis[9-11], thus, some recommended a routine IOC during LC[4,5,12]. Because majority of gallstones patients do not have choledocholithiasis, IOC will increase the patient' s cost and exposure to X-ray, however, some researches found that the value of IOC were limited[13-15], it is unnecessary to perform a routine IOC during LC. However, there are still 10-15 % of cholecystolithiasis patients who have choledocholithiasis[16]. Preoperative ERCP and IOC may be helpful to find choledocholithiasis[17-20].

Mahmud suggested that, some gallstones might slip into the cystic duct or the common bile duct during LC, and IOC is valuable of determing the choledocholithiasis, ERCP and EST were regarded as effective methods detecting choledocholithiasis[21]. Edye retrospectively analyzed 31 patients with choledocholithiasis treated by EST, and ERCP showed completely cleared common bile duct, but IOC during subsequent LC revealed common duct residual stones in 8 of these 31 patients. The author suggested that even after presumed endoscopic clearance of the bile duct stone, many patients (26 %) still harbored stones in common bile duct at the time of cholecystectomy. Therefore IOC during LC was recommended even after successful ERCP[22]. Some studies revealed that preoperative ultrasound is neither sensitive nor specific for detecting common bile duct dilatation or the presence of residual stones[23]. Some studies assessed the use of endoscopic retrograde cholangiopancreatography (ERCP), IOC, intraoperative laparoscopic ultrasonography (IOUS)[24-27]. Bege manifested that combined endoscopic and laparoscopic management of cholecystolithiasis and choledocholithiasis were a viable option and were optimized by endoscopic ultraosonography[28]. The combined procedures of endoscopic sphincterotomy and LC included one-stage treatment of cholelithiasis and choledocholithiasis, elimination of potential return to the operating room when postoperative ERCP were unsuccessful[29,30]. Ichihara concluded that intraoperative real time cholangiograms were helpful in detecting bile duct injuries or anomalies, and unsuspected bile duct stones[31].

We recommend that IOC during LC should be performed selectively. Digital C-arm can provide real-time imaging and obtain a clear cholangiogram easily. The protocol of selective IOC is still debatable. Snow analyzed the results of 2034 LC, and found that there were no false negative, bile duct injuries, or other complications attributable to routine IOC or selective IOC, and suggested that selective IOC were an effective method of verifying suspected choledocholithiasis and were safer and less expensive than routine IOC[32]. Abboud performed a meta-analysis of published data to evaluate preoperative indicators of choledocholithiasis, which included cholangitis, jaundice, dilated CBD on ultrasound, hyperbilirubinemia, elevated levels of alkaline phosphatase, pancreatitis, cholecystitis, and hyperamylasemia. The results showed that these predictors could be applied as guidelines for whether to investigate for duct stones before cholecystectomy[33]. Kim also suggested selective IOC, and the risk levels of the presence of choledocholithiasis were determined by the independent predictor including preoperative clinical, biochemical and sonographic variables[34]. However, Koo reviewed 420 cases of elective LC, IOC was routinely performed and acted as the reference standard for the presence of choledocholithiasis, and found that there were no predictive tests that could sufficiently increase an observer' s probability estimate of the presence or absence of choledocholithiasis to allow for "selective" IOC decisions[35].

By logistic regression analysis, our studies showed that sex, transaminase levels, alkaline phosphatase level, bilirubin level and common bile duct diameter on ultrasonography were independent predictors of choledocholithiasis. A scoring system was therefore designed with a total score of 11. Our prospective studies also showed that patients scoring more than 3 were at significant risk to have choledocholithiasis, and IOC should be performed during LC.

REFERENCES

1 **Huang ZQ.** Present status of biliary surgery in china. *World J Gastroenterol* 1998; **4 (Suppl 2):** 8-9
2 **Shi JS,** Ma JY, Zhu LH, Pan BR, Wang ZR, Ma LS. Studies on gallstone in China. *World J Gasteroenterol* 2001; **7:** 593-596
3 **Fujisaki S,** Tomita R, Koshinaga T, Fukuzawa M. Analysis of pancreaticobiliary ductal union based on intraoperative cholangiography in patients undergoing laparoscopic cholecystectomy. *Scand J Gastroenterol* 2002; **37:** 956-959
4 **Ludwig K,** Bernhardt J, Steffen H, Lorenz D. Contribution of intraoperative cholangiography to incidence and outcome of common bile duct injuries during laparoscopic cholecystectomy. *Surg Endosc* 2002; **16:** 1098-1104
5 **Ludwig K,** Bernhardt J, Lorenz D. Value and consequences of routine intraoperative cholangiography during cholecystectomy. *Surg Laparosc Endosc Percutan Tech* 2002; **12:** 154-159
6 **Podnos YD,** Gelfand DV, Dulkanchainun TS, Wilson SE, Cao S, Ji P, Ortiz JA, Imagawa DK. Is intraoperative cholangiography during laparoscopic cholecystectomy cost effective? *Am J Surg* 2001; **182:** 663-669
7 **Cai XJ,** Wang XF, Hong DF, Li LB, Li JD, Bryan F. The application of intraoperative cholangiography in laparoscopic cholecystectomy. *Zhonghua Waike Zazhi* 1999; **37:** 427-428
8 **Flum DR,** Koepsell T, Heagerty P, Sinanan M, Dellinger EP. Common bile duct injury during laparoscopic cholecystectomy and the use of intraoperative cholangiography: adverse outcome or preventable error? *Arch Surg* 2001; **136:** 1287-1292
9 **Cemachovic I,** Letard JC, Begin GF, Rousseau D, Nivet JM. Intraoperative endoscopic sphincterotomy is a reasonable option for complete single-stage minimally invasive biliary stones treatment: short-term experience with 57 patients. *Endoscopy* 2000; **32:** 956-962
10 **Mitchell SA,** Jacyna MR, Chadwick S. Choledocholithiasis: a controversy revisited. *Br J Surg* 1993; **80:** 759-760
11 **Kama NA,** Atli M, Doganay M, Kologlu M, Reis E, Dolapci M. Practical recommendations for the prediction and management of choledocholithiasis in patients with gallstones. *Surg Endosc* 2001; **15:** 942-945
12 **Waldhausen JH,** Graham DD, Tapper D. Routine intraoperative cholangiography during laparoscopic cholecystectomy minimizes unnecessary endoscopic retrograde cholangiopancreatography in children. *J Pediatr Surg* 2001; **36:** 881-884
13 **Li LB,** Cai XJ, Li JD, Mu YP, Wang YD, Yuan XM, Wang XF, Bryner B, Finley RK Jr. Will intraoperative cholangiography prevent biliary duct injury in laparoscopic cholecystectomy? *World J Gastroenterol* 2000; **6(Suppl 3):** 21
14 **Falcone RA Jr,** Fegelman EJ, Nussbaum MS, Brown DL, Bebbe TM, Merhar GL, Johannigman JA, Luchette FA, Davis K Jr, Hurst JM. A prospective comparison of laparoscopic ultrasound vs intraoperative cholangiogram during laparoscopic cholecystectomy. *Surg Endosc* 1999; **13:** 784-788
15 **Arul GS,** Rooney PS, Gregson R, Steele RJ. The standard of laparoscopic intraoperative cholangiography: a quality control study. *Endoscopy* 1999; **31:** 248-252
16 **Hong DF,** Gao M, Bryner U, Cai XJ, Mou YP. Intraoperative endoscopic sphincterotomy for choledocholithiasis during laparoscopic cholecystectomy. *World J Gastroenterol* 2000; **6:** 448-450
17 **Silverstein JC,** Wavak E, Millikan KW. A prospective experience with selective cholangiography. *Am Surg* 1998; **64:** 654-658
18 **Stuart SA,** Simpson TI, Alvord LA, Williams MD. Routine intraoperative laparoscopic cholangiography. *Am J Surg* 1998; **176:** 632-637
19 **Meyer C,** Le JV, Rohr S, Duclos B, Reimund JM, Baumann R. Management of choledocholithiasis in a single operation combining laparoscopic cholecystectomy and peroperative endoscopic sphincterotomy. *J Hepatobiliary Pancreat Surg* 2002; **9:** 196-200
20 **Halpin VJ,** Dunnegan D, Soper NJ. Laparoscopic intracorporeal ultrasound versus fluoroscopic intraoperative cholangiography: after the learning curve. *Surg Endosc* 2002; **16:** 336-341
21 **Mahmud S,** Hamza Y, Nassar AH. The significance of cystic duct stones encountered during laparoscopic cholecystectomy. *Surg Endosc* 2001; **15:** 460-462
22 **Edye M,** Dalvi A, Canin-Endres J, Baskin-Bey E, Salky B. Intraoperative cholangiography is still indicated after preoperative endoscopic cholangiography for gallstone disease. *Surg Endosc* 2002; **16:** 799-802
23 **Lichtenbaum RA,** Mcmullen HF, Newman RM. Preoperative abdominal ultrasound may be misleading in risk stratification for presence of common bile duct abnormalities. *Surg Endosc* 2000; **14:** 254-257
24 **Barwood NT,** Valinsky LJ, Hobbs MS, Fletcher DR, Knuiman MW, Ridout SC. Changing methods of imaging the common bile duct in the laparoscopic cholecystectomy era in Western Australia: implications for surgical practice. *Ann Surg* 2002; **235:** 41-50
25 **Biffl WL,** Moore EE, Offner PJ, Franciose RJ, Burch JM. Routine intraoperative laparoscopic ultrasonography with selective cholangiography reduces bile duct complications during laparoscopic cholecystectomy. *J Am Coll Surg* 2001; **193:** 272-280
26 **Liu TH,** Consorti ET, Kawashima A, Tamm EP, Kwong KL, Gill BS, Sellin JH, Peden EK, Mercer DW. Patient evaluation and management with selective use of magnetic resonance cholangiography and endoscopic retrograde cholangiopancreatography before laparoscopic cholecystectomy. *Ann Surg* 2001; **234:** 33-40
27 **Luo XZ,** Wang LS, Lin SZ. An analysis of the relationship between ultrasonography and laparoscopic cholecystectomy. *World J Gastroenterol* 1998; **4(Suppl 2):** 83
28 **Berdah SV,** Orsoni P, Bege T, Barthet M, Grimaud JC, Picaud R. Follow-up of selective endoscopic ultrasonography and / or endoscopic retrograde cholangiography prior to laparoscopic cholecystectomy: a prospective study of 300 patients. *Endoscopy* 2001; **33:** 216-220
29 **Kalimi R,** Cosgrove JM, Marini C, Stark B, Gecelter GR. Combined intraoperative laparoscopic cholecystectomy and endoscopic retrograde cholangiopancreatography: lessons from 29 cases. *Surg Endosc* 2000; **14:** 232-234
30 **Park AE,** Mastrangelo MJ Jr. Endoscopic retrograde cholangiopancreatography in the management of choledocholithiasis. *Surg Endosc* 2000; **14:** 219-226
31 **Ichihara T,** Suzuki N, Horisawa M, Kataoka M, Uchida Y, Sekiya M, Matsui T, Chen H, Sakamoto J, Nakao A, Koide A. The importance of the real-time fluoroscopic intraoperative direct cholangiogram in the laparoscopic cholecystectomy using a new strument. *Hepatogastroenterology* 1996; **43:** 1296-1304
32 **Snow LL,** Weinstein LS, Hannon JK, Lane DR. Evaluation of operative cholangiography in 2043 patients undergoing laparoscopic cholecystectomy: a case for the selective operative cholangiogram. *Surg Endosc* 2001; **15:** 14-20
33 **Abboud PA,** Malet PF, Berlin JA, Staroscik R, Cabana MD, Clarke JR, Shea JA, Schwartz JS, Williams SV. Predictors of choledocholithiasis prior to cholecystectomy: a meta-analysis. *Gastrointest Endosc* 1996; **44:** 450-455
34 **Kim KH,** Kim W, Lee HI, Sung CK. Prediction of choledocholithiasis: its validation in laparoscopic cholecystectomy. *Hepatogastroenterology* 1997; **44:** 1574-1579
35 **Koo KP,** Traverso LW. Do preoperative indicators predict the presence of choledocholithiasis during laparoscopic cholecystectomy? *Am J Surg* 1996; **171:** 495-499

Edited by Ren SY

P.O.Box 2345, Beijing 100023,China
Fax: +86-10-85381893
E-mail: wjg@wjgnet.com www.wjgnet.com

World J Gastroenterol 2003;9(4):868-870
World Journal of Gastroenterology
 ISSN 1007-9327

• CLINICAL RESEARCH •

Use of endoscopic naso-pancreatic drainage in the treatment of severe acute pancreatitis

Zhu-Fu Quan, Zhi-Ming Wang, Wei-Qin Li, Jie-Shou Li

Zhu-Fu Quan, Zhi-Ming Wang, Wei-Qin Li, Jie-Shou Li, Research Institute of General Surgery, Jinling Hospital, Medical College of Nanjing University, Nanjing 210002, Jiangsu Province, China
Correspondence to: Dr. Zhu-Fu Quan, Institute of General Surgery, Jinling Hospital, Medical College of Nanjing University, Nanjing 210002, Jiangsu Province, China. quanzf@×263.net
Telephone: +86-25-4810649 **Fax:** +86-25-4803956
Received: 2002-10-05 **Accepted:** 2002-11-06

Abstract

AIM: To review the experience on the use of endoscopic nasopancreatic drainage (ENPD) in the treatment of severe acute pancreatitis (SAP).

METHODS: Since March 1998, under the regular management of SAP with non-operative method, ENPD has been randomly used in 14 patients. The average age of the patients was 41.3±15.9 (years), with 8 males and 6 females. The time from onset to admission was 32.9±22.8 (hours). 8 cases were found to have gallbladder stone. The daily output of pancreatic fluid was measured. The body temperature, heart rate, WBC count, blood glucose, blood calcium, PaO_2, blood and urine levels of amylase were detected on the fifth day and compared with their respective data on the first day. Therapeutic results and hospitalization times were recorded.

RESULTS: The time of drainage was 7.3±4.0 days. The daily drainage outputs of the first five days were 236.4±176.6, 287.1±164.7, 284.6±216.4, 435.0±357.8 and 377.8±223.8 ml, respectively. The decreases in body temperature, heart rate, WBC counts, blood and urine levels of amylase and the increase in PaO_2 were significant on the fifth day when compared with those on the first day. Infection of pancreatic necrosis was found in one patient and controlled by anti-infectives. 6 out of 8 patients with gallbladder stone were operated during hospital stay. All patients were cured and diischarged and the average hospital stay was 28.1±11.6 days.

CONCLUSION: ENPD is an effective method for the drainage of pancreatic fluid and might have an important role in the treatment of SAP. Further observation, comparison and summary by this method are worthy to be considered.

Quan ZF, Wang ZM, Li WQ, Li JS. Use of endoscopic naso-pancreatic drainage in the treatment of severe acute pancreatitis. *World J Gastroenterol* 2003; 9(4): 868-870
http://www.wjgnet.com/1007-9327/9/868.htm

INTRODUCTION

Acute pancreatitis (AP) is a common clinical emergency. For the reason of urgency of episode, severity of patient' s condition, frequent complications and high mortality, extensive attention has been paid to severe acute pancreatitis (SAP) in clinical practice[1-10]. Since August 1995, we have adopted the principle of combination therapy mainly by non-operative methods, the therapeutic efficacy of SAP has been increased significantly and hospital stay has been shortened. Therein, the method of endoscopic naso-pancreatic drainage (ENPD) was used in 14 cases since March 1998,with significant results.

MATERIALS AND METHODS

General clinical data

A total of 14 patients were treated, with average age of 41.3±15.9 (27-77) years, 8 males and 6 females. From onset of the sisease to admission was 32.9±22.8 (6-72) hours. In 8 cases (8/14, 57.1 %), gallbladder stone was detected by B ultrasonography or computerized tomography (CT). All patients were diagnosed as SAP in accord with the diagnostic criteria set by Surgical Pancreatic Group of the Surgical Society of Chinese Medical Association[11,12]. Within 24 hours after hospitalization, their APACHE-II scores were ⩾8, Balthazar CT grades ⩾II, and all accompanied by one or more organ dysfunction.

Routine non-operative monitoring therapy

All patients in fasting were installed with gastric tube to decompress and drain gastrointestinal fluid, and were given oxygen therapy (nasal catheter oxygen inhalation, 5 L/min), prophylactic application of antibiotics and somatostatin (14 peptide or 8 peptide). At the same time, internal homeostasis including water-electrolyte balance, acid-base balance, and the change of organ functions such as heart, lung, liver and kidney were monitored. Proper supportive therapy was given on time if necessary.

Endoscopic nasopancreatic drainage (ENPD)

After hospitalization, with the use of fiberoptive duodenoscope spectacle (Olympus TJF-30 model), nasopancreatic drainage-tube was inserted through the scope in the ward instantly after admission. The procedure was as follows: after intramuscular injection of 50 mg meperidine and 10 mg 654-2 with topical anaesthesia of throat, the endoscope was advanced to duodenum, searching for the papilla. Once found, it was observed about its shape, size, and position of the orifice. A tube was inserted into pancreatic duct for 5-10 cm through the orifice. The catheter was 1.95 m in length, 1.95 mm in outside diameter and 1.70 mm in inside diameter with 3 to 5 side holes near the distal end. If pancreatic juice cound be drawn out, it indicated that insertion of the catheter was successful. The endoscope was then withdrawn and the drainage tube was guided from oral cavity to nasal cavity by a guiding catheter and fixed. Thereafter, the patency of the nasopancreatic tube was closely observed daily and was washed with gentamycin saline solution if necessary. When the abdominal symptoms and signs subsided, the tube was pulled out.

Observation index

Volume of the drainage from nasopancreatic tube was observed and recorded everyday. The body temperature, heart rate, WBC counts, blood glucose, blood calcium, PaO_2, and blood and urine levels of amylase were surveyed on the fifth day and compared with that on the first day. The therapeutic results and the time of hospital stay were recorded.

Data processing

All data were expressed as mean ±standard deviation, and *t*-test was used for statistical analysis.

RESULTS

Information of drainage by nasopancreatic tube

The pancreatic fluid of all patients drained out was feculent achromatic or white fluid in the first 1 to 3 days, and then turned to clear transparent pancreatic fluid. The time of nasopancreatic drainage was 7.3±4.0 days. The drainage output of pancreatic fluid during the first five days was shown in Figure 1. The radiogram of naso-pancreatic catheter in a patient was shown in Figure 2.

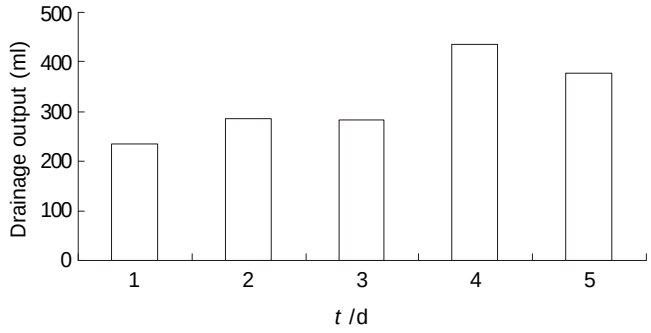

Figure 1 The drainage output of pancreatic fluid during the first five days.

Figure 2 The radiogram of naso-pancreatic catheter in a patient.

Changes of the relevant monitoring indices

The decrease of body temperature, heart rate, WBC count, blood and urine levels of amylase and the increase of PaO_2 were significant on the fifth day when compared with that on the first day. The change of blood glucose or blood calcium had no significant difference. The details were shown in Table 1.

Table 1 Changes in several related indexes

	The first day	The fifth day
Body temperature (℃)	38.2±0.6	37.2±0.8[b]
Heart rate (bpm)	102.3±17.0	82.9±14.5[b]
WBC count ($\times10^9$/L)	14.6±4.2	10.1±5.4[a]
Blood amylase (U/L)	695.7±445.2	82.6±47.1[b]
Urine amylase (U/L)	3174.1±2542.5	286.8±260.9[b]
PaO_2 (mmHg)	78.0±16.3	113.0±41.6[b]
Blood glucose (mmol/L)	10.0±4.9	8.6±3.3
Blood calcium (mmol/L)	2.1±0.2	2.2±0.2

[a]$P<0.05$, [b]$P<0.01$, *vs* the first day.

Therapeutic result of treatment and time of hospital stay

Bacterial infection of pancreatic necrosis was found in one patient and controlled after changing the anti-infectives. Cholecystectomy was performed in 6 patients with cholecystolithiasis before discharge. All patients were cured and the time of hospital stay was 28.1±11.6 days.

DISCUSSION

There has been a steady increase in the incidence or the admission rate of AP[13-15]. Generally, it is recognized that the pathogenesis of AP is correlated with the common channel of biliary and pancreatic ducts which is also called the common biliary pancreatic duct. The most common cause (60-80 %) is gallbladder stone and alcoholism[16]. The former cause was more extensively studied than the latter. Incarceration by the calculus which enters the common channel and/or the inflammatory reaction and tissue edema caused by the passage of the calculus have often been proposd as the mechanism of AP and we name this type of AP the gallbladder stone-originated AP.

The obstruction of common biliary pancreatic duct results in the bile flowing into the pancreatic duct, activating the pancreatic enzymes and then causing the occurrence of AP. This is the classical bile reflux-common channel theory. This theory does not explain why AP happens in patients who have no calculus incarceration in or obstruction of common biliary pancreatic duct. In our group, 8 out of 14 cases, which amounted to 57.1 %, were diagnosed as having with cholecystolithiasis. But no one showed incarceration of the calculus or obstruction of common biliary pancreatic duct. We found that there was no bile mixed in the pancreatic fluid in our SAP patients with or without cholecystolithiasis, although the initial drain was feculent.

Nevertheless, the experiment of Lerch, *et al*[17] made it clear that both pancreatic duct ligation alone and common biliary pancreatic duct ligation could cause the occurrence of AP, with pathological changes of similar severity. This result suggested that pancreatic duct obstruction, especially increase of pancreatic intraductal pressure was the main factor of the occurrence of AP. It may be the main mechanism in patients suffering from AP with or without cholecystolithiasis. Pancreatic ischaemia has an important role in the pathphysiology of AP[18,19]. Shi and his colleagues[20] reported that pancreatic duct obstruction was the first step causing ischaemia in AP and early decompression of the pancreatic duct prevented the early pancreatic ischaemia. The study of Choudari, *et al*[21] proved that improving drainage of the pancreatic ductal system by endoscopic means effectively relieved the pain and reduced the number of attacks of pancreatitis in the majority of patients with heriditory pancreatitis. Aiming directly on this mechanism, we used the method of ENPD in treating SAP patients. All the patients accepted the routine non-operative therapy. Amelioration of abdominal symptoms and signs was very rapid with the drainage. Comparing with that on the first day, the decrease in body temperature, heart rate, WBC counts, blood and urine levels of amylase and the increase in PaO_2 were significant on the fifth day. Although blood glucose decreased and blood calcium increased, but they had no statistic significance. Bacterial infection of pancreatic necrosis was found only in one patient and was controlled after changing the anti-infectives. All 14 patients of this group were cured.

Studies have shown that duration of the obstruction of common biliary pancreatic duct was related directly with the severity of pancreatic necrosis and prognosis of the patient. Removal of the obstruction or decreasing the pressure on time can prevent the appearance of pancreatic necrosis or its further

development. The earlier the time of removal of the obstruction or decreasing the pressure, the better the prognosis[16,22-24]. Beger, *et al*[25] found that if the course of AP was longer than 3-4 days, the pancreas would necrotize irreversibly. It is important in the therapy of SAP to remove the obstruction or lower the high pressure of the pancreatic duct as early as possible. The time from onset to admission was 32.9±22.8 (6-72) hours in this group and the application of ENPD was carried out in the ward immediately after the admission. This is another important factor to get the curative effect.

This is our preliminary experience of the clinical application of ENPD in the treatment of SAP. The real value of this this therapeutic modality should be further studied by strict randomised control study.

REFERENCES

1 **Howard TJ,** Temple MB. Prophylactic antibiotics alter the bacteriology of infected necrosis in severe acute pancreatitis. *J Am Coll Surg* 2002; **195**: 759-767

2 **De La Mano A,** Sevillano S, De Dios I, Vicente S, Manso MA. Low enzyme content in the pancreas does not reduce the severity of acute pancreatitis induced by bile-pancreatic duct obstruction. *Mol Cell Biochem* 2002; **240**: 75-81

3 **Srikanth G,** Sikora SS, Baijal SS, Ayyagiri A, Kumar A, Saxena R, Kapoor VK. Pancreatic abscess: 10 years experience. *ANZ J Surg* 2002; **72**: 881-886

4 **Ammori BJ,** Cairns A, Dixon MF, Larvin M, McMahon MJ. Altered intestinal morphology and immunity in patients with acute necrotizing pancreatitis. *J Hepatobiliary Pancreat Surg* 2002; **9**: 490-496

5 **Hartwig W,** Werner J, Muller CA, Uhl W, Buchler MW. Surgical management of severe pancreatitis including sterile necrosis. *J Hepatobiliary Pancreat Surg* 2002; **9**: 429-435

6 **Hartwig W,** Werner J, Uhl W, Buchler MW. Management of infection in acute pancreatitis. *J Hepatobiliary Pancreat Surg* 2002; **9**: 423-428

7 **Mayumi T,** Ura H, Arata S, Kitamura N, Kiriyama I, Shibuya K, Sekimoto M, Nago N, Hirota M, Yoshida M, Ito Y, Hirata K, Takada T. Evidence-based clinical practice guidelines for acute pancreatitis: proposals. *J Hepatobiliary Pancreat Surg* 2002; **9**: 413-422

8 **Balthazar EJ.** Complications of acute pancreatitis: clinical and CT evaluation. *Radiol Clin North Am* 2002; **40**: 1211-1227

9 **Balthazar EJ.** Staging of acute pancreatitis. *Radiol Clin North Am* 2002; **40**: 1199-1209

10 **Uhl W,** Warshaw A, Imrie C, Bassi C, McKay CJ, Lankisch PG, Carter R, Di Magno E, Banks PA, Whitcomb DC, Dervenis C, Ulrich CD, Satake K, Ghaneh P, Hartwig W, Werner J, McEntee G, Neoptolemos JP, Buchler MW. IAP Guidelines for the Surgical Management of Acute Pancreatitis. *Pancreatology* 2002; **2**: 565-573

11 **Surgical Pancreatic Group of the Surgical Society of Chinese Medical Association.** The clinical diagnosis and grading criteria of acute pancreatitis. *Zhonghua Waike Zazhi* 1997; **35**: 773-775

12 **Surgical Pancreatic Group of the Surgical Society of Chinese Medical Association.** The treatment guideline of severe acute pancreatitis. *Zhongguo Shiyong Waike Zazhi* 2001; **21**: 513-514

13 **Tinto A,** Lloyd DA, Kang JY, Majeed A, Ellis C, Williamson RC, Maxwell JD. Acute and chronic pancreatitis-diseases on the rise: a study of hospital admissions in England 1989 / 90-1999 / 2000. *Aliment Pharmacol Ther* 2002; **16**: 2097-2105

14 **Birgisson H,** Moller PH, Birgisson S, Thoroddsen A, Asgeirsson KS, Sigurjonsson SV, Magnusson J. Acute pancreatitis: a prospective study of its incidence, aetiology, severity, and mortality in Iceland. *Eur J Surg* 2002; **168**: 278-282

15 **Lopez MJ.** The changing incidence of acute pancreatitis in children: a single-institution perspective. *J Pediatr* 2002; **140**: 622-624

16 **Steer ML.** Pathogenesis of acute pancreatitis. *Digestion* 1997; **58** (Suppl 1): 46-49

17 **Lerch MM,** Saluja AK, Runzi M, Dawra R, Saluja M, Steer ML. Pancreatic duct obstruction triggers acute necrotizing pancreatitis in the opossum. *Gastroenterology* 1993; **104**: 853-861

18 **Zhou ZG,** Chen YD. Influencing factors of pancreatic microcirculatory impairment in acute panceatitis. *World J Gastroenterol* 2002; **8**: 406-412

19 **Zhou ZG,** Chen YD, Sun W, Chen Z. Pancreatic microcirculatory impairment in experimental acute pancreatitis in rats. *World J Gastroenterol* 2002; 8: 933-936

20 **Shi CX,** Chen JW, Carati CJ, Schloithe AC, Toouli J, Saccone GT. Effects of acute pancreatic duct obstruction on pancreatic perfusion: implication of acute pancreatic duct decompression. *Scand J Gastroenterol* 2002; **37**: 1328-1333

21 **Choudari CP,** Nickl NJ, Fogel E, Lehman GA, Sherman S. Hereditary pancreatitis: clinical presentation, ERCP findings,and outcome of endoscopic therapy. *Gastrointest Endosc* 2002; **56**: 66-71

22 **Runzi M,** Saluja AK, Lerch MM, Dawra R, Nishino H, Steer ML. Early ductal decompression prevents the progression of biliary pancreatitis: an experimental study in the opossum. *Gastroenterology* 1993; **105**: 157-164

23 **Feng BX,** Huang B, Zhai CB, Li DW, Yang LQ, Lin HJ. Role of pancreatic duct cannulation in the treatment of experimental acute haemorragic necrotizing pancreatitis of dogs. *Zhonghua Putong Waike Zazhi* 1998; **13**: 295-297

24 **Kueppers PM,** Russell DH, Moody FG. Reversibility of pancreatitis after temporary pancreaticobiliary duct obstruction in rats. *Pancreas* 1993; **8**: 632-637

25 **Beger HG,** Rau B, Mayer J, Pralle U. Natural course of acute pancreatitis. *World J Surg* 1997; **21**: 130-135

Edited by Xu JY

P.O.Box 2345, Beijing 100023,China
Fax: +86-10-85381893
E-mail: wjg@wjgnet.com www.wjgnet.com

World J Gastroenterol 2003;9(4):871-873
World Journal of Gastroenterology
 ISSN 1007-9327

• CLINICAL RESEARCH •

Local excision carcinoma in early stage

Ji-Dong Gao, Yong-Fu Shao, Jian-Jun Bi, Su-Sheng Shi, Jun Liang, Yu-Hua Hu

Ji-Dong Gao, Yong-Fu Shao, Jian-Jun Bi, Department of General Surgical Oncology, Cancer Hospital, Chinese Academy of Medical Sciences, Peking Union Medical College, Beijing 100021, China
Su-Sheng Shi, Department of Pathology, Cancer Hospital, Chinese Academy of Medical Sciences, Peking Union Medical College, Beijing 100021, China
Jun Liang, Yu-Hua Hu, Department of Radiotherapy Oncology, Chinese Academy of Medical Sciences, Peking Union Medical College, Beijing 100021, China
Correspondence to: Ji-Dong Gao, Department of General Surgical Oncology, Cancer Hospital, Chinese Academy of Medical Sciences, Peking Union Medical College, Beijing 100021, China. ab168@vip.sina.com
Telephone: +86-10-87708308
Received: 2002-12-22 **Accepted:** 2003-01-16

Abstract

AIM: To assess the validity of local excision for the early stage low rectal cancer as an effective treatment alternative to radical resection.

METHODS: A retrospective medical chart review was done in 47 patients with early stage low rectal carcinoma who underwent local excision from November 1980 through November 1999 at Cancer Hospital of Chinese Academy of Medical Sciences (CAMS). The patients were treated by either transanal (40 cases), trans-sacral (5 cases), or trans-vaginal (2 cases) excision of tumors and no death was related to surgery. Sixteen patients received postoperative radiotherapy.

RESULTS: T1 and T2 lesion was found in 36 (76.6 %) and 11 patients (23.4 %) respectively. The overall local tumor recurrence rate was 14.9 % (7/47), with an average recurrence time of 21 months. Among these 7 recurrent patients, there were 4 T1 and 3 T2 lesions. Microscopically, the surgical incisal margin was negative in 45 (95.7 %) and positive in 2 patients (4.3 %); Both of the later had developed local recurrence. The overall 5-year survival rate was 91.7 %, in which there were 94.4 % for T1 and 83.3 % for T2 tumors. T stage, intravessel tumor thrombosis, lymphocytic infiltration and histological grade were not found to be significant by related to the local recurrence and survival (P>0.05).

CONCLUSION: Local tumor excision was a safe procedure for the treatment of early stage low rectal carcinoma with minimal morbidity and mortality, which might serves as one of the primary surgical treatment methods for the disease of this kind.

Gao JD, Shao YF, Bi JJ, Shi SS, Liang J, Hu YH. Local excision carcinoma in early stage. *World J Gastroenterol* 2003; 9(4): 871-873
http://www.wjgnet.com/1007-9327/9/871.htm

INTRODUCTION

Abdominoperineal resection (APR) has traditionally been use to treat the Adenocarcinoma of the low rectum[1-2]. In which a permanent colostomy has to be performed, leading to the risk of complications, inconvenience of patients and even death[3,4]. More recently, local excision has been performed with the curative intent to remove the well-differentiated lesions that are less than 3 cm in diameter and limited to the mucosa or submucosa[5-7], which offers these patients fewer operative complications and long-term survival outcome[8-13]. The increasing evidence based on the local tumor recurrence and survival rates supports the use of local excision as a primary treatment modality in the selected patients[14-18].

The aim of the present study was to review our experience in the local excision of the early rectal cancers and to assess the validity of this therapeutic strategy as an effective treatment alternative to radical resection.

MATERIALS AND METHODS

Materials

Forty-seven 47 patients with early stage low rectal carcinomas were treated by local excision from November 1980 to November 1999 at the Department of General Surgical Oncology, Cancer Hospital of Chinese Academy of Medical Sciences (CAMS). They were 23 male and 24 female and with an average age 57 years (ranging from 31 to 80 years). The rectal carcinomas were located 3 to 8 cm from the anal verge (Table 1).

Table 1 Patient and treatment characteristics (n=47)

Characteristic	No. patients
Sex	
Male	23
Female	24
Surgical margin	
Negative	45
Positive	2
Radiotherapy	
No	31
Yes	16
T stage	
T1	36
T2	11
Grade	
Well differentiated	22
Moderately differentiated	23
Poorly differentiated	2
Surgical Procedure	
Transanal excision	40
Trans-sacral excision	5
Trans-vaginal excision	2

Treatment

Patients were treated by either transanal (40 cases), trans-sacral (5 cases), or trans-vaginal (2 cases) excision of tumors, in which 16 patients received postoperative radiotherapy.

Pathological diagnosis

All available pathohistological sections were reviewed by a single pathologist to assessed the depth and extent of tumor invasion, the lymphocytic infiltration, mucinous status, and the degree of tumor differentiation. The tumor was staged according to the American Joint Committee on Cancer Staging System (AJCC1996).

Statistical analysis

The end points of this study were local and distant tumor recurrence and patient survival. Obtained data were analyzed using the Statistical Package for the Social Sciences (Release 11.0, SPSS, Inc). Survival curves were estimated using the Kaplan-Meier method and were compared using the log-rank test. Significance was defined as $P<0.05$.

RESULTS

There was no death related to surgery. The most severe complication was the fistula formation, which was necessitated to perform a temporary diverting colostomy in two patients treated with trans-sacral excision. Other complications included bleeding in 2 patients and anal stricture in one patient (Table 1).

The median tumor diameter was 2.0 cm (ranging form 0.4 to 3 cm). Thirty-six patients (76.6 %) had T1 and 11 patients (23.4 %) had T2 lesion. The resected tumors in most cases were well or moderately differentiated, poorly differentiated were only seen in two patients. For those pathological sections were available, intravessel tumor thrombosis was identified in 10 patients (21.3 %) and lymphocytic infiltration in 8 patients (17.0 %). Tumor cells appeared on the surgical incisal margin were negative in 45 patients (95.7 %) and positive in 2 cases (4.3 %).

The average time for follow-up survey was 53 months. The overall local tumor recurrence rate was 14.9 % (7 patients) with the median recurrence time of 21 months (ranging from 12 to 48 months) postoperation. Among those with local recurrence, T1 and T2 tumors were found in 4 and 3 cases respectively. Five patients had immediate reoperation (APR or anterior resection). Both of the two patients with tumor cell positive incisal margin developed local recurrence. The overall 5-year survival rate was 91.7 %, in which there were 94.4 % for T1 and 83.3 % for T2 tumors.

T stage, intravessel tumor thrombosis, lymphocytic infiltration, histological grade and mucinous differentiation were not found to be significant predictors for local tumor recurrence and survival ($P>0.05$).

DISCUSSION

Abdominoperineal resection, the mainstay of treatment for rectal cancer nowadays, has been reported bearing a death rate of 2.3 % to 3.2 % and 30 % to 46 % postoperative complications in the patient. permanent colostomy, urinary and sexual dysfunction are common sequelae of radical proctectomy that impair seriously affecting the patient' s quality of life[1-4]. In the past, local excision was performed only if the patient was in poor medical condition or refused to have a colostomy. Recent data suggest that the combination of local excision and postoperative chemo-radiation therapy may be an option for some patients with early stage rectal cancer. Encouraging results of local treatment of early rectal cancer and the development of new diagnostic technology providing accurate preoperative staging have greatly increased the interest of surgical oncology in this therapeuticstrategy[14-19].

However, broad acceptance of local excision as the primary treatment rectal cancer has been limited by the high local tumor recurrence that was difficult to be interpreted because the literature was dominated by retrospective analyses of heterogeneous groups of patients. Included the patients with the tumors undifferentiated and penetrating the perirectal fat, with questionable or even positive tumor cell incisal margins, or with different surgical approaches, even palliative surgery[20,21]. Besides specific reference was not always made to the lymphatic and blood vessel invasion, and the role of salvage surgery after failed local excision has also not been clearly stated[22-26]. Therefore, There is an almost uniform agreement at present that only the well- or moderately differentiated T1 and T2 tumors, without blood vessel or lymphatic invasion or mucinous components could be treated by local excision with curative intent.

The present study there was no death related to the surgery, postoperative mortality. Complications occurring more and with a minimal in patients treated with trans-sacral excision was the fistula that was necessitated to perform a temporary diverting colostomy in two patients. Transanal excision was associated with less morbidity than any other local excision procedures.

Our data suggested that longer follow-up was necessary to identify those who would have a relapse, as shown by the fact that the median time for the local tumor recurrence in our study was about 21 months, with a range of 12 to 48 months postoperation. Recurrence rates were 11.1 % and 27.3 % in T1 and T2 tumors, respectively, which suggested that T stage was an important factor affecting recurrence.

The fact that both of the 2 patients with tumor cell positive incisal margin developed local recurrence suggested that tumor-free incisal margin and completely tumor excision was crucial for the prevention of local tumor recurrence, which was difficult to achieve for T3 lesion because the tumor had invaded the perirectal fat or anal sphincter. Therefore, if a tumor cell negative incisal margin could not be achieved in the operation, the patient was not considered as a good candidate for the local excision[27,28]. Statistical analysis showed that intravessel tumor thrombosis, lymphocytic infiltration, histologic grade and mucinous differentiation were not found to be the significant predictors for the local tumor recurrence and survival ($P>0.05$).

In summary, on the basis of our retrospective data, the sphincter-preserving local excision can be used as one of the primary surgical treatment methods for the early-stage low rectal cancer with minimal morbidity and mortality.

REFERENCES

1 **Nissan A,** Guillem JG, Paty PB, Douglas Wong W, Minsky B, Saltz L, Cohen AM. Abdominoperineal resection for rectal cancer at a specialty center. *Dis Colon Rectum* 2001; **44**: 27-35

2 **Zheng S,** Liu XY, Ding KF, Wang LB, Qiu PL, Ding XF, Shen YZ, Shen GF, Sun QR, Li WD, Dong Q, Zhang SZ. Reduction of the incidence and mortality of rectal cancer by polypectomy: a prospective cohort study in Haining County. *World J Gastroenterol* 2002; **8**: 488-492

3 **Luna-Perez P,** Rodriguez-Ramirez S, Vega J, Sandoval E, Labastida S. Morbidity and mortality following abdominoperineal resection for low rectal adenocarcinoma. *Rev Invest Clin* 2001; **53**: 388-389

4 **McLeod RS.** Comparison of quality of life in patients undergoing abdominoperineal extirpation or anterior resection for rectal cancer. *Ann Surg* 2001; **233**: 157-158

5 **Sengupta S, Tjandra JJ.** Local excision of rectal cancer: what is the evidence? *Dis Colon Rectum* 2001; **44**: 1345-1361

6 **Masaki T,** Sugiyama M, Atomi Y, Matsuoka H, Abe N, Watanabe T, Nagawa H, Muto T. The indication of local excision for T2 rectal carcinomas. *Am J Surg* 2001; **181**: 133-137

7 **Taylor RH,** Hay JH, Larsson SN. Transanal local excision of selected low rectal cancers. *Am J Surg* 1998; **175**: 360-363

8 **Bleday R,** Steele G Jr. Current protocols and outcomes of local

therapy for rectal cancer. *Surg Oncol Clin N Am* 2000; **9**: 751-758
9 **Rothenberger DA,** Garcia-Aguilar J. Role of local excision in the treatment of rectal cancer. *Semin Surg Oncol* 2000; **19**: 367-375
10 **Chorost MI,** Petrelli NJ, McKenna M, Kraybill WG, Rodriguez-Bigas MA. Local excision of rectal carcinoma. *Am Surg* 2001; **67**: 774-779
11 **Blair S,** Ellenhorn JD. Transanal excision for low rectal cancers is curative in early-stage disease with favorable histology. *Am Surg* 2000; **66**: 817-820
12 **Hall NR,** Finan PJ, al-Jaberi T, Tsang CS, Brown SR, Dixon MF, Quirke P. Circumferential margin involvement after mesorectal excision of rectal cancer with curative intent. Predictor of survival but not local recurrence? *Dis Colon Rectum* 1998; **41**: 979-983
13 **Chakravarti A,** Compton CC, Shellito PC, Wood WC, Landry J, Machuta SR, Kaufman D, Ancukiewicz M, Willett CG. Long-term follow-up of patients with rectal cancer managed by local excision with and without adjuvant irradiation. *Ann Surg* 1999; **230**: 49-54
14 **Wagman RT,** Minsky BD. Conservative management of rectal cancer with local excision and adjuvant therapy. *Oncology (Huntingt)* 2001; **15**: 513-519
15 **Daniels IR,** Simson JN. Local excision and chemoradiation for low rectal T1 and T2 cancers is an effective treatment. *Am Surg* 2000; **66**: 512
16 **Medich D,** McGinty J, Parda D, Karlovits S, Davis C, Caushaj P, Lembersky B. Preoperative chemoradiotherapy and radical surgery for locally advanced distal rectal adenocarcinoma: pathologic findings and clinical implications. *Dis Colon Rectum* 2001; **44**: 1123-1128
17 **Benson R,** Wong CS, Cummings BJ, Brierley J, Catton P, Ringash J, Abdolell M. Local excision and postoperative radiotherapy for distal rectal cancer. *Int J Radiat Oncol Biol Phys* 2001; **50**: 1309-1316
18 **Varma MG,** Rogers SJ, Schrock TR, Welton ML. Local excision of rectal carcinoma. *Arch Surg* 1999; **134**: 863-867
19 **Akasu T,** Kondo H, Moriya Y, Sugihara K, Gotoda T, Fujita S, Muto T, Kakizoe T. Endorectal ultrasonography and treatment of early stage rectal cancer. *World J Surg* 2000; **24**: 1061-1068
20 **Weber TK**, Petrelli NJ. Local excision for rectal cancer: an uncertain future. *Oncology (Huntingt)* 1998; **12**: 933-943
21 **Bouvet M**, Milas M, Giacco GG, Cleary KR, Janjan NA, Skibber JM. Predictors of recurrence after local excision and postoperative chemoradiation therapy of adenocarcinoma of the rectum. *Ann Surg Oncol* 1999; **6**: 26-32
22 **Graham RA**, Hackford AW, Wazer DE. Local excision of rectal carcinoma: a safe alternative for more advanced tumors? *J Surg Oncol* 1999; **70**: 235-238
23 **Benoist S**, Panis Y, Martella L, Nemeth J, Hautefeuille P, Valleur P. Local excision of rectal cancer for cure: should we always regard rigid pathologic criteria? *Hepatogastroenterology* 1998; **45**:1546-1551
24 **Mellgren A,** Sirivongs P, Rothenberger DA, Madoff RD, Garcia-Aguilar J. Is local excision adequate therapy for early rectal cancer? *Dis Colon Rectum* 2000; **43**: 1064-1071
25 **Wexner SD,** Rotholtz NA. Surgeon influenced variables in resectional rectal cancer surgery. *Dis Colon Rectum* 2000; **43**: 1606-1627
26 **Lopez-Kostner F,** Fazio VW, Vignali A, Rybicki LA, Lavery IC. Locally recurrent rectal cancer: predictors and success of salvage surgery. *Dis Colon Rectum* 2001; **44**: 173-178
27 **Kim CJ,** Yeatman TJ, Coppola D, Trotti A, Williams B, Barthel JS, Dinwoodie W, Karl RC, Marcet J. Local excision of T2 and T3 rectal cancers after downstaging chemoradiation. *Ann Surg* 2001; **234**: 352-358
28 **Beart RW Jr.** Predictors of recurrence after local excision. *Ann Surg Oncol* 1999; **6**: 26-32

Edited by Zhu L

P.O.Box 2345, Beijing 100023,China
Fax: +86-10-85381893
E-mail: wjg@wjgnet.com www.wjgnet.com

World J Gastroenterol 2003;9(4):874-877
World Journal of Gastroenterology
 ISSN 1007-9327

• CLINICAL RESEARCH •

Acaroid mite, intestinal and urinary acariasis

Chao-Pin Li, Yu-Bao Cui, Jian Wang, Qing-Gui Yang, Ye Tian

Chao-Pin Li, Yu-Bao Cui, Jian Wang, Qing-Gui Yang, Ye Tian, Department of Etiology and Immunology, School of Medicine, Anhui University of Science & Technology, Huainan 232001, Anhui Province, China
Correspondence to: Dr. Chao-Pin Li, Department of Etiology and Immunology, School of Medicine, Anhui University of Science & Technology, Huainan 232001, Anhui Province, China. yxfy@aust.edu.cn
Telephone: +86-554-6658770 **Fax:** +86-554-6662469
Received: 2002-11-11 **Accepted:** 2002-12-20

Abstract

AIM: To investigate epidemiology and pathogenic mite species of intestinal and urinary acariasis in individuals with different occupations.

METHODS: A total of 1994 individuals were tested in this study. History collection, skin prick test and pathogen identification were conducted. The mites were isolated from stool and urine samples by saturated saline flotation methods and sieving following centrifugation, respectively.

RESULTS: Among the 1994 individuals examined, responses to the skin prick test of "+++", "++", "+","±" and "-" were observed at frequencies of 3.96 % (79), 3.21 % (64), 2.31 % (46), 1.25 % (25) and 89.27 % (1780), respectively. A total number of 161 (8.07 %) individuals were shown to carry mites, with 92 (4.61 %) positive only for stool samples, 37 (1.86 %) positive only for urine samples and 32 (1.60 %) for both. The positive rate of mites in stool samples was 6.22 % (124/1994), being 6.84 % (78/1140) for males and 5.39 % (46/854) for females. No gender difference was observed in this study (χ^2=1.77, P>0.05). The mites from stool samples included *Acarus siro*, *TyroPhagus putrescentiae*, *Dermatophagoides farinae*, *D. pteronyssinus*, *Glycyphagus domesticus*, *G.ornatus*, *Carpoglyphus lactis and Tarsonemus granaries*. The positive rate of mites in urine samples was 3.46 % (69/1994). The positive rates for male and female subjects were found to be 3.95 % (45/1140) and 2.81 % (24/854) respectively, with no gender difference observed (χ^2=1.89, P>0.05). Mites species in urine samples included *Acarus siro*, *Tyrophagus putrescentiae*, *T. longior*, *Aleuroglyphus ovatus*, *Caloglyphus berlesei*, *C. mycophagus*, *Suidasia nesbitti*, *Lardoglyphus konoi*, *Glycyphagus domesticus*, *Carpoglyphus lactis*, *Lepidoglyphus destructor*, *Dermatophagoides farinae*, *D. pteronyssinus*, *Euroglyphus magnei*, *Caloglyphus hughesi*, *Tarsonemus granarus* and *T. hominis*. The species of mites in stool and urine samples were consistent with those separated from working environment. A significant difference was found among the frequencies of mite infection in individuals with different occupations (χ^2=82.55, P<0.001), with its frequencies in those working in medicinal herb storehouses, those in rice storehouse or mills, miners, railway workers, pupils and teachers being 15.89 % (68/428), 12.96 % (53/409), 3.28 % (18/549), 2.54 % (6/236), 5.10 % (13/255) and 2.56 % (3/117), respectively.

CONCLUSION: The prevalence of human intestinal and urinary acariasis was not associated with gender, and these diseases are more frequently found in individuals working in medicinal herb, rice storehouses or mills and other sites with high density of mites. More attention should be paid to the mite prevention and labor protection for these high-risk groups.

Li CP, Cui YB, Wang J, Yang QG, Tian Y. Acaroid mite, intestinal and urinary acariasis. *World J Gastroenterol* 2003; 9(4): 874-877
http://www.wjgnet.com/1007-9327/9/874.htm

INTRODUCTION

Various species of mites often infest stored foodstuffs and various drugs, and cause losses in food and drug products, especially in humid and warm area[1-9]. They are small creatures of about half a millimeter in body size and creamy white in color, proving difficult to be detected from drugs and food products. Therefore, the incidence of various forms of human acariasis presumably caused by the ingestion of mite-infested food is unusually high in China[10]. In this study we investigates the epidemiological characteristics and pathogenic mite species of intestinal and urinary acariasis in individuals with different occupations in Anhui Province.

MATERIALS AND METHODS

Population

A total of 1994 subjects with the average age of 35 years (6-63 years), 1 140 males and 854 females, were examined in this study, including medicinal herb storehouse workers (n=428), rice storehouse or mill workers (n=409), miners (n=549), railway workers (n=236), pupils (n=255) and teachers (n=117). Special attention was paid to individuals with intestinal or/and urinary symptoms.

Methods

History collection, skin prick test and etiological examination were carried out on the 1994 subjects.

History collection A questionnaire, administered by a nurse, was used to collect information from each subject investigated. Information was collected by means of in-person, telephone, interview, including age, gender, history of present illness, anamnesis, symptomatology (i.e. abdominal pain, diarrhea, abdominal cramps, urethremorrhage, urodynia, cloudy urine, frequency of micturition), onset date and duration of symptoms, personal habits, living environmental hygiene and the date of stool and urine sample collection.

Skin prick test Skin prick test were performed with the concentrations of 1:100 (W/V) of the test extract. After skin disinfection, a little of extract (about 0.01 ml) was dripped on skin surface of right forearm flexor, then a special disinfectant needle was used to prick into the skin through the drop of the extract. The depth of needle in skin was limited about 0.5-1 mm and there was no bloodshed. About 5 cm apart from the extract drop, normal saline in proximal and histamine in distalis were used for negative and positive control solution. The mean diameter of the wheals or areolae was measured 15-20 min after the test. The reactions with the mean diameter up to 1.5

mm, 2 mm, 3 mm, 5 mm and 10 mm were regarded as ±, +, ++, +++ and ++++, respectively.

The test extract was made according to NIBSC82/518 approved by World Health Organization (WHO) in 1984. The purified fraction was prepared as follows: the mites were then frozen and thawed several times after having been cultured in the initial medium for several months. A 48-hr maceration in a borate buffer (pH 8.5) was followed by centrifugation. The supernatant was neutralized and submitted to precipitation with a series of acetone. The fraction precipitated at 80 % acetone was isolated, washed and dried. This purified extract was lyophilized or stored as a solution in the presence of 50 % glycerol and 5 % phenol[11-14].

Etiological examination All individuals were asked to provide stool and urine samples for etiological examination. Mites in stool samples were separated by saturated saline flotation methods, and the mites were identified under microscope. Each stool sample was examined for three times Specimens containing adult or larval mites, eggs, or hypopus were considered positive.

Samples of the first urine in the morning and 24 hours' urine of all individuals were collected for separation of mites. After centrifugation and filtration with a copper sieve, they were examined under a microscope for adult or larval mites, eggs or hypopus.

Blood examination Leukocytes were also counted and sorted in 30 patients with mites detected.

Detection of mites from working environment Directicopy, waterenacopy and tullgren were used to identify mites from mill floor dust, stores of medicinal herbs including wolfberry fruit, ophiopogon root liquorice, boat-fruited sterculia seed and safflower.

Colonoscopy After defecation, the patients with mites found in their stools were examined by routine colonoscopy.

Cystoscopy After emiction, the patients with mites detected in their urine were examined by routine cystoscopy.

Statistical analysis

The positivity rates were expressed as percentages, and the statistical analysis was carried out by using χ^2 test. A probability value of less than 0.05 was considered statistically significant.

RESULTS

Skin prick test

The skin prick test was definitely positive in 189 subjects, with the results "+++", "++", "+", "±" and "-" observed in 79 (3.96 %), 64 (3.21 %), 46 (2.31 %), 25 (1.25 %) and 1 780 (89.27 %), respectively among the 1994 individuals examined.

Etiological examination

Of 1994 individuals investigated, mites were detected from stool or/and urine samples in 161 (8.07 %) subjects, with the positive rates in stool, urine and in both being 4.61 % (92), 1.86 % (37) and 1.60 % (32), respectively.

The positive rate of mites in stool samples was 6.22 % (124/1 994), with that for male and female subjects being 6.84 % (78/1 140) and 5.39 % (46/854), respectively. No gender difference was found in this series (χ^2=1.77, P>0.05). The mites from stool samples included *Acarus siro*, *TyroPhagus putrescentiae*, *Dermatophagoides farinae*, *D. pteronyssinus*, *Glycyphagus domesticus*, *G.ornatus*, *Carpoglyphus lactis* and *Tarsonemus granaries*. Among 124 cases with mites in stool samples, 54 (43.55 %) were positive for adult mites, 13 (10.48 %) for larval mites, 43 (34.68 %) for both adult and larval mites, 3 (2.42 %) for both adult mites and eggs, 6 (4.84 %) for adult and larval mites and eggs, 3 (2.42 %) for both larval mites and eggs and 2 (1.61 %) for both hypopus and eggs. Mite concentration was also estimated, being 1-2 /cm^3, 2-4 /cm^3 and >5 /cm^3 in 6, 30 and 88 cases, respectively.

Totally, mites were detected from urine samples at a frequency of 3.46 % (69/1 994). The positive rate for male and female subjects were 3.95 % (45/1140) and 2.81 % (24/854), respectively, with no gender difference found in this series (χ^2=1.89, P>0.05). The mites in urine samples were separated and identified, including *Acarus siro*, *Tyrophagus putrescentiae*, *T. longior*, *Aleuroglyphus ovatus*, *Caloglyphus berlesei*, *C. mycophagus*, *Suidasia nesbitti*, *Lardoglyphus konoi*, *Glycyphagus domesticus*, *Carpoglyphus lactis*, *Lepidoglyphus destructor*, *Dermatophagoides farinae*, *D. pteronyssinus*, *Euroglyphus magnei*, *Caloglyphus hughesi*, *Tarsonemus granarus* and *T. hominis*. Among the 69 positive cases, 19 cases (27.54 %) were found to be positive for adult mites, 18 (26.09 %) for larval mites, 11 (15.94 %) both adult and larval mites, 3 (4.35 %) for adult mites and eggs, 11 (15.94 %) adult and larval mites and eggs, 6 (8.70 %) for larval mites and eggs, and 1 (1.44 %) for both hypopus and eggs. The mite concentrations were shown to be <0.5 /ml, 0.6-1 /ml, 1.1-1.5 /ml and >1.5 /ml, respectively, in 32, 25, 10 and 2 cases, reflecting the verity infectiosity of mites among different individuals.

Relationship between skin prick test and etiological examination

The results of etiological examination are correlative to skin prick test. One hundred and sixty-one of the 189 cases (85.19 %) positive skin-prick reaction were found to be positive for mites in their stool or / and urine samples. The intensities of the skin prick reaction were also found to be associated to mite concentrations in stool or / and urine samples, with the reactions "+++", "++" and "+" corrective to 100 % (79/79), 90.63 % (58/64) and 37.50 % (24/46), respectively.

Blood examination

Leukocytes were counted and sorted in so cases, most of them being in the range of (5.55-10.4)×10^9/L with the exception of 4 cases [(11.0-12.9)×10^9/L]. The esoinophilic granulocyte count was high [(0.32-0.78)×10^9/L]. The average value of constituent ratio of eosinophilic granulocyte was 0.09 (0.04-0.11) and was higher than the normal range (P<0.01).

Mites separated from working environment

The samples of mill floor dust (30 shares), stores of medicinal herbs (146 species) including wolfberry fruit, ophiopogon root liquorice, boat-fruited sterculia seed, safflower and other working environmental foodstuffs were collected and used for mites isolation. Numbers of mites per gram were shown to be 91-1862, 21-186, 0-483, 10-348, 51-712, and 311-1193, in mill floor dust, traditional Chinese medicine stores, traditional Chinese herbs including candied fruit, dry fruit, brown sugar, and expired cake. Twenty-two species, from 9 families of mites were separated and identified out of them, including *Acaridae*, *Lardoglyphidae*, *Glycyphagidae*, *Chortoglyphidae*, *Carpoglyphidae*, *Histiostomidae*, *Pyroglyphidae*, *Tarsonemus*, *Cheyletus*. The mite species isolates from working environmentwere were shown to be similar to those from stored food staffs.

Relationship between acariasis and occupation

Of the 1994 subjects investigated, mites were detected in 68 individuals (15.89 %) working in traditional Chinese medical storehouses, and 53 rice storehouse or mill workers 53 (12.96 %), being higher than those with other occupations (Table 1).

Table 1 Prevalence of intestinal and urinary tract mite infection in individuals with different occupations

Occupations	*n*	Only in stool		Only in urine		Both in stool and urine		Total	
		n	%	*n*	%	*n*	%	*n*	%
Traditional medical storehouse workers	428	32	7.48	24	5.61	12	2.80	68	15.89[a]
Rice storehouse or mill workers	409	28	6.85	12	2.93	13	3.18	53	12.96[a]
Miners	549	16	2.91	0	0	2	0.36	18	3.28[a]
Railway workers	236	5	2.12	0	0	1	0.42	6	2.54[a]
Pupils	255	9	3.53	1	0.39	3	1.18	13	5.10[a]
Teachers	117	2	1.71	0	0	1	0.85	3	2.56[a]
Total	1994	92	4.61	37	1.90	32	1.65	161	8.07

[a]χ^2=82.55, P<0.001.

Colonoscopy

Colonoscopy performs in 16 patients with mites found only in stool, showing pale intestinal wall, punctate ulcer, and exfoliated cell from intestinal wall. In addition, live mites and eggs were observed in tissues, especially in marginal zone of ulcer.

Cystoscopy

Cystoscopy was performed in the 11 patients with mites only found in urine samples, showing Pachymucosa, uroepithelial hyperplasia, lymphocyte and plasmaocyte infiltration in membrana propria and a lot of dense pink abscess in the trigone. In addition, trabecularism of inner wall of urinary bladder changed slightly, local of lateral wall was congestive, and blood capillary was also congestive and dilated. By cystoscopy, 4 adult mites were found in 3 of 11 subjects, which were identified to be *Lardoglyphus konoi*, *Euroglyphus magnei*, *Tarsonemus granarus*, and neither larval mite nor egg was found.

DISCUSSION

The acaroid mite is a kind of arthropod and its geographic distribution appears to be global[15,16]. Acaroid mites infestation is a well-known problem for stored grain, often influencing quality and hygienic condition of the grain[1-9]. However, little is known about acariasis. Acaroid mite can survive in many environments including the storehouse, human and animal bodies. Its infestion in human can cause acariasis in several organs including the lung, intestine and urinary tract[17-26].

In this study, mites were identified in 124 of the 1994 stool samples. The mite species observed in stool samples included *Acaridae*, *Glycyphagidae*, *Carpoglyphidae*, *Pyroglyphidae and Tarsonemus*, being in accordance with those found in the working places of the patients. This confirmed that mites being able to live in intestinal tract and causing intestinal acariasis were transmitted through living environment and stored foods. The respiratory infection through the polluted air may also be an alternative pathway. Eight sampling sites had been set up in a traditional Chinese medicine plant, and 13 mites had been isolated from the dust samples collected from the 640 L volume of air in the working environment of the plant. When dust with mites ingested, some of mites might go into intestine through mouth, nasal cavity or gorge. The mites living in intestinal tract may stimulate mechanically and damage intestinal tissues with its gnathosoma, chelicera, feet, and other structures[27,28]. In addition, they may also intrude into mucous layer and deep tissues, and cause necroinflammation and ulcers[29-33]. This has been approved in this study by colonoscopy, with spotty necrosis, petechial hemorrhage and ulcer observed. The most frequent symptoms of the intestinal acariasis were abdominal pain, diarrhea and pyohemofecia [10, 34,45].

Urinary acariasis was caused by mites parasitizing in human urinary tract. Mite isolation from urine is essential for its diagnosis. In the present study, 1994 individuals with different occupation were surveyed 69 patients found from their urine samples, 17 mite species were identified, with most of them being *Acaridida*. Apparently the pathogenic mites come from environment. Regarding the transmission path, the following possibilities have been proposed. First, the insects may enter the urinary tract by crawling from vulva. Second, they may enter the body through skin and reach urinary tract in some way. Third, mites in respiratory or alimentary system may enter the blood circulation, and reach kidney and urinary tract[46-50]. Acarid in human urinary system may damage urethral epithelia, for the mites are good at digging. Furthermore, they can also invade loose connective tissue and small blood vessel in urinary tract, and caused an ulcer. Under cystoscopy, a lot of dense pink abscess were found in trigone of urinary bladder in this study.

The incidence of intestinal and urinary acariasis was shown in this study to vary greatly and was linked to occupations, being higher in individuals working in traditional Chinese medicine (16 %) and rice storehouses or mills (13 %) than in those with other occupations (2.5-8.1 %). The densities of mites in traditional Chinese medicine and rice storehouses were shown to be high. When peoples exposed to these environment for a long time, the possibility to be infected may be greater than those in environments with low densities of mites. It is important to note that some patients with acariasis have habits of having teas immersed by traditional Chinese herbs, such as Liriope longipedicellata, Radix glycyrrhizae, boat-fruited sterculia seed, and eating dried kern like dateplum persimmon, candied jujube and Crataegus cuneata. Therefore, the prevalence of acariasis was related to personal habits and densities of mites in working environment and stored foodstuffs.

REFERENCES

1 **Sun HL,** Lue KH. Household distribution of house dust mite in central Taiwan. *J Microbiol Immunol Infect* 2000; **33**: 233-236

2 **Croce M,** Costa-Manso E, Baggio D, Croce J. House dust mites in the city of Lima, Peru. *Investig Allergol Clin Immunol* 2000; **10**: 286-288

3 **Arlian LG,** Neal JS, Vyszenski-Moher DL. Reducing relative humidity to control the house dust mite *Dermatophagoides farinae*. *J Allergy Clin Immunol* 1999; **104:** 852-856

4 **Mumcuoglu KY,** Gat Z, Horowitz T, Miller J, Bar-Tana R, Ben-Zvi A, Naparstek Y. Abundance of house dust mites in relation to climate in contrasting agricultural settlements in Israel. *Med Vet Entomol* 1999; **13:** 252-258

5 **Arlian LG,** Neal JS, Vyszenski-Moher DL. Fluctuating hydrating and dehydrating relative humidities effects on the life cycle of *Dermatophagoides farinae* (*Acari: Pyroglyphidae*). *J Med Entomol* 1999; **36:** 457-461

6 **Racewicz M**. House dust mites (Acari: Pyroglyphidae) in the cities of Gdansk and Gdynia (northern Poland). *Ann Agric Environ Med* 2001; **8:** 33-38

7 **Solarz K.** Risk of exposure to house dust pyroglyphid mites in Poland. *Ann Agric Environ Med* 2001; **8:** 11-24

8 **Sadaka HA,** Allam SR, Rezk HA, Abo-el-Nazar SY, Shola AY. Isolation of dust mites from houses of Egyptian allergic patients and induction of experimental sensitivity by Dermatophagoides pteronyssinus. *J Egypt Soc Parasitol* 2000; **30:** 263-276

9 **Boquete M,** Carballada F, Armisen M, Nieto A, Martin S, Polo F, Carreira J. Factors influencing the clinical picture and the differential sensitization to house dust mites and storage mites. *J Investig Allergol Clin Immunol* 2000; **10:** 229-234

10 **Li CP,** Wang J. Intestinal acariasis in Anhui Province. *World J Gastroenterol* 2000; **6:** 597-600

11 **Nuttall TJ,** Lamb JR, Hill PB. Characterisation of major and minor *Dermatophagoides* allergens in canine atopic dermatitis. *Res Vet Sci* 2001; **71:** 51-57

12 **Basomba A,** Tabar AI, de Rojas DH, Garcia BE, Alamar R, Olaguibel JM, del Prado JM, Martin S, Rico P. Allergen vaccination with a liposome-encapsulated extract of *Dermatophagoides pteronyssinus*: a randomized, double-blind, placebo -controlled trial in asthmatic patients. *J Allergy Clin Immunol* 2002; **109:** 943-948

13 **Akcakaya N,** Hassanzadeh A, Camcioglu Y, Cokugras H. Local and systemic reactions during immunotherapy with adsorbed extracts of house dust mite in children. *Ann Allergy Asthma Immunol* 2000; **85:** 317-321

14 **Hillier A,** Kwochka KW, Pinchbeck LR. Reactivity to intradermal injection of extracts of *Dermatophagoides farinae*, *Dermatophagoides pteronyssinus*, house dust mite mix, and house dust in dogs suspected to have atopic dermatitis: 115 cases (1996-1998). *J Am Vet Med Assoc* 2000; **217:** 536-540

15 **Musken H,** Franz JT, Wahl R, Paap A, Cromwell O, Masuch G, Bergmann KC. Sensitization to different mite species in German farmers: clinical aspects. *J Investig Allergol Clin Immunol* 2000; **10:** 346-351

16 **van Hage-Hamsten M,** Johansson E. Clinical and immunologic aspects of storage mite allergy. *Allergy* 1998; **53**(Suppl 48): 49-53

17 **Beco L,** Petite A, Olivry T. Comparison of subcutaneous ivermectin and oral moxidectin for the treatment of notoedric acariasis in hamsters. *Vet Rec* 2001; **149:** 324-327

18 **Hiraoka E,** Sato T, Shirai W, Kimura J, Nogami S, Itou M, Shimizu K. A case of pulmonary acariasis in lung of Japanese macaque. *J Vet Med Sci* 2001; **63:** 87-89

19 **van der Geest LP,** Elliot SL, Breeuwer JA, Beerling EA. Diseases of mites. *Exp Appl Acarol* 2000; **24**: 497-560

20 **Hammerberg B,** Bevier D, DeBoer DJ, Olivry T, Orton SM, Gebhard D, Vaden SL. Auto IgG anti-IgE and IgG x IgE immune complex presence and effects on ELISA-based quantitation of IgE in canine atopic dermatitis, demodectic acariasis and helminthiasis. *Vet Immunol Immunopathol* 1997; **60:** 33-46

21 **Morris DO,** Dunstan RW. A histomorphological study of sarcoptic acariasis in the dog: 19 cases. *J Am Anim Hosp Assoc* 1996; **32:** 119-124

22 **Jungmann P,** Guenet JL, Cazenave PA, Coutinho A, Huerre M. Murine acariasis: I. Pathological and clinical evidence suggesting cutaneous allergy and wasting syndrome in BALB/c mouse. *Res Immunol* 1996; **147:** 27-38

23 **Jungmann P,** Freitas A, Bandeira A, Nobrega A, Coutinho A, Marcos MA, Minoprio P. Murine acariasis. II. Immunological dysfunction and evidence for chronic activation of Th-2 lymphocytes. *Scand J Immunol* 1996; **43:** 604-612

24 **Ponsonby AL,** Kemp A, Dwyer T, Carmichael A, Couper D, Cochrane J. Feather bedding and house dust mite sensitization and airway disease in childhood. *J Clin Epidemiol* 2002; **55:** 556-562

25 **Paufler P,** Gebel T, Dunkelberg H. Quantification of house dust mite allergens in ambient air. *Rev Environ. Health* 2001; **16:** 65-80

26 **Zhou X,** Li N, Li JS. Growth hormone stimulates remnant small bowel epithelial cell proliferation. *World J Gastroenterol* 2000; **6:** 909-913

27 **Fryauff DJ,** Prodjodipuro P, Basri H, Jones TR, Mouzin E, Widjaja H, Subianto B. Intestinal parasite infections after extended use of chloroquine or primaquine for malaria prevention. *J Parasitol* 1998; **84:** 626-629

28 **Barrett KE.** New insights into the pathogenesis of intestinal dysfunction: secretory diarrhea and cystic fibrosis. *World J Gastroenterol* 2000; **6:** 470-474

29 **He ST,** He FZ, Wu CR, Li SX, Liu WX, Yang YF, Jiang SS, He G. Treatment of rotaviral gastroenteritis with Qiwei Baizhu powder. *World J Gastroenterol* 2001; **7:** 735-740

30 **Zhou JL,** Xu CH. The method of treatment on protozoon diarrhea. *Shijie Huaren Xiaohua Zazhi* 2000; **8:** 93-95

31 **Lee JD,** Wang JJ, Chung LY, Chang EE, Lai LC, Chen ER, Yen CM. A survey on the intestinal parasites of the school children in Kaohsiung county. *Kaohsiung J Med Sci* 2000; **16:** 452-458

32 **Herwaldt BL,** de Arroyave KR, Wahlquist SP, de Merida AM, Lopez AS, Juranek DD. Multiyear prospective study of intestinal parasitism in a cohort of Peace Corps volunteers in *Guatemala*. *J Clin Microbiol* 2001; **39:** 34-42

33 **Komatsu S,** Nimura Y, Granger DN. Intestinal stasis associated bowel inflammation. *World J Gastroenterol* 1999; **5:** 518-521

34 **Davis MD,** Richardson DM, Ahmed DD. Rate of patch test reactions to a *Dermatophagoides* mix currently on the market: a mite too sensitive? *Am J Contact Dermat* 2002; **13:** 71-73

35 **Lebbad M,** Norrgren H, Naucler A, Dias F, Andersson S, Linder E. Intestinal parasites in HIV-2 associated AIDS cases with chronic diarrhoea in Guinea-Bissau. *Acta Trop* 2001; **80:** 45-49

36 **Menon BS,** Abdullah MS, Mahamud F, Singh B. Intestinal parasites in Malaysian children with cancer. *J Trop Pediatr* 1999; **45:** 241-242

37 **Vandenplas Y.** Diagnosis and treatment of gastroesophageal reflux disease in infants and children. *World J Gastroenterol* 1999; **5:** 375-382

38 **Germani Y,** Minssart P, Vohito M, Yassibanda S, Glaziou P, Hocquet D, Berthelemy P, Morvan J. Etiologies of acute, persistent, and dysenteric diarrheas in adults in Bangui, Central African Republic, in relation to human immunodeficiency virus serostatus. *Am J Trop Med Hyg* 1998; **59:** 1008-1014

39 **Spiewak R,** Gora A, Horoch A, Dutkiewicz J. Atopy, allergic diseases and work-related symptoms among students of agricultural schools: first results of the Lublin study. *Ann Agric Environ Med* 2001; **8:** 261-267

40 **Fan WG,** Long YH. Diarrhea in travelers. *Shijie Huaren Xiaohua Zazhi* 2000; **8:** 937-938

41 **Feng ZH.** Application of gene vaccine and vegetable gene in infective diarrhea. *Shijie Huaren Xiaohua Zazhi* 2000; **8:** 934-936

42 **Xiao YH**. Treatment of infective Diarrhea with antibiotic. *Shijie Huaren Xiaohua Zazhi* 2000; **8:** 930-932

43 **Walusiak J,** Palczynski C, Wyszynska-Puzanska C, Mierzwa L, Pawlukiewicz M, Ruta U, Krakowiak A, Gorski P. Problems in diagnosing occupational allergy to flour: results of allergologic screening in apprentice bakers. *Int J Occup Med Environ Health* 2000; **13:** 15-22

44 **Barret JP,** Dardano AN, Heggers JP, McCauley RL. Infestations and chronic infections in foreign pediatric patients with burns: is there a role for specific protocols? *J Burn Care Rehabil* 1999; **20:** 482-486

45 **Xia B,** Shivananda S, Zhang GS, Yi JY, Crusius JBA, Peka AS. Inflammatory bowel disease in Hubei Province of China. *China Natl J New Gastroenterol* 1997; **3:** 119-120

46 **Bertot GM,** Corral RS, Fresno M, Rodriguez C, Katzin AM, Grinstein S. Trypanosoma cruzi tubulin eliminated in the urine of the infected host. *J Parasitol* 1998; **84:** 608-614

47 **Snowden KF,** Didier ES, Orenstein JM, Shadduck JA. Animal models of human microsporidial infections. *Lab Anim Sci* 1998; **48:** 589-592

48 **Mqoqi NP,** Appleton CC, Dye AH. Prevalence and intensity of Schistosoma haematobium urinary schistosomiasis in the Port St Johns district. *S Afr Med J* 1996; **86:** 76-80

49 **Greiff L,** Andersson M, Svensson J, Wollmer P, Lundin S, Persson CG. Absorption across the nasal airway mucosa in house dust mite perennial allergic rhinitis. *Clin Physiol Funct Imaging* 2002; **22:** 55-57

50 **Obase Y,** Shimoda T, Tomari SY, Mitsuta K, Kawano T, Matsuse H, Kohno S. Effects of pranlukast on chemical mediators in induced sputum on provocation tests in atopic and aspirin-intolerant asthmatic patients. *Chest* 2002; **121:** 143-150

Edited by Su Q

P.O.Box 2345, Beijing 100023,China
Fax: +86-10-85381893
E-mail: wjg@wjgnet.com www.wjgnet.com

World J Gastroenterol 2003;9(4):878-880
World Journal of Gastroenterology
 ISSN 1007-9327

• CASE REPORT •

Primary biliary cirrhosis and ulcerative colitis: A case report and review of literature

Wen-Bin Xiao, Yu-Lan Liu

Wen-Bin Xiao, Yu-Lan Liu, Department of Gastroenterology, People' s Hospital, Peking University, Beijing 100044, China
Correspondence to: Dr. Wen-Bin Xiao, Department of Gastroenterology, People' s Hospital, Peking University, Beijing 100044, China. hhxwb@263.net
Telephone: +86-10-68314422 Ext 5726 **Fax**: +86-10-68318386
Received: 2002-11-26 **Accepted:** 2002-12-25

Abstract

AIM: To summarize the characteristics of patients suffered from primary biliary cirrhosis associated with ulcerative colitis.

METHODS: To report a new case and review the literature.

RESULTS: There were 18 cases (including our case) of primary biliary cirrhosis complicated with ulcerative colitis reported in the literature. Compared with classical primary biliary cirrhosis, the patients were more often males and younger similar. The bowel lesions were usually mild with proctitis predominated. While ulcerative colitis was diagnosed before primary biliary cirrhosis in 13 cases, the presentation of primary biliary cirrhosis was earlier than that of ulcerative colitis in our new case reported here. The prevalence of primary biliary cirrhosis among patients of ulcerative colitis was almost 30 times higher than in general population.

CONCLUSION: Association of primary biliary cirrhosis with ulcerative colitis is rare. It should be considered in the differential diagnosis of hepatobiliary disease in patients with ulcerative colitis, and vice versa.

Xiao WB, Liu YL. Primary biliary cirrhosis and ulcerative colitis: A case report and review of literature. *World J Gastroenterol* 2003; 9(4): 878-880
http://www.wjgnet.com/1007-9327/9/878.htm

INTRODUCTION

A variety of hepatobiliary diseases have been described in patients with ulcerative colitis (UC). The incidence is 3-15 % with persistent abnormal liver function tests, and up to 90 % with abnormal liver histology at surgery or autopsy[1]. These include primary sclerosing cholangitis, pericholangitis of the small bile ducts, chronic active hepatitis, cholangiocarcinoma and cirrhosis. The association of primary biliary cirrhosis (PBC) and UC has occasionally been reported[2-4]. We hereby presented an additional case.

CASE REPORT

A 50-year-old woman was admitted to our hospital because of skin pruiritus for two years. One year ago she was found to have jaundice and examined in another hospital. The results of all hepatitis virus test were negative, and she was diagnosed as cryptogenic hepatitis. Six months ago she had diarrhea 2-3 times per day. Upon physical examination icterus was evident on the skin and sclera. Hepatomegaly and splenomegaly were found. Blood routine test revealed hemoglobulin 106 g/L, WBC and platelet counts normal. ESR 78 mm/h. IgM elevated to 7.73 g/L, IgA and IgG normal. Liver function tests showed ALT 81 U/L, AST 139 U/L, serum total bilirubin 223.2 umol/L, direct bilirubin 138.3 umol/L and GGT 1042 U/L. Cholesterol was 12.2 mmol/L. Immunological tests, by indirect immunofluorescence were as follows: ANA, 1:10 positive, anti-mitochondria antibody (AMA), negative, anti-LK (anti-liver and anti-kidney) microsome antibody and anti-smooth muscle antibody negative. Hepatomegaly, splenomegaly and portal hypertension were seen in abdominal computed tomography (Figure 1). No intra- and extrahepatic bile duct abnormalities were found by ERCP. Liver biopsy disclosed an increased portal inflitration consisting of lymphocytes, plasmacytes, and scattered eosinophils with fibrosis and pseudolobulation. Two portal areas had hyperplastic ductule. The findings were compatible with PBC stage 3-4 (Figure 2). Colonoscopy showed up to 20 cm continuous lesions of the mucosa with numerous ulcers and adherent mucopurulent exudate (Figure 3). Histological examination demonstrated loss of goblet cells, neutrophilic microabscesses in the crypts, and inflitration with mononuclear cells and plasma cells in the lamina propria (Figure 4). Ulcerative colitis limited to rectosigmoid was diagnosed. Ursodeoxycholic acid (UDCA) was prescribed. One month later serum bilirubin and liver function tests returned to normal. But diarrhea persisted and sulfasalazine was given. The bowel symptoms were then relieved.

Table 1 Review of patients of PBC associated with UC[a]

References	Patient	Sex	Age (yr)	Comorbidity	AMA (titer)
3	1	F	65	Pancolitis, chronic pancreatitis	1/64
4	2	F	20	Proctitis	Strongly
4	3	M	22	Proctitis	1/160
4	4	M	44	Proctitis	1/320
4	5	F	28	Left-side colitis	1/200
5	6	F	49	Proctitis, chronic myelocytic leukemia	Positive
6	7	F	45	Proctitis,chronic pancreatitis	Positive
7	8	M	40	Left-side colitis	1/160
8	9	F	48	Pancolitis, renal cell carcinoma	1/160
9	10	M	58	Proctitis	1/160
9	11	F	68	Proctitis	1/160
10	12	F	43	Pancolitis	>1/160
11	13	M	61	Proctitis	Positive
Present	14	F	50	Proctitis	Negative

[a]Four cases with incomplete data were not shown here.

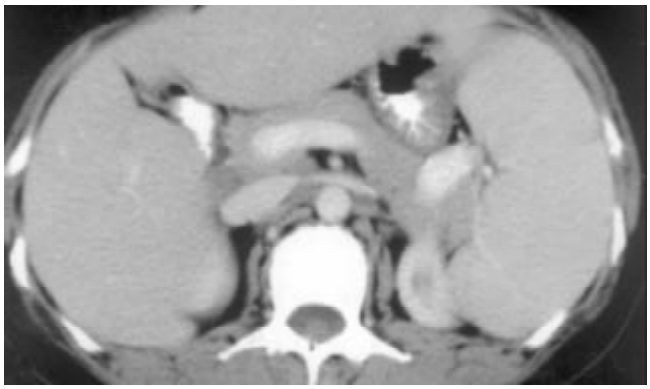

Figure 1 Abdominal CT disclosed hepatomegaly, splenomegaly and portal hypertension.

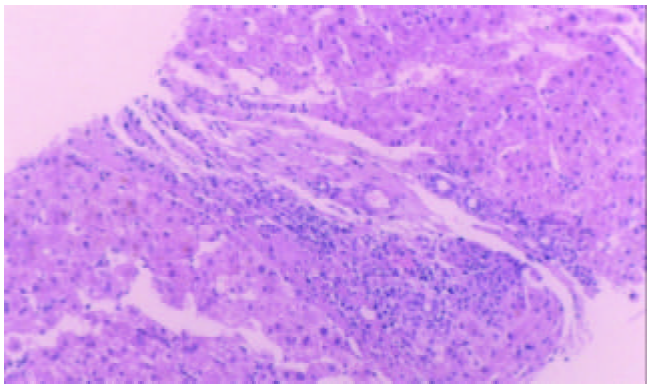

Figure 2 Liver biopsy revealed portal inflitration of lymphocytes, plasmacytes, and scattered eosinophils with fibrosis and pseudolobule (H&E, 10×10).

Figure 3 Colonoscopy showed continuous mucosal ulceration.

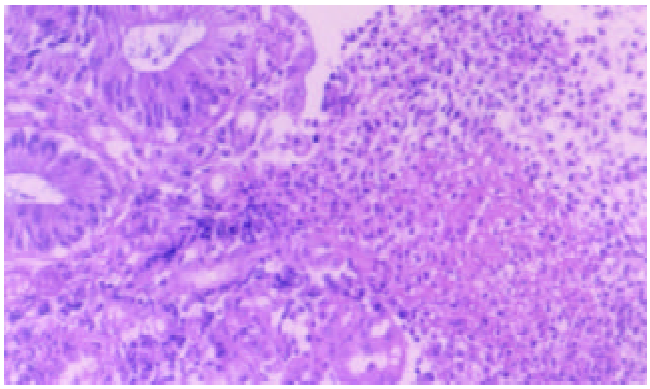

Figure 4 Histological examination demonstrated neutrophilic microabscesses in the crypts (H&E, 10×20).

DISCUSSION

Hepatobiliary diseases are commonly found in association with UC. Primary sclerosing cholangitis (PSC) involved the large bile ducts is the most common associated hepatopathology, affecting 2.4-7.5 % of UC patients. PBC is another autoimmune hepatobiliary disease similar to PSC. The typical features include skin pruiritus, with hyperbilirubinemia, increased IgM levels and hypercholesterolemia. AMA is present in about 95 % of patients, that is in about 5 % AMA is negative. Cholangiogram is normal. Granulomatous inflammation of the periportal areas is a typical finding. The clinical manifestation and histologic features of our patient were compatible with PBC, although AMA was negative.

PBC associated with UC is rare. There were 18 cases (including our case) reported in the literature. In 4 cases from Sweden and Taiwan data were incomplete. In the remaining 14 patients, their presentations were different from that of typical PBC without UC (Table 1). It is well known that PBC usually affects middle-aged women. The sex ratio is 10:1 (women to men), and the mean age at diagnosis was 57.5 years. It is quite obvious that these figures differ in the patients of table 1. The sex ratio was low (2:1) and the mean age was younger similar to that of UC. In addition, UC was mild and limited with proctitis predominating. Only 3 of 12 patients had pancolitis. Similarly, UC associated with PSC tends to be mild, but usually involving the whole bowel.

The prevalence of PBC in Europe is about 15/100 000. In a cohort of 412 cases of UC, 2 cases of PBC were diagnosed estimating the prevalence of PBC among these patients 485/100 1 000, almost 30 times higher as compared with the general population[2]. It is believed that both PBC and UC are autoimmune disease, and have similar pathogenesis. Associated autoimmune conditions are frequent in both PBC and UC. PBC and UC may be an additional example of a true association between syndromes of autoimmune etiology. But the detail remains to be clarified. In 13 out of the 14 patients UC were diagnosed many years before the diagnosis of PBC. Symptoms of PBC usually presented during the active stage of UC. In other words, PBC runs a course depending the activity of UC. So most authors considered PBC as the extraintestinal (hepatobiliary) manifestiation of UC. But in our case it is clear that the presentation of PBC is earlier than that of UC. We believe that UC also could be regarded as extrahepatic manifestation of PBC.

Treatment of these patients presents some difficulties. Prednisolone, which is indicated for the treatment of the active stage of UC, might lead to extensive osteroporosis in PBC. But as mentioned above, UC associated with PBC is usually mild, so sulfasalazine is the first choice. If the presentation of PBC is evident, UDCA could be added.

In conclusion the reported association between UC and PBC is rare, and it has not yet been established whether it occurs coincidently or is due to a common immunogenetic basis. PBC should be considered in the differential diagnosis of hepatobiliary disease in patients with UC, and vice versa. Liver biopsy and serum AMA are two diagnostic criteria that clearly distinguish PBC from PSC.

REFERENCES

1 **Monsen U**, Sorstad J, Hellers G, Johansson C. Extracolonic diagnoses in ulcerative colitis: an epidemiological study. *Am J Gastroenterol* 1990; **85**: 711-716

2 **Chien RN**, Sheen IS, Chen TJ, Liaw YF. A clinicopathological study in primary biliary cirrhosis. *J Formos Med Assoc* 1992; **91** (Suppl 2): S117-121

3 **Kato Y**, Morimoto H, Unoura M, Kobayashi K, Hattori N, Nakanuma Y. Primary biliary cirrhosis and chronic pancreatitis

in a patient with ulcerative colitis. *J Clin Gastroenterol* 1985; **7**: 425-427

4 **Bush A**, Mitchison H, Walt R, Baron JH, Boylston AW, Summerfield JA. Primary biliary cirrhosis and ulcerative colitis. *Gastroenterology* 1987; **92**: 2009-2013

5 **Akahoshi K**, Miyata Y, Hashimoto M, Koga S, Chijiiwa Y, Misawa T, Suematsu E, Nishimura J, Nawata H. A case of combined primary biliary cirrhosis, ulcerative colitis and chronic myelocytic leukemia. *Gastroenterol Jpn* 1992; **27**: 252-257

6 **Veloso FT**, Dias LM, Carvalho J, Fraga J, Saleiro J. Ulcerative colitis, primary biliary cirrhosis, and chronic pancreatitis: coincident or coexistent? *J Clin Gastroenterol* 1993; **16**: 55-57

7 **Lever E**, Balasubramanian K, Condon S, Wat BY. Primary biliary cirrhosis associated with ulcerative colitis. *Am J Gastroenterol* 1993; **88**: 945-947

8 **Satsangi J**, Marshall J, Roskell D, Jewell D. Ulcerative colitis complicated by renal cell carcinoma: a series of three patients. *Gut* 1996; **38**: 148-150

9 **Koulentaki M**, Koutroubakis IE, Petinaki E, Tzardi M, Oekonomaki H, Mouzas I, Kouroumalis EA. Ulcerative colitis associated with primary biliary cirrhosis. *Dig Dis Sci* 1999; **44**: 1953-1956

10 **Ohge H**, Takesue Y, Yokoyama T, Hiyama E, Murakami Y, Imamura Y, Shimamoto F, Matsuura Y. Progression of primary biliary cirrhosis after proctocolectomy for ulcerative colitis. *J Gastroenterol* 2000; **35**: 870-872

11 **Nakayama M**, Tsuji H, Shimono J, Azuma K, Ogata H, Matsumoto T, Aoyagi K, Fujishima M, Iida M. Primary biliary cirrhosis associated with ulcerative colitis. *Fukuoka Igaku Zasshi* 2001; **92**: 354-359

Edited by Xu JY

P.O.Box 2345, Beijing 100023,China
Fax: +86-10-85381893
E-mail: wjg@wjgnet.com www.wjgnet.com

World J Gastroenterol 2003;9(4):881-882
World Journal of Gastroenterology
 ISSN 1007-9327

• CASE REPORT •

Congenital H-type anovestibuler fistula

Mesut Yazlcl, Barlas Etensel, Harun Gürsoy, Sezen Özklsaclk

Mesut Yazlcl, Barlas Etensel, Harun Gürsoy, Sezen Özklsaclk, Department of Pediatric Surgery, Faculty of Medicine, Adnan Menderes University, Aydln, Turkey
Correspondence to: Mesut Yazlcl, Department of Pediatric Surgery, Faculty of Medicine, Adnan Menderes University, 09100 Aydln, Turkey. myazici@adu.edu.tr
Telephone: +90-256-2120020 **Fax:** +90-256-2120146
Received: 2002-12-22 **Accepted:** 2003-01-13

Abstract

The congenital H-type fistula between the anorectum and genital tract besides a normal anus is a rare entity in the spectrum of anorectal anomalies. We described a girl with an anovestibuler H-type fistula and left vulvar abscess. A 40-day-old girl presented symptoms after her parents noted the presence of stool at the vestibulum. On the physical examination, anus was in normal location and size, and had normal sphincter tone. A vestibuler opening was seen in the midline just below of the hymen. A fistulous communication was found between the vestibuler opening and the anus, just above the dentate line. There was a vulvar abscess which had a left lateral vulvar drainage opening 15 mm left lateral to the perineum. After the management of local inflammation and abscess, the patient was operated for primary repair of the fistula. A protective colostomy wasn't performed prior the operation. A profuse diarrhea started after 5 hours of postoperation. After the diarrhea, a recurrent fistula was occurred on the second postoperative day. A divided sigmoid colostomy was performed. 2 months later, and anterior sagital anorectoplasty was reconstructed and colostomy was closed 1 month later. Various surgical techniques with or without protective colostomy have been described for double termination repair. But there is no consensus regarding surgical management of double termination.

Yazlcl M, Etensel B, Gürsoy H, Özklsaclk S. Congenital H-type anovestibuler fistula. *World J Gastroenterol* 2003; 9(4): 881-882
http://www.wjgnet.com/1007-9327/9/881.htm

INTRODUCTION

The congenital H-type fistula between the anorectum and genital tract without anal atresia is a rare entity in the spectrum of anorectal anomalies. This type of anomaly has been termed as "double termination" of the alimentary tract in girls[1-3]. Most of the fistulas localized between the anorectum and vestibule of the vagina, and this type anomaly was described as Perineal Canal[1,2, 4-6]. We described a 40-day-old girl with a congenital anovestibuler H-type fistula complicated with a vulvar abscess.

CASE REPORT

A 40-day-old girl referred to our university medical center with a passage of stool through vestibulum as well as through the normal anal passage from birth. She had been swelling and tenderness on her left vulvar region for one week. On the physical examination, anus was at the normal location and size, and it had normal sphincter tone. A vestibuler opening was found in the midline just below of the hymen. With insertion of an 8 Fr catheter through the vestibuler opening, a fistulous communication was detected between the vestibule of the vagina and the anus at the dentate line. Nearly 3 mm to the left side of this opening, there was a second opening about 3 mm in diameter. A metal sound was inserted through this opening and it was found that it had a subcutaneous continuity with a vulvar abscess. This abscess was detected to drain through a cutaneous opening 15 mm lateral to the perineum (Figure 1). No associated anomaly was detected.

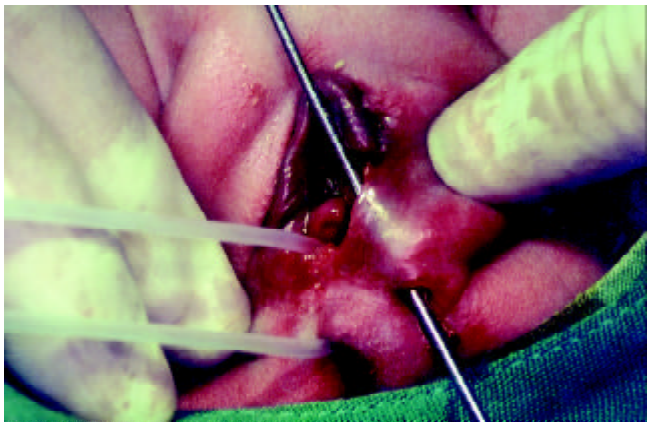

Figure 1 8 Fr catheter was placed in the perineal canal and metal sound was passed through vestibuler and cutaneous openings of the abscess.

After the management of local inflamation and abscess, the patient was operated for primary repair of the fistula. The bowel preparation was performed with saline enemas. A protective colostomy was not performed either prior or during the definitive operation. We used the technique of anterior sagittal anorectoplasty described by Kulshrestha *et al.* in 1998[1]. At the operation, a metal sound was passed through the fistula from the vestibule of the vagina into the anal canal in the lithotomy position. Then the perineal body that remained over the sound vertically was incised. This incision included skin, subcutaneous tissue, a few fibers of external sphincter muscle, wall of the fistulous tract and anal canal mucosa. The mucosa of the opened fistulous tract was dissected off the underlying muscle. Then, perineal reconstruction was performed by stitching the vestibule, perineal body, sphincter muscle and the anorectum with interrupted 4/0 PDS sutures. Perineal skin was closed with 4/0 Prolene. Five hours following the transfer of the patient to the ward, a profuse diarrhea started resulting in 16 defecations on the first postoperative day. Unfortunately, this caused a partial breakdown of the wound on the second postoperative day, which caused the recurrence of the fistula. And the divided sigmoid colostomy was performed.

Two months later, we operated with the same technique and this attempt was successful. One month following the repair of the fistula, we closed her colostomy and started a rectal dilatation program. Her first year postoperative follow-up was uneventful.

DISCUSSION

The incidence of double termination among female anorectal malformations ranged between 4-14 % in different Asian series[1,5-8]. On the basis of Wingspread classification, these H-type fistulas were divided into three groups according to their level. Low type double termination included cases in which the fistula was lying between the anal canal and the vestibule and this was named as "perineal canal". In the intermediate type, communication was found between the rectum and the vestibule. High type of double termination consisted of a fistula between the rectum and the vagina[1]. Our case had a low type double termination and an abscess which was detected in her vulvar region complicated her anomaly. When we reviewed the cases reported in the literature, we found out that Rintala *et al*. reported vulvar abscess formation in three girls with double termination[2]. In another report by Brem *et al.* abscess formation was claimed to be secondary to the infection in either a congenital blind-ending sinus or an existing fistula leading to additional openings[9].

On the other hand, high type of vestibuler fistula demands a more specific operation and it may be named as vestibulorectal pull-through procedure. Without protective colostomy, this type of repair is reported to have a fairly high recurrence rate[7]. Various surgical techniques have been described for low-type double termination repair. These techniques were utilized either with or without protective colostomy in different series. Chatterjee described a simple perineal procedure without colostomy and with good results[3]. Tsuchida *et al* did not use diversion during definitive procedure they named as "pull-through of the anterior wall of the rectum" in 3 of his 7 cases with perineal canal. Their results were satisfactory for both diverted and non-diverted cases. However, they were not as successful as above with their cases managed with another different simple repair technique and without diversion[5]. Kulshrestha *et al*. described anterior sagittal anorectoplasty in 1998 as a surgical technique for all types of double termination without colostomy and without no complications[1]. This series which were the most recent and had a successful outcome for the repair of perineal canal directed us to prefer this technique in our series. Furthermore, avoiding a colostomy in using this technique was another major factor for our selection.

Unfortunately, our case' s fistula recurred. This may have resulted not from insufficiency of the technique, but from some factors that did not take place in Kulshrestha' s series. A major reason for breakdown of the repair may be due to the unexpected and unwanted profuse diarrhea of the patient that started after 5 hours of the post-operation. The sufficiency of the technique may be thought of when one thinks that in the redo operation, it was proved to be a good result.

In conclusion, it is believed that definitive repair can be performed without protective colostomy when no abscess formation is present in the vulvar region. If an abscess is detected, it should be well managed before the operation.

REFERENCES

1 **Kulshrestha S**, Kulshrestha M, Prakash G, Gangopadhyay AN, Sarkar B. Management of congenital and acquired H-type anorectal fistulae in girls by anterior sagittal Anorectovaginoplasty. *J Pediatr Surg* 1998; **33**: 1224-1228

2 **Rintala RJ**, Mildh L, Lindahl H. H-type anorectal malformations: incidence and clinical characteristics. *J Pediatr Surg* 1996; **31**: 559-562

3 **Chatterjee SK**, Talukder BC. Double termination of the alimentary tract in female infants. *J Pediatr Surg* 1969; **4**: 237-243

4 **Rao KL**, Choudhury SR, Samujh R, Narasimhan KL. Perineal canal-repair by a new surgical technique. *Pediatr Surg Int* 1993; **8**: 449-450

5 **Tsuchida Y**, Saito S, Honna T, Makino S, Kaneko M, Hazama H. Double termination of the alimentary tract in females: a report of 12 cases and a literature review. *J Pediatr Surg* 1984; **19**: 292-296

6 **Wakhlu A**, Pandey A, Prasad A, Kureel SN, Tandon RK, Wakhlu AK. Anterior Sagittal anorectoplasty for anorectal malformations and perineal trauma in the female child. *J Pediatr Surg* 1996; **31**: 1236-1240

7 **Chatterjee SK**. Double termination of the alimentary tract-a second look. *J Pediatr Surg* 1980; **15**: 623-627

8 **Bagga D**, Chadha R, Malhotra CJ, Dhar A. Congenital H-type vestibuloanorectal fistula. *Pediatr Surg Int* 1995; **10**: 481-484

9 **Brem H**, Guttman FM, Laberge JM, Doody D. Congenital anal fistula with normal anus. *J Pediatr Surg* 1989; **24**: 183-185

Edited by Xu XQ

P.O.Box 2345, Beijing 100023,China
Fax: +86-10-85381893
E-mail: wjg@wjgnet.com www.wjgnet.com

World J Gastroenterol 2003;9(4):883-884
World Journal of Gastroenterology
 ISSN 1007-9327

• CASE REPORT •

A case of enterolith small bowel obstruction and jejunal diverticulosis

Buhussan Hayee, Hamed Noor Khan, Talib Al-Mishlab, John F McPartlin

Buhussan Hayee, Hamed Noor Khan, Talib Al-Mishlab, John F McPartlin, Department of Surgery, William Harvey Hospital, Ashford, Kent TN24, U.K.
Correspondence to: Dr. Hamed Khan, Flat 11, the Point, 6 Bellargate, Nottingham, NG1 1JN, U.K. hamed4Khan@aol.com
Telephone: +44 -115-9242809
Received: 2002-11-19 **Accepted:** 2003-01-13

Abstract

We reported a case of 79-year old woman with known large bowel diverticulosis presenting with small bowel obstruction due to stone impaction - found on plain abdominal X-ray. Contrast studies demonstrated small bowel diverticulosis. At laparotomy, the gall bladder was normal with no stones and no abnormal communication with small bowel - excluding the possibility of a gallstone ileus. Analysis of the stone revealed a composition of bile pigments and calcium oxalate. This was a rare case of small bowel obstruction due to enterolith formation - made distinctive by calcification (previously unreported in the proximal small bowel).

Hayee B, Khan HN, Al-Mishlab T, McPartlin JF. A case of enterolith small bowel obstruction and jejunal diverticulosis. *World J Gastroenterol* 2003; 9(4): 883-884
http://www.wjgnet.com/1007-9327/9/883.htm

INTRODUCTION

Diverticulosis of the small bowel (excluding Meckel' s) is uncommon - being found in less than 5 % of post-mortem examinations, although the prevalence increases with age[1]. The condition can be complicated by diverticulitis, haemorrhage or perforation[2,3]. Small bowel obstruction due to an enterolith formed and extruded from a diverticulum is a rare complication[4-6].

Enteroliths form in small bowel diverticula either *de novo* or around a central nidus such as a fruit stone or undigested vegetable matter (the latter is termed a bezoar). The usual composition of true enteroliths is choleic acid[7] - an end product of bile salt metabolism - postulated to form as a result of acidic pH shift within a small bowel diverticulum. Radiological diagnosis of such stones is rare, unless calcified (which usually occurs only in the more alkaline ileum)[7]. Diagnosis is therefore made at laparotomy with the presence of the stone, diverticula and the finding of a normal gall bladder (excluding a gallstone ileus). It is unclear how stones are extruded from small bowel diverticula lacking a muscular coat, but larger stones will be extruded and pass distally to cause obstruction - an enterolith ileus.

CASE REPORT

A 79-year-old lady presented with a two-day history of vomiting and central, colicky abdominal pain. She had been constipated prior to this episode and had taken senna with only a little effect on the previous day. She had a known history of sigmoid diverticular disease and had been admitted only once previously for suspected diverticulitis. She appeared dehydrated with fever of 37.6 degrees. Her abdomen was distended but soft with some central and left-sided tenderness. Bowel sounds were heard and digital rectal examination was unremarkable. Blood tests revealed a white cell count of 21.6×10^9/L without other abnormality. A plain abdominal film demonstrated opacity on the left side (Figure 1) and a gastrografin study revealed numerous small bowel diverticula of varying sizes. The opacity now was presumed to be a stone, was noted within the small bowel (Figure 2).

Figure 1 Radio-opaque stone was clearly seen in the plain abdominal radiograph (arrow).

Figure 2 Contrast study (105 mins) demonstrated multiple jejunal diverticula and minimal passage of barium beyond the mid-jejunum. Stone was still visible (arrow).

At laparotomy, the presence of large jejunal diverticula was confirmed and the stone was found impacted in the mid-

jejunum. The gall bladder appeared normal without stones. The stone approximately 3×4 cm and weighing 10.60 g appeared greyish and hard which was removed via a small enterotomy close to it. The patient made a good recovery from operation, delayed only by post-operative nausea. Analysis of the stone revealed a composition of bile pigments and calcium oxalate.

DISCUSSION

We reported the first case of proximal small bowel obstruction due to a calcified enterolith. It is postulated that diverticulas provide the more acidic environment necessary for choleic acid precipitation and stone formation[7]. However calcification cannot occur without an alkaline pH shift, which normally occurs in the ileum. Our case confirmed calcification occurring in the proximal small bowel which made this theory less definitive but facilitated the diagnosis.

The consensus management of enterolith ileus at laparotomy is to first attempt manual lysis of the stone without enterotomy and to milk the smaller parts into the colon where they are passed through rectum[8]. If this is proved to be impossible or inappropriate, the stone is removed through an enterotomy which is made in a less edematous segment of proximal small bowel.

The rarity of enterolith small bowel obstruction is well recognised with the condition occurring in conjunction with cases of diverticulosis. However the diagnosis should be considered in patients presenting with clinical features of small bowel obstruction without evidence of previous abdominal surgery or incarcerated hernia.

REFERENCES

1 **Noer T**. Non-Meckelian diverticula of the small bowel. *Acta Chir Scand* 1960; **120**: 175-179
2 **Longo WE**, Vernava AM 3rd. Clinical implications of jejunal diverticular disease. *Dis Colon & Rectum* 1992; **35**: 381-388
3 **Sibille A**, Willocx R. Jejunal diverticulitis. *Am J Gastroenterol* 1992; **87**: 655-658
4 **Yang HK**, Fondacaro PF. Enterolith ileus: a rare complication of duodenal diverticula. *Am J Gastroenterol* 1992; **77**: 621-624
5 **Ishizuka D**, Shirai Y, Hatakeyama K. Duodenal obstruction caused by gallstone obstruction into an intraluminal duodenal diverticulum. *Am J Gastroenterol* 1997; **92**: 182-183
6 **Klingler PJ**, Seelig MH, Floch NR, Branton SA, Metzger PP. Small intestinal enteroliths: unusual cause of small intestinal obstruction: report of three cases. *Dis Colon & Rectum* 1999; **42**: 676-679
7 **Shocket E**, Simon SA. Small bowel obstruction due to enterolith (bezoar) formed in a duodenal diverticulum: a case report and review of the literature. *Am J Gastroenterol* 1982; **77**: 621-624
8 **Yang HK**, Fondacaro PF. Enterolith ileus: a rare complication of duodenal diverticula. *Am J Gastroenterol* 1992; **87**: 1846-1848

Edited by Xu XQ